ISSN 0021-9673

VOL. 587 NO. 2 DECEMBER 20, 1991

THIS ISSUE COMPLETES VOL. 587

JOURNAL OF CHROMATOGRAPHY

INCLUDING ELECTROPHORESIS AND OTHER SEPARATION METHODS

ELSEVIER

JOURNAL OF CHROMATOGRAPHY

INCLUDING ELECTROPHORESIS AND OTHER SEPARATION METHODS

Scope. The *Journal of Chromatography* publishes papers on all aspects of chromatography, electrophoresis and related methods. Contributions consist mainly of research papers dealing with chromatographic theory, instrumental development and their applications. The section *Biomedical Applications*, which is under separate editorship, deals with the following aspects: developments in and applications of chromatographic and electrophoretic techniques related to clinical diagnosis or alterations during medical treatment; screening and profiling of body fluids or tissues with special reference to metabolic disorders; results from basic medical research with direct consequences in clinical practice; drug level monitoring and pharmacokinetic studies; clinical toxicology; analytical studies in occupational medicine.

Submission of Papers. Manuscripts (in English; *four* copies are required) should be submitted to: Editorial Office of *Journal of Chromatography*, P.O. Box 681, 1000 AR Amsterdam, Netherlands, Telefax (+31-20) 5862 304, or to: The Editor of *Journal of Chromatography, Biomedical Applications*, P.O. Box 681, 1000 AR Amsterdam, Netherlands. Review articles are invited or proposed by letter to the Editors. An outline of the proposed review should first be forwarded to the Editors for preliminary discussion prior to preparation. Submission of an article is understood to imply that the article is original and unpublished and is not being considered for publication elsewhere. For copyright regulations, see below.

Publication. The *Journal of Chromatography* (incl. *Biomedical Applications*) has 39 volumes in 1992. The subscription prices for 1992 are:

J. Chromatogr. (incl. *Cum. Indexes, Vols. 551–600*) + *Biomed. Appl.* (Vols. 573–611):
Dfl. 7722.00 plus Dfl. 1209.00 (p.p.h.) (total *ca.* US$ 4421.25)

J. Chromatogr. (incl. *Cum. Indexes, Vols. 551–600*) only (Vols. 585–611):
Dfl. 6210.00 plus Dfl. 837.00 (p.p.h.) (total *ca.* US$ 3488.50)

Biomed. Appl. only (Vols. 573–584):
Dfl. 2760.00 plus Dfl. 372.00 (p.p.h.) (total *ca.* US$ 1550.50).

Subscription Orders. The Dutch guilder price is definitive. The US$ price is subject to exchange-rate fluctuations and is given as a guide. Subscriptions are accepted on a prepaid basis only, unless different terms have been previously agreed upon. Subscriptions orders can be entered only by calender year (Jan.–Dec.) and should be sent to Elsevier Science Publishers, Journal Department, P.O. Box 211, 1000 AE Amsterdam, Netherlands, Tel. (+31-20) 5803 642, Telefax (+31-20) 5803 598, or to your usual subscription agent. Postage and handling charges include surface delivery except to the following countries where air delivery via SAL (Surface Air Lift) mail is ensured: Argentina, Australia, Brazil, Canada, China, Hong Kong, India, Israel, Japan*, Malaysia, Mexico, New Zealand, Pakistan, Singapore, South Africa, South Korea, Taiwan, Thailand, USA. *For Japan air delivery (SAL) requires 25% additional charge of the normal postage and handling charge. For all other countries airmail rates are available upon request. Claims for missing issues must be made within three months of our publication (mailing) date, otherwise such claims cannot be honoured free of charge. Back volumes of the *Journal of Chromatography* (Vols. 1–572) are available at Dfl. 208.00 (plus postage). Customers in the USA and Canada wishing information on this and other Elsevier journals, please contact Journal Information Center, Elsevier Science Publishing Co. Inc., 655 Avenue of the Americas, New York, NY 10010, USA, Tel. (+1-212) 633 3750, Telefax (+1-212) 633 3990.

Abstracts/Contents Lists published in Analytical Abstracts, Biochemical Abstracts, Biological Abstracts, Chemical Abstracts, Chemical Titles, Chromatography Abstracts, Clinical Chemistry Lookout, Current Contents/Life Sciences, Current Contents/Physical, Chemical & Earth Sciences, Deep-Sea Research/Part B: Oceanographic Literature Review, Excerpta Medica, Index Medicus, Mass Spectrometry Bulletin, PASCAL-CNRS, Pharmaceutical Abstracts, Referativnyi Zhurnal, Research Alert, Science Citation Index and Trends in Biotechnology.

See inside back cover for Publication Schedule, Information for Authors and information on Advertisements.

0021-9673/91/$03.50

This issue is printed on acid-free paper.

Printed in the Netherlands

CONTENTS

(Abstracts/Contents Lists published in Analytical Abstracts, Biochemical Abstracts, Biological Abstracts, Chemical Abstracts, Chemical Titles, Chromatography Abstracts, Current Contents/Life Sciences, Current Contents/Physical, Chemical & Earth Sciences, Deep-Sea Research/Part B: Oceanographic Literature Review, Excerpta Medica, Index Medicus, Mass Spectrometry Bulletin, PASCAL-CRNS, Referativnyi Zhurnal, Research Alert and Science Citation Index)

REGULAR PAPERS

Column Liquid Chromatography

Gas Chromatography

(Continued overleaf)

Contents (continued)

SHORT COMMUNICATIONS

Column Liquid Chromatography

Gas Chromatography

In articles with more than one author, the name of the author to whom correspondence should be addressed is indicated in the article heading by a 6-pointed asterisk (*).

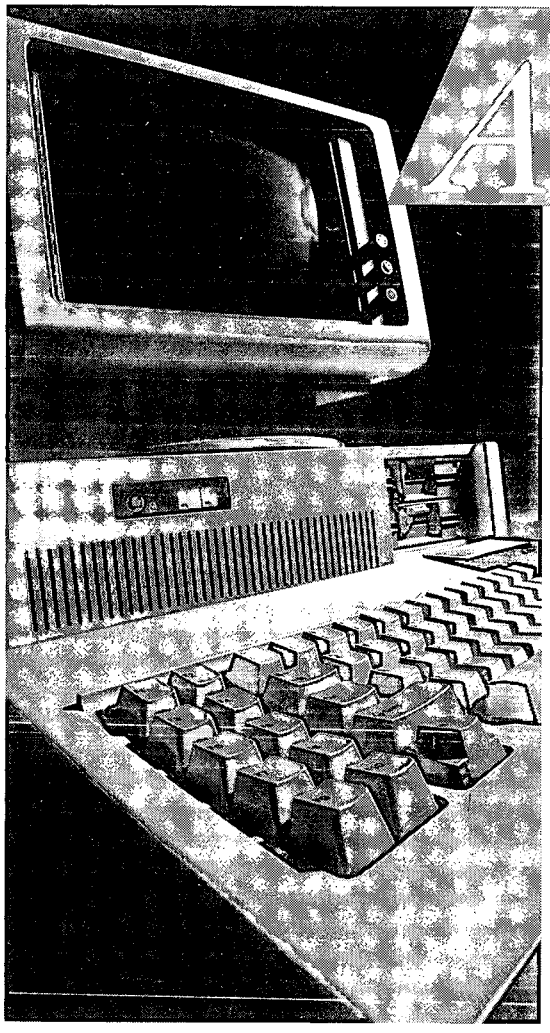

Access Elsevier Journals Online on STN International® !

On STN International, you can now access full-text articles from Analytica Chimica Acta, Journal of Organometallic Chemistry, Carbohydrate Research, and Applied Catalysis, four of the leading chemistry journals published by Elsevier Science Publishers B.V.

In the CJELSEVIER database, you'll find more than 2,400 citations added yearly, dating from 1990 to the present, with more than 50 new articles appearing weekly. The information in CJELSEVIER is some of today's most current — updates appear within the database BEFORE the journals are available!

In CJELSEVIER, you don't have to rely on an abstract or on keywords. On STN, the full-text articles are both searchable and displayable. You can quickly decide whether the material in the article is important to your work. In CJELSEVIER, you're getting complete information right from the start!

It's easy to begin searching the CJELSEVIER database on STN. Simply fill out the attached coupon. We will send you a complete packet of information on all the full-text chemistry databases on STN and an STN sign-up kit.

☐ **YES! I'd like further information on full-text chemistry searching on STN. Please rush my information kit to me.**

Name _____

Title _____

Organization _____

Address _____

_____

Telephone _____

Mail to: STN International, c/o CAS® Marketing Dept. 39990, P.O. Box 3012, Columbus, OH 43202 USA.

STN®
INTERNATIONAL
The Scientific & Technical Information Network

Physical Sciences Data Volume 43

Vapor-Liquid Equilibrium Data - Salt Effect

by **S. Ohe**, Department of Engineering, Science University of Tokyo, Japan

Vapor-liquid equilibrium (VLE) data of solutions are necessary for the design of distillation and absorption processes. VLE exhibits various characteristics depending on the type of solution. In the case of nonideal solutions, an azeotropic mixture is formed which cannot be separated by ordinary distillation. The mixture must be separated by adding a third component, called an entrainer, which has the capability of breaking the azeotropic point. In most cases, a volatile component is employed as an entrainer for an azeotropic mixture. However, salt is also effective in breaking the point; this is called the salt effect on VLE. Much has been observed on salt effect, however very few commercial distillation plants use this method. This book aims to cover all reported data found in journals on salt effect on VLE.

Prediction methods for VLE at low and high pressures for systems composed of volatile substances are used routinely, However, no method to predict the salt effect on VLE is in use, because salts show entirely different behavior from volatile substances. A method to predict salt effect based on preferential solvation was reported by the author in 1976. 30 systems were examined and the formation of preferential solvates between the salt and one of the volatile components was shown. Continuing the work, the formation of preferential solvates for almost all salt effect data has been examined. As a result of this work, it has been found that preferential solvates are formed without exception.

In this volume, the preferential solvation numbers determined by least squares method are shown by processing the data of salt effect on VLE.

Contents:

1991 xxxii + 360 pages
Price: US $ 218.00 / Dfl. 425.00
ISBN 0-444-98687-1

Co-edition with and distributed in Japan by Kodansha Scientific Ltd.

Elsevier Science Publishers

P.O. Box 211, 1000 AE Amsterdam, The Netherlands
P.O. Box 882, Madison Square Station, New York, NY 10159, USA

Discover new solutions

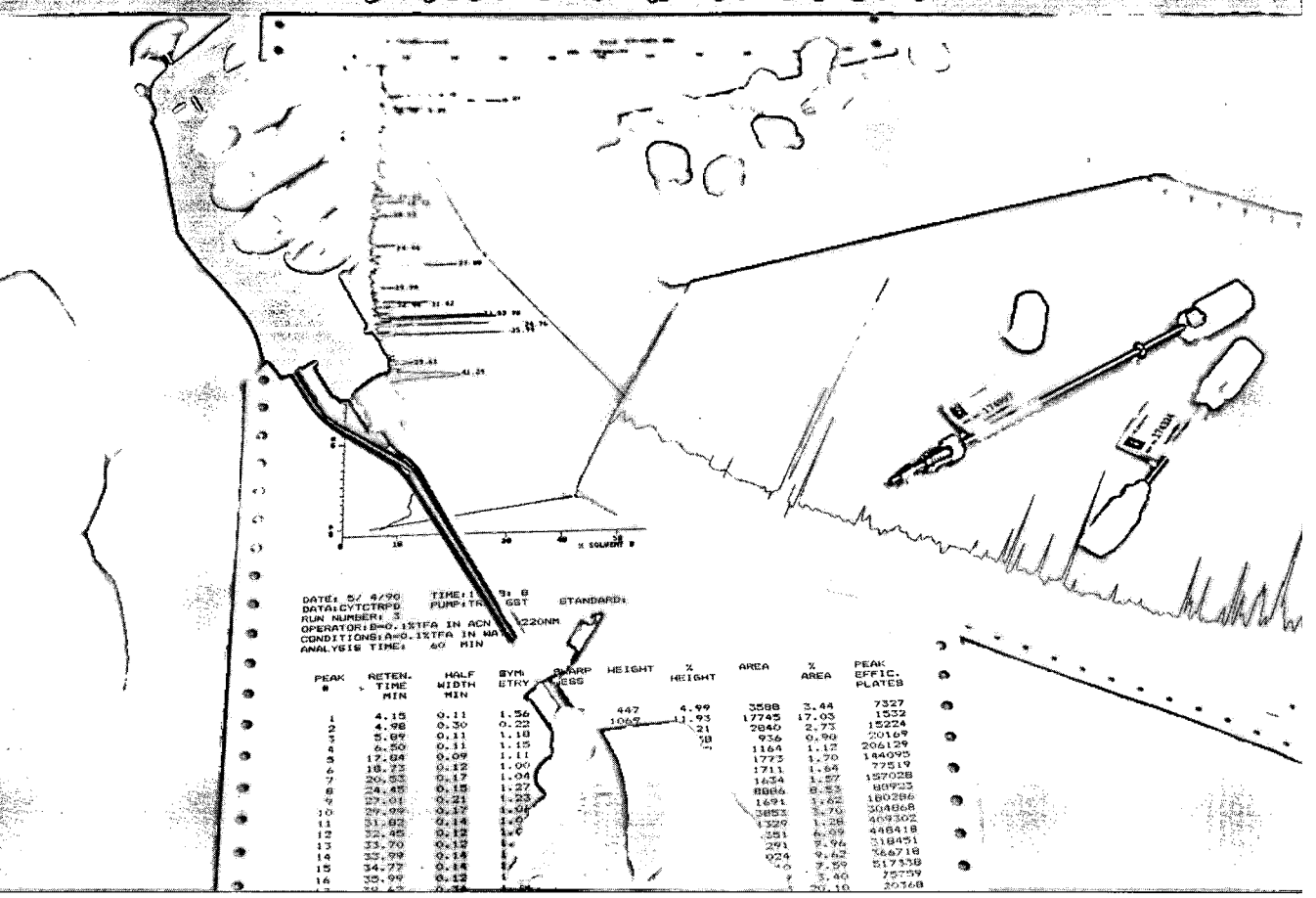

If a tiny sample is all you have, microbore HPLC is what you need

Since 1985, Isco's optimized systems have helped prove the benefits of true microbore HPLC. They'll give you manyfold improvement in mass sensitivity and resolution. Tremendous sample and solvent economy. Simple, direct interfacing to FAB-MS and other advanced spectrometers.

Now these systems offer new capabilities and options that make microbore HPLC more attractive than ever.

- New digital syringe pumps deliver totally pulseless flow with quartz-locked stability and precision—even at packed-capillary flow rates.
- It's easy to program precise, reproducible gradients for highest efficiency in demanding separations such as peptide mapping and protein sequencing.

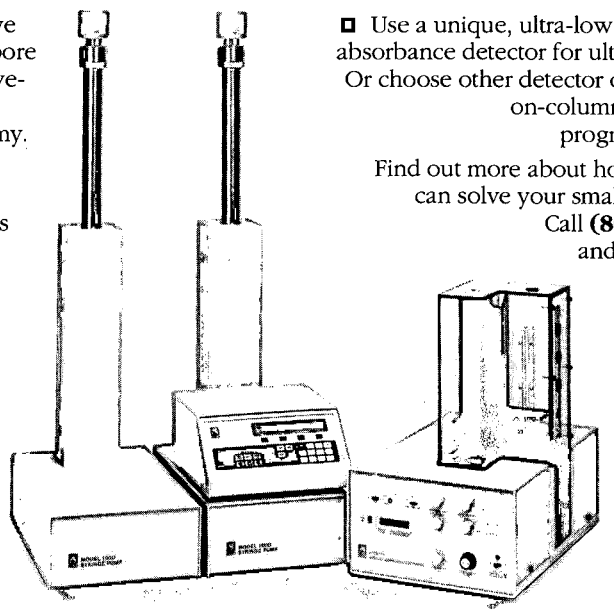

- Use a unique, ultra-low dispersion injector-absorbance detector for ultimate performance. Or choose other detector options for capillary on-column detection, or even programmable scanning.

Find out more about how microbore HPLC can solve your small-sample problems. Call **(800)228-4250** today and ask for Bulletin 50.

Isco, Inc.
P.O. Box 5347
Lincoln NE 68505, U.S.A.
Tel: **(800)228-4250**

Isco Europe AG
Brüschstr. 17
CH8708 Männedorf
Switzerland
Fax **(41-1)920 62 08**

ISCO

Journal of Chromatography, 587 (1991) 129–136
Elsevier Science Publishers B.V., Amsterdam

CHROM. 23 563

Deconvolution method for accurate determination of overlapping peak areas in chromatograms

Thomas J. Nelson

Neural Systems Section, National Institute of Neurological Diseases and Stroke, National Institutes of Health, Bethesda, MD 20892 (USA)

(First received February 13th, 1991; revised manuscript received June 11th, 1991)

ABSTRACT

A method is described for deconvoluting chromatograms which contain overlapping peaks. Parameters can be selected to ensure that attenuation of peak areas is uniform over any desired range of peak widths. A simple extension of the method greatly reduces the negative overshoot frequently encountered with deconvolutions. The deconvoluted chromatograms are suitable for integration by conventional methods.

INTRODUCTION

Although considerable effort has been expended over the years to improve the peak-resolving power of chromatographic techniques, one is frequently still faced with data-containing peaks which are incompletely separated from each other, or which contain large baseline drifts or other features which render accurate peak-area determination difficult. Conventional peak integration algorithms utilize running averages to compute baselines and simple tangent-skimming and perpendicular drop methods for separating peaks. Although robust, these algorithms are notoriously inaccurate [1,2], and require numerous parameters which must be determined and adjusted empirically for each chromatogram, a laborious and inexact process which in effect introduces numerous assumptions about peak width, peak shape, etc. In addition, as they generally rely on detecting points at which the first derivative (dy/dx) crosses zero to separate peaks, they are usually incapable of detecting peaks which are not separated by a horizontal region or valley.

An alternative approach is to deconvolute the chromatogram mathematically to remove all peaks above a certain threshold peak width (*i.e.*, below a threshold frequency). This also automatically flattens the baseline. In practice, however, attempts at deconvolution often produce unsatisfactory results, negative peaks or discrepancies in areas for peaks of different width. Other methods, such as moments analysis [3], orthogonal polynomial analysis of chromatogram segments [4,5] and an inverse diffusion model [6], have also been proposed for analyzing overlapping peaks. The relative advantages of several types of deconvolution methods have been compared [7]. In this paper, a straightforward method for deconvoluting chromatograms prior to integration is presented and its applicability to actual chromatographic analyses is discussed.

EXPERIMENTAL AND RESULTS

Two most commonly used mathematical techniques for deconvoluting sets of numbers are nonlinear least-squares (NLR) analysis [8] and the Fourier transform method. In least-squares analysis, the chromatographic data are fitted to a sum of several Gaussians, solving for $3n$ parameters (position, width and height) for each peak. Although successful for single peaks [9], NLR analyses typically fail to converge when more than three or four

peaks are involved. In the Fourier transform method, the data are converted to a set of complex frequencies, then divided by the transform of a transfer function, which is a function which represents the data smearing process [10] (since Fourier transforms yield complex numbers, complex division must be used). The new set of complex frequencies is then inverse transformed to obtain the deconvoluted data. This method is also considerably faster than NLR.

The principle of deconvolution is that convoluting two functions (b and c) is equivalent to multiplying their Fourier transforms (B and C), *i.e.*, if

$$a(x) = b(x) \otimes c(x)$$

then

$$A(\omega) = B(\omega)C(\omega)$$

The variance of the convolution product of the two functions is equal to the sum of the variances of the individual functions:

$$\sigma_a^2 = \sigma_b^2 + \sigma_c^2$$

Deconvolution is simply the reverse of this process, dividing the transform of the data by that of the transfer function, thereby subtracting its contribution to the variance.

As the observed peaks in a chromatogram are products created by the peak-smearing process which we desire to reverse, the transfer function should in some manner mimic the peak shape. Although peak shape has been modelled as a simple Gaussian [11], a combination of Gauss and Cauchy functions [12,13], a Gaussian in the presence of noise [14], a polynomial series [5], a combination of statistical moments [15] or an exponentially modified Gaussian [16–18], there are reasons for using a simple Gaussian curve. Diffusion processes and response time-limited detector response functions, which are the main contributors to peak broadening, are both Gaussian in form. Also, conveniently, the Fourier power spectrum of a Gaussian is another Gaussian, as well as a real function. This reduces the number of transforms needed in deconvolution from three to two, as the desired Gaussian can be easily generated when needed. Finally, Gaussians do not produce fast Fourier transform (FFT) oscillation artifacts, in contrast with a sharp threshold cut-off function or triangle function.

Unfortunately, performing a deconvolution as described above frequently yields unsatisfactory results, as the amplitudes of some frequencies in the transfer function may be extremely small, resulting in enormous amplitudes of high-frequency components of the deconvoluted data, possibly even exceeding the dynamic range of the computer. An alternative method, shown in Table I, involves creating a high-pass filter function based on a Gaussian, retaining its favorable characteristics such as an absence of oscillation artifacts, x-axis symmetry and steep fall-off, but having a wide plateau for high frequencies and attenuating low ones. The non-zero real and imaginary Fourier frequencies are then multiplied by this function, that is, by

$$f = [1 - \exp(-b_f x^2)]\{1 - \exp[-b_f(x - n)^2]\} \qquad x = 1, 2, \ldots, n \qquad (1)$$

where n is the number of data points and x is the index for the points for (in this case) the frequency domain (Fig. 1). The $\omega = 0$ frequency is set to zero. Strictly, this is a type of convolution rather than deconvolution, as it is a multiplication rather than division, but the effect is that of deconvoluting wide and narrow peaks as the term is frequently used in chromatography. Fig. 1 shows the function used, which is essentially a filter function. The adjustable, dimensionless exponential constant for the filter, b_f, is related to the attenuation for a peak component of

TABLE I

PROCEDURE FOR DECONVOLUTING CHROMATOGRAMS

Step	Action
1	Create Gaussian filter function of length n: $f = [1 - \exp(-b_f x^2)]\{1 - \exp[-b_f(x - n)^2]\}$ where b_f is an adjustable parameter and n is the number of data points in the chromatogram
2	Fourier transform the data
3	Calculate the new real and imaginary frequencies by multiplying the old frequencies $\omega^{(x)}$ by the filter function f and adding a fraction c of the original data frequencies ω_0^x: $\omega^{(x)\prime} = \omega^{(x)} f^{(x)} + c\omega_0^{(x)}, \quad x = 0, 1, 2, \ldots, n$
4	Inverse transform and apply a smoothing filter if necessary

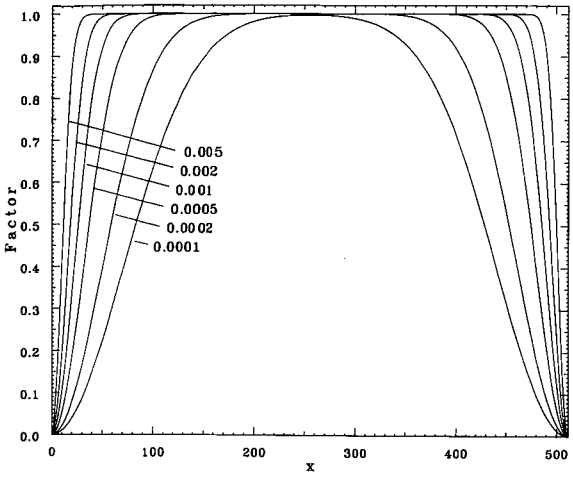

Fig. 1. Filter functions computed from Gaussians with an exponential coefficient (b_f) of 0.005, 0.002, 0.001, 0.0005, 0.0002 and 0.0001 for a chromatogram of 512 data points. The lowest frequencies (near both ends of the curve) are attenuated to a greater extent as the Gaussian becomes wider, whereas the highest frequencies (center) remain unchanged. The Nyquist (maximum) frequency is at $x = 256$. A simple step function cannot be used, as it would create artifactual sinusoids in the final result. The function also must be symmetrical in order to also handle negative frequencies, which are customarily placed in reverse order above the positive frequencies by an FFT.

frequency ω (ω = 1/peak width in x units) by the equation

$$b_f = -w^2 \ln(1 - a)$$

where a is the attenuation and w is the peak width at half-height expressed as a fraction of the total length of the chromatogram. This equation provides a useful approximation of attenuation. For example, if the maximum acceptable attenuation for the broadest peak is 0.95, and the broadest peak is 4% of the total length of the chromatogram, then b_f should be 0.004793 or greater. Peaks of width >8.3% of the total chromatogram will be attenuated by a factor of 2 or more. This value gives a good margin of safety, because for a typical high-pressure liquid chromatogram most of the peaks are <1% of the length of the chromatogram. Even values of b_f which result in significant attenuation of some broader peaks may still be useful, as peaks eluting at similar retention times usually have similar height/width ratios.

The relationship between attenuation and peak width can be estimated more accurately from considering the power spectrum of an entire individual peak. The power spectrum is generated by taking the modulus of the real and imaginary components of the transform. It can be shown that the $\omega = 0$ component (*i.e.*, the amplitude) of a power spectrum is equal to the area under the original peak (A_p) in the time domain, and conversely, the area of the power spectrum curve (in the frequency domain) is equal to the height of the original peak (h_p) times n, the number of data points. The power spectrum curve of a Gaussian peak is another Gaussian centered at $x = 0$, with an amplitude of A_p, or

$$y = A_p \exp(-b_2 x^2)$$

The exponential coefficients of a Gaussian curve and its corresponding power spectrum conveniently happen to be related by a simple inverse multiplied by π^2/n^2. Thus, the exponential parameter b_2, the exponential coefficient of the power spectrum, is calculated from b_p, the exponential coefficient of the original peak, by the equation

$$b_2 = \pi^2 / b_p n^2 \tag{2}$$

where b_p is related to the width of the original peak, w_p, by

$$b_p = 4 \ln 2 / w_p^2 \tag{3}$$

If the power spectrum is multiplied by the filter function (eqn. 1), it becomes

$$y = [1\text{-}\exp(-b_f x^2)] A_p [\exp(-b_2 x^2)]$$

or

$$y = A_p \{\exp(-b_2 x^2) - \exp[-(b_f + b_2) x^2]\} \tag{4}$$

The maximum value of this new curve, which occurs at a non-zero position, is equal to the area of the new deconvoluted peak. The maximum, found by setting dy/dx to zero, is at

$$x = \left[\frac{-1}{b_f} \cdot \ln\left(\frac{b_2}{b_f + b_2} \right) \right]^{\frac{1}{2}}$$

After substituting back into eqn. 4 to obtain the y value at this point, one obtains

$$y_{max} = A_{new} = A_p \left(1 - \frac{b_2}{b_f + b_2} \right) \left(\frac{b_2}{b_f + b_2} \right)^{b_2/b_f} \tag{5}$$

where the equality $\exp(a \ln b) = b^a$ was used to remove the exponential. This equation enables one

to calculate the area (A_{new}) of the new, attenuated Gaussian representing the deconvoluted peak.

It is also straightforward to calculate the height and width of the new peak, by integrating eqn. 4. However, the value obtained is the height measured from $y = 0$ and not from the negative minima on either side of the peak. Hence the calculated h_{new} would be an underestimate of the actual new height. The negative regions of the deconvoluted peak arise because the new power spectrum is slightly asymmetric.

From the above equations, it is possible to select a value for b_f to keep the area of a peak of any specified width from decreasing, within any desired tolerance.

For example, suppose that a chromatogram of length 512, with a typical peak width $w_p = 5$ and height $h_p = 7$, was to be deconvoluted using a b_f of 0.01. The area of the peak (estimated by numerical integration or FFT) would be 37.26. Using eqn. 3, b_p would be 0.1109. Then, using eqn. 2, one calculates b_2 to be 0.0003395. The new area would be 32.088 from eqn. 5. As this value is only 14% less than the starting value, the selection of 0.01 would be a suitable choice.

To test whether the deconvolution method can be used to obtain a calibration curve, samples containing hemoglobin, cytochrome *c* and various amounts of bovine serum albumin were subjected to size-exclusion high-pressure liquid chromatography (HPLC). The chromatograms were compressed to 512 data points and the areas of the peaks, which were partially overlapping, were measured before and after deconvolution. For the lowest albumin concentrations, area measurement by both the perpendicular drop and tangent-skin methods yielded less accurate results than measurement from the deconvoluted chromatograms. The areas after deconvolution were reduced by *ca.* 10% at all concentrations (Fig. 2), although at the lowest concentrations this effect was difficult to observe because of the greater uncertainty in estimating areas from the original chromatograms. In contrast, the peak in the deconvoluted chromatogram was clearly visible, even at the lowest concentrations (Fig. 2, inset).

Fig. 3a shows a chromatogram produced by an HPLC column under conditions of sample overloading, selected to show features of erratic baseline drift, unresolved peaks and a flat region bounded on one side by a sharp edge, all of which make integration difficult. Fig. 3b–d show the chromatogram deconvoluted with the method in Table I, using b_f values of 0.00005, 0.00015, 0.0005 and 0.0015. The peaks are resolved to a greater extent than the original, although in Fig. 3b and c the noise is also increased. Note the absence of oscillation artifacts in the flat region at the right. Fig. 3 also demonstrates the importance of selecting a value appropriate for the largest peak in the sample. In Fig. 3, the curve is too narrow, hence only the high-frequency noise is enhanced.

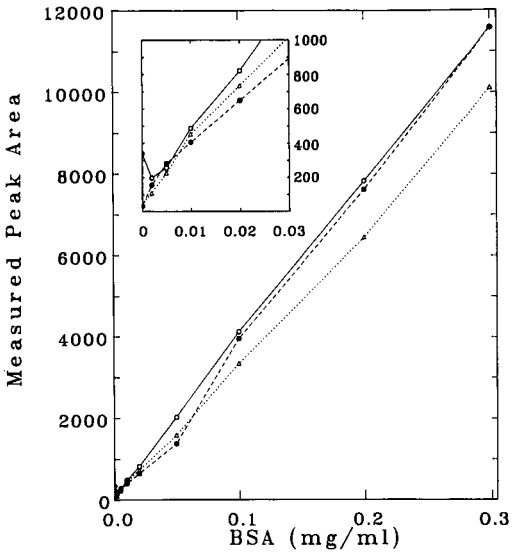

Fig. 2. Calibration curves derived from a set of chromatograms, measuring peak areas with the vertical drop method (○), tangential-skim method (●) or after deconvolution using a simple minimum-to-minimum method (△). The original chromatograms consisted of 0.1 mg/ml hemoglobin, 0.1 mg/ml cytochrome *c* and various concentrations of bovine serum albumin. The samples were chromatographed on a 250 × 4.6 mm I.D. size-exclusion HPLC column (Macrosphere GPC 60, 7 μm) eluted with 0.1 *M* potassium acetate (pH 7.4). Inset: enlargement of low-concentration region.

Also, there is a large negative overshoot near some of the larger peaks. This overshoot is one of the major drawbacks of deconvolution. Several sophisticated methods have been devised for removing these negative regions, which generally introduce a constraint function such as zero-clipping followed by several reiterations of the deconvolution [19]. However, a close examination of the transforms of the original deconvoluted chromatogram and one in

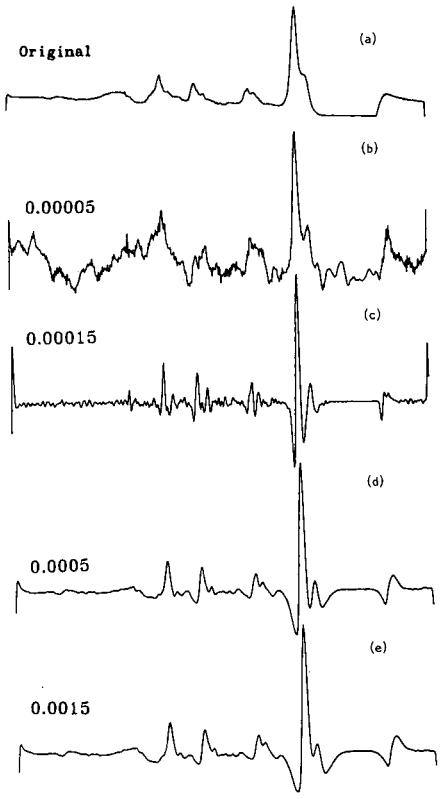

Fig. 3. Chromatograms deconvoluted by the method in Table I using different values for b_f. Thirty optic ganglia from squid (*Loligo paelei*) were homogeneized and chromatographed on DEAE-Sephacel. One fraction from this column was concentrated and re-chromatographed by HPLC on a column of AX-300, using a gradient of 0–0.6 *M* potassium acetate (pH 7.4) (0–20 min) and 0.6 M potassium acetate (20–60 min), and the absorbance was measured at 280 nm. The data set was compressed to 512 data points before processing.

which the negative regions have been artificially removed by subtraction would reveal that the desired changes are essentially an increase in the low-frequency regions which were attenuated by the deconvolution. Thus, a simple alternative method is to add back a portion of the frequencies of the original data. As shown in Fig. 4, even retaining a small fraction of original frequencies is sufficient to eliminate the negative regions, while the resolution is impaired to a lesser extent than if a wider curve were used (compare Figs. 3d and 4d). For integration purposes, in fact, it is actually not necessary to eliminate the negative regions, provided that the integration is performed between minima and not from the zero-crossings.

It is also possible to combine the retention of original frequencies by modifying the filter equation, as follows:

$$f = [1 - k\exp(-b_f x^2)]\,\{1 - k\exp[-b_f(x - n)^2]\}$$

The factor k ranges from 0 to 1 and determines the fraction of the low original frequencies to be discarded. If k is less than 1, the ends of the filter function (Fig. 1) approach 1-k instead of 0, and the $\omega = 0$ frequency should also be set to 1-k.

The most important criterion for integration purposes is the degree to which relative peak areas are preserved for peaks of different width. At the same time, extremely wide peaks (resulting from baseline shifts) should be attenuated. Fig. 5 shows the effect of different filter widths on the preserva-

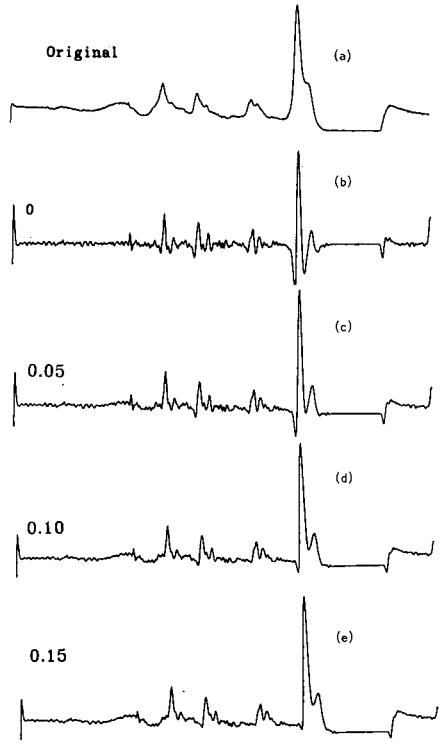

Fig. 4. Effect of adding increasing fractions of the original Fourier set during deconvolution, using a b_f value of 0.0002 in the chromatogram from Fig. 3. Adding 5% of the original frequencies eliminates the negative overshoot almost completely, whereas the resolution is only slightly impaired. As more of the original frequencies are added back, the baseline drift begins to reappear.

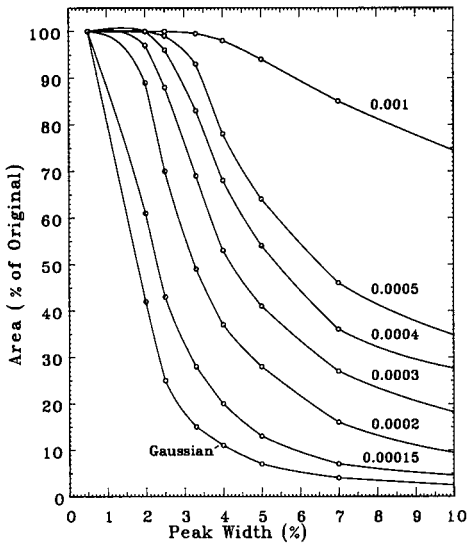

Fig. 5. Effect of width of the filter function used for deconvolution on attenuation of peaks of increasing width. A simulated chromatogram of 100 data points, containing peaks of various widths and area = 1, was deconvoluted using the method in Table I, and the areas in the deconvoluted chromatograms were computed. A broader function yields a wider plateau of low, constant attenuation. Fourier deconvolution using the standard method resulted in the curve marked "Gaussian" for all peak widths within a broad range. In contrast to the present method, the traditional Fourier deconvolution method does not produce a region over which attenuation is constant for different peak widths.

tion of peak areas with increasing peak width. Since for a typical HPLC trace the majority of peaks are less than 1% of the total length of the chromatogram, all but the narrowest peak produce satisfactory results, providing a fairly wide plateau. In contrast, results of a standard FFT deconvolution (using three Fourier transforms and complex division instead of the filtering method described here), are shown on the curve marked "Gaussian". The standard method attenuates peaks of increasing width to an increasing extent; hence the shape of this curve is relatively constant regardless of the width of the Gaussian transfer function used within almost the entire region of useful transfer function widths. Additionally, a peak whose width approached zero would also be enlarged to an unlimited extent, whereas in the present method its area would be unchanged.

The determine whether the recovered peak areas are dependent on the resolution between the components or their height ratios, a sequence of simulated chromatograms containing peaks of different heights and different degrees of separation was analyzed. Fig. 6 shows that, at the point at which the two peaks merge into a single peak, there is a slight decrease (up to 10%) in the total recovered area. The size of this decrease depends inversely on b_f, and results when the greater width of the unresolved peak shifts the filter function (Fig. 1) into a region of greater attenuation. Hence this effect can be minimized by a careful choice of b_f. The effect is also maximal when the two peaks are of identical size.

It is also possible to apply the deconvolution method iteratively, using partial retention of original frequencies and zero-clipping to reduce negative peaks. This results in chromatograms such as the one in Fig. 7. Although the peaks are all clearly resolved, their areas depend on the original peak width to a greater extent than the result from a single iteration, *i.e.*, the plateau in Fig. 1 is narrower. Hence, although it can help determine whether multiple overlapping peaks exist, and return their

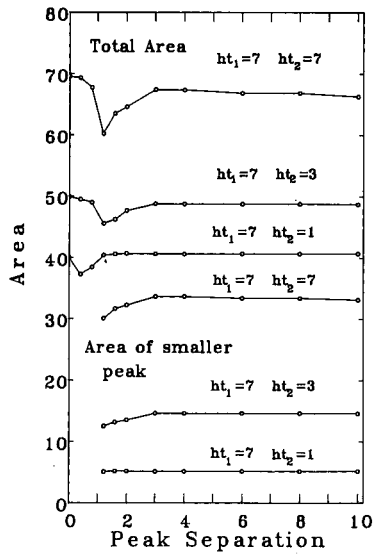

Fig. 6. Effect of the degree of peak separation and relative peak height on the recovered areas. Simulated chromatograms with peaks of constant peak heights with maxima separated by various distances were deconvoluted and the individual and total areas were measured. For some values of the deconvolution parameter b_f, a slight decrease in recovered area can occur when the two peaks are approximately one peak width apart. This effect is much less pronounced when the two peaks are of different sizes. The abscissa is peak separation in units of peak width.

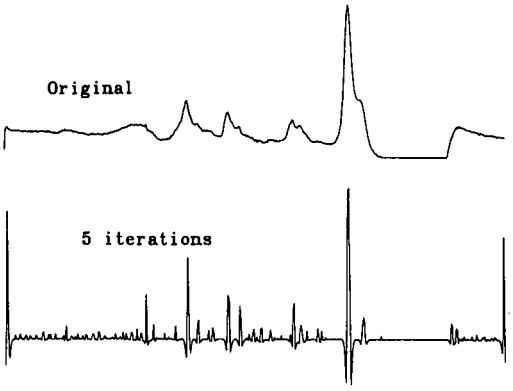

Fig. 7. Deconvolution of a chromatogram by the method in Table I applied for five iterations using a filter function based on $b_f = 0.0002$. The second to fifth iterations were carried out using a carry-over of 0.5 of the previous frequencies, and clipped at $y = 0$. All the peaks contain either one or two data points, making integration computationally trivial and allowing accurate determinations of retention times.

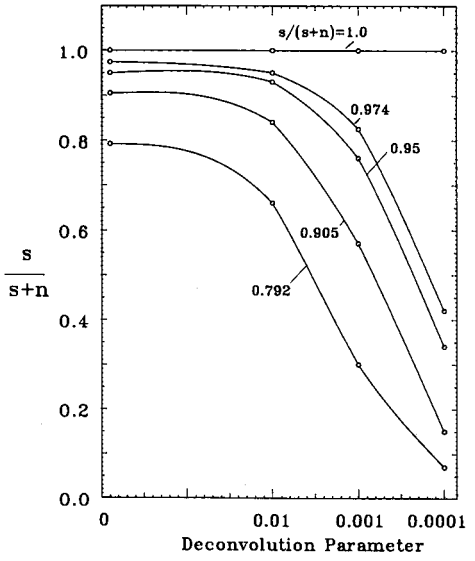

Fig. 8. Effect of chromatogram noise on the signal-to-noise ratio in the deconvoluted chromatogram. Simulated chromatograms containing 512 data points, with $S/(S + N)$ ratios of 1.0, 0.974, 0.95, 0.905 and 0.792, were deconvoluted using b_f values of 0.01, 0.001 and 0.001. Similated white noise was produced by adding random numbers to the chromatogram. Smaller values of b_f decrease the signal-to-noise ratio in direct proportion to their attenuating effect on the peak area (Fig. 5). No noise is added by the deconvolution, as indicated by the top curve.

retention time, area measurements from the reiterative method should be viewed with caution.

In some instances, deconvolution adds excessive high-frequency noise, which can usually be removed by data smoothing before or after the deconvolution.

The effect of noise on the deconvolution is shown in Fig. 8. Simulated chromatograms of 512 data points, containing numerous overlapping peaks were deconvoluted with different values of b_f. As b_f is decreased, the $S/(S + N)$ ratio (S = signal; N = noise) in the deconvoluted chromatogram becomes progressively lower than the original, because a greater proportion of the signal is being discarded. Hence, the decrease in the signal-to-noise ratio caused by using too low a value of b_f exactly parallels the decrease in area recovery caused by the same factor. In the case of zero noise, the $S/(S + N)$ ratio is unaffected by deconvolution.

More complicated functions than those described in Table I could equally well be applied to this method, as long they contain a flat region over a fixed range of higher frequencies and a smooth cut-off, and produce a small number of artifacts. It is envisaged that some of these other functions could produce an even sharper cut-off of peak widths whose areas are consistently retained.

ACKNOWLEDGEMENT

The helpful criticisms of Dr. Avrama Blackwell of the Environmental Research Institute of Michigan are appreciated.

REFERENCES

1 A. W. Westerberg, *Anal. Chem.*, 41 (1969) 1770–1777.
2 A. N. Papas and T. P. Tougas, *Anal. Chem.*, 62 (1990) 234–239.
3 E. Grushka, M. N. Myers and J. C. Giddings, *Anal. Chem.*, 42 (1970) 21–26.
4 H. J. G. Debets, A. W. Wijnsma, D. A. Doornbos and H. C. Smit, *Anal. Chim. Acta*, 171 (1985) 33–43.
5 P. J. H. Scheeren, Z. Klous and H. C. Smit, *Anal. Chim. Acta*, 171 (1985) 45–60.
6 R. Crandall, M. McClellan, S. Arch, J. Doenias and R. Piper, *Anal. Biochem.*, 167 (1987) 15–22.
7 L. M. Gugliotta, J. R. Vega and G. R. Meira, *J. Liq. Chromatogr.*, 13 (1990) 1671–1708.
8 D. W. Marquardt, *J. Soc. Ind. Appl. Math.*, 11 (1963) 431–441.
9 S. N. Chesler and S. P. Cram, *Anal. Chem.*, 45 (1973) 1354–1359.

10 W. H. Press, B. P. Flannery, S. A. Teukolsky and W. T. Vetterling, *Numerical Recipes: the Art of Scientific Computing*, Cambridge University Press, Cambridge, 1986, pp. 407–414.
11 E. Grushka, M. N. Myers and J. C. Giddings, *Anal. Chem.*, 42 (1970) 21–26.
12 R. D. B. Fraser and E. Suzuki, *Anal. Chem.*, 38 (1966) 1770–1773.
13 R. D. B. Fraser and E. Suzuki, *Anal. Chem.*, 41 (1969) 37–39.
14 J. M. Laeven and H. C. Smit, *Anal. Chim. Acta*, 176 (1985) 77–104.
15 E. Grushka, M. N. Myers, P. D. Schettler and J. C. Giddings, *Anal. Chem.*, 41 (1969) 889–892.
16 J. P. Foley and J. G. Dorsey, *J. Chromatogr. Sci.*, 22 (1984) 40–46.
17 R. Pauls and L. B. Rogers, 49 (1977) 625–628.
18 J. P. Foley and J. G. Dorsey, *Anal. Chem.*, 55 (1983) 730–737.
19 P. A. Jansson, *Deconvolution, with Applications in Spectroscopy*, Academic Press, Orlando, FL, 1984.

Journal of Chromatography, 587 (1991) 137–147
Elsevier Science Publishers B.V., Amsterdam

CHROM. 23 480

Physical and chemical characterization of a porous phosphate-modified zirconia substrate

Wes A. Schafer*,☆ and Peter W. Carr

Department of Chemistry and Institute for Advanced Studies in Bioprocess Technology, University of Minnesota, 207 Pleasant Street SE, Minneapolis, MN 55455 (USA)

E. F. Funkenbusch

3M Ceramic Technology Center, Bldg. 201-4N-01, 3M Center, St. Paul, MN 55144 (USA)

K. A. Parson

Department of Chemistry, Macalester College, 1600 Grand Ave., St. Paul, MN 55105 (USA)

(First received June 13th, 1991; revised manuscript received May 22nd, 1991)

ABSTRACT

A phosphate modification of previously described porous zirconium oxide high-performance liquid chromatographic support particles has been developed. Modification of the surface with inorganic phosphate alleviates the irreversible adsorption of proteins on the native oxide surface and makes the surface more biocompatible. X-ray photoelectron spectroscopic, solid-state ^{31}P NMR, elemental analysis, pH stability and ^{32}P phosphate release studies that have been used to characterize physically the surface of these modified particles are reported.

INTRODUCTION

We have recently reported on the development of acid- and base-stable porous zirconium oxide spherules as support particles for high-performance liquid chromatography (HPLC) [1,2] and previous work on the chromatographic utility of zirconium oxide, silica and glasses which contained an overlayer of zirconia was reviewed. The support particles consist of monoclinic zirconia crystals and can be produced with diameters ranging from 5 to 50 μm and pore diameters from 60 to 415 Å. The mechanical, chemical and thermal stability of monoclinic zirconia is the basis for our interest in developing and investigating porous zirconia spherules as HPLC supports. Zirconia particles with large pore diameters (>300 Å) are now available, making the investigation of protein separations on zirconia possible.

Zirconia particles have the extremely high pH stability typical of organic polymeric supports but maintain the high mechanical stability of silica and alimunia supports. Static pH stability studies [2] showed no evidence of dissolution of the zirconia particles at any pH (1–14), whereas more than 1% (w/w) of a 100-mg sample of alumina dissolved in 900-ml aliquots of aqeuous solutions at any pH < 3 or > 12. The use of silica-based supports is limited

☆ Present address: Merck, Sharp and Dohme Research Laboratories, P.O. Box 2000, R80Y-115, Rahway, NJ 07065, USA.

0021-9673/91/$03.50

to the Ph range 2–8 owing to their high solubility outside this range. Attempts to inhibit the dissolution of silica by the use of saturation columns [3], zirconia cladding [4] or acid–base treatment [5] have been only partly successful. Clearly, zirconia has distinct advantages over alumina and silica for both high- and low-pH applications.

Polymer-based supports have been developed which are stable over a much broader pH range than are silica and alumina. Such supports are, however, subject to shrinking and swelling, which may restrict diffusion [6] and cause higher column backpressures. The use of organic modifiers is also necessary to wet the polymer effectively [7]. These effects have adverse consequences on column efficiency.

Another disadvantage of silica-based supports is the strong interaction of amines with the residual silanol groups on the silica surface [8], leading to peak tailing, poor efficiency, low recoveries and hysteresis effects. Zirconia has no strong interactions with amines and their efficient separation is possible without the use of mobile phase additives [2].

Although zirconia has no strong interactions with amines, it does have a high affinity for many anions, especially phosphate [9,10]. Indeed, even a brief exposure of zirconium oxide to a dilute phosphate solution converts the support from an anion to a cation exchanger at pH 8. This can be reversed by rinsing the support with strongly alkaline solutions. Exposure of zirconia to samples containing certain anions such as phosphate will thus alter its chromatographic properties. This characteristic requires that such anions be removed from the sample matrix in a "clean-up" step or that their adsorption be blocked so as to maintain reproducible retention behavior of the zirconia. The presence of strong adsorption sites on the heterogeneous surface of the zirconia is also evident by the strong adsorption of certain anionic solutes in all modes of chromatography on zirconia. Elution of carboxylic and phosphonic acids requires the presence of an oxyanion as an additive in the mobile phase to avoid unacceptable peak broadening and low recoveries [1].

The surface of the zirconia particles is complex and several surface species have been identified, as depicted in Fig. 1. Infrared studies of zirconia have confirmed the presence of at least two types of surface hydroxyl species [11–13]: a terminal hydroxyl

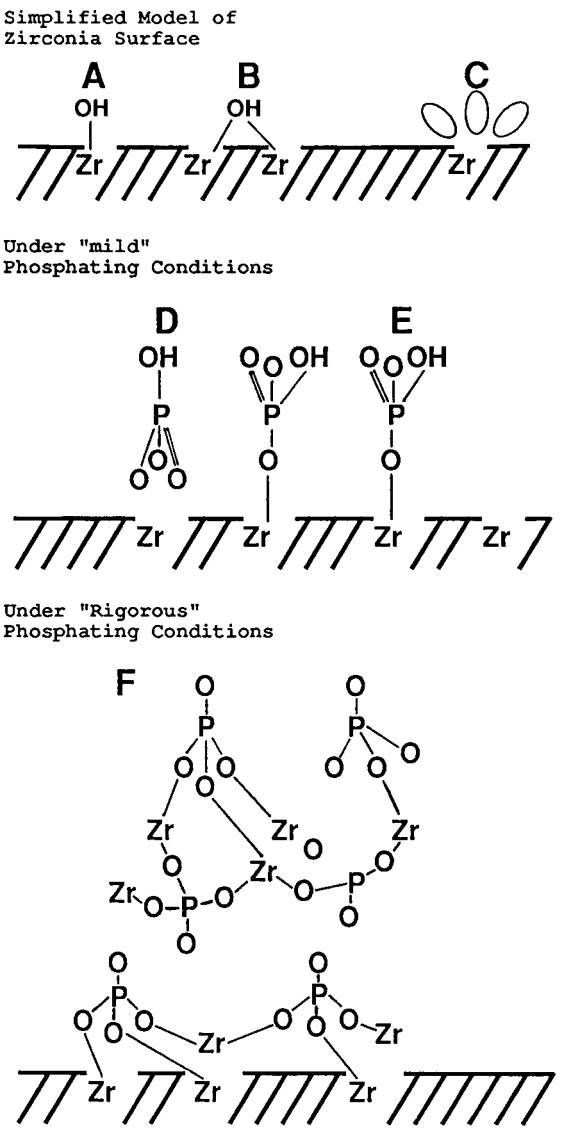

Fig. 1. Proposed models for the surface species of various phosphate-treated zirconias. (A) terminal hydroxide group; (B) bridging hydroxide group; (C) uncoordinated Lewis acid site; (D) physisorbed phosphate group; (E) esterified phosphate group covalently bound to the surface; (F) multi-layer zirconium phosphate area resulting from partial dissolution of the zirconia matrix.

(A), similar to the free silanol of silica, and a bridging hydroxyl (B), in which a single oxygen is shared by two zirconium atoms. As with other metal oxides, these surface hydroxyl groups are partly re-

sponsible for the amphoteric nature of the surface. They may be protonated or deprotonated depending on the solution pH, giving the zirconia anion- or cation-exchange properties, respectively:

$$Zr\text{-}OH_2^+ \rightleftharpoons Zr\text{-}OH + H^+ \rightleftharpoons Zr\text{-}O^- + 2H^+$$

Coordinatively bound water molecules may also contribute to the ion-exchange properties of the zirconia. The point of zero charge, *i.e.*, the pH at which zirconia has no net charge, is between 8 and 9.2 for the material used in these studies [1].

In addition to surface hydroxyls, the presence of coordinatively unsaturated zirconium(IV) ion sites (C in Fig. 1) on zirconia was confirmed by the use of a nitroxyl ion paramagnetic probe and ESR [14]. These very strong Lewis acid sites are similar to those found on alumina and are probably responsible for the strong interactions of certain anions with the surface of the zirconia.

These interactions persist even when bare zirconia particles are coated with a polymeric phase such as polybutadiene [1]. Whereas non-polar molecules such as benzene behave as expected, oxyanions such as benzoic acid did not elute from polybutadiene-coated zirconia. Ordinarily such polar molecules are less retained than non-polar solutes on a non-polar surface such as polybutadiene. These observations show the strength and persistence of surface interactions with the surface on zirconia despite the presence of a polymer coating. Indeed, it is unlikely that any polymer coating procedure will successfully block all of the adsorption sites. Rigney [1] found continued phosphate adsorption despite thick polybutadiene coatings of up to 1.7 nm. Similarly residual silanol groups continue to play a role in chromatographic separations on silanized supports despite years of work to alleviate these interactions [8].

The separation of proteins on zirconia has become feasible with the development of particles whose pores are large enough to avoid steric exclusion of these large molecules. Obviously, if the separation of small solutes containing a single oxyanion functionality requires the presence of inorganic phosphate in the mobile phase to block the strong interactions with the surface of zirconia, the separation of large biopolymers containing many such groups will be extremely problematic. Indeed, elution of myoglobin and bovine serum albumin from zirconia required a pH 10 buffer and then only partial separation was achieved. Very poor efficiency and peak shapes were observed despite the presence of phosphate in the mobile phase [1].

The aim of this work was to modify the surface of the zirconium oxide spherules reported previously [1,2] in order to remove the undesirable oxyanion interactions without compromising the mechanical and chemical stability of the particles. The strong affinity of zirconia for phosphate and the low solubility of zirconium phosphate [15] in water made a phosphate modification of the surface a reasonable approach. A phosphate modification of zirconia that effectively blocks the strong sites responsible for the oxyanion interactions would provide a more "bio-compatible" stationary phase, suitable for the separation of proteins and other biologically important molecules. The widespread use of the calcium phosphate hydroxyapatite in protein chromatography and zirconium phosphate for transition metal ion spearations also suggested that a phosphate-modified zirconia would be of interest as a chromatographic support.

This paper described the study of the preparation and physico-chemical characterization of phosphate-modified zirconia particles. Their chromatographic properties and utility in the separation of proteins are described in the following paper [29].

EXPERIMENTAL

Water was purified using a Barnstead Nanopure deionizing system with an organic free cartridge and a 0.2-μm final filter. All water was boiled and cooled prior to use in order to remove dissolved carbon dioxide. All chemicals were of analytical-reagent grade or better. Hydrochloric acid [7647-01-0] was obtained from EM Science (Gibbstown, NJ, USA), 50% sodium hydroxide solution [1310-73-2] from Curtin Matheson Scientific (Houston, TX, USA), tris(hydroxymethyl)aminomethane (Tris) [77-86-1] from Sigma (St. Louis, MO, USA), potassium phosphate dibasic [7758-11-4] and potassium chloride [7447-40-7] from Mallinkrodt (Paris, KY, USA), sodium acetate [127-09-3] and sodium borate [1330-43-4] from Fisher Scientific (Fairlawn, NK, USA), phenylphosphonic acid [1571-33-1] and zirconium phosphate from Pfaltz & Bauer (Waterbury, CT, USA) and phosphoric acid [7664-38-2]

from J.T. Baker (Phillipsburg, NJ, USA). Carrier-free [^{32}P]-orthophosphate was purchased from Amersham (Arlington Heights, IL, USA).

Zirconia particles were prepared by a proprietary process at the Ceramic Technology Center of 3M. Several batches of the zirconia particles with various physical properties were used throughout this work. The typical particle had a pore diameter of about 300 Å as determined by mercury porosimetry and a BET surface area of about 120 m^2/g. The particles are well defined spherules and the chief difference in the particles used here is the average particle size. For this work, larger particles (>20 μm) were used, but small (5-μm) well sized particles can be obtained for chromatographic purposes by particle size classification methods.

All particles were chemically pretreated before further modification in order to minimize any differences in the surface chemistry of the different batches of zirconia particles. Pretreatment with acid or base is known to affect the retention characteristics of inorganic supports, especially alumina [16]. Galkin *et al.* [17] noted differences in the reactivity of various zirconia surfaces toward phosphoric acid based on the number of condensed and free hydroxyls. In this study, all particles were immersed for 1 h in 0.1 *M* hydrochloric acid followed by 1 h in 0.1 *M* sodium hydroxide solution at room temperature and were swirled periodically. At the beginning of both the acid and base treatments, the particles were thoroughly degassed by sonication and application of a vacuum. The treatment was carried out in closed high-density polyethylene bottles rather than glass flasks to prevent precipitation or adsorption of dissolved silicates on the particles. In order to avoid the adsorption of carbonates, freshly boiled and cooled deionized water was used and the lower carbonate-containing 50% saturated sodium hydroxide solutions rather than sodium hydroxide pellets were used to prepare all alkaline solutions. The particles were thoroughly rinsed two or three times with 500-ml portions of deionized water after both the acid and base treatments.

During both the acid and base treatments, most of the particles settled to the bottom of the flask within about 10–15 min. However, up to about one third of the particles remained suspended for periods longer than 2 h in the water rinses, especially after the base treatment, probably owing to charging of the particles. The high ionic strength of the acidic and basic solutions supresses the repulsion between the particles. For expediency, larger particles (>20 μm) were rinsed in a sintered-glass funnel. A portion of the smaller particles was sacrificed with each water rinse rather than waiting for all of the particles to settle. The particles were either immediately subjected to the phosphate modification described below or they were dried in a vacuum oven at 60°C and stored in capped bottles.

The phosphate modification was carried out as follows: 15–25 g of pretreated zirconia particles were placed in a 500-ml round-bottomed flask. About 250 ml of 0.1 *M* phosphoric acid containing 1.0 *M* potassium chloride were added and the resultant slurry was thoroughly degassed by sonication and application of a vacuum. The potassium chloride was added to minimize any charging effects but other particles have been prepared without the addition of the salt and similar phosphorus to zirconium ratios were obtained. The potassium ion may also have a significant effect on the interlayer distance of any localized crystalline zirconium phosphate that might form. The slurry was warmed using a heating mantle such that the phosphoric acid solution refluxed for 4 h. Mixing was induced by "bumping" of the particles during reflux and by occasional swirling. Particles prepared in this manner are referred to as ZrP(0.1) and were used in all chromatographic studies unless indicated otherwise; the (0.1) denotes that the particles were treated with 0.1 *M* phosphoric acid and 1.0 *M* potassium chloride for 4 h.

A similar phase was also prepared in which 1.0 *M* phosphoric acid solution was substituted for the 0.1 *M* phosphoric acid–1.0 *M* potassium chloride solution. These particles were refluxed for only 1 h and are referred to as ZrP(1.0). Both the ZrP(0.1) and ZrP(1.0) particles had a "glue-like" appearance after phosphoric acid treatment. They became free-flowing particles after rinsing with HPLC-grade water and drying in vacuum.

Elemental analysis was done by placing 5-g samples of 100–400-μm zirconia particles in a filter flask containing 200 g of the appropriate phosphoric acid solution. The slurry was then subjected to vacuum in order to remove air from the pores and wet the surface with the acid solution. After degassing, the flask was maintained at the desired temperature for

the time period indicated. When the desired reaction time had elapsed, the particles were thoroughly rinsed with distilled water and dried for 24 h at 80°C. The surface area of each sample was determined by the BET nitrogen adsorption method. A portion of each sample was dissolved in hydrofluoric acid and analyzed by inductively coupled plasma (ICP) atomic emission spectroscopy. It should be noted that rinsing with water or neutral salts such as potassium chloride does not remove adsorbed phosphate from the surface of zirconia. Hence the elemental analysis studies (see below) probably represent the sum of both the adsorbed phosphate and covalently bound phosphate.

The pH stability of the phosphate modified zirconia particles in alkaline and acidic aqueous media was assessed in a static solubility study. About 1.5 g of the phosphate-modified zirconia [ZrP(0.1)] were weighed and placed in 500 ml of an aqueous solution at a known pH. Aqeous solutions of pH 1 and 3 were prepared by addition of hydrochloric acid to freshly boiled HPLC-grade water until the desired pH was obtained. Aqueous solutions of pH 11, 12 and 13 were likewise prepared by addition of carbonate-free sodium hydroxide to HPLC-grade water. Aqueous solution of pH 5, 8 and 10 were buffered with 10 m*M* sodium acetate, Tris and sodium borate buffers, respectively. Aliquots of 10 ml of the supernatant were collected from each of the samples decribed above after 1, 2, 4, 8 and 16 days. The pH of the solutions was redetermined after the last sample collection. The concentrations of phosphorus and zirconium in each of the supernatant samples were determined by ICP analysis. Samples were filtered to remove particulates using a Millipore Type HA 0.2-μm filter prior to analysis.

Phosphate-release and -exchange studies were performed using [^{32}P]phosphate-treated particles. About 7 g of zirconia (415 Å, 10–20-μm particles) were combined with 5 ml of HPLC-grade water and the resultant slurry was thoroughly degassed using house vacuum and sonication for about 5 min. The slurry was the added to a premixed solution of 1.0 ml of 1.0 mCi [^{32}P]phosphate in 100 ml of 0.10 *M* phosphoric acid–1.0 *M* potassium chloride and refluxed as before. After cooling, the mixture was filtered through Whatman No. 1 filter-paper on a Buchner funnel and washed with 2 l of 5 m*M* Tris (pH 8). The radioactivity remaining in aliquots of successive rinses was measured to determine when the inerstitial [^{32}P]phosphate had been removed. The radioactivity in the third rinse was less than 0.1% of that in the first, at which point rinsing was terminated. However, it is very likely that a significant amount of physisorbed phosphate remains after rinsing. The beads were dried overnight in a vacuum oven. A 200-mg amount of the dried particles was distributed into each of 24 tared 1.5-ml microcentrifuge tubes.

To each triplicate set of tubes was added 1.0 ml of 0.10 *M* phosphate buffer at one of eight different pHs from 1 to 14. The tubes were thoroughly vortexed and mixed continuously on a rocker. At various times after the addition of buffer, the tubes were removed from the rocker, centrifuged for 3 min at 6000 rpm and 50-μl aliquots of the supernatant were removed and added to 10.0 ml of scintillation fluor (Aquasol) for counting. Radioactivity was determined with a Packard Tricarb scintillation counter. Buffer was replaced to maintain a constant volume in the sample tubes. After the aliquots had been taken and the buffer replaced, the tubes were vortex mixed to resuspend the beads and returned to the rocker. Following removal of the 13-h aliquot, the tubes were centrifuged and, the buffer was decanted, discarded and replaced with fresh buffer. Subsequent samples of this supernatant buffer were removed and counted as described above. As ^{32}P has a relatively short half-life, all supernatant samples were counted consecutively on the same day at the end of the experiment to simplify the calculations.

X-ray photoelectron spectroscopy (XPS) was peformed on a Physical Electronics Industries (Eden, Prairie, MN, USA) Mode 555 ESCA/Auger system. Spectra were obtained with an Mg Kα source (15 kV, 2 mA) and a cylindrical mirror analyzer using a 100-eV pass energy for survey scans (1000–0 eV binding energy) and a 25-eV pass energy otherwise. Particles were held in place using aluminum tape.

Solid-state ^{31}P magic angle spinning (MAS) NMR spectra were obtained on an IBM Instruments NR/100 Fourier transform NMR spectrometer with the IBM Instruments NMR solids accessory. The instrument was calibrated with methyltriphenylphosphonium bromide at 20.43 ppm (*vs.* phosphoric acid at 0.00 ppm).

RESULTS AND DISCUSSION

Preparation and surface coverage

The extent of phosphate modification as a function of phosphoric acid concentation, reaction temperature and reaction time is shown in Table I. Not surprisingly, the phosphorus to zirconium P/Zr ratio increases with increasing phosphoric acid concentration and with increasing temperature. However, an analogous increase in the P/Zr ratio with time is only noted at the higher temperature of 100°C. This could be the result of kinetic limitations in the esterification of the phosphate with the surface hydroxyls. The fact that the amount of phosphate incorporated into the zirconia is independent of the reaction time at the lower temperature suggests that under these conditions phosphate is merely adsorbed on the zirconia surface and does not react to form covalent zirconium–phosphate bonds. The lack of any covalently bound phosphate in the materials produced at low temperature and at reaction times of the order of hours was confirmed by solid-state ^{31}P NMR studies (see below).

A theoretical maximum monolayer surface coverage of 4.9 m^2/g of phosphate on zirconia was calculated by assuming a face-centered cubic packing arrangement with a packing efficiency of 74% and a phosphate ion surface contact area of 25 $Å^2$. This assumes the most efficient packing geometry possible and hence probably overestimates the actual surace coverage. The surface contact area of the phosphate was calculated from the Van der Waals radius of oxygen and the average angle between the oxygen and phosphorus in phosphate. This value is considerably less than the 6.98 and 5.82 $\mu mol/m^2$ measured for the 1-h, 100°C, 1 molal phosphoric acid-treated and the 4-h, 100°C, 0.1 molal phosphoric acid-treated zirconia, respectively. This clearly suggests that at least some of the phosphate is incorporated into some form of zirconium phosphate and is neither adsorbed on the surface nor covalently bound surface sites.

It should be noted that elemental analysis does not distinguish between covalently bound phosphate and phosphate which is merely adsorbed on the surface. The high affinity of zirconium phosphate and phosphate ion has been observed in this laboratory and elsewhere [18].

BET surface area measurements were done to determine the effect of the modification on the surface

TABLE I

ELEMENTAL ANALYSIS OF VARIOUS PHOSPHATE-MODIFIED ZIRCONIAS

H_3PO_4 concentration (mol/kg)	Temperature (°C)	Time (h)	Specific surface area[a] (m^2/g)	P/Zr molar ratio[b]	Phosphate Surface coverage ($\mu mol/m^2$)
0.00	25	1	116	0.004	0.00
0.01	25	1	115	0.032	1.98
0.10	25	1	104	0.057	4.08
1.00	25	1	110	0.063	4.32
0.00	25	4	113	0.004	0.00
0.01	25	4	116	0.034	2.14
0.10	25	4	121	0.061	3.80
1.00	25	4	117	0.065	4.04
0.00	100	1	124	0.004	0.00
0.01	100	1	124	0.032	1.88
0.10	100	1	114	0.070	4.57
1.00	100	1	109	0.001	6.98
0.00	100	4	105	0.004	0.00
0.01	100	4	110	0.045	3.00
0.10	100	4	117	0.089	5.82
1.00	100	4	111	0.149	9.41

[a] As determined by BET nitrogen adsorption measurements.
[b] As determined by ICP spectroscopy.

area of the particles. As shown in Table I, there are only insignificant random changes in the surface area of the particles on treatment with phosphoric acid. This indicates that the pore structure of the particles is unaffected by the modification, *i.e.*, no significant decrease in pore volume has taken place.

Stability testing

In order to obtained a preliminary idea of the stability of the phosphate-modified zirconia, ZrP (0.1) was exposed to several solutions of various pH and the amounts of zirconium and phosphorus released were determined by ICP analysis of the supernatant and is shown in Fig. 2. An obvious relationship between the amount of released phosphate and the alkalinity of the solution is noted. Very little phosphate is desorbed in acidic solution whereas more than half of the total phosphate is desorbed at pH 13. The instability of zirconium phosphate at high pH has been noted previously [19].

The curves in Fig. 2 suggest a fast desorption process that is essentially complete by the second day, followed by a much slower release that continues throughout the duration of the study. This is especially evident in the neutral and alkaline pH solutions. After 16 days at pH 12.7, only *ca.* 3.1 μmol/m^2 of phosphate had desorbed from the surface. Even at high pH, the affinity of zirconia for phosphate is significant and indeed only half of the amount of phosphate incorporated into the phosphate-modified zirconia matrix had desorbed (see Table I).

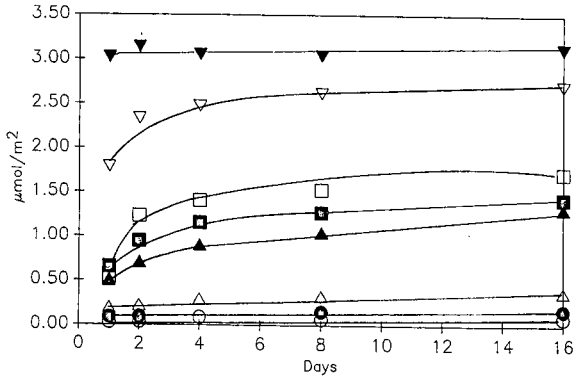

Fig. 2. Static pH stability of phosphate-modified zirconia , ZrP (0.1). Amount (μmol) of phosphate released into solution per squate meter of zirconia as a function of time and pH. ○ = pH 1.39 hydrochloric acid; ● = pH 3.18 hydrochloric acid; △ = pH 5.01, 10 m*M* sodium acetate buffer; ▲ = pH 7.95, 10 m*M* Tris buffer; □ = pH 9.83, 10 m*M* sodium borate buffer; ■ = pH 8.56 sodium hydroxide solution, originally pH 10.78; ▽ = PH 11.68 sodium hydroxide solution; ▼ = pH 12.68 sodium hydroxide solution.

Zirconium levels in all of the supernatants from the study above, except for the Tris-buffered (pH 8.00) samples shown in Fig. 3, were below the detection limit of 0.025 μg/ml of zirconium for ICP analysis. A similar study was undertaken on unmodified zirconia particles and no detectable zirconium was found. We assume that the Tris buffer is responsible for the presence of detectable amounts of zirconium in the supernatant. The three hydroxyl groups of the Tris may have enough chelating ability to solubilize the otherwise insoluble zirconium phosphate species in alkaline solutions. The stability of the unmodified zirconia particles in 10 m*M* Tris medium (pH 8.00) was then assesed by the method described above. No zirconium was found in the supernatant within the detection limits of the technique. This strongly suggests that the phosphate modification involves the breaking of zirconium–oxygen bonds in the zirconia matrix, thereby making the surface zirconia atoms susceptible to complexation by Tris. This is supported by the high surface coverages of phosphates determined earlier.

The effect of phosphate on the solubility of the support was investigated by adding 10 m*M* potassium phosphate to the Tris-buffered solution described earlier. As shown in Fig. 3, the added phosphate did indeed suppress the solubility of the zirconium phosphate but the level of zirconium solubility is still unacceptable. Based on this information,

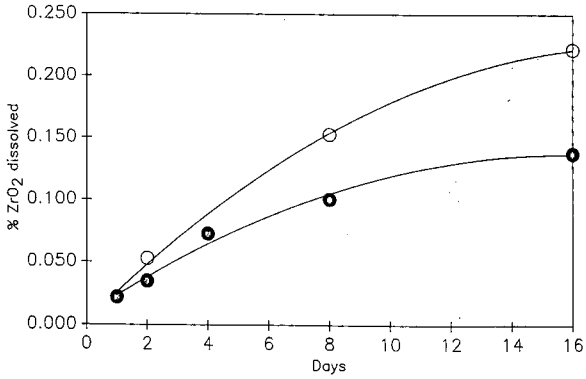

Fig. 3. Static pH stability study of phosphate-modified zirconia, ZrP(0.1). Amount (wt.%) of zirconia dissolved. ○ = pH 7.85, 10 m*M* Tris buffer; ● pH 7.98, 0 m*M* Tris, 10 m*M* potassium phosphate solution.

it is not advisable to use Tris or similar chelating buffers in the mobile phase with this support.

In order to assess the lability of the surface, the exchange rate of phosphate from radiolabeled ZrP (0.1) in buffered 0.2 *M* phosphate solutions was studied as a function of pH (see Experimental). As shown in Fig. 4, a considerable amount of phosphate (*ca.* 1.3 μmol/m^2) is exchanged for unlabeled solution-phase phosphate from pH 1 to 10. This is despite the fact that very little phosphate (<0.25 μmol/m^2) was found in the acidic solutions by ICP in the pH stability study described earlier. The data from this stability study are replotted *vs.* pH in Fig. 5 to be more analogous to the exchange experiment. It seems that at pH 10 and above, the competition between the solution-phase phosphate and hydroxide ion begins to favor the hydroxide ion. This results in the upward curvature of radioactive phosphate lost from the surface in Fig. 4 and the amount of phosphate which becomes soluble at pH 10 and above as seen in Fig. 5. The enhanced exchange rate of radiolabeled phosphate in acid suggests that a portion of the phosphate on the surface is labile and subject to exchange with phosphate in solution at lower pH. Note that no enhanced solubility of phosphate at lower pH was found in the stability study (Fig. 5).

Spectroscopic studies

Electron spectroscopy is a powerful surface analysis technique for the identification of elements and their chemical state [20]. Previous studies [21–23]

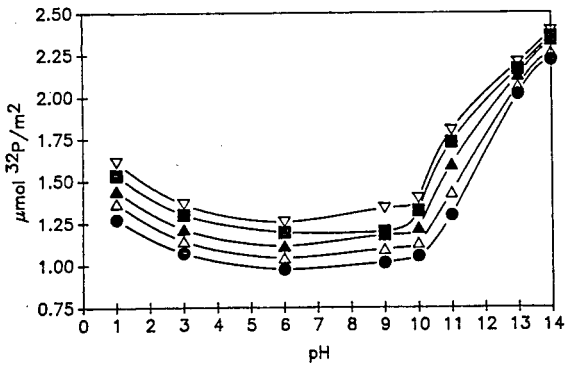

Fig. 4. Amount (μmol) of [^{32}P]phosphate exchanged as a function of pH. ● = 2 days; △ = 4 days; ▲ = 8 days; ■ = 18 days; ▽ = 29 days. Data for 7 g of radiolabeled ZrP(0.1) in 0.2 *M* potassium phosphate solutions buffered to the indicated pH.

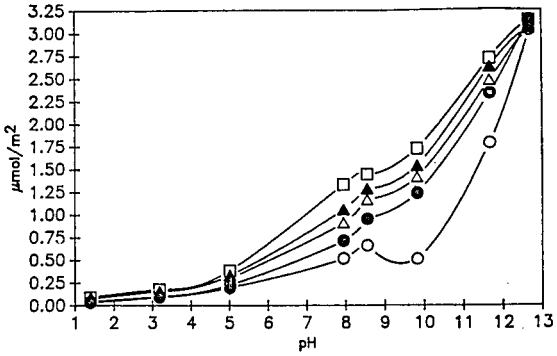

Fig. 5. Amount (μmol) of phosphate released as a function of pH. ○ = 1 day; ● = 2 days; △ = 4 days; ▲ = 8 days; □ = 16 days. Conditions as in Fig. 2.

have shown that the relative binding energy shifts of the oxygen and zirconium bands are dependent on the crystalline nature of the zirconium phosphate. Satellite structures and "shake-up" phenomena of the P 2*s* and Zr 3*d* bands are also influenced by the nature of the zirconium phosphate.

Neither the oxygen nor the zirconium bands in the spectra showed any asymmetry which might indicate the presence of more than one oxygen or zirconium state. It is likely that the contribution of the zirconia substrate in the phosphate-modified phases to the oxygen and zirconium bands masked any contribution from the phosphate surface species. However, close examination of the expanded spectra of the P 2*p* bands did show two distinct phosphorus chemical states in the phosphate-modified zirconia phases. The two phosphorus states are consistent with the presence of a covalently bound zirconium phosphate species on the surface and an adsorbed phosphate species.

MAS-NMR has proved to be a powerful technique for the characterization of solid [24–26]. The ^{31}P nucleus is NMR active ($S = 1/2$) with 100% abundance and thus is easily studied by NMR. Several solid-state ^{31}P NMR spectroscopic studies of α-$Zr(HPO_4)_2 \cdot H_2O$ [27] and γ-$Zr(HPO_4)_2 \cdot 2H_2O$ [28] and also amorphous zirconium phosphate have been reported. Solid-state ^{31}P NMR spectra of the phosphate-modified zirconia were obtained in order to characterize better the surface species present (see Fig. 6).

Amorphous zirconium phosphate gels exhibit three resonances at -11.8, -19.3 (major) and

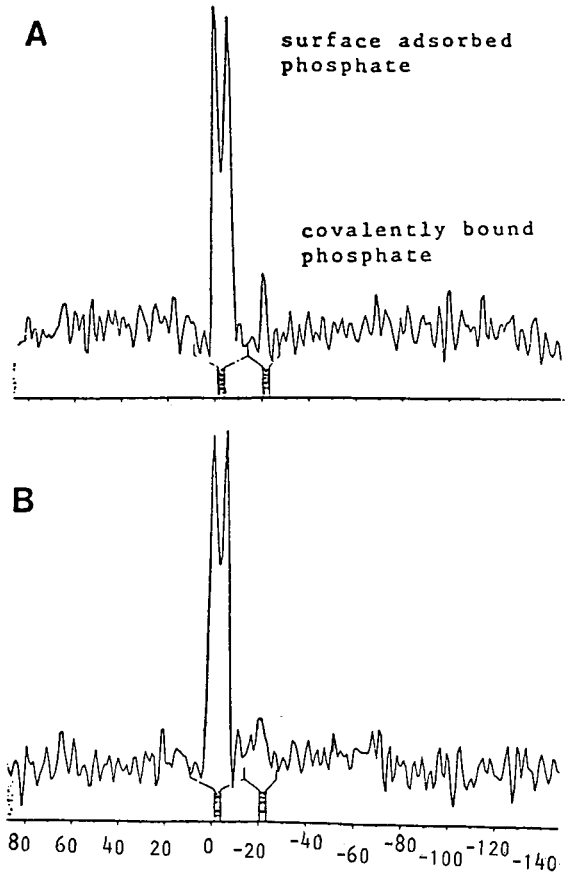

Fig. 6. Solid-state ^{31}P MAS-NMR spectra of phosphate-modified zirconia. (A) ZrP(1.0); (B) ZrP(0.1).

-25.5 ppm [27]. Despite its two crystallographically distinguishable phosphate groups, crystalline α-zirconium phosphate has a single resonance at -16.6 ppm [27] (-18.7 ppm [28]). The ^{31}P NMR spectrum of γ-zirconium phosphate does, however, contain two distinct resonances at -9.4 and -27.4 ppm [28] of equal intensity, suggesting that there is a significant chemical difference between the two phosphate groups in γ-zirconium phosphate and not simply a crystallographic difference.

No quantitative comparisons can be made between the two phosphate-modified zirconia phases ZrP(0.1) and ZrP(1.0) as different numbers of scans were used to obtain the two spectra. Quantitative comparisons between resonances in the same spectrum are also not possible as the relaxation times of the different phosphate species were not determined.

Based on these NMR spectra, it is not possible to distinguish between phosphate esterified onto surface hydroxyl groups and phosphate bound into a multi-layer zirconium phosphate matrix. NMR does, however, clearly show the presence of covalently bonded phosphate and phosphate adsorbed on the surface of the particles. Assignment of the covalently bound phosphate was made by comparison with crystalline zirconium phosphate. This information, combined with the kinetic effects noted in Table I, shows that phosphate adsorbs rapidly to the surface (under 3 h) at room temperature but the formation of covalent phosphate bonds requires the more rigorous conditions of lower pH, higher temperature (100°C) and longer exposure times.

^{31}P MAS-NMR spectroscopy was also used to investigate the alkaline instability of the phosphate-modified zirconia. As solid-state ^{31}P NMR spectroscopy is capable of distinguishing between adsorbed and covalently bound phosphate, it can be used to determine whether covalently bound phosphate is hydrolyzed or if the physically adsorbed phosphate is stripped from the surface by exposure to base.

The insure a good signal-to-noise ratio, particles with a larger surface area (50 m^2/g, 45-μm particles, 100 Å mean pore diameter) were used in this study. The pulse delay time of the instrument was also optimized to maximize the signal corresponding to the covalently bound phosphate. The particles were pretreated and modified with 1.0 *M* phosphoric acid as described earlier. These particles were statically exposed to 0.1 *M* sodium hydroxide solution for 3 days. Spectra of the two samples were obtained on the same day using the same instrument parameters. In this way the integrated peak areas of the two resonances corresponding to the surface-adsorbed phosphate and the covalently bound phosphate can be directly compared between the phosphate-modified zirconia and the base-treated phosphate-modified zirconia.

Examination of the spectra shown in Fig. 7 clearly shows that the covalent phosphate bonds were hydrolyzed by the alkaline conditions and that a large amount of the adsorbed phosphate desorbed.

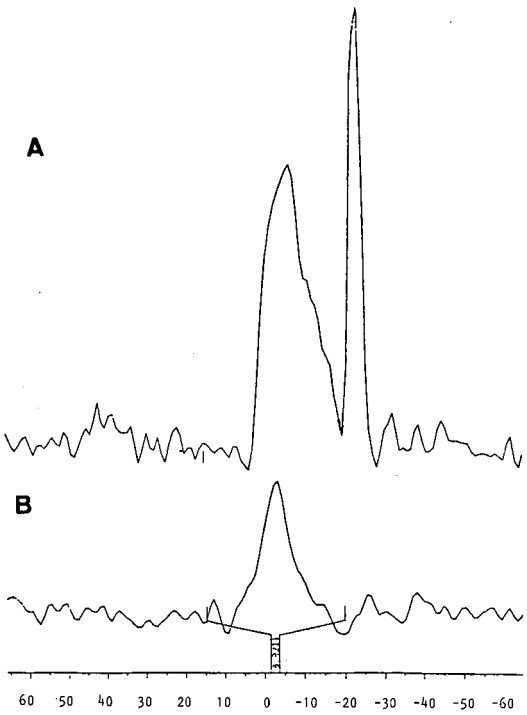

Fig. 7. Solid-state ^{31}P MAS-NMR spectra of ZrP(1.0). (A) Untreated; (B) after exposure for 3 days to 0.1 *M* sodium hydroxide solution.

CONCLUSIONS

Several spectroscopic techniques were used in the course of this work to characterize the surface species on phosphate-modified zirconia particles. These surface species are responsible for the chromatographic properties of the particles.

A simplified scheme of what we believe are the likely surface species on the unmodified zirconia particles is given at the top of Fig. 1. The terminal (A) and bridging hydroxyl (B) groups and the coordinatively unbound zirconium Lewis acid sites (C) are shown. Under the "mildest" phosphating conditions, *i.e.*, neutral pH, room temperature and short contact times, phosphate adsorbs on the surface of the particles (D), especially on the Lewis acid sites. At acidic pH and higher temperatures, esterification of the phosphate with surface hydroxyls (E) takes place as the kinetic bariers are overcome. Under the aggressive conditions of low pH, high phosphate concentration, high temperature and long reaction times, dissolution of the bulk zirconia matrix results with the "reprecipitation" of zirconium phosphates on the surface. Phosphate ions sorb on any exposed zirconium atoms in the precipitated zirconium phosphate.

Unfortunately, it is not feasible to remove the adsorbed phosphate from the surface of the particles to determine the amount of adsorbed phosphate, as the conditions necessary for the complete removal of the adsorbed phosphate also hydrolyze the covalently bonded phosphate. Thus elemental analysis cannot provide information on the presence or relative amounts of covalently bound phosphate. The solid-state ^{31}P NMR studies clearly show the presence of covalently bound phosphate and thus the surface is not merely covered with adsorbed phosphate. The elemental studies also show that the extent of the modification exceeds a monolayer. This suggests that the model depicted in Fig. 1F is reasonable. The release of zirconium ions into solution in the pH stability study of phosphate-modified zirconia in Tris buffer (Fig. 3) also suggests that the bulk zirconia matrix is attacked by phosphate.

It the support is to be regeneratable, the bulk zirconia support must not be involved, *ie.*, the modification must be a true surface modification which does not involve the breaking of zirconium oxygen bonds in the bulk zirconia matrix. ICP elemental analysis studies have shown that both the 0.1 and 1.0 *M* phosphoric acid treatments involve breaking zirconium–oxygen bonds in the bulk zirconia matrix and hence loss of the bulk support will occur on treatment with sodium hydroxide. Further study is needed to determine if it is possible to limit the modification to a monolayer and still block the sites responsible for the specific anion interactions.

ACKNOWLEDGEMENTS

The authors thank Tom Weber, John Blackwell and Dr. Alon McCormick of the University of Minnesota for many helpful discussions and information and Dr. Patrick Coleman of 3M for assistance in the ^{32}P phosphate release study. They also gratefully acknowledge financial support from 3M and the Institute for Advanced Studies in Bioprocess Technology at the University of Minnesota.

REFERENCES

1 M. P. Rigney, *Ph.D. Dissertation*, University of Minnesota, Minneapolis, MN, 1988.
2 M. P. Rigney, E. F. Funkenbusch, T. P. Weber and P. W. Carr, *J. Chromatogr.*, 499 (1990) 291–304.
3 J. G. Atwood, G. J. Schmidt and W. Slavin, *J. Chromatogr.*, 171 (1979) 109–115.
4 R. W. Stout, S. I. Sivakoff, R. D. Ricker, H. C. Palmer, M. A. Jackson and T. J. Odiorne, *J. Chromatogr.*, 352 (1986) 381–397.
5 J. Köhler and J. J. Kirkland, *J. Chromatogr.*, 385 (1987) 125–150.
6 F. Nevejans and M. Verzele, *Chromatographia*, 20 (1985) 173–178.
7 L. D. Bowers and S. Pedigo, *J. Chromatogr.*, 371 (1986) 243–251.
8 R. E. Majors, in Cs. Horváth (Editor), *High Performance Liquid Chromatography: Advances and Perspectives*, Vol. 1, Academic Press, New York, 1980.
9 K. A. Kraus, H. O. Phillips, T. A. Carlson and J. S. Johnson, in *Proceedings of the Second International Conference on the Peaceful Uses of Atomic Energy, Geneva, 1958*, United Nations, New York, 1958, paper 1832, pp. 3–16.
10 C. B. Amphlett, *Inorganic Ion Exchangers*, Elsevier, Amsterdam, 1964.
11 P. A. Agron, E. L. Fuller, Jr., and H. F. Holmes, *J. Colloid Interface Sci.*, 52 (1975) 553–561.
12 T. Yamaguchi, Y. Nakano and K. Tanabe, *Bull. Chem. Soc. Jpn.*, 51 (1978) 2482–2487.
13 N. E. Tret'yakov, D. V. Pozdnyakov, I. M. Oranskaya and V. N. Filimonov, *Zh. Fiz. Khim. (Engl. Transl.)*, 44 (1970) 596–600.
14 E. V. Lunina, A. K. Selivanovskii, V. B. Golubev, T. Y. Samgina and G. I. Markaryan, *Zh. Fiz. Chim. (Engl. Transl.)*, 56 (1982) 415–418.
15 G. Hevesy and K. Kimura, *J. Am. Chem. Soc.*, 47 (1925) 2540–2544.
16 H. Engelhardt and H. Elgass, in Cs. Horváth (Editor), *High Performance Liquid Chromatography: Advances and Perspectives*, Vol. 2, Academic Press, New York, 1980, pp. 57–111.
17 V. M. Galkin, L. M. Sharygin, V. E. Moiseev and V. P. Pyshkin, *Izv. Akad. Nauk SSSR, Neorg. Mater. (Engl. Transl.)*, 19 (1983) 1199–1202.
18 C. B. Amphlett, *Inorganic Ion Exchangers*, Elsevier, Amsterdam, 1964.
19 A. Clearfield, in A. Clearfield (Editor), *Inorganic Ion Exchange Materials*, CRC Press, Boca Raton, FL, 1982, pp. 1–74.
20 L. C. Feldman and J. W. Mayer, *Fundamentals of Surface and Thin Film Analysis*, Elsevier, New York, 1986.
21 G. Alberti, U. Costantino, G. Marletta, O. Puglisi and S. Pignataro, *J. Inorg. Nucl. Chem.*, 43 (1981) 3329–3334.
22 S. Pignataro, G. Marletta, O. Puglisi, U. Costantino and G. Alberti, *J. Electron Spectrosc. Related Phenom.*, 25 (1982) 49–57.
23 G. Marletta, O. Puglisi, S. Pignatori, G. Alberti and U. Costantino, *Polyhedron*, 2 (1983) 157–162.
24 D. J. O'Donnell, V. J. Bartuska, A. R. Palmer and D. W. Sindorf, *Am. Lab.*, 18 (1986) 96–111.
25 B. C. Gerstein, *Anal. Chem.*, 55 (1983) 781A.
26 B. C. Gerstein, *Anal. Chem.*, 55 (1983) 899A.
27 K. Segawa, H. Nakajima, S. Nakata, S. Asaoka and H. Takahashi, *J. Catal.*, 101 (1986) 81–89.
28 N. J. Clayden, *J. Chem. Soc., Dalton Trans.*, (1987) 1877–1881.
29 W. A. Schafer and P. W. Carr, *J. Chromatogr.*, 587 (1991) 149.

Journal of Chromatography, 587 (1991) 149–160
Elsevier Science Publishers B.V., Amsterdam

CHROM. 23 481

Chromatographic characterization of a phosphate-modified zirconia support for bio-chromatographic applications

Wes A. Schafer*,☆ and Peter W. Carr

Department of Chemistry and Institute for Advanced Studies in Bioprocess Technology, University of Minnesota, 207 Pleasant Street SE, Minneapolis, MN 55455 (USA)

(First received June 13th, 1990; revised manuscript received May 22nd, 1991)

ABSTRACT

A phosphate-modified zirconia was investigated for its potential use as a high-performance inorganic cation-exchange support for the separation of proteins. This phosphate modification effectively blocks the sites responsible for the strong interactions of certain Lewis bases with the zirconia surface. It provides a more "bio-compatible" stationary phase, resulting in high recoveries for proteins and enzymes and retention of their enzymatic activity. The stability, loading capacity, selectivity, efficiency and separation mechanism on the phosphate-modified zirconia are reported. These studies have shown that phosphate-modified zirconia is a useful high-performance ion-exchange support for the separation of cationic proteins and for blocking the sites responsible for the high affinity of zirconia towards certain anions. This makes the phosphate modification interesting in its own right and as an intermediate stage for the development of other zirconia-based chromatographic supports.

INTRODUCTION

As stated in the preceding paper [1], protein separations on porous zirconia have recently become feasible with the development of particles that are mechanically stable and have sufficiently wide pores to avoid steric exclusion of large biomolecules. Obviously, if the separation of small solutes containing a single carboxylate group requires the presence of inorganic phosphate in the mobile phase to block the strong interactions with the surface, the separation of large biopolymers containing many such groups will be extremely problematic. Indeed, in prior work [2], elution of myoglobin and bovine serum albumin from zirconia required a pH 10 eluent and the only partial separation was achieved. Very poor efficiency and peak shapes were observed for proteins despite the presence of phosphate in the mobile phase.

The aim of this work was to modify chemically the surface of zirconium oxide spherules in order to remove these undesirable interactions without seriously compromising the mechanical and chemical stability of the particle. The strong affinity of zirconia for phosphate [3] suggested that a phosphate modification of the surface should be a reasonable approach. A phosphate modification of the zirconia particles that effectively blocks the strong sites responsible for the Lewis base interactions might provide a more "bio-compatible" stationary phase, suitable for the separation of proteins and other biologically important molecules. The widespread use of the calcium phosphate hydroxyapatite in protein chromatography and zirconium phosphate for transition metal ion separations also suggested that a phosphate-modified zirconia should be of interest as a chromatographic support.

The poor mechanical stability of amorphous and crystalline zirconium phosphates has inhibited their use in high-performance liquid chromatography

☆ Present address: Merck, Sharp and Dohme Research Laboratories, P.O. Box 2000, R80Y-115, Rahway, NJ 07065, USA.

0021-9673/91/$03.50

(HPLC). Applications with low-pressure techniques such as paper chromatography and gas chromatography have been reported. There are numerous examples of the separation of transition metals on zirconium phosphates but they are beyond the scope of this work and the reader is referred to reviews on this subject [3–6].

Although a search of the literature revealed no studies on protein adsorption or separations on zirconium phosphates, the adsorption of amino acids on zirconium phosphates has been studied [7–9]. The mechanism of adsorption is dependent on the specific amino acid: basic amino acids such as histidine, lysine and arginine are intercalated into the interlayer region, whereas asparagine and alanine are adsorbed on the surface and not in the interlayer region of the zirconium phosphate. For those amino acids which are intercalated within the zirconium phosphate lattice, there is a corresponding loss of phosphate from the interlayer region of the zirconium phosphate which introduces defects into the lattice. This eventually leads to the collapse of the matrix at higher levels of intercalation. Significantly more lysine is adsorbed per gram of α-zirconium phosphate (1.8 mmol/g) than per gram of γ-zirconium phosphate (1.0 mmol/g). Differences in the interlayer spacing, amount of phosphate lost and maximum uptake of the amino acid between the α- and γ-zirconium phosphates show that the exact structure of the zirconium phosphate and the specific amino acid are important factors in the adsorption process. Owing to the higher surface area of the less crystalline zirconium phosphates, they have a higher capacity for the surface-adsorbed amino acids.

Paper impregnated with zirconium phosphate has been used in the separation of amino acids and alkaloids. Coussio *et al.* [10] studied the separation of several alkaloids on paper saturated with zirconyl oxychloride followed by a phosphoric acid treatment. By varying the concentration of zirconyl oxychloride used to saturate the paper, papers with differing capacities were produced. As most alkaloids do not adsorb appreciably on cellulose, adsorption was attributed to the impregnated zirconium phosphate. Catelli [11] investigated the separation of twelve amino acids on this phase but it lacked the selectivity to resolve them.

Zirconium phosphate has been investigated as a gas chromatographic support where the mechanical stability of the stationary phase is not a critical factor. A ligand-exchange separation of lower aliphatic amines using zirconium phosphate treated with copper(II) chloride was developed by Fujimura and Ando [12]. Allulli *et al.* [13] investigated microcrystalline $Zr(KPO_4)_2$ as a stationary phase in the separation of *n*-alkanes and some chlorohydrocarbons and thiols. Other classes of compounds gave asymmetric peaks and poor quantitative results.

Reversed-phase liquid chromatographic supports have been developed based on $Zr(O_3POR)_2$ where the alkyl group R is butyl, lauryl, octylphenyl or octadecyl [14,15]. As expected, these supports lack the mechanical stability necessary for high-performance supports. Rigney [2] investigated several methods of producing a reversed-phase zirconia-based support including the adsorption of organophosphates on porous zirconia spherules. However, these phases were not chemically stable in aqueous media.

Zirconium phosphate has been the most widely studied of the insoluble acid salts of tetravalent metals owing to its high ion-exchange capacity, although thorium, titanium and cerium phosphates [5] have also been investigated.

Calcium hydroxyapatite, $Ca_2(OH)_2(PO_4)_6$, has been extensively studied for the separation of proteins and other biologically important molecules such as nucleic acids [16–18]. The usual principles of ion exchange do not apply to hydroxyapatite chromatography [19–21] and indeed its popularity is probably due to its unique retention properties. The retention mechanism is complicated and several factors affect retention in hydroxyapatite chromatography, including overall and local charges on the protein, the composition of the loading and eluting buffers and the presence of sorbed counter ions on the support. General non-specific electrostatic interactions take place between the amino groups of proteins and the negative phosphate ions on the hydroxylapatite. The carboxyl groups of proteins may specifically complex with calcium sites provided that there are areas of significant carboxyl group density on the protein. The individual interactions are weak enough that many such interactions are required for retention. Small molecules are thus not generally retained on hydroxyapatite columns. There is, however, no correlation between the molecular weight and the retention of larger bio-

molecules on hydroxyapatite. Denatured proteins are generally much less retained than proteins in their native state [19].

A significant advantage of hydroxyapatite supports is their "bio-compatibility". Hydroxyapatite is a major component of bones and teeth, and synthetic hydroxyapatite have been used in prosthetics [22]. Typically a phosphate gradient at neutral pH is used to elute the proteins. Such gradients are much less likely to denature proteins than the conditions typically used in reversed-phase chromatography.

The usefulness of traditional hydroxyapatite chromatography is limited by practical considerations despite its unique retention characteristics. Retention characteristics on hydroxyapatite are extremely preparation dependent [23,24] and producing several batches of hydroxyapatite with the same retention characteristics has been problematic. The mechanical stability of conventional hydroxyapatite is poor and hydroxyapatite crystals break down even during gravity flow column operation, causing column bed collapse and a reduction in flow.

Recently, several manufacturers have introduced hydroxyapatite particles with improved mechanical and hydrodynamic properties, making hydroxyapatite HPLC possible [25–27]. These hydroxyapatite supports are limited, however, in several respects. They may only be used within the limited pH range of 5.5–10.5 and at pressures up to 3000 p.s.i. All of these columns require the use of expensive guard columns and the presence of phosphate and calcium ion in the mobile phase to prevent chemical degradation of the analytical column.

EXPERIMENTAL

All chemicals were of analytical-reagent grade or better. Calcium chloride dihydrate [10035-04-8] was obtained from Fisher Scientific (Fairlawn, NJ, USA), 50% sodium hydroxide solution [1310-73-2] from Curtin Matheson Scientific (Houston, TX, USA), concentrated hydrochloric acid [7647-01-0] from EM Science (Gibbstown, NJ, USA) and 3-[N-morpholino]propanesulphonic acid (MOPS) [1132-61-2] from Sigma (St. Louis, MO, USA). Potassium phosphate dibasic [7758-11-4], potassium phosphate monobasic [7778-77-0], potassium chloride [7447-40-7], potassium acetate [127-08-2], sodium phosphate dibasic heptahydrate [7782-85-6], ammonium phosphate dibasic [7783-28-0] and benzoic acid [65-85-0] were obtained from Mallinkrodt (Paris, KY, USA). Myoglobin (equine skeletal muscle), lysozyme (chicken egg white), α-chymotrypsin (bovine pancreas), ribonuclease A (bovine pancreas), bovine serum albumin (BSA), transferrin (human), cytochrome *c* (type VI from horse heart), β-lactoglobulin (bovine milk), insulin (bovine pancreas), alcohol dehydrogenase (equine liver), hemoglobin-A_0 (human), hemoglobin-A_2 (human) and hemoglobin-A_s (human) were obtained from Sigma and were used without further purification. The preparation of the 0.1 *M* phosphoric acid-treated zirconia was described in the preceding paper [1].

Several chromatographic systems were used throughout the course of this work. System I consisted of an IBM Instruments (Danbury, CT, USA) Model 9533 ternary liquid chromatograph with a Rheodyne (Berkeley, CA, USA) Model 7125 injector and an IBM Instruments Model 9522 fixed-wavelength UV absorbance detector (254 or 280 nm). System II consisted of a Perkin-Elmer (Norwalk, CT, USA) Series 3B binary gradient liquid chromatograph with a Rheodyne Model 7010 injector and a Perkin-Elmer LC-15 fixed-wavelength UV absorbance detector (254 or 280 nm). Unless indicated otherwise, an IBM Instruments Series 9000 laboratory computer with the chromatography applications package (version 1.4) was used for data collection with systems I and II. System III consisted of a Hewlett-Packard (Palo Alto, CA, USA) Model 1090L binary gradient liquid chromatograph with the Model 79847A autosampler, Model 79846A variable-volume injector and Model 79881A UV filter absorbance detector. A Hewlett-Packard Model 3393A reporting integrator was used for data collection. System IV consisted of a Hewlett-Packard Model 1090M ternary gradient liquid chromatograph with the Model 79847A autosampler, Model 79846A variable-volume injector and Model 79880A diode-array UV–VIS absorbance detector installed. A Hewlett-Packard Model 9133 ChemStation with HP 79995A chromatography software was used for data collection and control of the liquid chromatograph. For convenience, these systems will be identified by their assigned Roman numeral as described above.

Stainless-steel (316) column blanks (Alltech, Deerfield, IL, USA), 5 cm in length and 0.46 cm I.D.,

were used for high-pressure studies. Stainless-steel frits (2 μm) were used for small solute studies and 2-μm screens were used for protein separations to minimize the loss of protein. The particles were slurried in isopropanol and thoroughly degassed by sonication and application of a vacuum before packing. Particles with nominal pore diameters of 300 Å or greater were packed at 4500 p.s.i. using the stirred upward slurry technique, whereas particles with smaller pore diameters were generally packed at 6000 p.s.i.

During the course of this work, phosphate buffer gradients were routinely used. The blank gradient run contained two large system peaks: one peak at the beginning of the gradient and one peak after the gradient program returned to the initial phosphate concentration. The size of the first peak depends on the initial phosphate concentration of the gradient and disappears at initial phosphate concentrations of about 25 m*M*. Passing the phosphate buffer solutions over a Chelex 100 analytical-reagent grade chelating resin (Bio-Rad Labs., Richmond, CA, USA) before use decreased the background absorbance of the phosphate buffers but did not eliminate the system peaks.

Additional steps were then taken to reduce the amount of any impurities in the salts. These included rinsing all glassware with concentrated hydrochloric acid prior to use, the use of ultrapure sodium phosphate salts (99.999%) (Aldrich, Milwaukee, WI, USA) and the use of alternative phosphate sources such as ultrapure phosphoric acid. As there was no significant improvement in the size of the system peaks, the use of such expensive reagents was not justified and further studies were done using phosphate buffers prepared from analytical-reagent grade potassium salts. They were then passed over a Chelex-100 column. All buffer solutions were filtered for particulate matter using a Millipore (type HA) 0.45-μm membrane filter prior to use. To avoid the appearance of the large system peak at the beginning of the gradient, an initial phosphate concentration of 50 m*M* was used. Tentatively we assume that the isotherm for the adsorption of phosphate on the surface is saturated above about 25–50 m*M* and hence the system peaks disappear if the phosphate concentration is maintained above this level.

In situ column treatments were accomplished using an Altex (Beckman Instruments, San Ramon, CA, USA) Model 110A isocratic HPLC pump to flush the column with the appropriate solution. A Haake (Karlsruhe, Germany) Model FE circulating constant-temperature bath with a glass column jacket was used for elevated temperature studies. The pH of the mobile phase was measured at the detector outlet using a planar pH electrode system designed for this purpose (Lazar Model FTPH1).

The recovery of protein was studied by comparing the amount of protein collected in a control experiment in which the column was replaced with a zero dead volume detector to that obtained with the column in place. The samples were diluted to the same final volume and analyzed by the BCA assay for total protein (BCA and BCA Protein Assay Reagent, instructions 23230, 23225; Pierce, Rockford, IL, USA, enhanced method, 1986). The recovery of the activity of lysozyme was determined similarly using a standard enzyme assay (assay obtained from the customer service department of Sigma).

RESULTS AND DISCUSSION

To determine if phosphate-modified zirconia had any selectivity for different proteins, the chromatographic elution properties of myoglobin, lysozyme, α-chymotrypsin, ribonuclease A, cytochrome *c* and BSA were investigated. A typical chromatogram is shown in Fig. 1. Peak widths and shapes are generally acceptable although some distorted peaks are noted, especially for α-chymotrypsin and cytochrome *c*. Further improvements in particle size distribution, modification and column packing will hopefully improve the efficiency of the support. The broad α-chymotrypsin peak may be the result of self-digestion and the shoulder associated with cytochrome *c* peak is probably due to the presence of the reduced form. The first peak is a system pressure peak and is not completely resolved from the myoglobin peak. A 30-min linear gradient from 50 to 500 m*M* potassium phosphate (dibasic) adjusted to pH 7.0 with hydrochloric acid was used to effect the separation. This is a typical gradient used in hydroxyapatite chromatography of proteins [28]. Significantly broader peaks resulted when potassium acetate was substituted for potassium phosphate.

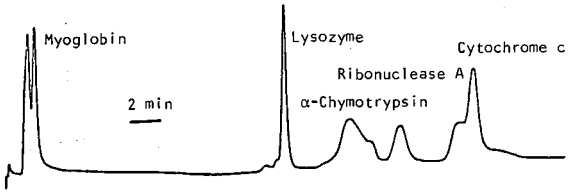

Fig. 1. Chromatographic separation of cationic proteins on phosphate-modified zirconia. Column: 6–11-μm, 300 Å phosphate-modified zirconia (5 × 0.46 cm I.D.). Mobile phase: 30-min linear gradient from 50 to 500 mM potassium phosphate dibasic (pH 7.0), 0.5 ml/min. System I (254 nm).

TABLE I

PHYSICAL PROPERTIES OF SELECTED PROTEINS

Protein	Mol. wt.	pI
Bovine serum albumin [29]	68 000	4.7
β-Lactoglobulin [30]	35 000	5.5
Insulin [30]	11 466	5.7
Alcohol dehydrogenase [30]	245 000	5.1
Myoglobin [30]	17 500	6.8–7.5
Ribonuclease-A [31]	14 700	9.3
α-Chymotrypsin [29]	25 000	9.8
Cytochrome c [29]	11 000	10.2
Lysozyme [29]	14 000	11.0

Retention mechanism

In order to characterize better the mechanism of retention of proteins on the phosphate-modified zirconia, isocratic retention data for several proteins as function of the potassium phosphate buffer concentration were obtained and are shown in Fig. 2. The molecular weights and isoelectric points of the proteins used in this study are given in Table I. The trends in retention suggest that retention is primarily due to cation exchange. At pH > 6, proteins with low pI values (*e.g.*, BSA, β-lactoglobulin, alcohol dehydrogenase and insulin) are not retained. In contrast, proteins with higher pI values are retained. Retention of retained proteins decrease with increasing competing ion concentration ([K^+]), which is also consistent with ion-exchange behavior.

Note that retention does not increase monotonically with the pI of the protein. This is a well known phenomena in ion-exchange chromatography [32] and shows that a "net point charge" model is not sufficient to describe the ion-exchange behavior of proteins. The effects of non-homogeneous charge distributions on proteins and specific protein interactions such as agglomeration and conformational changes must be considered [32–34].

To confirm that the retention of the proteins is a function of the potassium ion concentration of the mobile phase and not the phosphate ion concentration, a study similar to that shown in Fig. 2 was done. In this study a constant amount of phosphate

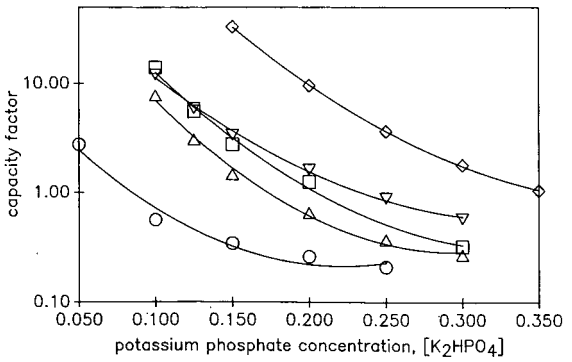

Fig. 2. Isocratic retention data for selected proteins on phosphate-modified zirconia. Column: 20-μm, 300 Å phosphate-modified zirconia (5 × 0.46 cm I.D.). Mobile phase: potassium phosphate dibasic (pH 6.0) at concentration given. System I. ○ = Myoglobin; △ = lysozyme; □ = α-chymotrypsin; ▽ = ribonuclease-A; ◇ = cytochrome c.

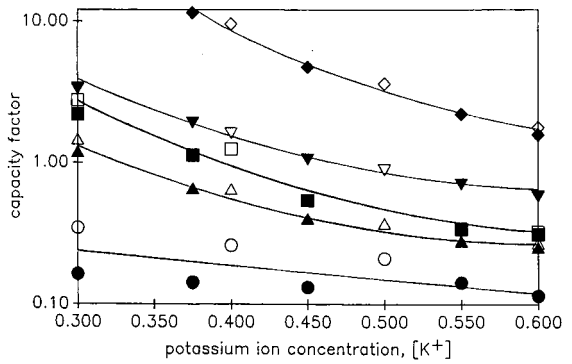

Fig. 3. Isocratic retention data as function of potassium ion concentration. Mobile phase: closed symbols, 0.15 M potassium phosphate dibasic (pH 6.0) with additional potassium chloride added to attain the indicated potassium ion concentration, 0.5 ml/min; open symbols, as in Fig. 2. Other parameters and symbols as in Fig. 2.

TABLE II

EFFECT OF VARIOUS CATIONS ON THE ISOCRATIC RETENTION OF SELECTED PROTEINS

Displacing cation	Capacity factor[a]		
	Lysozyme	Ribonuclease-A	α-Chymotrypsin
K^+	0.766 (6.91)	6.27 (6.87)	4.72 (6.87)
Na^+	3.17 (6.89)	10.28 (6.85)	9.99 (6.85)
NH_4^+	0.785 (6.90)	e.n.o.	18.97 (6.90)

[a] Capacity factors determined on 6–11-μm, 300 Å phosphate-modified zirconia, 5 × 0.46 cm I.D. column. Mobile phase: 200 m*M* phosphate buffer with counter ion listed, 0.5 ml/min. System I with HP 3388A recording integrator. Mobile phase pH given in parentheses.

ion (0.15 *M*) as potassium phosphate buffer was present in the mobile phase at all times. The potassium ion concentration of the mobile phase was adjusted by adding known amounts of potassium chloride. The retention data from this study are plotted with closed symbols in Fig. 3. Data from Fig. 2 are replotted with open symbols for comparison. The plot shows that the data from the two studies are in good agreement and the protein retention is independent of the relative amounts of phosphate and chloride, provided that the phosphate level is held above about 0.15 *M*. The scatter in the myoglobin data is attributed to the difficulty in accurately determining small capacity factors. The good agreement in the capacity factors for these two studies shows that the potassium ion is responsible for the elution of the proteins.

The effect of the specific displacing cation on the retention was also examined. Isocratic retention data for three proteins are given in Table II for the potassium, sodium and ammonium displacing cations. The data show that the displacing cation has a significant effect on retention, providing further evidence that the mechanism of retention is cation exchange. Potassium ion has the greatest displacing power of the three, followed by sodium. This trend is consistent with that found for protein chromatography on strong cation-exchange columns [35]. The retention of the proteins may thus be controlled by the choice of the phosphate counter ion and its concentration. More importantly, the potassium ion gives the largest selectivity for all three proteins shown here. As demonstrated by the capacity factors for sodium as the displacing ion, increased retention does not necessarily result in improved resolution. In this case, the potassium ion is obviously the best choice but sodium or ammonium may be better suited for other separations. The presence of phosphate in the mobile phase and the limited solubility of most phosphate salts restrict the number of displacing counter ions that may be used.

The pH of the mobile phase is expected to affect the retention of the proteins by two opposing mechanisms. As the phosphate groups associated with the zirconia surface are most likely responsible for the cation-exchange sites of the phosphate modified zirconia and bound phosphate is a weak ion exchanger, the pH of the mobile phase will determine the effective number of ion-exchange sites. As the pH of the mobile phase is lowered below one of the pK_a values of the surface-bound phosphate, an oxygen of the phosphate becomes protonated and thus reduces the number of possible ion-exchange sites. This, in turn, decreases the retention of proteins on the phase. The pH of the mobile phase also effects the charge on the proteins. The net charge of a protein becomes more positive as the pH of the mobile phase is decreased. In the absence of other effects, this should act to increase the retention of proteins.

To determine which of the above competing

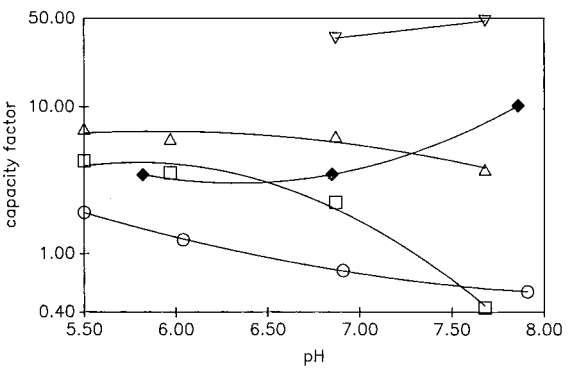

Fig. 4. Effect of mobile phase pH on the retention of selected proteins. Column: 6–11-μm, 300 Å phosphate-modified zirconia (5 × 0.46 cm I.D.). Mobile phase: open symbols, 200 m*M* potassium phosphate dibasic at pH indicated, 0.5 ml/min; closed symbols, 300 m*M* potassium phosphate dibasic at pH given, 0.5 ml/min. System I (254 nm). ○ = Lysozyme; □ = α-chymotrypsin; △ = ribonuclease-A; ▽ and ◆ = cytochrome *c*.

effects dominates the ion-exchange separation of proteins on the phosphate modified zirconia, the capacity factors of four well retained proteins were investigated as a function of mobile phase pH. The retention times of lysozyme, ribonuclease A, α-chymotrypsin and cytochrome *c* were determined isocratically with a 0.2 *M* potassium phosphate buffer solution at nominal pHs of 6.0, 7.0 and 8.0 and are given in Fig. 4.

As expected for complex biopolymers, the exact effect of pH is dependent on the individual protein. Retention increases with decreasing pH for all proteins except cytochrome *c*. We conclude that the protonation of these proteins has a larger effect on retention than does the protonation of the stationary phase. The behavior of cytochrome *c* cannot be explained by this argument. The decrease in retention of cytochrome *c* at the lower pH was confirmed with additional studies with 0.3 *M* potassium phosphate. As the dependence of protein retention on pH varies with the individual proteins, pH will be an important factor in the optimization of protein separations, especially in isocratic separations.

Attempts to separate proteins using a pH gradient were unsuccessful. Anionic proteins such as BSA, alcohol dehydrogenase and insulin were retained at low pH (2) and low phosphate conditions (50 m*M*), but all proteins eluted at the end of the linear gradient and were unresolved. The column thus shows no selectivity between anionic proteins with a pH gradient. BSA did not elute when a 50 m*M* (pH 3.0)–500 m*M* (pH 3.0) linear potassium phosphate gradient was used. This information combined with earlier observations that the mobile phase cation is responsible for the elution of proteins strongly supports the view that the predominant mechanism of retention is cation-exchange.

Phase stability

The stability of the phosphate-modified zirconia is an important consideration in determining its viability as a useful chromatographic support for routine analytical and preparative separations. As discussed above, one must maintain some minimum amount of phosphate in the mobile phase when calcium phosphate (hydroxyapatite) columns are used. Guard columns are recommended and the columns may only be used over a limited pH range.

The possible re-emergence of strong anionic interactions with the surface owing to the desorption of phosphate from the surface was an area of great concern as it would result in poor peak shapes and changing retention times. To determine if some minimum phosphate concentration must be maintained in the mobile phase for these supports, benzoic acid was used as a probe solute. Benzoic acid is not retained on a purely cationic stationary phase. If, however, significant amounts of phosphate were to be lost from the suface, the carboxylic acid group of the benzoic acid will interact with the bare zirconia support resulting in increased retention times and peak widths. By periodically determining the retention time and peak width of benzoic acid on a freshly packed phosphate-modified zirconia column while flushing the column continuously with a phosphate-free mobile phase, the amount of phosphate loss from the surface of the particles can be

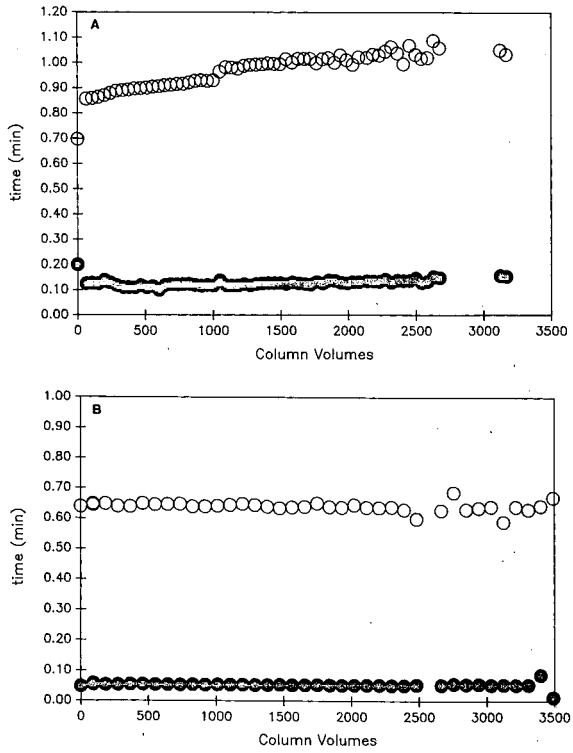

Fig. 5. Stability of the phosphate-modified zirconia using benzoic acid as a probe solute. Column: 10–15-μm, 300 Å phosphate-modified zirconia (5 × 0.46 cm I.D.). Mobile phase: (A) 1 m*M* MOPS buffer (pH 7.0), 0.5 ml/min; (B) 20 m*M* potassium phosphate dibasic (pH 7.0), 0.75 ml/min. System III (254 nm). ○ = Retention time; ● = peak width.

measured. The pH of the mobile phase without phosphate was buffered with 1 m*M* MOPS (pK_a = 7.2).

The retention time and to a lesser extent the peak width of the benzoic acid are affected as the support is exposed to phosphate-free mobile phase (see Fig. 5A). A reasonable explanation for the increase in retention time and peak width is that phosphate is being stripped from the surface exposing the underlying bulk zirconia matrix. Data for the study in which 20 m*M* phosphate was used in the mobile phase are plotted in Fig. 5B. The retention time and peak width of the benzoic acid remained constant throughout the study, indicating that the stationary phase is stable under these conditions. This clearly shows that the presence of 20 m*M* phosphate in the mobile phase is sufficient to maintain a reproducible behavior of the stationary phase.

The stability of the phosphate-modified zirconia in alkaline media was also assessed chromatographically. The retention times of three proteins, lysozyme, α-chymotrypsin and cytochrome *c*, were taken as a measure of the stability of the support to several alkaline treatments. Any significant changes in the retention times of the proteins after base treatment would indicate that the support is not stable under those particular base treatment conditions. Retention data are given in Table III for successively harsher alkaline treatments.

The column appeared to be fairly stable to flushing with 200 m*M* potassium phosphate (pH 11.9) for 1 h, although more extensive treatment would probably result in larger effects on retention as there is already evidence of a slight decrease in retention after 1 h. Previous chemical studies [1] have shown that the support is stable at pH < 10. Increasing the pH of the potassium phosphate solution to 13 had a dramatic effect on protein retention despite the presence of phosphate in the mobile phase. The retention dropped by over 30% for α-chymotrypsin and cytochrome *c*. This is consistent with phosphate desorbing from the surface of the particles as a result

TABLE III

CHROMATOGRAPHIC ALKALINE STABILITY STUDIES OF PHOSPHATE-MODIFIED ZIRCONIA[a]

Treatment conditions	Retention time (min)[a]		
	Lysozyme	α-Chymotrypsin	Cytochrome *c*
200 m*M* K_2HPO_4, pH 7.2, 2 h at 1 ml/min, R.T.[b]	1.223 (0.005)[c]	2.839 (0.07)	17.691 (0.04)
200 m*M* K_2HPO_4, pH 11.9, 1 h at 1 ml/min, R.T.	1.216 (0.003)	2.656 (0.001)	17.455 (0.015)
200 m*M* K_2HPO_4, pH 13.1, 1 h at 1 ml/min, R.T.	1.266 (0.001)	1.732 (0.005)	10.287 (0.01)
0.1 *M* KOH, 1 h at 1 ml/min, R.T.	1.263 (0.002)	1.746 (0.002)	10.015 (0.02)
0.1 *M* KOH, 1 h at 1 ml/min, R.T.	1.220 (0.05)	1.714 (0.004)	9.884 (0.04)
0.1 *M* H_3PO_4–1.0 *M* KCl, 24 h at 0.5 ml/min, R.T.	1.257 (0.002)	1.808 (0.03)	9.872 (0.008)
0.1 *M* H_3PO_4–1.0 *M* KCl, 4 h at 1.0 ml/min, 84°C	1.229 (0.002)	1.923 (0.01)	10.688 (0.03)
0.1 *M* H_3PO_4–1.0 *M* KCl, 12 h at 0.5 ml/min, 94°C	1.205 (0.02)	2.512 (0.01)	15.115 (0.04)

[a] Retention times determined after equilibrating the column with 200 m*M* K_2HPO_4 (pH 7.0) for 2 h at 1 ml/min. Column: 6–11-μm, 300 Å ZrP (0.1), 5 × 0.46 cm I.D. Flow-rate, 1.0 ml/min. System I.

[b] R.T. = Room temperature.

[c] Standard deviations for three injections given in parentheses.

of alkaline attack, resulting in a net decrease in the number of ion-exchange sites and thus a decrease in protein retention. Static stability studies [1] showed that significant amounts of phosphate are released at this pH. However, a comparable degradation in peak shape did not occur. As the peak shapes are not similarly affected, the sites responsible for strong oxyanion interactions appear to lose sorbed phosphate at a much lower rate than other sites on the surface. Additional treatments with potassium hydroxide in the absence of phosphate had little additional effect on protein retention, suggesting that the base-treated support is quasi-stable.

No specific studies to test the mechanical stability of the particles were carried out but it should be noted that during the course of this work (1.5 years) there was no case of bed collapse with routine use. The particles were routinely packed at 4500–6000 p.s.i. without evidence of particle disintegration. Based on these experiences, the mechanical stability of the particles is more than sufficient for high-pressure work.

Column regeneration studies

Attempts to regenerate the support *in situ* are also summarized in Table III. Neither the 24-h flush with neutral 200 m*M* potassium phosphate nor the 4-h flush with 0.1 *M* phosphoric acid–1.0 *M* potassium chloride solution at room temperature restored the original retention properties of the support. Improved retention of the proteins resulted from a 4-h, 84°C flush with 0.1 *M* phosphoric acid solution but the conditions were not sufficient to return the column to its original state. The 12-h, 94°C flush with 0.1 *M* H_3PO_4–1.0 *M* KCl also did not entirely return the column to its original state. The retention of the proteins is greatly increased by the treatment, however, and at least partial *in situ* regeneration of the support should be possible.

This study emphasized the importance of temperature in modifying the surface, as described previously [1]. Flushing the column with a phosphoric acid solution at room temperature had very little effect. Even the 84 and the 94°C treatments fell short of modifying the particles to the extent achieved by refluxing the particles. This is despite the much longer reaction time (12 *vs.* 4 h) for the 94°C case. The additional 10–12°C achieved by refluxing the particles in solutions at a high ionic strength appears to be significant in preparing the phosphate-modified zirconia.

TABLE IV

PROTEIN RECOVERIES ON PHOSPHATE-MODIFIED ZIRCONIA, ZrP (0.1)

Protein	Protein (mg)[a]		Recovery (%)
	Injected solution	Collected fraction	
Ribonuclease-A	0.182	0.173	95 (±5)
Lysozyme	0.207	0.196	95 (±5)
Cytochrome *c*	0.178	0.152	85 (±7)
Lysozyme enzymatic activity			
Total activity of the injected sample		57 (±8)[b]	
Total activity of the collected fraction		62 (±3)	

[a] As determined by the BCA total protein assay. Mean values given for three trials.

[b] Units as defined by the Sigma lysozyme assay.

Recovery studies

A good support must have high recoveries for the solutes it is intended to separate, *i.e.*, very little solute must remain in the column after a separation. Irreversibly bound protein will certainly affect the retention characteristics of the column. In some instances, the protein of interest is present in minute amounts and thus even small absolute amounts of irreversibly bound protein can significantly affect the yield. The protein recoveries are relatively high and could be 100% within the errors of measurement for lysozyme and ribonuclease A (see Table IV). Protein recovery studies should be done with as little protein as possible so that small amounts of adsorbed protein will still be significant in comparison with the amount injected. Although the BCA method significantly increases the detection limit of protein as compared with simply measuring the UV absorbance of the protein solution, it introduces considerable uncertainty in the measurements as it involves many steps.

Lysozyme was used to determine if the phosphate-modified zirconia denatured significant amounts of enzyme. Lysozyme is a "robust" enzyme and hence is not as sensitive a measure of the "bio-compatibility" of the support as we would have liked. However, most enzymes are anionic at neutral pH they are not retained on this support. The enzymatic activity of a

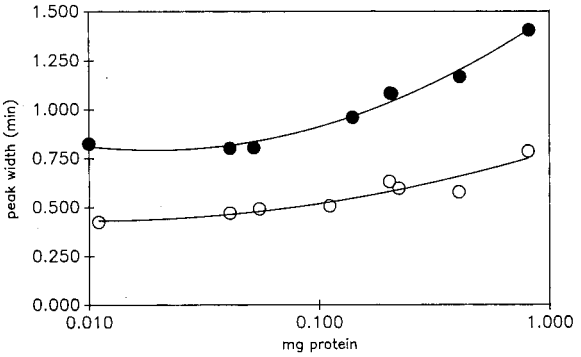

Fig. 6. Loading capacity of the phosphate-modified zirconia. Column: 6–11-μm, 300 Å phosphate-modified zirconia (5 × 0.46 cm I.D.). Mobile phase: 30-min linear gradient from 50 to 500 m*M* potassium phosphate dibasic (pH 7.0), 0.5 ml/min. System I (254 nm) with HP 3388A integrator. ○ = Lysozyme; ● = cytochrome *c*.

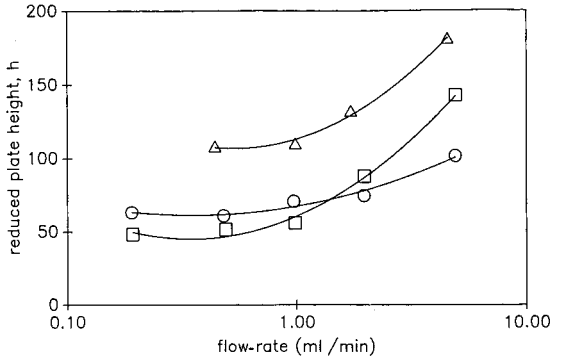

Fig. 7. Reduced plate height, *h*, *vs.* flow-rate for selected proteins on phosphate-modified zirconia. Column: 6–11-μm, 300 Å phosphate-modified zirconia (5 × 0.46 cm I.D.). System II with HP 9133 integrator. (△) Myoglobin, 50 m*M* potassium phosphate dibasic (pH 7.0), k' = 0.64; (○) lysozyme, 150 m*M* potassium phosphate dibasic (pH 7.0), k' = 2.17; (□) cytochrome *c*, 300 m*M* potassium phosphate dibasic (pH 7.0), k' = 6.89. 20-μl injections; 2 mg/ml protein solutions.

lysozyme solution, collected after elution from the support, was compared with an equal amount of the same lysozyme solution that was not exposed to the phosphate-modified zirconia. The data show that adsorption of lysozyme on phosphate-modified zirconia and subsequent desorption do not adversely affect its enzymatic activity. The higher total enzymatic activity of the lysozyme after exposure to the zirconia may be simply explained by the statistical error of the measurements. Alternatively, the phosphate-modified zirconia may have removed some inhibitors from the collected fraction.

Loading capacity and flow-rate studies

The loading capacity of the column was examined and the data are shown in Fig. 6. The plot shows that the column efficiency begins to suffer when more than about 50 μg of protein are injected. As these proteins are well resolved, they were injected as a mixture and thus the loading capacity of the column would be higher if the proteins were injected separately. This loading capacity corresponds to about 60 μg/ml of column volume or 1.49 μg/m^2 (comparisons based on the mass of stationary phase are inappropriate as zirconia is much denser than either silica or polymeric based phases). Loading capacities for comparable carboxymethylsilica-based columns are 30–300 μg/ml of column volume (data for Bio-Sil TSK CM-3-SW [36]). One particular high-performance hydroxyapatite support had a loading capacity of 120 μg/ml column volume [37].

The effect of flow-rate on the efficiency of the column was also examined. Proteins were used in this study as small cationic and anionic solutes are not well retained and proteins will be typically the species of interest. Plate heights were determined isocratically. The potassium phosphate concentration of the mobile phase was adjusted so that a range of capacity factors could be examined. The results are shown in Fig. 7.

The large reduced plate heights shown are not surprising as proteins are being used as probe molecules. Ion-exchange chromatography generally has lower efficiencies than other modes of chromatography [38]. The higher reduced plate heights observed for myoglobin may be due to specific effects with the stationary phase. Based on these

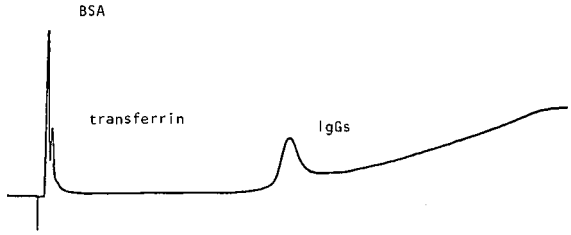

Fig. 8. Separation of IgGs from a modeled fermentation broth. Column: 6–11-μm, 300 Å phosphate-modified zirconia (5 × 0.46 cm I.D.). Mobile phase: 30-min linear gradient from 50 to 500 m*M* sodium phosphate buffer (pH 6.0), 0.5 ml/min. System I.

conditions, the efficiency of the column begins to decrease at an accelerated rate at flow-rates of 1.0 ml/min and higher (linear velocities of 0.12 cm/s and higher).

Applications

All of the separations and chromatographic studies discussed thus far were done in order to understand better the separation mechanism of the proteins on the phosphate-modified zirconia. To demonstrate some practical uses for the support, the preparative-scale separation of murine IgGs from a fermentation broth was examined. The fermentation broth was modeled by a solution of BSA, transferrin and a purified IgG sample generously provided by the Bioprocess Technology Institute at the University of Minnesota. The chromatogram is shown in Fig. 8. As expected, the anionic BSA and transferrin are unretained. The IgGs are retained and can be eluted from the column with the potassium phosphate buffer gradient. Triplicate injections of the same sample solution showed no significant changes in retention times or peak areas. Because only IgG is retained, the loading capacity of the support for this separation is very large.

CONCLUSIONS

These studies on the chromatographic characterization of phosphate-modified zirconia have shown that this substrate has potential as a support for HPLC, particularly for proteins with high p*I* values.

Cation-exchange is the mechanism of separation on this support. This limits the applicability of the support as most proteins and enzymes are anionic at neutral pH. The IgG preparative separation example demonstrates the utility of the support for solutes that are retained. As very few proteins are retained there is little difficulty in resolving the cationic protein of interest from the unwanted components of the sample matrix. Small solutes are likewise easily separated from proteins of interest as they are only retained at very low buffer concentrations.

These studies have shown that phosphate-modified zirconia is a useful high-performance cation-exchange support for the separation of proteins. The phase was found to have sufficient selectivity, efficiency and protein recovery while overcoming the strong oxyanion interactions associated with unmodified zirconia supports.

Phosphate-modified zirconia behaves as a classic cation exchanger and not as a mixed-mode medium analogous to hydroxyapatite, despite spectroscopic evidence of zirconium phosphate formation on the surface. There is no evidence that the support acts in a "hydroxyapatite-like" manner. It appears that interactions between proteins and the zirconium sites on the phosphate-modified zirconia are too strong to be chromatographically useful. Under the mobile phase conditions typically used in this work, it is likely that phosphate ions adsorb on and thus block the zirconium sites on the surface. The high affinity of zirconium phosphate for phosphate ion has been discussed earlier. This explains the cation-exchange-type behavior rather than a hydroxyapatite-like behavior.

The successful blocking of the strong oxyanion interaction sites on the zirconia surface makes the phosphate modification interesting as an intermediate phase in the development of other zirconia-based chromatographic phases. Strong interactions of solutes containing oxyanion functionalities with the bulk zirconia support persist even after zirconia particles have been coated with polybutadiene [2]. It is unlikely that any polymer coating will be dense enough to cover the surface entirely without severely limiting mass transport into the pores. Hence some modification of the zirconia surface will be necessary to block these interactions even when the particles are further modified by polymer coating. The phosphate modification described in this work can serve this purpose.

The susceptibility of the covalent phosphate bonds to hydrolysis at alkaline pH, as evidenced by the solid-state ^{31}P NMR studies [1], is the major drawback of the phosphate-modified zirconia. The chief advantage of the base zirconia support, *i.e.*, its pH stability (>10), is thus lost owing to the instability of the phosphate surface modification. As the phosphate modification is relatively easily done, it is possible at least partially to regenerate the column *in situ* by flushing with hot phosphoric acid solution. When the column becomes fouled, it can be flushed with sodium hydroxide solution to remove any irreversibly bound protein and the phosphate modification. The phosphate modification could then be reapplied by flushing the column with hot

phosphoric acid. The correct conditions for performing an *in situ* phosphate modification of the particles must also be determined.

Several other polybasic acid salts of zirconium have been examined as ion exchangers, including zirconium arsenate, molybdate, tungstate, antimonate, tellurate and silicate [3,4]. Recently, the synthesis of zirconium phosphoborate has been reported [39]. As sugars are known to form borate complexes and this has been successfully exploited in their separation [38], such a phase could be a convenient method for sugar separations.

In conclusion, phosphate-modified zirconia has been shown to be a viable high-performance support for the separation of cationic proteins. In order to take full advantage of the pH stability of the base support, the phosphate modification should be optimized so as to leave the bulk support untouched.

ACKNOWLEDGEMENTS

The authors thank Thomas Weber, John Blackwell and Dr. Alon McCormick of the University of Minnesota and Dr. Eric Funkenbusch of the 3M Ceramic Technology Center for many helpful discussions and suggestions. W.A.S. also gratefully acknowledges financial support from 3M and the Institute for Advanced Studies at the University of Minnesota.

REFERENCES

1 W. A. Schafer, P. W. Carr, E. F. Funkenbusch and K. A. Parson, *J. Chromatogr.*, 587 (1991) 137.
2 M. P. Rigney, *Ph.D. Dissertation*, University of Minnesota, Minneapolis, MN, 1988.
3 A. Clearfield, G. H. Nancollas and R. H. Blessing, in J. A. Marinsky and Y. Marcus (Editors), *Ion-Exchange and Solvent Extraction*, Marcel Dekker, New York, 1973.
4 C. B. Amphlett, *Inorganic Ion Exchangers*, Elsevier, Amsterdam, 1964.
5 V. Veselý and V. Pekárek, *Talanta*, 19 (1972) 219.
6 A. Clearfield, in A. Clearfield (Editor), *Inorganic Ion Exchanger Materials*, CRC Press, Boca Raton, FL, 1982.
7 T. Kijima, Y. Sekikawa and S. Ueno, *J. Inorg. Nucl. Chem.*, 43 (1981) 849–853.
8 T. Kijima, S. Ueno and M. Goto, *J. Chem. Soc., Dalton Trans.*, (1982) 2499–2503.
9 T. Kijima and S. Ueno, *J. Chem. Soc., Dalton Trans.*, (1986) 61–65.
10 I. D. Coussio, G. B. Marini-Bettòlo and V. Moscatelli, *J. Chromatogr.*, 11 (1963) 238–240.
11 P. Catelli, *J. Chromatogr.*, 9 (1962) 534–536.
12 K. Fujimura and T. Ando, *J. Chromatogr.*, 114 (1975) 15–21.
13 S. Allulli, N. Tomassini, G. Bertoni and F. Bruner, *Anal. Chem.*, 48 (1976) 1259–1261.
14 L. Maya, *Inorg. Nucl. Chem. Lett.*, 15 (1979) 207.
15 L. Maya and P. O. Danis, *J. Chromatogr.*, 190 (1980) 145–149.
16 R. K. Scopes, *Protein Purification: Principles and Practice*, Springer, New York, 2nd ed., 1987, pp. 175–176.
17 S. W. Compton and S. C. Engelhorn, *LC Mag.*, 1 (1983) 294–296.
18 G. Bernardi, *Methods Enzymol.*, 27 (1973) 471–479.
19 M. J. Gorbunoff, *Anal. Biochem.*, 136 (1984) 425–432.
20 M. J. Gorbunoff, *Anal. Biochem.*, 136 (1984) 433–439.
21 M. J. Gorbunoff and S. N. Timasheff, *Anal. Biochem.*, 136 (1984) 440–445.
22 M. Jarcho, *Clin. Orthoped. Relat. Res.*, 157 (1981) 259–278.
23 M. Spencer and M. Grynpas, *J. Chromatogr.*, 166 (1978) 423–434.
24 M. Spencer, *J. Chromatogr.*, 166 (1978) 435–446.
25 T. Kawasaki and W. Kobayashi, *Biochem. Int.*, 14 (1987) 55–62.
26 T. Kawasaki, S. Takahashi and K. Ikeda, *Eur. J. Biochem.*, 152 (1985) 361–371.
27 T. Kadoya, T. Isobe, M. Ebihara, T. Ogawa, M. Sumita, H. Kuwahara, A. Kobayashi, T. Ishikawa and T. Okuyama, *J. Liq. Chromatogr.*, 9 (1986) 3543–3557.
28 R. K. Scopes, *Protein Purification: Principles and Practice*, Springer, New York, 2nd ed., 1987, pp. 175–176.
29 T. Kadoya, T. Ogawa, H. Kuwahara and T. Okuyama, *J. Liq. Chromatogr.*, 11 (1988) 2951–2967.
30 P. G. Righetti and T. Caravaggio, *J. Chromatogr.*, 127 (1976) 1–28.
31 D. Malamud and J. W. Drysdale, *Anal. Biochem.*, 86 (1978) 620–647.
32 W. Kopaciewicz, M. A. Rounds, J. Fausnaugh and F. E. Regnier, *J. Chromatogr.*, 266 (1983) 3–21.
33 V. Lesins and E. Ruckenstein, *Colloid Polym. Sci.*, 266 (1988) 1187–1190.
34 W. R. Melander, Z. E. Rassi and C. Horváth, *J. Chromatogr.*, 469 (1989) 3–27.
35 F. E. Regnier, *Methods Enzymol.*, 104 (1984) 185–187.
36 *Bio-Rad HPLC Chromatography Catalog*, Bio-Rad Labs., Richmond, CA, 1989.
37 T. Kadoya, T. Isobe, M. Ebihara, T. Ogawa, M. Sumita, H. Kuwahara, A. Kobayashi, T. Ishikawa and T. Okuyawa, *J. Chromatogr.*, 9 (1986) 3543–3557.
38 L. R. Snyder and J. J. Kirkland, *Introduction to Modern Liquid Chromatography*, Wiley-Interscience, New York, 2nd ed., 1979.
39 P. S. Thind, S. K. Mittal and S. Gujral, *Synth. React. Inorg. Met.-Org. Chem.*, 18 (1988) 593–607.

Journal of Chromatography, 587 (1991) 161–169
Elsevier Science Publishers B.V., Amsterdam

CHROM. 23 586

Immobilization of Fv antibody fragments on porous silica and their utility in affinity chromatography

M. J. Berry*, J. Davies, C. G. Smith and I. Smith

Unilever Research, Sharnbrook, Bedfordshire MK44 1LQ (UK)

(First received May 13th, 1991; revised manuscript received June 24th, 1991)

ABSTRACT

Recent advances in molecular biology have allowed antibody binding domains to be cloned and expressed in *Escherichia coli*. The use of Fv antibody fragments as ligands in immunoaffinity chromatography is reported. Fv fragments specific for hen-egg lysozyme were immobilized on porous silica and used to recover antigen from spiked serum in a single step. Comparison with a conventional immunoadsorbent (whole antibodies immobilized on silica) showed the Fv-silica to have a fivefold superior capacity. Analysis of sectioned Fv-silica particles by immunoelectron microscopy indicated that captured antigen was evenly distributed throughout the internal porous structure of the particle.

INTRODUCTION

Immunoaffinity chromatography exploits the exquisite specificity of an antibody binding site. This means that very high resolution separations are achievable, typically in a single step. For example, the technique has been used to recover factor IX from serum fractions [1] and to separate different glycoforms of the same enzyme [2]. Another attraction is the enormous diversity of the immune system; it has been estimated to have the capacity for making 10^8 different antibody specificities [3]. In practical terms, this means that it is possible to raise monoclonal antibodies (usually from the mouse) which are uniquely specific for any enzyme, serum protein, carbohydrate, cell, virus or small organic that is likely to be encountered.

Immunoaffinity chromatography is widely used for laboratory-scale preparative work (typically with 4% agarose as the base medium), but is rarely used either for analytical applications or for industrial-scale processes. Reasons for this include the high cost of monoclonal antibodies and their low capacity on a weight for weight basis (antibodies have a molecular weight of 150 000 dalton and two binding sites). Another disadvantage of antibodies being such large ligands is that they need wide-pore chromatographic media for their efficient immobilization, and even then their presence may significantly reduce the pore size available for antigen exchange [4]. This may lead to problems such as poor specific capacity or band spreading. These effects have been demonstrated for immunoadsorbents made with "wide-pore" silicas (nominal pore size 200–500 Å) [4]. Wide-pore silicas are a popular choice for the analytical- and preparative-scale high-performance liquid chromatography (HPLC) of proteins owing to their nearly ideal properties of high mechanical strength, well defined pore size, freedom from swelling effects, resistance to enzymatic degradation and very low non-specific adsorption. The only negative aspect of silica-based media, their inability to withstand extensive treatment with 0.5 *M* sodium hydroxide solution, is no limitation for immunoaffinity chromatography where the proteinaceous ligand precludes the use of high-pH cleaning protocols. Moreover, there have been several recent reports describing the immobilization of antibodies and antibody fragments on silica for use in immunoaffinity chromatography [4–9].

0021-9673/91/$03.50

Recent progress in molecular biology has made it possible to produce antibody fragments in *Escherichia coli* [10–14]. One of the best described species is the Fv antibody fragment. Fv fragments consist of the variable domains of the heavy and light chains of the parent antibody and have a molecular weight of 25 000 dalton [11]. They have been shown to have a similar or slightly lower affinity than the parent antibody [10,11]. Several ingenious features have been designed into Fv fragments by protein engineers to facilitate their production and recovery. For example, Fv fragments have been made with a signal peptide sequence (the "pel B" sequence [15]) so that they are secreted by the host bacterium into the growth medium [10]. Another example is the provision of a histidine-rich "tail" to facilitate recovery from growth medium by immobilized metal affinity chromatography (IMAC) [13]. Fv antibody fragments offer an exciting opportunity in immunoaffinity chromatography: they may be produced cheaply in cultured media, they have more binding sites per milligram of protein than whole antibodies and they are sufficiently small to be immobilized within the pores of rigid chromatographic media such as silica without significantly reducing the pore size.

In this paper, we describe the immobilization of Fv fragments, specific for hen-egg lysozyme, on silica particles with 200 Å pore size. We used this immunoadsorbent to recover lysozyme from "spiked" serum and compared its performance (in a packed column) with that of a traditional immunoadsorbent consisting of silica and whole antibody. Also, the efficiency with which individual immunoadsorbent particles captured target antigen was analysed by immunoelectron microscopy of ultra-thin sections.

EXPERIMENTAL

Production of whole antibodies

A hybridoma cell line which produces an antibody specific for hen-egg lysozyme, the "D.1.3 antibody" [16], was obtained from Dr. G. Winter (MRC, Cambridge, UK). The hybridoma was reproduced in mice. Purified monoclonal antibodies were recovered from ascites using protein-A Sepharose.

Production of Fv antibody fragments

A vector encoding the Fv fragment of the D.1.3 antibody and tagged at its C-terminus with the "myc" peptide [17] was obtained from Dr. G. Winter [10]. The vector was transformed into *E. coli* (strain BMH 71-18) and grown in cultured medium according to the method of Ward *et al.* [10]. Secreted Fv fragments were recovered from the medium by affinity chromatography on lysozyme–Sepharose [10].

Preparation of tresylated silica

Preparative-grade epoxy silica (Sorbsil 40/60 C200) was obtained from Crosfield Chemicals (Warrington, UK). This material has a particle size range of 40–60 μm and a nominal pore size of 200 Å. Epoxy-silica was hydrolysed to the diol by the method of Mohan *et al.* [4]. Diol-silica was dried and then reacted with tresyl chloride (Fluka, Buchs, Switzerland) by a method based on that of Nilsson and Mosbach [18]. The modification was that triethylamine (0.6 mol% of tresyl chloride) and 4-dimethylaminopyridine (0.6 mol% of tresyl chloride) were used in place of pyridine. The optimum level of tresylation was determined with respect to capacity for antigen (low-level tresylation resulted in poor coupling of Fv fragments; very high tresylation resulted in good coupling of Fv fragments but unacceptable inactivation of their binding sites; a compromise was required). The amount of tresyl groups on the optimally activated silica was measured by fluorine determination (oxygen combustion–ion chromatographic procedure), and this was useful in reproducing the same result when a new batch of diol-silica was used.

Immobilization of immunoligands on tresylated silica

Two immunoadsorbent materials were made, one consisting of Fv antibody fragments and the other whole monoclonal antibody (MCA).

Approximately 1 g of tresylated silica was washed with saline (0.15 *M* sodium chloride solution) and then with coupling buffer (0.1 *M* $NaHCO_3$–0.5 *M* NaCl, pH 8.3). The washed silica was added to 4 ml of a *ca.* 1 mg/ml solution of the immunoligand (Fv or whole antibody) in coupling buffer. The slurry was rotated overnight at 4°C. The immunoadsorbent was blocked with blocking buffer (1 *M* ethanolamine–HCl, pH 8) and then washed three times

with 0.1 *M* Tris buffer (pH 8). The amount of ligand immobilized was determined by measuring the ligand concentration before and after coupling to silica using the BCA protein assay.

Running of immunoaffinity columns

A 1-g amount of each immunoadsorbent was conditioned in phosphate-buffered saline (PBS) and then packed in a glass column (Pharmacia C10/20) to give column dimensions of 40 mm × 10 mm I.D. Each column was loaded with a feedstock of 5% horse serum (Seralab), made up in PBS (0.01 *M* Na_2HPO_4/NaH_2PO_4–0.15 *M* NaCl, pH 7) and spiked with hen-egg lysozyme (Sigma) to a final concentration of 50 μg/ml (*ca.* 3000 U/ml). This feedstock was loaded until a stable breakthrough was reached; the columns were then washed back to the baseline with PBS. Flow-rates were kept at 85 ml/h throughout the experiments.

Bound protein was recovered by eluting with desorption buffer (4 *M* $MgCl_2$, pH 7) and dialysing the peak into PBS. The amount of recovered protein was determined by the BCA protein assay. Lysozyme activity was monitored across the chromatogram profile by assaying fractions using a suspension of *Micrococcus* (Sigma) according to the manufacturer's instructions. Non-specific binding was evaluated by passing the same feedstock down a "blank" column, which had been tresylated and blocked as above but no immunoligand was added.

The percentage recovery of lysozyme protein was also measured accurately by loading and eluting a known amount of FITC-labelled lysozyme [19,20] with spectrofluorimetric (Perkin-Elmer) detection.

Analysis of lysozyme within particles by immunoelectron microscopy

Immunoadsorbent particles were loaded with lysozyme by rotating slowly in a 1 mg/ml solution (in 0.1 *M* Tris buffer, pH 8) for 1 h at room temperature. They were then washed three times in Tris buffer. The washed particles were fixed in 1% paraformaldehyde–0.05% glutaraldehyde (made up in PBS, pH 7.6) for 2 h at 4°C. Following an overnight wash in PBS, the samples were dehydrated with 50, 70 and 90%, ethanol (15 min each) and absolute ethanol (2 × 30 min) and placed in several changes of hydrophilic resin: 3 parts LR Gold acrylic resin (London Resin, Woking, UK)–2 parts "low-acid grade"' glycol methacrylate (Polysciences, Warrington, PA, USA)–0.1% benzoin ethyl ether (Polysciences). The samples were finally embedded in the above resin in gelatin capsules and polymerized at room temperature by illumination with an ultraviolet light source (360 nm).

Ultra-thin sections of the particles were collected on Formvar (2% in amyl acetate)-coated nickel grids and placed in 10-μl aliquots of 1% ovalbumin (Sigma) in PBS–5% normal goat serum, for 30 min at room temperature. The grids were then transferred to 10-μl aliquots of a polyclonal rabbit anti-lysozyme antibody (an in-house preparation) diluted 1:5 in PBS–5% normal goat serum–0.1% Tween 20 (Sigma) and incubated overnight at room temperature in a moist dish (the rabbit anti-lysozyme antibody had been found to be able to pair with the D.1.3 anti-lysozyme monoclonal antibody in a sandwich ELISA on microtitre plates; results not shown). Following a thorough wash with PBS, the grids were placed in 10 μl aliquots of goat anti-rabbit–colloidal gold (5 nm diameter) (Biocell), diluted 1:200 in PBS–1% ovalbumin–5% normal goat serum for 60 min at room temperature. The grids were then thoroughly washed in PBS, followed by distilled water. The colloidal gold staining was silver enhanced using a silver enhancer kit (Biocell) for 2–3 min at room temperature. The grids were examined using a transmission electron microscope without further counterstaining.

Control particles (where the immunoligand had been omitted) were stained and examined by the same protocol.

RESULTS

Preparation and use of Fv-silica column

Approximately 3.4 mg of Fv polypeptide were found to have been immobilized on 1.0 g of Sorbsil. This immunoadsorbent was used to recover lysozyme from spiked serum in a single step. The breakthrough curve for lysozyme was sharp (Fig. 1A). The recovered lysozyme was found to be homogeneous by sodium dodecyl sulphate polyacrylamide gel electrophoresis (SDS-PAGE) (Fig. 2). The capacity of the column for lysozyme (determined by the breakthrough point) was 0.8 mg (16 ml × 50 μg/ml) of lysozyme protein. This corresponds to 48 000 lysozyme units (16 mls × 3000 U/ml). The

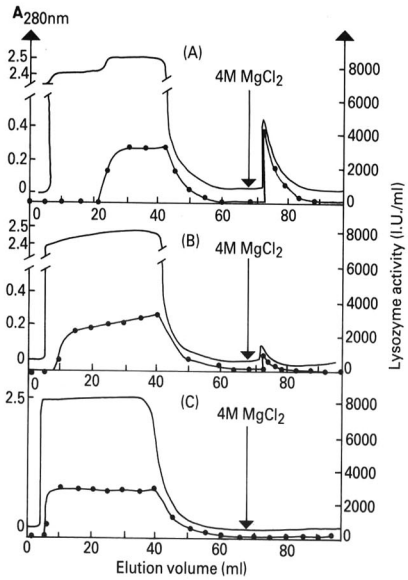

Fig. 1. (A) Recovery of hen-egg lysozyme from "spiked" serum using anti-lysozyme Fv fragments immobilised on Sorbsil C200 40/60. The feedstock was made up and loaded in PBS (0.01 *M* $NaHPO_4/NaH_2PO_4$–0.15 *M* NaCl, pH 7). Lysozyme was specifically eluted with 4 *M* $MgCl_2$ and dialysed into PBS. Total protein absorbance at 280 nm (top line) was monitored on-line; lysozyme activity (●) was monitored by assaying fractions. (B) Recovery of lysozyme from "spiked" serum using anti-lysozyme monoclonal antibodies immobilized on Sorbsil C200 40/60. (C) Interaction of "spiked" serum with a "blank" column (Sorbsil C200 40/60 which had been tresylated and blocked but on which no immunoligand had been immobilized).

amount of lysozyme recovered in the 4 *M* $MgCl_2$ fraction was 0.6 mg of lysozyme protein, as determined from the absorbance at 280 nm and the BCA protein assay (Pierce, Rockford, IL, USA). This fraction was determined to have a total acitivity of 14 400 U. This separation experiment was repeated twice and all the data agreed to within 5%. From these results, some parameters describing the performance of the immunoadsorbent were calculated as follows: recovery of lysozyme protein = (0.6/0.8) × 100 = 75%; recovery of lysozyme activity = (14.4/48) × 100 = 30%; and specific activity of immobilized Fv fragments = (0.8 × 25)/(3.4 × 14.3) × 100 = 41% (taking the molecular weight of lysozyme to be 14 300 dalton and the molecular weight of Fv to be 25 000 dalton). The recovery of lysozyme protein as determined by the FITC-labelled experiment was 78%. A summary of key data is given in Table I.

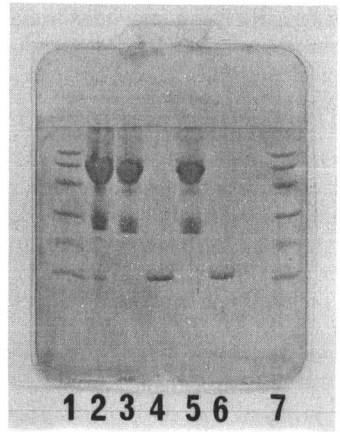

Fig. 2. SDS-PAGE of separation achieved with immobilized anti-lysozyme Fv fragments. Lanes: 1, 7 = Pharmacia low-molecular-weight standards (94 000, 67 000, 43 000, 30 000, 20 100, 14 400 dalton); 2, 3 = feedstock (5% horse serum "spiked" with 50 μg/ml of hen-egg lysozyme); 4 = lysozyme; 5 = column fall-through; 6 = lysozyme recovered from feedstock (4 *M* $MgCl_2$ fraction).

The "blank" column was found not to bind lysozyme or any serum proteins (Fig. 1C).

Preparation and use of MCA-silica column

Approximately 2 mg of monoclonal antibody (MCA) protein were found to have been immobi-

TABLE I

COMPARISON OF Fv FRAGMENTS AND WHOLE ANTIBODIES (MCA) IN IMMUNOAFFINITY CHROMATOGRAPHY

Affinity columns made with immobilized antibody fragments (Fv) and whole antibodies (MCA) were compared for their ability to recover antigen from spiked serum. Capacity for antigen was determined by breakthrough level (see Fig. 1); recovery of antigen protein was determined by following an FITC-labelled antigen.

Parameter	Fv fragment column	MCA column
Silica used (g)	1.0	1.0
Ligand used (mg)	4.0	4.0
Ligand coupled (mg)	3.4	2.0
Capacity for antigen (mg)	0.8	0.15
Antigen recovered (mg)	0.6	0.12
Recovery (%)	78	79

lized on 1.0 g of Sorbsil. This immunoadsorbent was used to recover lysozyme from spiked serum in a single step (Fig. 1B). There was a sharp breakthrough for lysozyme after reaching capacity and then a shallow "secondary breakthrough" (Fig. 1B). The capacity of the column for lysozyme (determined by the breakthrough point) was 0.15 mg (3 ml × 50 μg/ml). This correcponds to 9000 lysozyme units (3 ml × 3000 U/ml). The amount of lysozyme recovered in the 4 *M* $MgCL_2$ fraction was 0.12 mg of lysozyme protein, as determined by the absorbance at 280 nm and the BCA protein assay (Pierce). This fraction was determined to have a total activity of 3000 U. This separation experiment was repeated and all the data agreed to within 5%. From these results, some parameters describing the performance of the immunoadsorbent were calculated as follows: recovery of lysozyme protein = (0.12/0.15) × 100 = 80%; recovery of lysozyme activity = (3000/9000) × 100 = 33%; specific activity of immobilised antibodies = (0.15 × 75)/(2 × 14.3) × 100 = 39% (assuming antibodies to have a molecular weight of 150 000 dalton with two binding sites). The recovery of lysozyme protein as determined by the FITC-labelled experiment was 79%. A summary of key data is given in Table I.

Analysis of lysozyme within particles by immunoelectron microscopy

The immunoadsorbent particles consisting of Fv antibody fragments were found to have lysozyme bound to them evenly throughout their internal porous structure. A typical example is shown in Fig. 3A. The immunoadsorbent particles consisting of whole antibodies were found to have less lysozyme bound and in addition many of the particles were found to have most of their bound lysozyme at the surface of the particle. An example of this is shown in Fig. 3B. All negative control particles were found to give very low (or zero) background staining.

DISCUSSION

There are several reasons why Fv antibody fragments may be expected to be preferable to whole antibodies in immunoaffinity chromatography. First, we expect that Fv fragments will be cheaper to produce once their manufacture has been optimized, because they may be produced in *E. coli* in cheap baterial media whereas whole antibodies are expressed in mammalian cells in expensive tissue culture media. Second, Fv fragments have an increased capacity for antigen on a weight for weight basis (one binding site on a 25 000 dalton protein as opposed to two binding sites on a 150 000 dalton protein). Third, Fv fragments may be expected to be sufficiently small to be immobilized within the porous structure of "wide-pore" silica without significantly reducing the pore size. For example, the silica used in this study (Sorbsil C200 40/60) is a typical preparative-scale chromatographic medium. With a pore size of 200 Å, there is scarcely room to accommodate whole antibody (molecular diameter = 150 Å [10]) and still leave room to engage and bind antigen specifically (molecular diameter of lysozyme = 40 Å [21]). In contrast, the immobilization of Fv fragments (molecular diameter *ca.* 50 Å) would not be expected to reduce the pore size so drastically. Although silicas with larger pore sizes are available, these media have the drawbacks of reduced surface area (and therefore reduced capacity for ligand) and reduced tensile strength (and therefore reduced resistance to high pressures) [22]. For the purification of very large antigens, it may still be necessary to resort to silica with pore sizes in excess of 200 Å [4]; however, whatever the size of the target antigen, it should be possible to use a correspondingly smaller pore silica (with associated advantages) if Fv ligands are used in preference to whole antibodies. In this study, we set out to test whether these perceived advantages could be manifested as demonstrable performance improvements in column chromatography.

We made an immunoadsorbent consisting of Fv fragments immobilized on Sorbsil C200 and another consisting of whole monoclonal antibodies (MCA) immobilized on the same medium. A direct comparison indicated both immunoadsorbents to be capable of recovering target antigen (hen-egg lysozyme) from spiked serum in a single step; however, the immunoadsorbent made with Fv fragments had a five fold superior capacity (0.8 mg compared with 0.15 mg) for antigen. One reason for this was that more Fv had been immobilized than MCA (3.4 mg compared with 2 mg). This was thought to be because the Fv fragments had improved access to the internal porous structure of the silica (and therefore had more tresylated sites to re-

act with). This explanation was supported by the finding that antigen distribution within the Fv particle was even (it seems likely that for a small antigen such as lysozyme, the antigen distribution will closely mirror the immunoligand distribution). Another contributory explanation for the superior capacity of the Fv column is the increased number of binding sites per milligram of protein (as discussed above).

The specific activity of immobilized Fv fragments

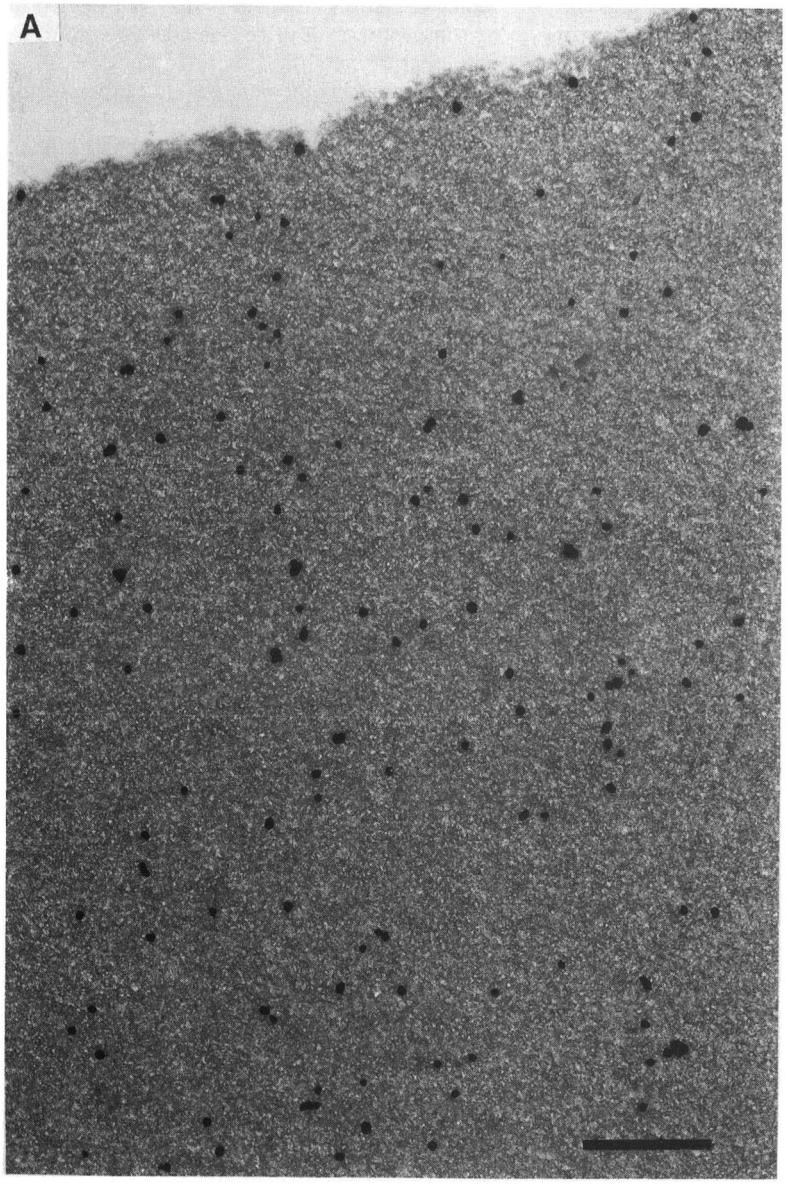

Fig. 3.

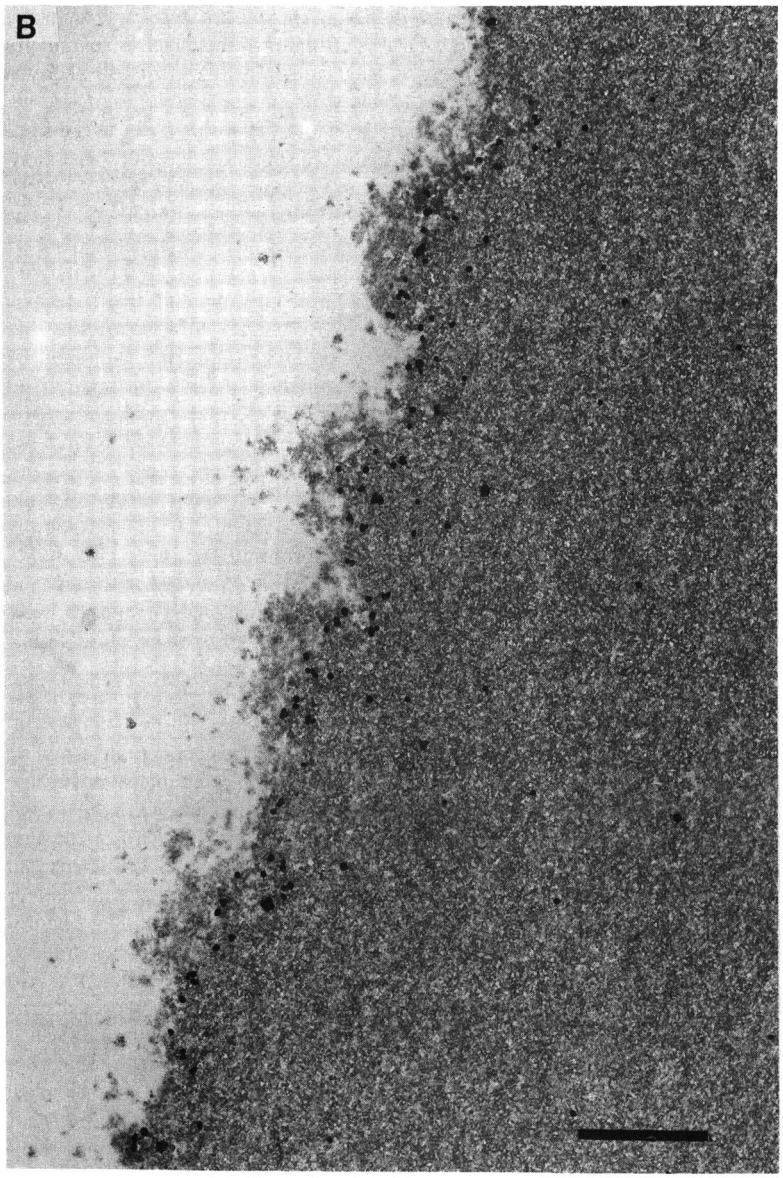

Fig. 3. (A) Immunoelectron micrograph of silica particle derivatized with anti-lysozyme Fv fragments. Particles were interacted with lysozyme, sectioned and then stained by labelling with rabbit anti-lysozyme followed by goat anti-rabbit–colloidal gold. Magnification 20 000 (bar = 1 μm). (B) Immunoelectron micrograph of silica particle derivatized with anti-lysozyme monoclonal antibodies. Particles were interacted with lysozyme, sectioned and then stained by labelling with rabbit anti-lysozyme followed by goat anti-rabbit–colloidal gold. Magnification 20 000 (bar = 1 μm).

and immobilized MCA was *ca.* 40%. Similar figures have been published by others for immobilized antibodies [1,6] and immobilized "Fab" fragments [6] (made by proteolytic digestion of whole antibodies). We believe that the specific activity achievable for immobilized Fv fragments could be increased by improving their orientation by incorporating a short, lysine-rich peptide "tail" at their C-terminus. Such a tail could be readily incorporated by recombinant DNA technology. In this study, we used the "myc" peptide as a linking tail, which only has one lysine [10].

An important result was that the Fv-silica immunoadsorbent produced a sharp breakthrough curve for lysozyme and a sharp elution peak. Taken in conjunction with the finding that bound lysozyme was evenly distributed within the silica particles, this is compelling evidence that lysozyme had unrestricted access to binding sites within the internal porous structure of the media. The MCA-silica immunoadsorbent also produced a sharp breakthrough curve and a sharp elution peak. This is in keeping with the view that most of the lysozyme purified by this immunoadsorbent was bound and released from the surface of the particle where the kinetics are known to be fast [23]. Support for this view is given by the distribution of antigen in the electron micrograph (Fig. 3B). An interesting finding was that the MCA-silica immunoadsorbent produced a shallow "secondary breakthrough" (Fig. 1B). It is possible that this secondary breakthrough is the result of a gradual filling of sites, deep within the particles, which are poorly accessed by antigen due to size restrictions. The presence of a few internal binding sites which would fit this description is suggested by the electron micrograph (Fig. 3B).

The aim of this study was to evaluate the utility of Fv fragments as affinity ligands, and in particular to compare their performance with that of whole antibodies on porous silica (we chose silica because we believe the long-term potential for Fv ligands is in preparative-scale systems and therefore we wanted to do our pilot project on a chromatographic medium which can be readily scaled up). We used Fv fragments specific for hen-egg lysozyme as these were the first to become available to us, and evaluated their ability to recover target antigen from 5% serum (this system was intended to model the recovery of a recombinant protein from tissue culture media). Using this model recovery system, we have been able to demonstrate two clear advantages of using Fv fragments in place of whole antibody: a superior capacity for antigen, and an improved access of antigen to internal binding sites in the silica particles. The only disappointing result was a moderate recovery of lysozyme protein (75–80%) and a poor recovery of lysozyme activity (30–33%). The loss of activity was because the eluent used (4 *M* $MgCl_2$) inactivated lysozyme. A preliminary screening could not identify an elution buffer which improved the recovery, and our conclusion is that this particular antibody (and corresponding Fv fragment) had too high an affinity for the preparative affinity purification of enzymes. As hen-egg lysozyme has no medical or commercial interest, we do not propose to try to improve its recovery. Moreover, our model has served its purpose and future work should concentrate on isolating Fv fragments of an appropriate specificity and affinity to achieve commercially viable separations and evaluating the performance of Fv ligands in high-performance and/or preparative chromatographic conditions.

Some groups have recently tried to mimic the antibody binding site by making short peptides corresponding to a single complementarity determining region [24]. An analogous attempt to mimic the binding site of the D.1.3 antibody was not successful in our hands (results not shown) and in any event it seems unlikely that such a reagent can match the specificity of an Fv carrying a full battery (i.e., six) of complementarity-determining regions. It is our belief that for high-resolution separations (such as separating isoenzymes and different glycoforms of the same protein), the Fv represents the smallest functional fragment of the antibody which is currently available. Moreover, the combination of silica with Fv fragments may be used to make high-resolution separation media with excellent flow-rates. This concept offers excellent opportunities for the use of immunoaffinity chromatography in rapid analytical separations and scaled-up industrial processes.

ACKNOWLEDGEMENT

We thank Dr. Ian Chappell for critically reading the manuscript.

REFERENCES

1 J. Tharakan, D. Strickland, W. Burgess, W. N. Drohan and D. Clark, *Vox Sang*, No. 1 (1990) 21.
2 M. J. Berry, *Anal. Proc.*, 28 (1991) 141.
3 P. G. Schultz, personal communication, 1990.
4 S. B. Mohan, J. M. Malhotra and A. Lyddiatt, in D. L. Pyle (Editor), *Separations for Biotechnology*, Elsevier, Amsterdam, 1990, p. 200.
5 L. R. Massom and H. W. Jarrett, *J. Chromatogr.*, 482 (1989) 252.
6 T. Hayashi, S. Sakamoto, M. Shikanabe, I. Wada and H. Yoshida, *Chromatographia*, 27 (1989) 569.
7 K. Nakamura, T. Hashimoto, Y. Kato, K. Shimura and K. Kasai, *J. Chromatogr.*, 510 (1990) 101.
8 J. Lin, I. Chang, J. D. Andrade, J. N. Herron and D. A. Christensen, *J. Chromatogr.*, 542 (1991) 41.
9 J. N. Lin, J. D. Andrade and I. Chang, *J. Immunol Methods*, 125 (1989) 67.
10 E. S. Ward, D. Gussow, A. D. Griffiths, P. T. Jones and G. Winter, *Nature (London)*, 341 (1989) 544.
11 A. Skerra and A. Pluckthun, *Science (Washington, D.C.)*, 240 (1988) 1038.
12 M. Better, C. P. Chang, R. R. Robinson and A. H. Horwitz, *Science (Washington, D.C.)*, 240 (1988) 1041.
13 A. Skerra, I. Pfitzinger and A. Pluckthun, *Biotechnology*, 9 (1991) 273.
14 R. E. Bird, K. D. Hardman, J. W. Jacobson, S. Johnson, B. M. Kaufman, S. Lee, T. Lee, S. H. Pope, G. S. Riordan and M. Whitlow, *Science (Washington, D.C.)*, 242 (1988) 423.
15 S. Lei, H. Lin, S. Wang, J. Callaway and G. Wilcox, *J. Bacteriol.*, 169 (1987) 4379.
16 A. G. Amit, R. A. Mariuzza, S. E. Phillipos and R. J. Poljak, *Science (Washington, D.C.)*, 233 (1986) 747.
17 S. Munro and H. Pelham, *Cell*, 46 (1986) 291.
18 K. Nilsson and K. Mosbach, *Eur. J. Biochem.*, 112 (1980) 397.
19 T. J. Gill, E. M. McLaughlin and G. S. Omen, *Biopolymers*, 5 (1967) 297.
20 R. Irwin and J. E. Churchich *J. Biol. Chem.*,. 246 (1971) 5329.
21 P. Claes, S. Fowell, A. Kenney, P. Vardy and C. Wollin, in D. L. Pyle (Editor), *Separations for Biotechnology*, Elsevier, Amsterdam, 1990, p. 611.
22 H. J. Ritchie, P. Ross and D. R. Ross, *Chromatogr. Anal.*, October (1990) 9.
23 F. E. Regnier, *Nature (London)*, 350 (1991) 634.
24 G. W. Welling, T. Geurts, J. Van Gorkum, R. A. Damhof and J. W. Drijfhout, *J. Chromatogr.*, 512 (1990) 337.

Journal of Chromatography, 587 (1991) 171–176
Elsevier Science Publishers B.V., Amsterdam

CHROM. 23 587

Optimization of oxidation of glycoproteins: an assay for predicting coupling to hydrazide chromatographic supports

Harvard W. Morehead* and Kenneth W. Talmadge

Bio-Rad Laboratories, 3300 Regatta Boulevard, Richmond, CA 94804 (USA)

Daniel J. O'Shannessy

Smith Kline–Beecham Pharmaceuticals, Department of Macromolecular Sciences, King of Prussia, PA (USA)

Christopher J. Siebert

Bio-Rad Laboratories, 3300 Regatta Boulevard, Richmond, CA 94804 (USA)

(First received February 5th, 1991; revised manuscript received June 12th, 1991)

ABSTRACT

A rapid, simple assay for aldehydes generated by oxidation of saccharide units in glycoproteins, using dyes containing hydrazide functionalities, is described. The assay is used, in conjunction with tests of biological activity, to predict oxidation conditions that will result in a maximum of active protein coupled to a hydrazide chromatographic support. Glycoproteins are labeled with Lucifer Yellow CH or Texas Red Hydrazide, and the extent of labeling is determined. Using the assay, it is shown that the efficiency of coupling to Affi-Prep Hydrazide is proportional to oxidation.

INTRODUCTION

Recently, several workers have reported the use of hydrazide-derivitized supports in the preparation of affinity chromatographic columns, where the coupled ligand is a glycoprotein (usually an antibody) [1–5] (for a recent review, see ref. 6). As these workers report, the primary attraction of the method is that the ligands are "oriented", with their active sites directed into solution, rather than randomly, as is the case in amine-directed coupling chemistries. Typically, the ligand is oxidized briefly under mild conditions with sodium periodate, to generate aldehydes from vicinal diols present on the saccharide units. The product is then made to react with the hydrazide functionalities present on the support, forming stable hydrazone linkages. The oxidation reaction is generally done "blind", that is, without analysis of the extent of oxidation in the product.

In our hands, the oxidation reaction has generally been reliable, yielding oxidized glycoproteins which couple to the support and produce affinity columns that behave as expected. Occasionally, however, a column exhibits a low coupling capacity. Under these circumstances, it has been difficult to determine whether this problem was the result of inadequate oxidation or an incomplete coupling reaction. Further, the optimum oxidation conditions for a new glycoprotein must be determined by trial and error, a process which can be expensive in terms of both time and material.

0021-9673/91/$03.50

An analysis of the extent of oxidation of the glycoprotein prior to coupling would overcome these problems. Avigad [7] reported a method based on analysis of formaldehyde released in the reaction, but it has the problems inherent in any indirect assay. Blotting techniques [8,9] have also been reported; however, they are cumbersome and are only semi-quantitative. O'Shannessy and Quarles [10] reported the use of immunoglobins labeled with fluorescent dyes in the direct immunofluorescence of cells. We report here the adaptation of this procedure to a simple, rapid, quantitative method for the determination of the extent of oxidation of glycoproteins.

EXPERIMENTAL

Reagents and chemicals

Human γ-globulins, horseradish peroxidase, bovine serum albumin, and [^{14}C]bovine serum albumin were obtained from Sigma (St. Louis, MO, USA). Sheep anti-bovine albumin was obtained from Bethyl Labs. (Montgomery, TX, USA). Immunoglobins were 3–4% carbohydrate; horseradish peroxidase had *ca.* 20% carbohydrate content. Lucifer Yellow CH and Texas Red Hydrazide were obtained from Molecular Probes (Eugene, OR, USA). Affi-Prep Hydrazide, Bio-Spin 6 desalting columns and the TMB peroxidase EIA substrate kit (containing 3,3′,5,5′-tetramethylbenzidine and hydrogen peroxide) were obtained from Bio-Rad Labs. (Richmond, CA, USA). Other chemicals were obtained from commercial sources and were of analytical-reagent grade or better.

Oxidation of glycoproteins

Proteins were dissolved in, or dialyzed against, acetate buffer (0.02 *M* sodium acetate–0.15 *M* NaCl, pH 5.0 adjusted with glacial acetic acid). Protein concentrations varied from 3.8 to 10 mg/ml, and are given in the figure legends. To begin the oxidation reaction, 40 μl of 0.25 *M* sodium periodate in water were added per 1 ml of sample solution. After incubation for various times in the dark at room temperature, the reaction was quenched by adding 56 μl/ml of ethylene glycol and incubating for $\geqslant 15$ min. The reaction by-products were then removed and the protein was exchanged into fresh acetate buffer, either by passage over a 10DG desalting column (Bio-Rad Labs.) or dialysis (Spectrapore 2, Spectrum Medical), and used immediately or stored at 4°C until used (generally no longer than overnight). Oxidized proteins are designated o-IgG (oxidized human γ-globulins), o-αBSA (oxidized sheep anti-bovine albumin) and o-HRP (oxidized horseradish peroxidase).

Dye labeling of oxidized immunoglobins

A mixture of 10 μl of Lucifer Yellow solution (5 mg/ml of Lucifer Yellow CH in acetate buffer) and 100 μl of oxidized protein solution was incubated for 2 h at room temperature. To solubilize any precipitate, 10 μl of 1 *M* Tris (pH 8.0) were added. To remove the excess dye, a 75–100-μl aliquot was then desalted by centrifugation with a Bio-Spin 6 column (0.3 ml gel volume) equilibrated in 0.1 *M* Tris–0.15 *M* NaCl (pH 8.0 adjusted with HCl). The Bio-Spin column is designed for rapidly desalting 50–100-μl samples in a table-top centrifuge. The eluate was diluted to 0.5–1 ml, as required. Absorbances at 428 and 280 nm were measured with a Perkin-Elmer Lambda 3 dual-beam spectrophotometer, and the extent of labeling was calculated as the ratio of dye (determined by the absorbance at 428 nm) to protein (determined by the absorbance at 280 nm, after subtracting the absorbance at 280 nm due to dye).

Dye labeling of oxidized HRP

To 100 μl of o-HRP solution, exchanged into coupling buffer (0.2 *M* sodium acetate–0.5 *M* sodium sulfate, pH 4.5 adjusted with glacial acetic acid) by passage over a Bio-Spin 6 column, 10 μl of Texas Red Hydrazide solution (6 mg/ml Texas Red Hydrazide in pyridine) were added. The reaction was incubated for 2 h at room temperature. A 100-μl aliquot was then passed over a Bio-Spin 6 column, diluted, and absorbances were measured at 403 and 590 nm. The extent of labeling was calculated as the ratio of dye (determined by the absorbance at 590 nm) to protein (determined by the absorbance at 403 nm).

Coupling of oxidized proteins to Affi-Prep Hydrazide

Approximately 0.5–3.0 ml of Affi-Prep Hydrazide was equilibrated with coupling buffer. The volume of settled gel was determined, and an equal volume of coupling buffer was added to prepare a 50% slurry. To begin the coupling reaction, two volumes

of coupling buffer and one volume of oxidized protein solution (o-IgG or o-HRP) were added to one volume of the slurry.

Alternatively, the gel was equilibrated in 1 *M* sodium sulfate–0.1 *M* sodium acetate (pH 4.5), a 50% slurry prepared and an equal volume of oxidized immunoglobin solution (o-αBSA) added.

In either instance, the mixture was gently mixed overnight at 4°C. The mixture was then transferred to a Poly-Prep column (Bio-Rad Labs.) and washed with 3–5 bed volumes of 0.1 *M* Tris (pH 8.0). The concentration of protein in the eluate was determined by measuring the absorbance at 280 nm (403 nm for o-HRP), and the amount of coupled protein was determined by difference.

Assay of sheep anti-bovine albumin activity

Microtiter plates were incubated with 50 μl per well of BSA solution (1 μg/ml bovine albumin in 0.1 *M* sodium carbonate, pH 8.8) overnight at 4°C. Then 200 μl of blocking solution [1 mg/ml of ovalbumin (Calbiochem) in PTT buffer (10 m*M* sodium phosphate–0.15 *M* sodium chloride–0.05% Tween 20–0.01% thimersol, pH 7.4)] were added for 60 min at room temperature. The wells were then emptied and rinsed twice with 200 μl of PTT buffer.

The protein solution to be assayed was diluted in PTT buffer containing 0.01 mg/ml of ovalbumin and 100-μl aliquots were placed in duplicate wells. The plates were incubated for 60–120 min at room temperature. The wells were then emptied, rinsed three times with 100 μl of PTT and blotted dry.

Rabbit anti-sheep IgG–HRP conjugate (Bio-Rad Labs.) was diluted 800–1600-fold in PTT containing 0.01 mg/ml ovalbumin and 100 μl of the resulting solution were added to each well. The plates were then incubated for 60 min at room temperature, washed three times with PTT buffer and blotted dry. A 100-μl aliquot of TMB peroxidase EIA substrate was added and incubated for 5–15 min. Finally, 100 μl of 0.5 *M* H_2SO_4 were added to stop the reaction. The wells were read at 450 nm with a Bio-Rad Model 3550 microplate reader.

Assay of sheep anti-bovine albumin activity on Affi-Prep Hydrazide

[^{14}C]Bovine serum albumin was diluted *ca.* 50-fold with unlabeled bovine albumin in PBN buffer (10 m*M* sodium phosphate–0.5 *M* sodium chloride, pH 7.0) to give a 2.0 mg/ml solution with a specific activity of 79 000 cpm/nmol. Samples of Affi-Prep Hydrazide to which o-αBSA had been coupled were suspended in an equal volume of PBN buffer, and 50-μl aliquots were incubated with 100 μl of BSA solution (1.70 nmol BSA; $1.3 \cdot 10^5$ cpm) for 5 h at room temperature. The samples were then washed twice with 4.0 ml of PBN buffer. The samples were suspended in 10 ml of scintillation cocktail and the bound radioactivity was counted.

Assay of horseradish peroxidase activity

Samples were diluted to $2 \cdot 10^{-6}$, $1 \cdot 10^{-6}$ and $5 \cdot 10^{-7}$ of the initial concentration with acetate buffer. Volumes of 20 μl of the resulting solutions were placed in microtiter plate wells and 180 μl of TMB peroxidase EIA substrate were added. Absorbances were read at 655 nm, with data collection beginning when the absorbance of the $1 \cdot 10^{-6}$ dilution of the unoxidized sample reached 0.25. Five data points were then taken at 5-min intervals. Activity was calculated as the slope of the absorbance *vs.* time plot and averaged for the three dilutions.

RESULTS AND DISCUSSION

Our primary intent was to develop an assay that would predict coupling of a sample of oxidized protein to a hydrazide support without consuming a great deal of time and material. Our initial efforts focused on the use of Texas Red Hydrazide as a label, owing to its relatively high molar absorption coefficient (8×10^4 at 580 nm), and because it contains a hydrazide functionality which would mimic the coupling chemistry of Affi-Prep Hydrazide. However, it is only slightly soluble in water, and causes precipitation problems when coupled to immunoglobins (data not shown). Although Lucifer Yellow CH's molar absorption coefficient is lower by a factor of 6.7, it is soluble in water, and causes only slight precipitates in highly oxidized immunoglobin samples; these can be resolubilized by increasing the pH of the solution. For horseradish peroxidase, however, Texas Red Hydrazide was retained as the label of choice, as the protein absorbs in the same region of the visible spectrum as Lucifer Yellow CH and precipitation was not a problem.

In addition to its visible (428 nm) absorbance, Lucifer Yellow CH also has an absorption band at

280 nm, the wavelength used to determine protein concentration. To correct for this, it was therefore necessary to determine the relative absorbance at 280 nm of the dye coupled to IgG. Four samples of o-IgG, oxidized for various times, were labeled and assayed with the Bradford protein assay [11] (Bio-Rad Labs.), and UV–VIS spectra were obtained (data not shown). The molar absorption coefficient at 280 nm for the protein was determined for unlabeled samples and used to determine the absorbance at 280 nm due to protein. The ratio of excess absorbance at 280 nm (due to dye) to the absorbance at 428 nm was 2.5 $\pm$ 0.1. This factor was used in subsequent experiments to correct for dye absorbance at 280 nm.

To determine the length of time required for the labeling reaction, aliquots of a single preparation of o-IgG were incubated for various times with Lucifer Yellow CH solution and the extent of labeling was determined as described above. The reaction with dye is essentially complete after 1.5–2 h (data not shown).

The primary applications of the assay are to readily optimize oxidation conditions for immunoglobin molecules, and, once optimized, insure that subsequent oxidations are reproducible. This requires that the extent of dye labeling is a reliable predictor of coupling efficiency. Also, retention of biological activity is a major consideration in the optimization of oxidation conditions. One wishes to maximize the coupling of the protein while minimizing the loss of activity due to destruction of labile amino acid residues. Although these residues, primarily aromatic and sulfur-containing amino acids, react slowly with periodate [12], they often are critical for activity.

To determine whether the assay fulfils these requirements, a series of oxidation, dyelabeling, and coupling experiments were performed on human γ-globulins, sheep anti-BSA, rabbit anti-bovine IgG and horseradish peroxidase. The glycoproteins were oxidized with sodium periodate for various lengths of time and then assayed for dye labeling and for coupling to Affi-Prep Hydrazide. In some instances the biological activity of the oxidized glycoprotein was measured before and after coupling to the solid support.

The correlation between Lucifer Yellow labeling and coupling to Affi-Prep Hydrazide for human IgG, oxidized for varying lengths of time, is shown in Fig. 1. With increasing oxidation and generation of aldehydes, there is a very close parallel between the dye labeling and coupling to the support.

The effect of oxidation time on dye labeling, coupling and biological activity of o-αBSA is shown in Fig. 2. Biological activity was evaluated in solution (before coupling) by ELISA, and after coupling using ^{14}C-labeled BSA. In Fig. 2a, the extent of dye labeling is compared with the extent of coupling to the gel; the correlation is very close. Fig. 2b presents biological activity data; a steady decrease in the activity of the samples before coupling is observed. The net effect of this loss of biological activity, combined with increasing coupling, is that the two nearly cancel. The predicted activity on the support, calculated as the product of the fractional coupling efficiency and the fractional BSA binding activity, is nearly constant after 15 min of oxidation. The activity actually observed on the support is slightly lower than predicted, particularly at the 15- and 30-min time points, but the prediction that the coupled activity does not decrease is borne out.

A similar experiment was conducted with rabbit anti-bovine IgG (o-αbIgG in Fig. 3); in this instance, however, the activity on the support peaked at 60

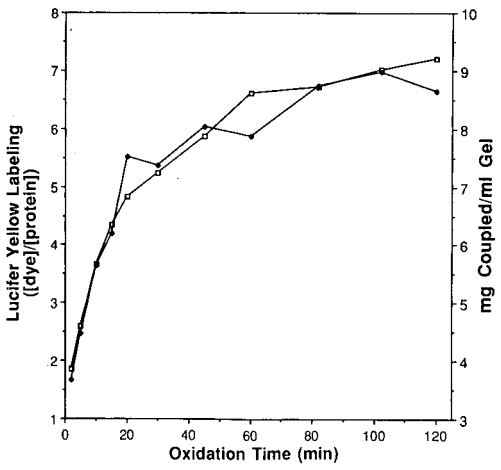

Fig. 1. Time course of oxidation of human γ-globulins. Human γ-globulins (10 mg/ml) were oxidized for various times and aliquots were labeled with Lucifer Yellow CH or coupled to Affi-Prep Hydrazide. The extent of labeling (□) and the amount of coupled o-IgG (◆) were determined for each time point.

min and declined thereafter (data not shown).

To determine if Lucifer Yellow CH labeling is a predictor of coupling to a hydrazide chromatographic support, the extent of protein oxidation was compared with the efficiency of coupling to a hydrazide support for a number of immunoglobins. Coupling is linearly correlated ($r^2 = 0.91$, using data from four experiments) with the number of dye molecules bound (Fig. 3). As different proteins have various numbers of carbohydrate moieties available, and couple to the support with various efficiencies, the values reported are relative to the respective maxima. The high correlation between relative oxidation and coupling is both gratifying and surprising, as the presumed mechanism of coupling requires only one aldehyde per molecule [13]. The assay, however, clearly gives a rapid indication of the relative amount of protein that one can expect to attach to the hydrazide support.

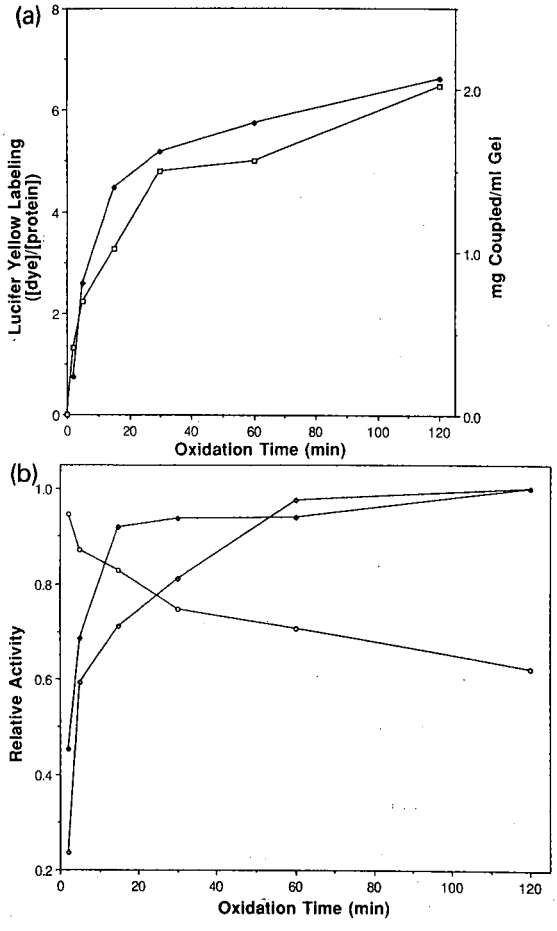

Fig. 2. Time course of oxidation of sheep anti-bovine albumin. (a) Sheep anti-bovine albumin (3.8 mg/ml) was oxidized for various times and aliquots were labeled with Lucifer Yellow CH or coupled to Affi-Prep Hydrazide. The extent of labeling (□) and the amount of coupled o-IgG (◆) were determined for each time point. (b) Activity of o-αBSA samples [(○) before and (◇) after coupling to Affi-Prep Hydrazide] were determined as described and normalized to the highest value (unoxidized material in the case of bulk). The predicted coupled activity (◆) was calculated as the product of the relative activity and the amount of protein coupled to the support.

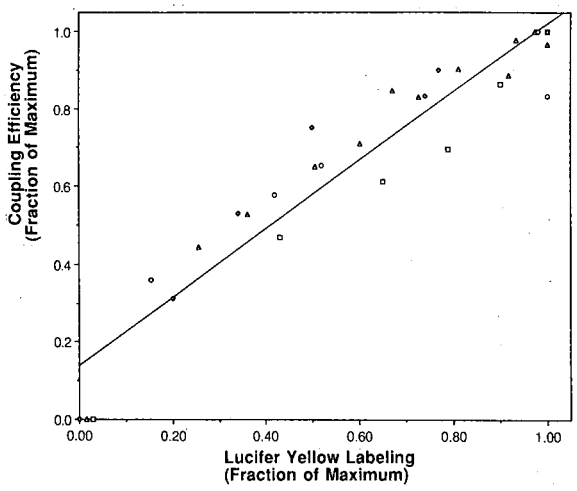

Fig. 3. Comparison of relative coupling efficiency and Lucifer Yellow labeling. Lucifer Yellow labeling and Affi-Prep Hydrazide coupling data from four immunoglobin oxidation time-course experiments were normalized, and a linear regression analysis performed on the resulting data. □, △ = o-IgG; ◇ = o-αBSA; ○ = o-αbIgG. $y = 0.13725 + 0.87945x$; $r^2 = 0.906$.

The assay is also useful for non-immunoglobin proteins; results for o-HRP are shown in Fig. 4. In this instance, the protein couples with high efficiency at relatively short oxidation times (86% of the input protein is coupled after only a 6.5-min oxidation time); the activity loss incurred from further oxidation therefore cannot be made up by increasing coupling, and the predicted and observed activities on the support agree well.

CONCLUSIONS

A simple assay, using hydrazide dyes to determine rapidly the extent of oxidation of glycoproteins, has been described. The results correlate well with the

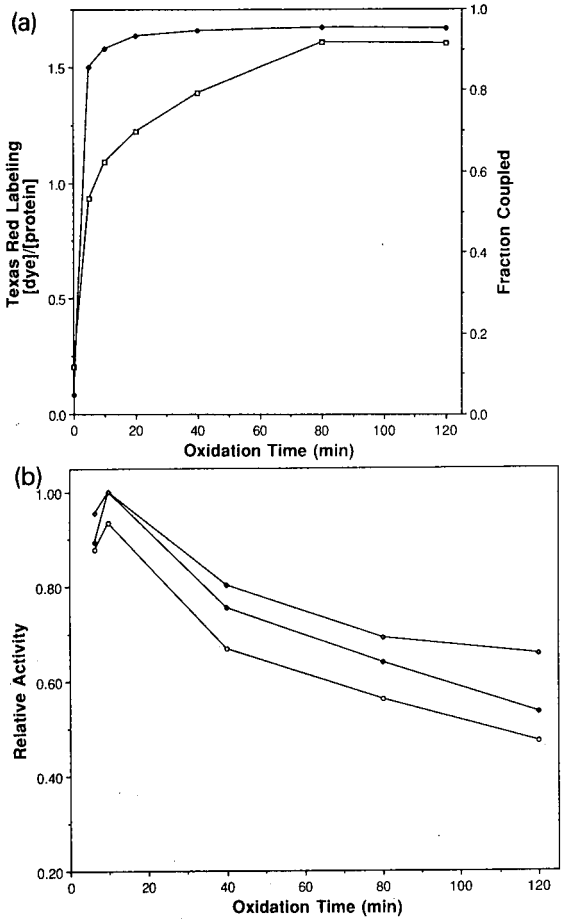

Fig. 4. Time course of oxidation of horseradish peroxidase. (a) Horseradish peroxidase (10 mg/ml) was oxidized for various times and aliquots were labeled with Texas Red Hydrazide or coupled to Affi-Prep Hydrazide. The extent of labeling (□) and the amount of coupled o-HRP (◆) were determined for each time point. (b) Activity of o-HRP samples [(○) before and (◇) after coupling to Affi-Prep Hydrazide] were determined as described and normalized to the highest value (unoxidized material in the case of bulk). The predicted coupled activity (◆) was calculated as the product of the relative activity and the amount of protein coupled to the support.

amount of protein coupled to a hydrazide chromatographic support.

Most important, the assay provides a convenient method of predicting the relative amount of protein that will couple to a hydrazide support under a given oxidation protocol. When combined with bioassay data, it can therefore be used to determine the optimum oxidation conditions, which will maximize the amount of biological activity on the column.

The assay simply involves the addition of a dye reagent to a small aliquot of the protein solution for a short period of time, rapid removal of the unbound dye with a Bio-Spin 6 column and reading the absorbance of the dyed protein. If the experimenter desires only a qualitative indication of the success of the oxidation reaction, the presence or absence of color in the Bio-Spin column eluate gives a simple yes/no answer.

ACKNOWLEDGEMENTS

The authors thank the staff of the Bio-Rad Quality Control Laboratory, where much of this work was done, for their kind hospitality in the aftermath of the October 17th, 1989, earthquake. We also thank Dr. Peter Schad for stimulating discussions and Dr. John Barich for a critical review of the manuscript.

REFERENCES

1 D. J. O'Shannessy and W. L. Hoffman, *Biotechnol. Appl. Biochem.*, 9 (1987) 488–496.
2 W. L. Hoffman and D. J. O'Shannessy, *J. Immunol. Methods*, 112 (1988) 113–120.
3 R. S. Matson and M. C. Little, *J. Chromatogr.*, 458 (1988) 67–77.
4 V. S. Prisyazhnoy, M. Fusek and Y. B. Alakhov, *J. Chromatogr.*, 424 (1988) 243–253.
5 M. C. Little, C. J. Siebert and R. S. Matson, *BioChromatography*, 3 (1988) 156–159.
6 D. J. O'Shannessy and M. Wilchek, *Anal. Biochem.*, 191 (1990) 1–8.
7 G. Avigad, *Anal. Biochem.*, 134 (1983) 499–503.
8 J. M. Gershoni, E. A. Bayer and M. Wilchek, *Anal. Biochem.*, 146 (1985) 59–63.
9 D. J. O'Shannessy, P. J. Voorstad and R. H. Quarles, *Anal. Biochem.*, 163 (1987) 204–209.
10 D. J. O'Shannessy and R. H. Quarles, *J. Appl. Biochem.*, 7 (1985) 347–355.
11 M. Bradford, *Anal. Biochem.*, 72 (1976) 248–254.
12 W. A. Krotoski and H. E. Weimer, *Arch. Biochem. Biophys.*, 115 (1966) 337–344.
13 D. J. O'Shannessy and R. H. Quarles, *J. Immunol. Methods*, 99 (1987) 153–161.

Journal of Chromatography, 587 (1991) 177–183
Elsevier Science Publishers B.V., Amsterdam

CHROM. 23 565

Recovery of sugar derivatives from 2-aminopyridine labeling mixtures for high-performance liquid chromatography using UV or fluorescence detection

Niels O. Maness☆, Edgar T. Miranda and Andrew J. Mort*

Department of Biochemistry, Oklahoma Agricultural Experiment Station, Oklahoma State University, Stillwater, OK 74078-0454 (USA)

(First received October 31st, 1990; revised manuscript received May 16th, 1991)

ABSTRACT

Labeling of reducing oligosaccharides with 2-aminopyridine by direct condensation to form a glycosylamine or by reductive amination to form a secondary amine has been used to allow the sensitive detection of oligosaccharides using both UV and fluorescence detection. For efficient labeling, a large excess of 2-aminopyridine is necessary in the derivatization mixture. The non-bound 2-aminopyridine absorbs and fluoresces near the wavelengths of the adducts and may obscure sample components. It must therefore be removed before the derivatives can be used for some chromatographic methods. It has been found that small cation-exchange columns (Extract-Clean columns from Alltech), if converted to the NH_4^+ form, bind free 2-aminopyridine but not labeled acidic oligosaccharides or neutral oligosaccharides of more than four residues. Thus, labeled oligomers can be obtained free enough of unbound 2-aminopyridine for fluorescence detection, by simple solid-phase extraction. As the 2-aminopyridine glycosylamine of oligosaccharides, and of galacturonic acid oligomers in particular, were found to be unstable, conditions for stable storage are presented. The conditions for complete hydrolysis of the 2-aminopyridine label from the glycosylamine are also presented if recovery of the native oligosaccharide after chromatographic purification is desired.

INTRODUCTION

Precolumn derivatization of reducing carbohydrates with 2-aminopyridine by direct condensation to form a glycosylamine or by reductive amination to form a secondary amine has allowed their rapid, reproducible and sensitive detection by high-performance liquid chromatography [1–3] and more recently by capillary zone electrophoresis [4]. The derivatives have also been used for the determination of oligosaccharide sequences [5–7]. For efficient labeling a large excess of 2-aminopyridine in the derivatization mixture is necessary. The non-bound 2-aminopyridine absorbs and fluoresces near the wavelengths of the adducts and may obscure sample components. We reported previously that precolumn derivatization of galacturonic acid oligomers by condensation reaction with 2-aminopyridine, and direct injection of an aliquot of the reaction mixture into a high-performance liquid chromatographic (HPLC) system, provides a method to determine oligogalacturonides differing in degree of polymerization [8]. Using UV detection, tailing of the 2-aminopyridine peak obscured the monomer and dimer of galacturonic acid, which eluted during the first 10–15 min of the chromatogram. We have since attempted to apply the technique using more sensitive fluorescence detection and found that interference from the 2-aminopyridine reagent front prevented detection of any labeled oligosaccharides. Additionally, 2-aminopyridine reagent is retained

☆ Present address: Department of Horticulture and Landscape Architecture, Oklahoma Agricultural Experiment Station, Oklahoma State University, Stillwater, OK 74078, USA.

0021-9673/91/$03.50

on some pellicular anion-exchange resin-based columns (PA-1; Dionex, Sunnyvale, CA, USA) and may co-elute with sample components.

In previous studies, a combination of ion-exchange and size-exclusion chromatography was used for the recovery of labeled sugars from 2-aminopyridine derivatization mixtures [9,10]. We report here that small cation-exchange columns (Extract-Clean columns from Alltech), if converted to the NH_4^+ form, bind free 2-aminopyridine but not labeled acidic oligosaccharides or neutral oligosaccharides of more than four sugar residues. Utilization of the procedure for both sample clean-up prior to chromatography and for removal of the 2-aminopyridine label following hydrolysis from glycosylamine adducts is discussed. Use of the procedure to recover the secondary sugar amines produced during reductive amination is also presented.

EXPERIMENTAL

Reagents and oligosaccharide standards

Pectic acid, sodium cyanoborohydride, 2-aminopyridine and curcumin were from Aldrich (Milwaukee, WI, USA) and lactose, maltotriose, maltotetraose, maltopentaose, maltohexaose, maltoheptaose, galacturonic acid and trigalacturonic acid from Sigma (St. Louis, MO, USA). Oligogalacturonides were prepared by autoclave hydrolysis of pectic acid as described by Robertsen [11]. The pH 2.0 supernatant was adjusted to 30 m*M* sodium acetate buffer (pH 5.2) and applied to a column of DEAE-Sephadex A-25 (90 mm × 50 mm I.D.) previously equilibrated using the same buffer. Oligogalacturonides were then eluted using stepwise increasing concentrations of potassium chloride in the same buffer. The fraction eluted with 375 m*M* potassium chloride (following a 350 m*M* potassium chloride elution), predominantly containing oligogalacturonides ranging from 8 to 16 sugar residues in length (determined as in ref. 8), was used. Purified tetra-, penta- and hexagalacturonic acid standards were prepared from an autoclave hydrolysate of pectic acid as described previously [12]. All other reagents were of analytical-reagent grade.

Preparation of oligosaccharide derivatives

Samples (10 μg–1 mg) were weighed on a Cahn 29 electrobalance and placed in 1-dram screw-capped vials or 1-ml Reacti-Vials (Pierce, Rockford, IL, USA). They were then derivatized by condensation reaction or by reductive amination with 2-aminopyridine. For condensation reaction, samples were dissolved in aqueous 2-aminopyridine labeling reagent (a minimum of 50 μl per mg sugar; prepared by dissolving 1 g of 2-aminopyridine in *ca.* 1 ml of water and adjusting the pH to 7.0 with glacial acetic acid, final volume 2.4 ml), sealed securely with Teflon-lined caps and incubated at 70°C overnight. For reductive amination, sodium cyanoborohydride was added to the 2-aminopyridine labeling reagent (1 mg per 50 μl) just prior to addition to samples, and reaction mixtures were incubated at 70°C overnight.

Solid-phase extraction of 2-aminopyridine from reaction mixtures

Cation-exchange Extract-Clean columns (100- and 500-mg packing sizes; exchange capacity 2–3 mequiv./g) were obtained from Alltech (Deerfield, IL, USA). Columns were converted to the ammonium form using concentrated ammonia solution (5 ml for 100-mg columns, 20 ml for 500-mg columns) and then rinsed with water (to pH 5–6) before the sample was applied. Aliquots of the 2-aminopyridine reaction mixtures (20 μl for 100-mg columns; 100 μl for 500-mg columns) were diluted 20-fold with 0.44 *M* acetic acid (final pH 4–5), applied to an Extract-Clean column and eluted with water. For evaluation of the percentage of adsorbed 2-aminopyridine, columns were eluted with 1 *M* sodim acetate buffer (pH 5.2) following the water elution. Appropriately sized aliquots were taken for sugar, 2-aminopyridine and borate assays. Columns were subsequently converted back to the ammonium form for re-use as described above.

Hydrolysis of 2-aminopyridine from glycosylamine derivatives

Glycosylamine derivatives were incubated in 100 m*M* acetic acid (200 μl per 0.1 mg of sugar) at 80°C for 1–23 h. Before cooling, the samples were diluted with 10% (v/v) acetic acid (100 ml per 0.1 mg of sugar) and applied to an Extract-Clean column. Sugars were eluted with two more volumes of water and then dried *in vacuo* at 40°C.

High-performance liquid chromatography

Liquid chromatographic separations were per-

formed using a Beckman (San Ramon, CA, USA) Model 334 gradient liquid chromatograph. The system consisted of a Model 421A system controller, two Model 110B high-pressure pumps, a Model 210A sample injector, a Model 163 variable-wavelength detector, a Model RF-535 variable excitation and emission wavelength fluorescence detector (Shimadzu, Kyoto, Japan) and a pulsed amperometric detector (PAD; Dionex) with a gold working electrode. Labeled sugars were detected by UV absorbance at 290 nm and by fluorescence with an excitation wavelength of 285 nm and an emission wavelength of 365 nm. Both labeled and non-labeled sugars were detected with PAD. Post-column delivery of 1 *M* sodium hydroxide solution through the PAD cell (total flow-rate 1.6 ml/min) was accomplished using a Dionex DQP-1 pump. The triple pulse sequence used for amperometric detection included the following potentials and durations: $E_1 = +0.05$ V ($t_1 = 480$ ms), $E_2 = +0.60$ V ($t_2 = 120$ ms) and $E_3 = -0.60$ V ($t_3 = 60$ ms). The integration sampling period was set at 200 ms and the response time at 3 s. Chromatographic data were integrated using an Apple IIe computer with chromatographic software. Eluents were prepared from analytical-reagent grade reagents and were filtered and degassed prior to use.

Gradient separations of sugars were conducted using either a CarboPac PA1 pellicular anion-exchange resin-based column (250 mm × 4 mm I.D.) with a CarboPac PA1 precolumn (Dionex) or a TSK DEAE 2SW anion-exchange silica-based column (250 mm × 4.6 mm I.D.) (Supelco, Bellefonte, PA, USA) at a flow-rate of 1 ml/min. Separations involving the TSK DEAE 2SW column were conducted as described previously [8]. Separations involving the CarboPac PA1 column were conducted as follows. Eluent A was water and eluent B was 1 *M* sodium acetate (pH 5.2). Elution of short oligogalacturonides [degree of polymerization (DP) 1–4] and of neutral maltose oligomers was accomplished using a linear gradient from 20 to 200 m*M* acetate in 25 min. Oligogalacturonides ranging from DP 5 to 10 were eluted using a linear gradient from 200 to 600 m*M* acetate over the same time period. Longer oligogalacturonides (DP 10–17) were separated using a linear gradient from 400 to 700 m*M* acetate in 30 min. The initial buffer concentration was maintained for 2 min following injection and prior to the start of the gradient. The final gradient conditions were maintained for 5 min and then the column was washed with 850 m*M* acetate for 15 min. The initial gradient conditions were then maintained for at least 12 min prior to injection of subsequent samples.

Other procedures

Sugar contents of fractions taken from Extract-Clean columns were determined using the phenol–sulphuric acid assay [13]. All assay volumes were half those given in ref. 13. Results were compared with calibration graphs prepared from corresponding sugar standards. The 2-aminopyridine contents of fractions were determined by measuring the UV absorbance at 290 nm. Aliquots of fractions were diluted appropriately and then brought to 1 ml in 200 m*M* sodium acetate (pH 5.2) for spectrophotometric analyses. Results were quantified using a molar absorption coefficient of $11.4 \cdot 10^3$ l mol^{-1} cm^{-1} for 2-aminopyridine. Borate content of appropriately sized aliquots from Extract-Clean fractions was determined spectrophotometrically using the curcumin procedure [14] with boric acid as standard. Assay mixture volumes were one tenth those given in ref. 14 and were conducted in 1.5-ml plastic microcentrifuge tubes.

RESULTS AND DISCUSSION

Various parameters were tested to assess the effectiveness and convenience of Extract-Clean columns for recovering labeled oligomers from derivatization mixtures. We attempted to devise a protocol that would enable us to remove the maximum proportion of unreacted 2-aminopyridine from the derivatization mixture of a wide range of oligosaccharides, but keep the concentration of the labeled sugars as high as possible. We also wanted to avoid having to test column eluates to locate the desired sugars. Our aim was to be able to derivatize samples of as small as a few picomoles, pass the entire reaction mixture through the column, know where the desired oligomers would elute and then be able to use the entire purified sample for chromatography using fluorescence detection.

Elution behavior of labeled sugars

In initial experiments, 20-μl aliquots of the reac-

tion mixture were loaded onto 100-mg Extract-Clean columns whose only pretreatment had been extensive washing with water to remove any breakdown products of the beads. In this form (H^+), 2-aminopyridine-labeled neutral oligomers, short labeled acidic oligomers and free 2-aminopyridine all bound to the column. As 2-aminopyridine and labeled sugars have different pK_a values, we next tried to adjust the pH of the eluent to obtain differential adsorption. With the columns in the H^+ form, the eluate acidified during exchange of the 2-aminopyridine for H^+ ions. To avoid this acidification and promote differential adsorption, we converted the columns to the ammonium form. In addition, we substituted acetic acid for hydrochloric acid when adjusting the pH of the 2-aminopyridine derivatizing reagent. Samples were thus eluted from the columns in ammonium acetate, which is volatile, allowing concentration of the sample prior to chromatography, if necessary.

Labeling mixtures (20 μl) were diluted with 0.44 *M* acetic acid to 400 μl, passed through 100-mg Extract-Clean columns and rinsed with four 400-μl aliquots of water. Bound components were subsequently eluted with 1 *M* sodium acetate buffer (pH 5.2). Each 400 μl of eluate was tested for the presence of sugar, 2-aminopyridine (bound + free) and borate. Borate is formed in the reductive amination reaction by breakdown of the cyanoborohydride.

Fig. 1A shows the elution behavior of a series of malto-oligomers linked non-reductively to 2-aminopyridine. Oligomers containing five or more sugar residues gave satisfactory recoveries (85% or more), whereas shorter oligomers adsorbed more firmly to the column. By analogy with the behavior (late elution) of aromatic amino acids on polystyrene-based cation-exchange columns, we expect that 2-aminopyridine interacts with the Extract-Clean column matrix by a hydrophobic effect as well as by an ionic effect with the sulphonate ion-exchange groups. We suspect that the hydrophobic interaction with the 2-aminopyridine label is weakened by the hydrophilic nature of sugars. For the neutral sugar oligomers with more than four sugars, their hydrophilicity overcomes the adsorptive interaction of the 2-aminopyridine label with the column matrix. The labeled oligogalacturonides did not bind to the columns under these conditions (Fig. 1B). Sugar recoveries for the secondary amine derivatives were

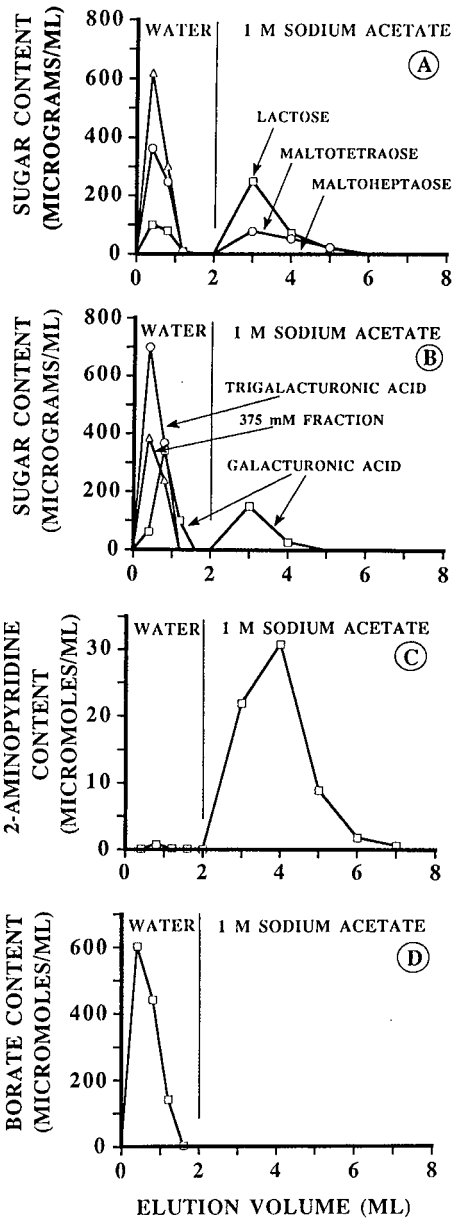

Fig. 1. Passage of various (A) neutral and (B) charged oligosaccharides, (C) 2-aminopyridine and (D) borate through Extract-Clean columns. Samples for A, B and C were prepared by non-reductive amination and sample for D was prepared by reductive amination. Sugar derivatives (20 μl) were diluted 20-fold with 0.44 *M* acetic acid, applied to 100-mg columns and eluted with 2 ml of water. Bound sample components were then eluted with 5 ml of 1 *M* sodium acetate buffer (pH 5.2). Fractions were analyzed for sugar, 2-aminopyridine and borate contents as described under Experimental.

generally lower than those for the corresponding glycosylamine derivatives. Almost all of the non-bound sugar eluted in the first 1.2 ml of eluate. Fig. 1C illustrates that essentially all of the 2-aminopyridine adsorbed to the column (at least 99%). However, none of the borate bound (Fig. 1D). As borate can interfere with chromatography by forming complexes with sugars, it may be necessary to remove borate by some other means. At least 70% of the borate can be removed by repeated evaporation with acidified methanol [15].

Degree of labeling of oligosaccharides with 2-aminopyridine

As non-labeled sugars would pass through the Extract-Clean columns without binding and thereby cause overestimation of the relative proportion of 2-aminopyridine-labeled sugar washing through the columns, we checked to see what proportion of the oligomers became labeled during the labeling reaction.

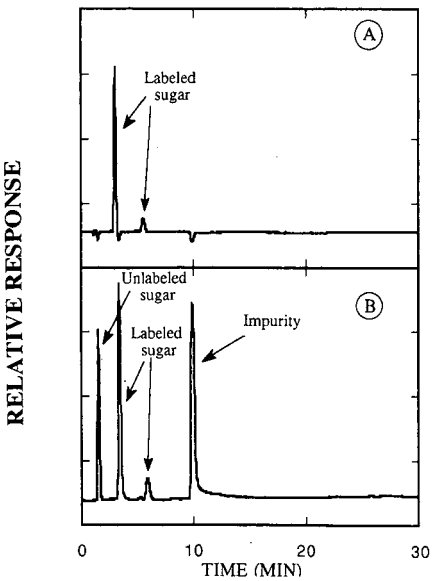

Fig. 2. Anion-exchange HPLC of labeled maltopentaose. Maltopentaose was derivatized by condensation, purified from the derivatization mixture with an Extract-Clean column and an aliquot (containing 9–10 nmol of oligosaccharide) was injected directly onto a Dionex PA-1 column (250 mm × 4 mm I.D.). The column effluent was monitored first (A) by UV absorbance at 290 nm and then (B) by pulsed amperometric detection. Non-labeled sugar eluted at about 2 min and labeled sugar at 3.5 and 6 min.

Non-reductively labeled maltopentaose was separated from the excess of 2-aminopyridine using Extract-Clean columns and aliquots were injected onto a PA-1 ion-exchange column. The effluent from the column passed first through a UV detector for detection of 2-aminopyridine and then through a pulsed amperometric electrochemical cell for detection of sugars. Fig. 2 shows the elution of labeled sugar in the UV trace (A) and the same plus non-labeled sugar in the electrochemical trace (B). By injection of the 2-aminopyridine reaction mixture alone, a peak eluting at 23 min was shown to be 2-aminopyridine. As the non-bound 2-aminopyridine was removed from the sample in Fig. 2 using an Extract-Clean column prior to injection, no free 2-aminopyridine peak was observed. The late elution of 2-aminopyridine from the polystyrene-based anion-exchange column supports our suggestion that 2-aminopyridine adsorbs to the Extract-Clean columns by more than just an ion-exchange interaction. Assuming a similar molar absorption coefficient for free and bound 2-aminopyridine and from a large number of independent injections, we can estimate that >95% of the 2-aminopyridine coming through the Extract-Clean column is bound to sugar. From the electrochemical trace (assuming that the molar responses are similar for labeled and non-labeled sugar), the peak area associated with the 2-aminopyridine sugar adduct represents 70–75% of the total peak area. We suspect that the actual proportion of sugar adduct to free sugar is greater than the 70–75% of peak area indicated. Preliminary evidence indicates that the 2-aminopyridine adduct of sugars exhibits a much lower electrochemical response than free sugars.

While investigating the degree of labeling for glycosylamine derivatives, we noticed that the degree of labeling of the purified oligomers decreased with time. After 1 day at room temperature these derivatives retained only *ca.* 75% of their original label. Hence it appeared that once the excess of 2-aminopyridine was removed, the glycosylamine came apart slowly. We investigated the lability of glycosylamines using maltopentaose and the pentagalacturonide at various pH values. As was pointed out by Her *et al.* [3], reversibility of the labeling could be useful if the oligosaccharide was needed in its original form after chromatography for further chemical characterization or testing of potential

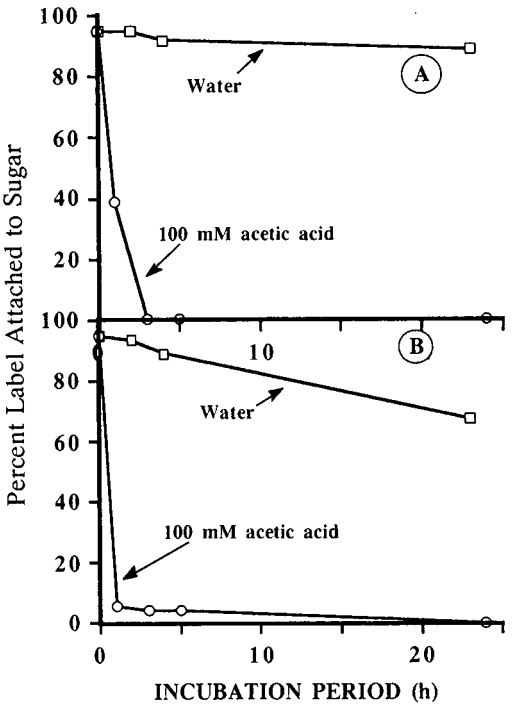

Fig. 3. Time course for hydrolysis of the glycosylamine derivatives of (A) maltopentaose and (B) trigalacturonic acid using 100 m*M* acetic acid at 80°C or water at room temperature. Samples were chromatographed as described in Fig. 2 and detected by UV absorbance at 290 nm. Values represent the percentage of 2-aminopyridine label remaining attached to sugar.

biological activity. Very mild acid hydrolysis was used to remove the 2-aminopyridine from the non-reductively labeled sugars. The time course for loss of label from both neutral and acidic oligomers after standing in the effluent from the Extract-Clean column (*ca.* pH 5) at room temperature, or after heating in 100 m*M* acetic acid at 80°C, is shown in Fig. 3. It is apparent that the neutral sugar glycosylamines are more stable than those of acidic oligomers, but that both types can be hydrolyzed rapidly in 100 m*M* acetic acid at 80°C. In addition to investigating the conditions for removal of the 2-aminopyridine label from glycosylamines, we also evaluated the conditions for retention of the label. After testing various conditions for the stable storage of the derivatives, we found that if the samples are frozen, especially at slightly elevated pH (6–8), they are more stable and should be useful for quantitative analysis.

Examples of the use of 2-aminopyridine-labeled oligosaccharides after elution from Extract-Clean columns

To determine if the method is useful for minute samples, it was applied to the preparation of 100-pmol samples of oligogalacturonides. Samples of pentagalacturonic acid were non-reductively aminated using 10-μl reaction mixtures. After the reaction they were diluted to 200 μl with 0.44 *M* acetic acid and then passed through 100-mg Extract-Clean columns. Only the first 600 μl of effluent were collected and kept in an ice-bath until used. Aliquots of 100 μl were injected onto a TSK DEAE 2SW column, eluted as described previously [8] and monitored with a fluorescence detector. The peak corresponding to free 2-aminopyridine at the elution volume (not retained by this column) was on scale at the same sensitivity setting needed to see the *ca.* 16 pmol of pentagalacturonide, which gave a peak about one quarter of full scale. The signal-to-noise ratio was about 25:1 for the pentagalacturonide.

Larger samples of non-reductively aminated oligogalacturonides and malto-oligomers recovered from Extrsct-Clean columns could be used directly for mass spectrometry after concentration by freeze-drying. However, additional sample clean-up was necessary before the reductively aminated oligomers gave good mass spectra owing to co-elution of borate with labeled sugars. Direct fractionation by reversed-phase chromatography of reductively aminated fragments of xyloglucans after removal of excess of 2-aminopyridine using an Extract-Clean column was possible, and fractions from the effluent were used directly for mass spectral identification [16].

CONCLUSIONS

Cation-exchange Extract-Clean columns in the ammonium form can be used efficiently to remove unreacted 2-aminopyridine from labeled sugars. However, borate co-elutes with the labeled sugars, and neutral oligosaccharides of less than five residues do not elute quantitatively. A sufficient amount of the excess of 2-aminopyridine is removed to allow the use of any kind of chromatography even with high-sensitivity fluorescence detection.

ACKNOWLEDGEMENTS

The authors thank Dr. Jerry Merz for providing chromatographic software and configuring the data acquisition hardware used in this study, Mr. Paul West for running the liquid secondary ion mass spectra, Dr. Bruno Moerschbacher for providing the batch-purified polygalacturonides and Ms. Dung Vu for technical support. The ZAB 2SE mass spectrometer used in the study was partially obtained via NSF grant BSS-8704089. This work was supported by DOE (US Department of Energy) grant No. DE GFD5 ER13496 and the Oklahoma Agricultural Experiment Station, Oklahoma State University. This is paper No. J-5844 of the Oklahoma Agricultural Experiment Station.

REFERENCES

1 S. Hase, T. Ikenaka and Y. Matsushima, *J. Biochem.*, 90 (1981) 407.
2 W. T. Wang, N. C. DeDopnne, B. Ackerman and C. C. Sweeley, *Anal. Biochem.*, 141 (1984) 366.
3 G. R. Her, S. Santikarn, V. N. Reinhold and J. C. Williams, *J. Carbohydr. Chem.*, 6 (1987) 129.
4 S. Honda, S. Iwase, A. Makino and S. Fujiwara, *Anal. Biochem.*, 176 (1989) 72.
5 V. N. Reinhold, E. Coles and S. A. Carr, *J. Carbohydr. Chem.*, 2 (1983) 1.
6 S. Hase and T. Ikenaka, *Anal. Biochem.*, 184 (1990) 135.
7 K. B. Lee, D. Loganathan, Z. M. Merchant and R. J. Linhardt, *Appl. Biochem. Biotechnol.*, 23 (1990) 53.
8 N. O. Maness and A. J. Mort, *Anal. Biochem.*, 178 (1989) 248.
9 N. Tomiya, M. Kurano, H. Ishihara, S. Tejima, S. Endo, Y. Arata and N. Takahashi, *Anal. Biochem.*, 163 (1987) 489.
10 H. Kiyohara and H. Yamada, *Carbohydr. Res.*, 193 (1989) 173.
11 B. Robertsen, *Physiol. Plant Pathol.*, 28 (1986) 137.
12 D. F. Jin and C. A. West, *Plant Physiol.*, 74 (1984) 989.
13 M. Dubois, K. A. Giles, J. K. Hamilton, P. A. Rebers and F. Smith, *Anal. Chem.*, 28 (1956) 350.
14 W. T. Dible, E. Truog and K. C. Berger, *Anal. Chem.*, 26 (1954) 418.
15 W. S. York, A. G. Darvill, M. McNeil, T. T. Stevenson and P. Albersheim, *Methods Enzymol.*, 118 (1986) 3.
16 Z. El Rassi, J. An, D. Tedford and A. Mort, *Carbohydr. Res.*, 215 (1991) 25.

Journal of Chromatography, 587 (1991) 185–191
Elsevier Science Publishers B.V., Amsterdam

CHROM. 23 539

High-performance liquid chromatographic column-switching technique for the determination of intermediates of anaerobic degradation of toluene in ground water microcosm

N. Chamkasem*,☆ and K. D. Hill

NSI Technology Services, P.O. Box 1198, Ada, OK 74820 (USA)

G. W. Sewell

R. S. Kerr Environmental Research Laboratory, US Environmental Protection Agency, Ada, OK 74820 (USA)

(First received December 12th, 1990; revised manuscript received May 23rd, 1991)

ABSTRACT

A reversed-phase liquid chromatographic column-switching system was used for the determination of phenol, benzoic acid and cresol (PBC) in the presence of toluene in ground water microcosm. A precolumn was connected in series with an analytical column via a column-switching valve. After the injection, as soon as PBC were eluted from the precolumn to the analytical column, the valve was switched so that the precolumn was between the analytical column and the UV detector. Toluene and other non-polar compounds were eluted from the precolumn in a very short time and detected along with the solvent front. Subsequently, PBC were separated on the analytical column and passed through the precolumn one more time before being detected by the UV detector. The total analysis time was 15 min. This technique facilitated the study of the basic mechanism and path way of anaerobic degradation of toluene in ground water aquifer.

INTRODUCTION

For high-performance liquid chromatographic (HPLC) analysis, isocratic elution is ineffective to separate compounds having widely disparate partition ratios (k). Gradient elution can provide a solution to this problem [1]. However, the column has to be brought back to its initial state to start reprogramming the solvent. The column-switching technique has been used to shorten the analysis time of complex mixtures without the use of gradient elution [2–4]. It was used with either one- or two-column configuration. Huber *et al.* [5] used column switching with a stop flow technique to determine toluene and the more-polar substituted phenols on a normal phase column. The separation time was reduced from 45 min to 8 min. Rocklin *et al.* [6] used a 4-way double stack slider-type valve with two cation columns to determine mono- and divalent cations in one run without stopping the flow of either column.

Alkylbenzenes are among the most tightly regulated classes of ground water contaminants. Fuel releases, either from leaking underground storage/transport systems or surface spills, are the most common route for alkylbenzenes to enter the subsurface environment. Alkylbenzenes constitute approximately 3 to 18% of petroleum-based fuels.

☆ Present address: California Department of Food and Agriculture, 3292 Meadowview Road, Sacramento, CA 95832, USA.

0021-9673/91/$03.50

The compounds of the so-called BTEX fraction (benzene, toluene, ethylbenzene and xylene) have relatively high solubility and mobility. The degradation of aromatic hydrocarbons has been extensively studied. For the last 10 years, laboratory and field evidences have shown that alkylbenzenes can be biodegraded under the anoxic conditions which are commonly found with fuel-contaminated aquifers [7–9]. As yet, little is known about the path ways used under anaerobic conditions or about the factors which limit or stimulate this activity. In our investigations on the fate of alkylbenzenes in the subsurface, we have used toluene as a model compound for biodegradation studies. It has been shown that phenol, benzoic acid and cresol (PBC) are all possible metabolic intermediates during anaerobic toluene degradation. A method for the determination of these intermediates, in the presence of toluene, is critical for researching the basic mechanisms and pathways involved.

The objective of this study was to develop a rapid HPLC method to determine PBC in ground water microcosms containing toluene. It is important that these compounds are quantified over the life of the experiment in order to identify changes in their concentrations. This will facilitate the study of the reduction process of toluene by anaerobic bacteria.

EXPERIMENTAL

Reagents and chemicals

Toluene, phenol, *m*-cresol and benzoic acid were purchased from Sigma (St. Louis, MO, USA). Analytical-reagent-grade phosphoric acid (H_3PO_4) (Fisher Scientific, Springfield, NJ, USA) was also used. Solvents used for chromatography were obtained as HPLC grade (Fisher Scientific, Fairlawn, NJ, USA). Water was purified in a Super-Q water purification system (Millipore, Bedford, MA, USA).

Reagent solutions

The mobile phase was prepared by mixing 250 ml of acetonitrile, 750 ml of water and 2 ml of H_3PO_4. It was sparged with helium at 10 p.s.i. for 15 min before use. A stock solution containing 500 ppm of phenol, benzoic acid and cresol was prepared in methanol–water (1:1, v/v). Working standard solutions were then prepared at the concentration range of 0.1–50 ppm by diluting the stock solution with water. Standard sulfate solution (1000 ppm) (Banco, Ft. Worth, TX, USA) was used to prepare the working standards range from 10 to 150 ppm.

Sample preparation

Aquifer solids were collected using the aseptic/anaerobic coring procedure as described by Leach *et al.* [10]. Sealed, collected cores were placed in an anaerobic chamber where 50 g of mixed, saturated core material were added aseptically to 160 ml of sterilized serum bottles, filled with 90 ml of a distilled water–sterile spring water (50:50, v/v) mixture (Byrd's Mill Spring-Municipal water supply for the city of Ada, OK, USA, pH 7.4, (total alkalinity 326 $CaCO_3$ equiv.) and amended with ammonium phosphate (10 m*M* ammonium and 5 m*M* phosphate final concentration) and sodium sulfate (1 m*M* final concentration). Reducing conditions were maintained by the addition of sodium sulfide (*ca.* 1 m*M* final concentration). Resazurin (0.0001%, w/v) was added as a redox indicator. Microcosms were inoculated with 10 ml of a toluene-degrading culture enriched from contaminated aquifer material. Microcosms were then spiked with toluene, phenol, cresol and benzoic acid or a mixture of these compounds (20 ppm total concentration), or were unamended. The bottles were sealed with PTFE-faced butyl rubber stoppers and aluminum crimp seals. Microcosms were incubated in an anaerobic chamber at 20°C and protected from light. Controls were constructed as above with the exception that the serum bottles were autoclaved for one hour on two successive days after core addition and before being filled and spiked. The microcosms were repetitively sampled by introduction of a syringe needle down the side of a partially opened stopper and removing an aqueous subsample. Sulfate concentrations in the microcosms were also determined in accordance with the US Environmental Protection Agency (EPA) method 375.2 [11].

Liquid chromatograph

The chromatograph consisted of a Model M590 pump (Waters Assoc., Milford, MA, USA), a Water autosampler Model 710B, a six-port automated column-switching valve (Waters), a Waters UV detector Model 484 at 200 nm. A NewGuard RP-18 precolumn with 7-μm particles (1.5 cm × 3.2 mm

I.D., Applied Biosystems, Santa Clara, CA, USA) for column 1 and an Econosphere C_{18} column with 3-μm particles (10 × 0.46 cm I.D., Alltech Assoc., Deerfield, IL, USA) for column 2 were used. The switching valve was controlled by time-programmable external events of the M590 pump and the autosampler. During the method development, three elution methods were performed, as follows.

Isocratic method. The mobile phase was acetonitrile–water (25:75, v/v) with 0.2% H_3PO_4 at a flow-rate of 1 ml/min. The switching valve was at the position 1 (Fig. 1) enabling column 1 to be between the injector and column 2. An aqueous solution containing 1 ppm of PBC and 25 ppm of toluene was injected (50 μl). The total analysis time was 40 min.

Gradient method. The conditions were similar to the isocratic method, except that gradient elution was used. A Model 600E pump (Waters) was used to generate a gradient program between solvent A (same as used in the isocratic method) and solvent B (acetonitrile) at a flow-rate of 1 ml/min. The gradient profile was shown in Table I. The total analysis time was 25 min.

Column-switching method. The column configuration during the analysis was also shown in Fig. 1. Other conditions were the same as in the isocratic method. The total run time was 15 min.

RESULTS AND DISCUSSION

PBC were quantified with the isocratic method on the reversed-phase column within 15 min using a weak mobile phase (25% acetonitrile). However, it took at least 35 min to elute toluene with the same conditions (Fig. 2). The gradient elution method, on the other hand, reduced the run time to 25 min. First, the isocratic elution was used to elute PBC and then the amount of acetonitrile in the mobile phase was increased to 100% to elute toluene. It

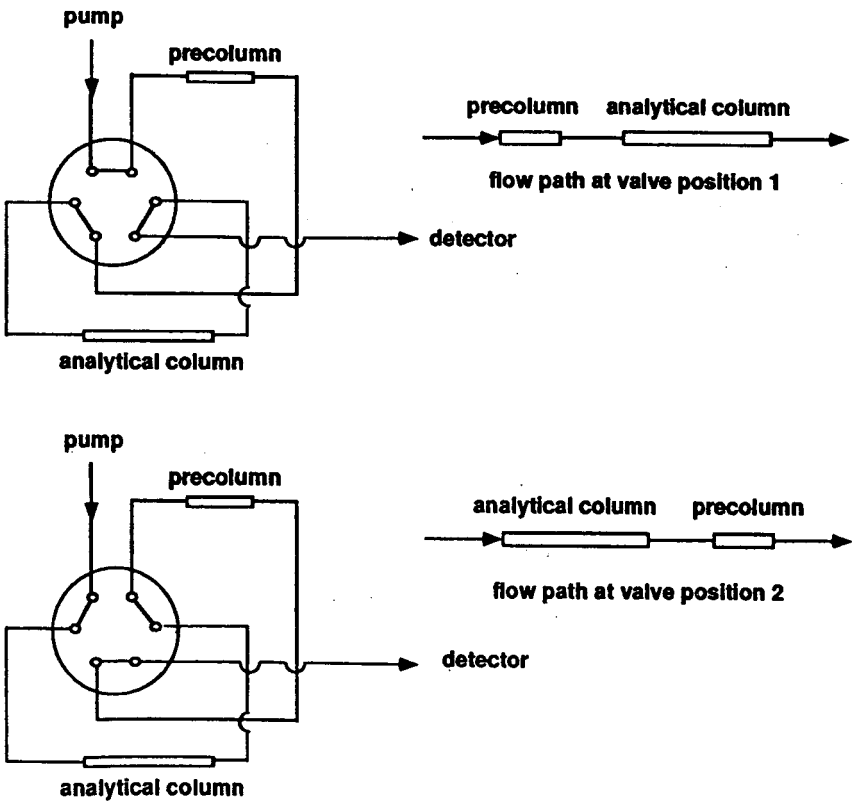

Fig. 1. Flow scheme of the six-port column-switching valves and mobile phase flow path.

TABLE I

GRADIENT PROFILE FOR THE GRADIENT METHOD

Time (min)	Flow-rate (ml/min)	Mobile phase A (%)	Mobile phase B (%)
Start	1	100	0
7.0	1	100	0
7.5	1	0	100
13.0	1	0	100
13.2	2	0	100
17.0	2	0	100
17.5	2	100	0
22.0	2	100	0
22.5	1	100	0
25.0	1	100	0

took 10 min at a flow-rate of 2 ml/min to bring back to its initial condition after toluene was eluted at 14 min (Fig. 2). By using the column-switching method, the total run time is 15 min for the PBC like the isocratic method while toluene was eluted close to the solvent front.

The strategy of the proposed column-switching technique was to elute polar compounds (PBC) from column 1 to column 2. Immediately after cresol was in column 2, the valve was switched so that the column 1 was between column 2 and the detector. Since column 1 was short, non-polar compounds, including toluene were eluted from the column quite rapidly and detected along with the solvent front. Subsequently, PBC were separated on the higher efficiency column (column 2) and column 1 one more time before they were quantified by the UV detector.

The mobile phase used in the column-switching method was the same as used in the isocratic method. It exhibited a good separation among PBC. The selection of column 1 was crucial to ensure that it separated PBC from toluene and allowed enough time for the valve switching. The NewGuard columns consisting of different packing materials (RP-2, RP-4, RP-8, phenyl, RP-18 and polymeric) were evaluated. An aqueous solution containing toluene and PBC was injected onto the NewGuard column and eluted with the isocratic mobile phase. The RP-18 exhibited the best retention of toluene (at 1.4 min) from cresol (0.8 min) which had the longest retention time among PBC (Fig. 3). Therefore, the RP-18 column was chosen for the experiment.

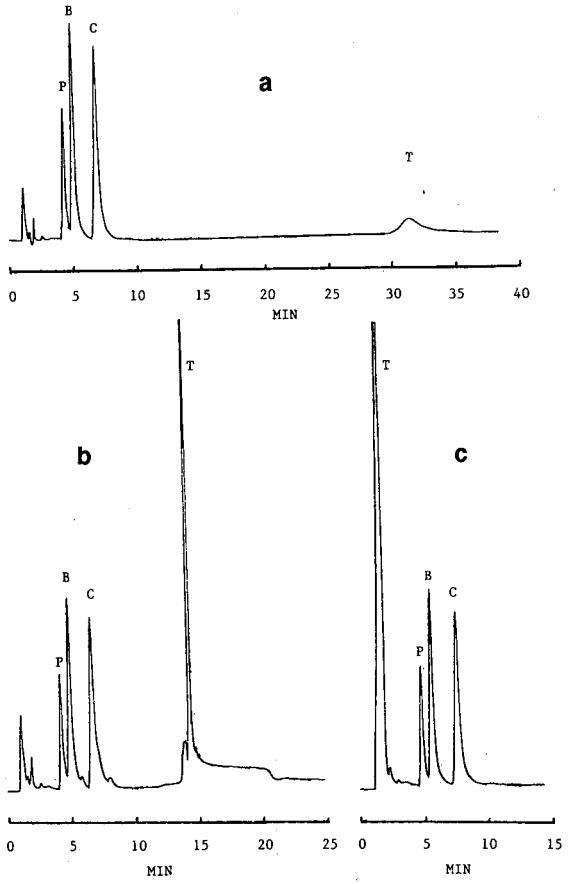

Fig. 2. Chromatograms of aqueous samples containing 1 ppm of PBC and 25 ppm of toluene using (a) isocratic method, (b) gradient method and (c) column-switching method. Peaks: P = phenol; B = benzoic acid; C = cresol; T = toluene.

Next, the proper switching time was examined by injecting 50 μl of PBC in aqueous solution (1 ppm) and varying the switching time after the injection from 0.6 to 1.4 min. The peak areas of PBC were recorded and plotted *versus* the switching times (Fig. 4). At 1.1 min after the injection, PBC were eluted from column 1 while toluene was still retained. Thus, the switching time at 1.1 was chosen. To observe the effect of toluene concentration on the column-switching method, the aqueous solution containing 1 ppm of PBC was added with toluene at concentrations of 0.5, 12.5, 25, 50 and 100 ppm. These samples were analyzed and the chromato-

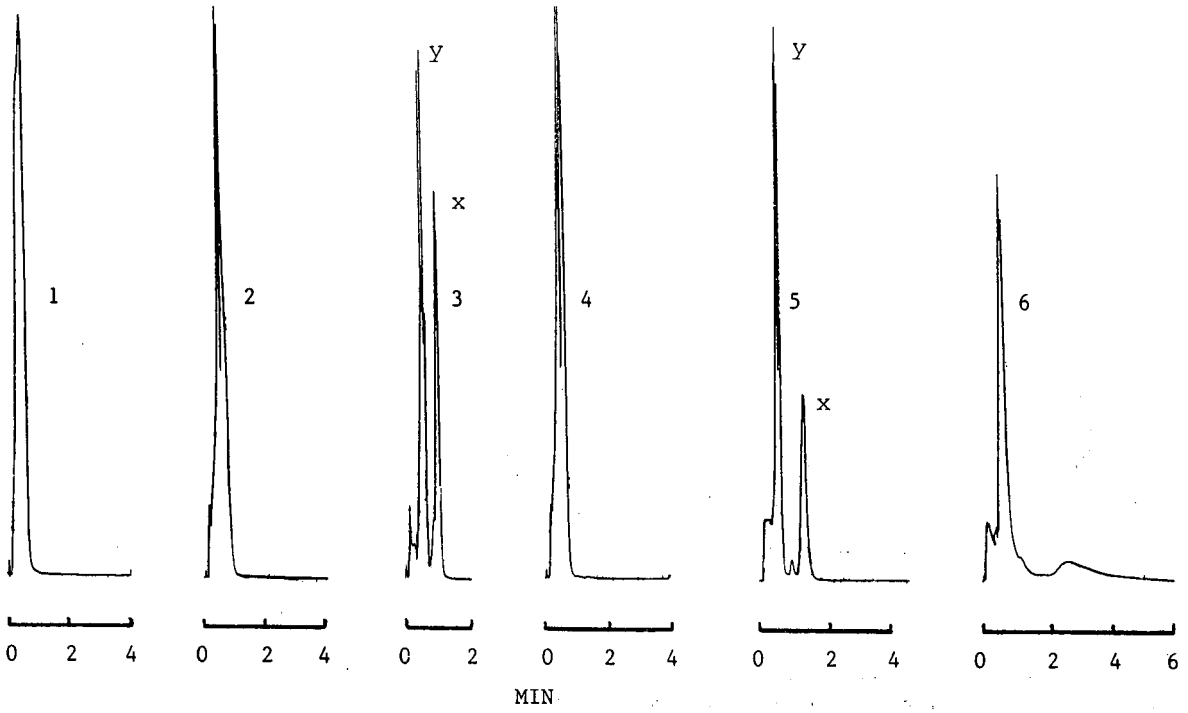

Fig. 3. Chromatograms of aqueous samples containing 1 ppm of PBC and 25 ppm of toluene using isocratic method on the NewGuard columns: (1) RP-2, (2) RP-4, (3) RP-8, (4) phenyl, (5) RP-18 and (6) polymeric. x = Toluene, y = PBC. Injection volume = 50 μl.

grams were examined (Fig. 5), The amount of toluene up to 100 times of the PBC concentration did not affect the separation of PBC.

It was highly recommended to pump at least 50 ml of acetonitrile through the columns after 25 injections to elute non-polar compounds from the reversed-phase column. Linearity data for concentrations of 0.1, 0.5, 1.5 and 10 ppm are shown in Table II. Concentrations as high as 50 ppm did not cause the carry-over in subsequent runs. The detection limit of the method was defined by the lowest amount that gave the signal three times higher than baseline noise. The recovery of the Bird's mill treated ground water spiked with 1 and 10 ppm of PBC is also shown in Table II. The accuracy is excellent with relative standard deviations range from 0.3 to 6.6%.

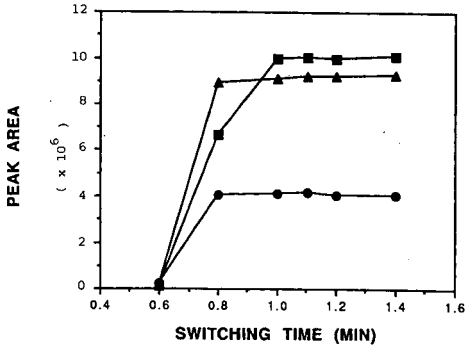

Fig. 4. Elution of PBC from the NewGuard column (RP-18) at different column-switching times. Samples: ● = phenol; ▲ = benzoic acid; ■ = cresol.

Suspension cultures of the sulfate-reducing, toluene-degrading consortium were able to degrade benzoic acid alone or preferentially in the presence of cresol and phenol (Fig. 6). The onset and cessation of benzoic acid removal correlated well to the reduction of sulfate (Fig. 7). The ratio of benzoic acid removed to sulfate reduced is close to the calculated values for the oxidation of benzoic acid to carbon dioxide coupled to sulfate reduction. Benzoic acid has been shown to be an intermediate of toluene, phenol, and cresol oxidation under anaerobic conditions by several groups and might be ex-

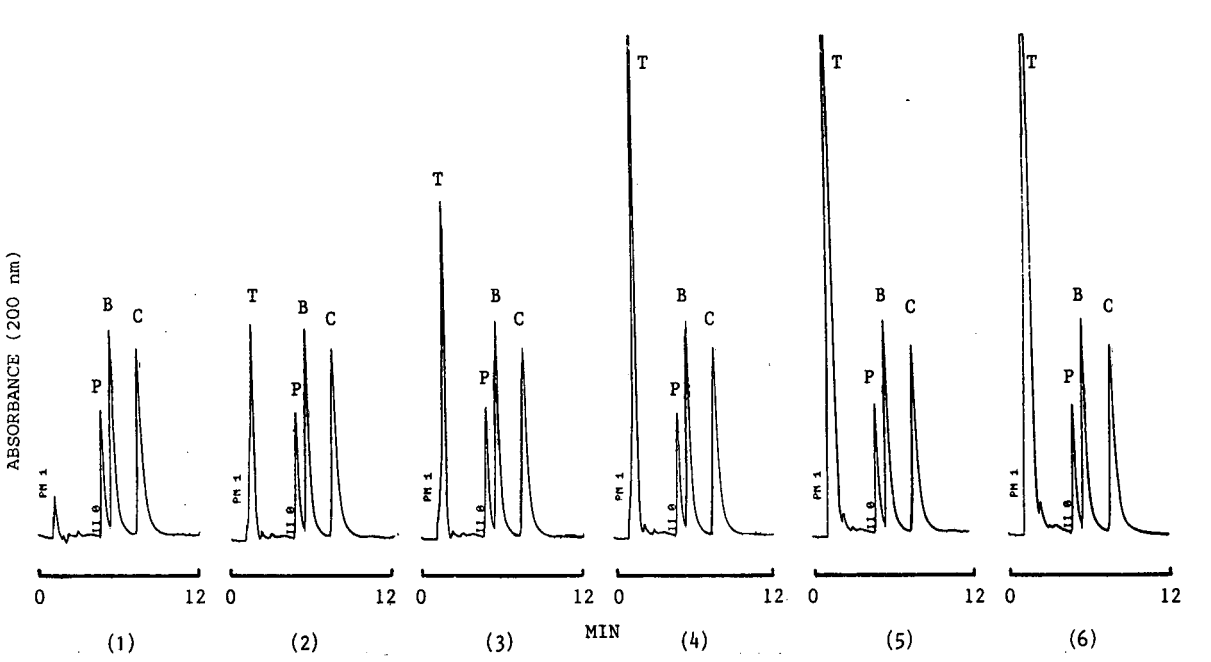

Fig. 5. Chromatograms of aqueous samples containing 1 ppm of PBC and toluene at the concentration of (1) 0 ppm, (2) 5 ppm, (3) 12.5 ppm, (4) 25 ppm, (5) 50 ppm and (6) 100 ppm. Injection volume = 50 μl.

pected to be the most easily degradable of the tested substrates [7,8,12,13]. Research continues to degradability of cresol and phenol in this system.

CONCLUSIONS

The use of the column-switching method permitted the determination of PBC in the presence of non-polar compounds particularly toluene under the isocratic condition in a very short time. It eliminated the need for re-equilibration of the analytical column and produced a constant spectral background. Complete analysis required less than 15 min. The method was simple, reproducible especially through automation with commercially available equipment. This technique could be also applied for

TABLE II

LINEARITY AND ACCURACY OF THE COLUMN-SWITCHING METHOD

Compound	Detection limit [a] (ppm)	Concentration range (ppm)	Linearity			Accuracy	
			Slope	Intercept	Correlation of coefficient	Mean[b]	Relative standard deviation (%)
Phenol	0.05	0.1–10	$1.69 \cdot 10^{-6}$	−0.13	0.998	97.41 (a)	0.64
						100.07 (b)	3.37
Benzoic acid	0.05	0.1–10	$1.51 \cdot 10^{-6}$	−4.49	0.999	100.98 (a)	6.59
						99.18 (b)	5.47
Cresol	0.05	0.1–10	$1.10 \cdot 10^{-6}$	−9.00	0.999	100.18 (a)	1.48
						99.22 (b)	0.34

[a] Signal-to-noise ratio = 3.

[b] (a) Spike level is 1 ppm with 6 replicates; (b) spike level is 10 ppm with 6 replicates.

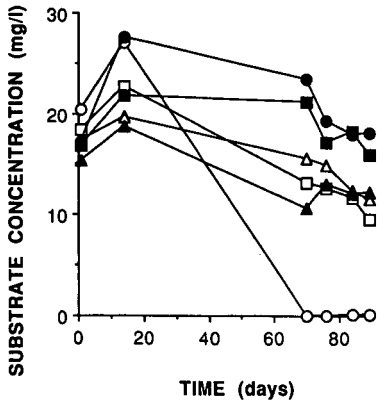

Fig. 6. Relationship between the incubation period and the concentration of PBC in the ground water microcosms. Samples: △ = phenol; □ = cresol; ○ = benzoic acid; ▲ = phenol control; ■ = cresol control; ● = benzoic acid control.

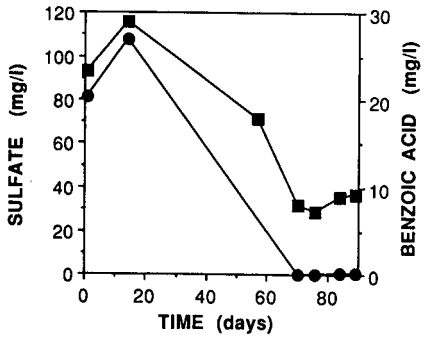

Fig. 7. Relationship between the incubation period and the concentration of sulfate (■) and benzoic acid (●) in the ground water microcosms.

the determination of other polar compounds in the present of non-polar interferences in an aqueous sample.

ACKNOWLEDGEMENT

We thank Dr. Jerry W. Anderson for constructive and valuable comments on the manuscript.

REFERENCES

1 L. R. Snyder, in Cs. Horváth (Editor), *High-Performance Liquid Chromatography —Advances and Perspectives*, Vol. 1, Academic Press, New York, 1980, p. 207.
2 J. W. Veals, and C. Lin, *Am. Lab.*, 20, No. 4 (1988) 42.
3 S. R. Binder, M. Regalia, M. Biaggi-McEachern and M. Mazhar, *J. Chromatogr.*, 473 (1989) 325.
4 C. J. Little and O. Stahel, *Chromatographia*, 19 (1984) 322.
5 J. F. K. Huber, R. van der Linden, E. Ecker and M. Oreans, *J. Chromatogr.*, 83 (1973) 267.
6 R. D. Rocklin, M. A. Rey, J. R. Stillian and D. L. Campbell, *J. Chromatogr. Sci.*, 27 (1989) 4.
7 D. R. Lovely and D. J. Lonergan, *Appl. Environ. Microbiol.*, 56 (1990) 1858.
8 D. Grbic-Galic and T. M. Vogel, *Appl. Environ. Microbiol.*, 53 (1987) 254.
9 B. H. Wilson, G. B. Smith and J. F. Rees, *Environ. Sci. Technol.*, 20 (1986) 997.
10 L. L. Leach, F. P. Beck, J. T. Wilson and D. H. Kampbell, *Proceedings of the Second National Outdoor Action Conferences on Aquifer Restoration, Ground Water Monitoring and Geophysical Methods, Las Vegas, NV, 1988*, Vol. 1, US EPA Environmental Monitoring Systems Laboratory, Las Vegas, NV, 1988.
11 *Methods for Chemical Analysis of Water and Wastes*, Office of Research and Development, US EPA Environmental Monitoring Systems Laboratory, Cincinnati, OH, 1983, p. 375.2.
12 X. Zhang, T. V. Morgan and J. Wiegel, *FEMS Microbiol. Lett.*, 67 (1990) 63.
13 B. R. S. Genthner, W. A. Price II and P. H. Pritchard, *Appl. Environ. Microbiol.*, 55 (1989) 1472.

Journal of Chromatography, 587 (1991) 193–203
Elsevier Science Publishers B.V., Amsterdam

CHROM. 23 578

High-performance liquid chromatography of phosphatidic acids and related polar lipids

S. L. Abidi

Food Quality and Safety Research, Agricultural Research Service, National Center for Agricultural Utilization Research, US Department of Agriculture, 1815 N. University Street, Peoria, IL 60614 (USA)

(First received March 15th, 1991; revised manuscript received June 18th, 1991)

ABSTRACT

The retention behavior of phosphatidic acids (PA) and phosphatidic acid methyl esters (PM) was studied by reversed-phase ion-pair high-performance liquid chromatography (HPLC). The HPLC systems consisted of mobile phases of acetonitrile–methanol–water containing tetraalkylammonium phosphates (TAAP) and stationary phases of alkyl-bonded silica and polystyrene–divinylbenzene resins. The lipid solutes were more strongly retained when using mobile phases containing larger TAAP at higher concentrations. The results are indicative of an ion-pair retention mechanism. Molecular species of PM were readily resolved despite the complete inseparability of PA under all conditions used. Except for tetrabutylammonium phosphate, there was a linear correlation between the logarithmic capacity factors (k') of PM (or PA) and the total number of carbon atoms of TAAP. The significant concentration dependence of separation factors for certain PM components was related to the size effect of TAAP. A normal-phase HPLC method for the separation of PA from other polar lipids is described.

INTRODUCTION

Phospholipids (PL) are widely distributed in plant and animal cells. These polar lipids play an important role in regulating the movement of charged and uncharged molecules. Soybean oil contains phosphatidic acid (PA), phosphatidylcholine (PC), phosphatidylethanolamine (PE) and phosphatidylinositol (PI) as the four major consitutents of its polar lipids. It also contains a small percentage of phosphatidylserine (PS). The change in PL composition with time has been related to the stability of soybean oil during storage [1]. The determination of PL in crude and degummed oil provides useful information on the extent of PL deterioration caused by stressed soybeans. As PA has been found to be the predominant product of PL decomposition, it was necessary to assess the variation in its molecular species distribution with the period of storage. To this end, an effective analytical method was required for the separation of PA components.

A number of techniques for the separation of molecular species of neutral PL (*i.e.*, PC and PE) are known and numerous reports on the reversed-phase high-performance liquid chromatography (HPLC) of PC and PE have been published [2–10]. Whereas the ionic charges in PC and PE are internally neutralized within the molecules, PA, PI and PS are all negatively charged compounds requiring external counter ions to form neutral species. Few studies have been conducted for the speciation of these negatively charged PL into molecular species using ion-pair methodology. Most recently, mixtures of soybean PI have been resolved by reversed-phase ion-pair HPLC [11]. Although sporadic reports on indirect determinations of PA derived from PC are available [12–14], methods for the direct determination of PA molecular species have remained obscure. This paper describes reversed-phase ion-pair HPLC techniques for the separation of molecular species of PA and its monomethyl ester, phosphatidic acid methyl ester (PM).

There are many publications [6,15–26] dealing with normal-phase HPLC separations of PL class-

es. However, the scarcity of published information on reproducible normal-phase HPLC methods for the separation of PA from other PL classes provided the impetus for this normal-phase HPLC work.

EXPERIMENTAL

Chemicals and reagents

Phospholipid standards PA, PC, PE, PI, PM and PS were obtained either from Avanti Polar Lipids (Pelham, AL, USA) or Sigma (St. Louis, MO, USA). Commercial PA and PM were used in all HPLC analyses. Both compounds were prepared from egg PC by the manufacturers. Commercial PM was prepared by methanolysis of PC in the presence of phospholipase D. Tetraalkylammonium phosphates were obtained from Regis (Morton Grove, IL, USA). HPLC-grade acetonitrile and methanol were purchased from J. T. Baker (Phillipsburg, NJ, USA). HPLC solvents tetrahydrofuran and ammonia solution were obtained from EM Science (Gibbstown, NJ, USA). Chloroform used in normal-phase HPLC was a product of Mallincrodt (Paris, KY, USA). A Waters–Millipore (Milford, MA, USA) Milli-Q water purifier was used for obtaining ultra-pure HPLC water.

High-performance liquid chromatography

In all reversed-phase HPLC experiments, a Spectra-Physics (San Jose, CA, USA) liquid chromatograph equipped with a Model SP8700 solvent delivery system was interfaced with an LDC Analytical (Riviera Beach, FL, USA) SpectroMonitor D variable-wavelength UV detector. For normal-phase HPLC work, a Varex (Rockville, MD, USA) Model ELSD II evaporative light-scattering (ELS) detector was used.

Reversed-phase HPLC mobile phases consisting of acetonitrile–methanol–water and various concentrations (0.1–5.0 m*M*) of quaternary ammonium phosphates were filtered, degassed and pumped through a column under isocratic conditions at a flow-rate of 1 ml/min. Normal-phase HPLC analyses were carried out by gradient elution with mobile phase solvents of (1) chloroform–tetrahydrofuran (THF) and (2) methanol–ammonia solution–chloroform at a flow-rate of 1 ml/min.

Several stationary phases were evaluated: (1) Waters NovaPak C_{18} (30 cm × 3.9 mm I.D.; 4 μm), (2) polymeric resins of macroporous polystyrene–divinylbenzene (MPD), PLRP-S-100 (25 cm × 4.6 mm I.D.; 5 μm) (Polymer Labs., Amherst, MA, USA), (3) EM Science LiChrosorb RP-18 (25 cm × 4.6 mm I.D.; 10 μm) (Alltech, Deerfield, IL, USA), (4) Brownlee Spheri-5 RP-8 (22 cm × 4 mm I.D.; 5 μm) (Applied Biosystems, Foster City, CA, USA), (5) Adsorbsphere HS C_{18} (25 cm × 4.6 mm I.D.; 5 μm (Alltech), (6) EM Science LiChrosorb Si-60 (25 cm × 4.6 mm I.D.; 10 μm) and (7) EM Science LiChrosorb Si-100 (25 cm × 4.6 mm I.D.; 5 μm).

Aliquots (5–10 μl of 1% solutions) of PL samples in chloroform were injected onto a column via a Rheodyne (Cotati, CA, USA) Model 7125 injector fitted with a 10-μl loop. Detector signals were monitored with an OminiScribe recorder (Houston Instruments, Houston, TX, USA).

RESULTS AND DISCUSSION

Reversed-phase high-performance liquid chromatography

Individual PL classes consist of molecular species that differ in the R^1 and R^2 groups of fatty acids, as shown in Fig. 1 for the strcture of PA. Notwithstanding the existence of non-polar tail groups in the fatty acid moieties, reversed-phase HPLC of PA in mobile phases containing no ion-pairing reagents produced unresolved peaks with little retention (Fig. 2A) owing to the influence of polar head groups of phosphoric acid derivatives. Much like phosphatidylinositols (PI), molecular species of PA including its monomethyl ester, PM, could be retained on a reversed-phase column only when cationic counter ions (ion-pairing reagents) were pres-

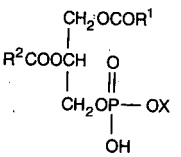

I . X = H

II . X = CH_3

Fig. 1. Structures of (I) phosphatidic acid (PA) and (II) phosphatidic acid methyl ester (PM). R^1 and R^2 are alkyl or alkenyl groups of fatty acids.

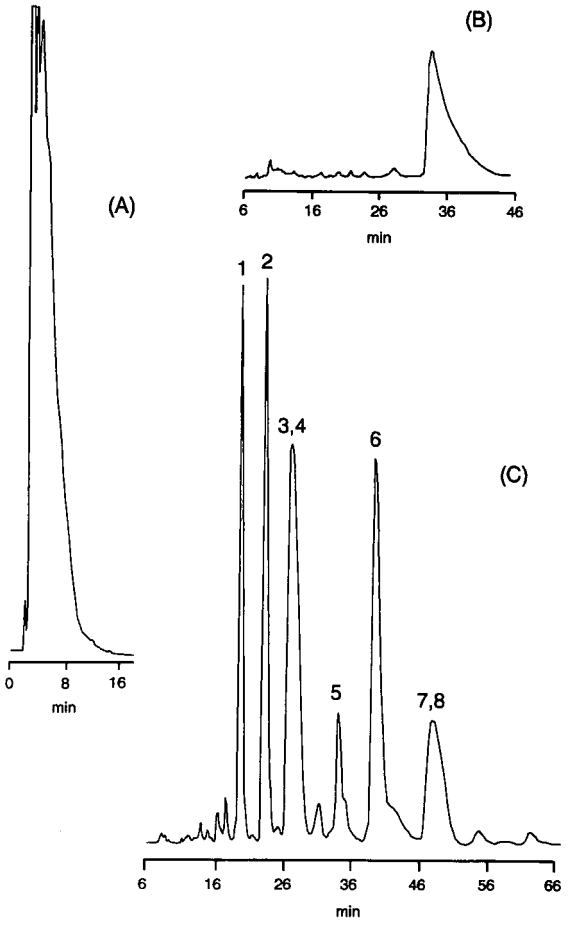

Fig. 2. Reversed-phase HPLC of (A) PM without an ion-pairing reagent, (B) PA with an ion-pairing reagent (5 m*M* PTAP) and (C) PM with an ion-pairing reagent (5 m*M* PTAP). Conditions: stationary phase, NovaPak C_{18}; mobile phase, acetonitrile–methanol–water (70:22:8); UV detection at 208 nm. Peaks: 1 = 16:0–20:4; 2 = 16:0–18:2; 3 + 4 = 16:0–18:1; 5 = 18:0–18:2; 6 = 18:1–18:1; 7 + 8 = 18.0–18:1, corresponding to R^1 and R^2 groups of fatty acids in PM (Fig. 1). Fatty acid designations: 16:0 = palmitic; 18:0 = stearic; 18:1 = oleic; 18:2 = linoleic; 20:4 = arachidonic.

ent in the mobile phases. In order to optimize the HPLC conditions and obtain various degrees of retention and separation of the compounds, a series of tetraalkylammonium phosphates (TAAP) were evaluated, including tetrabutylammonium phosphate (TBAP), pentyltriethylammonium phosphate (PTAP), hexyltriethylammonium phosphate (HTAP), heptyltriethylammonium phosphate (HTAP), octyltriethylammonium phosphate (OTAP) and dodecyltriethylammonium phosphate (DTAP). As there are two negative charges in the PA molecule, it requires two cationic ions for neutralization. In reversed-phase ion-pair HPLC of PA, an enhancement of analyte retention was invariably observed despite the inability of the HPLC systems to resolve PA molecular species (Fig. 2B). It is probable that concurrent ion-pair formation from doublely charged PA might be sterically disfavored, resulting in inadequate hydrophobic interactions in chromatographic processes. On the other hand, molecular species of phosphatidic acid methyl ester, PM, were separated on a reversed-phase column (Fig. 2C). In this instance, the singlely charged anion presumably formed an ion pair with a TAAP cation to facilitate hydrophobic interactions with the hydrophobic phase employed.

Results of the reversed-phase ion-pair HPLC of PM are summarized in Table I. The retention characteristics of PM components were markedly affected by both the size and concentration of quaternary ammonium counter ions present in the mobile phases. The capacity factors (k') of molecular species increased with an increase in the chain length of the alkyl group in an alkyltriethylammonium counter ion. There was a linear correlation between the logarithmic k' values and the total number of carbon atoms or the longest carbon chain length of alkyl groups in the TAAP counter ions (Fig. 3). The linear correlation data indicate that the total area of alkyltriethyl groups in TAAP is available for solvophobic interactions [27,28]. It should be pointed out that all but TBAP in the TAAP series are homologues of alkyltriethylammonium phosphates. The log k' values of PM in mobile phases containing TBAP were found to deviate from the correlation lines obtained with other TAAP in the series. Evidently, structural effects of TAAP on the k' values of PM were primarily controlled by the carbon chain length of the largest alkyl group of TAAP. These observations are in contrast with those in reversed-phase ion-pair HPLC of PI, where the k' values were entirely governed by the total number of carbon atoms in the tetraalkyl groups of TAAP [11]. Hence, among the investigated TAAP counter ions, HPLC of PM with TBAP (longest carbon chain length = 4) yielded the least retained components, whereas molecular species of PI were least retained in HPLC with mobile phases containing

TABLE I

EFFECTS OF THE CONCENTRATION AND THE TYPE OF QUATERNARY AMMONIUM COUNTER IONS ON THE CAPACITY FACTORS k' OF PHOSPHATIDIC ACID METHYL ESTER (PM)

HPLC conditions: stationary phase, NovaPak C_{18}; mobile phase, acetonitrile–methanol–water (70:22:8) containing a tetraalkylammonium phosphate (TAAP) at various concentrations. Commercial PM are derived from egg phosphatidylcholines. For abbreviations, see Results and Discussion. For peak identification, see Fig. 2C.

Counter ion	Concentration (mM)	Capacity factor, k'									
		Component									
		1	2	3	(α)	4	5	6	7	(α)	8
TBAP	5.0	5.60	6.68	7.48	(1.07)	8.02	10.7	12.5	15.7	(1.04)	16.4
	2.5	3.04	3.71	4.25	(1.06)	4.52	5.46	6.41	7.62	(1.04)	7.89
	1.25	2.30	2.84	3.44	(1.04)	3.58	4.39	5.33	6.34	(1.02)	6.50
HTAP	5.0	5.60	6.54	7.75	(1.00)	7.75	9.84	11.7	14.5	(1.00)	14.5
	2.5	3.31	3.98	4.86	(1.00)	4.86	6.14	7.48	8.97	(1.00)	8.97
	1.25	2.10	2.64	3.38	(1.00)	3.38	4.05	5.53	6.62	(1.00)	6.62
OTAP	5.0	9.51	11.7	13.9	(1.08)	15.0	18.5	22.4	27.0	(1.05)	28.4
	2.5	5.33	6.28	7.40	(1.07)	7.92	9.58	11.7	14.2	(1.03)	14.6
	1.25	3.13	3.90	4.91	(1.00)	4.91	5.93	7.77	9.44	(1.00)	9.44
DTAP	2.5	12.3	15.0	17.4	(1.08)	19.0	23.8	27.9	36.5	(1.07)	39.0
	1.25	7.08	8.70	10.2	(1.05)	10.7	12.7	15.8	188	(1.06)	19.9
	0.544	3.85	4.79	5.73	(1.00)	5.73	7.22	8.97	11.0	(1.00)	11.0

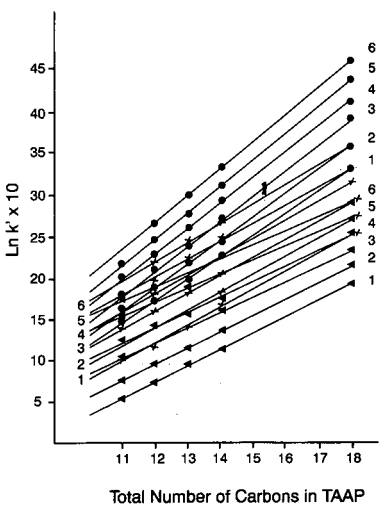

Fig. 3. Correlation of ln k' of six major molecular species of PM with the total number of carbon atoms in TAAP. Reversed-phase ion-pair HPLC conditions as in Fig. 2 except for TAAP concentrations: ● = 5 mM; × 2.5 mM; ▲ = 1.25 mM. UV detection at 208 nm.

PTAP (smallest total number of carbon atoms = 11) [11]. When TBAP was used as the counter ion, the retention of PI corresponded to a total of sixteen carbon atoms on correlation plots [11].

Separations of PM components 3, 4, 7 and 8 were particularly susceptible to variations in the structure of TAAP used in the mobile phases (Table I). The ammonium counter ions having a larger total number of carbon atoms, as in TBAP (C_{16}), OTAP (C_{14}) and DTAP (C_{18}), tended to offer better selectivity [higher values of separation factors (α)] for the lipid components of interest. Such structural effects appeared to diminish (lower α values) as the counter ion concentrations decreased (Table I). Component peaks 3 and 4 and 7 and 8 may be attributed to reverse positonal isomers. The k' values of PM analytes increased with increasing counter ion concentration. In general, the observed concentration effects of TAAP on the retention behavior of PM are similar to those found previously in HPLC of PI [11] and aminobenzoic acids [29], but are different

TABLE II

REVERSED-PHASE ION-PAIR HPLC OF PHOSPHATIDIC ACID ON OCTADECYLSILICA STATIONARY PHASES

Mobile phase: acetonitrile–methanol–water (70:22:8). The commercial phosphatidic acids are derived from egg phosphatidylcholine.

Stationary phase	TAAP concentration (m*M*)	Capacity factor, *k'*				
		Quaternary ammonium counter ion				
		TBAP	PTAP	HTAP	HPTAP	OTAP
LiChrosorb RP-18	5	4.03	8.17	8.54	9.36	9.78
	2.5	2.17	4.90	6.05	7.21	8.67
	1.25	2.08	2.83	3.60	4.63	5.75
NovaPak C_{18}	5	4.78	8.27	8.70	9.77	10.1
	2.5	2.34	5.10	6.68	7.89	9.87
	1.25	2.14	2.89	3.74	4.93	6.23

to those of aprotic ionic compounds [30,31]. The cationic counter ion effects (with respect to both the concentration and size of TAAP) discussed so far are indicative of an ion-pair retention mechanism by which solvophobic interactions of PM solutes with stationary phases are believed to proceed during HPLC separation processes.

Table II summarizes HPLC data for PA to show the influence of TAAP on the capacity factors, *k'*. The general trends of counter-ion effects on the retention of PA are similar to those noted in the HPLC of PM, even though there was no indication of component resolution of the former in all experiments performed. Correlation of ln *k'* values with the total number of carbons or the number of the carbons on the largest alkyl group in TAAP, excluding TBAP, yielded linear plots. It is unclear how TAAP participated in ion-pair formation with the double negative charges of PA molecules. Nevertheless, an ion-pair mechanism appeared to be

TABLE III

REVERSED-PHASE ION-PAIR HPLC OF PHOSPHATIDIC ACID METHYL ESTER (PM) UNDER VARIOUS CONDITIONS

Mobile phase: (A) and (B) acetonitrile–methanol–water (65.8:13.7:20.5); (C) and (D) acetonitrile–methanol–water (70:22:8). The source of PM is same as in Table I. For peak identification, see Fig. 2C.

Stationary phase	TAAP	Concentration (m*M*)	Capacity factor, *k'*									
			Component									
			1	2	3	(α)	4	5	6	7	(α)	8
(A) Spheri-RP-C_8 (5 μm)	DTAP	3.11	15.6	17.8	19.6	(1.14)	22.4	26.6	29.4	33.4	(1.13)	37.6
		0.78	4.61	5.20	5.82	(1.00)	5.82	7.19	8.24	9.68	(1.11)	10.7
(B) PLRP-S (5 μm)	DTAP	0.78	14.0	14.0	17.8	(1.08)	19.3	26.4	26.4	37.1	(1.00)	37.1
		0.195	6.41	6.41	7.89	(1.04)	8.19	11.9	16.5	11.9	(1.00)	16.5
(C) LiChrosorb RP-18 (10 μm)	HTAP	5.0	5.05	6.11	7.29	(1.00)	7.29	8.86	10.4	12.9	(1.00)	12.9
		2.5	3.21	4.00	4.93	(1.00)	4.93	5.86	7.14	8.57	(1.00)	8.57
(D) Adsorbsphere HS C_{18} (5 μm)	TBAP	5.0	13.4	15.9	18.1	(1.09)	19.7	23.7	27.6	32.3	(1.07)	34.4
		1.25	7.22	8.63	9.96	(1.06)	10.6	12.9	15.3	17.9	(1.06)	19.0
	PTAP	1.25	6.04	7.30	8.48	(1.00)	8.48	11.0	12.5	15.4	(1.00)	15.4

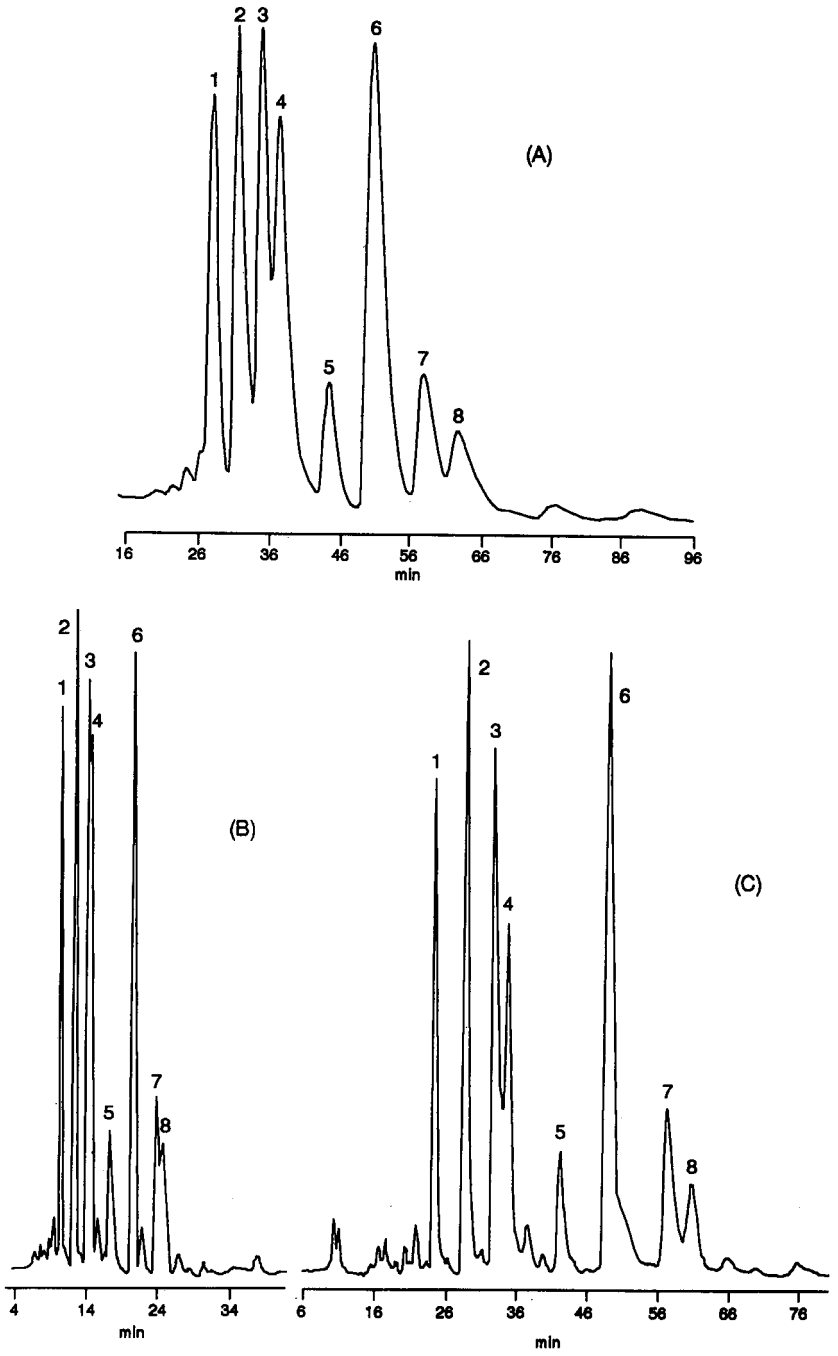

Fig. 4. Reversed-phase ion-pair HPLC separations of PM on various alkyl-bonded silica phases. Conditons: stationary phases, (A) octylsilica, Spheri-5 RP-8, (B) NovaPak C_{18}, (C) Adsorbsphere HS C18; mobile phases, (A) acetonitrile–methanol–water (65.8:13.7:20.5) containing 1.56 m*M* DTAP, (B) and (C) acetonitrile–methanol–water (70:22:8) containing 1.25 m*M* TBAP. UV detection at 208 nm.

TABLE IV

EFFECTS OF PHOSPHORIC ACID AND AMMONIA SOLUTION ON CAPACITY FACTORS, k', OF PM AND PA ON AN MPD PHASE IN REVERSED-PHASE ION-PAIR HPLC

HPLC conditions: stationary phase, MPD; mobile phase, acetonitrile–methanol–water (70:18:12) containing 5 m*M* dodecyltriethylammonium phosphate (DTAP). The sources of PM and PA are the same as in Tables I and II, respectively. For peak identification, see Fig. 2C.

Compound	Concentration (m*M*)	Capacity factor, k'								
		Component								
		1	2	3	4	5	6	7	8	PA
H_3PO_4	0.00	6.26	6.26	7.74	7.74	10.1	10.1	12.9	12.9	4.48
	5.00	8.33	8.33	9.37	9.37	12.9	12.9	16.8	16.8	9.96
	20.0	9.07	9.07	10.3	10.3	14.6	14.6	19.7	19.7	23.7
Ammonia solution	0.00	6.26	6.26	7.74	7.74	10.1	10.1	12.9	12.9	4.48
	15.0	4.93	4.93	6.56	6.56	9.22	9.22	11.3	11.3	3.74
	30.0	3.89	3.89	5.22	5.22	7.59	7.59	10.1	10.1	2.70

operative during chromatographic processes as reflected in the typical counter ion effects (Table II). As briefly stated earlier, the formation of ion pairs with both negative charges might be sterically unfavorable, leaving one unpaired acidic function that could inhibit hydrophobic interactions. Esterification of PA to its monoester PM removed one free charge and facilitated the separation of molecular species by ion-pairing retention processes. Hence, neutralization of charges in PA is an obvious prerequisite for the successful HPLC separation of its molecular species.

Table III shows the HPLC results for PM on various stationary phases. As expected, the capacity factors were higher on octadecylsilica phases than on stationary phases derived from macroporous polystyrene-divinylbenzene, MPD. In the former instances it was necessary to use lower members of TAAP in mobile phases for bringing peaks within reasonable retention times. However, the retention on octylsilica was lower (partly owing to smaller column dimensions) than on MPD, as demonstrated in the HPLC data in which the corresponding k' values of PM are compared under identical mobile phase conditions at a DTAP concentration of 0.78 m*M* (Table III). Of the silica-based stationary phases, Adsorbsphere HS C_{18} showed the greatest selectivity for PM components 3, 4, 7 and 8. This is attributed to its high carbon loading (20%), which favors hydrophobic interactions. With higher members of TAAP (total carbon number >16) in the series as counter ions, HPLC separations of component pairs 3–4 and 7–8 occurred with enhanced selectivity (higher α values). These results, coupled with the concentration dependence of the α values, are in agreement with earlier findings in analogous experiments where a higher efficiency column (NovaPak C_{18}, 4 μm) was used (Table I).

Fig. 4 compares separations of PM components on various alkyl-bonded silica phases. Although Spheri-5 RP-8, an octylsilica column, was made of relatively low carbon loading (9%) packings, significant enhancement (higher α values) in component separation (component pairs 3–4 and 7–8) was observed in experiments where DTAP was added to the mobile phases. Thus, with DTAP as counter ions, HPLC of PM led to reasonable separations of components 3, 4, 7 and 8, which remained unresolved or partially resolved in most instances.

In the light of the acidic properties of the title compounds and the stability of MPD over a wide pH range, we studied the retention behavior of PA and PM in acidic and basic media on this stationary phase. Table IV shows the effect of phosphoric acid and ammonia solution on the k' values in the reversed-phase ion-pair HPLC of the acidic polar lip-

ids. Generally, an increase in k' values of the analytes was demonstrated in HPLC with mobile phases containing higher concentrations of phosphoric acid. Conversely, an increase in the concentration of ammonia solution was accompanied by a small decrease in the k' values of the compounds analyzed. The pH dependence of both PA and PM in protic mobile phases is rationalized in terms of ion-suppression phenomena, frequently observed in the HPLC of ionic compounds [32,33]. As there was no evidence of participation of aromatic moieties of MPD in chromatographic interactions with analyte solutes, modifications of the mobile phase pH gave little improvement in column selectivity for the separation of PM molecular species. In comparison with results from the HPLC of PM, the concentration of phosphoric acid in the mobile phases had a greater influence on the retention of PA because of the doubly charged acidic characteristics of the parent compound.

Normal-phase high-performance liquid chromatography

Normal-phase HPLC separation of PA from other PL found in soybean oil has not been thoroughly investigated on account of its low natural abundance and some reported uncertainty associated with the HPLC behavior of the compound [6]. As PA is the major PL detected in degummed soybean oil, it was pertinent to include in this work the results of a normal-phase HPLC study. Table V presents separation data for PA and four other PL classes derived from soybeans. After initial attempts to reproduce a published procedure [21] failed to resolve the PL components with reported retention times (the published HPLC data [21] might have been obtained before equilibration of the HPLC system was reached), the mobile phase systems were modified as shown for systems A–F in Table V. Normally, baseline separations of PA from other PL were achieved with good reproduc-

TABLE V

NORMAL-PHASE HPLC SEPARATION OF MIXTURES OF SOYBEAN PHOSPHOLIPID CLASSES

HPLC conditions: gradient programs for changes in mobile phase solvents 1 and 2 with times (min) were run in one of the two modes 1→2→2→1 and 1→2→1 (arrows represent stepwise duration times) with duration times shown as (i) 20–20–20, (ii) 30–15–10, (iii) 40–20, (iv) 30–10–5 and (v) 35–10–5 min. For detailed description of gradient elution, see legend for Fig. 5. Mobile phases: (A) solvent 1 = $CHCl_3$, solvent 2 = CH_3OH–NH_3–$CHCL_3$ (92:7:1); (B) solvent 1 = $CHCl_3$–THF (4:1), solvent 2 = CH_3OH–NH_3–$CHCl_3$ (92:7:1); (C) solvent 1 = $CHCL_3$–THF (1:1), solvent 2 = CH_3OH–NH_3–$CHCL_3$ (92:7:1); (D) solvent 1 = $CHCl_3$–THF (1:1), solvent 2 = CH_3OH–NH_3CHCL_3 (92:4:4); (E) solvent 1 = $CHCl_3$–THF (1:1), solvent 2 = CH_3OH–$(C_2H_5)_3N$–$CHCl_3$ (92:4:4).

Stationary phase	Gradient elution	Capacity factor, k'								
		Phospholipid class								
		PE	(α)	PI	(α)	PS	(α)	PA	(α)	PC
LiChrosorb Si-60 (10 μm)	(A) (i) 20–20–20	8.52	(1.22)	10.4	(1.00)	10.4	(1.14)	11.9	(1.17)	13.9
	(ii) 30–15–10	10.2	(1.23)	12.5	(1.05)	13.1	(1.15)	15.0	(1.09)	16.3
	(iii) 40–20	13.0	(1.20)	15.6	(1.03)	16.1	(1.12)	18.0	(1.00)	18.0
	(B) (ii) 30–15–10	11.2	(1.15)	12.9	(1.11)	14.3	(1.09)	15.6	(1.15)	17.9
LiChrosorb Si-100 (5 μm)	(C) (i) 20–20–20	8.24	(1.10)	9.10	(1.02)	9.29	(1.18)	11.0	(1.18)	13.0
	(ii) 30–15–10	10.4	(1.13)	11.8	(1.03)	12.1	(1.17)	14.2	(1.16)	16.5
	(D) (i) 20–20–20	8.90	(1.04)	9.30	(1.06)	9.86	(1.18)	11.6	(1.20)	13.9
	(ii) 30–15–10	10.4	(1.07)	11.1	(1.06)	11.8	(1.19)	13.9	(1.19)	16.5
	(iv) 30–10–5	10.9	(1.05)	11.4	(1.06)	12.1	(1.21)	14.6	(1.16)	16.9
	(E) (ii) 30–15–10	9.10	(1.25)	11.4	(1.00)	11.4	(1.04)	11.9	(1.35)	16.1
	(iv) 30–10–5	8.81	(1.20)	10.6	(1.00)	10.6	(1.14)	12.1	(1.35)	16.3
	(v) 35–10–5	8.29	(1.48)	12.3	(1.00)	12.3	(1.07)	13.1	(1.35)	17.7

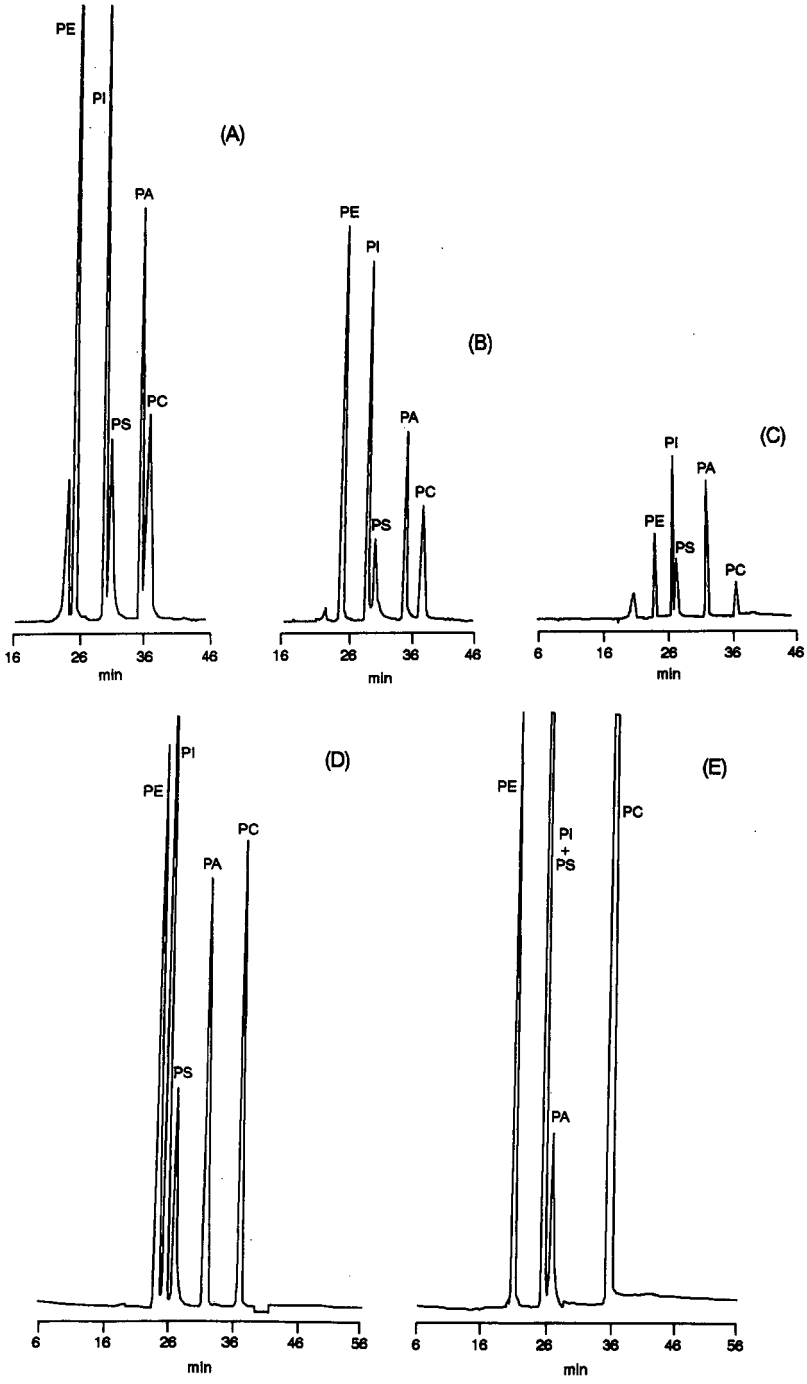

Fig. 5. Normal-phase HPLC separations of PL classes under gradient elution starting from solvent 1 to solvent 2 in 30 min, staying at solvent 2 for 15 min and then returning to solvent 1 in 10 min (solvent cycle 1→2→2→1, time period 30–15–10 min). HPLC conditions for (A), (B), (C), (D) and (E) as in Table V. ELS detector temperature for (A), (B), (C) and (D) 150°C and for (E) 160°C.

ibility and high efficiency. Normal-phase HPLC with mobile phases of different polarity and solvent strength yielded chromatographic profiles largely determined by the polarity of PL solutes. Under the conditions employed, the polar lipids exhibited polarity characteristics in the increasing order PE < PI < PS < PA < PC.

The data in Table V indicate that the mode of elution had a profound effect on the separation of negatively charged PL (PI, PS and PA). For a baseline separation of all five components, PE, PI, PS, PA and PC, the elution mode of choice was a gradient program of 1→2→2→1 (arrows represent stepwise duration times) in which solvent 1 [chloroform tetrahydrofuran (THF)] was pumped through a cycle via solvent 2 (methanol–ammonia solution–chloroform) with corresponding periods of 30, 15 and 10 min for the duration times (30 min from solvent 1 to solvent 2, 15 min hold at solvent 2, then 10 min from solvent 2 to solvent 1). Representative normal-phase HPLC chromatograms showing separations of PA from other PL under various conditions are given in Fig. 5. The order of elution, PE < PI < PS < PC, is the same as that obtained with Christie's systems [23,24]. Sphingomyelin would elute after PC in the present system. The extent of separation between PI and PS, which have close k' values, appeared to be more sensitive to the change in the mode of gradient elution than other adjacent pairs. Regardless of the stationary phases used, incorporation of THF [34] in mobile phases led to better dispersed chromatographic peaks of PA and PC [(A) (ii) *vs.* (B) (ii) and (C) *vs.* (D), Table V]. Further, separations of these two components were notably augmented by reducing the basicity of mobile phases, as indicated in experiments (D) *vs.* (E) and (E) *vs.* (F) in Table V. The chromatographic outcome can be explained in the context of decreasing polarity of PA (less ionized) in mobile phases containing decreased amounts of ammonia solution or in mobile phases whose ammonia contents are replaced with triethylamine of reduced basicity.

CONCLUSIONS

This reversed-phase ion-pair HPLC method represents the first direct approach to tackling the analytical problems associated with the separation of complex mixtures of molecular species derived from PA compounds. The ion-pairing technique provides a mean to delineate the chromatographic characteristics of polar lipids in general and other charged PL in particular. The correlations data can be used for the prediction of unknown k' values of PA and PM analyzed under given mobile phase conditions. For achieving separations under specific HPLC conditions, the method is versatile and can be applied to various analytical systems by optimizing reversed-phase HPLC variables such as stationary phase specfications, mobile phase compositions and types and concentrations of ion-pair reagents. The normal-phase HPLC–ELS detection method permits the simultaneous separation and quantification of PL classes in various samples of plant origin (*e.g.*, soybeans). The method is reliable and useful for the routine analysis of PL samples containing high levels of PA.

ACKNOWLEDGEMENT

The author thanks Kathy A. Rennick for technical assistance.

REFERENCES

1 T. L. Mounts and A. M. Nash, *J. Am. Oil. Chem. Soc.*, 67 (1990) 757.
2 N. A. Porter, R. A. Wolf and J. R. Nixon, *Lipids*, 14 (1979) 20.
3 F. B. Jungalwala, V. Hayssen, J. M. Pasquini and R. H. McCluer, *J. Lipid Res.*, 20 (1979) 579.
4 B. J. Comton and W. C. Purdy, *J. Liq. Chromatogr.*, 3 (1980) 1183.
5 M. Smith and F. B. Jungalwala, *J. Lipid Res.*, 22 (1981) 697.
6 G. M. Patton, J. M. Fasulo and S. J. Robins, *J. Lipid Res.*, 23 (1982) 190.
7 B. J. Compton and W. C. Purdy, *Anal. Chim. Acta*, 141 (1982) 405.
8 A. Cantafora, A. Di Biase, D. Alvaro, M. Angelico, M. Martin and A. F. Attili, *Clin. Chim. Acta*, 134 (1983) 281.
9 W. W. Christie and M. L. Hunter, *J. Chromatogr.*, 325 (1985) 473.
10 N. Sotirhos, C. Thorngren and B. Herslof, *J. Chromatogr.*, 331 (1985) 313.
11 S. L. Abidi, T. L. Mounts and K. A. Rennick, *J. Liq. Chromatogr.*, 14 (1991) 573.
12 J. G. Turcotte, J. Y. Hsieh and D. K. Welch, *Lipids*, 16 (1981) 761, and references cited therein.
13 J. Y. Hsieh, D. K. Welch and J. G. Turcotte, *J. Chromatogr.*, 208 (1981) 398.
14 Y. Nakagawa and K. Waku, *J. Chromatogr.*, 381 (1986) 225.
15 L. A. Dethloff, L. B. Gilmore and G. E. R. Hook, *J. Chromatogr.*, 382 (1986) 79.

16 P. Juaneda and G. Rocquelin, *Lipids*, 21 (1986) 239.
17 A. G. Andrews, *J. Chromatogr.*, 336 (1984) 139.
18 H. P. Nissen and H. W. Kreysel, *J. Chromatogr.*, 276 (1983) 29.
19 M. Seewald and H. M. Eichinger, *J. Chromatogr.*, 469 (1989) 271.
20 R. W. Gross and B. E. Sobel, *J. Chromatogr.*, 197 (1980) 79.
21 A. Stolyhwo, M. Martin and G. Guiochon, *J. Liq. Chromatogr.*, 10 (1987) 1237.
22 J. L. Perrin and A. Prevot, *Rev. Fr. Corps Gras*, 11 (1986) 437.
23 W. W. Christie, *J. Lipid Res.*, 26 (1985) 507.
24 W. W. Christie, *J. Chromatogr.*, 361 (1986) 396.
25 P. Juaneda, G. Rocquelin and P. O. Astorg, *Lipids*, 25 (1990) 756.
26 W. M. A. Hax and W. S. M. Geurts van Kessel, *J. Chromatogr.*, 142 (1977) 735.
27 H. Colin and G. Guiochon, *J. Chromatogr.*, 141 (1977) 289.
28 M. C. Hennion, C. Picard and M. Caude, *J. Chromatogr.*, 166 (1978) 21.
29 S. L. Abidi, *J. Liq. Chromatogr.*, 12 (1989) 595.
30 S. L. Abidi, *J. Chromatogr.*, 362 (1986) 33.
31 S. L. Abidi, *J. Chromatogr.*, 255 (1983) 101.
32 Z. Iskandarani and D. J. Pietrzyk, *Anal. Chem.*, 53 (1981) 489.
33 P. C. White and A. M. Harbin, *Analyst (London)*, 114 (1989) 877.
34 S. L. Abidi, *J. Chromatogr.*, 288 (1984) 277.

Journal of Chromatography, 587 (1991) 205–212
Elsevier Science Publishers B.V., Amsterdam

CHROM. 23 592

Determination of Cyasorb UV 1084 and its degradation products in low-density polyethylene film by high-performance liquid chromatography

S. G. Matz

Quantum Chemical Corp., Allen Research Center, P.O. Box 429566, 11530 Northlake Drive, Cincinnati, OH 45249 (USA)

(First received December 4th, 1990; revised manuscript received June 21st, 1991)

ABSTRACT

A reversed-phase high-performance liquid chromatographic (HPLC) method utilizing a photodiode-array detector was developed that is capable of identifying and quantifying Cyasorb UV 1084, a UV light stabilizer, and some of its UV and thermal decomposition products in low-density polyethylene (LDPE) resins in the presence of common antioxidants and UV stabilizers. Isopropanol extracts Cyasorb UV 1084 from the LDPE concentrate at greater than 95% efficiency. The overall precision of the method is very good, the relative standard deviation being less than 4%. This HPLC method was used to determine Cyasorb UV 1084 in concentrates and manufactured films. It was found that the level of Cyasorb UV 1084 in concentrates was as expected and had not degraded. However, lower than specified levels of Cyasorb UV 1084 were found in the manufactured film and clear evidence for thermal decomposition products was observed. This loss of Cyasorb UV 1084 apparently caused a shorter film life.

INTRODUCTION

UV light stabilizers and antioxidants are added to polyethylene to protect it from thermal and oxidative degradation at the elevated processing temperatures and oxidative degradation caused by exposure to the UV radiation from sunlight [1].

Cyasorb UV 1084, [2,2′-thiobis(4-*tert.*-octylphenolato)]-*n*-butylaminenickel(II), is used in low-, medium- and high-density polyethylene and in polypropylene as a UV light absorber, an antioxidant and a dye acceptor. The phenolic portion of the compound makes it a good heat stabilizer, and it is used as a stabilizer against UV light because of its light-absorbing capability.

Low-density polethylene (LDPE), used in agricultural mulches, greenhouse films or packaging that will be exposed to the outdoors, contains Cyasorb UV 1084 to protect it against high temperatures and UV radiation from the sun. Studies have demonstrated that film containing Cyasorb UV 1084 is stable for 12 months in Florida, whereas the film without stabilizer will last only about 2.5 months before it becomes brittle [2].

In our tests, commercially available co-extruded cast film was used. This film has a black layer and a white layer. The white layer contains about 2% Cyasorb UV 1084. Certain films contained a dark streaking due to die drool and were judged to be a problem owing to discoloration at high temperatures and deterioration when exposed to the Florida sun. The streaks were analyzed by X-ray diffraction and found to be nickel sulfide, one of the thermal decomposition product of Cyasorb UV 1084. Atomic absorption spectrometric (AAS) and UV analysis implied that the Cyasorb UV 1084 was present at the level expected. Mass spectrometric analysis indicated no significant differences between good and problem films, each giving similar decomposition products of the Cyasorb UV 1084 on heating in the probe. Fig. 1 shows the structures of Cyasorb UV 1084 and other thermal decomposition

0021-9673/91/$03.50

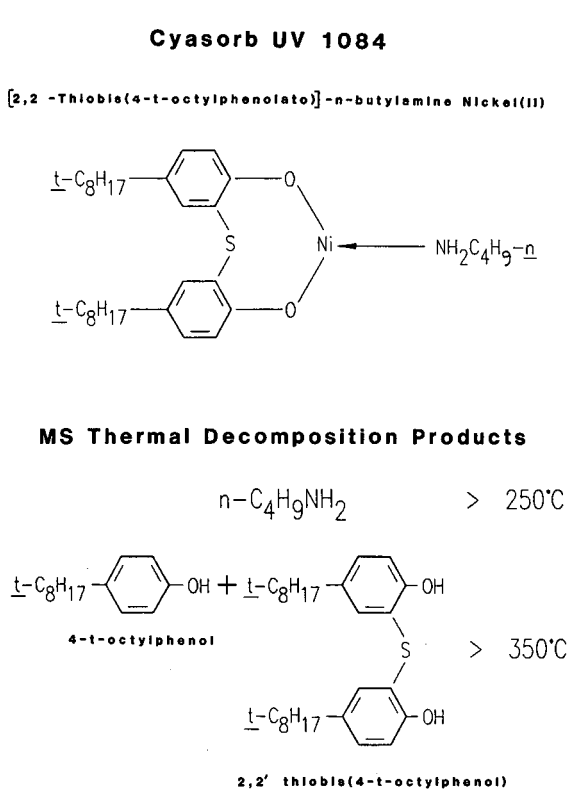

Fig. 1. Cyasorb UV 1084 and its thermal decomposition products identified by mass spectrometry. t = *tert.*

products determined by mass spectrometry. To understand what is occurring in the film, a high-performance liquid chromatographic (HPLC) method was developed to analyze for Cyasorb UV 1084 and its possible decomposition products in films and in concentrates, which comprise 20% of the white layer of the film.

EXPERIMENTAL

Chromatographic apparatus

The HPLC system used consists of a Model 712 WISP autosampler, a Model 600E gradient system with a column heater thermostated at 40°C, a Model 990 photodiode-array detector and an NEC Power Mate 2 data gathering station (Waters Assoc.). A Perkin-Elmer 3 × 3 C_{18} (3-μm particles) 3 cm × 4.6 mm I.D column was used. The mobile phase was either isopropanol–water–acetic acid (94.5:5.0:0.5) with isocratic elution at 2.0 ml/min, or a 2-min linear gradient at 1.0 ml/min from isopropanol–water–acetic acid (65:34.5:0.5) to isopropanol–acetic acid (99.5:0.5).

Chemicals

Cyasorb UV 1084 and 2,2-thiobis(4-*tert.*-octylphenol) were obtained from American Cyanamid (Wayne, NJ, USA), 4-*tert.*-octylphenol from Aldrich (Milwaukee, WI, USA), isopropanol (Omni-Solv) obtained from EM Science (Gibbstown, NJ, USA) and glacial acetic acid from Ashland Chemical (Columbus, OH, USA). Water was purified using a Milli-Q system (Millipore, Bedford, MA, USA).

Preparation of standard solutions

The standard solutions consisted of Cyasorb UV 1084, 2,2-thiobis(4-*tert.*-octylphenol) and 4-*tert.*-octylphenol dissolved in isopropanol. To dissolve the material completely, the solutions must be heated to about 40°C or placed in an ultrasonic bath.

Sample preparation

LDPE concentrate pellets or manufactured film were ground to 40 mesh using a Wiley mill. For those grinding experiments where liquid nitrogen was used to keep the samples from overheating, the sample pelets and film were ground in a liquid nitrogen-cooled Spex mill for 10 min. A 3-g sample of ground film or a 0.5-g sample of ground concentrate was refluxed with 100 ml of isopropanol for 1 h in a 250-ml flat-bottommed flask with a water-cooled condenser. For film samples, after cooling, the extract was filtered through a 0.2-μm filter. For concentrate samples, after cooling, the extract was diluted 1:10 with isopropanol before filtering to keep the Cyasorb UV 1084 signal in the linear calibration range.

Quantitative evaluation

Calibration graphs were constructed for each analyte in the concentration range 10–500 mg/l. A linear regression curve of concentration *versus* peak area was calculated. Eight complete replicate analyses were performed on two LDPE concentrates for the extraction recovery study for Cyasorb UV 1084 shown in Table I.

TABLE I

CYASORB UV 1084 RECOVERY STUDY

Extraction from an LDPE concentrate by refluxing with isopropanol for 1 h.

Concentrate	Parameter	Value
A	Mean Cyasorb UV 1084 (%)	9.69
	Standard deviation (%)	0.07
	Relative standard deviation (%)	0.72
	95% confidence limit for average (%)	9.69 ± 0.05
	n	8
B	Mean Cyasorb UV 1084 (%)	9.58
	Standard deviation (%)	0.38
	Relative standard deviation (%)	3.97
	95% confidence limit for average (%)	9.58 ± 0.33
	n	8

RESULTS AND DISCUSSION

Chromatographic separations

Cyasorb UV 1084 historically has been measured in polymers by determining nickel by AAS after ashing the polymer [3]. This method is fairly accurate and has the required sensitivity but lacks selectivity. Thus, all nickel-containing compounds in the polymer will be detected. This method, however, is not capable of determining the thermal decomposition products, 4-*tert.*-octylphenol and 2,2′-thiobis (4-*tert.*-octylphenol).

In 1977, an HPLC method was developed for the determination of Cyasorb UV 1084 [4]. A 1-g amount of powdered polyethylene sample was extracted for 6 h with 50 ml of chloroform. The extract was evaporated at low pressure and then dissolved in the mobile phase. It was separated on a Merkosorb Si 60 silica HPLC column using heptane–methylene chloride (2:1) as the mobile phase and a refractive index detector. A shorter extraction time and an improved separation of Cyasorb UV 1084 from interfering components were required to make the method practical for our purposes.

To improve the separation of Cyasorb UV 1084 from interfering antioxidants and its degradation products, a separation on a Perkin-Elmer 3 × 3 C_{18} column using isopropanol–water–acetic acid (94.5:5:0.5) at 2.0 ml/min as the mobile phase was developed. Acetate as acetic acid is added to sharpen any acid or phenolic components present in the sample. All components were detected at 226 nm, which is the absorbance maximum for Cyasorb UV 1084 in isopropanol. Using these isocratic conditions, Cyasorb UV 1084 produces a symmetrical but broad peak at 2.8 min.

Different separation conditions were needed to cause the 2,2′-thiobis(4-*tert.*-octylphenol) and 4-*tert.*-octylphenol peaks to be retained longer on the HPLC column and move them away from the solvent front. Using a Perkin-Elmer 3 × 3 C_{18} column, a 2-minute linear gradient at 1 ml/min provided the needed separation. The initial conditions were isopropanol–water–acetic acid (65:34.5:0.5) and the final conditions isopropanol–acetic acid (99.5:0.5). Fig. 2 is a chromatogram of a standard solution showing the separation of Cyasorb UV 1084, 2,2′-thiobis(4-*tert.*-octylphenol) and 4-*tert.*-octylphenol. Fig. 3 is a chromatogram of an extract from film 1 where 2,2′-thiobis(4-*tert.*-octylphenol) and Cyasorb UV 1084 can be seen. The first peak is the solvent front. The second peak is an unknown component, but is not 4-*tert.*-octylphenol. There are also a number of minor peaks that could possibly be impurities or other degradation products of the Cyasorb UV 1084. Using this gradient a number of common antioxidants and UV stabilizers can also be analyzed. Table II lists some common additives and their retention times. Early-eluting additives such as Irganox MD1024, Tinuvin P and Santanox R require a different gradient with initial conditions that are weaker than this gradient to produce retention on the column.

Using this gradient system, the baseline increases at wavelengths below 290 nm owing to increasing isopropanol absorption. Also, the Cyasorb UV

TABLE II

RETENTION TIMES (t_R) FOR COMMON POLYMER ADDITIVES

Additive	t_R (min)	Additive	t_R (min)
BHT	1.7	Irganox 1010	6.7
BHEB	2.0	Ethyl 330	7.0
Isonox 129	2.2	Irganox 1076	7.3
UV 531	4.0	Irgafos 168	7.7
Cyanox 1790	4.1	TNPP	8.8

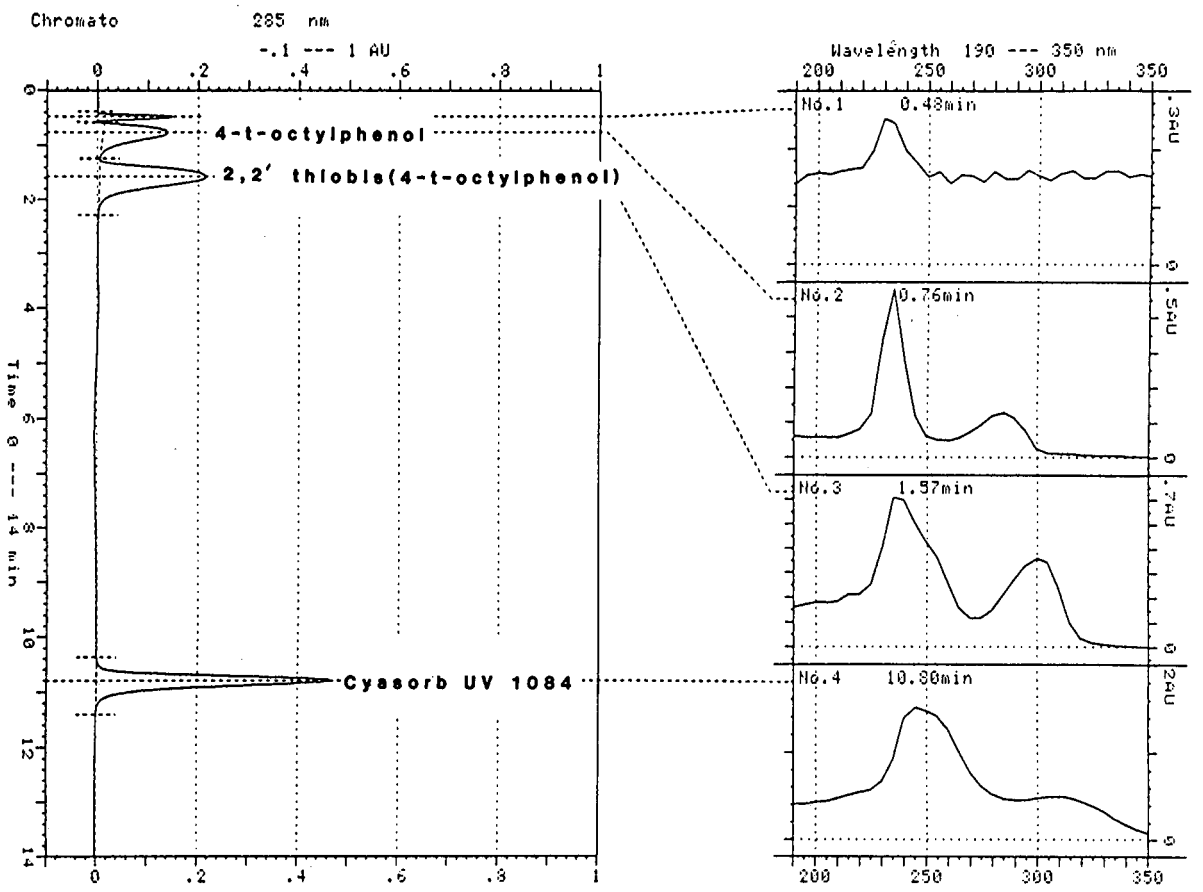

Fig. 2. Gradient separation of Cyasorb UV 1084 and two thermal decomposition products.

1084 signal drops significantly at wavelengths above 265 nm. A wavelength of 255 nm provides an acceptable compromise between background interference and component signal size. When using peak area to determine concentration, we found that peaks measured at 255 nm give the same results as those measured at 226 nm using the isocratic system. Hence, 255 nm was the wavelength chosen for determining Cyasorb UV 1084 and decomposition levels in a LDPE polymer.

Extraction

Various solvents were investigated for extracting Cyasorb UV 1084 from concentrates and films. Optimum extraction is achieved with a solvent that dissolves the component of interest and partially swells the polymer, enabling trapped component to be released. All extractions were carried out by reflux heating of sample ground to 40 mesh. Cyasorb UV 1084 is very soluble in polar chlorinated hydrocarbons such as methylene chloride and chloroform and non-polar hydrocarbons such as heptane and toluene. Methylene chloride was selected as one of the first solvents to try. Even after extended extraction times of up to 2 h, methylene chloride was found to be a poor extraction solvent. Also, solvent exchange was required before it could be injected onto the reversed-phase HPLC column owing to solvent immiscibility. Toluene, isopropanol, ethanol, methanol and acetonitrile were also investigated. Shaking with toluene at room temperature was found to extract about 90% of the Cyasorb UV 1084 from the colored concentrate but required solvent exchange before injection onto the reversed-

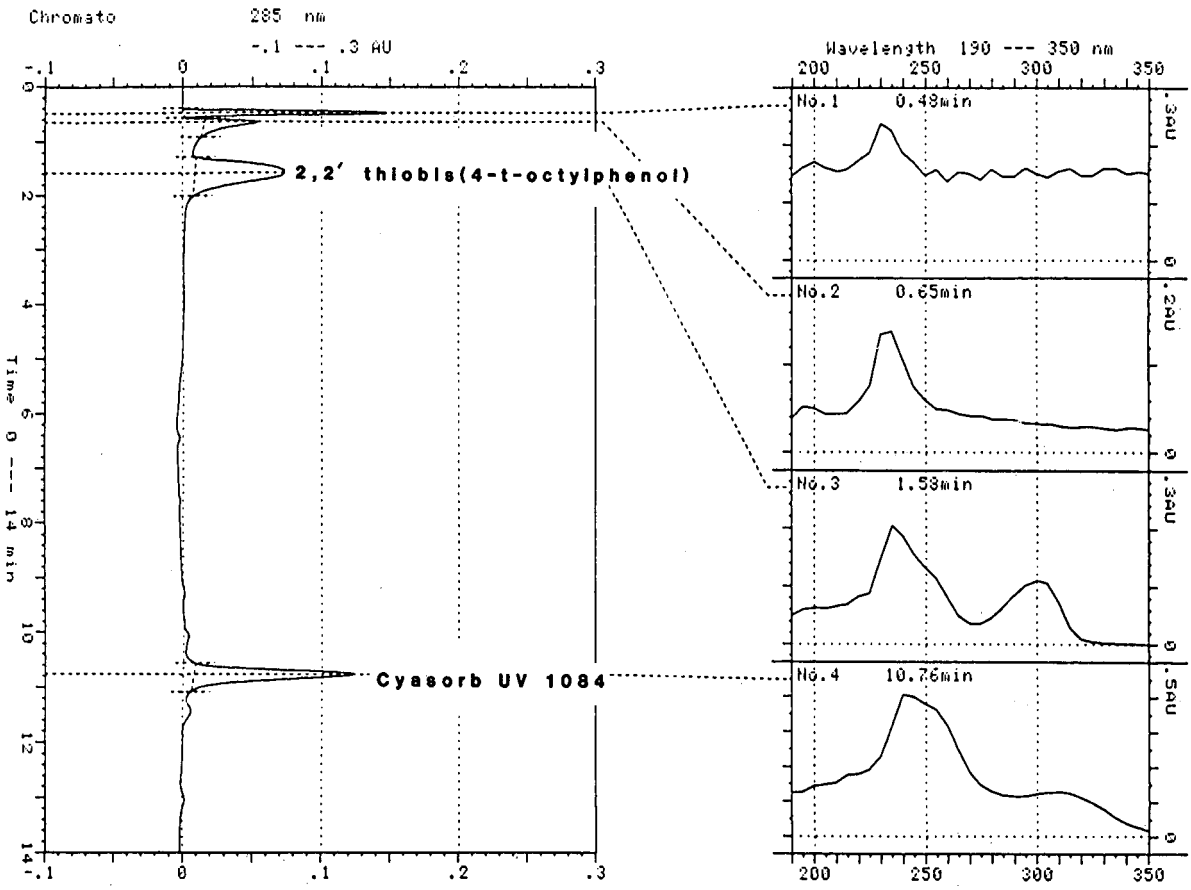

Fig. 3. Gradient separation of components in film 1 extract.

phase column. Typically, toluene can be diluted with a polar solvent such as methanol to cause the solution to be miscible with the mobile phase. In this instance the large solvent peak masks the two breakdown products even with weaker initial conditions of the gradient. Refluxing of LDPE with isopropanol for 1 h extracted 95% of the expected Cyasorb UV 1084 from the concentrate. A 2-h reflux failed to extract additional additive. To assure complete extraction, after refluxing the ground polymer was filtered from the extract, rinsed with fresh solvent, dried and refluxed a second time with fresh isopropanol. Table I shows the results for a single extraction of two concentrate samples, each containing about 10% of Cyasorb UV 1084. These data indicate that a single extraction is sufficient for the analysis. Previously extracted polymer samples were analyzed by AAS and IR spectrometry and verified that no Cyasorb UV 1084 remained after extraction. Acetonitrile and the other alcohols were found to have poorer extraction efficiencies than isopropanol. Therefore, isopropanol was chosen as the extraction solvent for Cyasorb UV 1084 in LDPE.

The co-extruded films were expected to contain 0.7–0.9% of Cyasorb UV 1084. All of the above solvents were tested using extraction times extended to 2 h owing to low recoveries. Using a 1-h isopropanol extraction only 0.44% of Cyasorb UV 1084 was found in film 1, which had not been exposed to weathering (Table III). Also, less than 10% of the expected Cyasorb UV 1084 was found in brittle weathered film 2. Film 3, the white layer of co-extruded film 1, was expected to contain about 1.8–

TABLE III

EXTRACTION RECOVERIES FOR AND AAS ANALYSIS OF THE FILM SAMPLES BEFORE AND AFTER EXTRACTION

Sample	Expected Cyasorb UV 1084 (%)	After extraction		Before extraction		
		Ni content found by AAS (ppm)	Cyasorb UV 1084 content based on Ni determination (%)	Ni content found by AAS (ppm)	Cyasorb UV 1084 content based on Ni determination (%)	Cyasorb UV 1084 found by HPLC (%)
Film 1	0.7–0.9	120	0.117	1001	0.974	0.440
Film 2	0.7–0.9	746	0.726	780	0.759	0.020
Film 3	1.8–2.0	180	1.75	1950	1.897	1.38

2.0% of Cyasorb UV 1084. This film was selected for analysis to determine if the carbon black or some other component in the black layer was impairing the extraction. Less than 50% of the expected amount was found as in the co-extruded films. Hence the components in the black layer do not appear to be the cause of the low recoveries of Cyasorb UV 1084. These results indicated either a poor extraction efficiency or possible degradation

Degradation of UV 1084

Film samples before and after extraction were submitted to nickel determination by AAS to determine the Cyasorb UV 1084 extraction efficiency. The results are given in Table III. All film samples before extraction had about the expected level of nickel. New film samples, 1 and 3, after extraction retained 9–12% of the original nickel. The weathered sample, film 2, still retained 95% of its original nickel. To determine if this residual nickel is due to the Cyasorb UV 1084, film 2 samples, before and after extraction, were analyzed by Fourier transform IR spectrometry. The extracted sample had no sharp band at 1600 cm^{-1} characteristic of Cyasorb UV 1084. Hence the nickel remaining in the film after extraction was not due to Cyasorb UV 1084 or its two decomposition products, 4-*tert.*-octylphenol and 2,2′-thiobis(4-*tert.*-octylphenol), as all would have a sharp aromatic band at 1600 cm^{-1}. As nickel sulfide was found in the films by X-ray diffraction, it is the most likely form of nickel in the films after extraction.

Two degradation products of Cyasorb UV 1084, 4-*tert.*-octylphenol and 2,2′-thiobis(4-*tert.*-octylphenol), were run on the isocratic HPLC system. When the spectrum of the early-eluting peak found in film extracts is superimposed on the spectrum of the two known degradation products there is a very good match of the unknown components and 2,2′-thiobis(4-*tert.*-octylphenol). This early-eluting peak was confirmed by mass spectrymetry to be 2,2′-thiobis(4-*tert.*-octylphenol).

In an attempt to degrade Cyasorb UV 1084, a solution of Cyasorb UV 1084 in isopropanol was placed in a quartz tube and irradiated with UV light for 48 h. No degradation was seen. The solution was then placed in a sunlit window, and within 4 weeks the Cyasorb UV 1084 had degraded. A chromatogram of this solution shows that the major component by retention time appears to be 2,2′-thiobis(4-*tert.*octylphenol) (Fig. 4). A normalized spectrum overlay of this component and 2,2′-thiobis(4-*tert.*-octylphenol) confirms its identity (Fig. 5). Mass spectrometric analysis also identified the major component in this solution as 2,2′-thiobis(4-*tert.*-octylphenol).

To be confident about our results, it was essential to know where the Cyasorb UV 1084 was breaking down: in the concentrate, in the film or during the analysis process. The various steps in the analysis where degradation could occur were examined. One possible cause fo the loss of the Cyasorb UV 1084 in the analysis is the milling step. During milling, the polymer can heat up, causing degradation and loss of certain additives. Samples were ground with and without liquid nitrogen cooling to determine whether the milling step was causing a breakdown of Cyasorb UV 1084. No significant difference was found between samples milled with or without liquid nitrogen. Another step where Cyasorb UV 1084 could

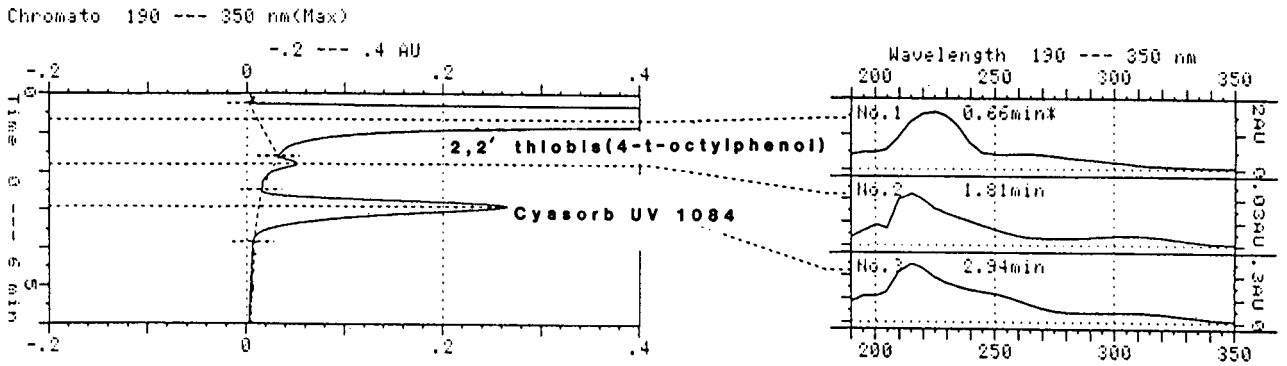

Fig. 4. Isocratic separation of the UV breakdown product of Cyasorb UV 1084.

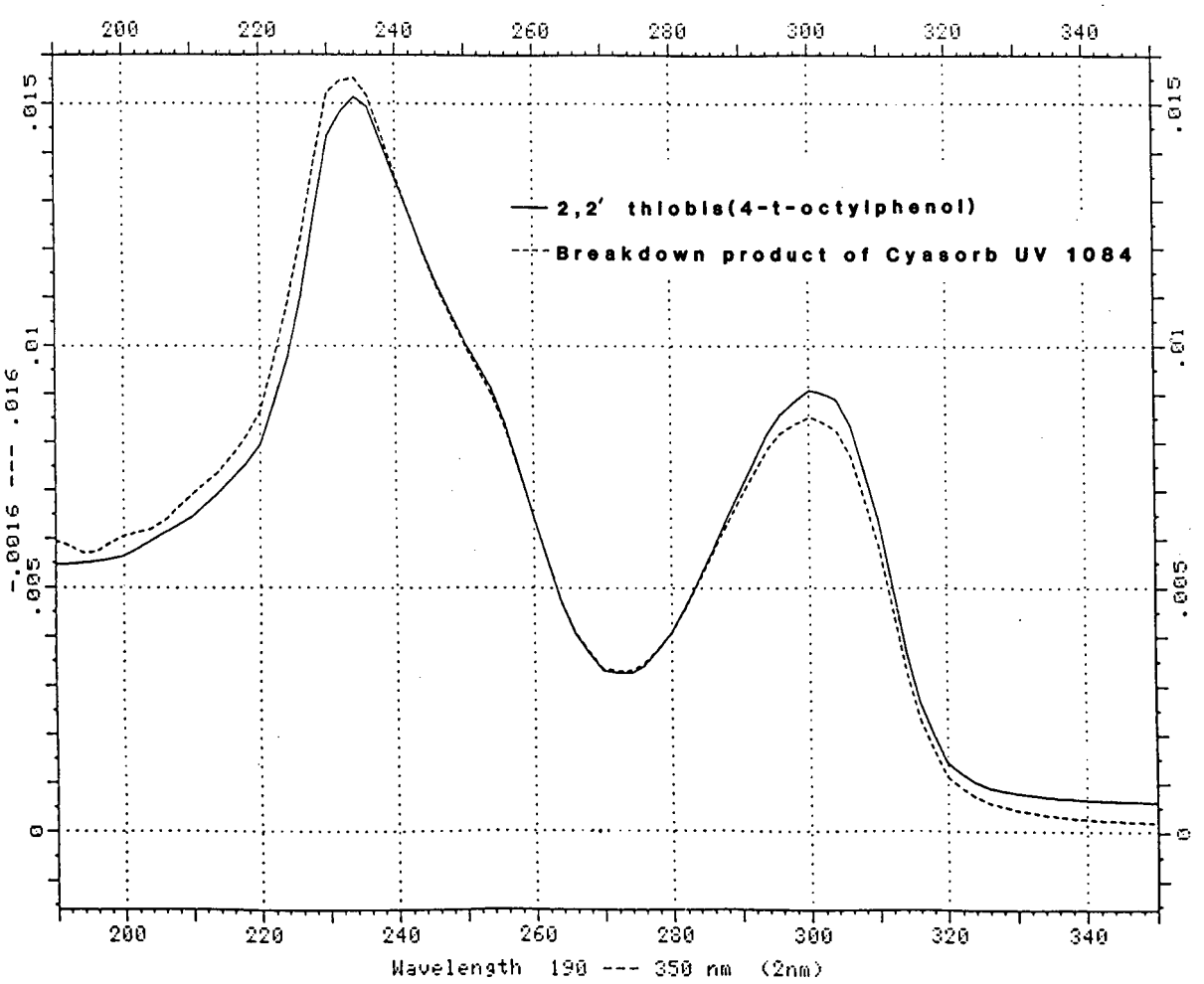

Fig. 5. Normalized overlay of the degradation product of Cyasorb UV 1084 and 2,2′-thiobis(4-*tert.*-octylphenol).

TABLE IV

CYASORB UV 1084 PRESENT IN NEW FILM DETERMINED BY AAS AND HPLC

All values in ppm.

Sample	AAS		HPLC	
	Ni level	Cyasorb UV 1084	Thiobis[a]	Cyasorb UV 1084
Film 4	847	8250	6870	110
Film 5	861	8390	3910	2280
Film 6	914	8900	4080	2250

break down is during the extraction. To check this, two experiments were run. Cyasorb UV 1084 was refluxed for 1 h in isopropanol and barefoot resin was refluxed for 1 h in an isopropanol solution containing Cyasorb UV 1084. No decrease in the Cyasorb UV 1084 signal or formation of degradation products was seen. We therefore found no evidence for Cyasorb UV 1084 degradation caused by the analytical procedure.

Solving the degradation problem

Using this HPLC method, we found no degradation in any of the concentrates used to make the films, but significant degradation was evident in film samples, including those not placed in sunlight. Hence we concluded that some of the Cyasorb UV 1084 degraded during the manufacture of the films. This resulted in lower than expected levels in the film, possibly causing early degradation of the films placed in sunlight. Table IV shows a comparison of the amount of Cyasorb UV 1084 in three new film samples based on their nickel contents determined by AAS and HPLC. Film 4 contains only 110 ppm of Cyasorb UV 1084 by HPLC or 1.3% of the original amount based on nickel results obtained by AAS; 83% degraded to 2,2′-thiobis(4-*tert.*-octylphenol) with the remaining 15.7% most likely being in an inorganic form such as nickel sulfide. Films 5 and 6 had 25–27% of the Cyasorb UV 1084 unchanged with 46–47% degrading to 2,2′-thiobis(4-*tert.*-octylphenol) and the remainder probably being present in an inorganic form.

CONCLUSIONS

Reversed-phase HPLC with photodiode-array detection is capable of separating, identifying and determining Cyasorb UV 1084 and its decomposition products, 4-*tert.*-octylphenol and 2,2′-thiobis (4-*tert.*-octylphenol). The extraction efficiency of Cyasorb UV 1084 from LDPE concentrates using isopropanol is greater than 95% with a relative standard deviation of less than 4%. This method is also capable of complete extraction of the Cyasorb UV 1084 and two of its major decomposition products in films.

Using this method, it was determined that the Cyasorb UV 1084 was unaltered and at the expected level in the concentrates. However, it had partially degraded to 2,2′-thiobis(4-*tert.*-octylphenol) during production of the film, which resulted in faster deterioration of the films when exposed to sunlight.

REFEFERENCES

1 R. G. Lichtenthaler and R. Ranfelt, *J. Chromatogr.*, 149 (1978) 553–560.
2 *Technical Bulletin D-43*, American Cyanamid Company, Polymer Products Division, Wayne, NJ, 1985.
3 T. R. Crompton, *Chemical Analysis of Additives in Plastics*, Vol. 46, Pergamon Press, Oxford, 2nd ed., 1975, pp. 17–29.
4 M. Dengreville, *Analysis*, 5 (1977) 195–202.

Journal of Chromatography, 587 (1991) 213–228
Elsevier Science Publishers B.V., Amsterdam

CHROM. 23 484

Hydrogen bonding

XVI. A new solute solvation parameter, π_2^H, from gas chromatographic data

Michael H. Abraham* and Gary S. Whiting

Department of Chemistry, University College London, 20 Gordon Street, London WC1H 0AJ (UK)

Ruth M. Doherty

Naval Surface Warfare Center, White Oak Laboratory, Silver Spring, MD 20910 (USA)

Wendel J. Shuely

US Army Chemical Research, Development and Engineering Center, Aberdeen Proving Ground, MD 21010 (USA)

(First received February 19th, 1991; revised manuscript received May 23rd, 1991)

ABSTRACT

The general solvation equation,

$\log V_G^0$ (or $\log L$) $= c + rR_2 + s\pi_2^H + a\alpha_2^H + b\beta_2^H + l \log L^{16}$

has been used to set up a new π_2^H parameter of solute dipolarity–polarisability, mainly through the extensive data of McReynolds and Patte *et al.* Values of π_2^H are tabulated for several hundred solutes, and two simple rules have been formulated to enable π_2^H to be estimated for many types of aliphatic functionally substituted compounds. A coherent set of effective solvation parameters, $\Sigma\pi_2^H$, $\Sigma\alpha_2^H$, $\Sigma\beta_2^H$, and also R_2 and $\log L^{16}$, allows the application of the general solvation equation to the characterisation of any gas–liquid chromatographic stationary phase.

INTRODUCTION

Previously, we have shown [1–3] that processes in which a solute is distributed between the gas phase and some condensed phase can usefully be described through the general solvation equation

$$\log SP = c + rR_2 + s\pi_2^* + a\alpha_2^H + b\beta_2^H + l \log L^{16} \quad (1)$$

Such processes include the solubility of a series of gaseous solutes in a given solvent [2], and chromatographic processes in which retention data are obtained for a series of compounds on a given stationary phase, at some constant temperature [3].

As regards gas–liquid chromatography (GLC), the dependent variable in eqn. 1 can be $\log L$ (or $\log K$), where L (or K) is the Ostwald solubility coefficient or gas–liquid partition coefficient, $\log V_G$, where V_G is either the specific retention volume referred to 273 K or the specific retention volume at the column temperature, or even $\log \tau$, where τ is the adjusted relative retention time [3]. All these dependent variables will give rise to the same values of

0021-9673/91/$03.50

r, s, a, b and l in eqn. 1, but will yield different values of the constant term. The explanatory variables in eqn. 1 are R_2, an excess molar refraction that can be determined experimentally [1], π_2^*, the solute dipolarity–polarisability, to which we shall refer later, α_2^H, an experimentally determined solute hydrogen-bond acidity [4], β_2^H, an experimentally determined solute hydrogen-bond basicity [5], and log L^{16}, where L^{16} is the solute Ostwald solubility coefficient on hexadecane at 298 K [6].

Of course, values of R_2, α_2^H, β_2^H and log L^{16} can be obtained through various approximations and estimations, all based on the original experimentally determined values. There are, however, difficulties with the solute parameter π_2^*. Originally [7,8] π_2^* was taken as identical with the Kamlet–Taft solvatochromic solvent parameter π_1^* for non-associated liquids only. As π_1^* is experimentally accessible only for compounds that are liquid at 298 K, values of π_2^* had then to be estimated not only for all associated compounds (including acids, alcohols, phenols and amides), but also for all compounds that are solid (or gaseous) at 298 K. In addition, there is present the inherent assumption that π_1^* is identical with π_2^* for non-associated liquids. We know that the Kamlet–Taft solvatochromic solvent basicity parameter β_1 is not exactly equivalent to the solute parameter β_2^H even for non-associated liquids [9], and it is possible that although π_2^* can be taken as equal to π_1^* for non-associated liquids as a generality, there may be a number of exceptions to this rule.

It seems necessary to set up a scale of solute dipolarity–polarisability based on some experimental procedure that will include, at least in principle, all types of solute molecule. The main purpose of this paper is to use the extensive sets of GLC data of McReynolds [10] and Patte *et al.* [11] to construct a new solute dipolarity–polarisability scale π_2^H for use in eqn. 1. At the same time, we shall set out an updated list of solute parameters that can be used in eqn. 1 to characterise GLC stationary phases and to interpret GLC retention data.

Since this work was started, Li *et al.* [12] have also concluded that the π_2^* scale derived from π_1^* is not very suitable for use in solvation equations such as eqn. 1, and have constructed an alternative π_2^c scale of solute dipolarity. We shall refer to this scale later.

RESULTS

McReynolds [10] determined V_G^0 values for up to 376 solutes on up to 77 stationary phases. Nearly all the phases were examined at a common temperature of 120°C. Of these 77 phases, 75 were found [3] to have no hydrogen-bond acidity at all, hence the $b\beta_2^H$ term in eqn. 1 drops out, and the log V_G^0 values can be correlated by the equation

$$\log V_G^0 = c + rR_2 + s\pi_2^* + a\alpha_2^H + l \log L^{16} \qquad (2)$$

We thus have a series of equations (n = 1–75), one for each stationary phase, where the constants c, r, s, a and l have been determined by multiple linear regression analysis (MLRA), using known values of the solute parameters R_2, π_2^*, α_2^H and log L^{16} for as many solutes as possible. Typically, around 150 solutes were included in each regression eqn. 2, generalised as

$$\log V_{G(n)}^0 = c_n + r_n R_2 + s_n \pi_2^* + a_n \alpha_2^H + l_n \log L^{16} \qquad (3)$$

It is convenient to subsume the constant c_n into the dependent variable to give 75 equations:

$$\begin{aligned} V_{n-1} &= r_{n-1}R_2 + s_{n-1}\pi_2^* + a_{n-1}\alpha_2^H + l_{n-1}\log L^{16} \\ &\vdots \\ V_{n-75} &= r_{n-75}R_2 + s_{n-75}\pi_2^* + a_{n-75}\alpha_2^H + \\ &\qquad l_{n-75}\log L^{16} \end{aligned} \qquad (4)$$

where

$$V_n = \log V_{G(n)}^0 - c_n \qquad (5)$$

We can now use the matrix defined by eqn. 4 in a vertical format, by regarding V_n for a given solute as the dependent variable and the constants r_n, s_n, a_n and l_n as four explanatory variables. In this new (vertical) MLR equation, R_2, π_2^*, α_2^H and log L^{16} for the particular solute now become the unknown coefficients to be evaluated by MLRA. As all the input data are now related purely to properties of the solute, we can replace π_2^* with an experimentally determined parameter, π_2^H:

$$V(\text{solute}) = V_n = R_2 r_n + \pi_2^H s_n + \alpha_2^H a_n + \log L^{16} l_n \qquad (6)$$

We carried out an analysis using eqn. 6, where the regression equation was forced through the origin, and obtained reasonable values of R_2, π_2^H, α_2^H and log L^{16} for the various solutes studied. However, as R_2

TABLE I

SOME CALCULATED PARAMETERS USING EQN. 7

Solute	π_2^H	α_2^H	Log L^{16}	n	S.D.
Pent-1-ene	0.09 ± 0.004 0.08[a]	0.00 ± 0.007 0.00[a]	2.040 ± 0.007 2.013[a]	36	0.014
Toluene	0.47 ± 0.004 0.55[a]	−0.01 ± 0.007 0.00[a]	3.327 ± 0.008 3.344[a]	73	0.017
Diethyl ether	0.27 ± 0.004 0.27[a]	−0.02 ± 0.007 0.00[a]	1.975 ± 0.008 2.061[a]	71	0.017
Butanone	0.69 ± 0.004 0.67[a]	0.00 ± 0.007 0.00[a]	2.282 ± 0.007 2.287[a]	71	0.016
n-Propyl acetate	0.61 ± 0.004 0.55[a]	0.00 ± 0.007 0.00[a]	2.847 ± 0.007 2.878[a]	73	0.016
Propan-1-ol	0.41 ± 0.009 0.40[a]	0.37 ± 0.006 0.33[a]	2.060 ± 0.006 2.097[a]	72	0.016

[a] Previous values, see ref. 1.

is either known or can easily be calculated for any solute[a], we can reduce the number of explanatory variables by incorporating R_2 into the dependent variable:

$$\log V^0_{G(n)} - c_n - r_n R_2 = V' = \pi_2^H s_n + \alpha_2^H a_n + \log L^{16} l_n \quad (7)$$

Again, the regression eqn. 7 is constrained to pass through the origin; we found that the results were much more self-consistent than when a constant term was allowed to float. We can check results using our preferred eqn. 7 by comparison of calculated solute parameters with known values, where available. Some typical results are given in Table I together with the standard deviation (S.D.) of the parameter, the number of stationary phases in the set (always less than 75, because not all solutes were examined on all phases by McReynolds), and the overall S.D. of the dependent variable V'. We do not give correlation coefficients because these have little meaning for a regression equation forced through the origin.

There are a number of deficiencies in McReynolds' data, especially those connected with interfacial adsorption, and it is clear that for certain combinations of solute and stationary phase, the retention data are inexact owing to sorption at the liquid interface. Hydrocarbons in very polar phases are a particularly well known example. We point out, however, that our vertical or "inverse" MLRA procedure yields solvation parameters that are effectively averages for a given solute over 30–70 stationary phases (see Table I). In the event, hydrocarbons such as alkanes and alkenes behave normally in our inverse MLRA (see Table II).

We list in Table II the π_2^H values that we obtained through eqn. 7. We note that the π_2^H values in Table II are effective π_2^H values for a situation in which a solute molecule is surrounded by an excess of solvent molecules, and so may be more correctly denoted as $\Sigma\pi_2^H$. Before discussing these π_2^H values, we first analyse the extensive GLC data of Patte *et al.* [11].

Patte *et al.* [11] obtained retention data for 240 solutes on five stationary phases. All these phases are non-acidic, and so we obtained [1] five regression equations of the following type, one for each phase:

$$\log L' = c + rR_2 + s\pi_2^* + a\alpha_2^H + l \log L^{16} \quad (8)$$

In eqn. 8, $\log L' = \log L - \log L(\text{decane})$, but this affects only the constant in the regression equations. We cannot apply the "reverse" MLRA we used for the McReynolds data set, because we would have

[a] Like the molar refraction itself, R_2, an excess molar refraction, is almost an additive quantity.

TABLE II

CALCULATED VALUES OF π_2^H AND LOG L^{16} VALUES

Compound	π_2^H			Log L^{16}	Compound	π_2^H			Log L^{16}
	Eqn. 7	Eqn. 16	Eqn. 8			Eqn. 7	Eqn. 16	Eqn. 8	
Alkanes					*Ethers (contined)*				
Ethane		0.03	0.11	0.492	Dibutyl ether	0.24	0.16	0.18	3.924
Propane		0.03	0.08	1.050	Dipentyl ether	0.27			4.875
Butane		0.03	0.05	1.615	Di-3-methylbutyl ether	0.21			4.538
2-Methylpropane		0.07	0.07	1.409	Dihexyl ether	0.27			5.938
Pentane		0.03	0.03	2.162	Di-2-ethyl-1-butyl ether	0.17			5.421
Hexane	0.02	0.03	0.02	2.688	Methyl propyl ether	0.30			2.090
2,3-Dimethylbutane	−0.01			2.495	Methyl butyl ether	0.30			2.630
Heptane		0.03	0.01	3.173	Methyl 2-methylpropyl ether	0.25			2.442
2,4-Dimethylpentane		−0.04	−0.02	2.809	Methyl *tert.*-butyl ether	0.29			2.378
Octane	0.01	0.03	0.00	3.677	Ethyl butyl ether	0.26			2.989
2-Methylheptane		0.08	0.01	3.480	Ethyl *tert.*-butyl ether	0.20			2.611
3-Methylheptane		0.07	0.03	3.510	Propyl isopropyl ether	0.19			2.771
Nonane		0.03	0.00	4.182	Isopropyl *tert.*-butyl ether	0.16			2.896
2,2,5-Trimethylhexane		0.16		3.530	Bis(2-ethoxyethyl)ether	0.79			4.592
Decane	0.03	0.03	−0.01	4.686	Ethyl vinyl ether	0.37			1.910
Undecane		0.03	−0.02	5.191	Butyl vinyl ether	0.34			2.970
Dodecane	0.03	0.03	0.03	5.696	2-Methylpropyl vinyl ether	0.29			2.746
Tridecane		0.03	−0.04	6.200	2-Ethyl-1-hexyl vinyl ether	0.32			4.682
Tetradecane	0.05	0.03	−0.03	6.705	2-Methoxyethyl vinyl ether	0.68			2.932
Hexadecane	0.07			7.714	Diallyl ether	0.38			2.430
Octadecane	0.05			8.722	Ethylene oxide	0.59			1.371
Cyclohexane		0.08	0.14	3.007	1,2-Propylene oxide	0.57			1.775
Hydrindane		0.19	0.22	4.530	1,2-Butylene oxide	0.55			2.350
Decalin		0.23	0.27	5.077	2-Methyl-1,2-propylene oxide	0.52			2.050
Alkenes					*trans*-2,3-Butylene oxide	0.52			2.140
Ethene		−0.13	0.32	0.289	*cis*-2,3-Butylene oxide	0.55			2.290
Propene		−0.09	0.25	0.946	1,3-Propylene oxide	0.61			2.086
But-1-ene		−0.05	0.21	1.491	1,3-Butylene oxide	0.52			2.360
Pent-1-ene	0.09	−0.05	0.19	2.047	Furan	0.54	0.39	0.51	2.140
Hex-1-ene		0.00	0.11	2.572	2-Methylfuran	0.50			2.430
Hept-1-ene		0.06	0.11	3.063	2-Acetyl-3-methylfuran		1.17		
Oct-1-ene		0.08	0.09	3.568	2-Acetyl-5-methylfuran		1.19		
cis-Oct-2-ene		0.11	0.12	3.683	2-Propanoyl-3-methylfuran		0.91		
2-Ethylhex-1-ene		0.16	0.13	3.510	Tetrahydrofuran	0.55			2.636
α-Pinene		0.30	0.18	4.200	2-Methyltetrahydrofuran	0.47			2.820
					2,5-Dimethyltetrahydrofuran	0.38			2.980
					1,4-Dioxane	0.75	0.69	0.74	2.892

Alkynes				
But-2-yne		0.17	0.37	1.856
Oct-1-yne		0.19	0.23	3.480
Oct-2-yne		0.16	0.31	3.850
Haloaliphatics				
1-Fluorooctane		0.30		3.850
Dichloromethane	0.66			2.019
Trichloromethane	0.65	0.25	0.36	2.480
Tetrachloromethane	0.35	0.28	0.35	2.823
1,2-Dichloroethane	0.74	0.35	0.55	2.573
1,1,2,2-Tetrachloroethane		0.32	0.65	3.803
1-Chlorohexane		0.27	0.36	3.710
Trichloroethene		0.34	0.33	2.997
Hexachlorobutadiene		0.62		
Bromoethane		0.30	0.42	2.120
1-Bromopentane		0.30	0.39	3.611
2-Bromooctane		0.33	0.28	5.110
Iodomethane		0.35	0.44	2.106
1-Iodobutane		0.38	0.39	3.628
2-Iodobutane		0.40	0.39	3.390
1,1-Difluorotetrachloroethane		0.41		2.970
1,2-Difluorotetrachloroethane		0.41	0.33	3.000
Aromatic hydrocarbons				
Benzene	0.48	0.53	0.47	2.803
Toluene	0.47	0.57	0.46	3.344
Ethylbenzene	0.47	0.56	0.46	3.789
o-Xylene	0.50	0.63	0.43	3.942
m-Xylene	0.47	0.60	0.46	3.864
p-Xylene	0.46	0.61	0.46	3.836
1,3,5-Trimethylbenzene		0.64	0.46	4.316
1,2-Diethylbenzene	0.50			4.690
1,3-Diethylbenzene	0.48			4.680
1,4-Diethylbenzene	0.47			4.680
Styrene		0.70	0.55	3.863
Phenylethyne		0.55	0.68	3.715
Haloaromatics				
1,2-Dichlorobenzene		0.65	0.70	4.489
Benzylchloride		0.69	0.78	4.320
Ethers				
Dimethyl ether	0.36			1.285
Diethyl ether	0.27	0.19	0.27	2.015
Dipropyl ether	0.23			2.954
Diisopropyl ether	0.16			2.482
Tetrahydropyran	0.49			3.057
3,4-Dihydropyran	0.51			2.910
Trioxane	1.02			2.650
Trimethyltrioxane (paraldehyde)	0.68			3.169
2-Methyl-2-ethyl-1,3-dioxolane	0.58			3.337
Anethole		1.02		
Dimethoxymethane	0.52			1.894
Methoxyethoxymethane	0.49			2.371
Methoxyisopropoxymethane	0.45			2.697
Diethoxymethane	0.45			2.789
Ethoxypropoxymethane	0.44			3.280
Ethoxyisopropoxymethane	0.41			3.093
Ethoxy-*sec.*-butyloxymethane	0.41			3.609
Dipropyloxymethane	0.42			3.762
Propoxy-*sec.*-butyloxymethane	0.40			4.037
Diisopropoxymethane	0.37			3.376
Dibutyloxymethane	0.43			4.726
Diisobutyloxymethane	0.37			4.331
Di-*sec.*-butyloxymethane	0.37			4.380
1,1-Dimethoxyethane	0.49			2.334
1,1-Diethoxyethane	0.41			3.066
1,1-Dipropoxyethane	0.37			3.964
1,1-Diisobutyloxyethane	0.26			4.491
1,1-Dimethoxypropane	0.46			2.841
1,1-Diethoxypropane	0.38			3.498
1,1-Dimethoxybutane	0.47			3.313
1,1-Dimethoxy-2-methylpropane	0.42			3.148
2,2-Dimethoxypropane	0.43			2.699
2,2-Diethoxypropane	0.32			3.304
1,1,3-Trimethoxybutane	0.69			3.962
Methyl phenyl ether		0.73	0.70	3.859
1,8-Cineole		0.47		4.290
Aldehydes				
Formaldehyde	0.73			0.730
Acetaldehyde	0.70	0.63	0.65	1.230
Propanal	0.65	0.59	0.62	1.815
Butanal	0.63	0.61	0.61	2.270
2-Methylpropanal	0.58	0.59	0.59	2.120
Pentanal	0.63			2.851
2-Methylbutanal	0.58			2.733
3-Methylbutanal	0.60	0.62	0.58	2.620
2,2-Dimethylpropanal	0.49			2.406
Hexanal	0.64	0.59	0.59	3.370
Heptanal	0.65	0.58	0.59	3.860
Octanal		0.57	0.57	4.380

(Continued on p. 218)

TABLE II *(continued)*

Compound	π_2^H			Log L^{16}
	Eqn. 7	Eqn. 16	Eqn. 8	
Aldehydes (continued)				
2-Ethylhexanal	0.56			4.179
Prop-2-ene-1-al (acrolein)	0.74	0.68	0.58	1.656
trans-But-2-ene-1-al	0.81	0.85	0.75	2.570
2-Methylprop-2-ene-1-al (methacrolein)	0.62			2.180
trans-Hex-2-ene-1-al		0.88	0.85	
2-Ethylbut-2-ene-1-al	0.68			3.436
trans-Hept-2-ene-1-al		0.85	0.84	
trans-Oct-2-ene-1-al		0.55		
2-Ethylhex-2-ene-1-al	0.62			4.371
Hexa-2,4-dienal	0.90			3.800
Furfural		0.97	1.05	3.262
Benzaldehyde		0.99	0.94	3.985
3-Methoxybutanal	0.85			
Ketones				
Propanone	0.73	0.77	0.66	1.696
Butanone	0.69	0.72	0.66	2.287
Pentan-2-one	0.66	0.70	0.66	2.755
Pentan-3-one	0.64			3.271
3-Methylbutan-2-one	0.63			2.692
Hexan-2-one	0.67	0.71	0.65	3.262
Hexan-3-one	0.62	0.65	0.58	3.271
3-Methylpentan-2-one	0.62			3.163
4-Methylpentan-2-one	0.62			3.089
3,3-Dimethylbutan-2-one	0.58			2.928
Heptan-2-one	0.67	0.69	0.64	3.760
Heptan-3-one	0.62			3.776
Heptan-4-one	0.61			3.705
4,4-Dimethylpentan-2-one	0.57			3.344
2,4-Dimethylpentan-3-one	0.52			3.403
Octan-2-one	0.68	0.68	0.65	4.257
Nonan-2-one	0.68	0.69	0.64	4.735
Nonan-5-one	0.61			4.698
Decan-2-one		0.67	0.65	5.245
Undecan-2-one		0.67	0.64	5.732
Dodecan-2-one		0.67	0.64	6.167
Cyclopentanone	0.84	0.83	0.86	3.221
Cyclohexanone	0.84	0.87	0.87	3.792
Cycloheptanone		0.84	0.86	4.376
Esters (continued)				
2-Ethyl-1-hexyl acetate	0.60			5.025
Cyclohexyl acetate	0.69			4.454
Methyl propanoate	0.62	0.56	0.58	2.431
Ethyl propanoate	0.58			2.807
Propyl propanoate	0.57			3.338
Isopropyl propanoate	0.52			3.028
Butyl propanoate	0.57			3.883
Isobutyl propanoate	0.54			3.635
Pentyl propanoate	0.58			4.331
3-Methylbutyl propanoate	0.56			4.153
2-Pentyl propanoate	0.52			4.024
2-Ethyl-1-hexylpropanoate	0.55			5.486
Methyl butanoate	0.61			2.893
Ethyl butanoate	0.56			3.271
Propyl butanoate	0.56	0.54	0.51	3.783
Isopropyl butanoate	0.51			3.482
Butyl butanoate	0.56			4.275
Isobutyl butanoate	0.54			4.097
Pentyl butanoate	0.57			4.764
3-Methylbutyl butanoate	0.55			4.597
2-Pentyl butanoate	0.51			4.472
2-Ethyl-1-hexyl butanoate	0.57			5.856
Methyl isobutanoate	0.56			2.636
Butyl isobutanoate	0.51			4.068
Isobutyl isobutanoate	0.49	0.56	0.46	3.885
3-Methylbutyl isopentanoate		0.55	0.55	4.371
Allyl formate	0.76			2.256
Allyl acetate	0.72			2.723
Allyl propanoate	0.67			3.241
Vinyl acetate	0.66			2.152
Vinyl butanoate	0.56			3.191
1-Propenyl acetate	0.67			2.741
Isopropenyl acetate	0.68			2.611
Methyl acrylate	0.68			2.360
Ethyl acrylate	0.64			2.758
2-Ethyl-1-hexyl acrylate	0.61			5.445
Propyl acrylate	0.62			3.260
Butyl acrylate	0.62			3.790
Methyl methacrylate	0.62			2.880

Cyclo-octanone		0.83	0.85	4.981
Cyclononanone		0.83	0.84	5.537
Cyclodecanone		0.83	0.84	6.063
Cycloundecanone		0.83	0.83	6.621
Cyclododecanone		0.83	0.83	7.222
Cyclotridecanone		0.82	0.82	7.783
Cyclotetradecanone		0.82	0.82	8.334
Carvone		0.86	0.98	5.330
But-3-ene-2-one	0.76			2.330
3-Methylbut-3-ene-2-one	0.68			2.691
Hex-5-ene-2-one	0.75			3.181
4-Methylpent-3-ene-2-one	0.70			3.300
Butane-2,3-dione	0.52	0.71	0.74	1.639
Pentane-2,3-dione	0.47			2.209
Pentane-2,4-dione	0.56			2.772
Acetophenone		1.09	0.99	4.483
Esters				
Methyl formate	0.72			1.285
Ethyl formate	0.67			1.845
Propyl formate	0.65	0.56	0.60	2.443
Isopropyl formate	0.62			2.230
Butyl formate	0.66			2.958
Isobutyl formate	0.62			2.789
sec.-Butyl formate	0.61			2.730
Pentyl formate	0.66			3.448
2-Pentyl formate	0.60			3.250
3-Pentyl formate	0.60			3.226
Hexyl formate	0.67			3.970
Methyl acetate	0.67	0.63	0.61	1.911
Ethyl acetate	0.62	0.60	0.59	2.314
Propyl acetate	0.61	0.60	0.57	2.819
Isopropyl acetate	0.57			2.546
Butyl acetate	0.61	0.59	0.58	3.353
Isobutyl acetate	0.58			3.161
sec.-Butyl acetate	0.56			3.054
tert.-Butyl acetate	0.50			2.802
Pentyl acetate	0.62	0.58	0.59	3.844
3-Methylbutyl acetate	0.60	0.59	0.53	3.740
2-Pentyl acetate	0.56			3.568
3-Pentyl acetate	0.56			3.679
2-Methyl-2-butyl acetate	0.51			3.340
Hexyl acetate	0.63			4.351
4-Methyl-2-pentyl acetate	0.55			3.822
2-Ethyl-1-butyl acetate	0.60			4.178
Heptyl acetate	0.63			4.865
Allyl acrylate	0.72			3.160
2-Methoxyethyl acetate	0.93			3.290
2-Ethoxyethyl acetate	0.87	0.68	0.79	3.747
3-Methoxy-1-butyl acetate	0.83			4.048
3-Methoxy-1-butyl acrylate	0.83			4.048
Methylene diacetate	1.16			3.419
Ethylene diacetate	1.20			3.937
Ethylene dipropanoate	1.05			4.914
Propylene diacrylate	1.10			4.979
Benzyl acetate		1.19	0.95	4.991
Methyl benzoate		0.77	1.11	4.634
Methyl salicylate		0.82		
Nitro compounds				
Nitromethane		0.73	0.86	1.892
Nitroethane		0.74	0.87	2.414
1-Nitropropane		0.71	0.86	2.894
2-Methyl-2-nitropropane		0.82	0.82	2.710
3-Nitrotoluene		1.08	1.05	5.062
Nitriles				
Acetonitrile		0.80	0.85	1.739
1-Cyanopropane		0.78	0.84	2.604
1-Cyanobutane		0.80	0.83	3.108
Benzonitrile		1.05	1.04	4.004
Amines				
sec.-Butylamine		0.21	0.47	2.410
Allylamine		0.29		2.268
Trimethylamine		0.47		1.620
Heterocyclics				
Pyridine		0.80	0.80	3.003
2,3,6-Trimethylpyridine		0.71		4.200
Pyrrole		0.61	0.65	2.865
Trimethylpyrazine		0.77		
2-Methyl-3-ethylpyrazine		0.73		
2-Methoxy-3-isobutylpyrazine		0.56		
2,4,5-Trimethyloxazole		0.68		
Carboxylic acids				
Acetic acid		0.68		1.750
Propanoic acid		0.60		2.290
Butanoic acid		0.56		2.830
2-Methylpropanoic acid		0.58		2.670
Pentanoic acid		0.58		3.380
2-Methylbutanoic acid		0.55		3.260
3-Methylbutanoic acid		0.56		3.140

(Continued on p. 220)

TABLE II *(continued)*

Compound	π_2^H			Log L^{16}
	Eqn. 7	Eqn. 16	Eqn. 8	
Carboxylic acids (continued)				
Hexanoic acid		0.62		3.920
2-Methylpentanoic acid		0.68		3.680
Heptanoic acid		0.58		4.460
Octanoic acid		0.56		5.000
Nonanoic acid		0.53		5.550
Decanoic acid		0.50		6.090
Undecanoic acid		0.46		6.640
Dodecanoic acid		0.43		7.180
3-Butenoic acid		0.62		
Phenyls				
2-Chlorophenol		0.66		4.937
Salicylaldehyde		0.98		4.750
Hydroxylic compounds				
Water	0.40			0.260
Methanol	0.39	0.46		0.970
Ethanol	0.40	0.41		1.485
Propan-1-ol	0.41	0.42		2.031
Butan-1-ol	0.42	0.41		2.601
2-Methylpropan-1-ol	0.38	0.42		2.413
Pentan-1-ol		0.41		3.106
2-Methylbutan-1-ol	0.39	0.41		3.011
3-Methylbutan-1-ol	0.39	0.42		3.011
2,2-Dimethylpropan-1-ol	0.33			2.650
Hexan-1-ol	0.42	0.40		3.610
2-Methylpentan-1-ol	0.40			3.530
3-Methylpentan-1-ol	0.44			3.500
4-Methylpentan-1-ol	0.43			3.500
2-Ethylbutan-1-ol	0.40			3.523
2,2-Dimethylbutan-1-ol	0.37			3.320
Heptan-1-ol	0.43	0.39		4.115
2,2-Dimethylpentan-1-ol	0.37			3.780
Octan-1-ol	0.43	0.39		4.619
2-Ethylhexan-1-ol	0.41			4.433
2-Ethyl-4-methylpentan-1-ol	0.39			4.266
Nonan-1-ol	0.39	0.39		5.124
Decan-1-ol		0.39		5.628
Undecan-1-ol		0.39		6.130
Dodecan-1-ol		0.38		6.640
Propan-2-ol	0.39	0.42		1.764
Hydroxylic compounds (contined)				
Prop-2-en-1-ol (allyl alcohol)	0.44	0.46		1.951
But-2-en-1-ol	0.49			2.618
But-3-en-1-ol	0.47			2.442
But-3-en-2-ol	0.43			2.206
2-Methylprop-2-en-1-ol	0.45			2.509
Pent-3-en-1-ol	0.50			3.064
Pent-4-en-1-ol	0.46			2.715
Pent-1-en-3-ol	0.43			2.752
2-Methylbut-3-en-2-ol	0.41			2.376
trans-Hex-2-en-1-ol		0.43		3.510
trans-Hept-2-en-1-ol		0.40		4.010
trans-Oct-2-en-1-ol		0.41		4.520
Prop-2-yn-1-ol	0.46			2.050
2-Methylbut-3-yn-2-ol	0.47			2.209
2-Chloroethanol	0.54			2.630
2-Methoxyethanol	0.59			2.490
2-Ethoxyethanol	0.56			2.815
2-Butoxyethanol	0.57			3.806
2-Allyloxyethanol	0.64			3.283
2-Methoxypropan-1-ol	0.58			2.793
2-Ethoxypropan-1-ol	0.56			3.115
3-Ethoxypropan-1-ol	0.57			3.426
1-Methoxypropan-2-ol	0.61			2.655
1-Propoxypropan-2-ol	0.57			3.495
3-Methoxybutan-1-ol	0.66			3.398
1-Ethoxypentan-3-ol	0.60			4.102
4-Methyl-4-methoxypentan-2-ol	0.65			3.963
3-Hydroxybutan-2-one	0.78			3.573
4-Hydroxybutan-2-one	0.85			3.160
3-Methyl-4-hydroxybutan-2-one	0.81			3.573
3-Methyl-3-hydroxybutan-2-one	0.75			2.951
4-Methyl-4-hydroxypentan-2-one	0.83			3.475
Thiols				
Ethanethiol		0.26	0.34	2.173
1-Propanethiol		0.25	0.34	2.685
2-Propanethiol		0.30	0.32	2.406
1-Butanethiol		0.28	0.33	3.243
2-Methyl-1-propanethiol		0.30	0.37	3.091
2-Methyl-2-propanethiol		0.28	0.29	2.558

Butan-2-ol	0.41	0.44	2.338
Pentan-2-ol	0.40		2.840
Pentan-3-ol	0.40		2.860
3-Methylbutan-2-ol	0.39		2.793
Hexan-2-ol	0.40	0.44	3.340
Hexan-3-ol	0.39	0.41	3.343
3-Methylpentan-2-ol	0.40		3.371
4-Methylpentan-2-ol	0.38		3.179
2-Methylpentan-3-ol	0.39		3.240
2,3-Dimethylbutan-2-ol	0.41		3.167
3,3-Dimethylbutan-2-ol	0.37		3.090
Heptan-2-ol	0.40		3.842
Heptan-3-ol	0.40		3.860
Heptan-4-ol	0.39		3.850
2,4-Dimethylpentan-3-ol	0.40		3.603
Octan-2-ol	0.41		4.343
2-Methylpropan-2-ol	0.38	0.50	1.963
2-Methylbutan-2-ol	0.41	0.47	2.630
2-Methylpentan-2-ol	0.40	0.48	3.081
3-Methylpentan-3-ol	0.45	0.47	3.277
2-Methylheptan-2-ol		0.47	3.990
3-Methylheptan-3-ol		0.46	4.000
3-Ethylpentan-3-ol	0.47		3.785
Cyclopropylcarbinol	0.57		2.675
Cyclopentanol	0.55	0.47	3.241
Cyclohexanol	0.57		3.758
2-Methylcyclohexanol	0.52		4.110
cis,cis-2,6-Dimethylcyclohexanol		0.43	
cis,trans-2,6-Dimethylcyclohexanol		0.45	
trans,trans-2,6-Dimethylcyclohexanol		0.51	
dl-α-Terpineol		0.57	
exo-Ethylfenchol		0.52	
1,2-Ethanediol	0.50		2.661
1,2-Propanediol	0.49		2.918
1,2-Butanediol	0.63		3.525
2-Methyl-1,2-propanediol	0.60		3.190
dl-2,3-Butanediol	0.62		3.250
meso-2,3-Butanediol	0.65		3.291
1,3-Propanediol	0.46		3.263
1,3-Butanediol	0.68		3.642
1,4-Butanediol	0.46		3.795
1-Pentanethiol	0.27	0.34	3.720
3-Methyl-1-butanethiol	0.27	0.18	3.360
1-Hexanethiol	0.26	0.35	4.220
1-Heptanethiol	0.27	0.33	4.720
1-Octanethiol	0.26	0.33	5.270
1-Nonanethiol	0.26	0.33	5.790
1-Decanethiol	0.25	0.33	6.318
Thiophenol	0.70	0.84	4.118
1,2-Ethanedithiol	0.43		
Benzylthiol	0.71		
Allylthiol	0.35	0.44	2.654
Sulphides			
Dithiapentane	0.68		
Dimethyl sulphide	0.40	0.37	2.238
Diethyl sulphide	0.37	0.34	3.104
Dipropyl sulphide	0.36	0.31	4.120
Methyl ethyl sulphide	0.28		2.730
Methyl propyl sulphide	0.38	0.34	3.240
Diisopentyl sulphide	0.44	0.28	5.540
Dibutyl sulphide	0.38	0.33	4.950
Diallyl sulphide	0.49		3.750
Propylene sulphide	0.39		2.870
Tetrahydrothiophene	0.47	0.50	3.660
Thiophene	0.50	0.50	2.943
2-Methylthiophene	0.55	0.53	3.302
2,5-Dimethylthiophene	0.60	0.49	3.806
Dimethyl disulphide	0.47	0.41	3.550
Diethyl disulphide	0.49	0.44	4.210
Dimethyl trisulphide	0.53		
Methyl thioacetate	0.65		
Methyl thiopropanoate	0.61		
Methyl thiobutanoate	0.59		
Methyl thiopentanoate	0.61		
Thiocyanates and isothiocyanates			
Phenyl isothiocyanate	1.00		
Allyl isothiocyanate	0.60		
Ethyl isothiocyanate	0.61		
Methyl thiocyanate	0.76		

only five data points in each regression, and no less than four explanatory variables. In principle, since we have five equations and (for each solute) four unknowns, *viz.*, R_2, π_2^*, β_2^H and log L^{16}, we could determine these unknowns through a set of simultaneous equations. This procedure proved to be useless, probably because there is not a wide enough range of constants in the five equations of the type of eqn. 8. However, Patte *et al.* [11] did manage to analyse the 240 × 5 data matrix to yield five characteristic solute parameters, denoted α, w, ε, π and β. In order to avoid confusion with our own parameters, we refer to Patte *et al.*'s set as αL, wL, εL, πL and βL. Each of these parameters for the 240 solute set can be examined via eqn. 1, where log $SP = \alpha L$, wL, etc. We found that αL was mainly a size factor and that βL was a general combination of factors. For the other three solute parameters of Patte *et al.* we obtained the following regressions:

$$\pi L = -0.040 + 0.342R_2 - 0.265\pi_2^* + 2.540\alpha_2^H \quad (9)$$

$$\varepsilon L = 0.165 + 2.796R_2 - 0.602\pi_2^* - 1.426\beta_2^H \quad (10)$$

$$wL = -0.081 - 1.700R_2 + 2.490\pi_2^* + 0.561\alpha_2^H \quad (11)$$

Eqns. 9–11 can be rearranged to yield

$$\alpha_2^H = 0.0218 + 0.0335wL - 0.0251\varepsilon L + 0.3722\pi L \quad (12)$$

$$\pi_2^*(\pi_2^H) = -0.0060 + 0.4755wL + 0.2826\varepsilon L + 0.0536\pi L \quad (13)$$

$$R_2 = 0.0492 + 0.1195wL + 0.4057\varepsilon L + 0.2014\pi L \quad (14)$$

If R_2 is known, as it usually is, then any two equations out of eqns. 9–11 will yield α_2^H and π_2^*. However, the best pair of equations to use is clearly eqns. 9 and 11, which yield

$$\alpha_2^H = 0.0187 - 0.0620R_2 + 0.0409wL + 0.3847\pi L \quad (15)$$

$$\pi_2^*(\pi_2^H) \simeq 0.0287 + 0.6954R_2 + 0.3932wL - 0.0789\pi L \quad (16)$$

Values of π_2^H calculated via eqn. 16 are listed in Table II. We can also simply take the set of five equations, eqn. 8, and, knowing R_2, log L^{16} and where necessary α_2^H, back-calculate values of π_2^H. For each solute the five back-calculated π_2^H values can be averaged, and this average is also given in Table II. The error in π_2^H between the five equations is *ca.* 0.03 unit. There are a few omissions in this set of π_2^H values; these arise through the lack of one or another of the remaining solute parameters.

Although the combination of solutes in the McReynolds and Patte *et al.* sets numbers several hundred, there are some notable omissions. First, most of the solutes are aliphatic, so that some of the simplest functionally substituted aromatic solutes are missing. Second, many of the polyhalogenated aliphatic solutes are either missing, or have π_2^H values that are discordant when calculated from the McReynolds or Patte *et al.* set. Finally, a number of important solutes such as nitroalkanes and nitriles need to be studied further.

Fellous *et al.* [13] listed GLC data for seventeen aromatic solutes on a number of stationary phases. In order to back-calculate π_2^H using the general solvation equation (eqn. 1), it is essential that the s coefficient be as large as possible, *i.e.*, that the stationary phase be polar. Results from the seven most polar phases used by Fellous *et al.* are given in Table III. There is generally good agreement with values listed in Table II.

Several workers have examined sets of halogenated or polyhalogenated solutes on various stationary phases [14–18]. In Table IV we give π_2^H values back-calculated from the general solvation regression equation (eqn. 1) and also from our own results on a variety of polar stationary phases.

McReynolds [10] did not examine any aliphatic nitro compounds or nitriles, but in Table II we give values of π_2^H for a few such compounds, obtained from Patte *et al.*'s data set. We examined both series of solutes on a number of stationary phases, and conclude that π_2^H is even larger than the values given in Table II. Our results suggest that for 1-nitroalkanes π_2^H is 0.95 and that for *n*-alkyl cyanides π_2^H is *ca.* 0.90 unit (see Table IV).

We have not detailed the α_2^H values calculated from eqn. 7 or 15 because these follow closely the original hydrogen-bond α_2^H values described before [4]. Only with the carboxylic acids do the new effective or $\Sigma\alpha_2^H$ values (0.60 unit) differ markedly from α_2^H (0.54 unit). In Table IV we collect all the $\Sigma\alpha_2^H$ values that correspond to the π_2^H values we have set out.

Although it was not our intention to construct a new $\Sigma\beta_2^H$ scale, we thought it prudent to check that

TABLE III

VALUES OF π_2^H FOR SOME AROMATIC COMPOUNDS CALCULATED FROM RESULTS OF FELLOUS *ET AL.* [13]

X in PhX	π_2^H	S.D.[a]	π_2^H (Table II)		
			Eqn. 7	Eqn. 16	Eqn. 8
H	0.53	0.02	0.48	0.53	0.47
CF_3	0.45	0.02			
CH_3	0.52	0.01	0.47	0.57	0.46
OCH_3	0.73	0.02		0.73	0.70
F	0.57	0.02			
Cl	0.67	0.01			
Br	0.73	0.01			
I	0.79	0.01			
CHO	0.99	0.01		0.99	0.94
SH	0.78	0.01		0.70	0.84
CO_2CH_3	0.85	0.01		0.77	1.11
CN	1.07	0.01		1.05	1.04
$COCH_3$	0.98	0.01		1.09	0.99
NH_2	0.96	0.02			
NO_2	1.10	0.01		1.08[b]	1.05[b]
CH_2OH	0.85	0.01			
OH	0.88	0.01			

[a] Average deviation from 7 results.
[b] For 3-nitrotoluene.

the combined solvation parameters do yield reasonable results in systems where solute basicity is important. We therefore give in Table IV preliminary $\Sigma\beta_2^H$ values, again based on our original β_2^H values [5]. We hope in the near future to report on a much more comprehensive list of effective or $\Sigma\beta_2^H$ values.

Finally, we include in Table II the log L^{16} values that we have used. Where these differ from previous values, the new set is to be preferred.

DISCUSSION

The "inverse matrix" method we have used to analyse the data of McReynolds is a novel approach to the extraction of solvation parameters from data on a large number of stationary phases. The method works very well, but is limited in scope to results for a given set of solutes on at least fifteen phases. Our back-calculation of parameters from regression equations based on Patte *et al.*'s data set, eqn. 8, is likely to be the most common procedure. In principle, as pointed out above, if three solvation parameters are unknown (*e.g.*, π_2^H, α_2^H and log L^{16} in eqn. 8), it is possible to calculate all three using three simultaneous equations derived from retention data on three phases. In practice, this method can hardly ever be used unless the three phases are specifically chosen to give rise to solvation equations with very different coefficients. In the event, all of our new π_2^H values have been obtained by either the inverse matrix method or simple back-calculation and averaging. Overall we think that the π_2^H values listed in Table IV are accurate to *ca* 0.02 unit, but not more.

As can be seen from the data collected in Table II, there is a compelling need to correlate and interpret π_2^H values in order to codify existing data and to help in the estimation of further values. An analysis of all of our results has led us to two very simple rules governing π_2^H values for aliphatic solutes:

Rule 1. In any homologous series of functionally substituted aliphatic compounds, π_2^H is constant except for the first one or two members of the series.

Rule 2. In any given series of functionally substituted aliphatic compounds, π_2^H decreases by 0.03 unit for each branch in a carbon chain.

We now examine these rules in turn. Rule 1 would be extremely valuable in the estimation of π_2^H values, because if π_2^H was known for a few members of a homologous series, then the same value could be applied to all other members. Unfortunately, Li *et al.* [12] apparently find that their own π_2^c parameter varies markedly along homologous series. Thus along the homologous series of *n*-alkylcarboxylic acids, π_2^c increases from 0.50 (acetic acid) to 0.72 (nonanoic acid) (see Table V), whereas our π_2^H value is constant at 0.60 unit after the first few members of the series. We note that π_2^c and π_2^H are "scaled" differently, so that for the present discussion only trends in these parameters are important. How the two sets of π_2 values in Table V both result in good fits to experimental data can be seen by inspection of the corresponding $\Sigma\alpha_2^H$ values, also given in Table V. Our constant π_2^H value is accompanied by a constant $\Sigma\alpha_2^H$ value, whereas Li *et al.*'s increase in π_2^c is counteracted by a decrease in $\Sigma\alpha_2^H$, so that both combinations of $\pi_2/\Sigma\alpha_2^H$ fit the experimental data with respect to the solvation eqn. 1. We suggest, however, that other experimental evidence supports the constancy of π_2^H and $\Sigma\alpha_2^H$. Thus, the dipole moment of the *n*-alkylcarboxylic acids (except for formic acid) remains constant [19], the gas-phase proton transfer acidities of acetic acid, propanoic

TABLE IV

RECOMMENDED SOLVATION PARAMETERS FOR USE IN EQN. 1[a]

Values in parentheses are approximate values.

Solute	$\Sigma\pi_2^H$	$\Sigma\alpha_2^H$	$\Sigma\beta_2^H$	Solute	$\Sigma\pi_2^H$	$\Sigma\alpha_2^H$	$\Sigma\beta_2^H$
Rare gas	0.00	0.00	0.00	Trichloromethane	0.49	0.15	0.02
Hydrogen	0.00	0.00	0.00	Tetrachloromethane	0.38	0.00	0.00
Oxygen	0.00	0.00	0.00	1,1-Dichloroethane	0.49	0.10	0.10
Nitrogen	0.00	0.00	0.00	1,2-Dichloroethane	0.64	0.10	0.11
Nitrous oxide	0.35	0.00	0.10	1,1,1-Trichloroethane	0.41	0.00	0.09
Carbon monoxide	0.00	0.00	0.04	1,1,2-Trichloroethane	0.68	0.13	0.08
Carbon dioxide	0.42	0.00	0.10	1,1,1,2-Tetrachloroethane	0.63	0.10	0.08
Alkane	0.00	0.00	0.00	1,1,2,2-Tetrachloroethane	0.76	0.16	0.12
Cycloalkane	0.10	0.00	0.00	Dibromomethane	0.67	0.10	0.10
Decalin	0.25	0.00	0.00	Tribromomethane	0.68	0.15	0.09
Hydrindane	0.20	0.00	0.00	Fluorobenzene	0.57	0.00	0.10
Ethene	0.10	0.00	0.07	Chlorobenzene	0.67	0.00	0.09
Other alkene	0.08	0.00	0.07	1,2-Dichlorobenzene	0.79	0.00	0.03
Cycloalkene	0.20	0.00	0.10	1,3-Dichlorobenzene	0.74	0.00	0.03
α-Pinene	0.24	0.00	0.10	1,4-Dichlorobenzene	0.69	0.00	0.03
Diene	0.23	0.00	0.10	2-Chlorotoluene	0.66	0.00	0.09
Ethyne	0.25	0.15	0.15	3-Chlorotoluene	0.67	0.00	0.09
Propyne	0.25	0.13	0.15	4-Chlorotoluene	0.67	0.00	0.09
But-1-yne	0.25	0.13	0.15	2,4-Dichlorotoluene	0.73	0.00	0.03
Other alk-1-yne	0.23	0.13	0.10	2,6-Dichlorotoluene	0.73	0.00	0.03
Alk-2-yne	0.30	0.00	0.10	3,4-Dichlorotoluene	0.79	0.00	0.03
Benzene	0.52	0.00	0.14	Bromobenzene	0.73	0.00	0.09
Toluene	0.52	0.00	0.14	1,2-Dibromobenzene	0.89	0.00	0.03
o-Xylene	0.54	0.00	0.17	1,3-Dibromobenzene	0.84	0.00	0.03
m-Xylene	0.52	0.00	0.17	1,4-Dibromobenzene	0.79	0.00	0.03
p-Xylene	0.52	0.00	0.17	Iodobenzene	0.79	0.00	0.09
Ethylbenzene	0.52	0.00	0.15				
n-Propylbenzene	0.52	0.00	0.15	Dimethyl ether	0.27	0.00	0.41
Isopropylbenzene	(0.51)	0.00	0.15	Di-*n*-alkyl ether	0.25[b]	0.00	0.45
1,2,3-Trimethylbenzene	0.54	0.00	0.20	Furan	0.53	0.00	0.15
1,2,4-Trimethylbenzene	0.52	0.00	0.20	2-Methylfuran	0.50	0.00	(0.15)
1,3,5-Trimethylbenzene	0.52	0.00	0.20	Tetrahydrofuran	0.52	0.00	0.48
n-Alkylbenzene	0.52	0.00	0.15	2-Methyltetrahydrofuran	0.48	0.00	0.55
Styrene	0.63	0.00	0.18	3,5-Dimethyltetrahydrofuran	0.38	0.00	0.55
Phenylethyne	0.58	0.12	0.21	Tetrahydropyran	0.47	0.00	0.55
Naphthalene	0.90	0.00	0.21	1,4-Dioxane	0.75	0.00	0.64
Fluoroalkane	0.35	0.00	0.10	Paraldehyde	0.68	0.00	
Chloromethane	0.43[b]	0.00	0.08	Methyl phenyl ether	0.73	0.00	(0.33)
Chloroalkane	0.40	0.00	0.10	Ethyl phenyl ether	0.72	0.00	(0.33)
Bromomethane	0.43[b]	0.00	0.10	Benzodioxane	1.01	0.00	
Bromoalkane	0.40	0.00	0.12	Formaldehyde	0.70	0.00	(0.33)
Iodomethane	0.43[b]	0.00	0.13	Acetaldehyde	0.67	0.00	0.45
Iodoalkane	0.40	0.00	0.15	*n*-Alkanal	0.65[b]	0.00	0.45
sec.-Chloroalkane	0.35[b]	0.00	0.12	Prop-2-en-1-al	0.74	0.00	0.45
sec.-Bromoalkane	0.35[b]	0.00	0.14	*trans*-Alk-2-en-1-al	0.80	0.00	0.45
sec.-Iodoalkane	0.35[b]	0.00	0.17	Benzaldehyde	0.99	0.00	(0.42)
tert.-Chloroalkane	0.25[b]	0.00	0.12	2-, 3- or 4-methylbenzaldehyde	0.95	0.00	(0.44)
tert.-Bromoalkane	0.25[b]	0.00	0.12	Propanone	0.70	0.04	0.51
tert.-Iodoalkane	0.25[b]	0.00	0.10	Butanone	0.70	0.00	0.51
Dichloromethane	0.57[b]	0.10	0.05	Alkan-2-one	0.68[b]	0.00	0.51

TABLE IV *(continued)*

Solute	$\Sigma\pi_2^H$	$\Sigma\alpha_2^H$	$\Sigma\beta_2^H$	Solute	$\Sigma\pi_2^H$	$\Sigma\alpha_2^H$	$\Sigma\beta_2^H$
Alkan-(3,4,5)-one	0.66[b]	0.00	0.51	Pyridine	0.82	0.00	
Cycloalkanone	0.86[b]	0.00	0.52	2-Methylpyridine	0.80	0.00	
Acetophenone	0.98	0.00	(0.51)	3-Methylpyridine	0.80	0.00	
				4-Methylpyridine	0.80	0.00	
Methyl formate	0.68	0.00	0.38	2,4,6-Trimethylpyridine	0.72	0.00	
Ethyl formate	0.66	0.00	0.38				
n-Alkyl formate	0.63[b]	0.00	0.38				
Methyl acetate	0.64	0.00	0.45	Acetic acid	0.65	0.61	0.41
Ethyl acetate	0.62	0.00	0.45	Propanoic acid	0.65	0.60	0.43
n-Alkyl acetate	0.60[b]	0.00	0.45	Butanoic acid	0.62	0.60	0.43
Methyl propanoate	0.60	0.00	0.45	*n*-Alkanoic acids	0.60[b]	0.60	0.43
Ethyl propanoate	0.58	0.00	0.45				
n-Alkyl propanoate	0.56[b]	0.00	0.45	Water	0.45	0.82	0.35
Vinyl acetate	0.64	0.00	0.42	Methanol	0.44	0.43	0.47
Methyl acrylate	0.66	0.00	0.42	Ethanol	0.42	0.37	0.48
Ethyl acrylate	0.64	0.00	0.42	Primary alcohols	0.42[b]	0.37	0.48
n-Alkyl acrylate	0.62[b]	0.00	0.42	Secondary alcohols	0.36[b]	0.33	0.56
Methyl benzoate	0.85	0.00	0.50	Tertiary alcohols	0.30[b]	0.31	0.60
n-Alkyl benzoates	0.80	0.00	0.50	Trifluoroethanol	0.60	0.57	(0.15)
				Hexafluoropropan-2-ol	0.55	0.77	(0.03)
Nitromethane	0.95	0.12	0.27	Decafluoroheptan-1-ol	0.55	0.60	0.22
Nitroethane	0.95	0.05	0.27				
1-Nitropropane	0.95	0.02	0.27				
1-Nitroalkane	0.95[b]	0.00	0.27	Phenol	0.88	0.60	
Nitrobenzene	1.10	0.00	0.27	*o*-Cresol	0.86	0.52	
2-, 3- or 4-nitrotoluene	1.10	0.00	0.27	*m*-Cresol	0.87	0.57	
				p-Cresol	0.87	0.57	
Acetonitrile	0.90	0.09	0.30	2,3-Dimethylphenol	0.82	0.53	
Propionitrile	0.90	0.02	0.35	2,4-Dimethylphenol	0.82	0.53	
n-Alkyl cyanide	0.90	0.00	0.36	2,5-Dimethylphenol	0.82	0.54	
Benzonitrile	1.07[b]	0.00	(0.30)	2,6-Dimethylphenol	0.82	0.39	
				3,4-Dimethylphenol	0.87	0.56	
Ammonia	0.35[c]	0.10	0.62	3,5-Dimethylphenol	0.87	0.57	
Primary *n*-alkylamines	0.35[c]	0.10	0.64	2,4,6-Trimethylphenol	0.83	0.37	
Dimethylamine	0.30[c]	0.08	0.67	Benzyl alcohol	0.85	0.39	
sec.-dialkylamines	0.30[c]	0.08	0.70				
Triethylamine	0.15[c]	0.00	0.81				
Aniline	0.96[c]	0.26	(0.53)	Carbon disulphide	0.21	0.00	0.07
o-Toluidine	0.94	0.23	(0.57)	Methanethiol	(0.35)	0.00	
m-Toluidine	0.94	0.23	(0.55)	1-Alkanethiol	0.35[b]	0.00	0.24
p-Toluidine	0.94	0.23	(0.57)	3-Methyl-1-butanethiol	0.18[d]	0.00	
2,6-Dimethylaniline	0.93	0.20	(0.60)	Thiophenol	0.78	0.12	(0.15)
N-Methylaniline	0.94	0.17	(0.47)	Di-*n*-alkyl sulphide	0.38[b]	0.00	0.32
N,N-Dimethylaniline	0.82	0.00	(0.48)	Tetraalkyltin	0.00	0.00	0.00

[a] Values of π_2^H (this work) derived from those in Tables II and III plus other values we have calculated. Values of $\Sigma\alpha_2^H$ and $\Sigma\beta_2^H$ are based on those given in refs. 4 and 5.
[b] Subtract 0.03 from π_2^H for each additional branch.
[c] Provisional values.
[d] See text.

acid and butanoic acid are almost the same (if anything, there is a slight increase in acidity along this series) [20] and the gas-phase hydrogen-bond acidity of propanoic acid is slightly less than that of acetic acid [21], not larger. As retention data can be accommodated as well by our constant π_2^H and $\Sigma\alpha_2^H$ values as by the variable parameters of Li *et al.*, we feel that Rule 1 is operative here.

There are other homologous series for which Li *et al.* found π_2^c to be a variable quantity, but for which $\Sigma\alpha_2^H = 0$, *e.g.*, the alkan-2-ones or the cycloalkanones where π_2^c increases sharply along the series. In

TABLE V

COMPARISON OF π_2^H WITH π_2^c FOR CARBOXYLIC ACIDS

R in ROC_2H	This work		Li *et al.* [12]	
	π_2^H	α_2^H	π_2^c	α_2^H
Methyl	0.65	0.61	0.50	0.72
Ethyl	0.65	0.60	0.61	0.67
n-Propyl	0.62	0.60	0.57	0.62
n-Butyl	0.60	0.60	0.56	0.62
n-Pentyl	0.60	0.60	0.60	0.52
n-Hexyl	0.60	0.60	0.64	0.47
n-Heptyl	0.60	0.60	0.68	0.41
n-Octyl	0.60	0.60	0.72	0.35

some other series, however, π_2^c decreases slightly (the alk-1-ene series), or remains approximately constant (the alkanal or the alkylbenzene series). For the cycloalkanone series, as an example, we feel that the difference between Li *et al.*'s result and our findings is not fundamental at all, but is probably due to small but systematic differences in the log L^{16} values. As the sign of the $s\pi_2$ and l log L^{16} coefficients is always positive, a systematic trend in π_2^c increasing, together with a trend in log L^{16} becoming slightly smaller than expected, would tend to cancel out. This can be seen by comparison of the figures in Table VI. Just as for the carboxylic acid results, the combination of π_2^c with Li *et al.*'s calculated log L^{16} values will lead to very nearly the same goodness-of-fit as our combination of π_2^H and log L^{16}. As it is always found that solute dipolarity, as the dipole moment, is constant along any homologous series, we again feel that Rule 1 applies to the various homologous series we have considered.

Rule 2 is not so well founded, and we think it possible that there will be exceptions or amendments to the rule. However, at the moment, we feel that application of Rule 2 does allow a very large number of π_2^H values to be estimated for aliphatic compounds. We note that the starting point for application of the rule is not always the simplest member of any series.

According to our results in Table II, the alkanols are a significant exception to Rule 2, as π_2^H seems roughly constant over non-branched and branched members. However, because the coefficients of π_2^H and α_2^H are both positive, and indeed follow each other for most stationary phases, there will be various combinations of π_2^H and α_2^H that give rise to the same (or very similar) goodness-of-fit in any given solvation equation. We have checked that π_2^H values for alkanols calculated using Rules 1 and 2, together with the α_2^H values listed in Table IV, yield regression eqations that are just as good as if π_2^H and α_2^H are allowed to "float". We give in Table IV our suggested π_2^H and α_2^H values for alkanols, noting that we have deliberately amended the first-calculated values in Table II.

We also find a few minor anomalies, with respect to Rule 2. Thus, π_2^H for isopentanethiol is 0.18 (using Patte *et al.*,'s set) rather than 0.32 as calculated by Rule 2. Whether or not this is the result of a systematic experimental error, or even of an incorrectly named compound, we cannot say. Interestingly, Li *et al.* [12] also found an anomalously low π_2^c value for isopentylthiol.

Finally, we can compare our π_2^H scale, as summarised in Table IV, with the π_2^c scale of Li *et al.*. We agree completely with Li *et al.* in that a new π_2 scale is needed in place of π_2^*. Apart from the difference in treatment of homologous series, the two scales are in approximate agreement. For 198 of the 203 compounds listed by Li *et al.* [12], we have π_2^H values, and find that

$$\pi_2^c = -0.103 + 0.845\pi_2^H \qquad (17)$$

with $r = 0.944$ and S.D. $= 0.083$ units. The intercept of -0.103 arises because Li *et al.* took cyclohexane as the zero ($\pi_2^c = 0.00$), but we take alkanes as zero. On the π_2^H scale, cyclohexane has $\pi_2^H = 0.10$ units.

TABLE VI

COMPARISON OF π_2^H WITH π_2^c FOR CYCLOALKANONES

n in $(CH_2)_nCO$	This work		Li *et al.* [12]	
	π_2^H	Log L^{16}	π_2^c	Log L^{16}
4	0.86	3.221	0.58	3.120
5	0.86	3.792	0.59	3.616
6	0.86	4.376	0.66	4.110
7	0.86	4.981	0.69	4.610
8	0.86	5.537	0.72	5.110
9	0.86	6.063	0.75	5.610
10	0.86	6.621	0.78	6.110
11	0.86	7.226	0.81	6.600

As mentioned above, we include in Table IV a provisional set of $\Sigma\beta_2^H$ values to use with our new π_2^H and our $\Sigma\alpha_2^H$ scale. In our view, it is most important that these three scales are constructed more or less simultaneously in order that they all be compatible. How well the scales listed in Table IV deal with various processes remains to be seen, but at the moment we can compare regressions of Patte *et al.*'s data using the Table IV values with our original regression equations. Details are given in Table VII and show that the new equations are much better than the old ones in terms of the correlation constant and standard deviation. However, the characteristic constants, *r*, *s*, *a* and *l*, are almost unchanged. Similarly, regression equations using McReynolds' data are much better than the original ones, whilst still giving very similar characteristic constants. Hence our analysis of the McReynolds' phases into clusters or groups remains unchanged, and it is not necessary to repeat the 75 regressions. We give in Table VII a few comparisons to show exactly the connection between the old and the new equations.

In conclusion, we have constructed a comprehensive π_2^H scale, based only on solute properties, for use in solvation equations. As the dependent variable, $\log L'$ or $\log V_G$, in the equations used to calculate π_2^H is a free energy-related term, then π_2^H also will be related to Gibbs energy. We are now in a position where the main terms in eqn. 1, *viz.*, π_2^H, $\Sigma\alpha_2^H$, $\Sigma\beta_2^H$ and $\log L^{16}$, are all related to Gibbs energy and hence form a thermodynamically consistent set of explanatory variables. The new π_2^H scale has an advantage in that the characteristic constants in all our previous equations remain the same, within any reasonable experimental error, so that our previous analyses and conclusions are unchanged.

TABLE VII

COMPARISON OF NEW AND OLD REGRESSIONS[a]

Phase	*c*	*r*	*s*	*a*	*l*	S.D.	*R*	No.
Patte *et al.*'s set								
Carbowax	−2.01	0.25	1.26	2.07	0.429	0.07	0.997	199
	−2.07	0.26	1.37	2.11	0.442	0.13	0.986	168
DEGS[b]	−1.77	0.35	1.58	1.84	0.383	0.07	0.997	199
	−1.83	0.35	1.70	1.92	0.396	0.15	0.981	168
PPE (6 rings)[b]	−2.51	0.14	0.89	0.67	0.547	0.06	0.997	199
	−2.55	0.19	0.98	0.59	0.552	0.11	0.991	168
TCEP[b]	−1.69	0.26	1.93	1.88	0.365	0.06	0.998	199
	−1.75	0.23	2.12	1.94	0.379	0.16	0.982	168
ZE7[b]	−1.99	−0.41	1.46	0.77	0.432	0.07	0.995	199
	−2.07	−0.38	1.61	0.70	0.442	0.13	0.983	168
The McReynolds' set at 120°C								
Apiezon J	−0.48	0.24	0.15	0.13	0.596	0.02	0.999	165
	−0.48	0.27	0.13	0.13	0.594	0.03	0.998	148
PPE (5 rings)	−0.69	0.14	0.92	0.61	0.560	0.02	0.999	168
	−0.70	0.21	0.88	0.54	0.564	0.06	0.994	155
Pluronic L72	−0.54	0.09	0.93	1.42	0.529	0.03	0.998	163
	−0.54	0.17	0.89	1.41	0.531	0.08	0.992	153
Carbowax 1540	−0.75	0.22	1.37	1.92	0.456	0.04	0.998	169
	−0.75	0.31	1.34	1.87	0.457	0.09	0.987	151
DEGS[b]	−0.97	0.26	1.76	1.80	0.375	0.05	0.995	158
	−0.99	0.43	1.74	1.68	0.379	0.11	0.975	145
ZE7[b]	−0.76	−0.42	1.55	0.78	0.448	0.07	0.991	170
	−0.82	−0.28	1.63	0.69	0.449	0.07	0.990	150

[a] The new constants in eqn. 1 are on the top lines and the old constants on the bottom lines; in all instances $b = 0$.

[b] Abbreviations: DEGS = diethylene glycol succinate; PPE = polyphenyl ether; TCEP = tricyanoethoxypropane; ZE7 = zonyl E-7.

ACKNOWLEDGEMENTS

We thank the US Army Research, Development and Standardisation Group for support under Contract DAJA 45-87-C-0004, and we are very grateful to Professor Peter W. Carr for a preprint of ref. 12.

REFERENCES

1 M. H. Abraham, G. S. Whiting, R. M. Doherty and W. J. Shuely, *J. Chem. Soc., Perkin Trans. 2*, (1990) 1451.
2 M. H. Abraham, G. S. Whiting, R. M. Doherty and W. J. Shuely, *J. Chem. Soc., Perkin Trans. 2*, (1990) 1851.
3 M. H. Abraham, G. S. Whiting, R. M. Doherty and W. J. Shuely, *J. Chromatogr.*, 518 (1990) 329.
4 M. H. Abraham, P. L. Grellier, D. V. Prior, P. P. Duce, J. J. Morris and P. J. Taylor, *J. Chem. Soc., Perkin Trans. 2*, (1989) 699.
5 M. H. Abraham, P. L. Grellier, D. V. Prior, J. J. Morris and P. J. Taylor, *J. Chem. Soc., Perkin Trans. 2*, (1990) 521.
6 M. H. Abraham, P. L. Grellier and R. A. McGill, *J. Chem. Soc., Perkin Trans. 2*, (1987) 797.
7 M. J. Kamlet, M. H. Abraham, R. M. Doherty and R. W. Taft, *Nature (London)*, 106 (1984) 464.
8 R. W. Taft, M. H. Abraham, G. R. Famini, R. M. Doherty, J.-L. M. Abboud and M. J. Kamlet, *J. Pharm. Sci.*, 74 (1985) 807.
9 M. H. Abraham, G. J. Buist, P. L. Grellier, R. A. McGill, D. V. Prior, S. Oliver, E. Turner, J. J. Morris, P. J. Taylor, P. Nicolet, P.-C. Maria, J.-F. Gal, J.-L. M. Abboud, R. M. Doherty, M. J. Kamlet, W. J. Shuely and R. W. Taft, *J. Phys. Org. Chem.*, 2 (1989) 540.
10 W. O. McReynolds, *Gas Chromatographic Retention Data*, Preston Technical Abstracts, Evanston, IL, 1966.
11 F. Patte, M. Etcheto and P. Laffort, *Anal. Chem.*, 54 (1982) 2239.
12 J. Li, Y. Zhang, A. J. Dallas and P. W. Carr, *J. Chromatogr.*, in press.
13 R. Fellous, L. Lizzani-Cuvelier and R. Luft, *Anal. Chim. Acta*, 174 (1985) 53.
14 P. Urone, J. E. Smith and R. J. Katnik, *Anal. Chem.*, 34 (1962) 476.
15 D. E. Martire and L. Z. Pollara, *J. Chem. Eng. Data*, 10 (1965) 40.
16 J. P. Sheridan, D. E. Martire and Y. B. Tewari, *J. Am. Chem. Soc.*, 94 (1972) 3294.
17 E. F. Meyer, K. S. Stec and R. D. Hotz, *J. Phys. Chem.*, 77 (1973) 2140.
18 G. Castello and T. C. Gerbino, *J. Chromatogr.*, 437 (1988) 33.
19 A. L. McClellan, *Tables of Experimental Dipole Moments*, Vol. 2, Rahara Enterprises, El Cerrito, CA, 1974.
20 J. E. Bartmess, *The Gas Phase Acidity Scale*, personal communication.
21 G. Caldwell and P. Kebarle, *J. Am. Chem. Soc.*, 106 (1984) 967.

Journal of Chromatography, 587 (1991) 229–236
Elsevier Science Publishers B.V., Amsterdam

CHROM. 23 485

Hydrogen bonding

XVII. The characterisation of 24 gas–liquid chromatographic stationary phases studied by Poole and co-workers, including molten salts, and evaluation of solute–stationary phase interactions

Michael H. Abraham* and Gary S. Whiting

Department of Chemistry, University College London, 20 Gordon Street, London WC1H 0AJ (UK)

Ruth M. Doherty

Naval Surface Warfare Center, White Oak Laboratory, Silver Spring, MD 20910 (USA)

Wendel J. Shuely

US Army Chemical Research, Development and Engineering Center, Aberdeen Proving Ground, MD 21010 (USA)

(First received February 19th, 1991; revised manuscript received May 23rd, 1991)

ABSTRACT

The general solvation equation

$$\log K = c + rR_2 + s\pi_2^H + a\alpha_2^H + b\beta_2^H + l \log L^{16}$$

has been used to characterise 24 gas–liquid chromatographic stationary phases for which Poole and co-workers have determined log K values for a series of solutes at 121.4°C. The explanatory variables are R_2, a solute excess molar refraction, π_2^H, the solute dipolarity, α_2^H and β_2^H, the solute hydrogen-bond acidity and basicity, and log L^{16}, where L^{16} is the solute gas–liquid partition coefficient on hexadecane at 25°C. It is shown that the $b\beta_2^H$ term is not significant for any phase, and that the molten salts are all strongly dipolar and basic, with large s and a constants. A term-by-term analysis of the solvation equation yields a quantitative measure of the contribution to log K of various solute–stationary phase interactions, and leads to an understanding of how these interactions affect solute retention. The use of the characteristic constants c, r, s, a, b and l in the selection of stationary phases for particular separations is described.

INTRODUCTION

There have been a number of interesting new developments in recent years in the characterisation of gas–liquid chromatographic (GLC) stationary phases. Poole and co-workers [1,2] have pointed out several deficiences in the McReynolds system of classification, and have suggested that the use of McReynolds numbers be abandoned. Following several other workers [3–5], Poole and co-workers suggested that the Gibbs energy of solvation of a gaseous methylene increment into a stationary phase, $\Delta G_s^{\circ}(CH_2)$, could be used as a measure of the "polarity" of the phase [1,2,6]. More recently, Poole

0021-9673/91/$03.50

and co-workers [7,8] defined a solvent strength parameter, *SSP*, as $SSP = \Delta G_s^{\ominus}(CH_2)/\rho_1$, where ρ_1 is the density of the stationary phase at the column temperature. Although $\Delta G_s^{\ominus}(CH_2)$, or alternatively *SSP*, might well be the best "single parameter" that can be used to classify stationary phases, it cannot possibly reflect the various solute–solvent interactions that determine the retention of a solute by a given stationary phase. The use of various test solutes as probes cannot be used to identify such interactions either, because there are no test solutes that possess, for example, a singular quality of "polarity" without also possessing some other quality. Thus a test solute such as 1-nitropropane, although certainly dipolar, is also basic, whereas a test solute such as butan-1-ol is acidic, basic and dipolar! Poole and co-workers [2,7,8] recognised this difficulty, although no easy solution to the problem seemed to be available.

In parallel with these studies, we have been developing the use of equations based on multiple linear regression analysis (MLRA) in order to identify and to quantify solute–solvent interactions as a means of classifying stationary phases. Our recommended solvation equation is

$$\log SP = c + rR_2 + s\pi_2^H + a\alpha_2^H + b\beta_2^H + l \log L^{16} \quad (1)$$

where *SP* can be the retention volume at the column temperature, the specific retention volume, the gas–liquid partition coefficient (*L* or *K*) or even the retention time or relative retention time corrected for gas hold-up, for a series of solutes on a given stationary phase [9–11]. All these quantities will yield the same characteristic constants *r*, *s*, *a*, *b* and *l*. Note that the retention index, *I*, cannot be used in eqn. 1 unless the alkane *b* values are also given. It is to be hoped that when *I* values are tabulated, workers will also include data that will enable the original retention values to be calculated.

The explanatory variables in eqn. 1 are solute properties as follows: R_2 is an excess molar refraction [9], π_2^H is our new solute dipolarity–polarisability parameter [12], α_2^H is the effective or summation hydrogen-bond acidity that could be denoted $\Sigma\alpha_2^H$ [12], β_2^H is the effective or summation hydrogen-bond basicity that could be denoted $\Sigma\beta_2^H$ [12] and L^{16} is the solute *L* or *K* value on *n*-hexadecane at 25°C [13]. Of course, most log L^{16} values have now been determined via back-calculation of retention data on various non-polar phases. The constants in eqn. 1 are found by MLRA, using log *SP* values for a series of varied solutes on a given stationary phase. As *r*, *s*, *a*, *b* and *l* quantitatively relate to stationary phase properties, they are denoted as "characteristic constants". In particular, the *r* constant refers to the ability of the phase to interact with solute π- and *n*-electron pairs, the *s* constant refers to the ability of the phase to take part in dipole–dipole and dipole–induced dipole interactions, the *a* constant refers to the interaction of the phase with solute hydrogen-bond acids and hence is a measure of the hydrogen-bond basicity of the phase, the *b* constant likewise measures the hydrogen-bond acidity of the phase and the *l* constant refers to the ability of the phase to separate adjacent members of a homologous series. The *l* constant should therefore be connected with $\Delta G_s^{\ominus}(CH_2)$, because the larger is *l* or $\Delta G_s^{\ominus}(CH_2)$ the greater will be the separation between adjacent homologues [11].

We have already shown how eqn. 1 can be used to characterise stationary phases in the McReynolds and Patte *et al.* series [9,11] and how retention data in these two series may then be used to obtain π_2^H and α_2^H solute parameters [12]. As these two activities are interdependent, it seems obligatory to test eqn. 1 with an independent set of retention data. We have chosen as a first test the retention data, as log *K* values, obtained by Poole and co-workers [7] on 24 stationary phases at 121.4°C. There are two main reasons for this choice. First, we believe the data obtained by Poole and co-workers [7] to be amongst the most reliable GLC data ever reported, with considerable care being taken to exclude contributions from interfacial adsorption. Second, the stationary phases studied by Poole and co-workers include seven molten salts, and it is of interest to analyse results on these novel stationary phases using the general solvation eqn. 1.

The stationary phases used by Poole and co-workers are shown in Table I, together with their $\Delta G_s^{\ominus}(CH_2)$ and *SSP* values [7]. Solute parameters were all taken from our previous compilation [12]; for convenience they are set out in Table II.

Note that not all solutes were examined on all phases, so that for any particular phase the number of solutes studied (No.) is less than 42. When we first applied eqn. 1 to Poole and co-workers' data

TABLE I

STATIONARY PHASES EXAMINED BY POOLE AND CO-WORKERS AT 121.4°C

Code	Stationary phase	$\Delta G_s^{\circ}(CH_2)$ (cal mol^{-1})	SSP
A	Squalane	−530	−728
B	SE-30	−463	−578
C	OV-3	−458	−523
D	OV-7	−467	−504
E	OV-11	−475	−478
F	OV-17	−470	−463
G	OV-22	−458	−439
H	OV-25	−431	−396
I	OV-105, poly(cyanopropylmethyldimethylsiloxane)	−461	−523
J	OV-225, poly(cyanopropylmethylphenylmethylsiloxane)	−418	−410
K	OV-275, poly(dicyanoallylsiloxane)	−265	−243
L	OV-330, a poly(dimethylsiloxane)–Carbowax copolymer	−418	−407
M	Poly(trifluoropropylmethylsiloxane), QF-1	−393	−337
O	Carbowax 20M	−400	−387
P	Poly(diethylene glycol succinate), DEGS	−324	−275
Q	1,2,3-Tris(2-cyanoethoxy)propane, TCEP	−280	−273
R	Poly(phenyl ether), five rings, PPE-5	−487	−436
S	Tetraethylammonium 4-toluenesulphonate	−286	−267
T	Tributylammonium 4-toluenesulphonate	−384	−384
U	Tetrabutylammonium 4-toluenesulphonate	−377	−377
V	Tetrabutylammonium picrate	−411	−381
W	Tetrabutylammonium methanesulphonate	−398	−406
X	Tetrabutylammonium N-(2-acetamido)-2-aminoethanesulphonate	−319	−312
Y	Tetrabutylammonium 3-[tris(hydroxymethyl)methylamino]-2-hydroxy-1-propanesulphonate	−290	−276

set, we noted that one of their solutes, oct-1-yne, was always out of line, and consistently behaved in a manner we expected of oct-2-yne. It was subsequently confirmed that the compound listed as oct-1-yne in their data set was indeed oct-2-yne [14]; hence in Table II we list oct-2-yne.

For each stationary phase, we analysed results using exactly the solutes studied by Poole and co-workers [7]. Of the 24 phases with an average of 35 solutes each, we excluded one data point only. The result for 2,6-dimethylaniline on phase V was out of line by over four standard deviations, with log K (obs.) = 2.947 and log K (calc.) = 3.416 units.

RESULTS AND DISCUSSION

As a necessary preliminary, we applied the full eqn. 1 to all 24 phases, and found that in no case was the b coefficient statistically significant as judged by the t-test. We can then revert to the simpler equation,

$$\log K = c + rR_2 + s\pi_2^H + a\alpha_2^H + l \log L^{16} \quad (2)$$

Results of application of eqn. 2 to all 24 phases are summarised in Table III, where we give the characteristic constants in eqn. 2, together with the overall standard deviation in log K, (S.D.), the overall correlation coefficient (R) and the number of data points or solutes in each regression (No.).

As judged by the values of S.D. and R, the regression equations for the 24 phases are of excellent quality. Most values of S.D. are <0.08 log unit, and for the four phases with S.D. >0.08, *viz.*, P. U. W and X, the errors in log K quoted by Poole and co-workers [7] are much larger than for the other phases. We can therefore conclude that the solvation parameters that we obtained previously, can, indeed, be used to characterise other GLC stationary phases. Whether such characterisation is useful or not will depend at least in part on whether the characteristic constants r, s, a and l in eqn. 2 make general chemical sense.

TABLE II

SOLUTE PARAMETERS USED IN REGRESSION EQN. 2

Solute	R_2	π_2^H	$\Sigma\alpha_2^H$	Log L^{16}
Heptane	0.000	0.00	0.00	3.173
Octane	0.000	0.00	0.00	3.677
Nonane	0.000	0.00	0.00	4.182
Decane	0.000	0.00	0.00	4.686
Undecane	0.000	0.00	0.00	5.191
Dodecane	0.000	0.00	0.00	5.696
Tridecane	0.000	0.00	0.00	6.200
Tetradecane	0.000	0.00	0.00	6.705
Pentadecane	0.000	0.00	0.00	7.209
Hexadecane	0.000	0.00	0.00	7.714
Butanone	0.166	0.70	0.00	2.287
Pentan-2-one	0.143	0.68	0.00	2.755
Hexan-2-one	0.136	0.68	0.00	3.262
Heptan-2-one	0.123	0.68	0.00	3.760
Octan-2-one	0.108	0.68	0.00	4.257
Nonan-2-one	0.119	0.68	0.00	4.735
Benzene	0.610	0.52	0.00	2.803
Butylbenzene	0.600	0.52	0.00	4.686
cis-Hydrindane	0.439	0.20	0.00	4.610
Oct-2-yne	0.225	0.30	0.00	3.850
Dodec-1-yne	0.133	0.23	0.13	5.657
Butan-1-ol	0.224	0.42	0.37	2.601
2-Methylpentan-2-ol	0.169	0.30	0.31	3.081
Dodecafluoroheptan-1-ol	−0.640	0.55	0.60	3.089
Octan-1-ol	0.199	0.42	0.37	4.619
Phenol	0.805	0.88	0.60	3.897
2,4,6-Trimethylphenol	0.860	0.83	0.37	5.185
Benzonitrile	0.742	1.07	0.00	4.004
1-Nitropropane	0.242	0.95	0.02	2.894
1-Nitropentane	0.210	0.95	0.00	3.938
Nitrobenzene	0.871	1.10	0.00	4.511
1,1,1,2-Tetrachlorethane	0.542	0.63	0.10	3.641
Pyridine	0.631	0.82	0.00	3.003
2,4,6-Trimethylpyridine	0.634	0.72	0.00	4.200
Aniline	0.955	0.96	0.26	3.993
N-Methylaniline	0.948	0.94	0.17	4.494
N,N-Dimethylaniline	0.957	0.82	0.00	4.754
2,6-Dimethylaniline	0.967	0.93	0.20	5.037
1,4-Dioxane	0.329	0.75	0.00	2.892
Methylphenyl ether	0.708	0.73	0.00	3.859
Di-*n*-hexyl ether	0.000	0.25	0.00	5.938
Benzodioxane	0.874	1.01	0.00	4.985
Nonanal	0.150	0.65	0.00	4.900

The rR_2 term generally makes only a minor contribution, but nevertheless the r constant seems well behaved. Phases with a substantial proportion of phenyl groups lead to an increase in the r constant, as expected if this is an index of π- and n-electron pair interaction. Thus, along the OV series of poly (methylphenylsiloxane), the r constant increases as the percentage of phenyl groups increases. The only substantially negative value of the r constant, with phase M, corresponds to the only phase that contains fluorine, again as expected.

More important is the $s\pi_2^H$ term, in which the s constant reflects dipole–dipole and dipole–induced dipole interactions, and so may be taken as a mea-

TABLE III

REGRESSION EQUATIONS FOR THE PHASES IN TABLE I

Code	c	r	s	a	l	S.D.	R	No.
A	−0.202	0.125	0.018	−0.097	0.581	0.033	0.9985	39
B	−0.194	0.024	0.190	0.125	0.498	0.022	0.9989	39
C	−0.181	0.033	0.328	0.152	0.503	0.021	0.9992	39
D	−0.231	0.056	0.433	0.165	0.510	0.025	0.9989	39
E	−0.303	0.097	0.544	0.174	0.516	0.029	0.9985	39
F	−0.326	0.128	0.612	0.147	0.509	0.036	0.9978	38
G	−0.328	0.201	0.664	0.190	0.489	0.034	0.9979	38
H	−0.273	0.277	0.644	0.182	0.472	0.042	0.9973	39
I	−0.212	−0.038	0.395	0.368	0.499	0.026	0.9987	39
J	−0.509	0.015	1.214	0.964	0.462	0.035	0.9979	39
K	−0.635	0.388	1.902	1.644	0.241	0.080	0.9935	32
L	−0.430	0.104	1.056	1.419	0.481	0.051	0.9954	36
M	−0.251	−0.362	1.101	0.054	0.416	0.077	0.9853	39
O	−0.558	0.285	1.292	1.803	0.450	0.059	0.9957	39
P	−0.498	0.351	1.683	1.718	0.311	0.096	0.9899	38
Q	−0.489	0.278	1.913	1.679	0.290	0.056	0.9972	40
R	−0.395	0.230	0.829	0.337	0.527	0.044	0.9972	39
S	−1.008	0.362	2.059	3.609	0.340	0.076	0.9941	29
T	−0.717	0.110	1.546	2.917	0.466	0.069	0.9922	30
U	−0.617	0.009	1.659	3.360	0.440	0.106	0.9885	34
V	−0.542	0.100	1.557	1.424	0.445	0.061	0.9935	36[a]
W	−0.631	0.095	1.595	3.408	0.437	0.097	0.9895	34
X	−0.666	0.283	1.809	3.417	0.329	0.100	0.9902	34
Y	−0.690	0.281	1.821	2.859	0.305	0.080	0.9932	29

[a] Excluding solute 2,6-dimethylanilline, which is out of line by over four standard devations; log K (calc.) = 3.416, log K (obs.) = 2.947

sure of stationary phase dipolarity. Of the conventional phases, phases K (OV-275), P (DEGS) and Q (TCEP) have the largest s constants of *ca.* 1.7–1.9 units. The ionic salts (S–Y) all have s constants that approach or equal those for the most dipolar conventional phases, and which are very much larger than those for the unsubstituted poly(methylphenylsiloxane) phases (C–H). The *SSP* parameter (see Table I) is very nearly the same, however, for phase H as for phases T–W.

All the phases in Tables I and III, other than squalane (A), are hydrogen-bond bases and so give rise to significant values of the a constant. Of the conventional phases K, L, O, P and Q are the most basic, and hence will preferentially interact with solutes that are hydrogen-bond acids. However, all the ionic salts except phase V are significantly stronger hydrogen-bond bases than any of the conventional phases. This is clearly due to the negatively charged counter anions. It is not coincidental that where charge dispersion in the anion is very large, as with phase V, the a constant decreases considerably.

The l constant, on its own, is equivalent to ΔG_s^0 (CH_2) in that both quantities describe the ability of a phase to separate adjacent members of a homologous series. For the 24 phases, we find that

$$\Delta G_s^0(CH_2) = -44.9 - 816\,l \qquad (3)$$

with S.D. = 17 cal mol^{-1}, R = 0.9739 and No. = 24. Thus our general solvation equation, eqn. 1 or 2, includes, via the l constant, all the information contained in $\Delta G_s^0(CH_2)$.

If the dependent variable, logSP, in eqn. 1 is based on retention times, then the characteristic constants r, s, a, b and l will be the same as if log$K$ had been used as the dependent variable. Only the c constant changes. For many purposes, the c constant is not needed in the set of characteristic constants, but if log$K$ is used as the dependent variable, combination of the c constant and the l constant can lead to extra information.

Suppose we consider only the rare gases and the

alkanes, for which $R_2 = \pi_2^H = \alpha_2^H = \beta_2^H = 0$, so that eqn. 2 then becomes

$$\log K \text{ (inert solute)} = c + l \log L^{16} \quad (4)$$

The value of c is now identical with log K for an inert solute with log $L^{16} = 0$, *i.e.*, a rare gas between krypton (−0.211) and xenon (0.378) or an alkane between methane (−0.323) and ethane (0.492). We can now combine the c constant and the l constant, via eqn. 4, to show exactly how the affinity of a stationary phase for an inert solute depends on the L^{16} value of the solute. In Fig. 1 is a plot of log K calculated through eqn. 4 against log L^{16} for a series of *n*-alkanes on phases R, T and Q. For any alkane, phase R always has the highest log K value, *i.e.*, the highest affinity, of the three phases. However, for phases T and Q there is a "cross-over" point between propane and *n*-butane, so that for small alkanes phase Q has more affinity, but for larger alkanes phase T has the greater affinity.

The l constant, as with $\Delta G_s^0(CH_2)$, gives only the slopes of the lines in Fig. 1. Combination of the l constant with the c constant leads to extra information on the affinity of the stationary phase for inert solutes.

We can quantify the interaction of solutes with stationary phases by calculating each term in eqn. 1 or, for the present purpose, each term in eqn. 2. The results are given in Table IV, using three particular solutes suggested by Poole and co-workers [7] as test probes. *n*-Butylbenzene was used as a test probe for dispersive interactions, octan-1-ol for solvent basicity, benzodioxane for solvent acidity (not relevant here) and nitrobenzene for "orientation interactions". However, examination of Table IV shows, as mentioned in the Introduction, that it is not possible to define a set of test probes in which each probe corresponds to a unique interaction. Thus, octan-1-ol, the test probe for solvent basicity (the α_2^H term), actually interacts with most solvents more through dipolar interactions (the $s\pi_2^H$ term) than through solute hydrogen-bond acid–solvent hydrogen-bond base interactions. It is useful to break down the l log L^{16} term into an exoergic dispersion contribution to the Gibbs energy of solution, leading to a positive contribution to log K, and an endoergic cavity contribution to the Gibbs energy of solution, leading to a negative contribution to log K. Abraham and Fuchs [15] dissected log L^{16} values into various contributions and if we calculate these for the test solutes in hexadecane, and assume that the proportions are relatively the same in the phases studied here, we obtain the results in the last two columns of Table IV. Now, even if these dispersive and cavity interactions are only very approximate, they do show, as we have suggested before [10], that the main exoergic contribution to solution of gaseous solutes in nearly all liquid phases (except water perhaps) is through solute–solvent dispersion interactions. Unfortunately, it is very difficult to devise a simple experimental solute parameter that will reflect only the ability of a solute to interact via dispersion forces. Hence our combined dispersion plus cavity term, logL^{16}, has to be used in the general solvation equation, and then broken down approximately into its constituents.

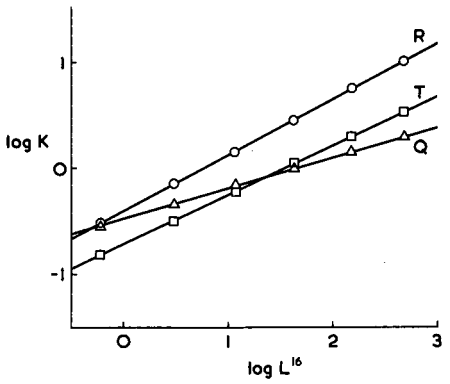

Fig. 1. Plot of log K against log L^{16} for the *n*-alkanes methane to hexane on phases R, T and Q.

Finally, we consider a few individual phases, and then show how the characteristic constants can be used to select phases for particular separations. Phases A–J are not exceptional; their dipolarities and hydrogen-bond basicities gradually increase along the series. Phase K has a very high dipolarity and basicity but the very low value of the l constant would tend to reduce the general usefulness of the phase. Phase M is exceptional, in that it has a moderate dipolarity ($s = 1.101$) but has effectively zero basicity, a most unusual occurrence. Of the molten salts, the tributylammonium salt, phase T, is of interest in that the Bu_3NH^+ group would be expected to be a powerful hydrogen-bond acid, but for this phase, as with all others, we find that the b constant is zero. No doubt intramolecular hydrogen bonding

TABLE IV

TERM-BY-TERM QUANTITATIVE EVALUATION OF THE SOLUTE-STATIONARY PHASE INTERACTIONS THAT CONTRIBUTE TO log K IN EQN. 2

Solute	Phase	c	rR_2	$s\pi_2^H$	$a\alpha_2^H$	$l \log L^{16}$	Dispersion[a]	Cavity[a]
Butylbenzene	C	−0.18	0.02	0.17	0	2.36	4.63	−2.27
	K	−0.64	0.23	0.99	0	1.13	2.22	−1.09
	M	−0.25	−0.22	0.57	0	1.95	3.83	−1.88
	Q	−0.49	0.17	0.99	0	1.36	2.67	−1.31
	R	−0.40	0.14	0.43	0	2.47	4.85	−2.38
	T	−0.72	0.07	0.80	0	2.18	4.28	−2.10
Octan-1-ol	C	−0.18	0.01	0.14	0.06	2.32	4.79	−2.47
	K	−0.64	0.08	0.80	0.61	1.11	2.29	−1.18
	M	−0.25	−0.07	0.46	0.02	1.92	3.96	−2.04
	Q	−0.49	0.06	0.80	0.62	1.34	2.77	−1.43
	R	−0.40	0.05	0.35	0.12	2.43	5.02	−2.59
	T	−0.72	0.02	0.65	1.08	2.15	4.44	−2.29
Nitrobenzene	C	−0.18	0.03	0.36	0	2.27	4.16	−1.89
	K	−0.64	0.34	2.09	0	1.09	2.00	−0.91
	M	−0.25	−0.32	1.21	0	1.88	3.45	−1.57
	Q	−0.49	0.24	2.10	0	1.31	2.40	−1.09
	R	−0.40	0.20	0.91	0	2.38	4.36	−1.98
	T	−0.72	0.10	1.70	0	2.10	3.85	−1.75

[a] These represent a breakdown of the $l \log L^{16}$ term according to ref. 15.

between the Bu_3NH^+ group and the counter anion takes place, so that the potential for intermolecular hydrogen bonding is reduced to zero. A comparison of the phases S, T and U shows that the a constant is reduced in phase T even though all three phases contain the 4-toluenesulphonate anion. This would be the result if there were intramolecular hydrogen bonding in phase T, because the anion would not then be totally available for intermolecular hydrogen bonding to a solute that was a hydrogen-bond acid.

For the separation of non-polar solutes, the only relevant characteristic constant is l. Phases A–F and R all have $l \geqslant 0.50$ and will be the best phases in the set to use. In order to separate compounds that are dipolar and non-acidic, a phase with a large s constant (and preferably a large l constant) is required. Phases J, L, M and O and the molten salts T, U, V and W are preferred here. These phases, except M, will also selectively absorb hydrogen-bond acids because they all have large a constants. To absorb acids rather than simply dipolar compounds requires $a \gg s$, if possible, and here the molten salts seem to be preferred (see Table IV).

In conclusion, we show that our general solvation equation, eqn. 1 or 2, can be used to analyse GLC retention data, both to classify stationary phases and to select phases for particular separations. The method is quantitative in that specific solute–stationary phase interactions can be identified and their contribution to the overall retention process can be evaluated (Table IV).

ACKNOWLEDGEMENTS

We thank the US Army Research, Development and Standardisation Group for support under Contract DAJA 45-87-C-004, and we are grateful to Professor Colin F. Poole for his helpful comments.

REFERENCES

1 C. F. Poole and S. K. Poole, *Chem. Rev.*, 89 (1989) 377.
2 S. K. Poole, B. R. Kersten and C. F. Poole, *J. Chromatogr.*, 471 (1989) 91.
3 J. Novak, *J. Chromatogr.*, 78 (1973) 269.
4 J. Novak, J. Ruzickova, S. Wicar and J. Janak, *Anal. Chem.*, 45 (1973) 1365.

5 R. V. Golovnya and T. A. Misharina, *Chromatographia,* 10 (1977) 658.
6 B. R. Kersten, C. F. Poole and K. G. Furton, *J. Chromatogr.,* 411 (1987) 43.
7 B. R. Kersten, S. K. Poole and C. F. Poole, *J. Chromatogr.,* 468 (1989) 235.
8 S. K. Poole and C. F. Poole, *J. Chromatogr.,* 500 (1990) 329.
9 M. H. Abraham, G. S. Whiting, R. M. Doherty and W. J. Shuely, *J. Chem. Soc., Perkin Trans. 2,* (1990) 1451.
10 M. H. Abraham, G. S. Whiting, R. M. Doherty and W. J. Shuely, *J. Chem. Soc., Perkin Trans. 2,* (1990) 1851.
11 M. H. Abraham, G. S. Whiting, R. M. Doherty and W. J. Shuely, *J. Chromatogr.,* 518 (1990) 329.
12 M. H. Abraham, G. S. Whiting, R. M. Doherty and W. J. Shuely, *J. Chromatogr.,* 587 (1991) 213.
13 M. H. Abraham, P. L. Grellier and R. A. McGill, *J. Chem. Soc., Perkin Trans. 2,* (1987) 797.
14 C. F. Poole, personal communication, 1990.
15 M. H. Abraham and R. Fuchs, *J. Chem. Soc., Perkin Trans. 2,* (1988) 523.

Journal of Chromatography, 587 (1991) 237–246
Elsevier Science Publishers B.V., Amsterdam

CHROM. 23 517

Identification of products resulting from carbonyl sulphide-induced degradation of diethanolamine☆

Olukayode Fatai Dawodu and Axel Meisen*

Department of Chemical Engineering, University of British Columbia, 2216 Main Mall, Vancouver, BC, V6T 1W5 (Canada)

(Received April 12th, 1991)

ABSTRACT

The degradation of aqueous diethanolamine (DEA) solutions due to carbonyl sulphide (COS) was studied by contacting the solutions (10–40 wt. %) in a well stirred, 600-ml stainless-steel autoclave with COS–nitrogen mixtures at temperatures ranging from 120 to 180°C. Combined gas chromatography-mass spectrometry, melting point determinations and elemental and infrared analyses were used to identify most of the major reaction products, *viz.*, monoethanolamine, ethylaminoethanol, ethyldiethanolamine, hydroxyethylacetamide, hydroxyethylpiperazine, ethanethioic acid S-hydroxyethylaminomethyl ester, bis(hydroxyethyl)ethylenediamine, bis(hydroxyethyl)piperazine, hydroxyethyloxazolidone, hydroxyethylimidazolidone, tris(hydroxyethyl)ethylenediamine, bis(hydroxyethyl)imidazolidone, acetaldehyde, acetone, butanone, acetic acid, ethanol, diethyl disulphide, dithiane and pyridines. In addition, a solid product containing sulphur was formed. The practical implications of the studies for gas plant operators are discussed.

INTRODUCTION

Acidic constituents (such as carbon dioxide, hydrogen sulphide, carbonyl sulphide and carbon disulphide) are frequently removed from natural, refinery and synthesis gases by counter-current contact with aqueous solutions of diethanolamine (DEA) in absorbers operating at elevated pressures and low temperatures. The amine solutions are subsequently regenerated by steam stripping at elevated temperatures and reduced pressures before recycling them to the absorbers.

In spite of its resistance to chemical breakdown, plant and laboratory experience indicate that, on prolonged use, DEA can undergo irreversible reactions. This phenomenon, which is called "degradation", not only leads to a loss of valuable amine, but may also contribute to operational problems such as equipment corrosion and fouling [1–4].

Previous studies [1,5–10] have provided appreciable insight into DEA degradation due to carbon dioxide (CO_2). The degradation is believed to occur primarily via DEA carbamate, which may be formed by the direct reaction of CO_2 with DEA. As hydrogen sulphide (H_2S) is incapable of forming carbamate-type compounds, it is generally agreed that H_2S does not cause the degradation of DEA, or in general, amines. The results reported by Choy [6] and Kim and Satori [7] suggest that H_2S in the presence of CO_2 hinders DEA degradation.

Compared with CO_2-induced degradation, little work has been reported on the degradation of DEA by carbonyl sulphide (COS). Orbach and Selleck [11] contacted pure COS with 20% (w/w) monoethanolamine (MEA) and 35% (w/w) DEA solutions in a bench-scale pilot plant simulating a typical, continuous absorption–regeneration process. The absorber and regenerator were operated at 40 and 104°C, respectively. Periodic analysis of the amine solutions using Kjeldahl analysis and acid titration revealed that, whereas MEA was substantially degraded, no loss of alkalinity occurred in the DEA solution over an 8-h period. Although the formation of a neutral product was reported, the

☆ This is an extended version of a paper presented at the *AIChE Spring National Meeting, Houston, TX, April 2–6, 1989.*

0021-9673/91/$03.50

amount was "too small to isolate and identify". Believing that this product was formed from small amounts of MEA in the initial DEA solution, they concluded that COS does not degrade DEA.

Pearce *et al.* [12] contacted, in a batch-mode, pure COS with 20 wt.% DEA solutions at temperatures ranging from 40 to 120°C. The solutions were subsequently analysed by infrared and mass spectrometry. Minor amounts of ethanol and oxazolidone were detected. However, they were insignificant compared with those formed when MEA was subjected to COS under similar operating conditions. Pearce *et al.* [12] also contacted COS with DEA continuously using a approach analogous to that of Orbach and Selleck [11]. The concentrations of the DEA solutions at the start and end of the experiments were determined by wet chemical analysis and found to be essentially the same. This again led to the conclusion that COS does not degrade DEA. A further conclusion was that COS underwent significant hydrolysis, as revealed by the presence of CO_2 and H_2S in the regenerator off-gas and the DEA solution leaving the absorber.

Notwithstanding the conclusions of the earlier studies, there are three reasons to believe that COS may degrade DEA: (i) COS may be hydrolysed to H_2S and CO_2, with the latter causing CO_2-induced degradation; (ii) previously used reaction times were too short, as amine degradation is a slow process; and (iii) past analytical techniqes were inadequate.

In connection with the first reason, Chakma's study [10] on the CO_2–methyldiethanolamine (MDEA) system revealed that degradation is possible via amine protonation and carbamate formation. As COS is hydrolysed in aqeuous systems to yield H_2S and CO_2, significant concentrations of H^+ and CO_2 can result, which lead to DEA degradation.

Second, Sharma [13] reported that the COS–DEA reaction to form thiocarbamate is more than two orders of magnitude slower than the CO_2–DEA reaction which produces DEA carbamate. As CO_2-induced degradation of DEA occurs primarily via the carbamate, it is likely that the COS-induced degradation of DEA via the thiocarbamates is correspondingly slower. The CO_2-induced degradation of DEA in itself is not a fast process. For instance, Kennard [9] found that at 120°C with a CO_2 partial pressure of 4.1 mPa and an initial DEA concentration of 30% (w/w), it took almost 20 h to obtain a 5% reduction in the amine concentration. During this period, only one degradation compound was detected at a concentration of about 1% (w/w). When CO_2–DEA degradation experiments were conducted over more than 8 days, significant accumulations of degradation compounds were noted at 120°C [7,9]. As Orbach and Selleck [11] conducted their DEA degradation experiments over 8 h, it is not surprising that significant amounts of degradation compounds could not be detected (the duration of the experimental runs performed by Pearce *et al.* [12] was not clearly indicated).

Third, the analytical techniques used previously may not have been sufficiently sensitive to detect the compounds arising from the degradation reactions. Gas chromatography (GC) and GC–mass spectrometry (GC–MS) using columns packed with Tenax GC [14] provide a more reliable and sensitive analysis of fresh and degraded alkanolamine solutions [7,15–19].

As the information in the literature on the COS-induced degradation of DEA is inconclusive and as such degradation is an important industrial problem, the present fundamental study was initiated.

EXPERIMENTAL

The degradation experiments were conducted by using a 600-ml stainless-steel reactor [8] which was partially filled with the amine solution of the desired concentration. The solution temperature was continuously measured by a J-type thermocouple and controlled within ± 0.5°C of the set point. The solution could be stirred at speeds up to 600 rpm and the system pressure was measured with a Bourdon pressure gauge graduated in 5 p.s.i. subdivisions. Liquid samples could be taken from the reactor by means of a stainless-steel sampling coil fitted with inlet and outlet valves. Pressure-lok syringes (supplied by Supelco, Oakville, Canada) were used for sampling the gas phase.

The following materials were used: DEA of 99+% purity was purchased from Aldrich (Milwaukee, WI, USA), COS from Matheson (Edmonton, Canada) with a purity of COS 97.7, CO_2 1.4, CS_2 0.19, H_2S 0.01, O_2 0.1 and CO and/or N_2 0.6 mol% and N_2 of 99+% purity from Medigas (Vancouver, Canada).

All compounds used for the calibration of the gas chromatograph were purchased from Aldrich, except hydroxyethyloxazolidone (HEOD), hydroxyethylimidazolidone (HEI), tris(hydroxyethyl)ethylene diamine (THEED) and bis(hydroxyethyl)imidazolidone (BHEI), which were not commercially available. HEOD was synthesized as described by Drechsel [20]. The final HEOD purity exceeded 97% as shown by GC analysis. The procedure described by Kennard [9] was used to synthesize THEED and gave a mixture containing about 48 mole% THEED, 47 mole% DEA and 5 mole% bis (hydroxyethyl)piperazine (BHEP). HEI was synthesized according to the procedure of Moller and Osberghaus [21]. The final product purity exceeded 97%. BHEI was formed by reaction of bis(hydroxyethyl)ethylenediamine (BHEED) with urea at 225°C for 4 h. This technique is an adaptation of the procedure for synthesizing HEI. The crude product mixture was purified by column chromatography using 70–230-mesh silica gel and water as solvent. A final product purity of 95+% was obtained.

Procedure for COS-induced DEA degradation

Typically, 250 ml of an aqueous DEA solution with the desired concentration were placed in the reactor, the stirrer was turned on and air was purged from the reactor by passing nitrogen through it for about 15 min. The reactor was then sealed and brought to the desired temperature; once a steady state had been achieved, COS was introduced through a stainless-steel tube connected to a pressurized COS cylinder fitted with a pressure regulator. The regulator was set so that its outlet pressure equalled the desired reactor pressure. The tube was left open and connected throughout the experiments to ensure a constant pressure in the reactor. The degradation experiments were conducted under the following operating conditions: DEA concentration, 10–40 wt.% (*ca.* 1–4 *M*); temperature, 120–180°C; and COS partial pressure, 0.3–1.17 MPa.

Chromatographic separation of reaction mixture

Liquid samples (typically 2 ml) were forced from the reactor at predetermined intervals into a stainless-steel sampling coil and quickly cooled to room temperature. Their constituents were then separated and determined using a Hewlett-Packard Model 5830A gas chromatograph equipped with an integrator terminal. The operating conditions were similar to those used by Kennard and Meisen [16] and Chakma and Meisen [19]: column, Tenax GC (60–80 mesh) packed in a 9 ft. × 1/8 in. I.D. stainless-steel column (supplied by Supelco); detector, hydrogen flame ionization, maintained at 300°C; temperature programme, isothermal at 150°C for 0.5 min, then increased to 300°C at 8°C/min; carrier gas, nitrogen at 23 ml/min; sample size, 0.001 ml.

Identification of degradation products

In order to identify the products of the degradation reactions, four successive methods were used.

GC. This technique (the details of which are described above) provides the retention times of the unknown compounds and, with the aid of relevant calibration data, the concentrations of the identified compounds.

GC–MS. A Hewlett-Packard Model 5985B GC–MS system was used and could be operated in both the electron impact (EI) and chemical ionization (CI) modes. The latter displays a prominent (usually the most abundant) protonated molecular ion $[M+1]^+$, from which the molecular weight of the unknown is inferred, whereas the former provides information on the fragmentation patterns, which are then compared with literature spectra [9,18,22,23].

GC–MS of silylated derivatives. To gain further insight into the structure of the degradation products, the degradation compounds were treated with trimethylsilylimidazole (TSIM) following a procedure similar to that employed by Chakma and Meisen [19] in order to replace active hydrogen atoms with trimethylsilyl groups. A 5-ml volume of a degraded solution was placed in a glass vial and saturated with potassium carbonate to dehydrate the sample. Isopropanol was then added to extract the degradation compounds from the mixture. The extract was transferred to another vial where the alcohol was removed by evaporation, leaving a viscous oil. An excess of TSIM was added to the oil and the mixture was thoroughly shaken and left for at least 1 h at room temperature to ensure complete derivatization. The derivatized sample was then analysed by GC–MS. GC was performed as described above, but a fused-silica megabore column (50% phenylmethylsilicone, 10 m × 0.53 mm I.D.) was used to separate the mixture because Tenax GC proved to

be unsuitable. As TSIM attacks primarily hydroxyl groups, the CI mass spectra could be used to determine the molecular masses of the silylated compounds and hence the number of hydroxyl groups per molecule. The silylating trimethylsilicon ion (TMS) has a molecular mass of 73 and replaces the hydrogen in OH groups. Thus silylation of a compound increases its molecular mass by $72n$, where n is the number of hydroxyl groups in the compound.

GC of degraded mixtures spiked with suspected compounds. Once GC–MS analysis had provided information on the possible identities of the degradation compounds, pure forms of these compounds were purchased or synthesized when commercially unavailable. The pure compounds were added to the degraded solutions and the spiked solution samples were then analysed by GC using the conditions given above. The resulting peak areas and retention times were compared with those for the unspiked sample. An increase in the area of a particular peak due to spiking, together with GC–MS analysis, can provide conclusive proof of the identity of an unknown compound.

RESULTS AND DISCUSSION

Before proceeding with the main experimental program, it was necessary to conduct some preliminary experiments aimed at evaluating the effects of certain operating variables on the degradation reactions.

Elevated temperatures were used in this study to speed up the degradation reactions. The result obtained under such conditions will only have industrial relevance if the alkanolamines are not thermally degraded and the reaction products are similar to those obtained at the lower temperatures commonly used in industry. Thermal degradation experiments, conducted by heating aqeuous solutions of DEA under a blanket of nitrogen, revealed no significant change in solution composition within 220, 60 and 48 h at temperatures of 150, 165 and 180°C, respectively [24]. Under these conditions, thermal degradation was negligible, and these findings agreed with the results of Kennard and Meisen [8]. As most of the high-temperature degradation runs were conducted within 48 h, the influence of thermal degradation on the results can be dismissed.

Typical chromatograms of aqueous DEA solutions degraded in the presence of COS are shown in Fig. 1. The qualitative similarity of the traces is obvious. This suggests that the basic reaction mechanism is not affected by temperature. As industrial DEA regenerators operate at reboiler temperatures of up to 140°C, the products obtained in this study should also be formed under industrial conditions.

Two runs were performed with and without a Pyrex liner in the reactor. The results indicated very similar products and hence the liner had a negligible effect on the reaction mechanism.

Degradation compounds

Fig. 2 shows the chromatograms of samples from a typical run conducted with a 40% (w/w) DEA solution at a COS partial pressure of 0.34 MPa and a temperature of 180°C. The gradual formation of reaction products is obvious. In addition, it was noted that the samples became more pungent and viscous as the degradation progressed. Some particulate matter was also found in the samples.

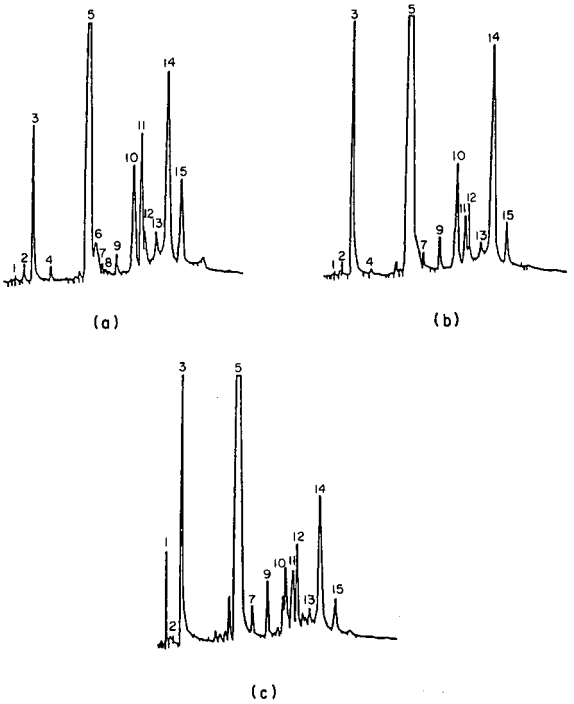

Fig. 1. Chromatograms of partially degraded DEA solutions of 4 *M* initial concentration. (a) 180°C, 0.34 MPa COS, time 30 h; (b) 150°C, 0.34 MPa COS, time 50 h; (c) 120°C, 0.68 MPa COS, time 215 h. For peaks, see Table I.

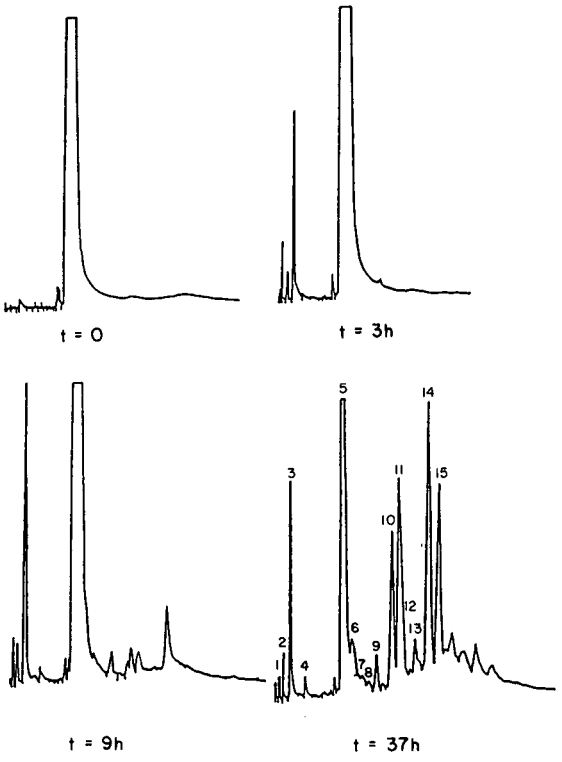

Fig. 2. Chromatograms showing the gradual formation of degradation products in a COS–DEA system (4 *M* DEA, 180°C, 0.34 MPa). *t* = time.

By following the techniques described above, the compounds responsible for the peaks labelled in Figs. 1 and 2 were identified and are listed in Table I. Figs. 3 and 4 show the various spectra for DEA and BHEI. For the compounds that are not available commercially (*e.g.*, BHEI), the library EI mass spectra refer to the spectra of the compound synthesized in the laboratory. The detailed spectra for the other compounds were provided by Dawodu [24].

A consistent pattern in the fragmentation of these hydroxylamino compounds is the loss of hydroxymethyl radicals (*m/e* 31) from the parent compounds to produce, in general, the most abundant ions. Ions of mass 30 for MEA, 58 for ethylaminoethanol (EAE), 74 for DEA, 72 for hydroxyethylacetamide (HEA), 102 for ethyldiethanolamine (EDEA), 143 for BHEP and BHEI, 100 for HEOD and 99 for HEI and hydroxyethylpiperazine (HEP) were generated in this manner. For BHEED and THEED, hydroxymethyl radicals were also lost, but the principal fragmentation resulted from the cleavage of the C–C bond between two nitrogen atoms giving ions with mass 74 for BHEED (N,N'-isomer) and 118 for THEED as the most abundant ions. The loss of water molecules also occurred. For example, ions of mass 74 lost water to give ions with a mass of 56 in the case of DEA. The molecular ion peaks are not prominent in most of the EI mass spectra because of the ease with which the hydroxymethyl groups break from the molecules. The characteristic peaks in the CI mass spectra of the hydroxylamino compounds are produced by the $[M+H]^+$, $[M+C_2H_5]^+$ and $[M-CH_5]^+$ ions. For the silyl derivatives, the CI mass spectra show prominent $[M+H]^+$, $[M+C_2H_5]^+$ and $[M-CH_3]^+$ ions. The $[M-CH_3]^+$ ion is characteristic of the silylating agent (TSIM). The previous, tentative identification [25] of peak 9 as bis(hydroxyethyl)aminoethanol (BHEAE) now appears to be invalid. The compound has a molecular mass (MW) of 149 as indicated by its CI mass spectrum (Fig. 5). Its silyl derivative has a molecular mass of 221, which suggests that it contains one hydroxyl group. The EI mass spectrum shows the most abundant ion as having a mass 74. Loss of the characteristic hydroxymethyl radical does not produce a prominent peak, even though the compound appears to have an hydroxyethyl attachment (deduced from the ion of mass 74). This, in addition to the prominent ion of mass 89 in the CI mass spectrum, suggests that the compound is not very stable and fragments on electron bombardment to give ions with a mass of 89 or, more likely, 74. Based on the available information, the most likely structure for this compound, ethanethioic acid S-[(2-hydroxyethyl) amino]methyl ester (ETAHEAME), is $CH_3C(O)SCH_2NHCH_2CH_2OH$. This compound is unavailable commercially and it was therefore not possible to compare its retention time under the present GC conditions with that of peak 9.

It also appears that triethanolamine (TEA) was formed as a degradation compound but could not be distinctively separated from BHEED under the analytical conditions used. This supposition arises from the fact that the GC analysis of the silyl derivatives showed a peak before BHEED, having a molecular weight of 365. This would suggest an underivatized hydroxylamino compound with a molec-

TABLE I

MAJOR DEGRADATION COMPOUNDS DETECTED IN THE COS–DEA SYSTEM

Peak No.	Retention time (min)	Characteristic EI ions	Molecular weight		n OH[b], (M* – M)/72	Identity
			M	M*[a]		
1	1.4– 1.5	43, 58	58			Acetone
2	2.2– 2.3	29, 43, 57, 72	72			Butanone
3	3.1– 3.3	30, 42, 61	61	133	1	MEA
4	5.2– 5.3	30, 56, 74 42, 58, 89	89	161	1	EAE
5	9.2–10.0	45, 56, 74	105	249	2	DEA
6	10.9–11.1	30, 56, 74, 102 45, 58, 88, 133	133	277	2	EDEA
7	11.5–11.6	30, 60, 73 43, 72, 85	103	175	1	HEA
8	12.0–12.1	42, 70, 112 56, 88, 130	130	202	1	HEP
9	13.4–13.5	56, 74, 118 61, 89, 149	149	221	1	ETAHEAME
10	15.2–15.5	44, 74, 100, 56, 88, 118, 127	148	292	2	BHEED
11	16.2–16.6	42, 70, 100, 125 56, 88, 113, 143 156, 174	174	318	2	BHEP
12	16.7–16.9	42, 74, 100 56, 88, 131	131	203	1	HEOD
13	18.2–18.4	42, 70, 99 56, 85, 130	130	202	1	HEI
14	19.7–19.8	42, 70, 100, 130 56, 88, 118, 143 174	192	408	3	THEED
15	21.0–21.3	42, 70, 114, 143 56, 99, 130, 174	174	318	2	BHEI

[a] M* is the molecular weight of the derivatized compound.

[b] n OH refers to the number of hydroxyl groups in each compound.

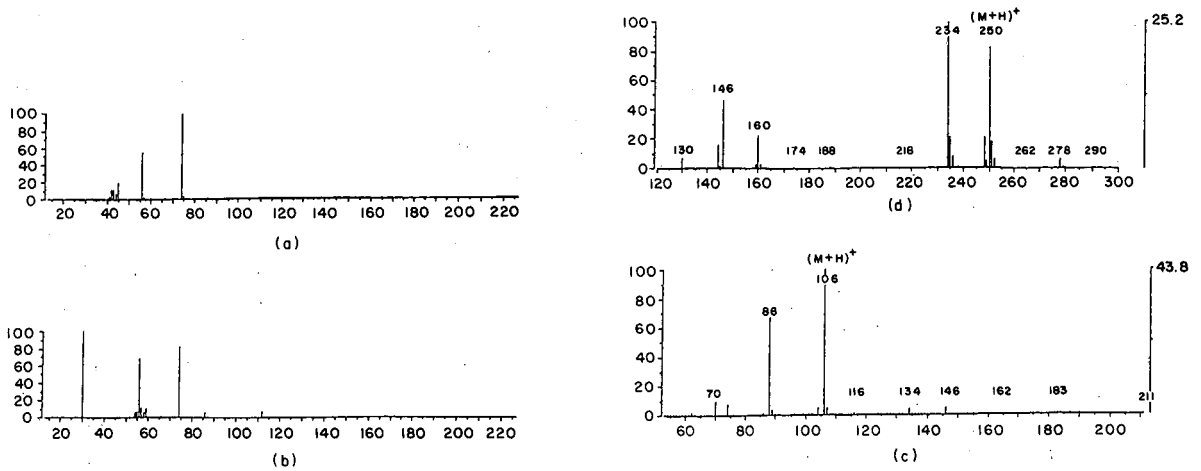

Fig. 3. Mass spectra of DEA. (a) EI spectrum; (b) EI library spectrum; (c) CI spectrum; (d) CI spectrum of silyl derivative.

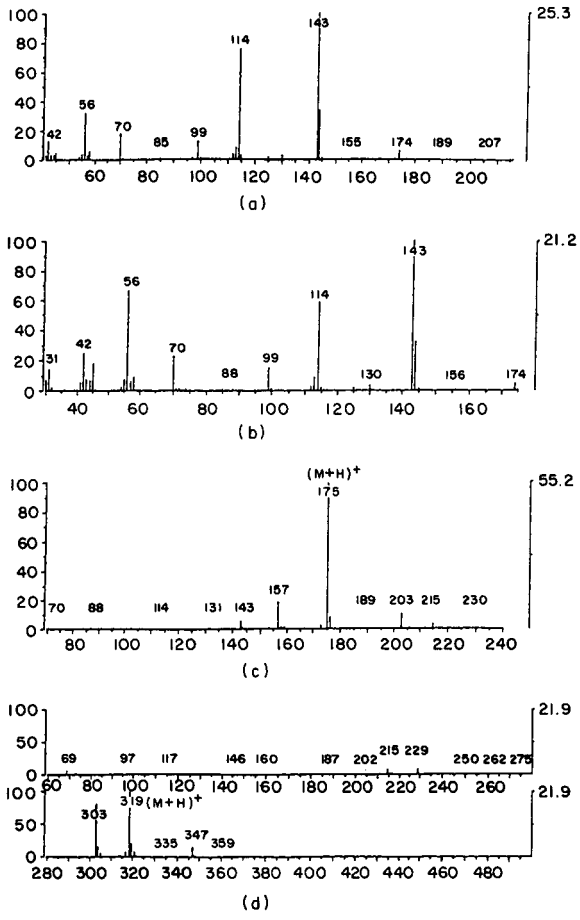

Fig. 4. Mass spectra of BHEI. (a) EI spectrum; (b) EI library spectrum; (c) CI spectrum; (d) CI spectrum of silyl derivative.

ular weight of 149 and three hydroxyl groups. Triethanolamine fits this structure.

The degradation compounds may be conveniently grouped into two categories: low-boiling degradation compounds which elute before DEA and high-boiling degradation compounds which elute after DEA. Other low-boiling degradation compounds include methanol, ethanol, acetaldehyde, acetic acid, methylpyridine, diethyl disulphide, ethyl methyl pyridine and 1,2-dithiane.

Analysis of the gas phase also revealed the presence of ethanol, acetone, butanone, higher molecular weight ketones and some of the other low-boiling degradation compounds found in the liquid phase.

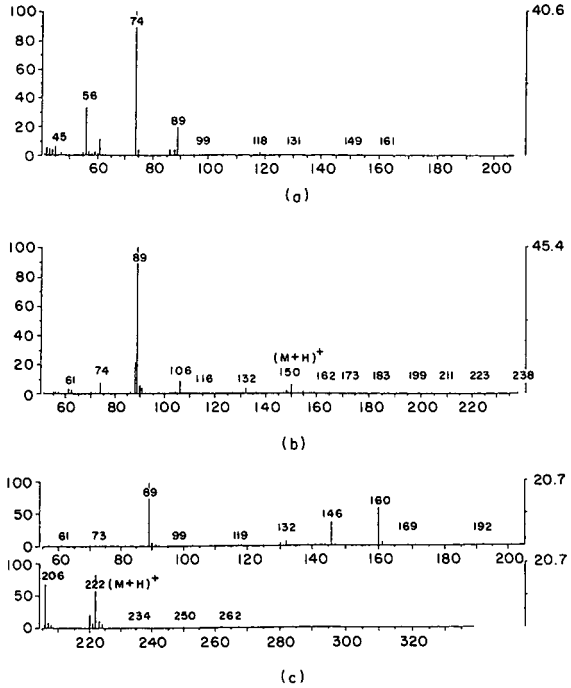

Fig. 5. Mass spectra of peak 9 identified as ETAHEAME. (a) EI spectrum; (b) CI spectrum; (c) CI spectrum of silyl derivative.

In addition to the water-soluble degradation compounds, an insoluble, sticky, light-brown solid product was formed. The product was insoluble in water, ethanol, methanol, toluene, diethyl ether, acetone and carbon disulphide (even at their boiling points). However, boiling dimethylformamide dissolved the product with precipitation occuring as soon as the solution was cooled. The insoluble nature of the solid suggests that it is a polymeric material.

The melting point of the solid was determined using a Kofler hot-stage microscope. A small chip of the solid product was placed on a slide on the hot bench and the temperature was raised at 4°C/min. At the melting temperature, the sample became fluid and the phase change was clearly visible. Four determinations were made for each sample and the average temperatures were recorded. The solid was found to melt in the range 124–138°C with most of it melting above 135°C. The broad melting range is an indication that the solid is impure.

The elemental composition of the solid was determined by the Canadian Microanalytical Laborato-

TABLE II

ELEMENTAL COMPOSITION OF SOLIDS GENERATED IN THE COS–DEA SYSTEM

Element	Composition			
	150°C		180°C	
	% (w/w)	Mole%	% (w/w)	Mole%
C	41.95	28.31	44.11	29.07
H	7.08	57.34	7.26	57.41
N	1.76	1.02	2.94	1.66
O	2.87	1.45	3.94	1.95
S	46.92	11.88	40.14	9.92
Total	100.58	100.00	98.39	100.00

ry (New Westminster, Canada) and the results are given in Table II. The composition of the solid depends on the operating conditions of the degradation runs. The percentage of sulphur decreased with increasing temperature whereas the reverse occurred for the other elements. This trend could be due to the fact that, except for sulphur, all other elements are contained in the amine whose initial concentration increases with increasing operating temperature (due to increased evaporation of water). In the same vein, increasing temperature limits the solubility of COS, and consequently the amount of sulphur available for reactions in the liquid phase. The differences in the elemental compositions could also be related to the purity of the solid produced under the various operating conditions. The degradation was more pronounced as the temperature increased, resulting in higher concentrations of the degradation products. As most of the products do not contain sulphur, the solid recovered from the run conducted at 180°C would contain more sulphur-free impurities (and thus have a lower sulphur content) than the solid recovered at lower temperatures. The ratios of the elements could be calculated from the elemental analyses given in Table II. For examples, in the solid generated in the runs at 180°C, the C/S, C/H, C/N, S/O, N/O, C/O, H/N and H/O ratios are 2.93, 0.50, 17.50, 5.09, 0.85, 14.93, 34.57 and 29.48, respectively. These ratios represent approximately an empirical formula of $C_{15}H_{30}NOS_5$ (empirical weight 400). The high empirical weight of the solid is consistent with its high melting point.

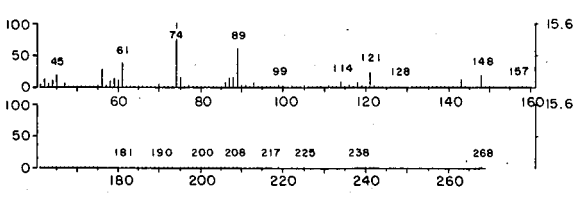

Fig. 6. EI mass spectrum of the solid.

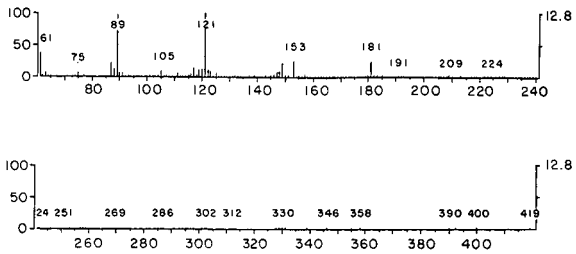

Fig. 7. CI mass spectrum of the solid.

Solid-probe EI and CI mass spectral analyses were performed on the solid product to determine the fragmentation pattern and the molecular weight; the results are shown in Figs. 6 and 7, respectively. The CI mass spectrum shows successive losses of ions of masses 28 and 32. As the solid is rich in sulphur, the ion of mass 32 is most likely sulphur. The ion of mass 28 could either be a carbonyl group (C=O) or an ethenyl (C_2H_4) group. However, the very low oxygen to sulphur ratio in the solids, the almost equal number of losses of masses 28 and 32 and the high carbon content of the solids point to an ethenyl group as the fragmenting group with mass 28 (IR analysis discussed below did not show any C=O bonding). It is difficult to identify a molecular ion peak from the CI trace because of the low abundances of the high-molecular-

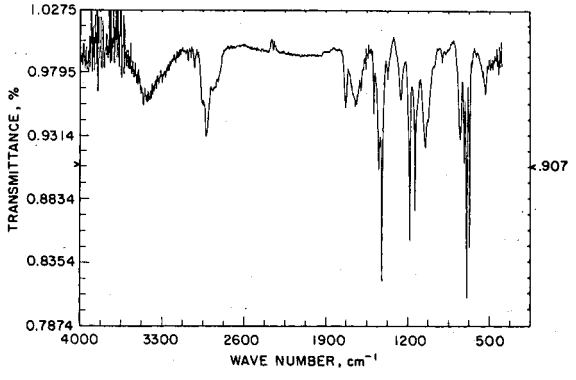

Fig. 8. Infrared trace of the solid.

TABLE III

FUNCTIONAL GROUP ASSIGNMENTS FOR THE SOLID

Literature IR [26,27]		Sample IR	
Group	Band (cm^{-1})[a]	Band (cm^{-1})[a]	Assignment
CH_2SCH_2	670– 760 (m)	672, 698 (m)	CH_2SCH_2
SH	815– 930 (w)	910 (w)	SH
	2420–2600 (w)	2500 (w)	SH
(CH_2NHCH_2)	3100–3500 (m)	3422 (w–m)	(CH_2NHCH_2)
	1480–1580 (w)	1492 (w)	
	1100–1200 (m)	1187 (m)	
	1080–1150 (m)	1143 (m)	
$-(CH_2)_1$	770– 785 (w–m)		
$-(CH_2)_2$	735– 745 (w–m)	754 (w)	$-(CH_2)_n$
$-(CH_2)_3$	725– 735 (w–m)	721 (w–m)	$(2 \leqslant n \leqslant 4)$
$-(CH)_2)_4$	720– 725 (w–m)	721 (w–m)	
(CH_2OH)	1400–1460 (w)	1424 (m)	CH_2OH
	1260–1350 (w)	1264 (w)	
	1010–1090 (s)	1053 (w)	
	3100–3500 (s)	3422 (w–m)	

[a] The letters, m, s and w refer to absorbances of moderate, strong and weak intensity, respectively.

weight ions. The most abundant peak has a mass of 121, suggesting a molecular weight of 120. The high melting point of the solids is inconsistent with this molecular weight. Further, the absence of ions of mass 149 (M + 29) makes a molecular mass of 120 very unlikely.

The pattern of successive losses of masses 28 and 32 in the CI mass spectra suggests a fragile linear structure containing several covalent bonds with sulphur interspersed between the ethenyl groups. The ease of bond breakage is, perhaps, the reason for not having a prominent molecular ion peak.

To gain an insight into the functional groups in the compound, IR absorption traces were obtained using potassium bromide pellets in a Bomem–Michelson 100 spectrophotometer. The resulting trace is shown in Fig. 8. It should be noted that the absorbances are of weak to medium intensities. Table III shows the assignment of functional groups to the absorption bands in the IR trace.

The analyses conducted allowed the identification of the fragments or functional groups that constitute the solid product. The insoluble nature of the solid and its level of purity were handicaps that prevented further analysis and a more conclusive identification.

The present results are at variance with previous findings of Orbach and Selleck [11] and Pearce *et al.* [12]. However, it is important to note that the degradation reactions were slow. Even under severe conditions (40% DEA, 180°C), only the low-boiling degradation compounds were formed in appreciable amounts within the first 6 h. At 120°C, only the low-boiling degradation compounds were detected within the first 24 h. As pointed out earlier, perhaps the inability of the previous investigators to detect degradation compounds in COS–DEA systems was due to the short experimental durations and inadequate analytical techniques.

Practical implications

The practical significance of COS-induced DEA degradation stems from the fact that degradation affects the absorption of acid gases, plant corrosion, equipment fouling and solution foaming. The major degradation compounds include MEA, BHEED, BHEP, HEOD, HEI, THEED and BHEI. Except for BHEI and HEOD these compounds are known to absorb acid gases (especially CO_2) and their presence will alter, but not eliminate, the absorptive capacity of DEA solutions. As MEA and diamines are known to be particularly corrosive at high temperatures, hot spots in the plant should be avoided. The most susceptible areas are the reboiler

and the rich side of the lean–rich DEA heat exchanger.

Formation of solid products may also create fouling deposits in piping, heat exchangers and reboilers. As a result, pressure drops will rise and heat-transfer coefficients will fall, leading to overall energy costs for the plants. Cleaning of piping and heat exchangers is also expensive. It is therefore advisable to provide efficient filtration systems.

There is a trend towards utilizing mixtures of alkanolamines for the removal of impurities from gas streams. The results of this study show that if the mixture consists of a primary and a secondary alkanolamine such as MEA and DEA, more degradation products will be formed compared with the single amine system. The increased degradation needs to be taken into consideration in deciding which alkanolamines are to be mixed.

CONCLUSIONS

COS can cause degradation of aqueous DEA solutions. Products not previously identified as degradation compounds in CO_2–DEA systems were detected. This is an indication that COS-induced degradation does not result, entirely, from CO_2 formed by the hydrolysis reaction. The degradation is slow, but may become significant under typical plant conditions, especially over extended periods of time. In addition to the water-soluble degradation compounds, a polymeric, insoluble, sulphur-rich solid product was formed.

ABBREVIATIONS

BHEED	Bis(hydroxyethyl)ethylenediamine
BHEI	Bis(hydroxyethyl)imidazolidone
BHEP	Bis(hydroxyethyl)piperazine
DEA	Diethanolamine
EAE	Ethylaminoethanol
EDEA	Ethyldiethanolamine
ETAHEAME	Ethane thioic acid S-[(2-hydroxyethyl)amino]methyl ester
HEA	Hydroxyethylacetamide
HEI	Hydroxyethylimidazolidone
HEOD	Hydroxyethyloxazolidone
HEP	Hydroxyethylpiperazine
MDEA	Methyldiethanolamine
MEA	Monoethanolamine
TEA	Triethanolamine
THEED	Tris(hydroxyethyl)ethylenediamine
TSIM	Trimethylsilylimidazole

ACKNOWLEDGEMENTS

The financial assistance provided by the Natural Sciences and Engineering Research Council of Canada and the Canadian Commonwealth Scholarship and Fellowship Plan is gratefully acknowledged.

REFERENCES

1 L. D. Polderman and A. B. Steele, *Oil Gas J.*, 54 (1956) 206.
2 K. L. Moore, *Corrosion*, 16 (1960) 111.
3 W. D. Hall, and J. G. Barron, in *Proceedings of the 31st Annual Gas Conditioning Conference, Norman, OK, March 2–4, 1981.*
4 A. Chakma and A. Meisen, *Ind. Eng. Chem., Prod. Res. Dev.*, 25 (1986) 627.
5 L. D. Hakka, K. P. Sing, G. L. Bata, A. G. Testart and W. M. Andrejchyshyn, *Gas Processing/Canada*, 61 (1968) 32.
6 E. T. Choy, *M. A. Sc. Thesis*, University of British Columbia, Vancouver, 1978.
7 C. J. Kim and G. Sartori, *Int. J. Chem. Kinet.*, 16 (1984) 1257.
8 M. L. Kennard and A. Meisen, *Ind. Eng. Chem., Fundam.*, 24 (1985) 129.
9 M. L. Kennard, *Ph.D. Thesis*, University of British Columbia, Vancouver, 1983.
10 A. Chakma, *Ph.D. Thesis*, University of British Columbia, Vancouver, 1987.
11 H. K. Orbach and F. T. Selleck, unpublished results, 1975 (quoted with permission of F. T. Selleck, Fluor Corp.).
12 R. L. Pearce, J. L. Arnold and C. K. Hall, *Hydrocarbon Process.*, 40 (1961) 121.
13 M. M. Sharma, *Trans. Faraday Soc.*, 61 (1965) 681.
14 R. van Wijk, *J. Chromatogr. Sci.*, 8 (1970) 418.
15 N. C. Saha, S. K. Jan and R. K. Dua, *Chromatographia*, 10 (1977) 368.
16 M. L. Kennard and A. Meisen, *J. Chromatogr.*, 267 (1983) 373.
17 G. D. Robbins and J. A. Bullin, *Energy Prog.*, 4 (1984) 229.
18 C. S. Hsu and C. J. Kim, *Ind. Eng. Chem., Prod. Res. Dev.*, 24 (1985) 630.
19 A. Chakma and A. Meisen, *J. Chromatogr.*, 457 (1988) 287.
20 E. K. Drechsel, *J. Org. Chem.*, 22 (1957) 849.
21 H. Moller and R. Osberghaus, *Ger. Offen.*, 2 746 650 (1979); *C.A.* 91 (1979) 128904u.
22 *Eight Peak Index of Mass Spectra*, Mass Spectrometry Data Centre, AWRE, Aldermaston, 2nd ed., 1974.
23 *EPA/NIH Mass Spectral Data Base*, National Standards Reference Data Service, National Bureau of Standards, Washington, DC, 1983.
24 O. F. Dawodu, *Ph.D. Thesis*, University of British Columbia, Vancouver, 1991.
25 O. F. Dawodu and A. Meisen, in *Proceedings of the 39th Annual Gas Conditioning Conference*, Norman, OK, 9–71, March 6–9, 1989.
26 W. W. Simmons (Editor), *The Sadtler Handbook of Infrared Spectra*, Sadtler Research Labs., Philadelphia, PA, 1978.
27 J. A. Dean, *Handbook of Organic Chemistry*, McGraw-Hill, New York, 1987, Ch. 6.

Journal of Chromatography, 587 (1991) 247–254
Elsevier Science Publishers B.V., Amsterdam

CHROM. 23 530

Analysis of keto acids as their methyl esters of 2,4-dinitrophenylhydrazone derivatives by gas chromatography and gas chromatography–mass spectrometry

Rafael Navarro-González*,☆, Alicia Negrón-Mendoza and Guadalupe Albarrán

Instituto de Ciencias Nucleares, UNAM, Circuito Exterior, CU, A. Postal 70-543, México, D.F. 04510 (México)

(First received January 25th, 1991; revised manuscript received June 5th, 1991)

ABSTRACT

The analysis of keto acids via reaction with 2,4-dinitrophenylhydrazine (DNP) and esterification with methanol–hydrochloric acid by gas chromatography and gas chromatography–mass spectrometry is described. The derivatives formed (DNPH) are moderately stable and are easy to analyse. The separation of eighteen biologically important keto acids is described. The utility of the method in biochemical studies is demonstrated by the facility of the analysis of keto acids from a plant extract of *Cnidoscolus urens*. A set of electron impact mass spectra of DNPH derivatives is presented.

INTRODUCTION

The analysis of keto acids is an important task in biochemical studies on cellular metabolism. Keto acids are formed as intermediates during metabolic inteconversions of sugars, carboxylic acids and amino acids. Several methods have been developed for the analysis of keto acids using certain types of derivatization [1–9]. Among them, the most widely employed is derivatization via dinitrophenylhydrazine (DNP) [10].

The 2,4-dinytrophenylhydrazone (DNPH) derivatives of keto acids can be used successfully for the isolation of these carboxylic acids from complex mixtures [11]. They have been analysed by spectroscopic techniques [11,12], paper chromatography [13], thin-layer chromatography [14,15] and high-performance liquid chromatography [4,16–18]. Direct separation of DNPHs by gas chromatography (GC) has been accomplished after converting them into methyl esters [19,20]. However, it must be pointed out that in all these chromatographic methods, the separations were complicated as some DNPHs exist as *syn–anti* isomers [13].

This paper describes a method for the analysis of a large number of keto acids as their methyl esters of DNPH derivatives by GC and GC mass spectrometry (MS). The electron impact mass fragmentation pattern of DNPH derivatives is examined, and a set of spectra is provided.

EXPERIMENTAL

Reagents

Keto acids were purchased from Sigma and DNP from Merck. Acetylsuccinic acid was synthesized as its dimethyl ester. Other reagents and solvents were

☆ Present address: Laboratory of Chemical Evolution, Department of Chemistry and Biochemistry, University of Maryland, College Park, MD 20742, USA.

0021-9673/91/$03.50

of the highest purity commercially available, and were used as received.

Derivatization of standard keto acids

DNPH derivatives were prepared via interaction of the keto acid (0.3 mmol) and DNP (0.5 mmol) in 15% aqueous perchloric acid (30 ml). The mixture was allowed to stand for 30 min at 20°C, then the derivatives were extracted with ethyl acetate (12 ml) by shaking for 3 min three times. The organic phase was evaporated to dryness and the residue was dissolved in 1.6 *M* hydrochloric acid in methanol (10 ml). Esterification was performed by heating the sample in a bath at 70°C for 1 h. After cooling, chloroform–water (4:1) (5 ml) was added and the DNPH derivatives were recovered in the organic phase. The products were recrystallized from benzene or ethyl acetate, and then analysed by GC, GC–MS and infrared spectrometry. This procedure is not affected if esterification is first performed followed by derivatization via DNP.

Derivatization and extraction of keto acids from biological material

Cnidoscolus urens, a typical plant from the Pedregal de San Angel on the south side of Mexico City, was used for this study. Leaves from *Cnidoscolus urens* were blended in doubly distilled water (pH 2–3) with a mixer immediately after harvesting. The homogenate was filtered and allowed to react with DNP as described in the previous section. After reaction, the DNPH derivatives of keto acids and other carbonyl compounds were extracted with ethyl acetate. The organic phase was washed three times with 1 *M* sodium carbonate (in a 3:1, v/v ratio) in order to extract the keto acids selectively. The aqueous phase was then acidified to pH 4–6 with concentrated hydrochloric acid and the keto acids were extracted with ethyl acetate. The organic layer was evaporated to dryness and subsequently esterified in 1.6 *M* hydrochloric acid in methanol (10 ml) as described in the previous section.

GC analysis

A Varian Aerograph Series 2400 gas chromatograph equipped with a flame ionizing detector and a Hewlett-Packard Model 3388A integrator terminal were employed. The chromatographic separation was carried out in a stainless-steel column (1.22 × 32 mm I.D.) packed with 3% OV-17 on Chromosorb W AW DMCS (80–100 mesh). The column temperature was programmed from 200 to 300°C at 6°C/min. The carrier gas was nitrogen at a flow-rate of 33 ml/min. The injector temperature was kept at 250°C. In order to increase the response and reproducibility of DNPH derivatives of keto acids, the detector temperature was maintained at 240°C. This temperature was based on the results of Papa and Turner [21], who found that a lower detector temperature produces an increased response and linearity, improved reproducibility and disappearance of extraneous peaks which are believed to be due to decomposition products of DNPH derivatives of aldehydes and ketones.

GC–MS analysis

GC–MS analysis was carried out on a Hewlett-Packard Model 5890 gas chromatograph coupled to a Hewlett-Packard Series HP-5970 mass detector operated at 70 eV. A PH-1 capillary column from Hewlett-Packard (12 m × 0.2 mm I.D.; film thickness 0.33 μm) was used. The carrier gas was helium at a flow-rate of 2 ml/min. The column temperature was programmed from 150 to 210°C at 6°C/min.

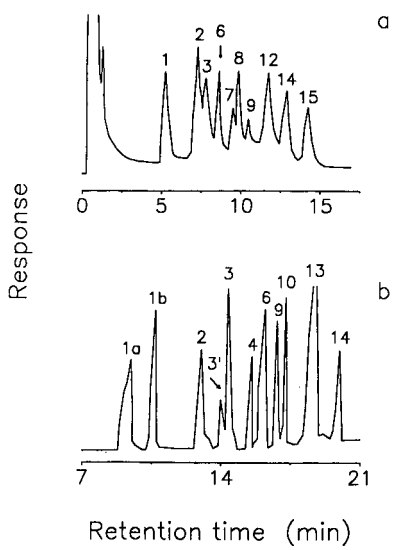

Fig. 1. Gas chromatograms of methyl esters of DNPH derivatives of keto acids: (a) 3% OV-17; (b) HP-1 column. Peak assignments as in Table I.

MS analysis

A VG Analytical Model 7070E mass spectrometer operated at 70 eV was used.

RESULTS AND DISCUSSION

The separation of eighteen biologically important keto acids was investigated. Table I summarizes their retention times for an OV-17 packed column and an HP-1 capillary column. In addition, Table I gives information concerning the molecular weights (MW) of the derivatives and the location of their mass spectra. The chromatographic separations for a variety of keto acids are shown in Fig. 1a and b for an OV-17 and a HP-1 column, respectively.

The method presented facilitates the examination of a wide variety of keto acids in a relatively short chromatographic time of less than 20 min. The detection limit for the determination of keto acids derivatives was established to be in the nanomole range.

Syn–anti isomers and their resolution have been reported in all chromatographic methods where keto acids are converted into DNPH derivatives [4,11–20]. In order to demonstrate whether or not

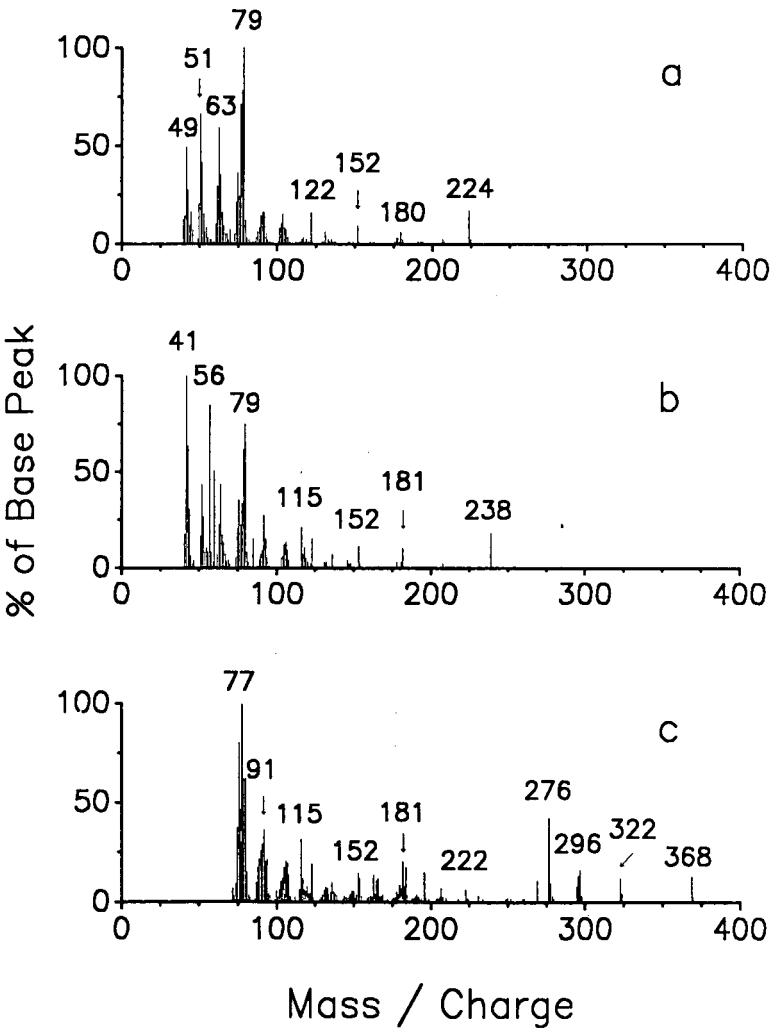

Fig. 2. Mass spectra of methyl esters of DNPH derivatives of β-keto acids: (a) acetoacetic acid, peak 1a; (b) acetoacetic, peak 1b, and β-ketoglutaric acids; (c) oxaloacetic acid (ethyl ester).

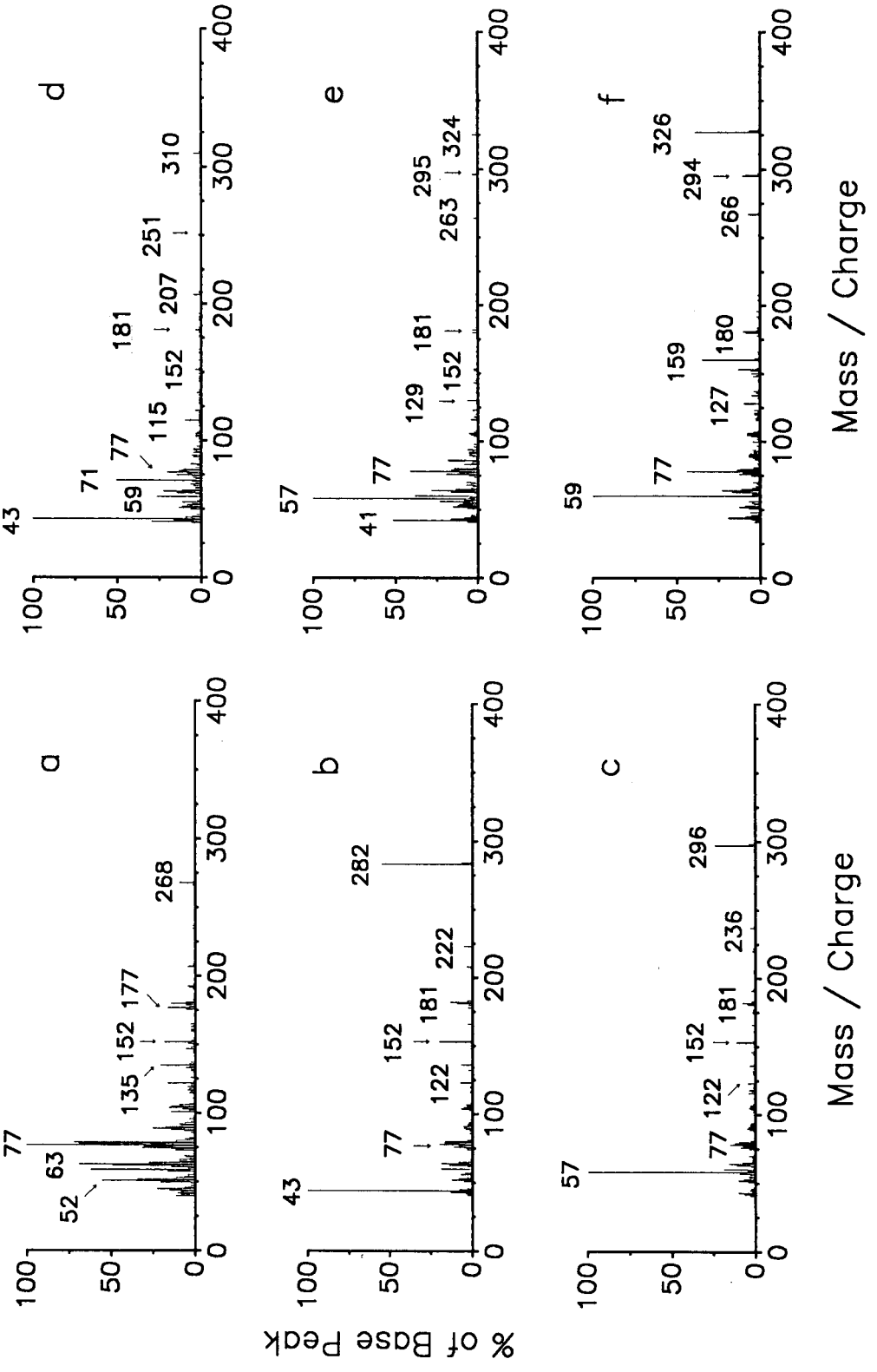
a
b
c
d
e
f
% of Base Peak
Mass / Charge
Mass / Charge

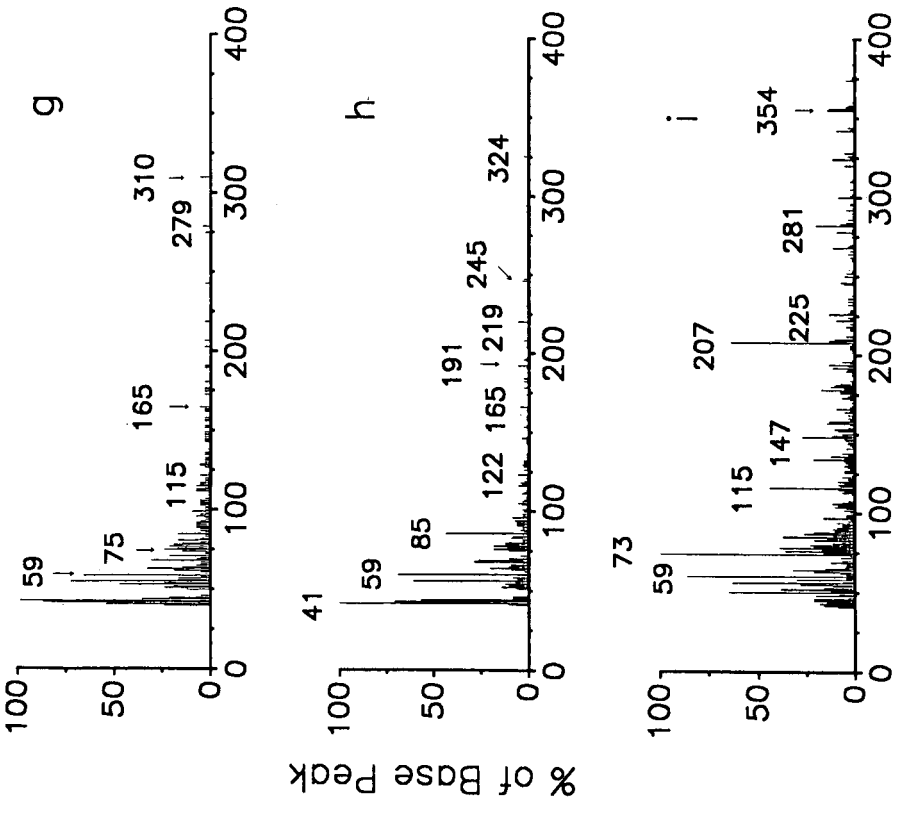

Fig. 3. Mass spectra of methyl esters of DNPH derivatives of keto acids: (a) glyoxylic acid; (b) pyruvic acid; (c) α-ketobutyric acid; (d) α-ketoisovaleric acid; (e) *d,l*-α-keto-β-methyl-*n*-valeric acid; (f) ketomalonic acid; (g) levulinic acid; (h) 4-acetyl-*n*-butyric acid; (i) α-ketoglutaric acid.

TABLE I

RELATIVE RETENTION TIMES OF METHYL ESTERS OF DNPH DERIVATIVES OF KETO ACIDS[a]

Peak No.	Keto acid	MW	Relative retention time		MS (Fig. No.)
			OV-17	HP-1	
1	Acetoacetic	296	0.7	0.7; 0.8	2a, 2b
2	Glyoxylic	268	1.0	1.0	3a
3	Pyruvic	282	1.1	1.1	3b
4	α-Ketobutyric	296	1.1	1.2	3c
5	α-Ketoisovaleric	310	1.2	–	3d
6	*d,l*-α-Keto-β-methyl-*n*-valeric	324	1.9	1.25	3e
7	Acetylsuccinic	368	1.95	–	
8	Acetopyruvic	296	1.4	–	
9	Ketomalonic	326	1.5	1.9	3f
10	Levulinic	310	1.5	1.95	3g
11	β-Ketoadipic	368	1.55	–	
12	Oxaloacetic	340	1.6	1.4	2c
13	4-Acetyl-*n*-butyric	324	1.7	1.45	3h
14	α-Ketoglutaric	354	1.8	1.5	3i
14a	β-Ketoglutaric	354	–	0.8	2b
15	α-Ketoadipic	368	1.9	–	

[a] Normalized to glyoxylic acid.

syn and *anti* isomers are resolved under the chromatographic conditions used here, it was necessary to separate each isomer of glyoxylic and pyruvic acid DNPHs according to the method of Katsuki *et al.* [11]. Each isomer was checked by spectroscopic measurements (300–500 nm) and the results obtained were similar to those of Katsuki and coworkers [11,12]. After esterification, the isomers were analysed by GC. The results showed that both isomers have equal retention times, and when *syn* and *anti* isomers were co-injected, they appeared as a single peak on an OV-17 column. Resolution of *syn–anti* isomers was only observed for pyruvic acid on an HP-1 column. This finding was further confirmed by GC–MS, where the spectra of both isomers (peaks 3′ and 3 in Fig. 1b) were identical.

The DNPH derivatives of hydroxypyruvic and oxalomalic acid could not be analysed by this technique as their melting points were higher than 300°C. The high melting point for hydroxypurivic acid DNPH is in agreement with the expected structure derived from the reaction of the acid with DNP, as an α-ketol structure undergoes double addition of DNP, leading to the formation of an osazone [22].

The analysis of β-keto acids was complicated owing to their instability in an acid medium leading to their decarboxylation. Table II summarizes the decarboxylation products for some unstable methyl ester DNPH derivatives of keto acids. For instance, decarboxylation of acetoacetic acid resulted in the formation of 2,4-dinitrophenylhydrazone derivatives of acetaldehyde and acetone, peaks 1a and 1b in Fig. 1, respectively. The identification of these compounds was confirmed by mass spectrometry (Fig. 2a and b); these spectra are identical with pub-

TABLE II

DECARBOXYLATION PRODUCTS OF SOME UNSTABLE METHYL ESTERS OF DNPH DERIVATIVES OF KETO ACIDS

Keto acid	Product[a]	Extent of decomposition
Acetoacetic	Acetaldehyde, acetone	Complete
Ketomalonic	Glyoxylic acid	Partial
Oxaloacetic	Pyruvic acid	Complete
β-Ketoglutaric	Acetone	Complete

[a] Detected as DNPHs.

lished mass spectra [23]. In a similar fashion, oxaloacetic decomposed completely into pyruvic acid. However, if the reaction of DNP is done with oxaloacetic acid diethyl ester, partial decarboxylation takes place. Fig. 2c shows the mass spectrum of the ethyl ester of the DNPH of oxaloacetic obtained directly from the crystallized product. The spectrum shows the presence of the molecular ions for oxaloacetic acid (MW 368) and pyruvic acid (MW 296).

The reaction of DNP with β-keto acids may lead to the formation of a cyclic structure (pyrazolones) [22]. Under our experimental conditions, the formation of such cylic compounds did not occur. However, some reported mass spectral data [20] indicate the existence of both linear and cyclic structures for oxalocetic acid.

Mass spectra for a variety of keto acids are given in Fig. 3. The masses of major fragmentation peaks characterizing the compounds are indicated. Common fragments for keto acids are at masses 63, 75, 77, 79, 91, 105, 127, 152 and 180. Most of the peaks

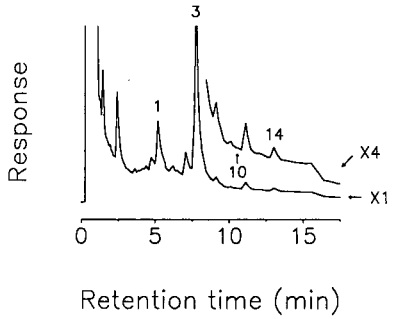

Fig. 4. Relationship between intensity of molecular ion peak and total number of carbon atoms present in the derivative. ○ = α-keto acid; △ = α-keto dicarboxylic acid; ▽ = γ-keto acid; □ = δ-keto acid.

in the lower part of the spectra are due to the DNP moiety, and are also characteristic of DNPHs of aldehydes and ketones [23].

The molecular ion (MI) peak was present in all instances. Its intensity was found to depend on the total number of carbon atoms present in the derivative (Fig. 4). The maximum intensity was pro-

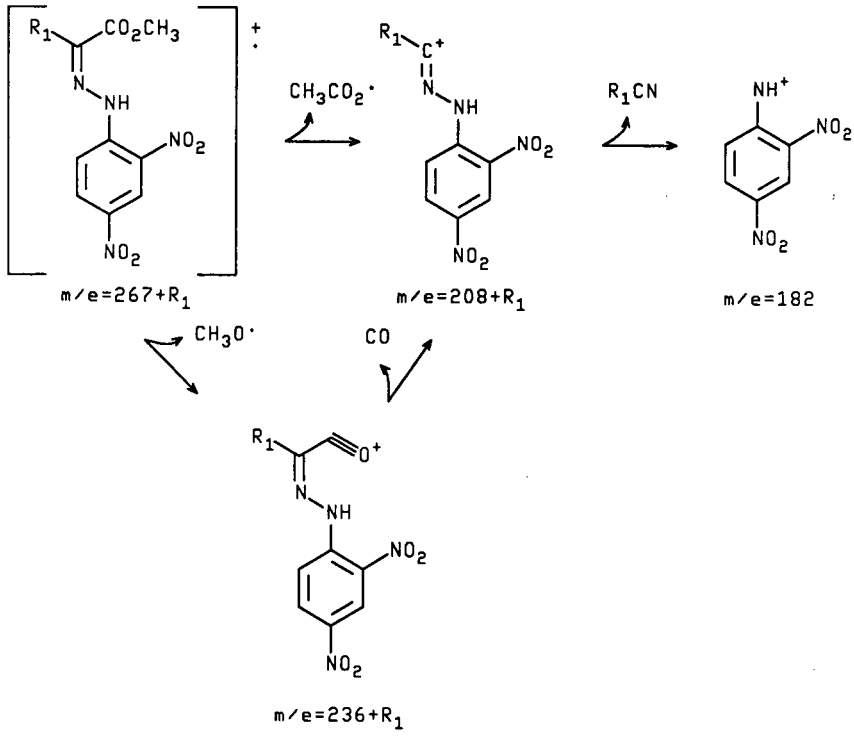

Fig. 5. Fragmentation pattern of methyl esters of DNPH derivatives of α-keto acids.

duced with pyruvic and ketomalonic acid (55% and 39%, respectively).

Characteristic peaks in the mass spectra of keto acids are at masses 55, 57 and 73 and at MI − 31, MI − 59, MI − 60 and MI − 73. These peaks are usually smaller than the peak at mass 59, and can be used as specific signs for identification of these compounds. Based on the MS data, a fragmentation pattern for methyl esters of the DNPHs of α-keto acids is given in Fig. 5.

The method presented for the detection, separation and identification of keto acids has the following advantages: (1) low GC and GC–MS running time; (2) good separation for a wide variety of keto acids; (3) no resolution of *syn–anti* isomers; (4) high detection sensitivity; and (5) ease of identification by MS. Therefore, this method can be adopted in studies of amino acid catabolism, maple syrup urine disease, diabetes and other metabolic or chemical studies. The adaptability of the method to biological material is illustrated by the analysis of keto acids present in leaves of *Cnidoscolus urens* (Fig. 6).

One disadvantage of the technique, which applies to all chromatographic separations of keto acids utilizing derivatization via DNP, is the decarboxylation of β-keto acids.

CONCLUSIONS

Derivatization of keto acids via DNP has been used successfully for their isolation from complex mixtures; however, it has been frequently criticized for imperfect qualitative and quantitative chromatographic analyses owing to the resolution of *syn* and *anti* isomers. This resolution leads to a greater number of peaks in the chromatogram and complicates the identification of keto acids [10,12]. The present method represents a definite improvement for the analysis of keto acids as there is no longer the problem of *syn* and *anti* isomer resolution. In addition, it offers the advantage of analysing a wide variety of keto acids in a short chromatographic time with a detection limit in the nanomole range.

The electron impact mass spectra for ten keto acids are provided. In addition, a mechanism for the fragmentation of methyl esters of the DNPHs of α-keto acids is presented.

This technique is now used routinely in our laboratory for the search for keto acids formed during the γ-radiolysis of aqueous solutions of organic compounds.

REFERENCES

1 P. G. Simmonds, B. C. Pettitt and A. Zlatkis, *Anal. Chem.*, 39 (1967) 163.
2 R. A. Chalmers and R. W. E. Watts, *Analyst (London)*, 97 (1972) 951.
3 S. P. Markey, *J. Chromatogr. Sci.*, 11 (1973) 417.
4 B. C. Hemming and C. J. Gubler, *Anal. Biochem.*, 92 (1979) 31.
5 K. Kobayashi, E. Fukui, M. Tanaka and S. Kawai, *J. Chromatogr.*, 202 (1980) 93.
6 O. A. Mamer, J. A. Montgomery and V. Y. Taguchi, *J. Chromatogr.*, 182 (1980) 221.
7 L. I. Woolf, C. Hasinoff and A. Perry, *J. Chromatogr.*, 231 (1982) 237.
8 A. P. J. M. De Jong, *J. Chromatogr.*, 233 (1982) 297.
9 L. Marai and A. Kuksis, *J. Chromatogr.*, 249 (1982) 359.
10 T. Hayashi, H. Todoroki and H. Naruse, *J. Chromatogr.*, 224 (1981) 197.
11 H. Katsuki, T. Yoshida, C. Tanegashima and S. Tanaka, *Anal. Biochem.*, 43 (1971) 349.
12 H. Katsuki, C. Kawano, T. Yoshida and S. Tanaka, *Anal. Biochem.*, 2 (1961) 433.
13 H. Katsuki, T. Yoshida, C. Tanegashima and S. Tanaka, *Anal. Biochem.*, 24 (1968) 1122.
14 P. Ronkainen, *J. Chromatogr.*, 28 (1967) 263.
15 N. Ariga, *Anal. Biochem.*, 49 (1972) 436.
16 H. Terada, T. Hayashi, S. Kawai and T. Ohno, *J. Chromatogr.*, 130 (1977) 281.
17 A. A. Quereshi, C. E. Elson and L. A. Lebeck, *J. Chromatogr.*, 249 (1982) 333.
18 B. S. Buslig, *J. Chromatogr.*, 247 (1982) 193.
19 H. Kallio and R. R. Linko, *J. Chromatogr.*, 76 (1973) 229.
20 H. Kallio, R. R. Linko, T. Pyysalo and I. Puntari, *Anal. Biochem.*, 90 (1978) 359.
21 L. J. Papa and L. P. Turner, *J. Chromatogr. Sci.*, 10 (1972) 744.
22 Q. Buckingham, *Q. Rev. Chem. Soc.*, 23 (1969) 37.
23 J. B. Stanley, D. F. Brown, V. J. Senn and F. G. Dollean, *J. Food. Sci.*, 40 (1975) 1134.

Journal of Chromatography, 587 (1991) 255–262
Elsevier Science Publishers B.V., Amsterdam

CHROM. 23 594

Quantitative measurements via co-elution and dual-isotope detection by gas chromatography–mass spectrometry

Lawrence C. Thomas* and Walter Weichmann

Department of Chemistry, Seattle University, Seattle, WA 98122 (USA)

(First received April 5th, 1991; revised manuscript received June 24th, 1991)

ABSTRACT

Dual-isotope measurements by gas chromatography–mass spectrometry (GC–MS) which mimic isotope dilution may suffer from irreproducibilities or unduly large uncertainties because of variations in ionization efficacies for the respective forms in the MS source. Such variations are sometimes avoided via extensive pretreatments and high-resolution GC separations. However, in some circumstances, an alternative approach is feasible which instead exploits the advantages of decreasing GC resolution. By forcing both forms of each analyte to co-elute, their ionization efficacies in the MS source will be virtually identical, thereby allowing for highly reproducible relative response ratios to be attained despite dramatically lowered GC resolution. The co-elution results described here are nearly as precise as results from moderate-resolution separations in the absence of interferents. Thus, dual-isotope GC–MS measurements with co-elution of the target analytes and their respective isotopically labeled internal standards offer a powerful alternative to the conventional approach of requiring expensive and labor-intensive additional pretreatments and separations; however, the effects of interferences may be exacerbated by the forced co-elution and must also be considered.

INTRODUCTION

Dual-label methods can be useful for measuring or comparing analytes [1–4]. Radioactive substances are often employed for dual-label measurements in order to exploit their good selectivities and high sensitivities. However, unless required because of their low limits of detection and freedom from interferences, radioactivity measurements are typically avoided because of potential health hazards or regulations. Consequently, methods utilizing non-radioactive isotopically labeled substances may be preferred, and GC–MS measurements can be used owing to the mass discrimination offered by mass spectrometry (MS). For example, MS with equilibrated mixtures of isotopically labeled compounds is a valuable approach for accurate analyses and has been used for many years [5].

Recently, dual-isotope techniques which mimic isotope dilution have become popular. Some gas chromatographic (GC)–MS approaches have been adopted for use in a variety of important environmental measurements, *e.g.*, via US Environmental Protection gency (EPA) Methods 1624 and 1625 [6]. Typically, for each analyte, a known amount of that analyte's selected isotopically labeled form is added to samples before pretreatment. The two analyte forms thereby undergo identical treatment because they exist together in the same conditions. A subsample of the prepared sample is then analyzed via GC–MS according to established protocols, with the analyte and its isotopically labeled form typically eluting separately and being measured via their respective characteristic m/z values.

Unfortunately, even those dual-isotope procedures are not always accurate, and it is recommended that other quantitative approaches be used if the two forms do not both show baseline separation from all potential interferents [6]. Such improved temporal resolution can sometimes be at-

0021-9673/91/$03.50

tained via modified pretreatment schemes and/or changes in instrumentation variables, but corresponding adaptations can be expensive and labor intensive. An alternative approach, detailed here, ensuring co-elution of the labeled and non-labeled forms, may offer sufficient data quality to avoid costly and time-consuming adaptations which are used to enforce baseline resolution of eluates.

THEORY: ASSURING CONSTANT RELATIVE SENSITIVITIES VIA CO-ELUTION

If an isotopically labeled, *e.g.*, deuterium-labeled, form of analyte i is added to sample n prior to pretreatment, then the peak area for its elution and measurement by GC–MS may be modeled as

$$A_{\text{ind}} = \frac{V_{sn} C_{ind} E_{ind} V_{\text{col},n} S_{ind} V_{\text{inj},n}}{V_{cn}(V_{\text{col}} + V_{\text{split}})_n V_{cn}} \int_{RT-bw}^{RT+bw} k_{ind}(I_{ind})_t \mathrm{d}t \quad (1)$$

with

$$(I_{ind})_t = (E_{\text{ion},ind})_t (E_{\text{ext},ind} E_{\text{sel},ind} P_{\text{mult},id} f_{\text{p}})_t \quad (2)$$

where A_{ind} is the peak area for analyte i from sample n and isotopic label d (which could be deuterium or ^{13}C or another isotope), V_s and V_c correspond to the original sample volume and the volume after pretreatment, C is the concentration of the specified analyte in the sample, E is the efficacy of the pretreatment as the fraction of the specified substance recovered, V_{col} and V_{split} correspond to carrier volumes which flow to the column and out of the split vent during the duration while the analyte resides in the injector, S is the fraction of the analyte which is in the carrier during the duration the analyte resides in the injector, V_{inj} is the volume of pretreated sample injected, RT is the retention time of the analyte, bw is some selected multiple of the analyte's peak width, k relates electrometer current to the monitored response, E_{ion} is the ionization efficiency in the source for the target analyte at the specified time t, E_{ext} and E_{sel} are efficiencies of extraction from the source and delivery to the first stage of the electron multiplier through the m/z selector and $P_{\text{mult}} f_{\text{p}}$ defines the response of the electron multiplier to incident selected ions.

Relative response factors (RRF) for naturally occurring analytes, indicated here as h, relative to the isotopically labeled form, d, can be defined for the overall pretreatment and measurement using known amounts of both forms in a reference sample, r:

$$RRF_{irhd} = (A_{irh}/C_{irh})(A_{ird}/C_{ird})^{-1} \quad (3)$$

In subsequent determination, a known amount of the isotopically labeled form is added to each sample before analysis, and the relative response factor may be assumed to be invariant; thus, for sample m, using a relative response factor determined from reference sample r:

$$C_{imh} = (C_{imd} A_{imh})(RRF_{imhd} A_{imd})^{-1} = (C_{imd} A_{imh})(RRF_{irhd} A_{imd})^{-1} \quad (4)$$

if both forms, h and d, are chemically identical through the pretreatment and delivery onto the separations column, and the measurements are not confounded by interferences. Thus, internal standard calculations are valid only if relative measurement sensitivities are stable.

More important for this discussion are special cases for which one ensures that the ionization efficiency of both forms in the source are effectively the same, *i.e.*, $E_{\text{ion},ih} = E_{\text{ion},id}$. For those situations, the response factor assumption is valid when

$$\frac{\int k_{imh}(E_{\text{ext},imh} E_{\text{sel},imh} P_{\text{mult},imh} f_{\text{p}})_t \mathrm{d}t}{\int k_{imd}(E_{\text{ext},imd} E_{\text{sel},imd} P_{\text{mult},imd} f_{\text{p}})_t \mathrm{d}t} \cdot \frac{\int k_{ird}(E_{\text{ext},ird} E_{\text{sel},ird} P_{\text{mult},ird} f_{\text{p}})_t \mathrm{d}t}{\int k_{irh}(E_{\text{ext},irh} E_{\text{sel},irh} P_{\text{mult},irh} f_{\text{p}})_t \mathrm{d}t} = 1 \quad (5)$$

That is, if ionization efficiencies are identical for the target analyte and its isotopomer standard, then internal standard quantitative calculations are appropriate if the relative instrumental responses are reproducible for both analyte and internal standard ions in the source.

However, the ionization efficiency for a specified species can vary dramatically with source pressure and concentrations of other species in the source. Consequently, if interferents co-elute with one of the analyte's forms but not the other, both source pressure and the presence of interferences may cause $E_{\text{ion},ih} \neq E_{\text{ion},id}$, and their relative response factors may therefore be irreproducible or unduly imprecise, perhaps precluding valid internal standard calculations if they elute separately.

The traditional approach to attempts for ensuring

$E_{ion,ih} = E_{ion,id}$ is to extensively pretreat samples and otherwise to separate measured species to yield baseline-resolved eluates, consistent with EPA recommendations [6], and to likewise ensure reproducible source pressures, gas-phase compositions in the source and measurement voltages. However, ensuring baseline resolution is not always feasible or economical, and thus an alternative approach might be used to ensure $E_{ion,ih} = E_{ion,id}$.

An alternative to assuring baseline separations is instead to force co-elution so that both forms of the target analyte are present together at the same time in the same ionizing environment. In such conditions their ionization efficiencies should be identical, neglecting tiny differences in ionization potentials due to differences in ground-state vibrational and rotational energies due to their different reduced masses. Of course, lowering GC resolution to assure co-elution may also cause interferences by other compounds which might contribute to the measured MS signal, and such interferences must be evaluated and compensated for the best results. Also, decreased GC resolution may sacrifice sensitivity and degrade limits of detection. However, because the internal standard and target analyte are chemically identical, fluctuations in ion source conditions may not affect their relative sensitivity, which is required for valid internal standard calculations for GC. Consequently, despite tradition, one might purposely decrease the GC resolution to cause co-elution of labeled and non-labeled forms of the target analytes in order to achieve valid quantitative analyses in dual-isotope procedures which mimic isotope dilution: effects of increased interferences and worse limits of detection due to lowered resolution must be considered and weighed against possible benefits of forced co-elution.

EXPERIMENTAL

Reagents

Anthracene and decadeuterated anthracene were purchased from Aldrich, both at >99% purity. All solvents used were of ChromAR grade from Mallinckrodt and helium carrier gas was >99.9995% pure.

Apparatus

A Hewlett-Packard Model 5971A mass-selective detector interfaced to a Hewlett-Packard Model 5890 Series II gas chromatograph was used, controlled and monitored by a Hewlett-Packard Model QS-20 Vectra computer. Helium was used as the carrier gas at 50 kPa pressure in the split–splitless inlet, yielding a 1.0 ml min^{-1} flow-rate out of the 12 m × 0.2 mm I.D. (0.33-μm film thickness) cross-linked methylsilicone fused-silica capillary column at 25°C. A splitting ratio of 60:1 was used, with a 1.0-min splitless period after each injection. Injection volumes of 1.0 μl were used, as indicated below.

Procedures

Separate solutions of natural isotopic abundance anthracene and decadeuterated anthracene were prepared, dissolving 1 mmol of each compound in 10 ml of methanol; other isotopes such as ^{13}C could likewise have been used, perhaps yielding improved results. These solutions were exposed to sunlight for 2 weeks, generating reaction products 9,10-dihydroanthracene [formula weight (FW) = 180 u], $9^1H,9^2H,10^1H,10^2H$-dihydrooctadeuteroanthracene (FW = 190 u), 9,10-anthracenedione (anthraquinone, FW = 208 u) and octadeuteroanthraquinone (FW = 216 u). The resulting solutions were mixed by volume, as indicated in Table I, and analyzed via two GC separation schemes: (a) isothermal at 160°C for 15 min after injection, then programmed from 160 to 250°C at 20°C min^{-1}, and (b) isothermal at 60°C for 5 min, then programmed to 120°C at 10°C min^{-1}, to 160°C at 2°C min^{-1} and to 250°C at 5°C min^{-1}. The former temperature programme caused co-elution of the deuterated and non-deuterated forms, and the latter allowed for their partial separations. Injections of 1 μl were used and ion currents monitored for selected m/z values over durations spanning the respective components' elutions: m/z = 180 and 190 for the dihydroanthracenes, m/z = 178 and 188 for the anthracenes and m/z = 208 and 216 for the anthraquinones. Five replicates were done for each solution tested, with respective integrated ion currents being calculated for each. For each replicate, ratios of the respective integrated ion currents for non-deuterated and deuterated components were found and corresponding average ratios and standard deviations were calculated.

RESULTS AND DISCUSSION

Deuterated d_{10}-anthracene, normal isotopic composition anthracene and their respective photolysis products, dihydroanthracene and anthraquinone, were separated and measured by GC–MS. Moderate-resolution GC allowed for the modest separation of the respective forms (see Figs. 1 and 2). Peak areas were calculated for each eluate via its parent m/z signal and within-run relative integrated responses compared for each eluate's natural and deuterated pair. For moderate-resolution separations, results within one set of replicates, mixed 1:1 (v/v), varied ($n = 5$): dihydroanthracene (m/z 180 : 190 = 1.436 ± 0.025), anthracene (m/z 178 : 188 = 1.155 ± 0.008) and anthraquinone (m/z 208 : 216 = 0.926 ± 0.011). These measurements were very reproducible, being made for pure solutions with no interferences detected other than the mutual overlap of the respective forms of the measured compounds. Baseline separations might produce better ratios, but these represent high-quality data.

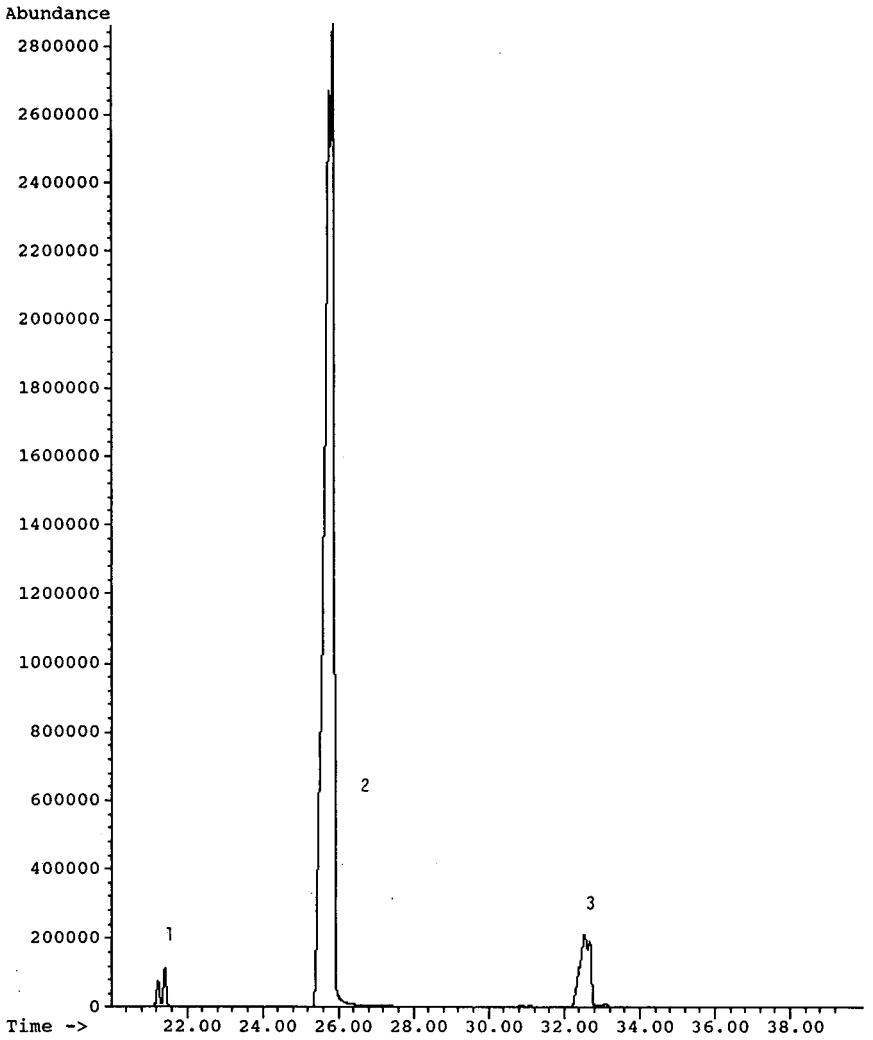

Fig. 1. Moderate-resolution GC–MS separation and measurements of non-deuterated and deuterated forms of (1) 9,10-dihydroanthracene, (2) anthracene and (3) 9,10-anthracenedione. This chromatogram is for the sum of all ion currents for m/z = 178, 180, 188, 190, 208 and 216 over the measurement duration. Time in min.

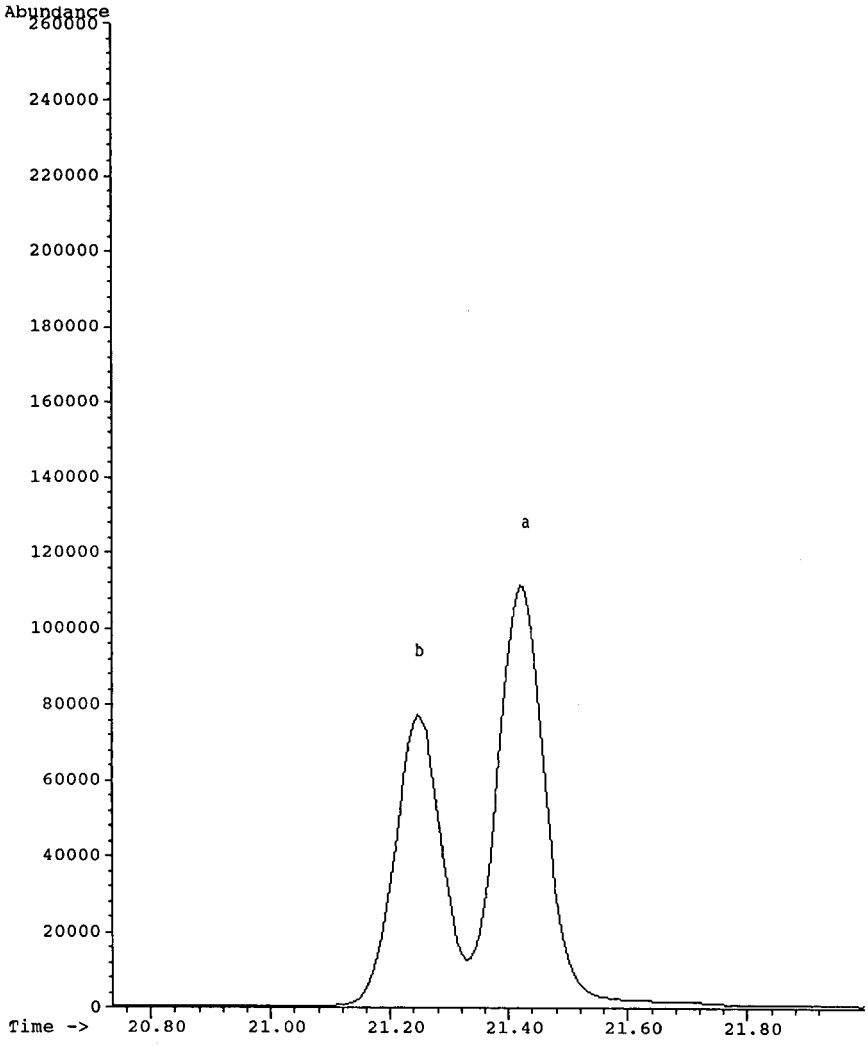

Fig. 2. Moderate-resolution GC–MS separation for selected ion measurements of (a) non-deuterated (m/z = 180) and (b) deuterated (m/z = 190) forms of 9,10-dihydroanthracene, showing nearly baseline resolution. Time in min.

The same solution, and others, were separated by low-resolution GC, yielding nearly complete co-elution of the respective deuterated *vs.* non-deuterated forms (see Figs. 3 and 4). The limits of detection were much worse for the lowered resolution separations and measurements, a disadvantage of the forced co-elution. However, the within-run relative integrated responses for sets of replicates (n = 5) varied by about the same amount as for moderate-resolution separations (see Table I). The relative responses were not as reproducible as those for moderate-resolution separations for pure solutions described above, partly owing to the much broader peak widths. However, the ratios for co-eluted forms were very reproducible and sufficient for good quantitative calculations, and might be superior to corresponding higher resolution measurements if significant interferences are present.

The dual-isotope example above indicates that good quantitative precision may be achieved despite the lowered resolution to achieve co-elution of target analytes and their isotopomer standards. Forcing

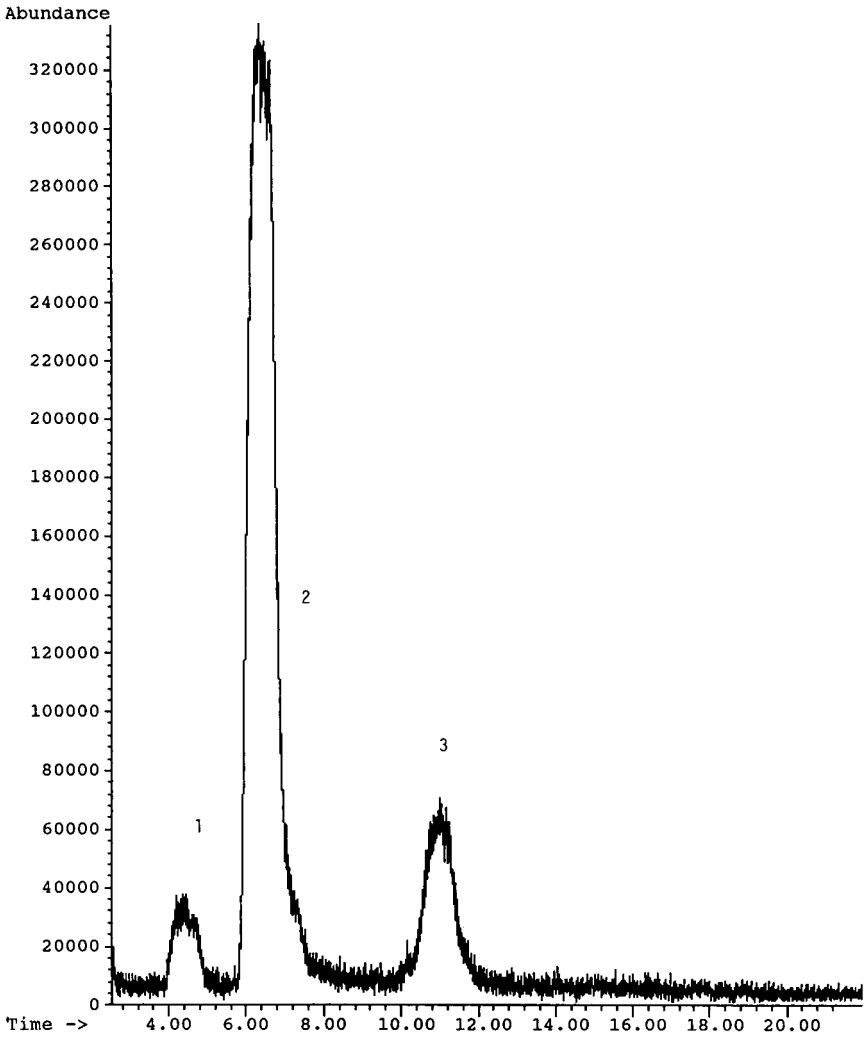

Fig. 3. Low-resolution GC–MS separation and measurements of both non-deuterated and deuterated forms of (1) 9,10-dihydroanthracene, (2) anthracene and (3) 9,10-anthracenedione. This chromatogram is for the sum of all ions for m/z = 178, 180, 188, 190, 208 and 216 over the measurement duration. Time in min.

identical ionization efficiencies via co-elution of the target analyte and its labeled isotopomer could thereby improve the precision and accuracy of ionization efficiencies which might otherwise vary dramatically. However, the feasible improvements are not without potential disadvantages, such as degradation of signal-to-noise ratios and correspondingly worse limits of detection, increased chances of errors in the selected m/z measurements owing to co-eluting interferents and possible isotope exchanges causing errors in selected m/z measurements and associated calculations. Compensation for isotopic abundances and assessment of interferences are typical problems in GC–MS, and using ^{13}C or other isotopes may be better than using deuterium, especially for avoiding isotope exchanges. These difficulties caused by co-elution are much like those encountered in direct-insertion MS, but the GC co-elution approach allows for the separation of analytes from solvents and other

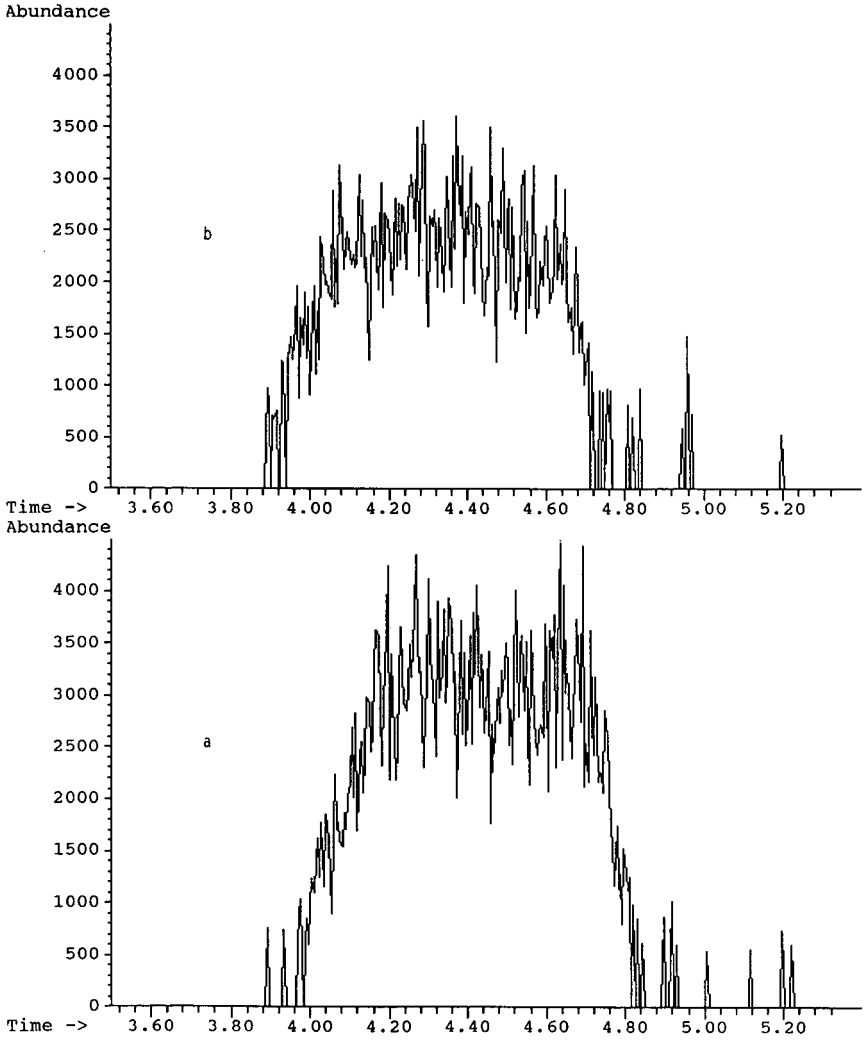

Fig. 4. Low-resolution GC–MS separation and selected ion measurements of (a) non-deuterated (m/z = 180) and (b) deuterated (m/z = 190) forms of 9,10-dihydroanthracene, showing nearly complete overlap of the eluates. Time in min.

major interferences which might preclude direct-injection or very low-resolution GC techniques.

The dual-isotope co-elution approach suggested here may require considerable compromise for its effective use. However, for situations in which direct-insertion MS is not feasible and for which higher resolution GC techniques yield intolerable fluctuations of source ionization efficiencies, forced co-elution of target analytes with their added isotopically labeled internal standards may in some instances allow for good quantitative GC–MS results.

ACKNOWLEDGEMENT

We thank the National Institutes of Health for their support of this and earlier work via grant number 1R15 GM36273-01A1.

TABLE I

RELATIVE RESPONSES FOR DEUTERATED *VS.* NON-DEUTERATED ELUATES FOR COELUTION OF TARGET ANALYTES

Relative concentration	Relative integrated response[a]		
	Dihydroanthracene[b]	Anthracene[b]	Anthraquinone[b]
3:1	3.720 ± 0.179	3.609 ± 0.078	3.002 ± 0.134
2:1	2.485 ± 0.106	2.450 ± 0.038	1.988 ± 0.064
1:1	1.178 ± 0.014	1.130 ± 0.039	0.906 ± 0.028
2:3	0.841 ± 0.018	0.772 ± 0.013	0.610 ± 0.018
1:2	0.674 ± 0.012	0.606 ± 0.013	0.477 ± 0.008
1:3	0.401 ± 0.005	0.339 ± 0.010	0.276 ± 0.009

[a] Area for non-deuterated form/area for deuterated form, average ± S.D. (n = 5).

[b] For dihydroanthracene m/z = 190 *vs.* m/z = 180, for anthracene m/z = 188 *vs.* m/z 178 and for anthraquinone m/z = 216 *vs.* m/z = 208 were measured.

REFERENCES

1 T. R. Roberts, *Radiochromatography*, Elsevier, Amsterdam, 1978.
2 L. C. Thomas and T. L. Ramus, *Anal. Chim. Acta*, 154 (1983) 143.
3 L. C. Thomas and T. L. Ramus, *Anal. Lett.*, 17 (1984) 2001.
4 L. C. Thomas and C. L. Wood, *J. Chromatogr.*, 522 (1990) 117.
5 A. V. Grosse, S. G. Hindin and A. D. Kirshenbaum, *Anal. Chem.*, 21 (1949) 386.
6 *Method 1624, Revision C and Method 1625, Revision C*, US Environmental Protection Agency, Washington, DC, 1988.

Journal of Chromatography, 587 (1991) 263–267
Elsevier Science Publishers B.V., Amsterdam

CHROM. 23 525

Behaviour of a common phthalate plasticizer (dioctyl phthalate) during the alkali- and/or acid-catalysed steps in an AOCS method for the preparation of methyl esters

N. C. Shantha and R. G. Ackman*

Department of Food Science and Technology, Technical University of Nova Scotia, P.O. Box 1000, Halifax, Nova Scotia, B3J-2X4 (Canada)

(First received July 5th, 1990; revised manuscript received May 31st, 1991)

ABSTRACT

It is shown that the alkali-catalysed methanolysis step of an official method for determination of long-chain marine oil fatty acids produced dimethyl and mixed alcohol esters from the plasticizer dioctyl [actually di(2-ethylhexyl)] phthalate. An independent boron trifluoride-catalysed methanolysis step produced a lower level of artifacts but the official two-step process gave an even higher conversion figure than either catalyst independently. The retention times for the dimethyl, mixed alcohol, and dioctyl phthalates are discussed in relation to methyl esters of common fatty acids on polyglycol wall-coated open-tubular gas–liquid chromatographic columns.

INTRODUCTION

Di(2-ethylhexyl) phthalate (DEHP) is a widely used plasticizer and a widespread contaminant in an increasingly plastic world. Classed among the phthalic acid esters (PAEs) it has been found to be a ubiquitous environmental contaminant [1–3] and has also been classified as a priority pollutant [4]. Many papers pertaining to DEHP have appeared in recent years as part of a voluminous literature relating to the biological activity and toxic effects of PAE [2,5–9].

Equally of importance are the problems arising in analytical laboratories due to contamination of various commercial reagents and equipment by the phthalates which could lead to errors in analytical results. Background contamination by phthalates is commonly encountered in the chromatographic analysis of lipid samples [10–12] and has also been reported in prostaglandin analysis [13]. Middleditch [3], in a book on analytical artifacts, listed in detail the various contaminating sources of DEHP and other phthalate esters. While most of the literature lists dibutyl phthalate (DBP) and DEHP as the major contaminants in lipid analyses, only a few papers actually speak about their transesterification products. Pascaud [12] used hydrochloric acid in methanol for transesterification and noted that phthalates were strongly resistant to transmethylation. Later, Ishida *et al.* [14] analysed by gas–liquid chromatography (GLC) the different products arising from the use of different acid-catalysed transesterification reagents on the phthalates. Both results indicated that dialkyl phthalates were transesterified very slowly to give the methyl ester products. The amounts of these transesterified products formed would differ with the nature of the reagent used.

In this study, DEHP was subjected to both the base- and acid-catalysed transesterification steps of the new American Oil Chemists' Society (AOCS) Official Method Ce-1b-89 [15], with slight modifications. The amounts of different phthalate ester products obtained by subjecting the DEHP sepa-

0021-9673/91/$03.50

rately to the base-catalysed and the acid-catalysed reagents, and to both reagents in sequence as given in the AOCS procedure, were determined by GLC and by thin-layer chromatography with flame ionization detection (TLC–FID) (the Chromarod/Iatroscan system). Their interference with the GLC analysis of fatty acid methyl esters on a polyethylene glycol-based capillary column (Supelcowax-10) is also discussed.

EXPERIMENTAL

Dioctyl phthalate [bis(2-ethylhexyl) phthalate] was purchased from Aldrich (Milwaukee, WI, USA). The standard was tested for purity by GLC and with the TLC–FID Iatroscan system. Dimethyl phthalate for use as reference standard was prepared by methylation of phthalic acid, which was available in the laboratory. The dioctyl phthalate (>99% purity) (*ca.* 25 mg) was treated with alcoholic sodium hydroxide and boron trifluoride–methanol according to AOCS method Ce-1b-89 with a few modifications. Thus the sample was treated with 0.5 *M* alcoholic sodium hydroxide for 2 min instead of the official 7 min and for 20 min with 12% boron trifluoride–methanol instead of 5 min [16]. The sample was subjected to three different transesterification conditions: (A) base-catalysed with sodium hydroxide in methanol, (B) acid-catalysed with boron trifluoride–methanol and (C) both base- and acid-catalysed transesterification according to the modified AOCS conditions described earlier. The reaction products were extracted with isooctane and injected three times into the GLC system. The reaction products were also analysed with the TLC–FID Iatroscan system. All experiments were carried out in duplicate.

GLC analysis was performed on a Perkin-Elmer Model 8420 gas chromatograph equipped with a digital integrator, using a Supelcowax-10 column (30 m × 0.32 mm I.D., phase thickness 0.25 μm) (Supelco, Bellefonte, PA, USA). The oven temperature was programmed from 195 to 240°C at 3°C/min after an initial hold of 8 min at 195°C, and was maintained at 240°C for 10 min. The other parameters were splitting ratio 1:32, helium flow-rate 1.2 ml/min and injection port temperature 250°C. The peak-area output was recorded on a Perkin-Elmer GP-100 graphic printer.

Gas chromatography–mass spectrometry (GC–MS) with electron impact ionization was performed on a Finnigan MAT (San Jose, CA, USA) Model 700 ion-trap detector (ITD) system interfaced with a Perkin-Elmer Model 990 gas chromatograph. The fused-silica capillary GLC column was fed through a heated transfer line directly into the ITD gas inlet. For GC–MS, the separations were performed on a methylsilicone DB-1 column (60 m × 0.25 mm I.D., phase thickness 0.25 μm) (J & W Scientific, Folsom, CA, USA). The oven temperature was programmed from 165 to 240°C at 3°C/min after an initial hold of 8 min and with a final hold of 48 min at 240°C. The helium pressure was 15 p.s.i. The data system consisted of an IBM 286 compatible DTK TECHDATA-1230C computer (Technida, Dartmouth, Canada). All studies were conducted with version 4.0 of the ITD software supplied by Finnigan. The ITD was tuned by using the procedure supplied by the manufacturer. The ITD was operated in the full-scan mode and scanned with a 1-s cycle time.

TLC–FID analysis was performed as described elsewhere [17]. Hexane–diethyl ether–formic acid (97:3:1, v/v/v) was used as the developing solvent system.

RESULTS AND DISCUSSION

Table I gives the composition of the different products formed when the dioctyl phthalate was subjected to the different transesterification conditions. Three peaks were observed in the GLC analysis of the reaction products. The peak due to 2-ethylhexanol eluting just after the solvent peak has been ignored. The earliest eluting phthalate peak had a retention time similar to that of methyl heptadecanoate (17:0) or methyl hexadecadienoate (16:2$n-4$) under the conditions of analysis [18], and was identified as dimethyl phthalate based on the mass spectra and comparison with the retention time of dimethyl phthalate standard.

The mass fragment corresponding to the acylium ion [$M^+ - 31$] at m/z 163 formed the base peak (Fig. 1), in keeping with the data published by Middleditch [3] and others [19]. However, we obtained a protonated parent ion at m/z 195 (Fig. 1) and not a parent ion at m/z 194 as published [3]. It is not unusual to obtain the M + 1 ion under electron impact

TABLE I

GLC ANALYSES OF THE DIFFERENT PHTHALATE ESTERS RESULTING FROM THREE TRANSESTERIFICATION CONDITIONS

Type of transesterification	Relative concentration of phthalates[a]		
	Dimethyl	Methyloctyl	Dioctyl
Base-catalysed	0.3 ± 0.001	14.2 ± 1.04	85.5 ± 1.18
Acid-catalysed	n.d.[b]	3.6 ± 0.29	96.4 ± 0.29
AOCS (modified)	1.8 ± 0.02	28.3 ± 1.55	69.9 ± 2.00

[a] Expressed as weight percent + S.D. (n = 6); theoretical response factor of the phthalates calculated with respect to methyl octadecanoate (18:0), based on ionizable carbon content.
[b] Not detected.

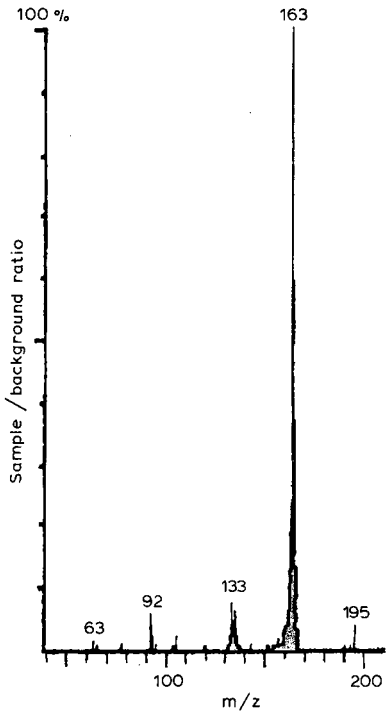

Fig. 1. Part of electron impact ionization mass spectrum of dimethyl phthalate obtained with a Finnigan MAT 700 ion-trap detector after passage through a Supelcowax-10 GC column as described.

in the ITD system [20,21]. The second-eluting peak, which fitted between the peaks for the methyl ester of the important eicosatetraenoic acid (arachidonic or 20:4$n-6$) and a later eluting (on polyglycols) eicosatrienoic acid (20:3$n-3$) was identified as methyloctyl phthalate based on the mass spectrum. Possibly it is a small component eluting at 13.34 min in a prior publication from this laboratory [22], with 20:4$n-6$ eluting at 13.21 min and 20:3$n-3$ at 13.56 min, and a similarly located but very large unknown component in Fig. 3 of a publication from another laboratory of the methyl esters of fatty acids from human plasma [23]. The protonated parent peak at m/z 293 was the base peak. The peak m/z 163 was, however, also prominent. The published mass spectral data for methyloctyl phthalate [3] show a very low-intensity parent peak at m/z 292.

These variations in the intensity of the peaks and the appearance of the protonated ions in this study from those published by Middleditch could be due to the different operating conditions used for spectra acquisition. A comparison of ion-trap mass spectra with quadrupole mass spectra has been presented in detail elsewhere [21].

The last-eluting peak, with a retention time greater than that of methyl tetracosenoate (24:1), was the unreacted dioctyl phthalate. This is also probably a major and late-eluting peak in the already mentioned Fig. 3 published elsewhere [23] for human plasma fatty acid methyl esters, with dioctyl partially converted to a methyloctyl phthalate. The mass spectra of authentic dioctyl phthalate, with the fragments at m/z 149, 167 and 279, was comparable to those published by Middleditch [3] and the protonated parent ion was observed at m/z 391.

The percentage composition of these products obtained by GLC (Table I) compares fairly well with those obtained from TLC–FID analysis (not shown). The three peaks resolved well on the Chromarods-SIII. The mobility decreased with decreasing chain length of the alcohol moiety, the dimethyl phthalate being the least and the dioctyl phthalate the most mobile.

This agrees with the elution order of a variety of phthalate esters in planar TLC on silica gel. The longer chain alcohol phthalates migrate close to methyl esters of common fatty acids [19]. This is in fact the key to a technique for eliminating phthalate esters from contaminated fatty acid methyl esters. Re-methanolysis with sodium methoxide converts all phthalate esters to dimethyl phthalate, which is much less mobile than the fatty acid methyl esters in TLC. The latter are not affected by the re-methan-

olysis and may be recovered from the TLC plate free from phthalate esters [19]. A more recent chromatographic separation of the phthalate esters [24] using a bonded methylphenylsilicone capillary column–quartz tube reactor–electron capture detection (ECD) system seems to be an interesting method for confirming alkyl phthalates. The quartz tube reactor maintained at a temperature of 900°C converts the phthalate esters to anhydrides and increases the sensitivity of the method for aliphatic phthalates.

Alkaline-catalysed transesterification, which is usually rapid [16,19,25], seemed to produce a relatively greater yield of the transesterified product when compared with acid-catalysed transesterification with boron trifluoride–methanol. Dimethyl phthalate was not observed in any detectable amounts following treatment of the dioctyl phthalate with boron trifluoride–methanol alone, and methyloctyl phthalate was also formed in low yield. The relatively higher yield of the transesterified products resulting from following the two-step modified AOCS procedure with contributions from both the acid- and the base catalysed reagents is not readily explained.

The modifications to the original published AOCS procedure [15] were not directed to reducing the yield of DEHP phthalate ester reaction products and the reasons for modifiying the reaction times [26] have been published in detail elsewhere [16].

All of the aliphatic fatty acids commonly encountered in food, plant or animal tissues are readily and almost totally transesterified by both base- and acid-catalysed reaction conditions. Although the 2-ethyl substituent could be involved in the slower reaction of these phthalate esters, the presence of the aromatic ring could also account for the resistance of DEHP to transesterification. Versino *et al.* [27] also observed that the presence of the aromatic ring in the dioctyl phthalate made it less biodegradable.

The proportion of the actual transesterified product of the dioctyl phthalate formed during the transesterification of oil samples contaminated with a small amount of the phthalate could differ, depending on the relative ratio of the dioctyl phthalate present and the reagent used. While the dioctyl phthalate eluting with a relatively greater retention time than the fatty acids of most interest (*e.g.*, docosahexaenoic acid or 22:6$n-3$) can probably be ignored in the GLC analysis of the fatty acid methyl esters on polygycol liquid phases, the dimethyl and the methyloctyl phthalate which elute along with the fatty acid methyl esters should be considered more carefully to avoid erroneous qualitative or quantitative results. The large number of liquid phases in common use in GLC [18] precludes the listing of definitive retention times, particularly as even changing the temperature on any one column could cause a shift of the aromatic esters relative to the common methyl esters of aliphatic acids. As methyl heptadecanoate (17:0) is often used as an internal standard in quantitative GLC [18,23], it is fortunate that only a small amount of dimethyl phthalate is formed with the popular boron trifluoride–methanol reagent. In high-performance liquid chromatographic analyses of fatty acids, as such or in the form of any aromatic derivative, similar problems could arise and the magnitude of the problem would depend on the type of detector in use.

Strictly, "dioctyl" phthalate should be based on *n*-octanol. However, the common phthalate ester commercially available is based on 2-ethyl-1-hexanol as the alkyl moiety. Similarly, "dibutyl" phthalate could refer to either esters of *n*-butanol or isobutanol (2-methyl-1-propanol), themselves sources of identification problems in the GLC of fatty acid methyl esters [10].

ACKNOWLEDGEMENT

This work was supported by a grant from the National Sciences and Engineering Research Council of Canada.

REFERENCES

1 I. Tomita, Y. Nakamura and Y. Yagi, *Ecotoxicol. Environ. Saf.*, 1 (1977) 275.
2 Y. Nakamura and I. Tomita, *Eisei Kagaku*, 33 (1987) 71; *C.A.*, 107 (1987) 53536.
3 B. S. Middleditch, *Analytical Artifacts —GC, MS, HPLC, TLC and PC (Journal of Chromatography Library*, Vol. 44), Elsevier, Amsterdam, 1989, pp. 78, 279 and 350.
4 A. D. Sauter, L. D. Betowski, T. R. Smith, V. A. Strickler, R. G. Beimer, B. N. Colby and J. E. Wilkinson, *J. High Resolut. Chromatogr. Chromatogr. Commun.*, 4 (1981) 366.
5 R. W. R. Baker, *Toxicology*, 9 (1978) 319.

6 J. A. Thomas, T. D. Darby, R. F. Wallin, P. J. Garvin and L. Martis, *Toxicol. Appl. Pharmacol.*, 45 (1978) 1.
7 T. Gray and M. Gray, *Food Chem. Toxicol.*, 26 (1988) 811.
8 C. J. A. Doelman, P. J. A. Borm and A. Bast, *Lancet*, 335 (1990) 725.
9 K. Bergman and L. Albanus, *Food Chem. Toxicol.*, 25 (1987) 309.
10 J. C. Pascal and R. G. Ackman, *Comp. Biochem. Physiol. B.*, 53 (1976) 111.
11 M. Ishida, K. Suyama and S. Adachi, *J. Chromatogr.*, 189 (1980) 421.
12 M. Pascaud, *Anal. Biochem.*, 18 (1967) 571.
13 J. Mai, J. E. Kinsella and J. S. Chou, *Lipids*, 15 (1980) 968.
14 M. Ishida, K. Suyama and S. Adachi, *J. Chromatogr.*, 294 (1984) 339.
15 *Offical Methods and Recommended Practices of the American Oil Chemists' Society*, AOCS, Champaign, IL, 4th ed., 1989, Official Method Ce 1b-89.
16 R. G. Ackman, A. M. Timmins and N. C. Shantha, *INFORM*, 1 (1990) 987.
17 N. C. Shantha and R. G. Ackman, *Lipids*, 25 (1990) 570.
18 R. G. Ackman, in R. J. Hamilton and J. B. Rossell (Editors), *Analysis of Oils and Fats*, Elsevier Applied Science Publ., London, 1986, Ch. 4, p. 137.
19 A. Shibahara, M. Nakanishi and G. Kajimoto, *Yukagaku*, 32 (1983) 18.
20 W. M. N. Ratnayake, A. Timmins, T. Ohshima and R. G. Ackman, *Lipids*, 21 (1986) 518.
21 R. P. Adams, *Identification of Essential Oils by Ion Trap Mass Spectroscopy*, Academic Press, San Diego, CA, 1989.
22 R. G. Ackman, *Acta Med. Scand.*, 222 (1987) 99.
23 W. Welz, W. Sattler, H.-J. Leis and E. Malle, *J. Chromatogr.*, 526 (1990) 319.
24 Atlas of Chromatograms, *J. Chromatogr. Sci.*, 27 (1989) 685.
25 C. D. Bannon, G. J. Breen, J. D. Craske, N. T. Hai, N. L. Harper and K. L. O'Rourke, *J. Chromatogr.*, 247 (1982) 71.
26 R. G. Einig and R. G. Ackman, *J. Am. Oil Chem. Soc.*, 65 (1988) 510.
27 C. Versino and M. Novaria, *J. Synth. Lubr.*, 4 (1987) 3.

Journal of Chromatography, 587 (1991) 268–270
Elsevier Science Publishers B.V., Amsterdam

CHROM. 23 725

Short Communication

Dehydrogenase-silica as a stationary phase for the separation of alcohols and ketones

Staffan Birnbaum

Department of Pure and Applied Biochemistry, Chemical Center, University of Lund, Box 124, S-22100 Lund (Sweden)

Kurt G. I. Nilsson*

Department of Biotechnology, Chemical Center, University of Lund, Box 124, S-22100 Lund (Sweden)

(First received July 3rd, 1991; revised manuscript received September 3rd, 1991)

ABSTRACT

Horse liver alcohol dehydrogenase was immobilized on tresyl-activated silica particles and slurry packed into a PTFE-coated stainless-steel column. The stationary phase enzyme column was used for the high-performance chromatographic separation of alcohols and ketones. Baseline resolution of the secondary alcohols terbutaline and bambuterol and their respective ketones was obtained. In addition, discrimination of closely related isomers, including the positional isomers of ethylphenethyl alcohol and the optical isomers of 1-phenyl-1-butanol, was achieved.

INTRODUCTION

Immobilized enzymes have been used in a number of applications, *e.g.*, in biosensors and for the selective synthesis of organic compounds. In 1983, the use of immobilized enzymes as selective adsorbents for the high-performance liquid chromatographic (HPLC) separation of organic compounds was reported [1]. More recently, immobilized hydrolytic enzymes, such as cellulase and a protease, chymotrypsin, were employed for the enantiomeric separation of various compounds [2,3]. In this paper, we show that dehydrogenase immobilized on silica can be used for the separation of alcohols and ketones and for the chiral discrimination of optically active alcohols.

EXPERIMENTAL

Silica particles (10 μm, 300-Å pores) were activated with tresyl chloride (116 mg/g silica) as described previously [4]. Sedimented silica (2.5 ml) was resuspended in a total volume of 4 ml with 5 m*M* hydrochloric acid. Horse liver alcohol dehydrogenase (HLADH, 100 mg), obtained from Boehringer, was dissolved in 4 ml of 0.5 *M* potassium phosphate (pH 7.9) and added to the activated silica particles. Coupling proceeded for 6 h at 4°C with mixing. The absorbance of the supernatant was negligible and thus the yield of immobilized HLADH was close to 100%. Subsequently, 1 ml of 1 *M* Tris–HCl (pH 8.8) was added to block remaining activated groups and incubated for an additional 12 h. The silica-bound HLADH was packed in a PTFE-coated stainless-steel column (50 × 4.6 mm

0021-9673/91/$03.50

I.D.) as described [1], connected to HPLC equipment and tested for its ability to separate a number of ketones and alcohols.

RESULTS

Active-site titration of the HLADH- silica with NADH in the presence of excess of isobutyramide gave a binding site concentration, e_0,of 0.43 mM. An initial test of the immobilized enzyme column with AMP gave a capacity factor, k', of 5.4. The capacity factor can be used to calculate the dissociation constant, K_d, of the retained compounds according to the equation

$$K_d = e_0/k'$$

if the binding site concentration, e_0, is much greater than the concentration of the substrate molecule, [S], which is to be chromatographed. Further discussion on the determination of K_d by chromatography is given in the literature [1]. The calculated K_d for AMP obtained in this study, 87 μM, agrees well with the value reported previously, 70 μM [1].

To test the ability of the immobilized enzyme column to resolve various alcohols and ketones, a mixture of β-adrenergic receptor active compounds, terbutaline and bambuterol, and their respective ketones were tested. Both the secondary alcohols and the corresponding ketones were completely resolved, as shown in Fig. 1, with k' values ranging from 0.79 for terbutaline to 4.43 for the ketone of bambuterol under the conditions described in Fig. 1.

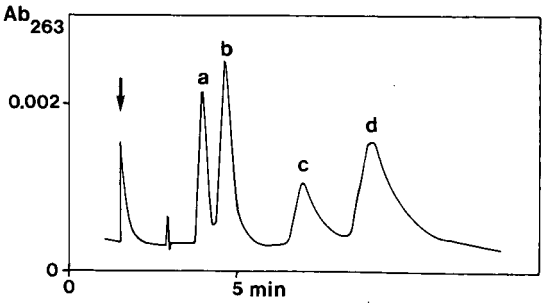

Fig. 1. Separation of β-adrenergic blocking agents, terbutaline (a) and bambuterol (b) and their respective ketones (c and d). Injection volume, 25 μl; mobile phase, 0.1 M potassium phosphate buffer (pH 7.5) containing 1 μM $ZnSO_4$; flow-rate, 0.5 ml/min. Sample concentrations of a, b, c, and d were 5, 25, 1 and 6 μg/ml, respectively.

Subsequently, the immobilized HLADH column was tested for its ability to separate various isomers of alcohols. Thus, the positional isomers of ethylphenethyl alcohol and the enantiomeric isomers of 1-phenyl-1-butanol were discriminated by the immobilized enzyme column with k' values as indicated in Table I.

HLADH contains two substrate-specific binding sites. Using eqn. 1 it can be calculated that K_d for the compounds listed in Table I are in the range 0.1–1.0 mM. This assumes that the analyte binds to the two substrate specific binding sites per immobilized enzyme molecule. It cannot be excluded, however, that interactions with other sites on the immobilized enzyme take place, although we have found that increasing the sample concentration above the calculated binding site concentration did lead to decreased retention times, which indicates, that the interaction is specific.

The immobilized enzyme column was used intermittantly during a period of 6 months. Between use, the HLADH-silica was stored at 4°C in the buffer that had been used. During this time the column retained its ability to separate the compounds above, even though the capacity fators decreased by about 50%.

DISCUSSION

Immobilized protein stationary phases, including enzymes, have previously been exploited for the separation of various organic compounds including racemic resolution of β-blockers [1–3,5]. As it has been reported previously that HLADH catalyses the stereoselective oxidation of secondary alcohols and that part of this selectivity can be attributed to different binding specificities of the enzyme for the different optically active alcohols and enantiomers

TABLE I

CAPACITY FACTORS, k', FOR VARIOUS ALCOHOLS ON HLADH-SILICA

Compound	k'
(±)-α-Ethylphenethyl alcohol	0.99
β-Ethylphenethyl alcohol	1.11
(R)-1-Phenyl-1-butanol	1.38
(S)-1-Phenyl-1-butanol	1.32

[6], we chose to investigate the ability of silica-bound HLADH to separate various β-blockers and their ketones and other primary and secondary alcohols. We found that HLADH-silica was able to separate completely a mixture of various secondary alcohols that are used as β-blockers in addition to their ketone intermediates. It is probable that the order of retention of these alcohols and ketones reflects in part the hydrophobic character of the substrate molecule, in agreement with that reported earlier [6]. In addition, we were able to separate closely related positional isomers of ethylphenethyl alcohol and to obtain racemic discrimination of the secondary alcohol 1-phenyl-1-butanol. It should also be possible to separate other alcohols, and also their oxidized or reduced intermediates, not tested here, including racemic mixtures of other optical isomers.

We are now examining other conditions in order to optimize and to extend this concept to alcohol dehydrogenases from other sources, including thermostable and secondary alcohol-specific dehydrogenases and other oxidoreductases. As there is a broad range of highly stable, especially thermostable, dehydrogenases available, in particular from microbial sources, it should be possible to prepare columns with higher stability and which can be used over a wide range of temperatures, solvents and solvent concentrations in comparison with previous chiral columns prepared from mammalian transport proteins [7,8].

ACKNOWLEDGEMENT

We are grateful for support from the Swedish National Board of Technical Development.

REFERENCES

1 K. Nilsson and P.-O. Larsson, *Anal. Biochem.*, 134 (1983) 60.
2 P. Erlandsson, I. Marle, L. Hansson, R. Isaksson and C. Pettersson, *J. Am. Chem. Soc.*, 112 (1990) 4573.
3 P. Jadaud, S. Thelohan, G. R. Schonbaum and I. W. Wainer, *Chirality*, 1 (1989) 38.
4 K. Nilsson and K. Mosbach, *Biochem. Biophys. Res. Commun.*, 102 (1981) 449.
5 C. L. Davies, *J. Chromatogr.*, 531 (1990) 131.
6 C. L. Stone, T.-K. Li and W. F. Bosron, *J. Biol. Chem.*, 264 (1989) 11112.
7 S. Allenmark, *J. Liq. Chromatogr.*, 9 (1986) 425.
8 J. Hermansson, *Trends Anal. Chem.*, 8 (1989) 251.

Journal of Chromatography, 587 (1991) 271–275
Elsevier Science Publishers B.V., Amsterdam

CHROM. 23 759

Short Communication

Efficient substitution of 1,1′-carbonyldiimidazole activated cellulose and Sepharose matrices with amino acyl spacer arms

S. C. Burton, N. W. Haggarty and D. R. K. Harding*

Separation Science Unit, Department of Chemistry and Biochemistry, Massey University, Palmerston North (New Zealand)

(First received December 31st, 1990; revised manuscript received September 23rd, 1991)

ABSTRACT

Previous procedures for addition of the spacer arm, 6-aminocaproic acid, to 1,1′-carbonyldiimidazole (CDI) activated matrices used dilute, largely aqueous reaction conditions. Only 20–50% of the activated groups were substituted. Treatment of CDI activated matrices in an organic solvent, with a concentrated aqueous solution of sodium 6-aminocaproate, allowed efficient (up to 95%) substitution of CDI activated groups. The substitution efficiency of aminocaprylic acid was also improved considerably using an organic solvent although the maximum efficiency was lower (66%). The new procedure allows reproducible levels of spacer arm substitution to be obtained. A benzamidine affinity resin prepared by the new method had a 50% higher capacity for trypsin than one prepared by the original method.

INTRODUCTION

1,1′-Carbonyldiimidazole (CDI) activation of hydrophilic matrices is a useful technique for affinity chromatography because it produces an uncharged, relatively stable urethane link between matrix and ligand [1–4]. Previous work demonstrated that very high levels of CDI activation (up to 10 mmol/g) could be obtained on cellulose and agarose matrices. However, substitution of activated matrices with a spacer arm or ligand was inefficient (typically in the range of 20 to 40% and occasionally up to 50% [4–6]. This phenomenon was particularly noticeable with the use of dilute buffered solutions of amino acyl spacer arms. The inefficiency of coupling resulted in poorly reproducible substitution levels.

Of particular concern has been the coupling of spacer arms, aminocaproic and aminocaprylic acid. This report investigates their coupling to activated matrices in a range of solvent environments to determine whether reduction of water content improves efficiency. Other variables tested were: reaction time, ratio of moles of spacer arm added to moles of active groups and solvent type. The results reported here present an improved method for the attachment of ligands with limited solubility in organic solvents.

EXPERIMENTAL

Perloza bead cellulose was purchased from Tessek (Prague, Czechoslovakia); Sepharose CL 6B from Pharmacia (Uppsala, Sweden); trypsin (type IX), CDI, 6-aminocaproic acid, 7-aminocaprylic acid, 1-ethyl-3-(3-dimethylamino-propyl)carbodiimide (EDC) and dimethyl sulphoxide (DMSO)

0021-9673/91/$03.50

(99+%) from Sigma (St. Louis, MO, USA); and *p*-aminobenzamidine from Aldrich (Germany). Dioxane, acetone and N,N-dimethylformamide (DMF) were analytical reagent grade and ethanol was technical grade. DMF was degassed and then distilled under vacuum from calcium hydride before use. Lithium, sodium and potassium aminocaproate salts were prepared by dissolving 6-aminocaproic acid in an equimolar amount of 1 *M*-LiOH, NaOH and KOH respectively, and freeze-drying the solutions.

CDI activation of matrices and titration methods were similar to the method of Bethell *et al.* [1]. Carbon dioxide was not titrated. Imidazole released by hydrolysis of active groups was titrated between pH 5 and pH 8.5 after carbon dioxide removal. The carboxyl groups of spacer arm substituted matrices were titrated to pH 8 with 0.1 or 1 *M* NaOH using a Radiometer autotitrator. Titrated samples were washed, oven-dried and weighed.

Solvent exchange

The matrix was washed sequentially with deionised water, dioxane–water (25:75), dioxane–water (50:50), dioxane–water (75:25) and 100% dioxane. A minimum of 5 matrix volumes was used for each stage. The final 100% dioxane washes were analytical grade to ensure minimal water content. For some experiments dioxane was replaced by acetone to solvent exchange the matrix to the anhydrous state.

Mixing procedure

All reactions were mixed mechanically at room temperature in sealed vessels. CDI activation mixtures were agitated mildly using an Ika Vibra-mix shaker. Spacer arm–activated matrix mixtures were mixed by rotation on a Ballmill roller.

CDI activation

CDI was added to the solvent-exchanged matrix and mixed for 1.5 h. The mixture was transferred to a sintered glass funnel and washed with 10× resin volumes of solvent (acetone or dioxane) to remove unreacted CDI and imidazole produced by the reaction. Weighed samples were taken from the activated matrix. One sample was kept for titration. The other samples were either maintained in the organic solvent used for CDI activation or solvent exchanged to another solvent, water or a solvent–water mixture. Activation levels of 2.5–3.5 mmol/g dry matrix were obtained using 0.7–1 g CDI per g dry matrix (determined from known wet weight:dry weight ratios).

Spacer arm addition

A 5-fold excess of 6-aminocaproic acid (5 mmol of spacer arm per mmol of active group on the matrix) was the standard amount used. A 3-fold excess of aminocaprylic acid was used because of its lower aqueous solubility. The surplus of spacer arm removed the need for additional buffering and ensured a reproducible, complete reaction. A 50% solution of aminocaproic acid, pH 11.3, was produced using 10 *M* NaOH and water. These pH conditions were higher than those used previously [1,2,5] and were chosen so that 80 to 90% of amino groups were in the reactive (unprotonated) form. Aminocaprylic acid is less soluble and was prepared as a 20% solution at the same pH.

The CDI-activated matrix in the appropriate organic solvent was mixed with spacer arm solution for 0.5–24 h. Afterwards mixtures containing organic solvent were solvent exchanged to water as described previously. All matrices were then washed thoroughly with deionised water. The substitution of spacer arm groups on the matrix was determined by titration (ml NaOH)/g dry weight of matrix. The dry weight value included the weight of spacer arm groups attached to the matrix. For comparison with the original CDI substitution, corrected spacer arm substitution values were calculated using corrected dry weights (dry weight − weight of spacer arm groups). The accuracy of the corrected values were validated in one experiment (Table I).

Ligand binding and capacity testing

Two samples of 6-aminocaproate bead cellulose were used to produce affinity matrices for trypsin. For each sample a slurry was prepared (5 g wet weight of resin in 2 ml of water) and the pH adjusted to 4.7 with 1 *M* HCl. The affinity ligand (*p*-aminobenzamidine hydrochloride, 0.2 g dissolved in 2 ml water) and the condensation agent (EDC, 0.2 g dissolved in 0.5 ml water) were each pH adjusted to 4.7 and added to the slurry. The slurry was maintained at pH 4.7, while mixing, at room temperature for 48 h [7]. Both samples were retitrated

TABLE I

VERIFICATION OF CORRECTED SUBSTITUTIONS AND COMPARISON OF SOLVENTS

Weighed samples of CDI-activated matrices in dioxane were solvent exchanged using mixtures of either DMSO, DMF or water with dioxane to produce samples in 100% DMSO, 100% DMF, 100% water, 50% dioxane and the original 100% dioxane form. Another sample (CDI*), solvent exchanged to 100% water, was used to determine the concentration of activated groups on the matrix. W. W. is the original wet weight of CDI-activated matrix in dioxane, D.W. is the dry weight of the sample. Titre/D.W. is the titrated substitution whereas substitution* is the corrected substitution. The accuracy of the corrected values is indicated by the correlation between corrected substitution percentages and percentages of substitution per gram wet weight.

Sample	W.W.	Titre	D.W.	Titre/W.W.		Titre/D.W.		Substitution*	
	(g)	(ml 1 *M* NaOH)	(g)	ml/g	%	ml/g	%	mmol/g	%
CDI*	3.035	0.895	0.3518	0.295		2.54		2.54	
Dioxane	3.034	0.753	0.4679	0.248	84	1.61	63	2.26	89
Dioxane 50%	3.010	0.575	0.4438	0.191	65	1.30	51	1.69	66
Water	3.033	0.437	0.4239	0.144	49	1.03	40	1.27	50
DMSO	3.056	0.844	0.4972	0.276	94	1.70	67	2.44	96
DMF	3.145	0.820	0.5049	0.261	89	1.62	64	2.29	90

to ensure completeness of carboxyl group substitution.

Resin capacity was tested by frontal analysis [8] on 1-ml samples packed in 2-ml polystyrene columns. Equilibration, loading and washing buffer was 25 m*M* Tris, 10 m*M* $CaCl_2$ (pH 8.2). Trypsin was eluted with 0.05 *M* formic acid and total protein (mg) determined by UV spectroscopy at 280 nm and bicinchoninic acid assay [9].

RESULTS AND DISCUSSION

Spacer arm solubility

The solubilities of lithium, sodium and potassium aminocaproate salts were tested in a range of solvents to see if a nonaqueous or near nonaqueous medium could be used for coupling. Solubilities were generally poor in the absence of water. Addition of a small volume of water dramatically improved solubility. Therefore it was essential to dissolve the spacer arm in a small volume of water before addition to the activated matrix. The concentrated solutions used did not appear to precipitate when added to organic media. Aminocaprylate was also dissolved in water prior to addition to organic media. Water could not be eliminated from the reaction mixture, in either case, but could be kept to a minimum.

Comparison of coupling efficiency in different environments

Initial studies used dioxane as solvent. Reducing the water content of the reaction mixture resulted in a steady improvement in the efficiency of substitution on both cellulose and agarose matrices (Table II). For bead cellulose the substitution efficiency using aminocaproic acid was 63% in water, 82% in dioxane–water (50:50) and 93% when water content was minimised. For Sepharose CL-6B the respective substitution efficiencies were 50%, 76% and 96%. Thus using a CDI-activated matrix in 100% dioxane and treating this with a concentrated aqueous solution of sodium aminocaproate produced 90–95% substitution of active groups.

Bead cellulose samples in DMSO or DMF had similar substitution efficiency to dioxane samples (96% and 90%, respectively) using minimum water content. In this experiment the values for water, water–dioxane (50:50) and minimum water were 50%, 66% and 89%, respectively (Table I). Comparison of results for bead cellulose in dioxane from separate experiments (Table I, Table II) showed that variation between samples was least when water content was minimised. The substitution efficiency obtained using acetone as organic solvent was intermediate between aqueous and dioxane samples. Bead cellulose substitution values ranged from 73 to 79% with minimum water whereas in 100% water the corresponding values where 56 to 59%. Sam-

TABLE II

COUPLING YIELDS OF CDI-ACTIVATED CELLULOSE AND SEPHAROSE WITH 6-AMINOCAPROIC ACID

CDI-activated matrices in 100% dioxane, dioxane–water (50:50) or 100% water were mixed with spacer arm solutions and substitution determined by titration. Corrected substitutions were determined using a corrected dry weight (dry weight − weight of spacer arm attached). Reaction efficiency was calculated using corrected substitution values.

Matrix	Active groups (mmol/g)	Media water (%)	Titrated substitution (mmol/g)	Corrected substitution (mmol/g)	Efficiency (%)
Bead cellulose	3.5	100	1.6	2.2	63
		50	1.88	2.85	82
		0	2.05	3.25	93
Sepharose CL-6B	2.47	100	1.01	1.23	50
		50	1.4	1.87	76
		0	1.67	2.38	96

ples in acetone developed a brown colour. This did not occur in the other solvents, suggesting a side-reaction and/or decomposition was occurring, presumably via enolisation of the acetone. The coloured products were soluble and readily washed out. The percentage substitutions using ethanol were lower than aqueous results and are not recorded here.

For bead cellulose, using aminocaprylic acid, the substitution efficiency could be improved from 27% in water to 66% when water content was minimised. The lower efficiency compared to the aminocaproic acid example was accounted for by the greater volume of water required to solubilise the 7-carbon spacer arm.

The use of a concentrated spacer arm solution improved the efficiency of active group substitution compared to previous results [5,6], even when the CDI-activated matrix was in aqueous media. The increased efficiency obtained by using an organic solvent to minimise the water content of the reaction mixture could be due to a higher molar ratio of spacer arm to water. This would favour spacer arm substitution of active groups rather than base-catalysed hydrolysis. Moreover the organic solvent is likely to affect the rates of the competing substitution and hydrolytic reactions and hence the percentage of active groups substituted.

Therefore the choice of solvent is important. The protic solvents (ethanol and water) gave the lowest results. The aprotic solvents (acetone, dioxane, DMSO and DMF) gave the highest results. The inference is that replacement of water with an aprotic solvent alters the relative rates of the hydrolytic and substitution reactions. Aprotic solvents increase the enthalpy of anionic forms and increase entropy. Overall the free energy differences between ground state and transition state for the reactions are apparently modified to favour the substitution reaction [10]. The more polar aprotic solvents (DMSO and DMF) are the best choices to solvate the CDI-activated matrix because solvent shock damage upon addition of the aqueous solution is less likely. If dioxane is used, the spacer arm solution can be diluted with solvent prior to addition to the matrix.

Other variables

The effect of reaction time and spacer arm concentration was also studied. The shortest time used for the reaction was 30 min. The reaction proceeded to effective completion within this time whether the solvent used was water or acetone. Only a 3–4% variation occurred from 0.5–20 h.

A 3- to 5-fold excess of aminocaproic acid (over active groups) was required for maximum substitution efficiency. For bead cellulose in acetone the substitution efficiences were 60% (1), 72% (2), 75% (3), 79% (4) and 79% (5 equivalents).

Trypsin-binding capacity

Two samples of CDI-activated bead cellulose (1.4 mmol/g) were substituted with aminocaproic acid; the first in dilute aqueous reaction conditions [5], the second using dioxane and minimising water content. The uncorrected spacer arm substitutions were 0.42 mmol/g and 1.09 mmol/g, respectively.

Following coupling with *p*-aminobenzamidine the samples were capacity tested by frontal analysis. The capacities for trypsin were 18 mg/ml and 28 mg/ml, respectively. Otherwise their chromatographic behaviour was the same. Thus the new technique allowed a considerable improvement in capacity without apparent side-effects.

Several advantages result from efficient substitution of a CDI-activated matrix. CDI is a moderately expensive, unstable compound requiring special storage conditions (below 0°C, sealed from atmosphere). A reduced requirement for CDI with increased efficiency of substitution is obviously an advantage. Aminocaprylic acid is expensive and efficient use will provide a considerable cost saving. If the substitution of the CDI-activated matrix is low for any reason (*e.g.* unreactive CDI, poor solvent exchange) efficient substitution of activated groups is more likely to yield a useful product. Extremely high substitution levels can be obtained using this technique. Such high levels of substitution can be undesirable for affinity chromatography [11,12]. However for some applications, highly substituted matrices allow very high capacities to be obtained [13]. The example of trypsin capacity quoted above demonstrates how capacity can be increased by efficient substitution. Alternatively lower substitutions may be obtained with more precision by minimising the hydrolysis reaction. This new method for spacer arm addition to a CDI-activated matrix does not require any additional steps compared to previous techniques. It can produce a significant cost saving when scale-up is considered.

REFERENCES

1 G. S. Bethell, J. S. Ayers, W. S. Hancock and M. T. W. Hearn, *J. Biol. Chem.*, 254 (1979) 2572.
2 M. T. W. Hearn, G. S. Bethell, J. S. Ayers and W. S. Hancock, *J. Chromatogr.*, 185 (1979) 463.
3 M. T. W. Hearn, E. L. Harris, G. S. Bethell, W. S. Hancock and J. S. Ayers, *J. Chromatogr.*, 218 (1981) 509.
4 M. T. W. Hearn, *Methods Enzymol.*, 135 (1987) 102.
5 G. S. Bethell, J. S. Ayers, M. T. W. Hearn and W. S. Hancock, *J. Chromatogr.*, 219 (1981) 353.
6 G. S. Bethell, J. S. Ayers, M. T. W. Hearn and W. S. Hancock, *J. Chromatogr.*, 219 (1981) 361.
7 C. R. Lowe and P. D. G. Dean, *Affinity Chromatography*, Wiley, London, 1974, Ch. V, pp. 222–224.
8 J. Turková, *Affinity Chromatography*, Elsevier, Amsterdam, 1978, Ch. 9, pp. 203–223.
9 P. K. Smith, R. I. Krohn, G. T. Hermanson, A. K. Mallia, F. H. Gartner, M. D. Provenzano, E. K. Fujimoto, N. M. Goeke, B. J. Olson and D. C. Klenk, *Anal. Biochem.*, 150 (1985) 76.
10 J. B. F. N. Engberts, in F. Franks (Editor), *Water: A Comprehensive Treatise*, Plenum Press, New York, 1979, Ch. 4.
11 M. T. W. Hearn, P. K. Smith, A. K. Mallia and G. Hermanson, in I. Chaiken, M. Wilchek and I. Parikh (Editors), *Affinity chromatography and Biological Recognition*, Academic Press, New York, 1983, pp. 135–142.
12 M. T. W. Hearn, *J. Chromatogr.*, 376 (1986) 245.
13 N. W. Haggarty, S. Burton, B. D. Hock and D. R. K. Harding, in P-L. Yu (Editor), *Fermentation Technologies: Industrial Applications*, Elsevier, London, 1990, Section 5, p. 407.

Journal of Chromatography, 587 (1991) 276–279
Elsevier Science Publishers B.V., Amsterdam

CHROM. 23 713

Short Communication

Interfacial effects in size-exclusion chromatography of latex

M. Potschka

Porzellangasse 19, A-1090 Vienna (Austria)

(First received June 11th, 1991; revised manuscript received August 28th, 1991)

ABSTRACT

The retention volume in size-exclusion chromatography (SEC) depends on both the size of the particle proper and the interfacial mutual repulsion of the surfaces, *i.e.*, between the pore wall and the surface of the particles. The presence of some interfacial repulsion is crucial to obtain a pure SEC mode of elution. It is therefore always present and should not be neglected as is usually done. Analysis of published data shows that the interfacial repulsion is well described by the Dejaguin–Landau–Verwey–Overbeek (DLVO) theory of colloidal stability, and its properties can therefore be studied in detail via chromatography. It is shown that interfacial repulsion depends on the size of the latex beads ans attains large values for larger beads. For a given size of the bead it depends strongly on its charge up to a limit of saturation, as predicted by DLVO theory.

INTRODUCTION

In size-exclusion chromatography (SEC), macromolecules or particles flow through a porous matrix and permeate all volumes accessible to their centres of gravity. For solutes comparable in size to the pore size, this accessible volume depends strongly on size and shape and hence larger particles elute first. In SEC proper, particles do not adhere to the matrix at all.

It was previously established [1–3] that universal calibration in SEC needs to account for both the effective hydrodynamic shape of the solute, which freely permeates the pores, and an interfacial wall effect. Whenever the interaction energy between the pore surface and the particles surface is attractive at some distance and the approach to this steric position is not kinetically inhibited by a high activation barrier, non-SEC modes determine elution. Electrostatic repulsion is a very effective means of preventing this adsorption and thus of establishing pure SEC conditions. A low ionic strength then is superior to high salt concentrations. However, the wall effect then becomes large at low ionic strength and must be explicitly accounted for, whereas it is usually neglected at high ionic strength or with neutral solutes. A universal calibration is therefore characterized by a total radius R:

$$R = R_{SEC} + R_{IF} = R_{SEC} + \kappa^{-1}\bar{x} \quad (1)$$

where $\bar{x}$ is the average electrostatic repulsion distance at equilibrium in multiples of Debye length κ, R is the total solute radius, R_{IF} is the interfacial contribution to R and R_{SEC} is the rotationally averaged mean radius of the solute, similar to or even identical with R_η, the equivalent body radius defined by intrinsic viscosity. For a detailed discussion of eqn. 1, see ref. 3. For spheres R_{SEC} is simply the radius of the bead and may also be determined by electron microscopy, even though

0021-9673/91/$03.50

hydrodynamic radii may slightly differ from the microscopic dimensions of dried beads.

Styring *et al.* [4] presented the same rationale but did not analyse their data further for latex spheres on porous glass packings along these lines. The analysis of the wall effect based on their data is presented in this paper.

EXPERIMENTAL AND RESULTS

All data reported in the following are based on elution volumes measured and tabulated by Styring *et al.* [4], who also prepared the materials. A polystyrene seed latex (L1) was prepared in Aerosol-MA80 detergent solution similar to the method of Woods as modified by Styring *et al.* [4]. This latex was then either grown stepwise to larger sizes in Aerosol-MA80 solutions according to Dodge [7] (L-series) or was overcoated stepwise with poly(methyl methacrylate) in detergent-free solution according to Chainey and Hearn [8] (M-series), as detailed by Styring *et al.* [4]. Optionally latices were exhaustively dialysed against pure water to remove all detergent. When later run on the SEC columns in the presence of sodium dodecyl sulphate (SDS) or Ultrawet-K detergent, dialysed latices gave identical results to non-dialysed latices. This suggests that Aerosol-MA80 has little influence on the different properties of the two types of latices. However, higher concentrations of initiator present during polystyrene seed growth might have incorporated more charged residues into the polystyrene latices than into the methacrylate latices. The sizes of the latices were determined by electron microscopy and are given in Tables 1 and 6 in ref. 4. The differently sized latices were run on a porous glass column at different ionic strength in the presence of detergent. Elution volumes are tabulated in Table 8 in ref. 4.

To apply the rationale of analysis devised by the present author [1–3], these primary data need to be converted into effective radii R via a universal calibration of their column set-up. The best choice is data obtained at 111 mM ionic strength in the presence of Ultrawet-K as surfactant (Table 10 in ref. 4), even though measurements made in SDS will be analysed below. There may be small differences in the viscosity radius R_η in these different solvents. However, an even larger error is introduced by using the electron microscopically determined latex radii R_{EM} (Tables 1 and 6 in ref. 4) instead of R_η. By later taking only differences in R for the salient conclusions, however, this reduces to a minor order correction. Fig. 1 shows the universal calibration obtained for their particular mixed bed CPG–Fractosil porous glass column used in these experiments.

Using Fig. 1, one can now convert all elution volumes for different latices and ionic strength (Table 8 in ref. 4) into radii. Fig. 2 shows the data for the surfactant-coated polystyrene–latex spheres for each solute (L1–L6) as a function of total ionic strength. This includes the concentration of SDS monomer and yields values slightly higher than those listed in ref. 4, which are based on support electrolyte alone. The data are scattered and may even reveal some non-linearity; however, for simplicity a first analysis is done in terms of a linear function of $I^{-1/2}$. Most likely deviations at high ionic strength originate from the commencement of adsorption noted by Styring *et al.* [4]. Fig. 3 shows the same analysis for poly(methyl methacrylate)-coated latex spheres. Comparing Fig. 2 with Fig. 3, it is obvious that the charge effect of the methacrylate surface is less than that for pure polystyrene, indicating that less surfactant has been adsorbed on the methacrylate surface than on pure polystyrene. It may be, however, that the prime difference is not

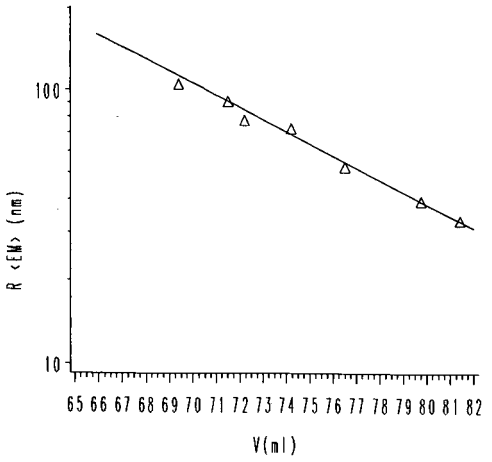

Fig. 1. Universal calibration of the mixed-bed CPG–Fractosil column used by Styring *et al.* [4] based on their data for I = 111 mM (Table 10 in ref. 4). The electron microscopically determined radii R_{EM} are presumably slightly smaller than the viscosity radii R_η, but errors will have little effect in the present context.

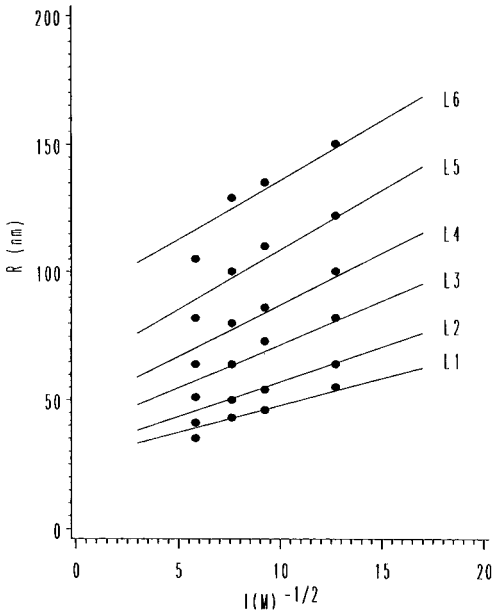

Fig. 2. Total size R of surfactant-coated polystyrene latex beads (L) as a function of ionic strength. Measurements were made at 0.0295, 0.0173, 0.0117 and 0.0062 M ionic strength with 0.0017 M SDS and various amounts of sodium nitrate. Elution volumes from Tables 8 in ref. 4 were converted into radii via universal calibration (Fig. 1).

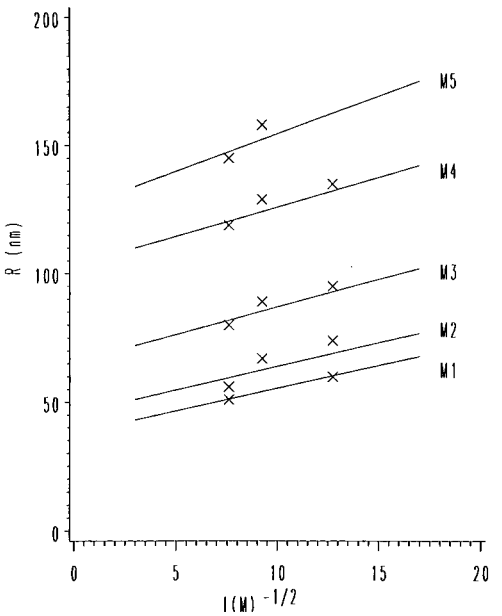

Fig. 3. Total size R of methacrylate-coated polystyrene latex beads (M) as a function of ionic strength. Measurements were made at 0.0173, 0.0117 and 0.0062 M ionic strength with 0.0017 M SDS and various amounts of sodium nitrate. Elution volumes from Table 8 in ref. 4 were converted into radii via universal calibration (Fig. 1).

SDS adsorbed from the elution fluid but different amounts of ionic residues incorporated during manufacture (see above). Alternatively, some Aerosol-MA80, which is used during manufacturing of the polystyrene latex but not for the methacrylate coating step, may have become entangled in the particle structure and thus not able to dialyse.

The average electrostatic repulsion distance $\bar{x}$, which measures the wall effect, is obtained from the slopes in Figs. 2 and 3 according to eqn. 1 since κ depends on $I^{1/2}$ [3]:

$$\bar{x} = 3.3 \cdot \frac{dR}{dI^{-1/2}} \qquad (2)$$

where the numerical factor assumes an aqueous eluent at room temperature; $\bar{x}$ is a universal parameter as it no longer depends on ionic strength but only on matrix charge and the size and charge of the solute polyelectrolyte.

The final result is shown in Fig. 4, which presents

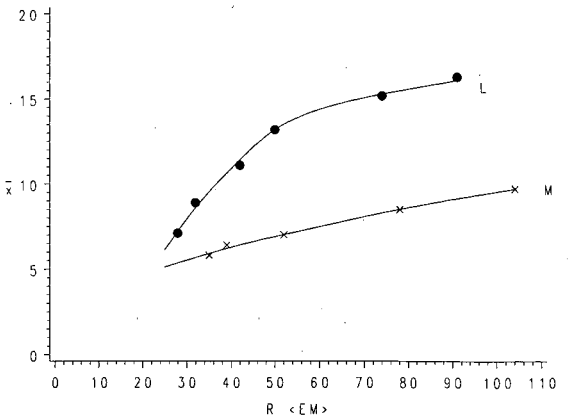

Fig. 4. Dependence of repulsion distance $\bar{x}$ in units of Debye length, obtained from the slopes of Figs. 2 and 3 according to eqn. 2, on the size of the latex beads, R_{EM}. This electron microscopic radius is here taken to be similar to R_{SEC}. (●) Surfactant-coated polystyrene latex spheres (L) based on data in Fig. 2; (×) methacrylate-coated polystyrene latex spheres (M) based on data in Fig. 3.

$\bar{x}$ as a function of the microscopic particle dimensions. In addition to this size dependence, $\bar{x}$ critically depends on the surface charge of both the solute and pore wall. The latter is the same for both types of latices, hence the difference reflects the different surface charge on the latex. Presumably the methacrylate surface is nearly uncharged whereas the polystyrene-based surface contains a very high charge density due to surfactant molecules. It is possible that the surface potential of these polystyrene beads is saturated, which would yield the maximum wall effect for the given column, but one cannot exclude that the maximum effect is even larger.

DISCUSSION

The present analysis of the data of Styring *et al.* [4] according to the rationale developed previous [1–3] confirms that wall effects in SEC depend greatly on the size of the solute particle. Comparison of the present data with those previously obtained on TSK-6000 PW [3] reveals that the porous glass is more highly charged than the TSK-6000 PW, which does, however, contain significant residual charges. The TSK PW material was argued to contain a hairy surface of polymer fibres protruding from the nodules that form the pores [3]. The present data with porous glass thus establish the wall effect with guaranteed geometrically smooth pore surfaces. It further has the advantage of avoiding any complications in analysis originating from the asymmetric shape of the sample (DNA) in one of the previous studies [3]. The magnitude of the wall effect is in line with the theory of surface forces as discussed in detail previously [3].

The present analysis demonstrates that SEC may be used to characterize the polyelectrolyte properties of macromolecules and particles. In fact, the adsorption of methacrylate-coated polystyrene at high ionic strength [4] is a direct consequence of the lower charge density of these particles compared with surfactant-coated polystyrene and is probably not a chemical property of the methacrylate.

In previous studies [1–3], the linear eqn. 1 was found to be well suited to describe the data. Some of the present data, in contrast, show a definite curvature (Fig. 3), suggesting a more complicated dependence on ionic strength. This possibility was anticipated previously on theoretical grounds [3]. The scatter of the data is such, however, that it seems inadvisable to propose a multi-parameter fit. Deviations from linearity are most significant above 15 mM ionic strength and might also originate from the commencement of adsorption. If so, this would suggest that the $I^{-1/2}$ law applies only at lower ionic strength. In this case the $\bar{x}$ values for methacrylate might be even lower whereas the polystyrene data remain as analysed.

Apparently more highly charged, the magnitude of interfacial effects is larger for polystyrene latex on controlled-pore glass than for similarly sized DNA and viruses on TSK-6000PW. A previous study of latex by hydrodynamic chromatography even reported interfacial effects equivalent to about 27 Debye length [5].

The repulsion distance $\bar{x}$ reflects a delicate balance between electrostatic repulsion and Van der Waals attraction in line with Dejaguin–Landau–Verwey–Overbeek theory. It may not be explained solely by electrostatic terms, thus confirming previous conclusions [3]. It must be emphasized that the wall effect, analysed here in terms of ionic strength-dependent elution of polyelectrolytes, is not limited to charge effects. As Van der Waals forces are generally attractive, the very existence of an SEC mode of elution for neutral molecules requires that solvation forces are repulsive, again establishing a repulsion distance, *i.e.*, a wall effect. This wall effect may differ for solutes of different chemical nature and for the same solutes in different solvents.

This study extends previous analyses of interfacial effects [2,3,5,6]. The salient conclusions are that interfacial effects are large contributors to the total observation and are large in absolute terms, they increase dramatically with increasing size of the solute particles and for a given size they increase with increasing charge density (up to a limit of saturation).

REFERENCES

1 M. Potschka, *Anal. Biochem.*, 162 (1987) 47.
2 M. Potschka, *J. Chromatogr.*, 441 (1988) 239.
3 M. Potschka, *Macromolecules*, 24 (1991) 5023.
4 M. G. Styring, J. A. J. Honing and A. E. Hamielec, *J. Liq. Chromatogr.*, 9 (1986) 3505.
5 H. Small, *Adv. Chromatogr.*, 15 (1977) 113.
6 P. L. Dubin, C. M. Speck and J. I. Kaplan, *Anal. Chem.*, 60 (1988) 895.
7 J. S. Dodge, M. E. Woods and I. M. Krieger, *J. Paint Technol.*, 42 (1970) 71.
8 M. Chainey, J. Hearn and M. C. Wilkinson, *Brit. Polym. J.*, 13 (1981) 132.

Journal of Chromatography, 587 (1991) 280–283
Elsevier Science Publishers B.V., Amsterdam

CHROM. 23 672

Short Communication

A high-performance liquid chromatographic method for the monitoring and quantification of the synthesis of *p*-hydroxyphenylacetamide

Jitendra S. Wagh, Asmita A. Mokashi and Arunabha Datta*

Alchemie Research Centre, P.B. No. 155, Thane-Belapur Road, Thane-400 601, Maharashtra (India)

(First received April 23rd, 1991; revised manuscript received August 6th, 1991)

ABSTRACT

p-Hydroxyphenylacetamide (HPAD) is the precursor for the synthesis of the β-blocker atenolol. A high-performance liquid method using methanol–water–tetrahydrofuran–acetic acid (35:65:1:1, v/v) as the mobile phase, a Novapak-C_{18} column and detection at 254 nm was developed for the monitoring and quantification of the synthesis of HPAD. The method allows the simultaneous determination of the product, the starting material and the intermediates and thereby permits the optimization of the reaction parameters to obtain impurity-free HPAD.

INTRODUCTION

Atenolol is a potent β-blocker commonly prepared by the reaction of epichlorohydrin with *p*-hydroxyphenylacetamide (HPAD) and its subsequent condensation with isopropylamine [1,2]. There are several routes for the synthesis of HPAD [3–5], but in this study a four-step synthesis starting from *p*-hydroxyacetophenone (PHA) was adopted [6] (Fig. 1).

After optimization of the high-performance liquid chromatographic (HPLC) conditions, the product was found to give rise to four well resolved peaks, which were identified and subsequently quantified. These results permitted the optimization of the synthesis parameters to obtain pure samples of HPAD.

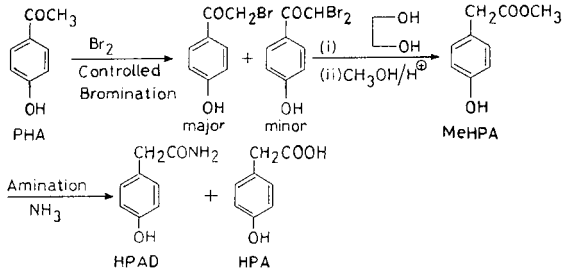

Fig. 1. Reaction scheme for the synthesis of HPAD from PHA.

EXPERIMENTAL

Reagents

The following reagent were used: *p*-hydroxyphenylacetic acid (HPA) (Sigma, St. Louis, MO, USA), *p*-hydroxyacetophenone (PHA) (Boehringer, Ingelheim, Germany), *p*-nitroacetophenone [internal

0021-9673/91/$03.50

standard (I.S.)] (Riedel-de Haën, Hannover, Germany), methyl ester of HPA (MeHPA) (synthesized from HPA in our laboratory) and hydroxyphenylacetamide (HPAD) (ICI, Mereside, UK).

Instrumentation

The HPLC system consisted of a Model 6000 alternating pump, a Novapak-C_{18} column (4-μm particle size) (150 mm × 3.9 mm I.D.), a Model 481 UV detector (all from Waters Assoc., Milford, MA, USA), a Rheodyne injector with a 10-μl loop and a Hewlett-Packard Model 3394A integrator.

Chromatographic analyses

The mobile phase was methanol–water–tetrahydrofuran–acetic acid (35:65:1:1, v/v) at a flow-rate of 1 ml/min. The detection wavelength was 254 nm and the sample size was 10 μl throughout.

Nine standard calibration mixtures with different concentrations of HPA, PHA, MeHPA and HPAD with *p*-nitroacetophenone as the internal standard were prepared and analysed by HPLC. Calibrations graphs were constructed for each analyte and the response factors determined from the slope. Synthetic mixtures of all four analytes were then prepared and analysed using the same system and the validity of the response factors was examined by checking the mass balance. The analysis of reaction mixtures and the final assay of pure HPAD were done using the same system.

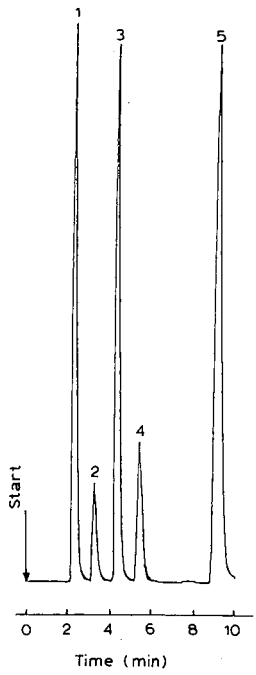

Fig. 2. Typical chromatogram of a synthetic mixture of analytes with an internal standard: (1) HPAD (4.94 μg); (2) HPA (0.86 μg); (3) PHA (0.29 μg); (4) MeHPA (1.61 μg); (5) I.S. (0.29 μg).

RESULTS AND DISCUSSION

The results for HPAD, HPA, PHA and MeHPA are given in Table I. It is evident that the response factor of PHA is significantly higher than those of the other analytes, being about 20 and 17 times those of MeHPA and HPA, respectively. It was therefore essential to take the response factors into account when determining the concentration of each constituent of the mixture.

A typical chromatogram of a synthetic mixture of the analytes is shown in Fig. 2; all the peaks are baseline resolved. The calibration for each analyte

TABLE I

RELATIVE RETENTION TIMES (*RRT*), RESPONSE FACTORS (*RF*), CAPACITY FACTORS, RESOLUTION (R_s) AND LINEARITY RANGE OF THE CONSTITUENTS OF THE HPAD SYNTHESIS ROUTE

Compound	*RRT*	*RF*	Capacity factor	R_s	Linearity range (μg)
HPAD	0.22	0.039	0.41	–	0.32 – 5.13
HPA	0.33	0.044	1.14	2.45	0.33 – 3.00
PHA	0.44	0.762	1.90	2.55	0.71 – 1.54
MeHPA	0.58	0.038	2.80	2.18	0.32 – 2.73
I.S.	1	1	5.52	5.63	–

TABLE II

LINEARITY OF RESPONSE FOR THE DIFFERENT ANALYTES

Compound[a]	Sample No.	Area / Area I.S.	Conc. / Conc. I.S.	Area ratio / Conc. ratio	Compound[a]	Sample No.	Area / Area I.S.	Conc. / Conc. I.S.	Area ratio / Conc. ratio
HPA	1	0.053	1.17	0.045	MeHPA	1	0.042	1.13	0.037
	2	0.109	2.34	0.046		2	0.085	2.25	0.021
	3	0.157	3.51	0.045		3	0.128	3.38	0.038
	4	0.210	4.68	0.045		4	0.183	4.50	0.040
	5	0.254	5.85	0.043		5	0.217	5.63	0.039
	6	0.312	7.02	0.044		6	0.261	6.76	0.039
	7	0.356	8.19	0.043		7	0.303	7.88	0.038
	8	0.405	9.36	0.043		8	0.348	9.01	0.039
	9	0.463	10.53	0.044		9	0.394	9.57	0.041
HPAD	1	0.072	1.12	0.064	PHA	1	0.545	0.60	0.905
	2	0.103	2.25	0.046		2	0.951	1.21	0.792
	3	0.193	4.49	0.043		3	1.412	1.81	0.779
	4	0.283	6.75	0.042		4	1.904	2.41	0.788
	5	0.348	8.99	0.039		5	2.321	3.01	0.771
	6	0.450	11.24	0.040		6	2.868	3.62	0.792
	7	0.523	13.49	0.039		7	3.164	4.22	0.749
	8	0.060	15.74	0.038		8	3.640	4.75	0.766
	9	0.706	17.99	0.039		9	4.131	4.43	0.761

[a] Regression equations:

$y = (5.181 \cdot 10^{-3}) + (4.319 \cdot 10^{-2})C_{HPA}$

$y = (2.421 \cdot 10^{-2}) + (3.738 \cdot 10^{-2})C_{HPAD}$

$y = (-5.508 \cdot 10^{-3}) + (4.011 \cdot 10^{-2})C_{MeHPA}$

$y = (7.854 \cdot 10^{-3}) + (7.476 \cdot 10^{-1})C_{PHA}$.

was done for the concentration ranges given in Table I and the response was found to be linear for all four analytes (Table II). The inter-assay precision of the method was established by triplicate analyses of synthetic mixtures of different compositions and the percentage error was found to be generally less than 1% with a maximum error of 1.09% (Table III).

The results of the analysis of actual reaction mixtures is shown in Table IV, where the difference between the percentage concentration of each analyte determined from the zero method (area percentage) and that obtained after taking the relevant response factors into account is clearly evident. The results of the analysis of reaction mixtures were in good agreement with the yields obtained after isolating

TABLE III

RESULTS OF THE ANALYSIS OF SYNTHETIC MIXTURES OF THE ANALYTES

Averages of triplicate determinations.

HPAD (%)			HPA (%)			MeHPA (%)			PHA (%)		
Taken	Found	Error	Taken	Found	Error	Taken	Found	Error	Taken	Found	Error
63.90	63.78	0.12	11.50	11.13	0.37	20.84	20.78	0.06	3.76	3.77	0.01
65.62	65.13	0.49	8.33	8.33	0.00	17.90	16.81	1.09	8.18	7.62	0.56
59.19	58.87	0.32	21.31	21.50	0.19	8.48	8.43	0.05	11.00	10.22	0.78

TABLE IV

RESULTS OF THE ANALYSIS OF REACTION MIXTURES FOR THE SYNTHESIS OF HPAD

Sample	Analyte	Area (%)	Actual [a] (%)
I	HPAD	78.00	87.00
	HPA	4.50	4.78
	PHA	17.22	1.00
	MeHPA	–	–
II	HPAD	90.40	90.95
	HPA	3.50	3.13
	PHA	6.00	0.32
	MeHPA	–	–

[a] After correction with respective response factors.

the product. The presence of HPA in the reaction mixture (Table IV) suggested the possible hydrolysis of MeHPA to HPA and the synthesis parameters were accordingly optimized to minimise this hydrolysis.

The method described is effective for monitoring the synthesis and for the final assay of the product. With minor modification it should also be possible to use this method for monitoring the synthesis of HPAD by other routes. In fact, a similar system has been used for monitoring the synthesis of HPAD starting from sodium hydroxymandelate and involving HPA as an intermediate [7].

ACKNOWLEDGEMENTS

The authors thank Dr. B. N. Roy for his support, ICI India for financial assistance and Dr. A. Kumar and Mr. R. A. Rane for providing authentic analytes and samples.

REFERENCES

1 A. M. Barret, J. Carter, R. Hull, D. J. Le Count and C. J. Squire, (to ICI) *U.S. Pat.*, 3 663 607(1972).
2 A. M. Barret, J. Carter, R. Hull, D. J. Le Count and C. J. Squire, (to ICI) *U.S. Pat.*, 3 836 671 (1974).
3 G. M. Sharma and P.R. Burkholder, *Tetrahedron Lett.*, 42 (1967) 4147.
4 J. Lange and T. Urbanski, *Diss. Pharm. Pharmacol.*, 20 (1968) 607.
5 O. Yone-mitsu and S. Naruto, *Chem. Pharm. Bull.*, 19 (1971) 1158.
6 A. Kumar and R. A. Rane, *Indian Pat. Appl.*, 135/CAL/89 (1990).
7 A. K. Mandal, S. W. Mahajan and D. G. Jawalkar, *Indian Pat. Appl.* 897/CAL/89 (1989).

Journal of Chromatography, 587 (1991) 284–287
Elsevier Science Publishers B.V., Amsterdam

CHROM. 23 724

Short Communication

Clean-up procedure for partially methylated alditol acetate derivatives of polysaccharides

David M. Gibeaut and Nicholas C. Carpita*

Department of Botany and Plant Pathology, Purdue University, West Lafayette, IN 47907 (USA)

(First received April 9th, 1991; revised manuscript received September 3rd, 1991)

ABSTRACT

After derivatization of polysaccharides for glycosyl linkage analysis, considerable contamination is often present. We have devised a simple phase partition system which extracts virtually all phthalate esters and baseline contaminants into a carbon tetrachloride phase, but yields greater than 95% recovery of partially methylated alditol acetate derivatives in a methanol–water (40:60) phase.

INTRODUCTION

Gas chromatography of partially methylated alditol acetate (PMAA) derivatives used in linkage analysis of polysaccharides often requires injection of dilute samples. As a result, a high concentration of contaminants, introduced during the derivatization procedure, compromises chromatograms with low signal-to-noise ratios. In an effort to remove these contaminants, particularly abundant when using *n*-butyllithium in hexane to form the Li^+-methylsulfinylmethanide carbanion, we explored several clean-up and solvent extraction schemes. Carbon tetrachloride is a useful solvent for phthalate esters, known contaminants of methylation procedures [1], and PMAA derivatives of sugars are soluble in methanol. However, carbon tetrachloride and methanol are miscible. Therefore, we sought an immiscible second phase of methanol–water which would still carry the sugar derivatives. We chose a two-phase system of methanol–water (40:60), saturated with carbon tetrachloride. This system separated derivatives from contaminants with greater than 95% recovery of PMAA derivatives in the methanol–water phase after a single extraction. The carbon tetrachloride phase contained phthalate esters of known origin, and unknown contaminants contributing to a high baseline. A portion of the PMAA derivatives of terminal sugars from sucrose and the hexa- and pentaacetate derivatives of neutral sugars were also found in the carbon tetrachloride phase, but good recovery of these could be obtained by adjusting the solvent ratio.

EXPERIMENTAL

Preparation of plant oligo- and polysaccharides

Cell walls from cariocha bean (*Phaseolus vulgaris* L. cv. Cariocha) were prepared from flour made by pulverizing the seeds in a coffee grinder. The flour was homogenized in 50 m*M* N-tris(hydroxymethyl) methyl-2-aminoethanesulfonic acid (TES)–NaOH, 30 m*M* ascorbic acid, 1.5% sodium dodecyl sulfate (SDS), pH 7.2, and washed sequentially in SDS buffer followed by water. Starch was removed by three successive extractions with 90% dimethyl sulfoxide

0021-9673/91/$03.50

(DMSO) [2] until the wall preparations were iodine-negative. The chelator-soluble pectins were extracted with trans-1,2-diaminocyclohexane-N,N,N',N'-tetraacetic acid (CDTA) [3], and esterified pectins and some hemicelluloses were extracted under nitrogen atmosphere with 1.0 *M* NaOH, containing 3 mg/ml $NaBH_4$ to prevent end elimination [4]. The majority of the hemicelluloses were extracted under nitrogen atmosphere with 4 *M* NaOH containing 3 mg/ml $NaBH_4$ for 18 h, neutralized with glacial acetic acid, dialyzed against running deionized water, and lyophilized. The 4 *M* NaOH fraction was used in this analysis.

Radioactive cell wall samples of maize seedlings were obtained as described [5]. Radioactive sucrose from ^{14}C-labeled tissue slices from Jerusalem artichoke (*Helianthus tuberosus* L. cv. Bianca) tubers were isolated and characterized as described [6].

Preparation of partially methylated alditol acetate derivatives

Simplified procedures were developed for methylation of polysaccharides with the Li^+-methylsulfinylmethanide carbanion made from *n*-butyllithium and DMSO [7–9]. About 1 mg of carbohydrate and a small stir bar were placed in 15-ml thick-walled glass tubes and stored in a vacuum dessicator over P_2O_5 overnight. The next day, the tubes were sealed with serum sleeve stoppers, evacuated, and 1.0 ml of anhydrous DMSO was added by syringe. The tubes were sonicated for 1 h in a water bath that warmed to 50°C. Nitrogen was introduced by means of a syringe needle with a second needle inserted for escape flow. The solutions were stirred, and 0.5 ml of 2.5 *M* *n*-butyllithium in hexanes was added slowly. After the solution had cleared, but before the color darkened (about 1 h) 0.5 ml of CH_3I was added. Nitrogen flow was stopped and stirring was continued for 1 h in the sealed tubes. Reactions were stopped with 5 ml of water, and the derivatives were extracted two times from the mixture with 1.0 ml chloroform. The chloroform phase was washed five times with water and then dried in 1-dram borosilicate glass vials sealed with PTFE-lined caps.

The partially methylated derivatives from cell wall polysaccharides were hydrolyzed in 1.0 ml 2 *M* trifluoroacetic acid (TFA) at 120°C for 90 min; whereas the derivatives of sucrose were hydrolyzed in 1.0 ml of 1 *M* TFA at 70°C for 30 min to minimize decomposition of the fructofuranosyl units. After hydrolysis, 1.0 ml of *tert.*-butyl alcohol was added and the mixtures were dried under a stream of nitrogen. The partially methylated sugars, L-[U-^{14}C]arabinose and *myo*-[U-^{14}C]inositol were reduced and acetylated as described [8,10]. Fully derivatized sugars were transfered in dichloromethane to 0.5-ml conical vials, and dried with a stream of nitrogen before the clean-up procedure.

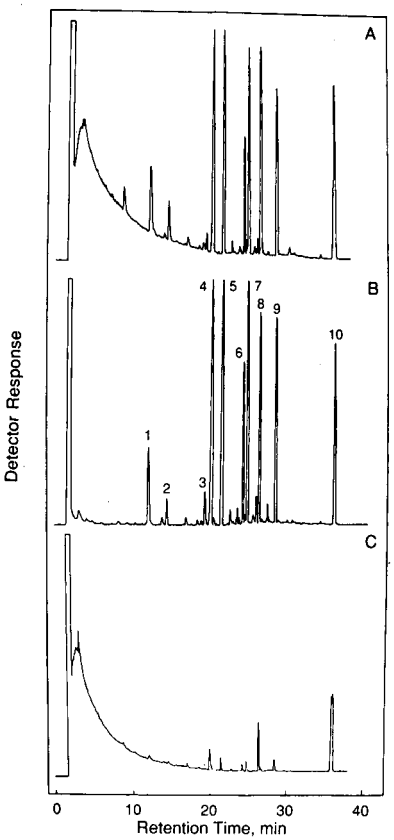

Fig. 1. Flame ionization detector response showing the removal of baseline components in the chromatographic separation of PMAA derivatives of bean cell wall. The sample was divided equally before the clean-up procedure, and samples were injected representing equal quantities of sample. The solvent volumes used for clean-up were 10 μl carbon tetrachloride and 100 μl methanol–water (40:60). (A) Before clean-up. (B) After clean-up. (C) Carbon tetrachloride phase of the clean-up from B. Glycosyl residue: 1 = terminal-arabinose; 2 = terminal-xylose; 3 = terminal-galactose; 4 = 5-arabinose; 5 = 2-xylose + 4-xylose; 6 = 2,5-arabinose; 7 = 4-glucose; 8 = arabinose pentaacetate; 9 = 4,6-glucose; 10 = *myo*-inositol hexaacetate.

Clean-up procedure

Spectrophotometric grade solvents and deionized water (18 MΩ) were used in the extraction procedures. A stock solution was prepared by adding equal volumes of carbon tetrachloride and methanol–water (40:60, v/v) in a reagent bottle. The stock solution was shaken and allowed to separate for several hours. It was necessary to saturate the two solvent phases because a considerable amount of carbon tetrachloride entered the methanol–water phase. Routinely, 10 μl of the carbon tetrachloride phase and 100 μl of the methanol–water phase were added to 0.5 ml-conical vials containing derivatives. The vials were vortex-mixed and then centrifuged at 2 000 *g* for 10 min to quickly separate the two phases. The upper, methanol–water phase containing the derivatives was pipetted into a clean vial and dried with a stream of nitrogen. For determination of extraction efficiency samples of radioactive sugar derivatives were extracted and the two phases were assayed by liquid scintillation spectroscopy.

Gas chromatography

Separations were carried out with a Hewlett-Packard 5840A gas chromatograph. Samples in ethyl acetate were injected in the split mode (split ratio *ca.* 10:1) and detected by flame ionization. The derivatives were separated on a SP-2330 fused-silica capillary column, 30 m × 0.25 mm I.D., 0.20 μm film (Supelco, Bellfonte, PA, USA) temperature programmed from 160 to 210°C at 2°C/min then to 240°C at 5°C/min with a 10-min hold at the upper temperature. The carrier gas was helium at 180 kPa.

RESULTS AND DISCUSSION

Removal of contaminants from PMAA derivatives of plant polysaccharides

A cell wall sample was divided equally after derivatization but before the clean-up procedure to demonstrate the removal of contaminants (Fig. 1). The chromatogram of a sample before clean-up shows an elevated baseline that does not return to the initial level until many of the PMAA derivatives have eluted. However, the cleaned sample recovered from the methanol–water phase shows baseline resolution throughout the chromatogram. The baseline contaminants, phthalate esters (gas chromatography–electron impact mass spectrometry base peak *m/z* 149), and a portion of the *myo*-inositol hexaacetate were partitioned into the carbon tetrachloride phase.

Extraction efficiency

Recovery was quantified with radioactive samples (Table I). Comparison of a first and second

TABLE I

EXTRACTION EFFICIENCY OF A TWO-PHASE, CARBON TETRACHLORIDE/METHANOL–WATER (40:60), CLEAN-UP PROCEDURE FOR THE REMOVAL OF CONTAMINANTS FROM THE DERIVATIZATION PROCEDURE OF PARTIALLY METHYLATED ALDITOL ACETATES

Radioactive samples were extracted and assayed as described in the Experimental section. Alditol acetate derivatives of arabinose and inositol do not require clean-up, but demonstrate selective partitioning. PMAA derivatives of terminal glucose and fructose from sucrose are not as well recovered as derivatives of linked sugars.

	Solvent ratio carbon tetrachloride–methanol[a]	Recovery (%)			
		Maize cell wall (PMAA)	Arabinose (pentaacetate)	Inositol (hexaacetate)	Sucrose (PMAA)
First extraction[b]	(10:100)	94.6	49.2	73.8	77.1
Second extraction[b]	(10:100)	95.4	52.0	77.7	79.9
One extraction[c]	(5:100)	97.8	70.7	84.0	89.3
One extraction[d]	(5:500)	99.6	93.0	96.4	98.5

[a] Volumes in μl.

[b] Derivatized samples were extracted ("first extraction") and the phases separated; then the methanol–water phase was re-extracted ("second extraction") with additional carbon tetrachloride.

[c,d] Equivalent samples were extracted once with different volumes of solvents.

extraction demonstrated that derivatives were recovered consistently between extraction in all samples and that loss into the carbon tetrachloride phase was not from breakdown products of the sugars. Recovery of PMAA derivatives of cell walls was quite high with each extraction. However, with a 10:100 solvent ratio there was a greater loss of both fully acetylated sugars and PMAA derivatives of terminal sugars from sucrose. We then found that the ratio of volumes was important to improving recovery. By reducing the volume of the carbon tetrachloride phase and increasing the volume of methanol–water, we showed that all derivatives could be recovered with good efficiency. Of course, rather than increasing the volume of the methanol–water phase, re-extraction of the carbon tetrachloride phase with fresh methanol–water would yield equal results with less volume of methanol–water.

This clean-up procedure is rapid and can be accomplished with minimal selective loss of PMAA derivatives. After clean-up, baseline resolution is achieved throughout the chromatogram and elimination of contaminants should greatly increase column life.

ACKNOWLEDGEMENTS

Thanks to Dr. Tullia M. C. C. Filisetti-Cozzi for a sample of the bean cell wall preparation. Supported by Grant DE-FG02-88ER13903 from the US Department of Energy. Journal paper No. 12 925 of the Purdue University Agriculture Experiment Station.

REFERENCES

1 R. J. Henry, P. J. Harris, A. B. Blakeney and B. A. Stone, *J. Chromatogr.*, 262 (1983) 249.
2 N. C. Carpita and J. Kanabus, *Anal. Biochem.*, 161 (1987) 132.
3 M. C. Jarvis, *Plant Cell Environment*, 7 (1984) 153.
4 G. O. Aspinall, C. T. Greenwood and R. J. Sturgeon, *J. Chem. Soc.*, (1961) 3667.
5 D. M. Gibeaut and N. C. Carpita, *Plant Physiol.*, 97 (1991) 551.
6 N. C. Carpita, F. Keller, D. M. Gibeaut, T. L. Housley and Ph. Matile, *J. Plant Physiol.*, 138 (1991) 204.
7 A. L. Kverheim, *Acta Chem. Scand., Ser B*, 41 (1987) 150.
8 N. C. Carpita and E. M. Shea, in C. J. Bierman and G. A. MacGinnis (Editors), *Analysis of Carbohydrates by GLC and MS*, CRC Press, Boca Raton, FL, 1989, p. 155.
9 E. M. Shea, D. M. Gibeaut and N. C. Carpita, *Planta*, 179 (1989) 293.
10 A. B. Blakeney, P. J. Harris, R. J. Henry and B. A. Stone, *Carbohydr. Res.*, 113 (1983) 291.

Journal of Chromatography, 587 (1991) 288–291
Elsevier Science Publishers B.V., Amsterdam

CHROM. 23 588

Short Communication

Separation of functionalized dextrins by reversed-phase high-performance liquid chromatography

E. Andriamboavonjy*, E. Flaschel and A. Renken

Institute of Chemical Engineering, Swiss Federal Institute of Technology, CH-1015 Lausanne (Switzerland)

(First received April 24th, 1990; revised manuscript received June 18th, 1991)

ABSTRACT

Functionalized linear dextrins were separated on a preparative scale by high-performance liquid chromatography on RP-18 phases with water as the eluent. These dextrins were obtained by the transfer of α-cyclodextrin to glucosides by means of a cyclodextrin-glycosyltransferase of *Klebsiella pneumoniae* M5 aI. Product recovery was readily achieved owing to the simple eluent used.

INTRODUCTION

Functionalized dextrins can be produced by enzymatic transfer of cyclodextrins (CD_n containing n units of glucose) to an acceptor. The reaction is catalyzed by cyclodextrin-glycosyltransferase (CGT) and may be schematically described as:

$$CD_n + A \rightleftharpoons A\text{-}G_n \quad (1)$$

$$A\text{-}G_n + A \rightleftharpoons A\text{-}G_i + A\text{-}G_{(n-i)} \quad (2)$$

where $A\text{-}G_i$ are coupling products which consist of an acceptor molecule (A) and i, n units of glucose (G).

The CGT from *Klebsiella pnemoniae* catalyzed only the transfer of CD_6 (α-CD) to an acceptor molecule which contains D-glucose with the reducing C-1 position blocked and the C-4 position underivatized [1]. The transfer products may be used for different applications. The series of substituted malto-oligosaccharides (for example *p*-nitrophenyl α-malto-oligosaccharides) is used for determining glucosidases and amylases [2–4]. Erlose, a transglycosylation product from the transfer of CD_6 to sucrose, is a low-cariogenic sweetener [5]. Glycosylmoranoline derivatives are used as antidiabetes drugs [6].

The separation and analysis of dextrins from enzymatic or chemical digests according to their degree of polymerization (DP) is important in the food industry. Liquid chromatography using water or aqueous solutions as the eluent is usually applied. Different approaches may be distinguished: low-pressure gel-permeation chromatography using a polyacrylamide gel [7] or a cross-linked dextran gel [8] as the stationary phase; low- [9] and high-pressure liquid chromatography [10] on cation- [9–12] or anion- [13,14] exchange resins; high-performance liquid chromatography (HPLC) using aminopropyl-bonded silica as the stationary phase [12,15,16]. Preparative separation of malto-oligosaccharides has been described for HPLC using C_{18}-bonded and aminopropyl silica gel [12]. Recently, reversed-phase columns in HPLC have been used to separate normal and branched cyclodextrins [17].

Reversed-phase chromatography with pure water

0021-9673/91/$03.50

as the eluent combines two advantages: the use of an eluent that is both non-toxic and cheap.

The aim of this study was to test reversed-phase HPLC with respect to its suitability for the preparative separation of functionalized dextrins.

EXPERIMENTAL

Apparatus

The HPLC system consisted of a Hewlett-Packard Model 1084A pump (Palo Alto, CA, USA)

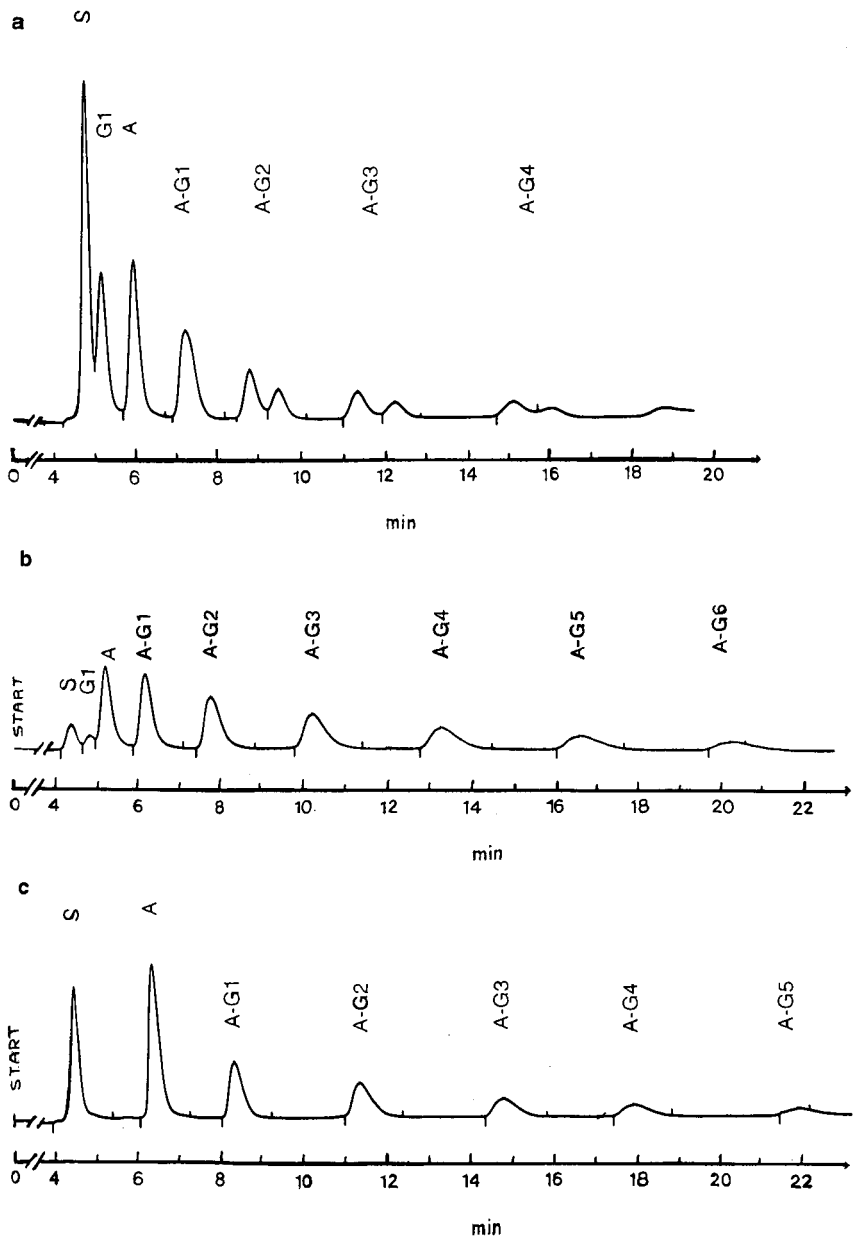

Fig. 1. Separation of functionalized dextrins from transfer reactions of α-CD on various acceptors (A). Detector attenuation, 32; sample size, 500 μl. S, salt; $[\alpha\text{-CD}]_0$, initial concentration of α-CD; $[A]_0$, initial concentration of acceptor. (a) A = maltose ($[\alpha\text{-CD}]_0$ = 9.05 m*M*; $[A]_0$ = 20.03 m*M*). (b) A = maltitol ($[\alpha\text{-CD}]_0$ = 8.93 m*M*; $[A]_0$ = 18.52 m*M*). (c) A = saccharose ($[\alpha\text{-CD}]_0$ = 8.74 m*M*; $[A]_0$ = 25.14 m*M*).

with an integrator, a Model ASI 45 automatic sampler (Kontron, Zürich, Switzerland), a Rheodyne Model 7000 sample injection valve (Berkeley, CA, USA) with a 500-μl loop and an Erma Optical Works Model 7510 refractive index detector (Tokyo, Japan). A commercial column from Macherey Nagel (Oensingen, Switzerland), 250 × 10 mm I.D., was packed with Nucleosil 7 C_{18}: particle diameter, 7 μm; pore diameter, 10 nm. As a precaution, a 2-μm filter from Rheodyne was placed between the sampler and the column.

Materials

The transfer reactions catalyzed by CGT from *K. pneumoniae* M5 aI (EC 2.4.1.19) were performed in a strirred glass vessel equipped with a thermostat and a magnetic stirrer. Before the addition of enzyme (0.49 kU/l) (determined by a cyclization test) [18], a volume of 100 ml of an aqueous solution containing α-CD (kindly provided by Consortium für Elektrochemische Industrie, Munich, Germany) and an acceptor was equilibrated at 40°C and adjusted to pH 7. After incubation for 25 min, the reaction was stopped by decreasing the pH from 7 to 3 by addition of 0.1 *M* hydrochloric acid.

The acceptors used were maltose from Carl Roth (Karlsruhe, Germany), maltitol from Fluka (Buchs, Switzerland) and saccharose from Serva (Heidelberg, Germany).

Standard solutions of maltodextrins were prepared with glucose from Merck (Darmstadt, Germany), maltotriose from Sigma (St. Louis, USA) and maltotetraose, maltopentaose and maltohexaose from Boehringer (Mannheim, Germany).

TABLE I

CONCENTRATION OF DEXTRINS FROM A TRANSFER REACTION OF α-CD ON MALTITOL

($[\alpha\text{-CD}]_0$ = 20.93 m*M*; $[A]_0$ = 54.43 m*M*).

Oligosaccharide	Concentration (m*M*)
A	18.31 ± 1.09
A-G_1	13.94 ± 0.14
A-G_2	9.66 ± 0.13
A-G_3	6.57 ± 0.12
A-G_4	4.44 ± 0.32
A-G_5	2.99 ± 0.12
A-G_6	<1.90

Chromatographic conditions and measurements

Distilled and degassed water was used as the eluent in all the experiments. The separations were carried out at ambient temperature and the detection was at 40°C with a flow-rate of 3 ml/min.

Samples were filtered through 0.2-μm filters from Schleicher & Schuell (Dassel, Germany) prior to analysis. Production of these dextrins by enzymatic transfer of α-CD has been studied by analyzing the reaction mixtures by HPLC on an aminopropyl silica column with 65% (v/v) aqueous acetonitrile solution [1]. Maltitol and saccharose series were separated under the same chromatographic conditions in order to identify the composition of the mixtures before using the RP column.

RESULTS AND DISCUSSION

Fig. 1 shows typical chromatograms illustrating the resolution and separation of functionalized dextrins by HPLC. The retention time increased with the degree of polymerization. The α- and β-anomers of maltosaccharides beyond maltotriose (A-G_1) (Fig. 1a) were resolved at ambient temperature. The retention times for oligosaccharides of the same DP were different. Fig. 1b and c shows remarkable differences in the retention of coupling products from maltitol and saccharose. The time needed to separate dextrins up to DP 7 = A-G_5 was 17 and 22 min for derivatives of maltitol and saccharose, respectively.

Table I shows the composition of a solution obtained from a transfer experiment in the presence of α-CD and maltitol. The carbohydrate content was estimated by the external standard method taking maltitol as the reference substance and using relative peak areas.

Table II shows the resolution (R_s) of adjacent peaks for the same transfer products as in Table I but for different dilutions. In general, a satisfactory resolution was obtained for each pair of saccharides ($R_s > 1$) [19]. The least well resolved was the pair maltitol–A-G_1, but resolution was still acceptable for concentrations up to 6.5 mg of each constituent.

CONCLUSIONS

The present study has shown that RP-18 phases may be advantageously applied for the preparative-

TABLE II

RESOLUTION OF FUNCTIONALIZED DEXTRINS OBTAINED FROM A TRANSFER REACTION (TABLE I)

Dilution factor is calculated as $V_s/(V_s + V_w)$, where V_s is the volume of mixture of saccharides from transfer reaction and V_w is the volume of distilled water.

Dilution factor	R_s				
	A->A-G_1	A-G_1->A-G_2	A-G_2->A-G_3	A-G_3->A-G_4	A-G_4->A-G_5
0.167	1.39	2.15	2.73	2.50	2.23
0.200	1.58	2.14	2.66	2.73	2.11
0.250	1.39	2.07	2.25	2.37	2.08
0.333	1.33	1.82	2.22	2.17	2.79
0.500	1.31	1.79	2.11	1.92	1.58
1.0	0.98	1.40	1.71	1.59	1.40
2.0	0.73	1.22	1.28	1.35	1.18

scale separation of functionalized dextrins. The separation is fast, and the dextrins may be recovered entirely when distilled water is used as the mobile phase. To prevent column overloading, an excess of acceptor should be avoided during the enzymatic reaction. Cyclodextrins adsorb strongly on the RP-18 phase. Therefore it is necessary to eliminate them, preferably prior to the chromatographic separation. This can be done by precipitation with organic solvents. Thus, CD_6 was eliminated to a great extent by trichloroethane precipitation. Long-term experiments (5–6 weeks) with repeated injection have revealed a certain instability of the RP-18 phase used in the presence of water. In consequence, an end-capped stationary phase or a self-adjusting column adaptor would be beneficial.

REFERENCES

1 D. Spiesser, *Ph.D. Thesis No. 695*, EPF Lausanne, 1987.
2 K. Wallenfels, P. Földi, H. Nierman, H. Bender and D. Linder, *Carbohydr. Res.*, 61 (1978) 359.
3 K. Wallenfels, *DE 27 52 501*, 31.5.1978.
4 K. Wallenfels, *DE 30 00 292*, 9.7.1981.
5 K. Takeuchi, S. Sakai and T. Miyaki, (Hayashibara Biochemical Labs.), *Fr 2 572 079*, 15.4.1984.
6 S. Nippon, *DE 36 34 496*, 16.4.1987.
7 G. Trenel, M. John and D. Dellweg, *FEBS Lett.*, 2 (1968) 74.
8 P. Nordin, *Arch. Biochem. Biophys.*, 99 (1962) 101.
9 M. Schmidt, M. John and C. Wandrey, *J. Chromatogr.*, 213 (1981) 151.
10 K. Brunt, *J. Chromatogr.*, 246 (1982) 145.
11 J. Havlicek and O. Samuelson, *Carbohydr. Res.*, 22 (1972) 307.
12 K. B. Hicks and S. M. Sondey, *J. Chromatogr.*, 389 (1987) 145.
13 J. I. Ohms, J. Zec, J. V. Benson and J. A. Patterson, *Anal. Biochem.*, 20 (1967) 51.
14 R. Oshima, N. Takai and J. Kumanotini, *J. Chromatogr.*, 192 (1980) 452.
15 C. A. White, P. H. Corran and J. F. Kennedy, *Carbohydr. Res.*, 87 (1980) 165.
16 N. W. H. Cheetham, P. Sirimanne and W. R. Day, *J. Chromatogr.*, 207 (1981) 439.
17 K. Koizumi, Y. Kubota, T. Utamura, S. Hizukuru and J.-I. Abe, *J. Chromatogr.*, 437 (1988) 47.
18 J.-P. Landert, E. Flaschel and A. Renken, in J. Szejtli (Editor), *Proceedings of the First International Symposium on Cyclodextrins, Budapest, 1981*, Reidel, Dordrecht, 1982, pp. 89–94.
19 J. M. Miller, *Chromatography Concepts and Contrasts*, Wiley-Interscience, New York, 1988, pp. 14–18.

Journal of Chromatography, 587 (1991) 292–296
Elsevier Science Publishers B.V., Amsterdam

CHROM. 23 729

Short Communication

Rapid high-performance liquid chromatographic determination of fatty acid profiles of lipids by conversion to their hydroxamic acids

George Gutnikov* and John R. Streng

Department of Chemistry, California State Polytechnic University, Pomona, CA 91768 (USA)

(First received September 11th, 1990; revised manuscript received August 27th, 1991)

ABSTRACT

A simple and rapid procedure is described for the determination of fatty acid profiles of lipids by reversed-phase high-performance liquid chromatography with UV detection. Rapid derivatization of esterified fatty acids to their hydroxamic acids was achieved in a single step at room temperature in *ca.* 1 min by conducting the reaction in solvents of low acidity. The long-chain hydroxamic acids (C_8 to C_{24}) were separated on a commercial C_{18} column with a low Fe(III) content, which minimized peak distortion due to strong complexation. The detection limit (2 × baseline noise) was 150 pmol at 213 nm. This method was applied successfully to the analysis of various lipid samples.

INTRODUCTION

The characterization of lipid samples by their fatty acid (FA) profile has acquired considerable significance in a variety of fields. Although gas chromatography (GC) has been used predominantly for such determinations, there has been increasing interest in applying high-performance liquid chromatography (HPLC) for this purpose. In recent years, numerous HPLC methods have been reported utilizing precolumn derivatization for UV detection. A variety of UV-chromophore-containing derivatives have been prepared including phenacyl and substituted phenacyl esters [1–3], 2-nitrophenylhydrazides [4], naphthaliminoethyl [5] and *p*-nitrobenzyl esters [6]. All of the above methods involve derivatization of the *free* fatty acids, and thus require a prior saponification step when determining *esterified* fatty acids.

The ready convertibility of fatty acid esters to their hydroxamic acids (HAs), which absorb strongly in the low-wavelength UV region [7,8] (ε 1000 l mol^{-1} cm^{-1} at 213 nm, 2450 l mol^{-1} cm^{-1} at 206 nm), together with the ability to accelerate this reaction by base catalysis [9], prompted us to investigate this approach to FA profiling. Hamilton *et al.* [10] had reported a rather complex reaction scheme involving on-column conversion of fatty acids to hydroxamic acids, followed by chromatography of their ferric chelates. However, these peaks exhibited considerable tailing. The hydroxamic acids themselves were not monitored because they yielded even more distorted peak shapes, which were ascribed to iron impurities in the column packing. During this investigation, these problems were overcome, allowing the succesful chromatography of the FA hydroxamic acids.

The method described herein is rapid, uses only

0021-9673/91/$03.50

conventional chromatographic equipment, and for natural lipid samples affords results that are in good agreement with those obtained by an established GC method.

EXPERIMENTAL

Reagents and chemicals

Fatty acid methyl esters (FAMEs) and triglycerides were purchased from Sigma (St. Louis, MO, USA). The FAMEs reference mixture was obtained from Nu-Chek Prep (Elysian Park, MN, USA). Methanol and acetonitrile (HPLC grade) and 2-propanol were acquired from Fisher Scientific (Fair Lawn, NJ, USA). Sodium methoxide (25%, w/w) and *tert.*-butyl methyl ether were purchased from Aldrich (Milwaukee, WI, USA). Hydroxylamine hydrochloride was obtained from J. T. Baker (Phillipsburg, NJ, USA). Anhydrous sodium perchlorate was purchased from G. Frederick Smith (Columbus, OH, USA). All were used without further purification.

The hydroxamation reagent, 1.5 *M* hydroxylammonium perchlorate, was prepared by adding 18.6 g of sodium perchlorate to 100 ml of *tert.*-butanol and stirring to comminute and partially dissolve the solid. Finely ground hydroxylamine hydrochloride (10.5 g) was dried for 1 h at 110°C and, after cooling, added, along with one drop of sodium methoxide solution, to the stirring sodium perchlorate suspension. After allowing the mixture to stir at least 4 h at room temperature, the suspension was centrifuged and the reagent solution decanted from the resulting sodium choride solid.

Oleo-, linoleo- and linolenohydroxamic acid were synthesized from the methyl esters following the procedure of Hung [11] with modification. All were recrystallized from hexane at −15°C.

Derivatization procedure

A sample of fat or oil (5–10 mg) was placed in a PTFE-lined screw-capped vial (45 × 10 mm) and dissolved in 1 ml of *tert.*-butyl methyl ether. A 6-μmol amount of methyl nonadecanoate was added as internal standard. A 150-μl volume of the hydroxamation reagent was pipetted in, followed by 150 μl of 25% sodium methoxide solution, and the mixture was shaken for a few seconds to ensure mixing. After 1 min, 2 ml of quench solution (5%, v/v, glacial acetic acid in methanol) was added and a 10-μl aliquot of this mixture was injected directly into the liquid chromatograph for analysis.

HPLC analysis

Analyses were carried out using a Model 1090 liquid chromatograph (Hewlett-Packard, Palo Alto, CA, USA) equipped with a filter-photometric detector. Separations were performed on a reversed-phase column (250 × 4.6 mm I.D.) obtained from Alltech Assoc. (Deerfield, IL, USA) packed with Nucleosil C_{18} (Macherey-Nagel, Düren, Germany), 5 μm particle size. Column temperature was maintained at 40°C. The absorbance was monitored at 213 nm, and the detector signals were fed to a Model 3392A (Hewlett-Packard) integrator. Samples were injected via a Model 7125 rotary injector valve (Rheodyne, Cotati, CA, USA) fitted with a 10-μl loop.

Analyses were performed by gradient elution, using a methanol–aqueous buffer solvent system at a flow-rate of 1.0 ml/min. The aqueous buffer was prepared as 20 m*M* sodium dihydrogenphosphate adjusted to pH 3 with concentrated phosphoric acid. A 125-μl volume of 1% (w/w) sodium nitrate per liter was added to match the absorbance of methanol at 213 nm. Solvents were degassed continuously by helium sparging.

GC analysis

Analyses were carried out using a Model 5880 gas chromatograph (Hewlett-Packard) equipped with a flame ionization detector. FAME separations were performed on a DB-23 column (J&W Scientific, Folsom, CA, USA). Lipid samples were derivatized to methyl esters by the method of Christie [12] with modification.

RESULTS AND DISCUSSION

Reaction conditions

The conversion of esters to their hydroxamic acids is commonly conducted in hydroxylic solvents such as methanol in the presence of a strong base catalyst such as methoxide ion, and usually requires lengthly reaction times [13]. Since methanol is a relatively acidic solvent, less acidic reaction media were studied as a means of in increasing the relative base strength of methoxide and thereby accelerating

the rate of hydroxamation. The order of decreasing acidity, methanol > 2-propanol > *tert.*-butanol > *tert.*-butyl methyl ether, was accompanied by a concomitant increase in reaction rate. Hydroxamation proceeds particularly rapidly in *tert.*-butyl methyl ether, which also serves as an excellent solvent for non-polar lipids. Under the conditions recommended, the derivatization reaction is complete within 1 min, with 84% yield.

Chromatographic conditions

The elution of hydroxamic acids on commercial reversed-phase columns often gives rise to distorted peaks, which have been attributed to chelation with Fe(III) impurities in the silica support [14]. This is supported by the fact that other substances that form strong Fe(III) complexes behave similarly [15]. In our previous work [8], no appreciable peak distortion had been observed in the chromatography of hydroxamic acids on a 10-μm C_{18} reversed phase synthesized from silica that had been thoroughly acid-washed prior to bonding [16]. However, to attain the greater resolution required for complex HA mixtures, a number of commercial 5-μm reversed-phase columns were investigated. Most were found to be unsatisfactory because of peak distortion. Remedial measures for improving peak shape, such as washing the column with EDTA solution or adding it to the eluent [17], as well as by controlling eluent pH and buffer strength, failed to resolve the problem. However, a commercial reversed-phase column (Nucleosil C_{18}) based on a silica with the lowest reported metal content [18] provided satisfactory results with aqueous methanol eluents, and was utilized for the analyses reported herein. Acceptable peak shape was not obtained, however, from aqueous acetonitrile eluents.

Alternatively, a polymeric reversed-phase column (Hamilton PRP-1, 150 × 4.1 mm, 5 μm) afforded excellent peak symmetry for the individual hydroxamic acids in both methanol and acetonitrile eluents. The resolution achieved with this column, however, was marginal, particularly for complex HA mixtures. Nevertheless, if higher resolution can be achieved, polymeric reversed-phase columns offer three distinct advantages over silica-based ones for HA separations: (i) the absence of iron impurities; (ii) lack of residual hydroxyl groups; (iii) the use of acetonitrile eluents which would permit monitoring at lower wavelengths with resultant higher sensitivity (ε 5600 l mol^{-1} cm^{-1} at 195 nm).

For FA profiling, lipid samples and a standard FAME mixture were derivatized and chromatographed under identical conditions. Fig. 1 presents a chromatogram of a standard mixture of C_{10} to C_{24} FA hydroxamic acids eluted with a linear methanol–aqueous buffer gradient (70–95% methanol in 45 min). Gradients with lower initial methanol content were used for samples containing lower carbon number fatty acids.

The retention times of the HA derivatives vary directly with the number of carbon atoms and inversely with the number of double bonds in the FA moiety. In contrast to other reported FA derivatives, the HA chromophoric group adds no carbon atoms to the original FA species and therefore does not diminish the inherent reversed-phase chromatographic selectivity derived from the carbon backbone of the sample FAs. This effect is demonstrated

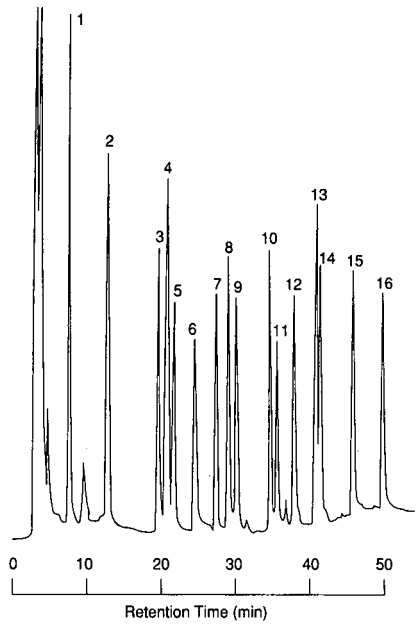

Fig. 1. Chromatogram of the hydroxamic acid derivatives of a FAME mixture separated on a reversed-phase column (Nucleosil) with a methanol–phosphate buffer gradient (70–95% methanol) and UV detection at 213 nm. Peaks: 1 = capric; 2 = lauric; 3 = myristic; 4 = linolenic; 5 = palmitoleic; 6 = linoleic; 7 = palmitic; 8 = oleic (*cis*-18:1); 9 = elaidic (*trans*-18:1); 10 = stearic; 11 = eicosenoic; 12 = nonadecanoic (internal standard); 13 = arachidic; 14 = erucic; 15 = behenic; 16 = lignoceric. Each peak corresponds to 10–30 nmol fatty acid.

TABLE I

ANALYSIS OF NU-CHEK FAME REFERENCE MIXTURE 17A

FAME	Content (%, w/w)		
	Actual	GC	HPLC
Myristic (14:0)	1.0	0.9	0.8
Palmitic (16:0)	4.0	3.7	4.2
Stearic (18:0)	3.0	2.9	2.8
Arachidic (20:0)	3.0	2.8	2.8
Behenic (22:0)	3.0	2.8	2.8
Lignoceric (24:0)	3.0	2.4	2.8
Oleic (18:1)	45.0	46.5	46.0
Linoleic (18:2)	15.0	15.0	15.2
Linolenic (18:3)	3.0	2.9	3.8
Erucic (22:1)	20.0	19.8	18.8

by the excellent resolution of the *cis–trans* isomers of $C_{18:1}$ in Fig. 1.

Quantitative analysis

Quantitative data for references and samples were calculated from individual UV response factors and/or calibration curves obtained from the derivatization of increasing amounts of a mixed FAME standard solution. Differences in individual molar absorptivities of the unsaturated species are thus easily compensated for in this simple calibration process.

The minimum detectable quantity of an individual fatty acid was determined by injecting serial dilutions of a myristic acid methyl ester derivative solution until the quantity corresponding to a peak height of 2× baseline noise was calculated (150 pmol).

In order to verify accuracy, a FAME reference mixture (Nu-Chek 17A) was analyzed by an established GC procedure [12] and this HPLC method. The results (Table I) demonstrate good agreement between the two methods.

Analysis of natural lipid samples

Lipid samples from a variety of plant and animal sources were derivatized and quantified by HPLC and GC. They included fats and oils containing a wide range of saturated and unsaturated fatty acids (C_8–C_{24}). Table II lists the FA profiles as weight percentages of four lipid samples.

In conclusion, direct derivatization of the esterified fatty acids in lipids can be used to rapidly determine FA profiles, eliminating the need for lengthly sample preparation steps. It has now been demonstrated that reversed-phase chromatography with sensitive UV detection can be successfully applied to the separation of FA hydroxamic acids.

TABLE II

DETERMINATION OF FA PROFILES OF LIPID SAMPLES BY GC AND HPLC

Fatty acid	Content (%, w/w)							
	Corn oil		Peanut oil		Coconut oil		Butter fat	
	GC	LC	GC	LC	GC	LC	GC	LC
8:0					8.0	8.4	1.4	1.0
10.0					6.0	5.9	3.0	3.5
12:0					44.9	45.2	3.5	4.3
14:0					17.9	18.4	12.6	13.7
16:0	11.1	12.4	9.8	10.6	10.0	9.4	32.6	37.0
18:0	2.0	1.7	2.6	2.2	3.3	2.5	14.0	13.3
20:0	0.5	0.8	1.3	1.5				
22:0			3.4	3.1				
24:0			1.7	1.5				
16:1							1.5	tr
18:1	25.5	27.1	48.1	48.8	7.4	7.2	30.0	25.5
18:2	60.0	56.8	31.3	30.8	2.5	2.9	2.1	0.8
18:3	0.9	1.3					1.2	0.9
20:1			1.5	1.5				

ACKNOWLEDGEMENTS

We wish to express our appreciation to Professor H. Engelhardt (University of the Saarland, Saarbrücken, Germany) for helpful discussion and to Mr. Mark T. Bunker (Hamilton Co., Reno, NV, USA) for the loan of the polymeric columns.

REFERENCES

1 J. Halgunset, E. W. Lund and A. Sunde, *J. Chromatogr.*, 237 (1982) 496.
2 R. Wood and T. Lee, *J. Chromatogr.*, 254 (1983) 237.
3 E. Vioque, M. P. Maza and F. Millan, *J. Chromatogr.*, 331 (1985) 187.
4 H. Miwa and M. Yamamoto, *J. Chromatogr.*, 351 (1986) 275.
5 Y. Yasaka, M. Tanaka, T. Shono, T. Tetsumi and J. Katakawa, *J. Chromatogr.*, 508 (1990) 133.
6 F. Funazo, M. Tanaka, Y. Yasaka, H. Takigawa and T. Shono, *J. Chromatogr.* 481 (1989) 211.
7 R. Karlicek and V. Jokl, *Chem. Zvesti*, 34 (1980) 762.
8 G. Gutnikov and L.-B. Hung, *Chromatographia*, 19 (1984) 260.
9 G. Gutnikov and G. Schenk, *Anal. Chem.*, 34 (1962) 1316.
10 R. J. Hamilton, S. F. Mitchell and P. A. Sewell, *J. Chromatogr.*, 395 (1987) 33.
11 L.-B. Hung, *M. S. Thesis*, California State Polytechnic University, Pomona, CA, 1983.
12 W. W. Christie, *Gas Chromatography and Lipids*, Oily, Ayr, 1989.
13 H. Henecka and P. Kurtz, in E. Müller (Editor), *Houben-Weyl, Methoden der Organishen Chemie*, Vol. 8, Thieme, Stuttgart, 4th ed. 1952, p. 684.
14 J. D. Glennon, M. R. Woulfe, A. T. Senior and N. NiChoileain, *Anal. Chem.*, 61 (1989) 1474.
15 P. C. Sadek, C. J. Koester and L. D. Bowers, *J. Chromatogr. Sci.*, 25 (1987) 489.
16 H. Engelhardt, University of the Saarland, Saarbrücken, personal communication, 1988.
17 M. Verzele and M. De Potter, *J. Chromatogr.*, 166 (1978) 320.
18 M. Verzele, M. De Potter and J. Ghysels, *J. High Resolut. Chromatogr. Chromatogr. Commun.*, 3 (1978) 151.

Journal of Chromatography, 587 (1991) 297–299
Elsevier Science Publishers B.V., Amsterdam

CHROM. 23 742

Short Communication

Improved high-performance liquid chromatographic separation for the analysis of oxalate in fungal culture media

M. V. Dutton, R. A. Rastall and C. S. Evans*

School of Biological and Health Sciences, The Polytechnic of Central London, 115 New Cavendish Street, London W1M 8JS (UK)

(First received June 11th, 1991; revised manuscript received September 12th, 1991)

ABSTRACT

A rapid method to determine oxalate concentrations in liquid culture media of wood-rotting fungi has been developed using reversed-phase high-performance liquid chromatography. Separation was achieved on a Shandon Hypercarb column using 0.2 *M* orthophosphoric acid as the mobile phase, oxalate was detected at 210 nm. Oxalate was well resolved from other components in the culture medium, this enabled an accurate quantification of oxalate concentration in the range of 0.005–2 m*M*.

INTRODUCTION

The quantitative measurement of oxalate is required in many areas of biological research, such as medicine (urine and plasma analysis), the food and brewing industry and agriculture.

Many methods have been described for the detection of oxalate, the majority of which are based on enzyme assays, involving either oxalate oxidase [1] or oxalate decarboxylase [2]. These are highly specific reactions, but susceptible to interference in crude samples, therefore initial extraction and purification of oxalate is frequently required.

Gas–liquid chromatographic procedures have also been employed which require complex extraction and derivatisation of oxalate prior to analysis [3–6].

Of the numerous high-performance liquid chromatographic (HPLC) methods available, few are suitable for rapid analysis of a large number of biological samples. Many are time consuming, requiring pre-column removal of interfering substances, [7–9], in some cases with oxalate eluting close to the void peak preceding monocarboxylic acids such as formate and acetate. Many methods have detection problems due to sensitivity or selectivity, requiring derivatisation of oxalate prior to detection, such as precolumn derivatisation with *o*-phenylenediamine [10], or postcolumn derivatisation based on complexing with Fe^{3+} ions [11].

This paper describes a rapid, simple method to determine levels of oxalate in cultures of wood-rotting fungi by HPLC using a porous graphitic carbon column.

EXPERIMENTAL

Reagents

All reagents were prepared using HPLC-grade water supplied by Rathburn (Walkerburn, UK), HiPerSolv-grade orthophosphoric acid and Ana-

0021-9673/91/$03.50

laR-grade oxalic acid were purchased from BDH (Poole, UK).

Standards of oxalate were prepared in the range 0.005–2 m*M*.

Apparatus and procedure

A 20-μl aliquot of either sample or standard was injected onto a 10 cm × 4.6 mm I.D. graphitised carbon Hypercarb column (Shandon Scientific, Runcorn, UK), using a Merck–Hitachi LiChro-Graph HPLC System. Separation was achieved using 0.2 *M* orthophosphoric acid as the mobile phase.

The flow-rate of the mobile phase was maintained at 1 ml min^{-1} and separated compounds were detected at 210 nm.

Culture media preparation

Stationary cultures of the basidiomycete fungus, *Coniophora marmorata* 410 (Building Research Establishment, Department of the Environment) were grown in a defined liquid culture medium [12], using 10 g glucose as carbon source, for 35 days at 25°C.

Growth medium was collected and filtered to remove biomass. Aliquots (2 ml) were boiled for 5 min and subsequently centrifuged at 16 000 *g* for 10 min to remove denatured proteins from the media. The supernatant was filtered through a 0.45-μm membrane filter (Whatman, Maidstone, UK) prior to injection onto the column.

RESULTS AND DISCUSSION

Under the conditions described it was possible to determine oxalate levels in the culture medium. With 0.2 *M* orthophosphoric acid as eluent good resolution of oxalate from other components in the culture medium was achieved. At lower eluent concentrations (0.05 *M*) oxalate eluted as two peaks, which may be attributable to the differing pK_a values of the two carboxylic acid groups.

Linear regression analysis

Regression analysis was carried out on peak area against analyte concentration for oxalate. The correlation coefficient was 0.998 over the concentration range 0.005–2 m*M*. The detection limit was 0.1 nmoles on column in standard aqueous solutions and 1 nmole in culture medium.

Reproducibility

The variations in peak area were measured for an

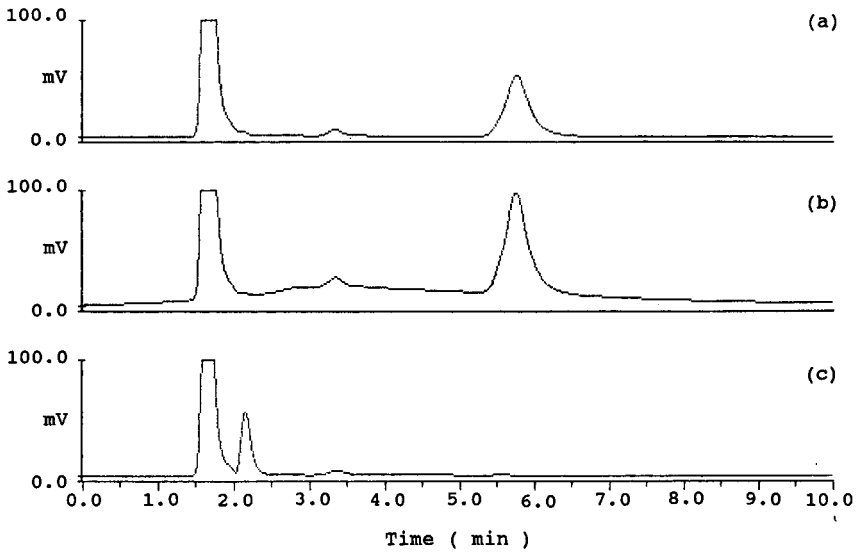

Fig. 1. Chromatogram of separation of oxalate in culture media: (a) after growth of *C. marmorata*, for 35 days at 25°C in a glucose–salts medium [12]; (b) spiked with 0.5 mmol of authentic oxalate; (c) degraded by the addition of 0.1 mg of oxalate decarboxylase in 0.2 ml of 0.2 *M* acetate buffer, pH 3.7, incubated at 37°C for 1 h. The peak at retention time 2.2 min corresponds to acetate from the acetate-buffered enzyme solution.

oxalate standard, and the cooefficient of variation between triplicate injections was found to be low (0.26%–1.28%), and between 10 different batches of eluent and oxalate standard was 4.84%. Standard oxalate solutions should be prepared fresh or kept at 4°C for a maximum of seven days to maintain the low coefficient of variation. Degradation of oxalate in solution has been reported [13].

Culture media analysis

The presence of oxalate in fungal culture media was identified by retention time and confirmed by spiking experiments with authentic oxalate and subsequent degradation with oxalate decarboxylase. Fig. 1 shows a representative chromatogram of the separation of oxalate in culture media after growth of *C. marmorata*, spiked with 0.5 mmol of oxalate, and its subsequent degradation by the addition of 0.1 mg of oxalate decarboxylase incubated at 37°C for 1 h. Some variation in retention time was apparent possibly as a result of other analytes present in the medium.

CONCLUSIONS

Oxalate has been satisfactorily resolved in fungal culture media without the need for isolation of oxalate and subsequent derivatisation, using reversed-phase HPLC on a Hypercarb column. Analysis was rapid and simple to perform thus facilitating analysis of a large number of samples.

As concentrated acids can be used as eluents on Hypercarb columns, separation is effected which would not be possible on acid-soluble silica columns. This method may therefore be useful for the determination of oxalate in other biological matrices.

ACKNOWLEDGEMENTS

This work was supported by AFRC (UK) Research grant PG44/525, and Shandon Scientific Ltd. who supplied the Hypercarb column.

REFERENCES

1 M. F. Laker, A. F. Hofmann and B. J. D. Meeuse, *Clin. Chem.*, 26 (1980) 827.
2 W. B. Jakoby, *Methods Enzymol.*, 5 (1962) 637.
3 S. L. Mackenzie, D. Tenaschuk and G. Fortier, *J. Chromatogr.*, 367 (1986) 181.
4 H. Ohkawa, *J. Assoc. Off. Anal. Chem.*, 68 (1985) 108.
5 A.D. Corcia, R. Samperi, G. Vinci and G. D'Ascenzo, *Clin. Chem.*, 28 (1982) 1457.
6 B. Fabig, K. Vielhauer, A. M. Moawad and W. Achtnich, *Z. Pflanzenernaehr. Bodenkd.*, 152 (1989) 261.
7 L. Larsson, B. Libert and M. Asperud, *Clin. Chem.*, 28 (1982) 2272.
8 K. Kataoka, M. Takada,Y. Kato, M. Iguchi, K. Kohri and T. Kurita, *Urol. Res.*, 18 (1990) 25.
9 G. Gu and C. K. Lim, *J. Chromatogr.*, 515 (1990) 183.
10 F. A. Martz, M. F. Weiss and R. L. Belyea, *J. Dairy Sci.*, 73 (1990) 474.
11 A. Millan, J. M. Grases and F. Grases, *J. Chromatogr.*, 529 (1990) 402.
12 G. Fahraeus and B. Reinhammer, *Acta Chem. Scand.*, 21 (1967) 2367.
13 F. Heinz and G. Kohlbecker, in H. U. Bergmeyer (Editor), *Methods of Enzymatic Analysis*, Vol. VI, 3rd ed., VCH, New York, 1984, p. 649.

Journal of Chromatography, 587 (1991) 300–305
Elsevier Science Publishers B.V., Amsterdam

CHROM. 23 702

Short Communication

Separation of taxol from related taxanes in *Taxus brevifolia* extracts by isocratic elution reversed-phase microcolumn high-performance liquid chromatography

S. D. Harvey* and J. A. Campbell

Pacific Northwest Laboratory, Battelle Boulevard, P.O. Box 999, Richland, WA 99352 (USA)*

R. G. Kelsey and N. C. Vance

US Department of Agriculture, Pacific Northwest Research Station, 3200 Jefferson Way, Corvallis, OR 97331 (USA)

(First received April 4th, 1991; revised manuscript received August 20th, 1991)

ABSTRACT

Previous attempts to resolve the closely related taxanes cephalomannine and taxol by reversed-phase high-performance liquid chromatography (HPLC) on octadecyl silica columns have not been successful. In the present study, high-resolution HPLC on microcolumns packed with octadecyl silica was evaluated for the separation of the aforementioned taxanes. Due to the enhanced separation efficiency of this technique, baseline resolution between cephalomannine and taxol was readily achieved under isocratic elution conditions. Chromatographic profiles of *Taxus brevifolia* twig and needle foliage extracts are presented that illustrate this separation.

INTRODUCTION

Taxol is a taxane diterpene amide produced by the Pacific yew (*Taxus brevifolia*) [1]. This natural product shows promise for the treatment of a variety of human cancers, including leukemia and certain ovarian, breast and lung tumors [1–3]. The mode of action of taxol stems from the unique propensity of this compound to promote microtubule formation and inhibit post-mitotic spindle disassembly [4]. Phase II clinical tests of taxol, which are currently in progress, will require kilogram quantities of pure compound [5]. Presently, taxol is available only from limited natural sources. Efforts to synthesize taxol have not been fruitful, primarily because of difficulties encountered in forming the taxane skeleton [6]. For this reason there has been a great deal of interest in isolating other taxanes from *T. brevifolia* for use as intermediates in the synthesis of taxol. Taxol is isolated from the bark of *T. brevifoolia* by extraction, solvent partitioning and preparative-scale chromatography [7]. Taxol constitutes less than 0.01% of the bark on a dry weight basis [5]. The processing of bark from 2000 to 3000 trees is required to produce approximately 1 kg of taxol [3]. The sheer magnitude of required plant material has prompted ecological concerns about the poten-

* Operated for the US Department of Energy by Battelle Memorial Institute under Contract DE-AC06-76RLO 1830.

tial impact of massive harvesting on Pacific yew populations. The limited geographical distribution, the slow maturation, and specific niche requirements of this species all contribute to these concerns. Bark stripping holds no advantage over lumbering, as the bark-stripped trees eventually perish. Isolation of taxol from portions of the tree that are capable of regrowth (such as the needle foliage) would be particularly attractive, since harvesting would not decimate the stock. It seems likely that future research will focus on genetic methods aimed at maximizing taxol yield as well as detailed analytical studies focusing on taxol distribution within the plant.

Analysis of taxol in crude bark extracts of *T. brevifolia* presents a challenge for the separation scientist because a bewildering array of indigenous components is present. Analysis of needle foliage extracts becomes even more difficult due to the presence of large amounts of photosynthetic pigments and cuticular waxes. Taxol is one of a series of compounds contained in *T. brevifolia* extracts that share the taxane ring system. One of these taxanes, cephalomannine, is present in significant quantities and is difficult to separate from taxol [5]. The structures of taxol and cephalomannine are shown in Fig. 1. Past work by Witherup and co-workers investigated the utility of high-performance liquid chromatography (HPLC) for the analysis of taxol in bark [5] and needle foliage extracts [8]. Chromatography on 25 cm × 4.6 mm I.D. columns packed with 8-μm particles of octadecyl-, cyanopropyl- or phenyl-bonded silica was studied under either isocratic or gradient reversed-phase elution conditions. These authors found that the added selectivity of the phenyl or cyanopropyl silica was necessary to provide baseline resolution between taxol and cephalomannine. Baseline resolution between these two compounds was not achieved on the octadecyl silica stationary phase [5].

Although cyanopropyl- and phenyl-bonded silica columns provide the requisite resolution between taxol and cephalomannine, there are several shortcomings associated with the separation of crude extracts on these columns. Many extract components elute after taxol when separated on phenyl or cyanopropyl silica columns. As a consequence, extended gradient runs are required to ensure elution of strongly retained components. Additionally, elution of taxol and cephalomannine occur on a background that is significantly above the initial baseline. This baseline offset is most likely caused by elution of numerous unresolved matrix components. Further development of separations on octadecyl silica has not been pursued due to the initial failure of conventional columns to provide resolution between cephalomannine and taxol. However, provided that the column efficiency is sufficient to allow resolution between taxol and cephalomannine, separations on octadecyl silica may prove advantageous over separations performed on cyanopropyl- or phenyl-bonded silica.

The present study evaluates high-resolution microcolumn HPLC on octadecyl silica, as described by Novotny [9,10], Yang [11], and others [12–14], for the separation of taxol in crude *T. brevifolia* extracts. This technique utilizes fused silica tubing (1 m × 250 μm I.D.) that is slurry packed with 5-μm particles to provide columns that approach separation efficiencies of 100 000 theoretical plates [15]. High-resolution microcolumn HPLC has been applied to a variety of complex environmental [16,17] and biological [11,18] samples allowing for separations that cannot be achieved within the resolution constraints imposed by columns of conventional (25 cm × 4.6 mm I.D.) dimensions. In addition to

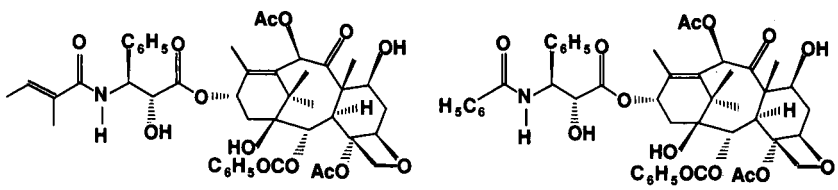

Fig. 1. Structures of cephalomannine and taxol. Ac = Acetyl.

the enhanced resolution, microcolumn separations offer a number of inherent advantages including minute sample volume requirements, enhanced mass flow detection sensitivity, and the feasibility of utilizing expensive "exotic" mobile phases [9]. Importantly, the low flow-rates characteristic of microcolumn HPLC greatly simplify introduction of the column eluate to mass spectrometric analyzers [19,20].

The objective of the present study was to evaluate high-resolution microcolumn HPLC as applied to the analysis of taxol in crude twig and needle foliage extracts of *T. brevifolia*. With over five times the available separation efficiency, as compared to columns of conventional dimensions packed with 8-μm particles, it becomes possible to resolve taxol and cephalomannine on octadecyl silica under isocratic elution conditions.

EXPERIMENTAL

Cephalomannine and taxol standards

Standards of taxol were donated by Dr. D. Ellis of the Department of Horticulture, University of Wisconsin, USA, and the National Cancer Institute (NCI), Bethesda, MD, USA. Cephalomannine was donated by NCI.

Tissue collection and extraction

T. brevifolia selected for analysis were located on the Oregon State University, McDonald Experimental Forest, near Covallis. In October 1990, branches from five trees were harvested and returned immediately to laboratory where twigs from 1989 and 1990 and their needles were separated for each tree. Tissues were placed in an oven maintained at 50°C to dry overnight. Dry tissues were ground with a Wiley mill to pass a 20-mesh screen and stored for less than a week at room temperature until extracted.

Extraction of tissue samples was in accordance with the procedure set forth by Witherup *et al.* [5]. Before weighing, each sample was redried for 1 h at 50°C and cooled to room temperature. Approximately 2 g were accurately weighed into a flask, covered with 20 ml of methanol, and placed on a shaker at room temperature for 1 h. The supernatant was decanted and centrifuged to remove large particulates. A 10-ml aliquot of the methanol extract was evaporated to dryness at 40°C under vacuum. The residue was next partitioned between methylene chloride and water (10 ml each). A measured aliquot of the methylene chloride layer was then dried under vacuum. Samples were reconstituted with methanol and filtered through a 0.45-μm nylon 66 filter (Alltech, Deerfield, IL, USA) immediately before analysis.

Microcolumn instrumentation and modifications

The microcolumn HPLC system consisted of an Isco μLC-500 syringe pump (Lincoln, NE, USA) and Schoeffel Model 770 detector (Westwood, NJ, USA) that was modified to meet the technique's stringent low-dead-volume requirements. The modified flow cell was centered within a screw-mounted aluminum block that contained a 345-μm machined slit. This block housed a length of 250 μm I.D. fused silica (345 μm O.D.) that had a 1.0-cm section of polyimide coating removed to serve as a low-dead-volume quartz cell. A section of 50 μm I.D. (189 μm O.D.) fused silica was inserted into the 250-μm tube up to the point of the quartz window. This insert was secured to the 250-μm tube with epoxy and further minimized the detector dead volume.

Column preparation and evaluation

Fused-silica tubing of 344 μm O.D. × 250 μm I.D. and 189 μm O.D. × 50 μm I.D. was obtained from Polymicro Technologies (Phoenix, AZ, USA). Columns (1 m × 250 μm I.D.) were slurry packed with Spherisorb 5-μm ODS-2 (Phase Separations, Norwalk, CT, USA) and evaluated according to the methods described by Borra *et al.* [15]. The column bed was held in place by a porous PTFE frit, which in turn was held stationary by a length of 50-μm fused silica inserted into the 250-μm column and cemented with epoxy to prevent leaking [21]. The column was joined to the detector cell by butting the ends of the 50-μm fused-silica tubes together within a snug-fitting PTFE sheath [22].

Chromatographic conditions

All injections were accomplished by the stopped-flow technique [13]. Capillary injection volumes were kept below 200 nl. Mobile phases, prepared from Burdick & Jackson (Muskegon, MI, USA) HPLC-grade solvents, were filtered through

0.45-μm nylon 66 filters and degassed with helium flow prior to use. Columns were evaluated with a mobile phase consisting of acetonitrile–water (60:40). During evaluation, the mobile phase was delivered at a constant flow-rate of 1.5 μl/min and components detected by UV absorption at 254 nm. For analysis of *T. brevifolia* extracts, the mobile phase composition was methanol–water–acetonitrile (30:30:40) delivered at a constant pressure of 3500 p.s.i. This corresponded to a flow-rate of approximately 2.5 μl/min. The separated *T. brevifolia* components were detected by absorption at 225 nm.

RESULTS AND DISCUSSION

Column evaluation was conducted with a standard mixture containing acidic, basic, and neutral compounds as described previously [15]. The chromatogram of the test mixture is presented in Fig. 2. A theoretical plate calculation performed on the phenanthrene peak indicated a separation efficiency of 85 000 plates. This separation efficiency falls within the range of 70 000 to 90 000 theoretical plates that is typically realized for 1-m columns packed with 5-μm particles. This efficiency was judged adequate for the ensuing taxol separations. Separations performed on the microcolumn system described above offered at least 5.44 times the separation efficiency compared to the columns containing 8-μm material that were utilized by Witherup *et al.* [5].

A variety of chromatographic conditions were evaluated for the separation of cephalomannine and taxol standards. The objective was to obtain baseline resolution between these taxanes under isocratic elution conditions within a reasonable analysis time. Injections of pure standards with a methanol–water–acetonitrile (30:30:40) mobile phase, delivered at 3500 p.s.i., revealed that cephalomannine eluted with a retention time of 57.5 min, whereas taxol eluted at 61.2 min. The chromatogram shown in Fig. 3 illustrates a separation of a mixture containing cephalomannine and taxol standards. These taxanes were separated by 3.7 min under the chromatographic conditions employed. The ability of microcolumn HPLC to provide baseline resolution between these compounds is a direct consequence of the higher resolution available from the technique. Previous studies have shown that the related taxanes 10-deacetylcephalomannine, baccatin III, and 10-deacetylbaccatin III are readily resolved and elute well before cephalomannine on columns packed with octadecyl silica [5].

Analysis of *T. brevifolia* extracts proceeded under the chromatographic conditions described above. A representative chromatogram of twig extract is presented in the top of Fig. 4. The peaks labeled 1 and 2 correspond to the retention times of cephalomannine and taxol, respectively. The identity of these peaks was further established by co-elution of the respective taxane standards with these peaks. The bottom of Fig. 4 presents a chromatogram resulting

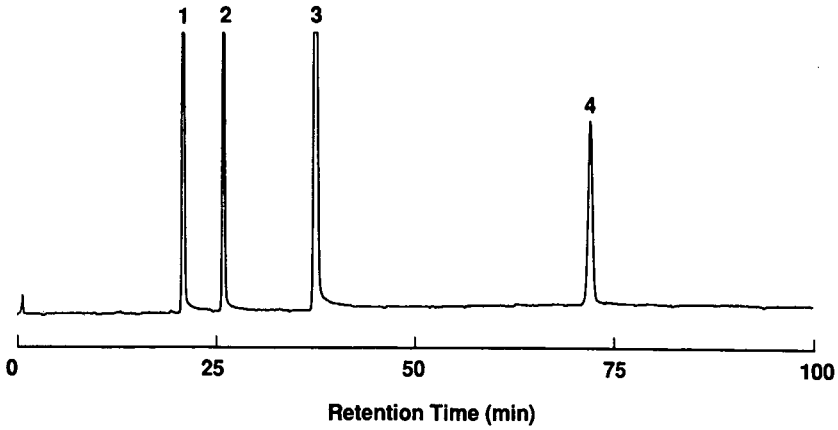

Fig. 2. Chromatogram of column evaluation test mixture. Peaks: 1 = *m*-cresol; 2 = nitrobenzene; 3 = diphenylamine; 4 = phenanthrene.

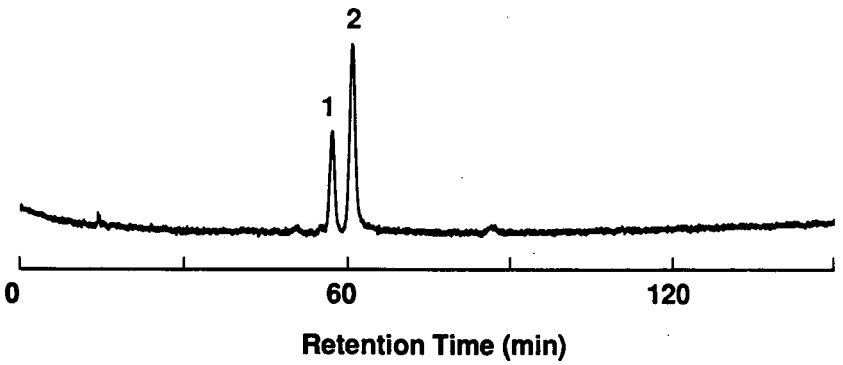

Fig. 3. Separation of cephalomannine (1) and taxol (2) standards.

from an injection of needle foliage extract. The identity of cephalomannine and taxol in this extract was also verified by co-injection experiments. The higher complexity of the needle foliage extract is clearly evident by comparison of the two chromatograms in Fig. 4. Cephalomannine and taxol are baseline resolved in extracts from both twigs and needles and, judging from the symmetrical peaks, appear to elute free of perceptible interferences. It appears that microcolumn HPLC on octadecyl silica has the separation power necessary for quantification of taxol in crude extracts of *T. brevifolia*. Despite this capability, however, it remains desirable to develop an intermediate normal-phase clean-up of crude extracts prior to reversed-phase chromatographic analysis. An intermediate orthogonal separation would be expected to remove considerable matrix interferences.

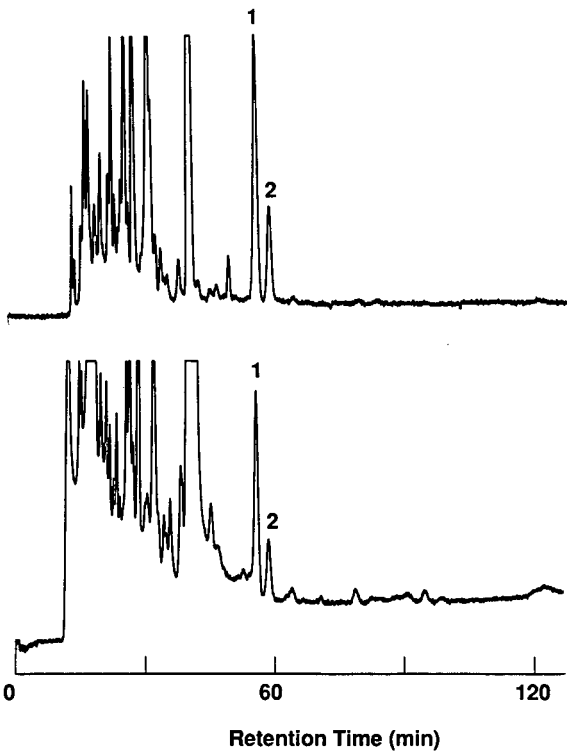

Fig. 4. Chromatographic profiles of *T. brevifolia* twig (top) and needle foliage (bottom) extracts. Peaks 1 and 2 correspond to cephalomannine and taxol, respectively.

The separations obtained in this study offer several unique attributes over those performed on cyanopropyl- and phenyl-bonded silica. Chromatograms in Fig. 4 were allowed to proceed for 2 h to demonstrate that very little material contained in the crude *Taxus* extracts elute after taxol. This elution pattern stands in sharp contrast to separations performed on cyanopropyl- and phenyl-bonded silica columns. High-resolution separations on octadecyl silica result in elution of taxol and cephalomannine within a clean retention window that is considerably removed from the majority of matrix components. Additionally, cephalomannine and taxol elute in a region that has a minimal baseline offset. Microcolumn sample analysis times of slightly over 60 min were approximately equal to previously reported gradient elution methods performed on conventional columns.

Although the objective of the above separations was the separation of taxol and cephalomannine, the same microcolumn techniques would be valuable for analysis of *T. brevifolia* extracts for other

known and hitherto unidentified taxanes. Toward this end, the implementation of high-resolution separations combined with either electrospray ionization [20] or continuous flow fast atom bombardment [19] mass spectrometry would be particularly powerful for structural elucidation. In addition, a variety of mass spectral techniques could be employed to minimize or eliminate matrix interferences during quantification. Our laboratory is presently engaged in this pursuit.

These studies have demonstrated the ability of microcolumn HPLC to provide resolution between closely related natural products that cannot be obtained on columns of conventional dimensions packed with the same octadecyl silica stationary phase. The conclusions of this study do not serve to undermine the sound approach of exploiting optimal selectivity available from different bonded stationary phases, but rather emphasizes that such an approach will always be more effective when used in conjunction with high-resolution chromatographic techniques. Recent advances in microcolumn HPLC separations include descriptions for preparing a variety of bonded-phase columns [23], applications of paired-ion mobile phase modifers [24], and further refinement of gradient elution strategies [25,26]. Progress in these directions ensures that the flexibility responsible for the popularity of conventional HPLC will also be available for high-resolution microcolumn techniques. This emerging technology can be expected to have a significant impact on the isolation and identification of natural products.

REFERENCES

1 M. C. Wani, H. L. Taylor, M. E. Wall, P. Coggon and A. T. McPhail, *J. Am. Chem. Soc.*, 93 (1971) 2325.
2 W. P. McGuire, E. K. Rowinsky, N. B. Rosenshein, F. C. Grumbine, D. S. Ettinger, D. K. Armstrong and R. C. Donehower, *Ann. Intern. Med.*, 111 (1989) 273.
3 E. K. Rowinsky, L.A. Cazenave and R. C. Donehower, *J. Natl. Cancer Inst.*, 82 (1990) 1247.
4 P. B. Shiff, J. Fant and S. B. Horwitz, *Nature (London)*, 277 (1979) 665.
5 K. M. Witherup, S. A. Look, M. W. Stasko, T. G. Mc Cloud, H. J. Issaq and G. M. Muschik, *J. Liq. Chromatogr.*, 12 (1989) 2117.
6 F. Gueritte-Voegelein, D. Guenard and P. Poitier, *J. Nat. Prod.*, 50 (1987) 9.
7 D. G. I. Kingston, D. R. Hawkins and L. Ovington, *J. Nat. Prod.*, 45 (1982) 466.
8 K. M. Witherup, S. A. Look, M. W. Stasko, T. J. Ghiorzi, G. M. Muschik and G. M. Cragg, *J. Nat. Prod.*, 53 (1990) 1249.
9 M. V. Novotny, *Science (Washington, D.C.)*, 246 (1989) 51.
10 M. Novotny, *J. Microcol. Sep.*, 2 (1990) 7.
11 F. J. Yang, *J. Chromatogr.*, 236 (1982) 265.
12 R. P. W. Scott and P. Kucera, *J. Chromatogr.*, 185 (1979) 27.
13 Y. Hirata and M. Novotny, *J. Chromatogr.*, 186 (1979) 521.
14 T. Takeuchi and D. Ishii, *J. Chromatogr.*, 213 (1981) 25.
15 C. Borra, S. M. Han and M. V. Novotny, *J. Chromatogr.*, 385 (1987) 75.
16 M. V. Novotny, A. Hirose and D. Wiesler, *Anal. Chem.*, 56 (1984) 1243.
17 F. Andreolini, C. Borra, D. Wiesler and M. Novotny, *J. Chromatogr.*, 406 (1987) 375.
18 F. Andreolini, S. C. Beale and M. Novotny, *J. High Resolut. Chromatogr. Chromatogr. Commun.*, 11 (1988) 20.
19 J. S. M. de Wit, C. E. Parker, K. B. Tomer and J. W. Jorgenson, *Biomed. Environ. Mass Spectr.*, 17 (1988) 47.
20 R. D. Smith, J. A. Olivares, N. T. Nguyen and H. R. Udseth, *Anal. Chem.*, 60 (1988) 436.
21 D. C. Shelly, J. C. Gluckman and M. V. Novotny, *Anal. Chem.*, 56 (1984) 2990.
22 Y. Hirata, *J. Microcol. Sep.*, 2 (1990) 214.
23 F. Andreolini, C. Borra and M. Novotny, *Anal. Chem.*, 59 (1987) 2428.
24 J. F. Banks, Jr. and M. Novotny, *J. Chromatogr.*, 475 (1989) 13.
25 J. F. Banks, Jr. and M. Novotny, *J. Microcol. Sep.*, 2 (1990) 84.
26 F. Andreolini and A. Trisciani, *J. Chromatogr. Sci.*, 28 (1990) 54.

Journal of Chromatography, 587 (1991) 306–313
Elsevier Science Publishers B.V., Amsterdam

CHROM. 23 714

Short Communication

Applicability of high-performance liquid chromatography–continuous-flow fast atom bombardment mass spectrometry for simultaneous quantitation of multiple neurochemicals

Yasushi Ikarashi and Yuji Maruyama*

Department of Neuropsychopharmacology (Tsumura), Gunma University School of Medicine, 3-39-22 Showa-machi, Maebashi-shi, Gunma 371 (Japan)

(First received February 2nd, 1991; revised manuscript received August 27th, 1991)

ABSTRACT

A method is described for the analysis of multiple neurochemically important compounds. The technique involves high-performance liquid chromatographic separation in combination with ultraviolet and continuous-flow fast atom bombardment mass spectrometric detection. High-performance liquid chromatographic elution behaviour and relative detection responsiveness as correlated with chemical structure are also presented.

INTRODUCTION

The complexity of the interactions which take place between various neurochemical systems during behavioral, pharmacological or psychological investigations requires that a comprehensive analytical strategy be used in order to study these phenomena. In one approach to this problem, simultaneous quantitative determination of multiple neurochemicals is utilized to provide a profile of the changes which are occurring in the central nervous system. Instrumental techniques such as gas chromatography (GC), GC–mass spectrometry (GC–MS) and high-performance liquid chromatography (HPLC) have been widely used for this purpose. In particular, recent developments in HPLC technology make it possible to separate and quantitate numerous organic compounds without requiring extensive sample preparation or chemical derivatization. Moreover, the combination of HPLC with MS permits the analysis of polar, non-volatile or thermally labile substances which are not amenable to GC–MS techniques. As an alternative to thermospray [1,2] or moving-belt [3–5] interfaces, we utilize direct sample introduction into an HPLC–continuous-flow fast atom bombardment (CF-FAB)-MS system [6,7] to accomplish these measurements. We have recently reported on our use of this method for quantitative analysis of acetylcholine (ACh) in rat brain regions [8].

In the present report we describe our results for analysis of 29 standard neurochemicals which have been evaluated for their LC elution behavior and suitability for quantitation by HPLC–CF-FAB MS. Furthermore, we show correlations between individual chemical structure and sensitivity by this technique.

0021-9673/91/$03.50

EXPERIMENTAL

Chemicals

A list of the standard compounds used in this investigation is presented in Table I. DOPAC, nMET and DOMA were purchased from Aldrich (Milwaukee, WI, USA); all of the other standards were obtained from Sigma (St. Louis, MO, USA). HPLC solvents and other reagents were of the highest purity available from commercial sources.

Continuous-flow FAB LC–MS system

A block diagram of the HPLC–CF-FAB-MS system is shown in Fig. 1. (Note that the manufacturer, JEOL, uses the term "FRIT-FAB LC–MS" for this technique.) Details about this system were recently presented by Ikarashi *et al.* [8]. HPLC separation was accomplished with an octadecyl silane semi-micro column (SFPAC-ODS05 S15 column, 15 cm × 1.7 mm I.D., 5 μm particle size, JEOL, Tokyo, Japan). Binary gradient elution was performed with mobile phase A comprised of 0.2% (v/v) trifluoroacetic acid (TFA) in water containing 1% glycerol, and mobile phase B consisting of 0.2% TFA in methanol containing 1% glycerol. The separation was initiated with 100% A, and the content of B was linearly increased from 0 to 40% over a period of 15 min. The flow-rate was maintained at 0.15 ml/min. After passing through the UV detector, the effluent from the column was mixed with a 1%

TABLE I

HPLC RETENTION TIME OF SELECTED NEUROCHEMICALS USING UV AND MASS SPECTROMETRIC DETECTION

Compound	Abbreviation	Mol. wt.	Retention time (min)[a]	
			UV	MS
Choline	Ch	104	n.d.	3.6 ± 0.2
Norepinephrine	NE	169	2.4 ± 0.1	3.7 ± 0.5
Octopamine	OCT	153	3.2 ± 0.1	4.4 ± 0.4
3,4-Dihydroxymandelic acid	DOMA	184	3.4 ± 0.1	n.d.
Epinephrine	EP	183	3.7 ± 0.2	4.9 ± 0.4
Ethylhomocholine	EHC	132	n.d.	5.1 ± 0.2
3,4-Dihydroxybenzylamine	DHBA	139	4.2 ± 0.2	5.5 ± 0.4
Acetylcholine	ACh	146	n.d.	5.7 ± 0.3
Normetanephrine	NMN	183	4.7 ± 0.2	5.9 ± 0.4
Synephrine	SYN	167	5.3 ± 0.2	6.7 ± 0.4
Dopamine	DA	153	5.8 ± 0.2	7.2 ± 0.4
Metanephrine	MN	197	6.4 ± 0.5	8.1 ± 0.6
Deoxyepinephrine	DEP	167	6.5 ± 0.5	8.1 ± 0.5
3,4-Dihydroxyphenylalanine	DOPA	197	7.0 ± 0.5	8.5 ± 0.5
Tyramine	TYM	137	7.0 ± 0.4	8.5 ± 0.5
Phenylethanolamine	PEOHA	137	n.d.	8.9 ± 0.4
Tyrosine	TYR	181	8.7 ± 0.2	10.0 ± 0.4
3-Methoxytyramine	3-MT	167	8.7 ± 0.2	10.0 ± 0.5
5-Hydroxytryptamine	5-HT	176	8.9 ± 0.2	10.3 ± 0.4
N-Methyl-5-hydroxytryptamine	nMET	190	9.3 ± 0.3	10.7 ± 0.5
Homovanilic acid	HVA	182	10.0 ± 0.3	11.5 ± 0.4
5-Hydroxytryptophan	5-HTP	220	10.4 ± 0.3	11.7 ± 0.3
Phenylalanine	PHE	165	n.d.	12.1 ± 0.2
Phenylethylamine	PEA	121	n.d.	12.3 ± 0.2
5-Hydroxytryptophol	5-HTOL	177	11.0 ± 0.4	12.6 ± 0.4
3,4-Dihydroxyphenylacetic acid	DOPAC	168	11.9 ± 0.5	13.2 ± 0.4
5-Hydroxyindoleacetic acid	5-HIAA	191	13.4 ± 0.2	14.8 ± 0.4
Tryptamine	TM	160	13.5 ± 0.2	14.8 ± 0.3
Tryptophan	TRP	204	14.1 ± 0.2	15.4 ± 0.5

[a] n.d. = not detected; values represent the mean ± standard deviation for five separate injections.

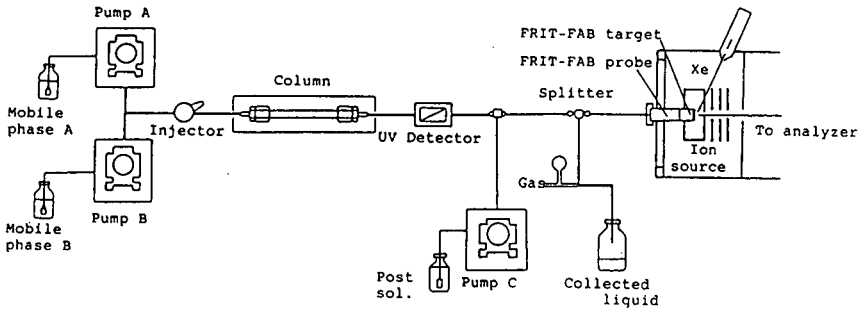

Fig. 1. Block diagram of the HPLC–CF-FA-MS system. For more details about the instrumentation, see ref. 8.

glycerol–methanol solution and introduced into the interface region (the splitter, connector and CF-FAB probe) at a final flow-rate of 0.25 ml/min, the maximum flow-rate which could be readily accomodated by the vacuum system. Approximately 8 μl/min of the effluent were transmitted into the mass spectrometer, and the remainder was collected. Mass spectra were acquired on a JEOL Model JMS-AX505W mass spectrometer in combination with a JEOL Model JMA-OA 5000 data system which was used for mass spectra data processing. MS conditions were as follows: ion source temperature, 50°C; accelerating voltage, 3 kV; conversion dynode voltage, −10 kV; electron multiplier voltage, 1.2 kV; resolution, 1000. A liquid nitrogen trap in the ion source region was used to improve the speed of evaporation. The mass spectrometer was either scanned from 30 to 800 a.m.u. (positive-ion detection) for qualitative analyses or operated in the selected-ion monitoring (SIM) mode for quantitative determinations. A JEOL atom gun was used with xenon (5 keV) for FAB from the surface of the flow FAB probe.

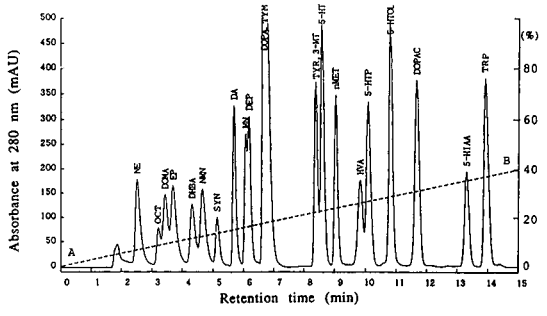

Fig. 2. HPLC pattern with UV detection for the standard compounds listed in Table I. Column specifications and composition of mobile phase are given in the Experimental section. A 5-nmol aliquot of each compound was injected.

RESULTS AND DISCUSSION

After HPLC separation of the standard compounds, initial detection was accomplished by UV

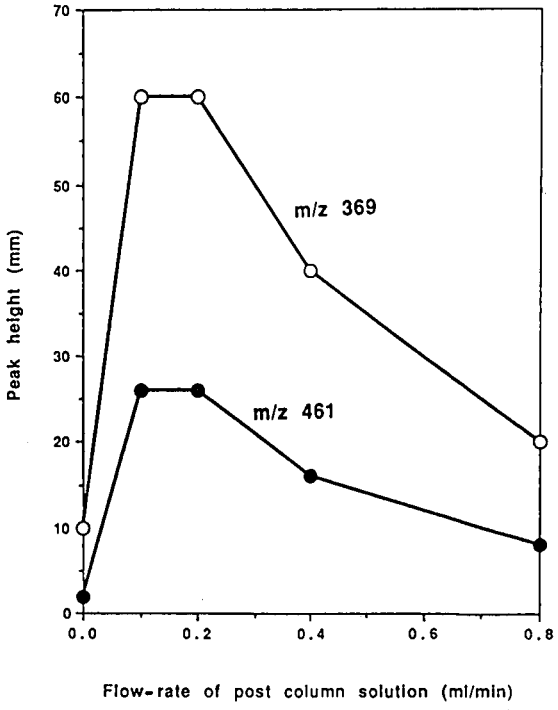

Fig. 3. Effect of post-column addition on the intensity of matrix ions in HPLC–CF-FAB-MS. Composition of mobile phases is given in the Experimental section. Solution added post-column consisted of 1% glycerol in methanol (v/v).

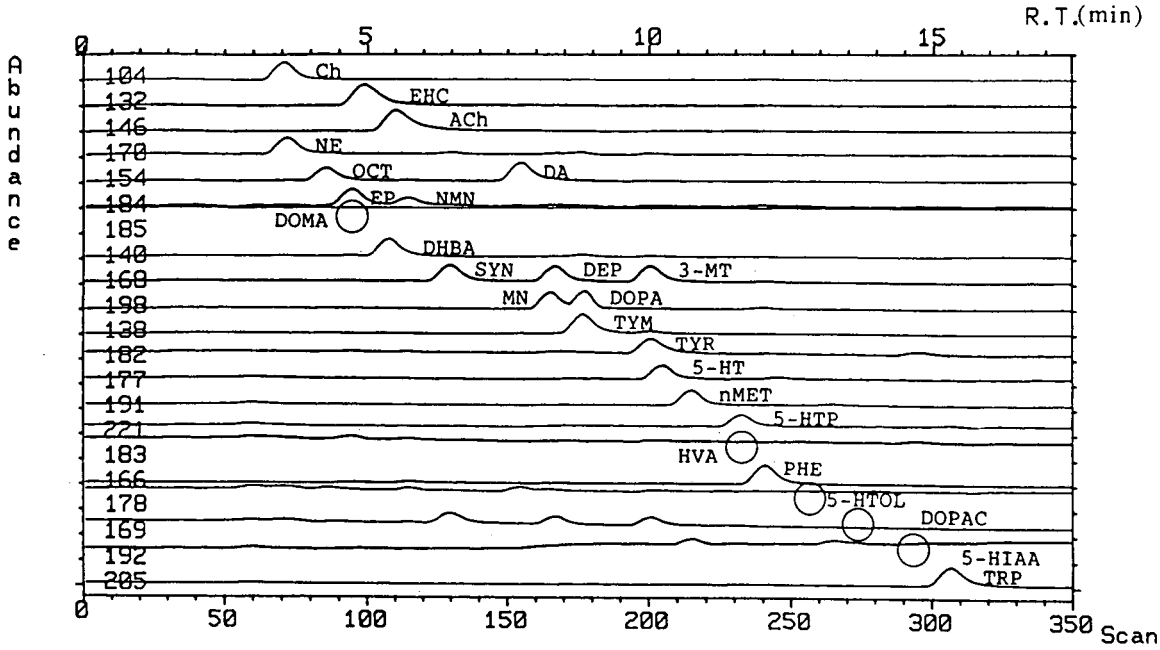

Fig. 4. Mass chromatograms for HPLC–CF-FAB-MS analysis of the standard compounds listed in Table I. Column specifications and composition of mobile phase are given in the Experimental section. A 5-nmol aliquot of each compound was injected. Positions on the traces marked with a circle represent the retention time for compounds not detected for the sample size used in this analysis.

since most of the neurochemicals of interest to us absorb near 280 nm. We found that, when only solvent A was utilized, retention times were extremely long, and broad peaks were observed for the strongly retained compounds. Gradient addition of methanol containing 0.2% TFA along with 1% glycerol led to faster elution of these substances. After examining various mixing rates for the two solvent systems, we ascertained that the linear gradient system of 0–40% solvent system B gave optimal separation in an acceptable amount of time. A typical HPLC profile using UV detection is shown in Fig. 2. Peaks for Ch, ACh, EHC and PHE were not observed at 280 nm because these compounds lack a chromophore at that wavelength; consequently, MS was used for detection of these substances. With the solvent system described above, HPLC separation of the analytes was completed within 15 min. As can

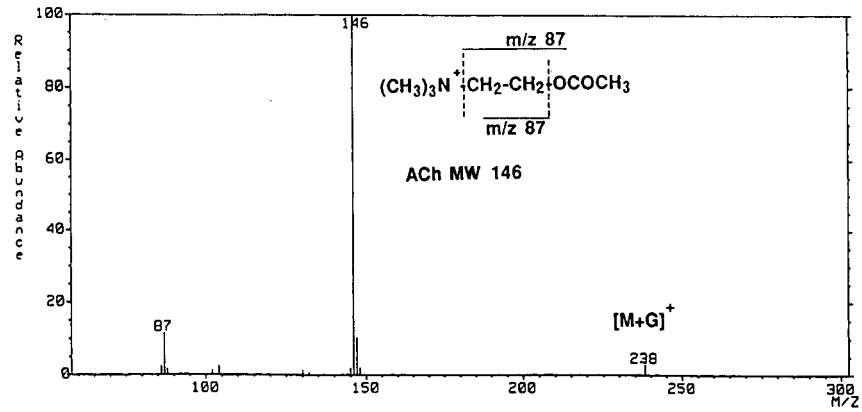

Fig. 5. CF-FAB mass spectrum of acetylcholine (ACh); G = glycerol.

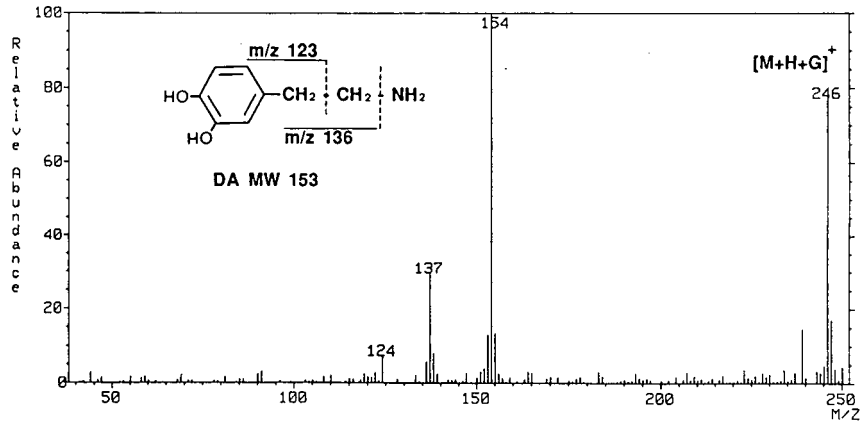

Fig. 6. CF-FAB mass spectrum of dopamine (DA); G = glycerol.

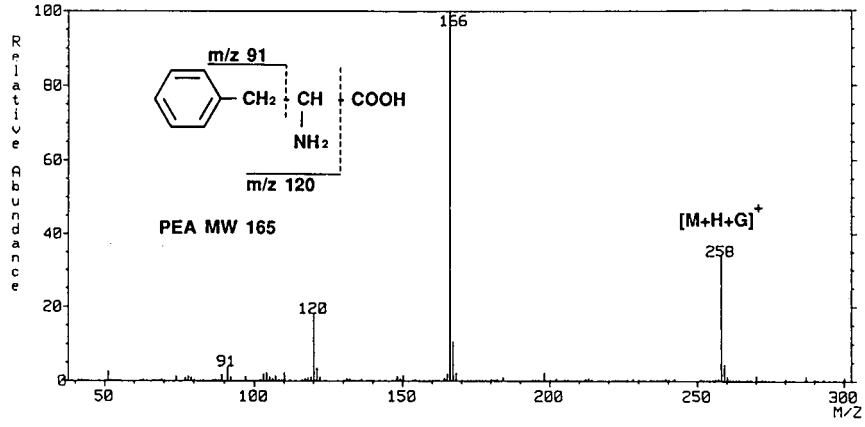

Fig. 7. CF-FAB mass spectrum of phenylalanine (PHE); G = glycerol.

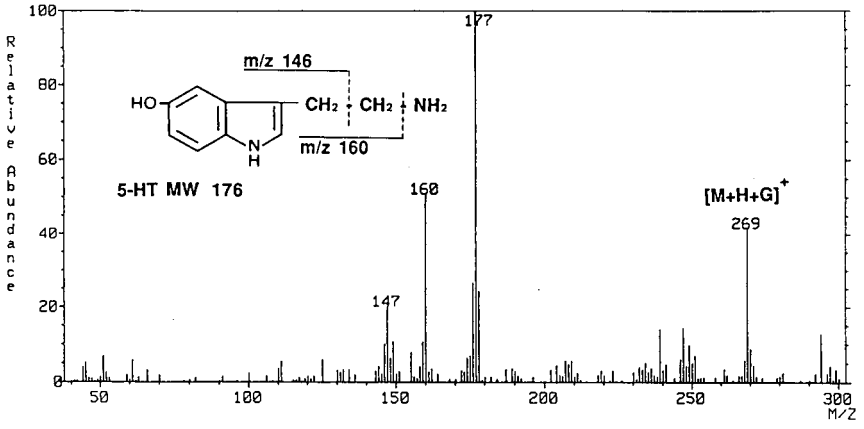

Fig. 8. CF-FAB mass spectrum of serotonin (5-HT); G = glycerol.

TABLE II

RELATIVE RESPONSE OF SELECTED NEUROCHEMICALS TO DETECTION BY FRIT-FAB-MS

Compound[a]	Monitored ion (*m/z*)	Peak area[b]	Response[b,c] (%)
ACH	146	42832	100.0
EHC	132	39187	91.5
PEA	122	25123	58.7
Ch	104	19184	44.8
PHE	166	14675	34.3
PEOHA	138	13523	31.6
TM	161	6046	14.1
3-MT	168	5449	12.7
TRP	205	4427	10.3
DEP	168	4216	9.8
SYN	168	4019	9.4
TYM	138	3838	9.0
MN	198	3762	8.8
EP	184	2889	6.7
DA	154	2386	5.6
TYR	182	2334	5.4
nMET	191	2033	4.7
OCT	154	1520	3.5
NMN	184	1361	3.2
DOPA	198	1337	3.1
NE	170	1313	3.1
5-HT	177	1033	2.4
DHBA	140	920	2.1
5-HTP	221	762	1.8
HVA	183	390	0.9
5-HIAA	192	239	0.6
5-HTOL	178	214	0.5
DOPAC	169	55	0.1
DOMA	185	n.d.	n.d.

[a] Abbreviations as shown in Table I.
[b] n.d. = Not detected.
[c] Response relative to ACh.

be seen from the chromatogram in Fig. 2, the close similarities in chemical structures of many of the compounds makes it difficult to obtain complete HPLC separation, as evidenced by closely eluting or overlapped peaks. However, the use of CF-FAB-MS for detection eliminates this problem. By using SIM, differentiation between these compounds can be readily accomplished even without baseline HPLC separation. Moreover, even for isobaric sets of compounds such as OCT and DA (mol wt. 153), EP and NMN (mol. wt. 183), SYN, DEP and 3-MT (mol. wt. 167) and MN and DOPA (mol. wt. 197) the HPLC retention times are sufficiently separated that the specificity afforded by MS permits facile peak identification.

In order to increase efficiency and ion stability, it was necessary to employ post-column addition of a mixture of 1% glycerol in methanol. The effect of flow-rate of the post-column solution on the production of matrix ions by CF-FAB was examined by monitoring the intensities of ions at *m/z* 369 (protonated glycerol tetramer) and *m/z* 461 (protonated glycerol pentamer). As shown in Fig. 3, the maximum peak heights for both of these ions were obtained when the flow-rate was 0.1–0.2 ml/min.

The mass chromatograms obtained for HPLC–CF-FAB-MS analysis of the selected neurochemicals are presented in Fig. 4. For the quaternary ammonium compounds Ch, ACh and EHC molecular cations ($[M]^+$) at *m/z* 104, 146 and 132, respectively, were monitored. For the other neurochemicals, protonated molecular ions ($[MH]^+$) were detected. The retention times of the compounds being tested, as recorded by UV and CF-FAB-MS are listed in Table I. As can be seen in the table, longer retention times were observed for the peaks detected by MS (Fig. 4) as compared with UV (Fig. 2) because of the additional length of tubing in between the UV detector and the CF-FAB probe.

CF-FAB mass spectra of representative compounds are shown as follows: ACh (quaternary amine), Fig. 5; DA (catecholamine), Fig. 6; PHE (amino acid), Fig. 7; and 5-HT (indoleamine), Fig. 8. Proposed cleavages for each analyte are illustrated for each structure; however, details of the fragmentation mechanisms have not yet been comprehensively investigated. From the spectra it can be seen that the base peak was either $[M]^+$ or $[MH]^+$, depending on the compound class.

In order to ascertain the sensitivity of CF-FAB-MS for our compounds of interest, 5 nmol of each substance were injected into the HPLC system, and the retrieved area for each base peak was measured after SIM. The results are summarized in Table II. The data show that the highest sensitivity was obtained for quaternary ammonium compounds such as ACh and EHC. The detection limit for ACh was less than 1 pmol. The poorest sensitivities were found for compounds such as HVA, 5-HIAA, 5-HTOL, DOPAC and DOMA, all of which lack an amino group. These compounds were either not observed or were only marginally detected at the 5-

TABLE III

RELATIONSHIP BETWEEN CHEMICAL STRUCTURE AND RESPONSE FOR ANALYSIS BY CF-FAB-MS

Compound	R_1	R_2	R_3		Peak area	Response (%)
Quaternary ammonium compounds						
AcH	CH_3	$OCOCH_3$		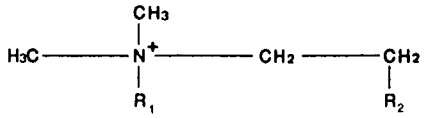	42 832	100.0
EHC	C_2H_5	CH_2OH			39 187	91.5
Ch	CH_3	OH			19 183	44.8
Catechol analogues						
PEA	H	H	H	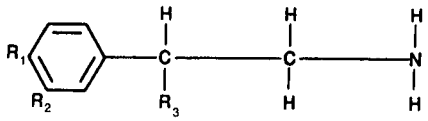	25 123	100.0
PEOHA	H	H	OH		13 523	53.8
TYM	OH	H	H		3838	15.3
DA	OH	OH	H		2386	9.5
NE	OH	OH	OH		1313	5.2
Indole analogues						
TM	H	H	H	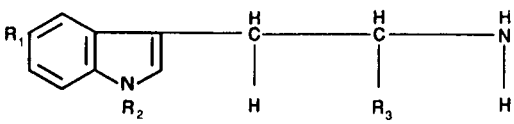	6046	100.0
TRP	H	H	COOH		4427	73.2
nMET	OH	CH_3	H		2033	33.6
5-HT	OH	H	H		1033	17.1
5-HTP	OH	H	COOH		764	13.6

nmol level. We found approximately a 1000-fold difference in sensitivity between ACh and DOPAC.

From a review of our data, we ascertained that the sensitivity of individual compounds using our CF-FAB-MS method could be correlated with chemical structure. For example, the response for PHE [C_6H_5–CH_2–$CH(NH_2)$–COOH] was almost ten times greater than for DOPA [$C_6H_3(OH)_2$–CH_2–$CH(NH_2)$–COOH], with the structures of these related compounds differing only by the presence of two hydroxyl groups on the phenyl side-chain of DOPA. In the current study, it was apparent that compounds with alcoholic or phenolic substituents tended to exhibit lower responsiveness by CF-FAB-MS; in general, the greater the hydrophobic nature of a compound, the stronger the signal CF-FAB-MS. This trend is substantiated by the data presented in Table III for representative quaternary ammonium, catechol and indole analogues.

In conclusion, we present methodology for LC separation and CF-FAB-MS quantitation of multiple neurochemically important compounds. We believe that this technique will be quite valuable for monitoring changes in the central nervous system during behavioral, pharmacological and psychological investigations if the sensitivity of the technique can be improved. In future studies we plan to explore the use of packed capillary columns for HPLC separation in order to eliminate the need for post-column splitting. In addition, we will examine the use of negative-ion detection in conjunction with CF-FAB-MS analysis of these compounds in an effort to enhance the sensitivity for the more hydrophilic analytes and to obtain more uniform responsiveness for the different structural analogues.

ACKNOWLEDGEMENT

The authors thank Dr. Susan Weintraub for help with this manuscript.

REFERENCES

1 C. R. Blakley and M. L. Vestal, *Anal. Chem.*, 55 (1983) 750.
2 R. D. Voyksner and C. A. Haney, *Anal. Chem.*, 57 (1985) 991.

3 R. P. W. Scott, C. G. Scott, M. Munroe and J. Hess, Jr., *J. Chromatogr.*, 99 (1974) 395.
4 M. J. Hayes, E. P. Lankmayer, P. Vouros, B. L. Karger and J. M. McGuire, *Anal. Chem.*, 55 (1983) 1745.
5 D. E. Games, *Biomed. Mass Spectrom.*, 8 (1981) 454.
6 T. Mizuno, T. Kobayashi, Y. Ito and D. Ishii, *Mass Spectros.*, 35 (1987) 9.
7 Y. Ito, T. Takeuchi and D. Ishii, *J. Chromatogr.*, 358 (1986) 201.
8 Y. Ikarashi, K. Itoh and Y. Maruyama, *Biomed. Environ. Mass Spectrom.*, 20 (1991) 21.

Journal of Chromatography, 587 (1991) 314–317
Elsevier Science Publishers B.V., Amsterdam

CHROM. 23 610

Short Communication

Analytical and quantitative studies of californin and protopin in aerial part extracts of *Eschscholtzia californica* Cham. with high-performance liquid chromatography

Jean-Pierre Rey*, Joël Levesque and Jean-Louis Pousset

Laboratoire de Pharmacognosie, Faculté de Médecine et de Pharmacie, 34 Rue du Jardin des Plantes, 86034 Poitiers Cedex (France)

François Roblot

Laboratoire de Pharmacognosie, Faculté de Pharmacie, Rue J. B. Clément, 92296 Chatenay-Malabry (France)

(First received April 26th, 1991; revised manuscript received July 2nd, 1991)

ABSTRACT

In the medicinal plant *Eschscholtzia californica* Cham., californin and protopin are mainly responsible for the sedative and spasmolytic effects. A selective high-performance liquid chromatographic method for the determination of these two alkaloids in plant extracts on a normal-phase column is described that allows their characterization and determination in medicinal plant drugs containing *Eschscholtzia californica* Cham. The most appropriated process for conceiving an *Eschscholtzia* liquid remedy seems to be a weak aqueous alcoholic preparation (30% ethanol) containing 1% of tartaric acid (total alkaloid efficiency = 0.405% dry material).

INTRODUCTION

As part of a study of the application of high-performance liquid chromatography (HPLC) to the analysis of medicinal plant extracts with sedative properties, we have examined the components of *Eschscholtzia californica* Cham. This plant contains many alkaloids, the main ones being protopin ($C_{20}H_{19}NO_5$), first isolated in 1871 by Hesse from opium, then later identified among various Fumariaceae species (fumarin) and other Papaveraceae [1], and californin (=eschscholtzin or crychin) ($C_{19}H_{17}NO_4$), belonging to the pavin group, isolated in 1964 by Gertig [first named alkaloid ("Fz")] [2] and then by Manske and Shin, who named it eschscholtzin [3]. The latter alkaloid is specific in the *Eschscholtzia* genus.

Yellow poppy has been thoroughly studied for its sedative power [1,4–8], which is attributed to the alkaloids present acting with synergistic effects. Numerous studies on protopin and also on *Fumaria* and *Eschscholtzia* spp., have been made using thin-layer chromatography (TLC) [2,9–13], no work has been reported on the determination of these alkaloids with HPLC. We describe here a quantitative HPLC method for the determination of protopin and californin, which can be used as specific tracers in flowered aerial parts of the plant.

0021-9673/91/$03.50

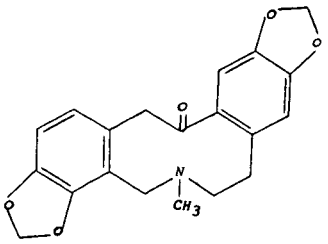

Protopin (= Fumarin)

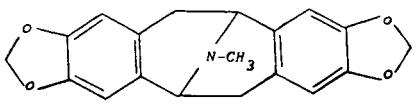

Californin (= Eschscholtzin ; Crychin)

EXPERIMENTAL

TLC

Silica gel Si 60 F_{254} plates were obtained from Merck (Darmstadt, Germany). The mobile phase was chloroform–methanol–acetic acid (80:15:5, v/v/v) and detection was effected with Dragendorff's reagent [14].

HPLC

A varian model 5000 chromatograph was used, equipped with a Rheodyne Model 7161 injector and a photodiode-array detector (Merck L3000) under computer control (Merck HPLC Manager). Analyses were conducted at 20°C.

Preparative HPLC was carried out with a Lichrosorb Si 60 column (250 × 10 mm I.D.; film thickness 7 μm) (Merck). The mobile phase was chloroform–methanol (99:1, v/v), at a flow-rate of 4 ml/min, and UV detection at 254 nm was applied.

Analytical HPLC was carried out on two columns. A normal-phase Lichrosorb Si 60 column (250 × 4 mm I.D., film thickness 7 μm) (Merck) was used with a Lichrosorb Si 60 precolumn (4 × 4 mm I.D. film thickness; 5 μm) (Merck). The mobile phase was chloroform–methanol (90:10, v/v) containing 0.1% of trifluoroacetic acid (TFA) at a flow-rate of 1 ml/min. The injection volume was 10 μl and UV detection at 292.5 nm was applied. The second column was a reversed-phase Lichrosorb RP-18 (250 × 4 mm I.D. film thickness 7 μm) (Merck) with a LiChrosorb RP-18 precolumn (25 × 4 mm I.D.; film thickness 5 μm) (Merck). The mobile phase was acetonitrile–water (65:35, v/v) containing 0.1% of TFA at a flow-rate of 1 ml/min. The injection volume was 10 μl and UV detection at 292.5 nm was applied.

Alkaloid extraction

A 500-g amount of flowered aerial parts harvested in Maine et Loire (France), dried at room temperature and finely powdered, was moistened with dilute ammonia solution and kept for 2 h before Soxhlet extraction with chloroform (5 l). The organic solution was evaporated under reduced pressure at 40°C to a final volume of about 100 ml, and then extracted with 5 × 50 ml of 0.25 M sulphuric acid. The acidic layers were mixed and filtered. After alkalinization with ammonia (pH 10), they were extracted with 4 × 50 ml of chloroform. The organic layers were washed with 70 ml of distilled water, filtered and evaporated under reduced pressure, affording a residue (2.18 g) corresponding to the total alkaloid fraction (0.456% dry material).

Californin separation

A 1-g amount of the total alkaloid fraction diluted with chloroform was placed on a column containing 20 g of silica gel 60 (grain size 0.063–0.2 mm; 70–230 mesh ASTM) for column chromatography (Merck) and 100-ml fractions were collected. Elution was effected with pure chloroform for fractions I–VII (18 mg) and with chloroform–methanol (95:5, v/v) for fraction VIII (513 mg), IX (170 mg) and X (9.6 mg). The whole of fraction VIII was diluted with 1.5 ml of chloroform and then injected on to the preparative HPLC column. Fractions of 4 ml were recovered according to the following scheme: chloroform–methanol (99:1, v/v), fractions 1–25; chloroform–methanol (98:2, v/v), fractions 26–48; chloroform–methanol (95:5, v/v), fractions 49 to completion.

The product was checked using analytical HPLC. Fractions 9–24, mixed and evaporated to dryness, gave 224 mg of pure compound. ^{1}H and ^{13}C NMR

spectrometry (Bruker AC 200 P), mass spectrometry (MS) (Nermag R1010 C), melting point determination, UV spectrophotometric analysis and TLC allowed its identification as californin: m.p. 128°C (methanol); ^1H and ^{13}C NMR spectra identical with the literature [3]; electron impact m/z 323 ($M^{+\cdot}$), 188 (100%); UV λ_{max} [chloroform–methanol–TFA (90:10:0.1, v/v/v)], 245 and 292.5 nm; TLC, R_F (californin) = 0.58 and R_F (protopin) = 0.14.

RESULTS

We started to investigate reversed-phase HPLC (RP-18) with acetonitrile–water as the mobile phase containing from 35 to 70% of acetonitrile, and in addition several kinds of acids such as 1% phosphoric acid or acetic acid. The best results, obtained with acetonitrile–water (65:35, v/v) containing 0.1% of TFA were insufficient for a quantitative study.

We then tried normal-phase HPLC on Si 60 with chloroform–methanol (90:10, v/v) containing 0.1% of TFA, which resulted in considerable improvement in the chromatographic profile. TFA was chosen because of its low absorbance in the UV region. Moreover, it increases the column efficiency and improves the column resolution in both the reversed-phase [15] and normal-phase modes.

The calibration graphs show a linear correlation between the amounts of the two alkaloids injected and the intensity of the absorption at 292.5 nm [correlation coefficient (r^2) 0.9978 for protopin and 0.9942 for californin]. Identification and determination of the two alkaloids were attempted (three consecutive times) on the total alkaloid fraction of different samples: fresh flowered aerial parts (Fig. 1); spray-dried fresh flowered aerial parts; dried flowered aerial parts; dried plant aqueous alcoholic extract (30% ethanol containing 1% of tartaric acid); and dried plant aqueous acidic extract (1% tartaric acid).

Quantitative analysis gave the results summarized in Table I.

DISCUSSION

This study has shown the simplicity, speed and reliability of HPLC for the determination of californin and protopin in *Eschscholtzia californica* Cham. extracts. The method is suitable for the systematic monitoring of sedative phytotherapeutic medicines. A quantitative study on various samples demonstrated the existence of chemotypes in this genus, correlated with a variable alkaloid ratio. The most appropriate process for obtaining an *Eschscholtzia* liquid remedy seems to be a weak aqueous alcoholic preparation (30% ethanol) containing 1% of tartaric acid.

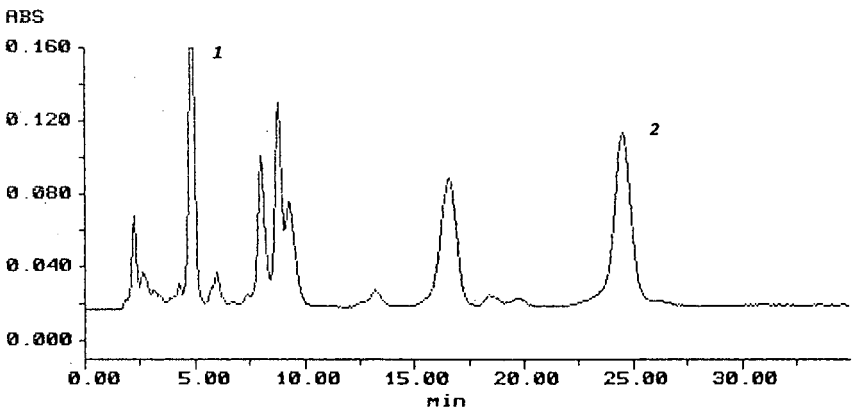

Fig. 1. Chromatogram of a total alkaloid fraction of fresh aerial parts of *Eschscholtzia californica* Cham. Peaks: 1 = californin; 2 = protopin. Conditions: column, LiChrosorb Si 60 (250 × 4 mm I.D.; film thickness 7 μm); precolumn, LiChrosorb Si 60 (4 × 4 mm I.D.; film thickness 5 μm); mobile phase, chloroform–methanol (90:10, v/v) + 0.1% TFA; flow-rate, 1 ml/min; UV detection at 292.5 nm.

TABLE I

VARIATION OF ACTIVE PRINCIPALS CALIFORNIN AND PROTOPIN WITHIN EXTRACTION PROCESSES

Extract	Total alkaloid efficiency (% dry material)	Amount of californin (mg per 100 g total alkaloids)	Amount of protopin (mg per 100 g total alkaloids)	Protopin: californin ratio
Fresh plant	0.471	23.5 ± 0.5	17.5 ± 1.3	0.74
Spray-dried	0.483	17.4 ± 0.3	16.5 ± 1.8	0.94
Dried plant	0.456	34.9 ± 0.2	10.1 ± 0.05	0.29
Aqueous alcoholic acidic extract	0.405	19.9 ± 0.8	2.2 ± 0.1	0.11
Aqueous acidic extract	0.273	11.3 ± 1.7	1.3 ± 0.2	0.11

ACKNOWLEDGEMENTS

Thanks are due to Laboratoire Pharmaceutique Florina (Valanjou) and Agrocinq (Toulouse) for providing pure protopin and financial support.

REFERENCES

1 R. H. Cheney, *Q. J. Crude Drug. Res.*, 3 (1963) 413.
2 H. Gertig, *Acta Pol. Pharm.*, 21 (1964) 59 and 127; 22 (1965) 271, 443, 462 and 473.
3 R. H. F. Manske and K. H. Shin, *Can J. Chem.*, 43 (1965) 2180 and 2183.
4 F. F. Vincieri, S. Celli, N. Mulinacci and E. Speroni, *Pharmacol. Res. Commun.*, 20 (1988) 41.
5 P. Delaveau, *Acta Pharm.*, 208 (1984) 33.
6 S. S. Lamba and R. W. Trottier, *Q. J. Crude Drug Res.*, 15 (1977) 25.
7 A. H. Dil, *Thérapie*, 28 (1973) 767.
8 R. Badacci, *Phytotherapy*, 9 (1984) 31.
9 B. Sener, *Int. J. Crude Drug. Res.*, 21 (1983) 135 and 272.
10 M. E. Popova, V. Simanek, J. Nouak, L. Dolejs, P. Sedmera and V. Preininger, *Planta Med.*, 48 (1983) 272.
11 V. B. Pandey, K. K. Seth and B. Das Gupta, *Pharmazie*, 37 (1982) 453.
12 M. E. Popova, A. N. Boeva, L. Dolejs, V. Preininger, V. Simanek and F. Santavy, *Planta Med.*, 40 (1980) 156.
13 J. Suspulgas, M. Lalaurie, G. Privat and R. Got, *Trav. Soc. Pharm. Montpellier*, 21 (1961) 28.
14 A. Baerheim Svendsen and R. Verpoorte, *Chromatography of Alkaloids, Part A: Thin-layer Chromatography (Journal of Chromatography Library*, Vol. 23A), Elsevier, Amsterdam 1983, pp. 11 and 502.
15 M. B. Radosevich and N. E. Delfel, *J. Chromatogr.*, 368 (1986) 443.

Journal of Chromatography, 587 (1991) 318–320
Elsevier Science Publishers B.V., Amsterdam

CHROM. 23 658

Short Communication

Separation of *Strychnos nux-vomica* alkaloids by high-performance liquid chromatography

Bratati De*

Department of Botany, University of Calcutta, 35 Ballygunge Circular Road, Calcutta 700 019 (India)

N. G. Bisset

Pharmacognosy Research Laboratories, Chelsea Department of Pharmacy, King's College London, University of London, Manresa Road, London SW3 6LX (UK)

(First received April 25th, 1991; revised manuscript received July 25th, 1991)

ABSTRACT

The common alkaloids present in *Strychnos nux-vomica* L. were separated using normal-phase high-performance liquid chromatography.

INTRODUCTION

Various methods of analysis of *Strychnos nux-vomica* L. alkaloids involving strychnine and brucine by high-performance liquid chromatography (HPLC) have been reported. Wu and Siggia [1], Twitchett [2] and Murgia and Walton [3] separated a number of alkaloids including strychnine. Verpoorte and Baerheim Svendsen [4], Dennis [5] and Hayakawa *et al.* [6] separated *S. nux-vomica* alkaloids including strychnine and brucine. However, none of these studies dealt with the separation of the two major alkaloids of *S. nux-vomica* (strychnine and brucine) and of the more important minor bases (icajine, novacine, vomicine, pseudostrychnine, pseudobrucine, α-colubrine and β-colubrine). This paper describes the separation of all these alkaloids and the determination of strychnine and brucine.

EXPERIMENTAL

Apparatus

The HPLC system consisted of a Millipore-Waters (Milford, MA, USA) Model 510 pumping system, a Waters UCK 029970 injector, a Waters automated gradient controller and a Waters Model 440 absorbance detector. The detector output was recorded with an SE 120 BBC Goerz Metrawatt chart recorder.

Chemicals

Chloroform for HPLC (Spectrochem, Bombay, India), cyclohexane for HPLC (S.D. Fine Chem, Boisar, India) and redistilled and filtered diethylamine of AnalaR grade (BDH, Poole, UK) were used. Strychnine and brucine (Smith, Stanistreet, Calcutta, India) were used without further purification.

0021-9673/91/$03.50

Chromatographic procedure

A Waters μPorasil column (30 cm × 3.9 mm I.D.) (particle size 10 μm) was used. Separations were performed at 20°C. The mobile phase was chloroform–cyclohexane–diethylamine (60:40:1) and was mixed in batches of 300 ml. The flow-rate was 0.5 ml/min. The eluate was monitored at 280 nm. For assays the chart speed was set at 0.1 cm/min.

Calibration

A stock standard solution of strychnine or brucine was prepared by dissolving 5 mg of the alkaloid in 10 ml of chloroform. A 1-ml of the stock solution was diluted to 5 ml with chloroform and volumes of 10, 15, 20, 25 and 30 μl were injected. Calibration graphs were obtained by plotting peak height (y) against concentration (x) (strychnine: regression equation $y = 35.2x - 1.6$, correlation coefficient 0.9926; brucine: regression equation $y = 20.4x + 3.2$, correlation coefficient 0.9983).

Method of extraction and analysis of nux-vomica tincture

A 5-ml volume of mother tincture of nux-vomica was evaporated to dryness and the dry tincture was transferred to a separating funnel with 5 × 10 ml of 10% glacial acetic acid. The acidic solution was made alkaline with 25% ammonia solution and was extracted with 5 × 30 ml of chloroform. The combined chloroform extracts were evaporated to dryness and the dry extract was transferred to a 10-ml volumetric flask with chloroform for HPLC and diluted to volume with chloroform. A 0.5-ml volume of this solution was transferred to a 5-ml volumetric flask and diluted to volume with chloroform. Volumes of 30 μl were injected for assay.

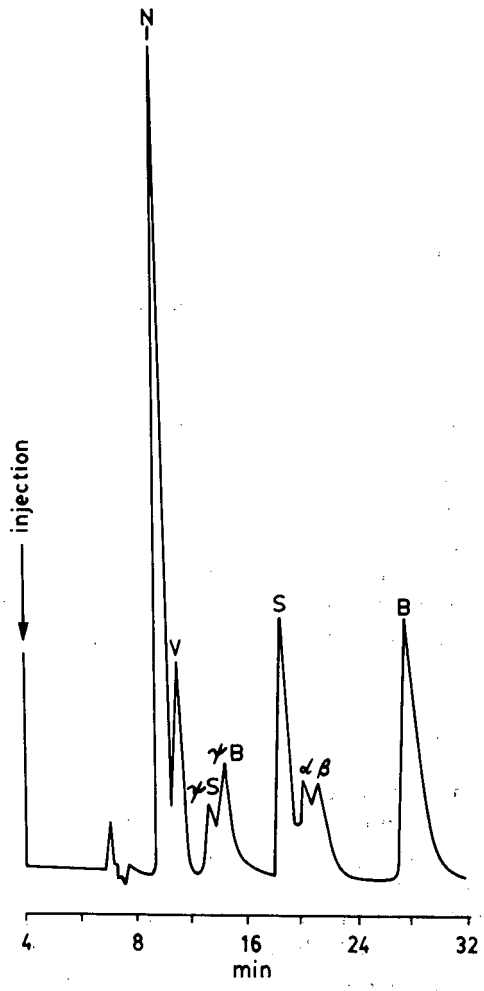

Fig. 1. Chromatogram of *Strychnos nux-vomica* alkaloids. N = Novacine; I = icajine; V = vomicine; ψS = pseudostrychnine; ψB = pseudobrucine; S = strychnine; α = α-colubrine; β = β-colubrine; B = brucine.

TABLE I

CAPACITY FACTORS OF ALKALOIDS

Alkaloid	k'	Alkaloid	k'
Icajine	0.67	Strychnine	2.13
Novacine	0.67	α-Colubrine	2.4
Vomicine	0.86	β-Colubrine	2.6
Pseudostrychnine	1.2	Brucine	3.66
Pseudobrucine	1.4		

TABLE II

RECOVERIES OF STRYCHNINE AND BRUCINE

Parameter	Strychnine	Brucine
Amount taken (mg)	5.00	5.00
Mean recovery (mg) (n = 3)	4.83	4.93
Standard deviation (mg)	0.125	0.094
Standard error of mean	0.07	0.05
Recovery (%)	96.6	98.6
Coefficient of variation (%)	2.59	1.91

TABLE III

DETERMINATION OF STRYCHNINE AND BRUCINE IN NUX-VOMICA TINCTURE

Alkaloid	Sample	Mean weight in 10 ml of tincture ± standard deviation (mg) (n = 3)	Concentration (%, w/v)	Coefficient of variation (%)
Strychnine	A	4.13 ± 0.125	41.3	3.03
	B	4.30 ± 0.16	43.0	3.72
Brucine	A	6.30 ± 0.29	63.0	4.6
	B	6.10 ± 0.14	61.0	2.3

For recovery tests, solutions of strychnine (20 mg) and brucine (20 mg) in 10 ml of chloroform were prepared and 2.5 ml of the solutions were added to 5 ml of nux-vomica tincture, dried and then extracted following the above procedure. Volumes of 30 μl were injected for assay.

Recoveries were calculated from the difference between the amount of strychnine or brucine present in the mother tincture and that in the same sample with known amounts of the two alkaloids added.

RESULTS AND DISCUSSION

Using the experience acquired during the thin-layer chromatographic analysis of tertiary nux-vomica alkaloids [7], different proportions of chloroform–cyclohexane–diethylamine were tried as mobile phases. Chloroform–cyclohexane–diethylamine (60:40:1) gave the best results, strychnine and brucine being separated with no interfering peaks. The most important alkaloids of nux-vomica extract were separated, except icajine and novacine, which showed the same retention time. This separation was found to be reproducible. Elution with baseline separation of a synthetic mixture of the authentic alkaloids was completed within 30 min (Fig. 1). The capacity factors (k') for different alkaloids are given in Table I. A higher proportion of chloroform in the mobile phase did not separate all the alkaloids completely and a reduction in the chloroform concentration resulted in an increase in peak width.

Detection was carried out at 280 nm despite the fact that the UV absorbance maximum of strychnine is 254 nm, because the diethylamine in the mobile phase had a UV cut-off point (λ_{max}) higher than 254 nm and thus interfered with the detection of the alkaloids.

The recoveries of strychnine and brucine were 96.6% and 98.6%, respectively. The results of recovery tests are given in Table II.

Strychnine and brucine were determined in two samples of nux-vomica tincture. The results are given in Table III.

ACKNOWLEDGEMENT

B.D. is grateful to Dr. S. C. Pakrashi, Director, Indian Institute of Chemical Biology, Calcutta, India, for making available the facilities of the Institute.

REFERENCES

1 C. Y. Wu and S. Siggia, *Anal. Chem.*, 44 (1972) 1499.
2 P. J. Twitchett, *J. Chromatogr.*, 104 (1975) 205.
3 E. Murgia and H. F. Walton, *J. Chromatogr.*, 104 (1975) 417.
4 R. Verpoorte and A. Baerheim Svendsen, *J. Chromatogr.*, 109 (1975) 441.
5 R. Dennis, *J. Pharm. Pharmacol.*, 36 (1984) 332.
6 J. Hayakawa, N. Noda, S. Yamada and K. Uno, *Yakugaku Zasshi*, 104 (1984) 57.
7 J. D. Phillipson and N. G. Bisset, *J. Chromatogr.*, 48 (1970) 493.

Journal of Chromatography, 587 (1991) 321–324
Elsevier Science Publishers B.V., Amsterdam

CHROM. 23 749

Short Communication

Determination of carbendazim in blueberries by reversed-phase high-performance liquid chromatography

Rodney J. Bushway*, Heather L. Hurst, Jasotha Kugabalasooriar and Lewis B. Perkins

Department of Food Science, 102 B Holmes Hall, University of Maine, Orono, ME 04469 (USA)

(First received July 3rd, 1991; revised manuscript received September 17th, 1991)

ABSTRACT

A fluorescent reversed-phase high-performance liquid chromatographic method was developed for the analysis of carbendazim in blueberries. Recoveries of fortified blueberries at 27 and 810 ng/g were more than adequate with good precision. Forty commercial blueberry samples were analyzed and the amount of carbendazim ranged from none detected (detection limit of 15 ng/g) to 155 ng/g. Confirmation of carbendazim in the blueberry samples was made by enzyme immunoassay and UV photodiode array.

INTRODUCTION

Carbendazim (methyl benzimidazole-2-yl carbamate) and benomyl (methyl 1-(butylcarbamoyl) benzimidazole-2-yl carbamate), systemic benzimidazole fungicides, are used as either preharvest or postharvest treatment on fruit and vegetables to prevent Botrytis and rotting during refrigeration [1]. Since benomyl metabolizes quite rapidly to carbendazim in fruits and vegetables [2,3], it is usually quantified as carbendazim. Tolerances range from 0.2 to 35 ppm. There has been some long standing concern as to the safety of carbendazim [4,5]. Because of possible health effects [4,5], widespread use [6] and insufficient residue data [6], there is a need to monitor carbendazim in food commodities.

Previous methods for carbendazim analysis in foods have focused on spectrophotometric and chromatographic procedures [1,5,7,8]. However, high-performance liquid chromatography (HPLC) has become the method of choice for benzimidazole fungicides [5,7,8]. Of these HPLC procedures none included the analysis of carbendazim in blueberries.

This paper describes a reversed-phase fluorescence HPLC method for the analysis of carbendazim in blueberries (fresh, frozen, highbush and lowbush) that is extemely sensitive.

EXPERIMENTAL

Materials and chemicals

Solvents were HPLC grade (VWR, Boston, MA, USA) except for the methanol used for the extraction which was ACS grade (Fisher Scientific, Fairlawn, NJ, USA). Carbendazim was obtained from the US Environmental Protection Agency (Research Triangle Park, NC, USA), Acid almunia was from Sigma (St. Louis, MO, USA) and the basic alumina from Fisher Scientific.

Blueberries were obtained from local stores and processors. Enviroguard carbendazim enzyme immunoassay kits were purchased from Millipore Corporation (Bedford, MA, USA).

Apparatus

The HPLC system consisted of a Waters Assoc.

0021-9673/91/$03.50

(Milford, MA, USA) 510 pump, a Valco pneumatic injector (VICI Instruments, Houston, TX, USA), a Waters 470 Fluorescence detector, a Hewlett-Packard (Avondale, PA, USA) 1040A photodiode array detector and a Hewlett-Packard 3396A integrator.

Chromatography

An Ultracarb 30 ODS column (stainless steel, 15 cm × 4.6 mm I.D.) (Phenomenex, Torrance, CA, USA) was employed for the separation along with a mobile phase comprised of acetonitrile–methanol–water–monoethanolamine (135:30:235:0.05) at a flow-rate of 1.0 ml/min. When UV detection was used 25 μl of sample was injected at a wavelength of 286 nm and 0.04 a.u.f.s. As for fluorescence, the excitation was set at 286 nm and the emission at 310 nm. A 5-μl volume was injected into the fluorescence system because of its greater sensitivity. Linearity for the fluorescence detector was from 0.25 ng to 500 ng injected while the UV was from 1.25 ng to 2500 ng injected.

Extraction procedure

The extraction procedure was a modification of the method of Gilvydis and Walters [8]. A 50-g amount of blueberries was blended with 100 ml of methanol for 5 min. (If one wants to make sure that all benomyl is converted to carbendazim, then 10 ml of 1 *M* hydrochloric acid may be added to the methanol before blending). The extract was vacuum filtered through No. 42 filter paper and the filter cake rinsed with an additional 50 ml of methanol before transferring the filtrate to a 500 ml sepatory funnel containing 100 ml of 1% NaCl. A pH adjustment was made by adding 40 ml of 2.0 *M* NH_4Cl (pH 9.5) to the separatory funnel. This mixture was partitioned twice with 100 ml aliquots of dichloromethane. The combined dichloromethane fractions were dried over Na_2SO_4 and evaporated to dryness using a rotary evaporator at 40°C. A 2-ml volume of acetonitrile–methanol (50:50) was used to dissolve the residue followed by 2 ml of water. A 1-ml aliquot of this dissolved residue was passed through an alumina column made with a Pasteur pipette that contained 5 mm of acid alumina and 5 mm of basic alumina. A 5- or 25-μl aliquot was injected into the HPLC system depending upon the system employed.

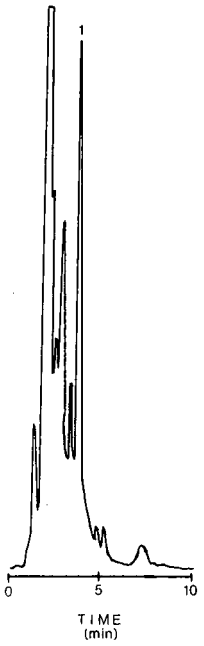

Fig. 1. Chromatogram of an extracted unfortified blueberry sample. Column, Ultracarb 30 ODS; flow-rate, 1 ml/min; wavelength 286 nm excitation and 310 nm emission; eluent, acetonitrile–methanol–water–monoethanolamine (135:30:235:0.05). Peak: 1 = carbendazim.

RESULTS AND DISCUSSION

A typical HPLC chromatogram of an unfortified blueberry extract is shown in Fig. 1. Chromatographic time is rapid with a retention time of 3.5 min and a complete clearance time from other compounds of 8 min. The resolution of the carbendazim peak was 90% from other components present in the blueberry samples. As for peak confirmation two techniques were used to ascertain that the peak at 3.5 min was carbendazim and that there were no co-eluting substances.

First, UV spectra from 190 nm to 350 nm were taken for each carbendazim peak at the up slope, pinnacle and down slope using a photodiode detector. All three spectra for each blueberry sample were the same and agreed with the carbendazim standard. The sensitivity needed for carbendazim confirmation by photodiode array was at least 6 ng carbendazim injected.

The second confirmation technique employed was an enzyme immunoassay for carbendazim. All blueberry samples were analyzed by enzyme immunoassay, including the 20 samples that were shown to contain no detectable residues by HPLC and the agreement between the fluorescent HPLC and immunoassay was excellent. A correlation coefficient of 0.98 was obtained which indicates that the carbendazim peak from the HPLC procedure was free from interfering substances. Furthermore, these results suggest that the immunoassay is a good confirmation technique for carbendazim. The sensitivity needed for carbendazim confirmation by enzyme immunoassay was a sample containing at least 15 ng/g carbendazim.

A recovery study was performed using organic blueberries fortified at 27 and 810 ng/g carbendazim. The blueberries were spiked at the two concentrations on each of six days. Results are shown in Table I. Average recovery for the 27-ng/g fortification was 94% with a coefficient of variation (C.V.) of 14% while the recovery for the 810-ng/g spike was 76% with a C.V. of 3.8%. These recoveries are good and the day to day reproducibility is excellent.

Forty blueberry samples were analyzed using the fluorescent HPLC method. The results are given in Table II. Of these samples, 20 contained measurable levels of carbendazim while the other 20 had no detectable amounts of carbendazim at a detection limit of 15 ng/g. This detection limit was based on a 5-μl injection into the fluorescent system and yielded a signal five times higher than the organic blueberry extract.

TABLE I

RECOVERY OF CARBENDAZIM FROM FORTIFIED ORGANIC BLUEBERRIES

Each spiked sample was extracted on different days.

Sample	Recovery (27 ng/g) (%)	Recovery (810 ng/g) (%)
1	89	76
2	86	73
3	76	74
4	100	76
5	103	77
6	112	81
Mean	94	76
C.V. (%)	14	3.8

TABLE II

CARBENDAZIM LEVELS IN COMMERCIAL BLUEBERRY SAMPLES

Sample	Carbendazim (ng/g)	Sample	Carbendazim (ng/g)
1	59	12	33
2	55	13	23
3	25	14	40
4	54	15	39
5	33	16	102
6	37	17	155
7	37	18	96
8	58	19	78
9	41	20	23
10	59	21–40	ND[a]
11	58		

[a] ND = none detected at a detection limit of 15 ng/g.

Approximately 9 samples per day can be run through the entire procedure. The limiting step is the partitioning with dichloromethane (since it takes much time to wait for the layers to partition after shaking) but this step is really necessary to clean up the sample from interfering substances so that a detection limit of 15 ng/g can be achieved. Since the carbendazim tolerance for blueberries is 7 ppm, it seems ridiculous to obtain such a low detection limit. However, there is an increased interest to know what the actual amounts of pesticides are in food so that the toxicologists and epidemiologists will have accurate data to design and do their studies. Presently, in the USA scientists dealing with the toxicity of pesticides in food assume that each pesticide used on food is present at its tolerance level and as can be seen with blueberries this is not the case. Thus, wrong assumptions can lead to incorrect conclusions.

ACKNOWLEDGEMENT

This manuscript is No. 1600 of the University of Maine Agricultural Experiment Station.

REFERENCES

1 A. Monico-Pifarre and M. Xirau-Vayreda, *J. Assoc. Off. Anal. Chem.*, 73 (1990) 553.
2 C. A. Peterson and L. V. Edgington, *J. Agr. Food Chem.*, 17 (1969) 898.
3 J. J. Sims, H. Mee and D. C. Erwin, *Phytopathology*, 59 (1969) 1775.
4 *Regulating Pesticides in Food–The Delaney Paradox*, National Academy Press, Washington, DC, 1987.
5 F. Sanchez-Rasero, T. E. Romero and C. G. Dios, *J. Chromatogr.*, 538 (1991) 480.
6 P. C. Bardalaye and W. B. Wheeler, *J. Chromatogr.*, 330 (1985) 403.
7 R. J. Bushway, S. A. Savage and B. S. Ferguson, *Food Chemistry*, 35 (1990) 51.
8 D. M. Gilvydis and S. M. Walters, *J. Assoc. Off. Anal. Chem.*, 73 (1990) 753.

Journal of Chromatography, 587 (1991) 325–328
Elsevier Science Publishers B.V., Amsterdam

CHROM. 23 712

Short Communication

Determination of sun-screen agents in cosmetic products by micellar liquid chromatography

Frank P. Tomasella*,☆, Pan Zuting☆☆ and L. J. Cline Love

Department of Chemistry, Seton Hall University, South Orange, NJ 07079 (USA)

(First received May 23rd, 1991; revised manuscript received August 28th, 1991)

ABSTRACT

A micellar liquid chromatographic method was developed for the quantitative determination of sun-screen agents in cosmetic products. The qualitative analysis of parabens is also feasible. Excellent linearity was obtained (r = 0.999) and recoveries were generally greater than 98%. A variety of commercial formulations were analyzed.

INTRODUCTION

Micellar chromatography continues to find unique applications. Recent applications include the use of micellar chromatography in the quantitation of hydrophobicity [1], determination of heavy-metal cations [2] and the determination of drug substances in biological fluids [3–6]. The solubilizing ability is one of the micelles most important property which allows for the direct quantitation of an analyte contained within a complex matrix.

With greater regulation of over-the-counter (OTC) products by the Food and Drug Administration (FDA), a facile analytical method for the determination of sun-screen agents in cosmetic products is desirable. Determinations based on reversed-phase high-performance liquid chromatography (HPLC) have been reported [7–9]. Due to the complex nature of the cosmetic preparation, the sample preparation may require an extraction step. A micellar solution would solubilize the cosmetic formulation allowing for the direct analysis of the active sun-screen agents.

A simple analytical method based on micellar HPLC which allows for qualitative and quantitative determination of 2-ethylhexyl-*p*-dimethylaminobenzoate (PABA), 2-ethylhexyl-*p*-methoxycinnamate (EMC) and 2-hydroxy-4-methoxybenzophenone (oxybenzone) in OTC sun-screen preparations will be described. PABA, EMC and oxybenzone are the leading UV absorbers in cosmetic products. The method makes use of external standards thus minimizing sample preparation even further.

EXPERIMENTAL

Instrumentation

A modular component HPLC system was used consisting of a Spectra-Physics SP8700 pump (San Jose, CA, USA), a Schoeffel Spectroflow Monitor SF 770 variable-wavelength detector and a Rhe-

☆ Present address: Bristol-Myers Squibb, P.O. Box 191, New Brunswick, NJ 08903, USA.
☆☆ Present address: Department of Chemistry, Wuhan University, Wuhan, Hubei 430072, China.

0021-9673/91/$03.50

odyne sample injector (Cotati, CA, USA) equipped with a 20-μl injection loop. The column was a Shandon (Sewickley, PA, USA) C_8 Hypersil WP300, 10 μm (250 × 4.6 mm I.D.). A Model 5000 Fisher Recordall strip chart recorder (Springfield, NJ, USA) was used to record the chromatograms.

Reagents

The sodium dodecyl sulfate (SDS), was electrophoresis grade obtained from Bio-Rad Labs. (Richmond, CA, USA) and used as received. The isopropanol, triethylamine and phosphoric acid, 85% (Fisher Scientific) were used as received. The methyl 4-hydroxybenzoate and propyl 4-hydroxy-benzoate (Aldrich, Milwaukee, WI, USA) were used as received. The PABA, EMC and oxybenzone were courtesy of Van Dyk & Co. (Belleville, NJ, USA).

Chromatographic conditions

A 0.10 *M* SDS solution, containing 0.3% (v/v) triethylamine, pH adjusted to 3.0 with phosphoric acid, was used as the micellar solution. The mobile phase was SDS–isopropanol (90:10, v/v). A flow of 1.5 ml/min was used. The column temperature was ambient. Detection wavelength was either 254 or 300 nm. Strip chart recorder speed was 0.25 cm/min.

Standard solution

About 30 mg oxybenzone and either 300 mg PABA or 300 mg EMC were transferred into a 50-ml volumetric flask, dissolved and diluted to volume with methanol. A volume of 5.0 ml of the solution was transferred to a 50-ml volumetric flask and diluted to volume with the mobile phase.

Simulated sun-screen preparation

Accurately weigh 9.0 g of commercial skin lotion which does not contain sun-screen agents into a 50-ml beaker. To the lotion is added 0.30 g oxybenzone and either 0.70 g EMC or 0.70 g PABA. The mixture is allowed to stir at 40–50°C for 1 h.

Sample preparation

Accurately weigh 1.0–1.5-g sample of sun-screen lotion into a 50-ml volumetric flask. The sample is dissolved with isopropanol and diluted to volume. A volume of 5.0 ml of the solution is diluted to a 50-ml volumetric flask with mobile phase. An aliquot of the solution is filtered through a 0.45-μm membrane filter prior to HPLC analysis.

RESULTS AND DISCUSSION

PABA, EMC and oxybenzone are active ingredients in sunscreen products because of their relatively high molar absorptivities in the ultraviolet range. In ethanol or methanol, PABA and oxybenzone have wavelength maximum values of 310 and 290 nm, respectively [10]. The analytical wavelength of 254 nm was initially selected as cited by Tan *et al.* [11]. Fig. 1 depicts a chromatogram of a commercial preparation containing methyl- and propylparaben, PABA and oxybenzone. As evident, good resolution of the compounds is obtained. The qualitative analysis of parabens which are utilized as antimicrobial agents [12] in cosmetic preparations is feasible. *p*-Hydroxybenzoic acid possesses a maximum absorbance at 246 nm [13]. At 254 nm a qualitative method of determining parabens with a quantitative determination of sun-screen agents is feasible. The drawback of the analysis is the poor response factor of PABA and EMC at this wavelength as compared to the response factor of oxybenzone.

To insure accurate quantitation, the analytical wavelength of 300 nm resulted in a greater response

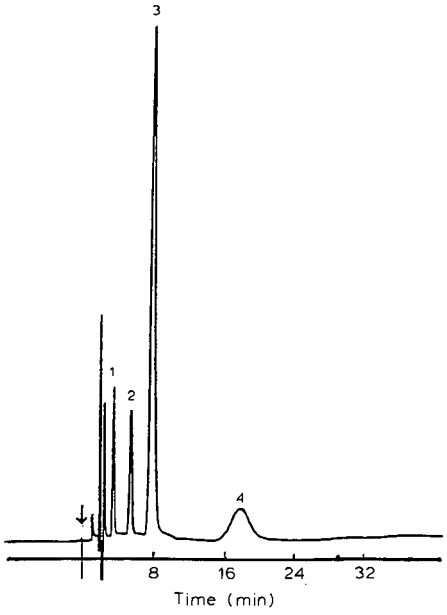

Fig. 1. Typical chromatogram of a commercial sun-screen preparation obtained by setting the detector at 254 nm. Peaks: 1 = methylparaben; 2 = propylparaben; 3 = oxybenzone; 4 = PABA. Chromatographic conditions as in text.

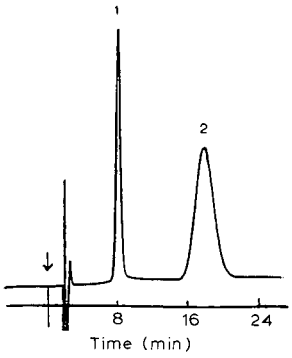

Fig. 2. Typical chromatogram of a commercial sun-screen preparation obtained by setting the detector at 300 nm. Peaks: 1 = oxybenzone; 2 = PABA.

factor of the analytes. The chromatogram of a commercial preparation containing oxybenzone and PABA is depicted in Fig. 2 which shows the enhanced response factor of PABA at 300 nm. Good resolution of the sun-screens is evident but the qualitative analysis of the parabens is diminished at the higher wavelength. The retention times under the experimental conditions described, were 3.92, 17.36 and 19.40 min for oxybenzone, PABA and EMC, respectively.

Quantitative analysis is obtained by the use of an external standard method which further simplified the sample preparation. Calibration curves were constructed for each of the three sun-screens. Excellent linearity was obtained throughout the investigated range of commercial preparations for PABA, oxybenzone and EMC. Typical sun-screen concentrations in a commercial preparation are as follows: 1.4–8.0% PABA, 2.0–7.5% EMC and 2.0–6.0% oxybenzone. Correlation coefficients $r = 0.9999$ were achieved for PABA, oxybenzone and EMC.

Recovery studies were performed by adding known amounts of sun-screen in the concentration range of a typical preparation to a commercial skin lotion preparation which does not contain sun-screens as part of the formula. The results of the analysis which were calculated using the calibration curves described above are summarized in Table I. As is evident, good recoveries and precision were obtained.

The method was applied to a variety of commercial preparations with a sun protection factor (SPF) ranging from 4 to 15. A SPF of 2 to 4 provides minimal sunscreen protection. Where as, a SPF of 8 to 15 provides greater sun-screen protection. Table II provides the results of the analysis of the commer-

TABLE I

RECOVERY DATA FROM SIMULATED FORMULATIONS

Each value is the mean of three determinations.

Compound	Amount added (mg/g sample)	Recovery (%) + S.D.
Lotion A		
Oxybenzone	10.7	97.7 ± 2.4
EMC	18.3	99.3 ± 2.5
Lotion B		
Oxybenzone	6.26	99.5 ± 2.5
PABA	14.4	98.2 ± 2.2

TABLE II

ANALYSIS OF COMMERCIAL SUN-SCREEN PRODUCTS

Representing three vendors (1, 2 and 3).

Compound	SPF	Amount found (%, w/w)
Lotion 1A	4	
Oxybenzone		1.35 ± 0.03
PABA		3.22 ± 0.08
Lotion 1B	8	
Oxybenzone		3.08 ± 0.08
PABA		6.36 ± 0.16
Lotion 1C	15	
Oxybenzone		2.92 ± 0.07
PABA		7.00 ± 0.18
Lotion 2A	4	
Oxybenzone		0.89 ± 0.02
EMC		3.02 ± 0.08
Lotion 2B	15	
Oxybenzone		2.72 ± 0.07
EMC		6.79 ± 0.17
Lotion 3A	8	
Oxybenzone		2.05 ± 0.05
PABA		4.38 ± 0.12
Lotion 3B	15	
Oxybenzone		3.04 ± 0.08
PABA		5.36 ± 0.13

cial preparations along with the SPF claimed by the manufacturer.

The HPLC assay reported here is suitable for routine analysis of sunscreen agents. The method is facile and reproducible. No deterioration of the column was detected due to the direct injection of a cosmetic matrix. The study exceeded 200 injections onto the column.

REFERENCES

1 M. G. Khaledi and E. D. Breyer, *Anal. Chem.*, 61 (1989) 1040.
2 T. Okada, *Anal. Chem.*, 60 (1988) 2116.
3 L. J. Cline Love and J. J. Fett, *J. Pharm. Biomed. Anal.*, 9 (1991) 323.
4 F. Palmisano, A. Guerrieri, P. G. Zambonin and T. R. I. Cataldi, *Anal. Chem.*, 61 (1989) 946.
5 J. Haginaka, J. Wakai, H. Yasuda and T. Nakagawa, *Anal. Chem.*, 59 (1987) 2732.
6 F. J. DeLuccia, M. Arunyanart and L. J. Cline Love, *Anal. Chem.*, 57 (1985) 1564.
7 L. Gagliardi, G. Cavazzutti, L. Montanarella and D. Tonelli, *J. Chromatogr.*, 464 (1989) 428.
8 K. Ikeda, S. Suzuki and Y. Watanabe, *J. Chromatogr.*, 482 (1989) 240.
9 Y. Maeda, M. Yamamoto, K. Owada, S. Sato, T. Masui, H. Nakazawa and M. Fujita, *J. Chromatogr.*, 410 (1987) 413.
10 Food and Drug Administration, *Fed. Reg.*, 43 (1979) 38264.
11 H. S. Tan, R. Sih, S. E. Moseley and J. L. Lichtin, *J. Chromatogr.*, 291 (1984) 275.
12 F. F. Cantwell, *Anal. Chem.*, 48 (1976) 1854.
13 A. M. Wahbi and M. A. H. Barary, *Anal. Chem.*, 16 (1983) 1617.

Journal of Chromatography, 587 (1991) 329–332
Elsevier Science Publishers B.V., Amsterdam

CHROM. 23 717

Short Communication

Assay for thiomersal (thimerosal) with adaptation to the quantitation of total ethylmercury available in degraded samples

J. E. Parkin

School of Pharmacy, Curtin University of Technology, Kent Street, Bentley, Western Australia 6102 (Australia)

(First received May 16th, 1991; revised manuscript received August 29th, 1991)

ABSTRACT

A simple adaptation of a previously reported chromatographic procedure for thiomersal (thimerosal) is reported. This involves the sequential analysis of a degraded sample of thiomersal with and without the addition of excess thiosalicylic acid. This enables the total amount of available ethylmercuric ion and thiomersal to be quantitated and by difference the amount of free ethylmercuric ion. The antimicrobial significance of the results is briefly discussed.

INTRODUCTION

Thiomersal (thimerosal) (TM) (I, Fig. 1) is an antimicrobial preservative used in pharmaceutical systems [1]. It consists of the sodium salt of a complex formed between thiosalicylic acid (TSA) (II) and the ethylmercuric (EtHg) ion (III). It is rapidly degraded by light [2–9] and among the identified degradation products are TSA [2,10–12] 2,2′-dithiosalicylic acid [10–13] and EtHg complexed with various species such as chloride (if present), hydroxide and with excess TM via the carboxylate group [2] and metallic mercury [11].

Davies *et al.* [7] have demonstrated that degraded samples of TM possess enhanced levels of antimicrobial activity, and, on the basis of demonstrating that disodium edetate decreased the activity, have suggested that the EtHg ion is the more active antimicrobial species in degraded samples. This suggestion is in keeping with the proposed mechanism-of-action of mercurial antiseptics [14].

A number of assays employing high-performance liquid chromatography (HPLC) have been applied to the quantitation of TM [3,6,9,11,12,15–19]. All,

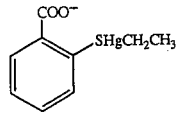

I

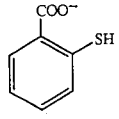

II

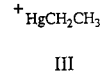

III

Fig. 1. Structures. I = Thiomersal (TM); II = thiosalicylic acid (TSA); III = ethylmercuric ion (EtHg).

0021-9673/91/$03.50

except one recently reported from these laboratories [9], measure intact TM without consideration of the relative levels of EtHg ion and TSA ligand in the system, the measured concentrations, in degraded samples, being limited by the stoichiometric ratio of the two species in solution.

The assay reported from these laboratories [9] quantitates TM (in undegraded samples) or total EtHg ion (in degraded samples) by reaction of the EtHg ion species in the system with dithiocarbamate complexing agents. By applying the analytical method in conjunction with the conventional method of Lam *et al.* [17], which measures intact TM, it is possible to quantitate, in degraded samples, the relative amounts of TM and free EtHg ion by difference. A disadvantage of this procedure is that it requires the application of two HPLC assays concurrently each requiring different chromatographic conditions.

This paper outlines a simple adaptation of the method of Lam *et al.* [17] which enables intact TM and TM plus EtHg ion to be measured using a single HPLC system by sequential assays.

EXPERIMENTAL

Materials

TM and TSA (Sigma, St. Louis, MO, USA) and EtHg chloride (TCI, Tokyo, Japan) were used as supplied. All other chemicals were analytical or HPLC grade.

Chromatographic equipment and conditions

The liquid chromatograph consisted of a pump (501, Waters Assoc., Milford, MA, USA), 20-μl loop injector (Rheodyne 7125, Cotati, CA, USA), variable-wavelength absorbance detector (484, Waters Assoc.) and integrating recorder (3396A, Hewlett-Packard, Palo Alto, CA, USA) together with a column of octadecyl silica (Waters Assoc.) 30 cm × 3.9 mm I.D., 10 μm particle size. The mobile phase consists of 2.74 g of monosodium phosphate and 2.49 g of disodium phosphate in acetonitrile–water (15:85, v/v) at a flow-rate of 1.5 ml min^{-1}. The monitoring wavelength was 254 nm.

Sample preparation

To 1 ml of sample to be analysed was added either acetonitrile–water (30:70, v/v) (1 ml) or an 0.02% (w/v) solution of TSA in acetonitrile–water (30:70 v/v) (1 ml). The solutions were mixed and analysed immediately.

Standard curve for TM

Freshly prepared solutions of TM (0.5, 1.0, 1.5, 2.0, 2.5, 3.0, 3.5 · 10^{-4} *M*) were submitted to analysis. The coefficient of variation (C.V.) at 1.5 · 10^{-4} *M* was determined using 6 replicate determinations.

Standard curve for EtHg chloride

Freshly prepared solutions of EtHg chloride (0.4, 0.8, 1.2, 1.6 and 2.0 · 10^{-4} *M*) were submitted to analysis. The C.V. at 1.2 · 10^{-4} *M* was determined using 6 replicate determinations.

Effect of sodium chloride on assay for TM

Freshly prepared solutions of TM (1.5 · 10^{-4} *M*) with and without sodium chloride (0.9%, w/v) were submitted to analysis involving addition to excess TSA.

Comparison of results for assay with that of dithiocarbamate method

A freshly prepared solution of TM (1.5 · 10^{-4} *M*) plus EtHg chloride (0.1 · 10^{-4} *M*) was submitted to analysis by both the assay involving addition of excess TSA and the previously reported method involving piperidinedithiocarbamate [9] using TM as the standard.

Photodegradation of TM

A sample of TM (0.01%, w/v; 2.47 · 10^{-4} *M*) in sodium chloride (0.9%, w/v) in a borosilicate glass flask was stored in direct sunlight and samples were withdrawn at 15, 30, 45, 60, 75, 90, 105 and 120 min and immediately submitted to HPLC analysis by both methods. A sample photodegraded for 60 min was submitted to analysis for total EtHg ion by both the method reported here and that using piperidinedithiocarbamate [9].

RESULTS AND DISCUSSION

The chromatographic conditions employed were identical to those of Lam *et al.* [17]. The method differs by preparing samples either by dilution (1:1) with acetonitrile–water (30:70 v/v) which enables TM to be quantitated or by dilution (1:1) with ace-

TABLE I

DATA FOR ASSAYS OF THIOMERSAL AND ETHYLMERCURIC CHLORIDE

Area response = slope × concentration (M) + intercept.

	Slope × 10^{10}	Intercept × 10^{6}	r	n	Concentration range (M)
TM without excess TSA	3.44	−0.184	0.9998	7	$0–3.5 \cdot 10^{-4}$
TM with excess TSA	3.48	−0.233	0.9997	7	$0–3.5 \cdot 10^{-4}$
EtHg chloride with excess TSA	3.39	−0.123	0.9998	5	$0–2.0 \cdot 10^{-4}$

tonitrile–water (30:70, v/v) containing TSA (0.02%, w/v) which quantitates TM plus EtHg ion (Fig. 2). At this concentration of TSA, there is a 5.25-fold excess of TSA to EtHg (when TM is present at a nominal concentration of 0.01% (w/v) ($2.47 \cdot 10^{-4}$ M) and total available EtHg ion is the limiting factor of the stoichiometric ratio of species present. The high affinity of the organomercuric ion for thiol groups assures quantitative conversion of the EtHg ion from its various complexed forms in the system to the TM complex [20,21].

When both diluent systems were applied to freshly prepared standards of TM identical calibration lines were obtained for the assays with and without TSA and for EtHg chloride with TSA (Table I). The C.V. values at $1.5 \cdot 10^{-4}$ M for TM with and without TSA were ± 1.02% and 0.87%, respectively, and for EtHg chloride the C.V. was ± 1.72% at a concentration of $1.2 \cdot 10^{-4}$ ($n = 6$ in all cases).

The assay suffers no interference from sodium chloride, a common component of pharmaceutical products which is known to complex with the EtHg ion [mean and C.V. for TM ($1.5 \cdot 10^{-4}$ M) with and without sodium chloride (0.9%, w/v) ($n = 4$): $\bar{x} = 1.48 \cdot 10^{-4}$ M ± 0.48% and $\bar{x} = 1.51 \cdot 10^{-4}$ M ± 0.62%]. The assay involving the addition of excess TSA affords identical results for samples containing TM ($1.5 \cdot 10^{-4}$ M) plus EtHg chloride ($0.1 \cdot 10^{-4}$ M) when compared with the previously reported method involving chromatography of the piperidinedithiocarbamate complex of total EtHg ion [9] [mean and C. V. ($n = 4$) for TSA assay; $1.58 \cdot 10^{-4}$ M; ± 1.10% and for the piperidinedithiocarbamate assay: $1.59 \cdot 10^{-4}$ M; ± 0.92%], the samples being compared against TM as a standard.

When photodegraded samples of TM were submitted to analysis both with and without excess TSA results were obtained demonstrating the presence of substantial amounts of free EtHg ion (Fig. 3). A photodegraded sample (sunlight for 1 h) of

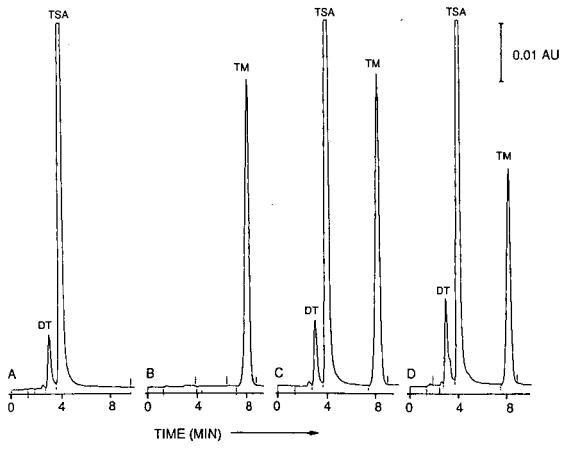

Fig. 2. Representative chromatograms derived by application of the assay. (A) TSA blank; (B) TM ($3 \cdot 10^{-4}$ M) without excess TSA; (C) TM ($3 \cdot 10^{-4}$ M) with excess TSA; (D) EtHg chloride ($2 \cdot 10^{-4}$ M) with excess TSA. DT = 2,2'-Dithiosalicylic acid contaminant in the thiosalicylic acid; TSA = thiosalicylic acid; TM = thiomersal.

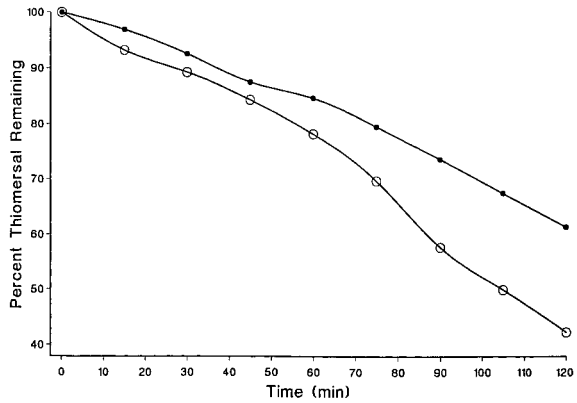

Fig. 3. Results of a typical experiment involving photodegradation of thiomersal in direct sunlight. ● = Concentration of TM with excess TSA; ○ = concentration of TM without excess TSA. The difference represents the amount of free EtHg ion.

TM (0.01%, w/v) when analysed by both the previously reported dithiocarbamate assay and the assay involving the addition of excess TSA gave identical results ($8.52 \cdot 10^{-3}$ and $8.44 \cdot 10^{-3}$%, w/v, remaining respectively calculated as TM). Under the conditions used for this degradation no free TSA was formed. This would be expected if excess EtHg ion were present. With consideration to the mode-of-action of antibacterial organomercurials [7,14] the formation of significant levels of excess EtHg ion would account for the enhanced antimicrobial activity of degraded samples of TM and the assay involving addition of TSA may more correctly reflect analytically the level of antimicrobial activity.

In conclusion, it should be noted that this simple adaptation applied to the method of Lam *et al.* [17] should be readily adaptable to a number of the other reported HPLC methods.

REFERENCES

1 *The Pharmaceutical Codex*, The Pharmaceutical Press, London, 11th ed., 1979, p. 940.
2 F. Tanaka and M. Mitsuno, *Ann. Rept. Takeda Res. Lab.*, 10 (1951) 65; C.A., 47 (1953) 4860 c.
3 B. J. Meakin and Z. M. Khammas, *J. Pharm. Pharmacol.*, 30 (1978) 52P.
4 C. M. McTaggart, J. Ganley, T. Eaves, S. E. Walker and M. J. Fell, *J. Pharm. Pharmacol.*, 31 (1979) 60P.
5 S. Pinzanti and M. Casini, *Farmaco, Ed. Prat.*, 35 (1980) 92; *Anal. Abstr.*, 39 (1980) 3E66.
6 S. N. Ibrahim, N. Stroud and B. J. Meakin, *J. Pharm. Pharmacol.*, 33 (1981) 7P.
7 D. J. G. Davies, Y. Anthony and B. J. Meakin, *Expo. – Congr. Int. Technol. Pharm. 3rd.*, 4 (1983) 238.
8 I. Ahmed. *Pharm. Res.*, 6 (1989) S19.
9 J. E. Parkin, *J. Chromatogr.*, 542 (1991) 137.
10 V. M. Trikojus, *Nature (London)*, 158 (1946) 472.
11 M. J. Reader and J. B. Lines, *J. Pharm. Sci.*, 72 (1983) 1406.
12 G. Anderman, J. Spittler and P. Jonvell, *Labo–Pharma —Probl. Techn.*, 32 (1984) 838, *Int. Pharm. Abstr.*, 25 (1988) 2501773.
13 E. Lüdtke and R. Pohloudek-Fabini, *Pharmazie*, 32 (1977) 625.
14 A. E. Elkhouly and R. T. Yousef, *J. Pharm. Sci.*, 63 (1974) 681.
15 C.-C. Fu and M. J. Sibley, *J. Pharm. Sci.*, 66 (1977) 738.
16 R. C. Meyer and L. B. Cohn, *J. Pharm. Sci.*, 67 (1978) 1636.
17 S. W. Lam, R. C. Meyer and L. T. Takahashi, *J. Parenter. Sci. Technol.*, 35 (1981) 262.
18 M. J. Reader, *J. Pharm. Sci.*, 73 (1984) 840.
19 G. C. Visor, R. A. Kenley, J. S. Fleitman, D. A. Neu and I. W. Partridge, *Pharm. Res.*, 2 (1985) 73.
20 R. B. Simpson, *J. Am. Chem. Soc.*, 83 (1961) 4711.
21 D. L. Rabenstein, *Acc. Chem. Res.*, 11 (1978) 100.

Journal of Chromatography, 587 (1991) 333–337
Elsevier Science Publishers B.V., Amsterdam

CHROM. 23 687

Short Communication

High-performance liquid chromatographic method for the determination of free gossypol in chicken liver

N. A. Botsoglou

Laboratory of Nutrition, School of Veterinary Medicine, Aristotelian University, 54006 Thessaloniki (Greece)

(First received March 20th, 1991; revised manuscript received August 13th, 1991)

ABSTRACT

A high-performance liquid chromatographic method for the determination of free gossypol in chicken liver at levels down to 0.5 ppm has been developed. Tissue was deproteinized with acetonitrile in presence of ascorbic acid and the filtrate was subjected to hydrolysis with hydrochloric acid. The liberated pure gossypol was partitioned into chloroform and analysed by gradient elution on a 10-μm C_{18} column. The overall recovery was 83.5 ± 2.6%, with an overall relative standard deviation of 9%.

INTRODUCTION

Cottonseed meal, a by-product of the cottonseed oil industry, is an important protein supplement for livestock feeding. Its utilization, however, is limited by the presence of gossypol (1,1′,6,6′,7,7′-hexahydroxy-5,5′-diisopropyl-3,3′-dimethyl-2,2′-binaphthalene-8,8′-dicarboxaldehyde), a compound with well documented toxic effects on animal species [1–3].

Following feeding to animals, gossypol is absorbed from the digestive tract and retained in the tissues where it occurs in both the free and protein-bound form. In liver tissue where the deposition of the free form appears particularly high, concentrations up to 323 and 94 ppm have been found in freeze-dried samples from pigs [4] and cows [5], respectively, and up to 415 ppm have been detected in fresh trout liver [6]. High gossypol concentrations in animal tissues may represent a concern for public health, considering the most harmful effect of gossypol, cardiotoxicity; in China, a low birthrate and high incidence of heart problems have been associated with gossypol in raw cottonseed oil [7], and hypokalaemic paralysis, an infrequent side-effect, was the major drawback of the use of gossypol (20 mg/day for 75 days) as an antifertility agent in men [8].

It seems, however, that the spectrophotometric method [9] used to determine gossypol in animal tissues overestimates the true concentrations. This method, which is based on the reaction of the aldehyde groups of gossypol with aniline to form dianilinogossypol, suffers from interferences from extraneous materials affecting the absorbance values [9]. False-positive readings have been reported for tissues that were known to be free from gossypol; diaphragm muscle and bile from animals fed gossypol-free diets [4] were found to contain as much as 24.5 and 100.3 ppm of gossypol, respectively. There has therefore been increasing interest in the development of more reliable methods.

Considerable progress has been made recently with the use of liquid chromatography (LC). Vari-

0021-9673/91/$03.50

ous LC methods allowing the accurate, precise and sensitive determination of gossypol in human plasma have been presented [10–13]. A survey of the literature, however, shows that such a method is not available for animal tissues.

This paper describes a high-performance liquid chromatographic (HPLC) method that has been developed for the determination of gossypol in chicken liver.

EXPERIMENTAL

Instrumentation

HPLC was carried out on a Perkin-Elmer (Norwalk, CT, USA) system consisting of a Series 3 modular chromatograph equipped with two reciprocating pumps controlled by mirocomputer, a power solvent mixer, an LC-100 column oven, an LC-55-B UV–VIS spectrophotometer and a Model 023 variable-span recorder. A Perkin-Elmer LC-55-S digital scanner permitted the monitoring of corrected spectra of the eluted compounds under stop-flow conditions; trapping of the eluates in the flow cell could be effected by shutting off the pump power and, simultaneously, closing a stop-flow valve located before the Rheodyne Model 7105 injector.

Injections were made on a 25 × 0.46 cm I.D. column laboratory packed with Spherisorb ODS-2, 10 μm (Phase Separations, Norwalk, CT, USA). Packing was accomplished at pressure of 42.8 MPa by the downwards slurry-packing technique on a Magnus Scientific (Aylesbury, UK) P6060 HPLC slurry-packer using as the suspending medium methanol–water (80:20 v/v) containing 0.0002 g/ml of sodium acetate [14].

Homogenization of tissue samples was performed in a domestic blender and hydrolysis of the extracts in a Tamson (Zoetermeer, Netherlands) Model T.X.V. 45 constant-temperature water-bath (accuracy ±0.1°C).

Chemicals and reagents

Analytical-reagent grade ascorbic acid, acetonitrile, chloroform, hydrochloric (37% min.) and phosphoric acid were obtained from Merck (Darmstadt, Germany), HPLC-grade methanol from Prolabo (Paris, France) and gossypol–acetic acid (89.62% pure gossypol) from Makor Chemicals (Jerusalem, Israel). Stock solutions of gossypol were prepared by weighing *ca.* 25 mg of gossypol–acetic acid and diluting to 50 ml with acetonitrile. Aliquots of these solutions were further diluted with acetonitrile to give working solutions that contained pure gossypol in the range 0.8–8 μg/ml. Working solutions were prepared daily and protected from light throughout the analysis.

Sample preparation

A 2-g sample of chicken liver was blended for 2 min with 50 ml of acetonitrile–water (40:10, v/v) containing 2% of ascorbic acid. After the precipitated proteins has settled, the supernatant liquid was filtered through Whatman No. 40 paper, discarding the first 5 ml of the filtrate. A 25-ml aliquot of the clear extract was pipetted into a 50-ml volumetric flask and 0.05 ml of hydrochloric acid was added. The flask was placed in a 65°C water-bath, stoppered after equilibration for 5 min and then heated for 100 min. After cooling to room temperature, the flask contents were transferred into a 250-ml separating funnel and 50 ml of 0.3% aqueous ascorbic acid followed by 0.5 ml of hydrochloric acid were added. The suspension formed was extracted with 25 ml of chloroform and the separated bottom layer was filtered through anhydrous sodium sulphate on Whatman No. 40 paper into a 100-ml flask to be further evaporated under vacuum at 35°C. Traces of solvents were expelled with a stream of nitrogen and the remaining residue was dissolved in $\geqslant 1$ ml of acetonitrile, the volume depending on the expected gossypol content of the processed sample.

Chromatography and quantification

Aliquots (25 μl) of sample extracts were injected into the chromatograph and analysed at a mobile phase flow-rate of 1.5 ml/min, a detection wavelength of 254 nm, a chart speed of 15 cm/h and a recorder sensitivity of 0.050 a.u.f.s. Chromatography was performed at 30°C to isolate the column from fluctuations in ambient temperature.

The mobile phase consisted of two solvents, methanol and water, both containing 0.1% of phosphoric acid. The water used in the mobile phase was glass-distilled water that had been further purified by passing it through a C_{18} column. Elution of gossypol was carried out by programming the metha-

nol–water mobile phase composition (v/v) as follows: 2 min isocratic at 82:18; 2 min linear gradient to 92:8; 5 min isocratic at 92:8; 3-min purge at 99:1, and 10-min equilibration at 82:18. After each day's work, the column was flushed with water until free from acidity and maintained filled with methanol.

Calibration graphs were prepared daily by running 25-μl aliquots from the series of the working solutions and plotting the recorded peak heights versus the amount of gossypol injected. The concentration of gossypol in the samples was calculated by reference to this calibration graph and multiplication by appropriate dilution factor as follows:

$$\text{Gossypol in samples (ppm)} = (QV \cdot 2)/(0.025\ W)$$

where Q = amount of gossypol found (ng), V = volume of final sample dilution (ml) and W = weight of sample (g).

RESULTS AND DISCUSSION

As gossypol is easily oxidized in aqueous solution, attempts were made to protect the compound against oxidative degradation from the very beginning of sample handling. Wang *et al.* [11] reported that a considerable loss of gossypol in human plasma kept at 0°C for 6 h occurs unless reduced glutathione is added. A series of pertinent experiments with liver samples showed that addition of 2% of ascorbic acid to the extraction solvent could efficiently protect gossypol, increasing its recovery from 10% to more than 80%.

The extraction of gossypol from liver samples was carried out with aqueous acetonitrile, a solvent which effectively precipitates proteins. With this solvent, further clarification of the homogenates such as that proposed by Smith [9], for extracting gossypol from animal tissues with an ethanol–water–diethyl ether–acetic acid solvent mixture, was not needed as clear filtrates were taken after a 1-min settling time. These observations concur with those of Wang *et al.* [11] and Wu *et al.* [12], who also used acetonitrile for deproteinization purposes in the determination of gossypol in human plasma, while Sattayasai *et al.* [10] deproteinized human plasma by using ethanol.

Purification of the protein-free filtrates was performed by partitioning them between chloroform and water, a procedure that has been effectively applied in the determination of total gossypol in cottonseed meals [15]. With this procedure, however, gossypol could not be partitioned into chloroform although this solvent quantitatively extracts the compound from its aqueous solutions provided that acid has been added to suppress gossypol ionization. As this might be due to the well known tendency of gossypol to form complexes with various metal ions [16], amino acids, phospholipids [17], etc., a debinding process was evaluated. Sattayasai *et al.* [10] reported that some chelating agents such as EDTA disodium salt can break gossypol complexes into pure gossypol, which can be easily extracted, and in previous work [18] it was found that an acid hydrolysis procedure at 65°C for 60 min can debind gossypol from cottonseed meal extracts. Application of these procedures in liver analysis showed that both worked equally well as far as the recovery was concerned, provided that the hydrolysis time was prolonged to 100 min. The EDTA procedure, however, increased the level of endogenous compounds that were coextracted with gossypol.

HPLC of the injected samples was initially performed under isocratic conditions using a mobile phase of methanol–water (88:12, v/v) containing 0.1% of phosphoric acid. The addition of the acid eliminated peak tailing by suppressing the ionization of the phenolic hydroxyl groups of gossypol, but the separation of the compound from other constituents could not be effected. To improve the resolution, the mobile phase composition was altered to contain less methanol but, surprisingly, even at 87% methanol the gossypol peak almost disappeared. Therefore, a short isocratic step at 82% methanol was finally used to elute the less retained compounds, and a rapid linear gradient to 92% methanol followed by an isocratic run was then applied to elute gossypol at 8.1 min without affecting its peak shape (Fig. 1a). With this solvent programme, however, further purification of the distilled water used in the mobile phase was essential, as otherwise a baseline rise appeared midway through each run even when no sample had been injected. This rise was found to be due to UV-absorbing impurities in the distilled water that concentrated on the top of the column during the equilibration period and eluted once the gradient was started.

Under the mentioned conditions, gossypol could

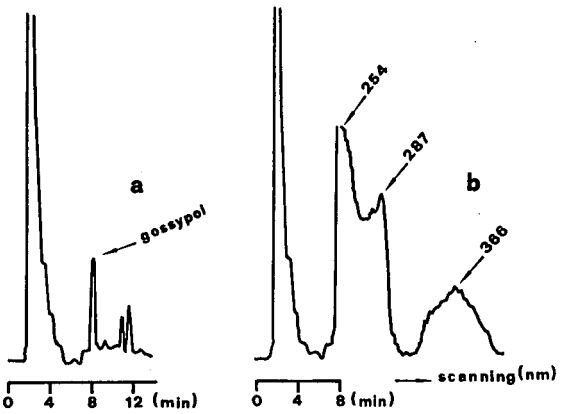

Fig. 1. (a) Typical chromatogram of chicken liver spiked with 2.4 ppm of gossypol and (b) absorbance scan of gossypol peak apex for sample spiked with 5.8 ppm of gossypol. HPLC conditions: solvent programme as in text using methanol and water, each containing 0.1% of phosphoric acid; column, 25 × 0.46 cm I.D., C_{18}, 10 μm; temperature, 30°C; flow-rate, 1.5 ml/min; detection wavelength, 254 nm; recorder sensitivity, 0.050 a.u.f.s.; chart speed, 15 cm/h; injection volume, 25 μl.

be determined in chicken liver at levels down to 0.5 ppm. Characterization of the recorded peak was based on the retention behaviour of the compound, but further characterization could be made possible by on-line scanning of the peak apex (Fig. 1b) and comparison of the spectral scan with the published absorption curve [19], provided that the sample contained more than 5 ppm of gossypol.

Regression analysis of the data obtained by running a series of working solutions showed the response to be linear within the range studied [0.050 a.u.f.s., $y = -0.24 + 0.421x$, correlation coefficient (r) = 0.9999, where y represents the peak height in mm and x the amount of gossypol injected in ng]. Therefore, the recovery of gossypol could be evaluated by adding various amounts of working solutions to liver samples and analyzing three replicates. The concentrations examined ranged from 1.4 to 44.8 ppm. Least-squares and regression analysis of the data (Table I) showed that the relationship between the added and found amounts was adequately described by a linear regression (r = 0.9987). Hence the slope (0.835 ± 0.026) of the regression line (y = −0.08 + 0.835x) could be used as an estimate of the overall recovery (83.5 ± 2.6%) in the determination of gossypol in chicken liver.

TABLE I

RECOVERY DATA FOR THE DETERMINATION OF GOSSYPOL IN CHICKEN LIVER

Concentration added (ppm)	Mean concentration found[a] (ppm)	Mean recovery (%)
1.4	1.2 ± 0.06	85.7
2.8	2.2 ± 0.15	78.6
5.6	4.3 ± 0.36	76.8
11.2	9.7 ± 0.40	86.6
22.4	18.2 ± 0.71	81.2
44.8	37.4 ± 1.43	83.5

[a] Mean of three (2-g) replicates ± S.D.

TABLE II

PRECISION DATA FOR THE DETERMINATION OF GOSSYPOL IN CHICKEN LIVER

Day	Concentration of gossypol found (ppm)	Mean concentration (ppm)	S.D.	R.S.D.[a] (%)
1	2.6, 2.6, 3.1, 2.9, 2.9, 2.9	2.8	0.20	7.1
2	3.2, 3.3, 3.2, 2.6, 3.0, 2.7	3.0	0.29	9.7
3	3.0, 3.4, 3.1, 3.3, 3.3, 3.0	3.2	0.17	5.3

Variance estimates

Source	R.S.D.[a] (%)
Within-day	7.5
Between-days	5.0
Overall	9.0

[a] Relative standard deviation.

The precision of the method was also studied by assaying, on each of three different days, six liver samples spiked with gossypol at the 3.7 ppm level and submitting the data (Table II) to analysis of variance and expected mean squares for the one-way classification-balanced design [20]. The within-day precision was found to be 7.5%, the between-days precision 5.0% and the overall precision 9.0% (relative standard deviation).

In conclusion, the results show that the proposed HPLC method is an efficient means of determining free gossypol in chicken liver. As the method can easily be applied to the analysis of other tissues, it offers the opportunity to study the deposition of the compound in chickens fed cottonseed meal diets.

REFERENCES

1 R. A. Phelps, *World's Poult. Sci.*, 22 (1966) 86.
2 L. M. Hudson, L. A. Kerr and W. R. Maslin, *J. Am. Vet. Med. Assoc.*, 192 (1988) 1303.
3 S. E. Morgan, *Vet. Clin. North Am., Food Anim. Sci.*, 5 (1989) 251.
4 M. P. Sharma, F. H. Smith and A. J. Clawson, *J. Nutr.*, 88 (1966) 434.
5 T. O. Lindsey, G. E. Hawkins and L. D. Guthrie, *J. Dairy Sci.*, 63 (1980) 562.
6 J. N. Roehm, D. J. Lee and R. O. Sinnhuber, *J. Nutr.*, 92 (1967) 425.
7 P. R. Cheeke and L. R. Shull, *Natural Toxicants in Feeds and Poisonous Plants*, Avi, Westport, CT, 1985, p. 345.
8 S. Z. Qian and Z. G. Wang, *Annu. Rev. Pharmacol. Toxicol.*, 24 (1984) 329.
9 F. H. Smith, *J. Am. Oil. Chem. Soc.*, 42 (1965) 145.
10 N. Sattayasai, J. Sattayasai and V. Hahnvajanawong, *J. Chromatogr.*, 307 (1984) 235.
11 M.-Z. Wang, D.-F. Wu and Y.-W. Yu, *J. Chromatogr.*, 343 (1985) 387.
12 D.-F. Wu, M. M. Reidenberg and D. E. Drayer, *J. Chromatogr.*, 433 (1988) 141.
13 D. Wu, Y. Yu and D. Zheng, *Yaoxue Xuebao*, 23 (1988) 927.
14 J. H. Knox, J. N. Done, A. F. Fell, M. T. Gilbert, A. Pryde and R. A. Wall, in J. H. Knox (Editor), *High-Performance Liquid Chromatography*, Edinburgh University Press, Edinburgh, 1978, p. 151.
15 N. A. Botsoglou and D. C. Koufidis, *J. Assoc. Off. Anal. Chem.*, 73 (1990) 447.
16 R. Adams, T. A. Geissman and J. D. Edwards, *Chem. Rev.*, 60 (1960) 555.
17 F. H. Matson, J. B. Martin and R. A. Volpenheim, *J. Am. Oil Chem. Soc.*, 37 (1960) 154.
18 N. A. Botsoglou, *J. Agric. Food Chem.*, 39 (1991) 478.
19 V. L. Frampton, J. D. Edwards and H. R. Henze, *J. Am. Chem. Soc.*, 70 (1948) 3944.
20 G. T. Wernimont, in W. Spendley (Editor), *Use of Statistics to Develop and Evaluate Analytical Methods*, Association of Official Analytical Chemists, Arlington, VA 1987, pp. 112–143.

Journal of Chromatography, 587 (1991) 338–342
Elsevier Science Publishers B.V., Amsterdam

CHROM. 23 700

Short Communication

Preconcentration technique for introducing gaseous or volatile compounds into a capillary gas chromatographic column

Tomoya Kohno and Kazuhiro Kuwata*

Environmental Pollution Control Centre, 1-3-62 Nakamichi, Higashinari-ku, Osaka City 537 (Japan)

(First received May 23rd, 1991; revised manuscript received August 20th, 1991)

ABSTRACT

A convenient cryofocusing technique was developed for introducing a gas or vapour sample into a capillary column. Precise temperature control was attained at the trapping segment down to −165°C in a gas chromatographic oven by controlling the flow-rate of liquid nitrogen to the trap. Gas samples, including low-boiling compounds, such as ethane, ethylene, propane, hydrogen sulphide and methanethiol, were accurately determined by cryofocusing at −165°C and by capillary gas chromatography.

INTRODUCTION

A number of cryofocusing techniques have been applied in capillary gas chromatographic (CGC) analyses of volatile compounds to give the highest attainable resolution [1–11]. These techniques ensure a better inlet-plug profile during injection into a capillary column. Conventional cryofocusing kits are usually installed outside the oven as they are relatively large and of high heat capacity in condensation and thermal desorption processes. Moreover, the vapours thermally desorbed from the trap should be re-focused at the head of the capillary column by cooling the GC oven to −98 to −50°C with a cryogen [5–8]. These procedures may be laborious, and impractical for automated analyses with reasonable accuracy. Recently, innovative multi-dimensional high-resolution GC [12,13] and cryostat systems [14–17] have been developed to enrich minor components with wide ranges of volatility and polarity. Several kits are commercially available, but they are expensive, large and complicated in operation.

This paper describes a convenient and inexpensive cryostat system that overcomes the disadvantages of conventional techniques. The cold trap used is small, light and of a low heat capacity, and is easily installed inside any GC oven. The cryofocusing tube can be cooled to any desired temperature down to −165°C by differentially controlling the flow-rate of liquid nitrogen to the cold trap. Automatic operation was readily available for determining low-boiling compounds.

EXPERIMENTAL

Standard reagents, gases and materials

Reagents and standard gases (100 ppm) were obtained from Wako (Osaka, Japan) and GL Science (Tokyo, Japan), respectively. The gas samples were

0021-9673/91/$03.50

prepared for test by diluting the standards with air to 0.5–1.0 ppm (v/v) in Flek samplers (polyester film bags) (Ohmi Odor Air Service, Shiga, Japan).

Cryostat system

Fig. 1 shows the cryostat system. The cold trap consists of a stainless-steel "mist feeder", a PTFE cooling tube, stainless-steel connection tube and a fine sheath thermocouple. A 250 mm × 0.53 mm I.D. × 0.7 mm O.D. fused-silica tube (Supelco, Bellefonte, PA, USA) and a 250 mm × 0.53 mm I.D. × 0.7 mm O.D. Pora-PlotQ porous-layer open-tubular (PLOT) column (Chrompack, Middelburg, Netherlands), inserted through the cooling tube, were used as cryofocusing tubes for trapping low-boiling compounds. Only a 10-cm segment of the cryofocusing tube was cooled in the cooling zone. The cryofocusing tube was connected with an analytical wide-bore open-tubular column or a capillary column by using a Supelco glass seal connector.

The internal pressure of the liquid-nitrogen container drove liquid nitrogen to the cold trap. The internal pressure was generated by switching a Skinner (New Britain, CT, USA) Model 16DK1050-GB three-way solenoid valve A to introduce 2.5–5.0 p.s.i. of nitrogen gas adjusted by a pressure regulator. On the other hand, the pressure was released at a limited rate by using a Skinner Model B2DA1052-GB two-way valve B under the command of an Omron (Kyoto, Japan) Model E5BX-A temperature monitor sending quick switching signals. The temperature monitor, where a desired temperature was set, closed valve B when it detected a higher temperature than the set temperature. The flow-rate of cryogen to the trap was thus increased. On the other hand, the monitor opened valve B to reduce the flow-rate when a lower temperature was detected. The cooling time and period were programmed in the microprocessor together with the GC control parameters.

Analytical apparatus

Fig. 2 shows the major components of the analytical system. A Valco Instruments (Houston, TX, USA) Model 1/16-V-6P six-way switching valve and a 1-, 2- or 9-ml sampling loop made of stainless-steel or PTFE tubing were used for sample introduction. They were placed in an oven heated at 165 and 120°C for hydrocarbons and sulphur compounds, respectively.

For the determination of low-boiling hydrocarbons, a Hewlett-Packard (Avondale, PA, USA) Model 5880A gas chromatograph was equipped with (1) a 30 m × 0.53 mm I.D. OV-1 wide-bore

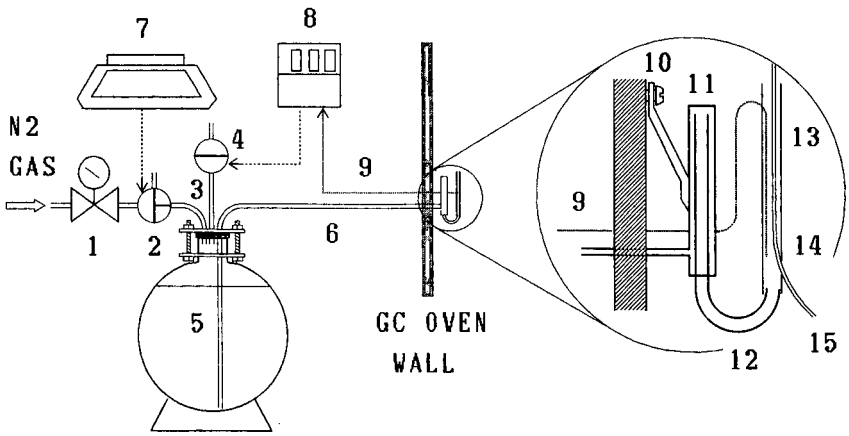

Fig. 1. Cryostat system. 1 = Pressure regulator (selectable in the range 2.5–5.0 p.s.i. according to the GC oven temperature and the desired trap temperature); 2 = three-way solenoid valve A; 3 = connection tube (2.0 mm I.D. × 3.2 mm O.D. SUS316 stainless-steel open tube); 4 = two-way solenoid valve B; 5 = 5-l liquid nitrogen container (a vacuum bottle plugged with a silicone-rubber stopper fixed with screw clamps); 6 = liquid-nitrogen carrier tube (ca. 600 mm × 2 mm I.D. × 3.2 mm O.D. PTFE tube); 7 = GC control microprocessor; 8 = temperature monitor; 9 = fine sheath thermocouple; 10 = screw clasp; 11 = mist feeder (125 mm × 4.5 mm I.D. × 6.4 mm O.D. SUS316 stainless-steel end-stopped tube); 12 = connection tube (150 mm × 2.0 mm I.D. × 3.2 mm O.D. SUS 316 stainless-steel open tube); 13 = cold trap (a 100 mm × 3.2 mm I.D. × 4.0 mm O.D. PTFE open tube); 14 = 0.5–0.7 mm diameter pin-hole; 15 = cryofocusing tube.

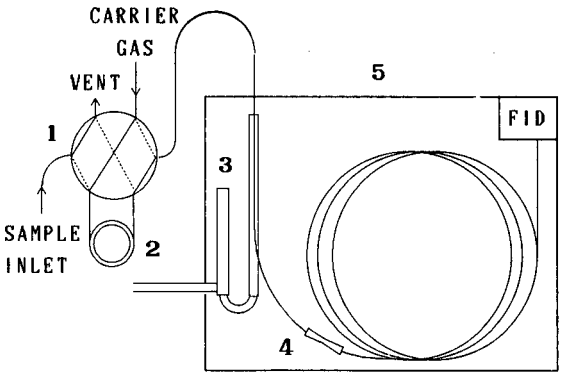

Fig. 2. Analytical system. 1 = Sampling valve; 2 = 1-, 2- or 9-ml sampling loop; 3 = cryofocusing system; 4 = glass seal connector; 5 = gas chromatograph with detector.

open-tubular (OVWOT) column or (2) a 30 m × 0.25 mm I.D. OV-1 capillary (OVC) column (Ohio Valley, Marietta, OH, USA) and a flame ionization detector. For the former column, the temperature was 30°C for 1 min, then programmed at 5°C/min to 100°C (250°C for the analysis of industrial emissions), and the carrier was 4.5 ml/min of nitrogen. For the latter column, the temperature was 30°C for 2.2 min, then programmed at 5°C to 100°C (250°C for the analysis of industrial emissions), and the carrier was 1.0 ml/min of nitrogen. The detector temperature was 250°C.

For the determination of sulphur compounds, a Varian (Walnut Creek, CA, USA) Model 1440 gas chromatograph was equipped with a 30 m × 0.53 mm I.D. OVWOT column and a flame photometric detector. The column temperature was 30°C for 3 min, then programmed at 5°C/min to 100°C, the carrier was 4.5 ml/min of nitrogen and the detector temperature was 160°C.

Analytical procedure

The cold trap was cooled to −165°C. A 1-, 2- or 9-ml volume of an air sample was taken in a sampling loop and transported into the cold trap with a carrier volume more than double the sample volume. Cooling was stopped and GC analysis was started. The components were identified by their retention times and determined from their peak areas.

RESULTS AND DISCUSSION

Cryostat system

The configuration of the proposed trap was effective in avoiding gradient cooling of the cryofocusing tube due to coarse cryogen droplets and did not affect the GC oven temperature. Fig. 3 shows temperature-control aspects at the cold trap. The trap temperature reached the desired temperature (−65 to −165°C) within 2 min after the start of the cooling. The temperature recovered to the oven temperature (30°C) within 2 min after stopping the cooling. A temperature dip was observed at the trap soon after the start of cooling, owing to heat conductance across the wall of the liquid-nitrogen carrier tube. This dip had no adverse effects on the analysis.

The temperature of the cooling zone depended strictly on the flow-rate of liquid nitrogen driven to the trap. The internal pressure of the liquid-oxygen container was differentially controlled by introducing 2.5–5.0 p.s.i. of nitrogen gas (determined considering the GC oven temperature and the trap temperature) into the container and by releasing the nitrogen from the container at a limited rate from valve B under the command of the temperature monitor. As a result, the temperature was precisely controlled down to −165°C. The temperature monitor indicated −165 ± ⩽2°C when it was set to −165°C. The cold trap could also be cooled to below −165°C. However, coarse cryogen droplets appeared on the thermocouple and disturbed the temperature monitor. Precise temperature control became more difficult at lower temperatures.

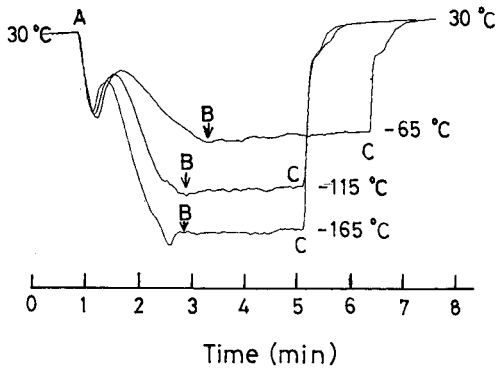

Fig. 3. Temperature-control aspects at the cold trap. (A) Cooling "on"; (B) sample introduction; (C) cooling "off".

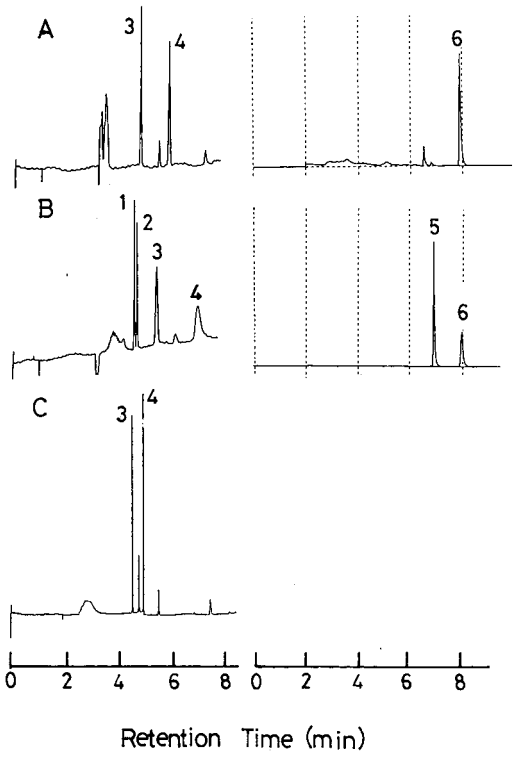

Fig. 4. Chromatograms of low-boiling compounds. Sample volume: 1 and 9 ml for analysis of hydrocarbons and sulphur compounds, respectively. For A, B and C, see Table I. Peaks: 1 = ethane (1 ppm); 2 = ethylene (1 ppm); 3 = propane (1 ppm); 4 = butane (1 ppm); 5 = hydrogen sulphide (0.8 ppm); 6 = methanethiol (0.5 ppm).

The cold trap and the carrier tube were of low heat capacity. Only the necessary amount of the cryogen was directed to the trap from the container. As a result, consumption of the cryogen was minimized. The trap had no effect on the GC oven temperature. A 180-ml volume of liquid nitrogen was consumed in a single run, requiring cooling for 5 min at −165°C. This is a very low consumption of the cryogen compared with conventional techniques.

The cryosat system was automatically operated by the microprocessor, using the low-pressure driving gas without direct handling of the cryogen during the analysis. The system was therefore safe in use.

Introduction of low-boiling compounds into a capillary column

The cryofocusing effects and the analytical accuracy were investigated by using gas samples containing 0.5–1.0 ppm (v/v) of low-boiling compounds such as C_1–C_4 aliphatic hydrocarbons, hydrogen sulphide and methanethiol. Fig. 4 shows chromatograms of these compounds and Table I indicates the analytical accuracy. The PLOT column was effective for cryofocusing the low-boiling compounds except methane. Ethane, ethylene and higher boiling hydrocarbons were well trapped in the cryofocusing tube at −165°C and accurately de-

TABLE I

ANALYTICAL ACCURACY FOR LOW-BOILING COMPOUNDS

S.D. = standard deviation; R.S.D. = relative standard deviation; n.d. = not detectable.

Compound[a]	Parameter[b]	A[c]	B[c]	C[c]
Ethane	S	n.d.	10.0 ± 0.07 (0.7)	n.d.
	PW	–	0.030 ± 0.0008	–
Ethylene	S	n.d.	10.1 ± 0.11 (1.1)	n.d.
	PW	–	0.026 ± 0.0009	–
Propane	S	15.8 ± 0.28 (1.8)	15.0 ± 0.17 (1.3)	15.7 ± 0.42 (2.7)
	PW	0.040 ± 0.0014	0.084 ± 0.0084	0.017 ± 0.013
Butane	S	18.0 ± 0.20 (1.1)	14.0 ± 0.096 (6.9)	17.9 ± 0.48 (2.7)
	PW	0.061 ± 0.0023	0.326 ± 0.0178	0.016 ± 0.0005
Hydrogen sulphide	S	n.d.	55.1 ± 4.20 (7.6)	n.d.
	PW	–	0.044 ± 0.0055	–
Methanethiol	S	33.7 ± 1.23 (3.6)	28.8 ± 1.50 (5.2)	n.d.
	PW	0.068 ± 0.0045	0.092 ± 0.0084	–

[a] Concentrations of ethane, ethylene, propane and butane = 1 ppm (v/v), hydrogen sulphide = 0.8 ppm and methanethiol = 0.5 ppm.
[b] S = Signal output of area ± S.D. (R.S.D., %) (average of five runs); PW = peak width ± S.D. (min) (average of five runs).
[c] Combination of a cryofocusing tube and an analytical column; (A) FST and OVWOTC; (B) PLOTC and OVWOTC; (C) FST and OVCC. Sample volume: 1 and 9 ml for hydrocarbons and sulphur compounds, respectively. For GC conditions, see text.

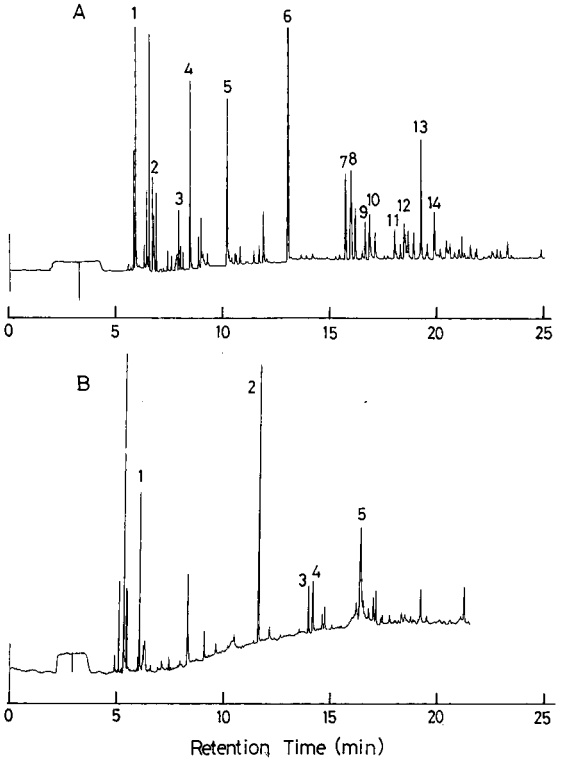

Fig. 5. Analyses of ambient air samples polluted by industrial emissions. For analytical conditions, see text. (A) Emission gas from a steel baking–coating process. Sample volume, 2 ml. Peaks: 1 = propionaldehyde (301 ppb, v/v); 2 = isopropanol (80 ppb); 3 = butyraldehyde (34 ppb); 4 = ethyl acetate (140 ppb); 5 = *n*-butanol (280 ppb); 6 = toluene (430 ppb); 7 = ethylbenzene (71 ppb); 8 = *m,p*-xylene (92 ppb); 9 = *o*-xylene (30 ppb); 10 = butyl Cellosove (79 ppb); 11 = benzaldehyde (32 ppb); 12 = *m*-ethyltoluene (32 ppb); 13 = pseudocumene (80 ppb); 14 = hemimellitene (43 ppb). (B) Emission gas from a photogravure printing works. Sample volume, 2 ml. Peaks: 1 = 2-propanol (15 ppb); 2 = toluene (56 ppb); 3 = ethylbenzene (14 ppb); 4 = *m,p*-xylene (19 ppb); 5 = *o*-xylene (7.4 ppb). All values (ppb) in American billion (10^9).

termined by GC with the OVWOT column. The detection limits of the hydrocarbons were 19–30 pg at three times the signal-to-noise ratio. Hydrogen sulphide and methanethiol were also well determined. The higher boiling organics were also effectively trapped on an ordinary fused-silica column. A higher trap temperature could therefore be selected for the determination of higher boiling organics to save the cryogen.

Application to analysis of environmental gas samples

Ambient air samples polluted by industrial emission sources were analysed by using the system with a 2-ml sampling loop (see Fig. 2) for hydrocarbons, aldehydes and others. Fig. 5 shows chromatograms for the succesful analysis of polluted air samples. Sharp and highly-resolved peaks were obtained for lower boiling compounds compared with conventional analysis.

CONCLUSIONS

The proposed cryofocusing system is convenient and useful for introducing low-boiling compounds except methane into a capillary column. The temperature of the 10-cm cryofocusing segment is accurately controlled at any desired temperature down to −165°C. Automatic operation can be programmed using a GC control microprocessor or other controller together with the GC operating parameters. The cryofocusing kit is easy to instal in any GC system. Operation is safe as there is no direct handling of the cryogen. The system may be useful for the determination of volatile organics in industrial emissions and air samples.

REFERENCES

1 P. Werkoff and W. Bretshneider, *J. Chromatogr.*, 405 (1987) 1.
2 R. D. Cox and R. F. Earp, *Anal. Chem.*, 54 (1982) 2265.
3 A. J. Netravaka and A. M. M. Rao, *Chromatographia*, 22 (1986) 183.
4 N. Schmidbauel and M. Oehme, *J. High. Resolut. Chromatogr. Chromatogr. Comm.*, 9 (1986) 502.
5 R. R. Arnts, *J. Chromatogr.*, 329 (1985) 399.
6 M. Ternonia and G. Alaerts, *J. Chromatogr.*, 328 (1985) 367.
7 J. F. Pankow, M. P. Ligocki, M. E. Rosen, L. M. Isabelle and K. M. Hart, *Anal. Chem.*, 60 (1988) 40.
8 W. A. McClenny, J. D. Pleil, M. W. Holdren and R. W. Smith, *Anal.Chem.*, 56 (1984) 2947.
9 W. F. Burns, D. T. Tinger, R. C. Evans and E. H. Bates, *J. Chromatogr.*, 269 (1983) 1.
10 B. E. Foulger and P. G. Simmonds, *Anal. Chem.*, 51 (1979) 1089.
11 S. Mitra and J. B. Phillips, *J. Chromatogr. Sci.*, 26 (1988) 620.
12 C. Bicchic, A. D'Amato, C. Frattini, G. M. Nago and A. Pisciotta, *J. High Resolut. Chromatogr.*, 12 (1989) 705.
13 S. Wu, W. H. Chatham and S. O. Farwell, *J. High Resolut. Chromatogr.*, 13 (1990) 229.
14 J. F. Pankow, *Development of purge-and-trap with whole-column cryotrapping for the analysis of groundwater contaminated with organic compounds*, PB Rep. (USA), PB-90-159245, Washington, DC, 1989, p. 36.
15 A. Van Es, J. Janssen, C. Cramers and J. Rijks, *J. High Resolut. Chromatogr. Chromatogr. Commun.*, 11 (1988) 852.
16 J. P. E. M. Rijks and J. A. Rijks, *J. High Resolut. Chromatrogr.*, 13 (1990) 261.
17 M. F. Mehran, M. G. Nickelsen, N. Golkar and W. J. Cooper, *J. High Resolut. Chromatogr.*, 13 (1990) 429.

Journal of Chromatography, 587 (1991) 343–346
Elsevier Science Publishers B.V., Amsterdam

CHROM. 23 758

Short Communication

Study of the response of three liquid crystals as stationary phases for the gas chromatography of some cyclic monoterpene volatile oil constituents with short retention times

T. J. Betts

School of Pharmacy, Curtin University of Technology, GPO Box U1987, Perth, W. Australia (Australia)

(First received July 22nd, 1991; revised manuscript received September 19th, 1991)

ABSTRACT

Eight cyclic monoterpene volatile oil constituents of short retention time were studied using three liquid crystals as gas chromatographic stationary phases in packed columns. Two phases (below) exhibited a different solute elution sequence after melting and supercooling. The third, bis-(methoxy-benzylidineanil-chloroaniline), did not, but still showed fairly good resolution. However, azoxydiphenetole offered the identification advantage of considerable changes in solute relative retention times, with melted *vs.* unmelted ratios of × 1.5 to × 3.0. Cineole and terpinolene were distinctive in giving for this ratio only × 0.9 on bis-(methoxy-benzylidineanil-bitoluidine). The results suggest that various parts of the melted or unmelted liquid crystal molecules participate in retaining the various solutes.

INTRODUCTION

In a previous study [1] of three liquid crystal stationary phases in packed columns used for gas chromatography it was noted that only on one of them, bis-(methoxy-benzylidineanil-bitoluidine), $(MBT)_2$, see Fig. 1, did cineole and caryophyllene give lower relative retention times to linalol on the melted, supercooled phase than on the unmelted liquid crystal at the same temperature. Most solutes were found to give higher relative retention times on melting the liquid crystals [1,2], including limonene on $(MBT)_2$. This author has previously used a liquid crystal phase to study some volatile oil constituents with short retention times such as cineole and limonene, although this was a mixed lyotropic phase [3]. The three packed columns of thermotropic liquid crystals (see Fig. 1) allowed a study of eight such quickly-emerging oil constituents on unmelted and melted supercooled phases to lead to deductions on the retention mechanisms of these liquid crystals and to see if there was any other case of the anomalous cineole-behaviour. The ability of the phases to resolve these eight cyclic substances, five with very similar molecular structure and boiling points, was also of interest.

EXPERIMENTAL

Apparatus

A Pye Unicam GCD gas chromatograph fitted with a flame ionization detector and a wide-range

0021-9673/91/$03.50

Acronym of liquid crystal and m.p. °C		Chemical formula	Chemical feature
$(MBCA)_2$	154	$(CH_3O-C_6H_4-CH=N-C_6H_3Cl-)_2$ bis-(methoxy-benzylidineanil-chloroaniline)	Anil dimer without spacing atoms between the central aromatic rings
$(MBT)_2$	181	$(CH_3O-C_6H_4-CH=N-C_6H_4-CH_2-)_2$ bis-(methoxy-benzylidineanil-bitoluidine)	Anil dimer with two central spacing methylene groups between aromatic rings
ADP	138	$(C_2H_5O-C_6H_4-N=)_2\rightarrow O$ azoxy-diphenetole	Azoxy compound with two central spacing nitrogen atoms between aromatic rings

Fig. 1. Details of liquid crystal stationary phases used. Note all are terminal di-ethers.

amplifier with a Hewlett-Packard 3380A recorder/integrator were used.

A packed glass column of 3% azoxy-diphenetole (ADP) was used, 1.5 m × 4 mm I.D, prepared as described previously [1]. A 20 ml min^{-1} flow of nitrogen was used as mobile phase. A similar column of 3% bis-(methoxy-benzylidineanil-chloroaniline), $(MBCA)_2$, was also studied using a slower flow of nitrogen, 8 ml min^{-1}. The 3% $(MBT)_2$ column was 1.5 × 2 mm I.D., and also had a nitrogen flow of 8 ml min^{-1}. All three columns had received previous careful use: none was "naive".

A Technoterm 7300 probe was used to observe oven temperatures to ± 0.1°C. Conditions used are given in the tables.

Materials and methods

The liquid crystals were from TCI, Tokyo.

p-Cymene, α-phellandrene*, α-terpinene, and γ-terpinene were from TCI. 1,8-Cineole (Faulding), limonene and α-pinene (BDH) and terpinolene* (Shanghai Essential Oils) were also used. See Fig. 2 for formulae. Materials marked * were impure, and the main peak was used. Injections were made from a microsyringe which had been filled, then "emptied".

Terpinolene (185^{0a}) has a 4-8 double bond.
γ-Terpinene (183^{0}) has a 4-5 double bond.
Limonene (176^{0}) has an 8-9 double bond.
α-Terpinene (174^{0}) has a 3-4 double bond.
α-Phellandrene (175^{0a}) has a 5-6 double bond.
α-Pinene (156^{0}) has a 6-8 bond.
Cineole (176^{0}) has a 1-8 *ether* bond and is fully saturated.
p-Cymene (177^{0}) has a fully *aromatic* ring.

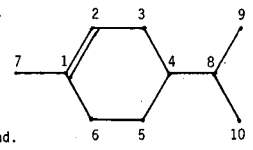

Fig. 2. Formulae of solutes used, with boiling points taken from ref. 5, except those marked *a* which come from ref. 6.

Holdup times were determined by extrapolating to methane the retention times of *n*-heptane and *n*-hexane plotted on logarithmic graph paper.

RESULTS AND DISCUSSION

Average results are given in Tables I and II. Due to the various melting points of the liquid crystals, different temperatures were used for each. α-Pinene, α-phellandrene, limonene and γ-terpinene retain this elution sequence in both tables, with the other four solutes changing positions.

Unlike the other two phases studied here, $(MBCA)_2$ after melting gave no change in the retention times for the eight solutes compared to its "unmelted" state. Their sequence was like that from the other two unmelted phases (Table I) with cineole last. The other di-anil liquid crystal $(MBT)_2$ on melting showed only slight, but definite, changes in relative retention times (from just over × 0.9 to × 1.2), and a different solute sequence, with cineole not last (Table II). With a similarly changed solute sequence, ADP on melting gave a considerable increase in relative retention times from × 1.5 to × 3.0. Thus ADP offers the greater chance for solute identification using the melted *vs.* unmelted phase observations: cineole distinctively changes only × 1.5; three solutes change about × 1.9; another three about × 2.6; and × 3.0 indicates *p*-cymene. Only terpinolene was found to behave like cineole and show a lower relative retention time to linalol on $(MBT)_2$ after melting. Cineole gave the lowest increase on melted ADP, but here behaves differently to terpinolene.

On the three "unmelted" phases (Table I), if the distinctively fastest α-pinene is ignored, $(MBT)_2$ clearly gives the poorest resolution with the longest

TABLE I

RELATIVE RETENTION TIMES (LINALOL = 1.00) ON COLUMNS OF 3% UNMELTED LIQUID CRYSTALS

Solute	ADP at 125°C	$(MBCA)_2$ at 120°C[a]	$(MBT)_2$ at 150°C
Cineole	0.19	0.32	0.44
Terpinolene	0.15	–[b]	0.44
γ-Terpinene	0.14	0.25	0.44
p-Cymene	0.12	0.24	0.43
Limonene	0.12	0.21	0.40
α-Phellandrene	0.13	0.19	0.39
α-Terpinene	0.11	0.20	0.38
α-Pinene	0.06	0.09	0.23

[a] $(MBCA)_2$ gave the same results after heating above its melting point and slowly supercooling to this temperature.
[b] No main peak discernable from impure solute.

time (0.44) being only about 115% of the shortest (α-terpinene). The other two phases show a time range of 160% or more, although $(MBCA)_2$ exhibits a better distribution of solute peaks. But ADP has the advantage of its two conditions, melted and unmelted.

To a considerable extent, the solutes studied emerge from the packed columns in the sequence of their boiling points (Fig. 2), particularly from the unmelted liquid crystals. Thus α-pinene is always quickest, as it is on conventional phases [4]. The ether cineole, however, is last from unmelted liquid crystals, reflecting its affinity for their ether structures (see Fig. 1) although this is not so apparent on $(MBT)_2$. On melted, supercooled liquid crystals the rigid structure of cineole probably becomes dominant, so it is one of the quickest solutes to emerge after the similarly box-like α-pinene, these two being unable to penetrate the liquid phase well. Terpinolene is similarly rigid due to its 4–8 double bond (see Fig. 2) and this sees it pass through these melted liquid crystals just after cineole, in contrast to being about last on the unmelted phases. Terpinolene, with the highest boiling point, is the last from conventional non-polar and polar phases [4]. The branched three-carbon side chains of the other solutes (see Fig. 2) can rotate allowing various molecular conformations, some of which presumably fit more readily into the melted liquid crystals. *p*-Cymene has the extra affinity of being an aromatic substance like the liquid crystals, and this is revealed by the melted phases retaining it longest (Table II). However, γ-terpinene, with its two unconjugated unsaturated groups on opposite sides of the ring, behaves very similarly to *p*-cymene. On the melted, supercooled liquid crystals, the least strongly retained solutes are, together with the three "rigid" molecules, those with conjugated double-bonds in their ring: α-phellandrene and α-terpinene. Thus the unconjugated double bond systems of limonene and γ-terpinene may allow them to be more strongly retained.

Why do the two similar anil phases behave differently? $(MCBA)_2$ behaves only like an unmelted liquid crystal here, although it has shown a "super-

TABLE II

RELATIVE RETENTION TIMES (LINALOL = 1.00) ON COLUMNS OF 3% MELTED, SLOWLY SUPERCOOLED LIQUID CRYSTALS, AND RATIOS TO THE UNMELTED VALUES

Solute[a]	ADP at 125°C		$(MBT)_2$ at 150°C	
	Time	Ratio	Time	Ratio
p-Cymene	0.36	× 3.0	0.53	× 1.2
γ-Terpinene	0.35	× 2.5	0.53	× 1.2
Limonene	0.32	× 2.7	0.49	× 1.2
α-Terpinene	0.29	× 2.6	0.43	× 1.1
Terpinolene	0.29	× 1.9	0.42	× 0.9
Cineole	0.28	× 1.5	0.41	× 0.9
α-Phellandrene	0.25	× 1.9	0.41	× 1.0
α-Pinene	0.12	× 2.0	0.23	× 1.0

[a] Solutes named in italics are in a different sequence to the unmelted phase (Table I).

cooled melted" response with other solutes [1]. It is the only one of the three liquid crystals used here without a central "spacer" of atoms between the aromatic rings. $(MBT)_2$ has $-Ar-CH_2-CH_2-Ar-$ present, and ADP has $-Ar-N=N-Ar-$ which may account for the two types of behaviour of solutes on these phases: there is no central space in $(MBCA)_2$ for them to fit into. Therefore it seems that various parts of the liquid crystal molecules participate in retaining different solutes: the terminal ether groups, and the central aromatic rings with or without spacing atoms between them. Some parts may be more effective in either the melted or the unmelted condition.

In other work by this author [1] a commercially available polysiloxane liquid crystal capillary seemed unsuitable for the analysis of these monoterpenes. It is unlikely that the three liquid crystals used here can be used for capillaries. But in packed columns they could supplement work with conventional phase capillaries. A column of ADP can be used for two different analyses without change (before and after melting) to provide an "extra dimension" in identification of these compounds.

ACKNOWLEDGEMENT

Thanks to Mr. B. Mackinnon for preparing the columns.

REFERENCES

1 T. J. Betts, *J. Chromatogr.*, 588 (1991) 231.
2 T. J. Betts, C. M. Moir and A. I. Tassone, *J. Chromatogr.*, 547 (1991) 335.
3 T. J. Betts, *J. Chromatogr.*, 467 (1989) 272.
4 N. W. Davies, *J. Chromatogr.*, 503 (1990) 1.
5 S. Budavari (Editor), *The Merck Index*, Merck & Co., Rahway, NJ, 11th ed., 1989.
6 R. C. Weast (Editor), *CRC Handbook of Chemistry and Physics*, CRC Press, Boca Raton, FL, 47th ed., 1966.

Journal of Chromatography, 587 (1991) 347–350
Elsevier Science Publishers B.V., Amsterdam

CHROM. 23 674

Short Communication

Simultaneous stereoanalysis of 2-alkyl-branched acids, esters and alcohols using a selectivity-adjusted column system in multi-dimensional gas chromatography

Volker Karl, Hans-Georg Schmarr and Armin Mosandl*

Institut für Lebensmittelchemie, Johann Wolfgang Goethe-Universität Frankfurt, Robert-Mayer-Strasse 7–9, W-6000 Frankfurt/Main (Germany)

(First received May 28th, 1991; revised manuscript received August 8th, 1991)

ABSTRACT

The direct and simultaneous stereodifferentiation of 2-methylbutanoic acid, 2-methylbutanoic acid methyl and ethyl esters and the corresponding alcohol 2-methylbutane-1-ol from complex matrices is achieved, using selectivity-adjusted multi-dimensional gas chromatography with perethylated β-cyclodextrin as the chiral stationary phase.

INTRODUCTION

Enzymatic reactions are commonly characterized by high stereoselectivity. In this respect, the evaluation of fruit-specific enantiomeric distributions has proved to be an appropriate criterion to differentiate natural flavour compounds from those of synthetic origin. Enantioselective multi-dimensional gas chromatography (MDGC) [1,2] is well established as a technique for the assignment of the origin of γ(δ)-lactones and also many chiral monoterpene compounds of essential oils [3–5].

In many instances, several chiral volatile compounds with different functionalities mainly contribute to the characteristic flavour of fruits and other foodstuffs. Hence chiral stationary phases of versatile enantioselectivity are highly desirable in capillary gas chromatography (cGC). Recently, the first simultaneous stereodifferentiation of all aroma-relevant γ(δ)-lactones from different fruits was described as the latest advance in the analytical differentiation between "natural" and "nature-identical" flavour compounds [6]. Using perethylated β-cyclodextrin as the chiral stationary phase, 2-methylbutanoic acid (**4**), 2-methylbutanoic acid methyl (**1**) and ethyl esters (**2**) and the corresponding alcohol 2-methyl-1-butanol (**3**), some of the most important chiral compounds of apple aroma, were separable into their mirror images [7,8].

This paper describes the direct and simultaneous chirality evaluation of all these substances from complex flavour extracts, using selectivity-adjusted MDGC.

EXPERIMENTAL

Sample preparation

Commercially available apple aroma concentrate A (B) was extracted with pentane–dichloromethane (2:1) under acidic conditions.

0021-9673/91/$03.50

Multi-dimensional gas chromatography

A Siemens SiChromat 2–8 double-oven system equipped with a "live-switching" coupling piece and two flame ionization detectors was used with hydrogen as the carrier gas and with split injection.

Open-tubular columns

Duran glass tubing (Schott Ruhrglas, Mainz, Germany) was drawn into capillaries of 0.23 or 0.32 mm I.D. using a Shimadzu GDM 1 glass-drawing machine. Acid leaching, rinsing and deactivation were performed as described [9–12].

Precolumn system

A 25 m × 0.23 mm I.D. restriction capillary, deactivated with diphenyltetramethyldisilazane (Fluka, Buchs, Switzerland) was coupled with a press-fit connection and a 5-cm fused-silica capillary to a 25 m × 0.32 I.D. glass capillary, deactivated with hexamethyldisilazane, coated with an 18.8% solution of PS-255 (a methylsilicone; Fluka) and 1.5% dicumyl peroxide (Aldrich, Milwaukee, WI, USA) in *n*-pentane–dichloromethane (1:1, v/v).

Main column system I

A 38 × 0.23 mm I.D. glass capillary column, deactivated with phenyldimethyldisilazane (Fluka), was coated with a 0.33% solution of heptakis (2,3,6-tri-O-ethyl)-β-cyclodextrin (33% in OV-1701-vi) in *n*-pentane–dichloromethane (1:1, v/v) [10,11]. The chiral stationary phase was synthesized as described [12].

Main column system II

Non-chiral main column. A 3 m × 0.32 mm I.D. fused-silica capillary coated with a 0.25-μm thick film of DB-1701 (J&W, Carlo Erba, Hofheim, Germany) was used.

Chiral main column. See main column system I.

Heart cutting

The chronological order of the "heart cuts" was as follows, with the cut time adapted to the amounts of the substances: **3**, 14.45–14.55; **1**, 18.15–18.45; **2**, 24.75–25.05; and **4**, 25.80–26.50 min.

RESULTS AND DISCUSSION

The enantiomeric distribution of chiral flavour

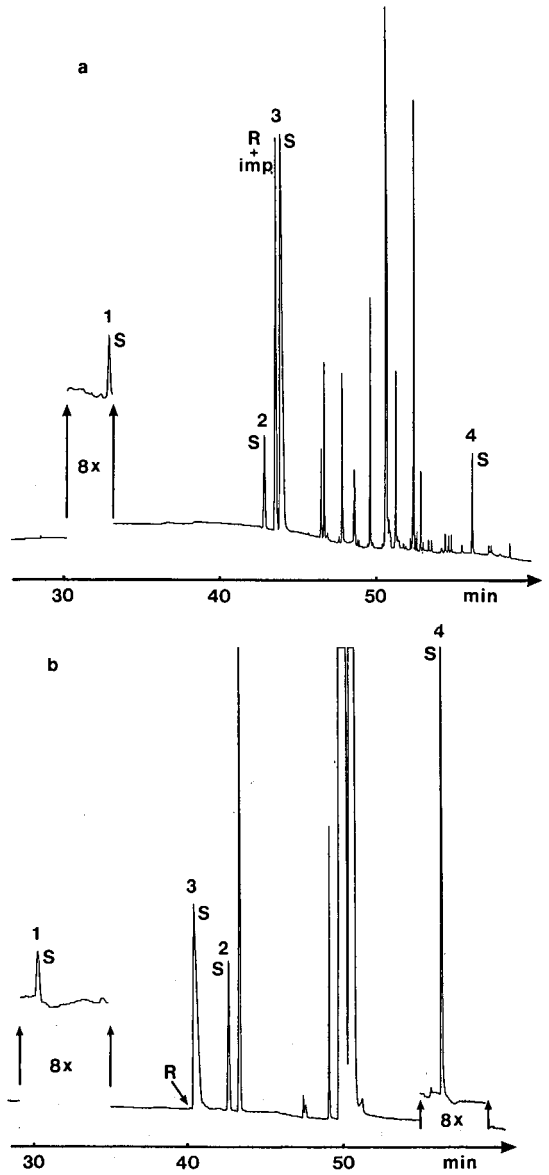

Fig. 1. (a) Enantioselective MDGC analysis of a genuine apple aroma concentrate A (main column system I). Temperature programme of the precolumn: 60°C isothermal for 20 min, then increased at 8°C/min to 240°C. Temperature programme of the main column: 40°C isothermal for 40 min then increased at 2°C/min to 50°C, 10°C/min to 90°C, 1.5°C/min to 105°C and 15°C/min to 210°C. (b) Enantioselective MDGC analysis of the same apple aroma concentrate (main column system II). Temperature programme of the precolumn: 60°C isothermal for 20 min, then increased at 8°C/min to 240°C. Temperature programme of the main column: 40°C isothermal for 35 min, then increased at 2°C/min to 50°C, 15°C/min to 90°C, 1.5°C/min to 110°C and 15°C/min to 210°C.

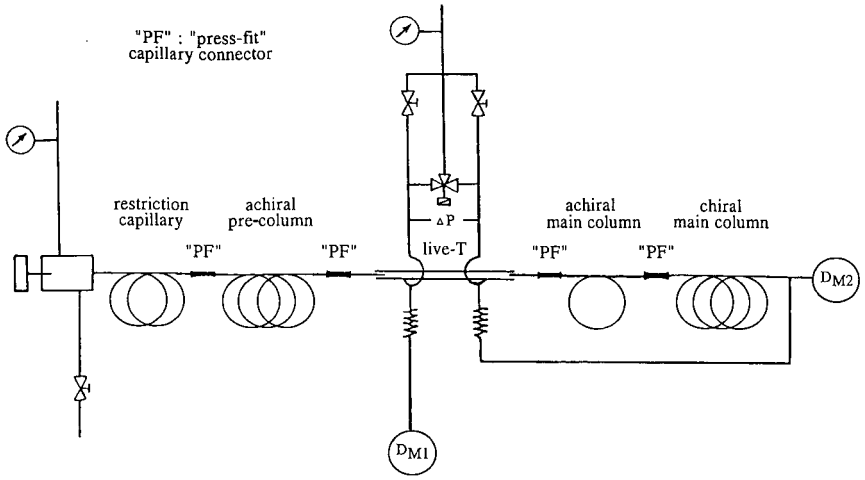

Fig. 2. Column switching in the applied MDGC system.

compounds in natural products reflects the enantiospecificity of their biogenesis. Therefore, the screening of enantiomer composition is a convenient method for differentiating between natural and nature-identical flavour compounds. Compounds **1–4** are well known to be some of the most important flavour compounds of apple aroma and their enantioselective analysis has been reported recently using heptakis (2,3,6-tri-O-ethyl)-β-cyclodextrin as a chiral CGC phase [8].

MDGC with a Superox 0.6 non-chiral precolumn and perethylated β-cyclodextrin as the chiral main column was applied previously to investigate the enantiomeric distribution of **1** and **2** [8]. However, this column combination was not suitable for separating the isomeric alcohol 3-methyl-1-butanol (isoamyl alcohol), also a well known component of apple aroma, from the stereoisomers of **3**. Therefore, the column combination had be optimized.

A column coated with a thick film of methylsilicone PS-255 seemed suitable as the precolumn in MDGC for further investigations. The stereoisomeric alcohols were separated at an elution temperature of about 60°C. Using the new column combination, all enantiomers of a standard mixture were baseline resolved. On analysing an apple aroma extract A for the mentioned chiral aroma compounds, the limitations of this configuration were established. Fig 1a shows the chromatogram obtained. The esters **1** and **2** and the acid **4** are detected as pure *S*-enantiomers. The enantiomer distribution of **3** seems to be different. A "single cut" of the alcohol indicated that this would be a misinterpretation; in fact, **3** has a nearly pure *S*-configuration. This means that unknown substances being transferred from the precolumn co-elute with **3** after their passage through the chiral main column. Obviously, the selectivities of the pre- and the main columns were too different.

Different columns with various polarities and columns coated with thick films of mixed stationary phases were tested to overcome this problem, without success.

An alternative approach was to adapt the pre- and the main columns by the additional insertion of a short non-chiral main column, coupled directly to the chiral main column with a press-fit connection (Fig. 2). A test with a 3 m × 0.32 mm I.D. fused-silica capillary coated with Supelcowax 10M (film thickness 0.25 μm) was not successful. The elution temperature of **4** was too high for the stereodifferentiation on perethylated β-cyclodextrin as the chiral stationary phase. Subsequently a 3 m × 0.32 mm I.D. fused-silica capillary coated with DB-1701 (film thickness 0.25 μm) was used. This combination was expected to be useful as the chiral material was dissolved in OV-1701-vi also.

The insertion of this short column had a very significant effect on the resulting chromatogram. The elution order of **3** and **2** is changed (Fig. 3). The

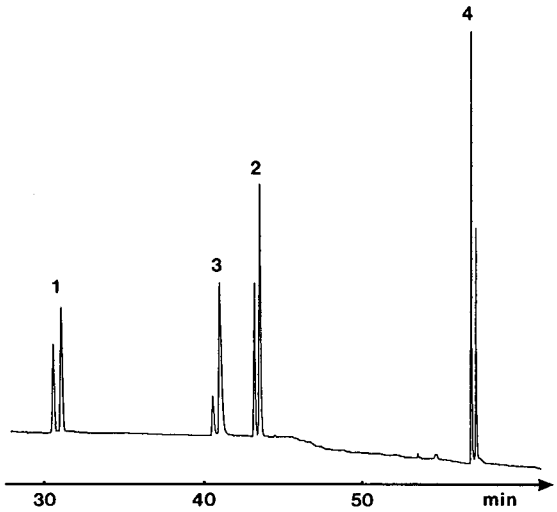

Fig. 3. Simultaneous enantioselective MDGC analysis of a standard mixture of methyl 2-methylbutanoate (**1**), ethyl 2-methylbutanoate (**2**), 2-methyl-1-butanol (**3**) and 2-methylbutanoic acid (**4**), all compounds *S*-enriched (main column system II). Temperature programme as in Fig. 1b.

resolution of the enantiomers is not affected by this added non-chiral main column.

Repeated analysis of the same apple aroma extract showed an improved accuracy. The enantiomer distribution of all the investigated compounds is now exactly determined (Fig. 1b).

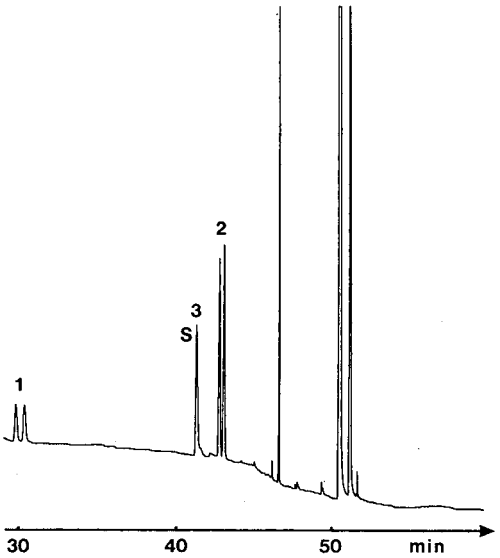

Fig. 4. Enantioselective MDGC analysis of an apple aroma concentrate B, adulterated by synthetic racemates of **1** and **2** (main column system I). Temperature programme as in Fig. 1b.

The analysis of another apple aroma concentrate (B) showed the improved speed of differentiation between natural and nature-identical compounds **1–3** (Fig. 4). After extraction with *n*-pentane–dichloromethane (2:1), the addition of nature-identical **1** and **2** was clearly detected by only one MDGC analysis.

CONCLUSIONS

Enantioselective inclusion GC with heptakis (2,3,6-tri-O-ethyl)-β-cyclodextrin as the chiral phase is an effective method for differentiating the mirror images of 2-methylbutanoic acid (**4**), the esters **1** and **2** and the corresponding alcohol **3**.

MDGC employing the heart-cutting technique from a suitable non-chiral precolumn onto a chiral main column, coated with perethylated β-cyclodextrin as the chiral stationary phase, allows the direct and simultaneous evaluation of the chirality of **1–4** from complex flavour matrices when an additional short nonchiral main column is inserted. The described modification of the main column system proved to be an efficient approach to realizing the simultaneous evaluation of the chirality of flavour compounds with different functionalities.

REFERENCES

1 C. Wang, H. Frank, G. Wang, L. Zhou, E. Bayer and P. Lu, *J. Chromatogr.*, 262 (1983) 352.
2 G. Schomburg, H. Husmann, E. Hübinger and W. A. König, *J. High Resolut. Chromatogr. Chromatogr. Commun.*, 7 (1984) 404.
3 E. Guichard, A. Kustermann and A. Mosandl, *J. Chromatogr.*, 498 (1990) 396.
4 K. Hildenbrand, N. Christoph and A. Bernreuther, *Dtsch. Lebensm.-Rundsch.*, 86 (1990) 39.
5 P. Kreis, U. Hener and A. Mosandl, *Dtsch. Aporth.-Ztg.*, 130 (1990) 985.
6 D. Lehmann, C. Askari, D. Henn, F. Dettmar, U. Hener and A. Mosandl, *Dtsch. Lebensm.-Rundsch.*, 87 (1991) 75.
7 A. Mosandl, K. Rettinger, B. Weber and D. Henn, *Dtsch. Lebensm.-Rundsch.*, 86 (1990) 375.
8 K. Rettinger, V. Karl, H.-G. Schmarr, F. Dettmar, U. Hener and A. Mosandl, *Phytochem. Anal.*, 2 (1991) 184.
9 K. Grob, *Making and Manipulating Capillary Columns for Gas Chromatography*, Hüthig, Heidelberg, 1986, p. 124.
10 V. Schurig and H.-P. Nowotny, *J. Chromatogr.*, 441 (1988) 155.
11 H.-P. Nowotny, D. Schmalzing, D. Wistuba and V. Schurig, *J. High Resolut. Chromatogr.*, 12 (1989) 383.
12 C. Askari, U. Hener, H.-G. Schmarr, A. Rapp and A. Mosandl, *Fresenius' J. Anal. Chem.*, 340 (1991) 768.

Journal of Chromatography, 587 (1991) 351–354
Elsevier Science Publishers B.V., Amsterdam

CHROM. 23 693

Short Communication

Thin-layer chromatographic separations of lantadenes, the pentacyclic triterpenoids from lantana (*Lantana camara*) plant

Om Prakash Sharma* and Rajinder Kumar Dawra

Biochemistry Laboratory, Indian Veterinary Research Institute, Regional Station, Palampur, Kangra Valley, H.P.-176 061 (India)

(First received June 21st, 1991; revised manuscript received August 15th, 1991)

ABSTRACT

Seven solvent systems of varying suitability are reported for the thin-layer chromatographic separation of lantadenes isolated from the heptatotoxic plant *Lantana camara* var. *aculeata*. Hexane–methanol–ethyl acetate (85:10:5) was found to be the most suitable for the separation of lantadene A, B, C, D, reduced lantadene A and reduced lantadene B. Lantadenes could be detected on thin layers of silica gel G using Liebermann–Burchard reagent, vanillin–sulphuric acid and primulin sprays.

INTRODUCTION

Lantana (*Lantana camara*) triterpenoids constitute a group of pentacyclic compounds called lantadenes, some of which have been shown to elicit hepatotoxicity in animals [1]. In the course of investigations on the purification and characterization of these compounds [2,3], a need arose to develop thin-layer chromatographic (TLC) procedures for the selection of liquid chromatographic systems and monitoring of column effluents, crystallization and purity. Lantadene A (LA), lantadene B (LB), lantadene C (LC), lantadene D (LD), reduced lantadene A (RLA) and reduced lantadene B (RLB) are the lantana triterpenoids which are of biological significance [1]. Previously, we have reported some solvent systems for the resolution of lantadene A from a number of other pentacyclic compounds [4]. Lantadenes differ from the latter compounds in having a side-chain at C-22 (Fig. 1). None of the systems individually was sufficient for the resolution of all the lantadenes, which have very similar polarities (Fig. 1). Here, we report the evaluation of various solvent systems, using silica gel G thin layers, for the resolution of putative hepatotoxins and related compounds from the lantana plant.

EXPERIMENTAL

Silica gel G was obtained from Sisco Research Labs. (Bombay, India). The solvents were of analytical-reagent grade and were freshly distilled before use. Lantadene A, B, C and D, reduced lantadene A and reduced lantadene B were prepared from *Lantana camara* var. *aculeata* (Red Flower variety) as described previously [2,3,5]. The identity of the compounds was confirmed by comparison with authentic standards and spectroscopic analysis. Cho-

0021-9673/91/$03.50

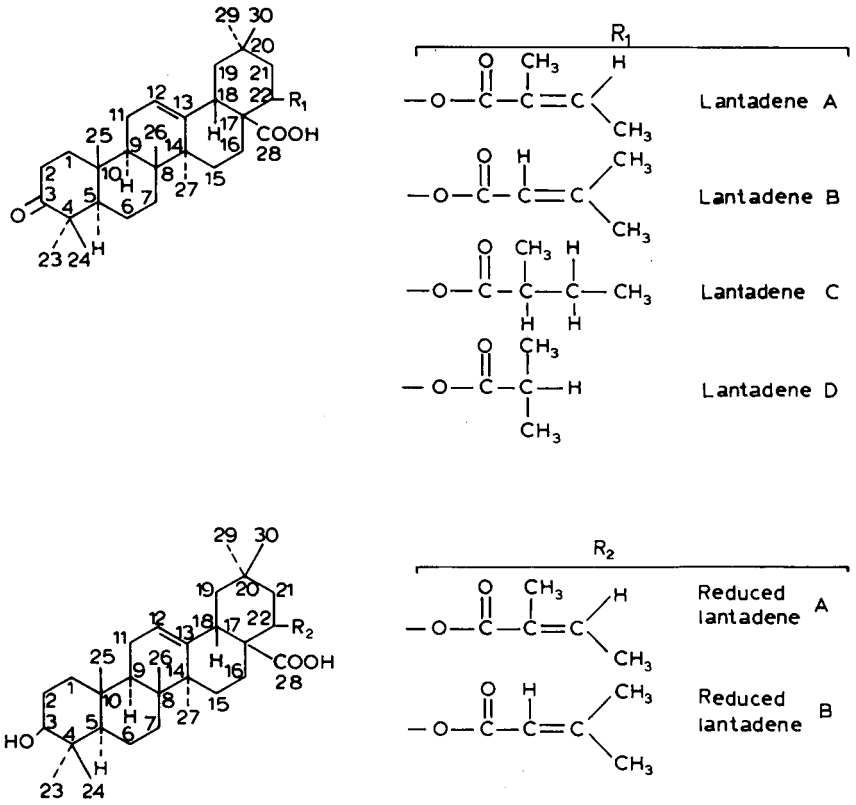

Fig. 1. Structures of lantadenes.

lesterol was purchased from E. Merck (Darmstadt, Germany) and primulin from Sigma (St. Louis, MO, USA).

Thin-layer plates (200 × 200 mm) were coated with silica gel G to a thickness of 0.2 mm, air dried and activated at 110°C for 1 h [6]. Solutions of lantadenes and cholesterol (4 mg/ml) were prepared in chloroform–methanol (2:1) and 10-μl aliquots of each solution were applied to the plate. The following solvent systems were used: (I) light petroleum (b.p. 60–80°C)–ethyl acetate–acetic acid (88:10:2); (II) benzene–methanol–ethyl acetate (85:10:5); (III) chloroform–methanol (97:3); (IV) diisopropyl ether–acetone (70:30); (V) light petroleum (b.p. 60–80°C)–benzene–ethyl acetate–acetic acid (40:80:28:2); (VI) benzene–diethyl ether (70:30); and (VII) hexane–methanol–ethyl acetate (85:10:5).

The chromatograms were developed at room temperature (ca. 25°C) in 250 × 250 × 120 mm glass tanks, saturated using Whatman filter-paper [6], and air dried. The spots were detected as follows.

(a) Exposure of the developed plates to iodine vapour in an iodine-saturated chamber for *ca.* 10 min yielded yellow spots.

(b) Liebermann–Burchard spray reagent (LBR) was prepared by mixing 90 ml of acetic anhydride with 10 ml of sulpuric acid with cooling [7,8]. The sprayed plates were heated at 110°C and observed after 5 and 10 min for the appearance of spots. The plates were examined at 366 nm using a UV cabinet. Spots for 3-hydroxylantadenes (RLA and RLB) and cholesterol appeared within 5 min; they were purple and reddish purple and gave golden and pinkish yellow fluorescence, respectively, at 366 nm. The sports for 3-keto compounds, *viz.*, LA, LB, LC and LD, appeared after heating for 10 min and were brownish purple.

(c) Vanillin–sulphuric acid spray reagent was prepared by dissolving 0.5 g of vanillin in 100 ml of sulphuric acid–ethanol (40:10) [6]. The sprayed plates were heated at 120°C, observed after 5 and 10 min and examined at 366 nm using a UV cabinet. The rate of appearance of spots for the different compounds and their colours were the same as with LBR.

(d) A stock solution of primulin was prepared by dissolving 0.1 g of primulin in 100 ml of water. To prepare the spray reagent, 1 ml of stock solution was diluted with 100 ml of acetone–water (4:1). Immediately after spraying, the wet chromatograms were observed at 366 nm in a UV cabinet [9]. All the lantadenes and cholesterol gave pale blue fluorescent spots.

RESULTS AND DISCUSSION

The R_F values of different compounds are known to vary considerably with various factors such as layer thickness, chamber saturation, air humidity and source of adsorbents [6]. Hence it is advisable to use hR_{st} values relative to some suitable reference compound of comparable structure [6]. The hR_{st} values for the lantadenes in relation to cholesterol as a reference compound are given in Table I.

All the solvent systems except V were suitable for the resolution of LA and LB. LA, LB and LC had the same hR_{st} value in solvent system V. Solvent systems I, V and VII gave very compact spots and thus the resolution was very sharp. Solvent system II also gave fairly compact spots but less so than those obtained with I, V and VII. The separations of LA and LC and of LB and LD were difficult. Only solvent systems VI and VII resolved LA and LC, VII being the most suitable. LB and LD could be separated in solvent systems IV, V, VI and VII. Like LA and LB, RLA and RLB could be separated in all the solvent systems except V. Two other solvents systems, light petroleum (b.p. 60–80°C)–ethyl acetate (60:40) and hexane–ethyl acetate (60:40), were fairly useful for the separation of LA and LB and of RLA and RLB, but they had limited utility for the resolution of other combinations of lantadenes. Amongst all the solvent systems, only VII was suitable for the separation of all the lantadenes investigated. The only limitation of this system was that the differences in the hR_{st} values of LA and LC and of RLA and RLB were very small (Table I). This problem could be overcome by applying "long-run" TLC [10] using 400 × 200 mm plates. This was more advantageous than "multiple-development" TLC recommended by some workers for difficult separations [6].

All the solvent systems used were suitable for the

TABLE I

hR_{st} VALUES FOR LANTADENES USING CHOLESTEROL AS A REFERENCE COMPOUND

The hR_{st} value for cholesterol was taken as 100. The R_F values for cholesterol in the different solvent systems were: I, 0.48; II, 0.82; III, 0.88; IV, 0.89; V, 0.55; VI, 0.70; and VII, 0.79.

Compound	hR_{st}						
	I	II	III	IV	V	VI	VII
Lantadene A (22β-angeloyloxy-3-oxoolean-12-en-28-oic acid)	99	84	60	78	109	51	30
Lantadene B (22β-dimethylacryloyloxy-3-oxoolean-12-en-28-oic acid)	85	74	48	70	109	46	21
Lantadene C (22β-(*S*)-2′-methylbutanoyloxy-3-oxoolean-12-en-28-oic acid)	99	84	60	78	109	50	33
Lantadene D (22β-isobutyroyloxy-3-oxoolean-12-en-28-oic acid)	85	74	48	58	102	43	25
Reduced lantadene A (22β-angeloyloxy-3β-hydroxyolean-12-en-28-oic acid)	69	68	43	78	95	43	19
Reduced lantadene B (22β-dimethylacryloyloxy-3β-hydroxy-12-en-28-oic acid)	63	58	32	70	95	36	16

separation of RLA and RLB from cholesterol. The difference in the hR_{st} values of LA, LC and cholesterol was only marginal in system I. Similarly, the difference in hR_{st} values of LD and cholesterol was very small in system V (Table I). The order of appearance of coloured spots using both LBR and vanillin–sulphuric acid sprays was: cholesterol > 3-hydroxylantadenes > 3-ketolantadenes. These spray reagents gave spots of different colours with 3-hydroxy- and 3-ketolantadenes. In addition, the spots for 3-hydroxylantadenes gave a golden fluorescence at 366 nm, which further facilitated their differential identification. The primulin spray gave the same type of spots (pale blue) with all the lantadenes and cholesterol. However, this detection system had the advantage of being non-destructive [8,9] and hence was suitable for preparative TLC.

All the lantadenes and cholesterol could be detected at levels down 2 μg using primulin and vanillin–sulphuric acid spray. The detection limit for all the compounds using LBR was 5 μg. Detection using iodine vapour was comparatively less sensitive. 3-Ketolantadenes could be detected at levels down to 5 μg, but the detection of 3-hydroxylantadenes and cholesterol required nearly 10-μg applications on the plates.

The reported TLC procedures would be useful in tackling different separation problems in the preparation of lantadenes and related compounds from the lantana plant. They would also find use in investigations on the metabolism and disposition of lantadenes in animal systems.

ACKNOWLEDGEMENT

We thank the Director of the Institute for providing the facilities for this work.

REFERENCES

1 O. P. Sharma and P. D. Sharma, *J. Sci. Ind. Res.*, 48 (1989) 471.
2 O. P. Sharma, R. K. Dawra and H. P. S. Makkar, *Toxicol. Lett.*, 37 (1987) 165.
3 O. P. Sharma, R. K. Dawra and D. Ramesh, *Phytochemistry*, 29 (1990) 3961.
4 O. P. Sharma and H. P. S. Makkar, *J. Chromatogr.*, 196 (1980) 515.
5 D. H. R. Barton, P. De Mayo and J. C. Orr, *J. Chem. Soc.*, (1956) 4160.
6 E. Stahl. *Thin Layer Chromatography, a Laboratory Handbook*, Springer, New York, 1969.
7 C. H. Brieskorn and H. Herring, *Arch. Pharmacol. Berlin*, 292 (1959) 485.
8 O. P. Sharma, H. P. S. Makkar and R. K. Dawra, *Anal. Biochem.*, 128 (1983) 474.
9 R. S. Wright, *J. Chromatogr.*, 59 (1971) 220.
10 O. P. Sharma, R. K. Dawra and H. P. S. Makkar, *Vet. Human Toxicol.*, 31 (1989) 10.

Journal of Chromatography, 587 (1991) 355–358
Elsevier Science Publishers B.V., Amsterdam

CHROM. 23 683

Short Communication

Chromatographic behaviour of the antidegradant ethoxyquin and its transformation products

L. Taimr* and M. Prusíková

Institute of Macromolecular Chemistry, Czechoslovak Academy of Sciences, 162 06 Prague 6 (Czechoslovakia)

(First received May 22nd, 1991; revised manuscript received August 9th, 1991)

ABSTRACT

An antidegradant, 6-ethoxy-2,2,4-trimethyl-1,2-dihydroquinoline (ethoxyquin) and the products formed during its oxidation, hydrolysis or reduction were analysed by thin-layer and high-performance liquid chromatography. Attention was concentrated on the stability of the compounds during analysis.

INTRODUCTION

6-Ethoxy-2,2,4-trimethyl-1,2-dihydroquinoline (ethoxyquin, EQ, compound **1**) is used as an antioxidant and antiozonant for rubber and as a feed additive. A number of transformation products of EQ have been reported [1], some of which have been investigated chromatographically [2], although a thorough reviw of the chromatographic properties of such compounds has not yet been performed.

This study considered compounds **1**–**12** shown in Fig. 1. Phenetidine (**2**) is a frequent impurity in technical EQ; the other compounds (**3**–**12**) are oxidation products of EQ under various conditions [1] and leucoforms of these compounds.

EXPERIMENTAL

Materials

Chromatographically pure compounds were used in the analyses. EQ, a light brown oil, was obtained by the repurification [1] of Vulkanox EC (Bayer, Leverkusen, Germany). Phenetidine (**2**) was obtained from Fluka. 2,2,4-Trimethyl-6-quinolone (**3**) (lemon yellow crystals, m.p. 56–57°C) was prepared [1,3] by the oxidation of compound **4** with silver (I) oxide. 6-Hydroxy-2,2,4-trimethyl-1,2-dihydroquinoline (**4**) (white crystals, m.p. 179–182°C with partial decomposition) was prepared [1,3] by the hydrolysis of EQ with hydrogen bromide. 2,2,4-Trimethyl-6-quinolone-N-oxide (**5**) (ochre yellow crystals, m.p. 94–95°C) was prepared [1] by the oxidation of compound **3** with *m*-chloroperbenzoic acid. 6-Ethcxy-2,2,4-trimethyl-1,2-dihydroquinoline-N-oxyl (**6**) (dark brown to violet crystals, m.p. 70.5–71.5°C) ws prepared [1] by the oxidation of EQ with *m*-chloroperbenzoic acid. 6-Ethoxy-2,2,4-trimethyl-8-quinolone (**7**) (red crystals, m.p. 122–124°C) was prepared [1] by the oxidation of EQ with Fremy's salt. 6-Ethoxy-8-hydroxy-2,2,4-trimethyl-1,2-dihydroquinoline (**8**) (almost white crystals, m.p. 104–106°C) was prepared [1] by the reduction of compound **7** with $Na_2S_2O_4$. 2,4-Dimethyl-6-ethoxyquinoline (**9**) (almost white crystals, m.p. 87°C) was prepared [4] by the oxidation of EQ with oxygen. 8-(6-Ethoxy-2,2,4-trimethyl-1,2-dihydro-1-

0021-9673/91/$03.50

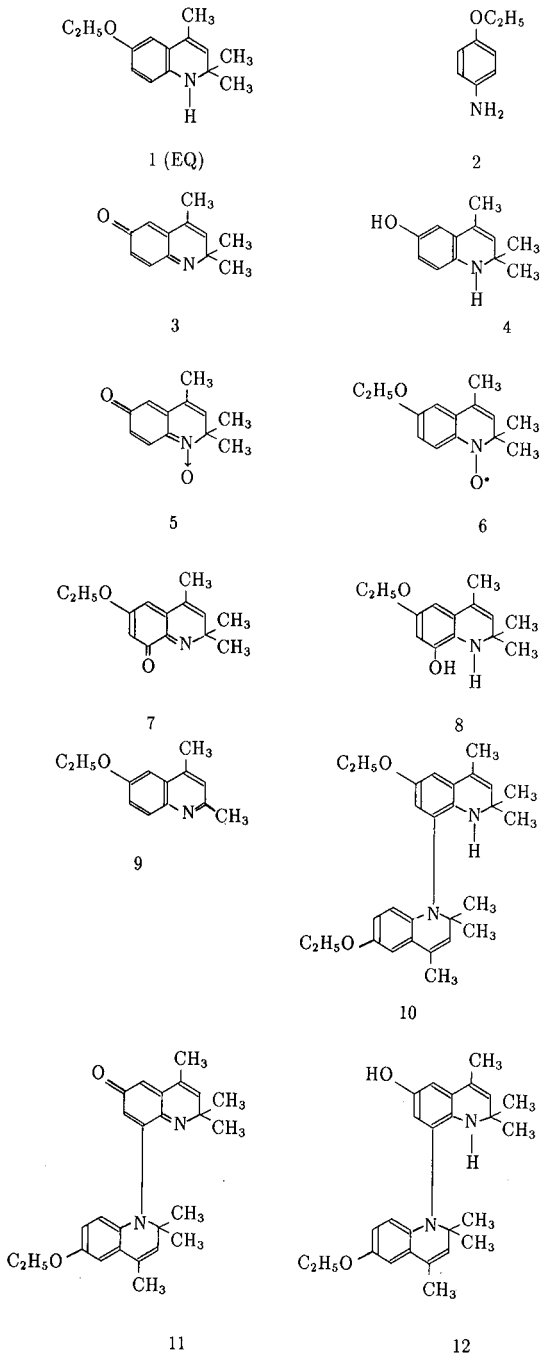

Fig. 1. Structures of compounds **1–12**.

quinolyl)-6-ethoxy-2,2,4-trimethyl-1,2-dihydroquinoline (**10**) (almost white crystals, m.p. 110°C) was prepared [1] by the oxidation of EQ with silver (I) oxide. 8-(6-Ethoxy-2,2,4-trimethyl-1,2-dihydro-1-quinolyl)-2,2,4-trimethyl-6-quinolone (**11**) (almost black needles, m.p. 152–153°C) was prepared [1] by the oxidation of EQ with lead (IV) oxide. 8-(6-Ethoxy-2,2,4-trimethyl-1,2-dihydro-1-quinolyl)-6-hydroxy-2,2,4-trimethyl-1,2-dihydroquinoline (**12**) (light coloured glassy substance) was prepared [1] by the reduction of compound **11** with $Na_2S_2O_4$.

Procedures

Thin-layer chromatography (TLC) was carried out on precoated silica gel plates (Silufol UV 254 with a luminescent indicator). The neutral mobile phases were: M_1, benzene–diethyl ether (9:1, v/v); M_2, benzene–diethyl ether (4:1, v/v); M_3, benzene–diethyl ether (1:1, v/v); M_4, diethyl ether; and M_5, benzene–acetone (1:1, v/v). The basic mobile phases were freshly prepared each time by shaking the following solvents with concentrated aqueous ammonia: M_6, benzene; M_7, benzene–diethyl ether (9:1, v/v); M_8, benzene–diethyl ether (1:1, v/v); and M_9, diethyl ether. An acid permanganate solution was obtained by dissolving 8 g of $KMnO_4$ in 500 ml of water and adding 1.5 ml of concentrated sulphuric acid; the excess of the reagent was removed with water after the plate had been sprayed.

Liquid chromatography took place on a silica gel column (two columns 150 × 3 mm connected in series, packed with Separon SIX, 5μm; Laboratory Instruments, Prague, Czechoslovakia). The neutral mobile phases were mixtures of hexane containing isopropyl alcohol in the following amounts: 0.1, 0.5 and 4% (v/v) (phases M_{10}, M_{11} and M_{12}); the basic mobile phases were mixtures of hexane with 0.1% (v/v) triethylamine, again containing isopropyl alcohol at 0.1, 0.5 and 4% (v/v) (phases M_{13}, M_{14} and M_{15}). The flow-rate of the mobile phases was 1 ml/min; the pressure was 140 bar. The temperature of the column was 24°C. All compounds were detected by a differential UV detector operating at 254 nm.

RESULTS AND DISCUSSION

Information on the composition of unknown mixtures containing the transformation products of EQ can be obtained by TLC. In this study compounds **1–12** were analysed using precoated silica

TABLE I

R_F VALUES IN TLC IN NEUTRAL (M_1–M_5) AND BASIC (M_6–M_9) MOBILE PHASES

Compound	R_F								
	M_1	M_2	M_3	M_4	M_5	M_6	M_7	M_8	M_9
1	0.37[a]	0.51	0.63	0.81	0.73	0.28	0.48	0.62	0.92
2	0.10[a]	0.13[a]	0.24[a]	0.33[a]	0.44[a]	0.08	0.17	0.29	0.56
3	0.08	0.15	0.33	0.51	0.60	0.05	0.17	0.37	0.65
4	0.10[a]	0.21[a]	0.40[a]	0.65[a]	0.63	0.02	0.05[c]	0.21[c]	0.52[c]
5	0.07	0.11	0.23	0.33	0.58	0.03	0.12	0.25	0.42
6	0.28[c]	0.40[c]	0.56[c]	0.73[c]	0.70[c]	0.19	0.39	0.54	0.80
7	0.01	0.02	0.05	0.08[a]	0.33[a]	0.00	0.01	0.05	0.11
8	0.16[a]	0.32[a]	0.59	0.75	0.63	0.00	–[c]	–[c]	–[c]
9	0.04	–[b]	–[b]	–[b]	–[b]	0.04	0.15	0.31	0.58
10	0.68	0.73	0.77	0.92	0.81	0.57	0.73	0.77	0.96
11	0.26	0.42	0.60	0.75	0.76	0.14	0.38	0.58	0.82
12	0.36	0.51	0.64	0.83	0.70	0.07	0.25	0.51	0.79

[a] Spot is slightly elongated towards the start.
[b] Spot is strongly elongated.
[c] Compound undergoes chemical changes during measurement.

gel plates with detection at 254 nm (Table I). Neutral or basic mobile phases were used. It is known that in TLC on a silica gel medium, basic compounds form asymmetrical spots with the tail orientated towards the initial position. In these instances R_F depends on the amount of compound initially present. This unfavourable behaviour is suppressed in the basic system. Ammonia was chosen because in two-dimensional TLC the neutral mobile phase can be used again in the second direction after the ammonia has evaporated.

The basic system is necessary for the TLC separation of compound **9**, because in neutral mobile phases this compound either remains at the initial position (M_1, Table I) or forms a long band. The presence of ammonia favourably affects the separa-

TABLE II

DETECTION OF COMPOUNDS IN TLC

Compound	Colour of spot in neutral mobile phases			Colour of spot in basic mobile phases		Luminescence at 366 nm[a]	Acid $KMnO_4$
	Immediately after analysis	After 1 h	After 20 h	Immediately after analysis	After 1 h		
1	Colourless	Grey–yellow	Grey–brown	Colourless	Yellow–grey	Blueish	+
2	Colourless	–	Grey–brown	Colourless	Light brown	–	+
3	Lemon yellow	Lemon yellow	Grey–yellow	Light yellow	Grey, green–yellow	–	+
4	Colourless	Grey	Grey–brown	Colourless	Grey, green–yellow	Blueish	+
5	Yelow	Yellow	Yellow	Yellow	Yellow	–	+
6	Brown–red	Brown–orange	Grey, yellow–orange	Red	Brown	–	+
7	Red	Red	Red	Red–orange	Red	–	+
8	Colourless	Red–brown	Red–brown	–	–	Blue	+
9	Colourless	Colourless	Colourless	Colourless	Colourless	Intense blue	–
10	Colourless	Grey–pink	Grey red	Colourless	Grey–red	Blueish	+
11	Blue	Blue	Blue	Blue	Blue	–	+
12	Colourless	Light blue	Blue	Colourless	Blue	Blueish	+

[a] All compounds quench the luminescence of the indicator at 254 nm.

TABLE III

ELUTION TIMES IN HPLC IN NEUTRAL (M_{10}–M_{12}) AND BASIC (M_{13}–M_{15}) MOBILE PHASES

Compound	Elution time (min)					
	M_{10}	M_{11}	M_{12}	M_{13}	M_{14}	M_{15}
1	46	8	5	13	6	–
2	–	30	11	–	28	14
3	–	32	8	37	10	6
4	–	–	17	–	–	21
5	–	–	11	–	34	11
6	–	11	7	15	7	5
7	–	–	14	–	–	11
8	–	–	7	–	–	13
9	–	34	9	43	13	7
10	15	–	–	6	–	–
11	–	13	6	24	8	5
12	–	28	7	–	–	8
Benzene	4	4	4	4	4	4

tion of other compounds by causing them to form rounder spots (Table I). The basicity of most of the compounds studied is so low, however, that in these instances neutral mobile phases, which are more convenient, can be used successfully.

Another reason for the application of both neutral and basic mobile phases is the low stability of some of the compounds under investigation, which in some instances is more significant in one or the other of these phases. For example, compound **6** in contact with silica gel decomposes [1], with the formation of EQ (**1**), nitrone **5** and some other compounds. The decomposition takes place gradually in the TLC analysis in neutral mobile phases, whereas the decomposition is suppressed in basic mobile phases. The opposite behaviour is observed with compounds **4**, **8**, and **12**, which in the basic medium are readily oxidized in air. The ease of oxidation increases in the order compound **12**, **4**, then **8**. Compound **8** is also partly oxidized in neutral mobile phases.

The R_F values of the compounds under investigation are summarized in Table I and increase with increasing ether content in the mobile phase (series M_1–M_4 and M_6–M_9). In the basic systems, in which the silica gel surface has been partly deactivated with ammonia and moisture, the R_F values are higher than in neutral systems at the same diethyl ether content. The M_5 phase is qualitatively different.

Detection of the compounds under study proceeds without difficulty (Table II). Many of the compounds are coloured or become coloured when the chromatogram is stored in the laboratory under scattered light. This behaviour is characteristic for each compound. Compounds **5** and **9** are stable. All compounds can be identified by a UV detector. With the exception of compound **9**, all can also be detected using an acid permanganate solution. Compound **9** has a characteristic intense light blue luminescence at 366 nm.

Similarly to separation by TLC, liquid chromatographic analysis was also performed using both neutral and basic mobile phases (triethylamine, Table III). The basic mobile phases are not absolute necessary for the compounds investigated in this study, although knowledge of their chromatographic behaviour is useful because basic conditions may be required by the presence of other compounds in the analysis of more complicated mixtures.

REFERENCES

1 L. Taimr, M. Prusíková and J. Pospíšil, *Angew. Makromol. Chem.*, 190 (1991) 53; and references cited therein.
2 S. Kato and K. Kanohta, *J. Chromatogr.*, 324 (1985) 462.
3 Yu. A. Ivanov, N. L. Zaitchenko, S. V. Rykov, O. Ya. Grinberg, A. A. Dubinskii, S. D. Pirozhkov, E. G. Rozantsev, J. E. Pokrovskaya and A. B. Shapiro, *Izv. Akad. Nauk SSSR, Ser. Khim.*, (1979) 1800.
4 T. D. Nekipelova and A. B. Gagarina, *Dokl. Akad. Nauk SSSR*, 231 (1976) 392.

Journal of Chromatography, 587 (1991) 359–363
Elsevier Science Publishers B.V., Amsterdam

CHROM. 23 703

Short Communication

Optimization of separation of rare earths in high-performance thin-layer chromatography

Qin-Sun Wang* and Dong-Ping Fan

National Laboratory of Elemento-Organic Chemistry, Nankai University, Tianjin 300071 (China)

(First received May 16th, 1991; revised manuscript received August 20th, 1991)

ABSTRACT

A computer-assisted method is presented for simultaneous two-factor optimization (acidity and extractant concentration) for the optimum separation of ten rare earths (La, Ce, Pr, Nd, Sm, Eu, Gd, Tb, Ho and Er) by high-performance thin-layer chroamtography. The method is based on a polynomial estimation from seven preliminary experiments according to a hexagon design. The computer scanning technique was used in two-dimensions. The R_F difference was used as the selection criterion. Good agreement was obtained between predicted data and experimental results.

INTRODUCTION

In recent years, several papers have been published on the advanced separation of rare earths by thin-layer chromatography (TLC) [1–8]. Mostly the mobile phase used was a mixture that included an organic solvent, extractant and acid. Generally, the composition of the mobile was tested empirically for synergistic effects. This was carried out on a trial-and-error basis, which leads to results often not as good as might be expected in an optimum separation. Systematic strategies to optimize mobile phase composition in high-performance TLC (HPTLC) has rapidly gained widespread acceptance. Sequential simplex [9,10] window diagram [11,12], overlapping resolution map [13,14] and statistical scanning techniques [15] have been employed for optimization of HPTLC. Recently we have described a computer-assisted optimization of two-factor selectivity in HPTLC [16].

In general, the mobile phase systems have usually involved an organophosphorus extractant, an oxygen-containing solvent (ether or ketone) and an acid for the separation of rare earths by TLC. This work was undertaken in order to develop a simpler and more convenient system for the separation of rare earths by HPTLC. A computer-assisted optimization method is presented for simultaneous two-factor (acidity and extractant concentration) optimization of the separation of ten rare earths (La, Ce, Pr, Nd, Sm, Eu, Gd, Tb, Ho and Er) by HPTLC.

The principle of the method is based on a polynomial between the retardation factor, R_F, and the two factors considered. In order to investigate the effect of two variables in HPTLC and their possible interaction, a Dochlert matrix design (Fig. 1) was adopted as the optimization strategy [17]. Seven preliminary experiments represent the three different levels in which the R_F values were obtained. These values were then substituted into the following equation, in order to establish the values of the constants:

0021-9673/91/$03.50

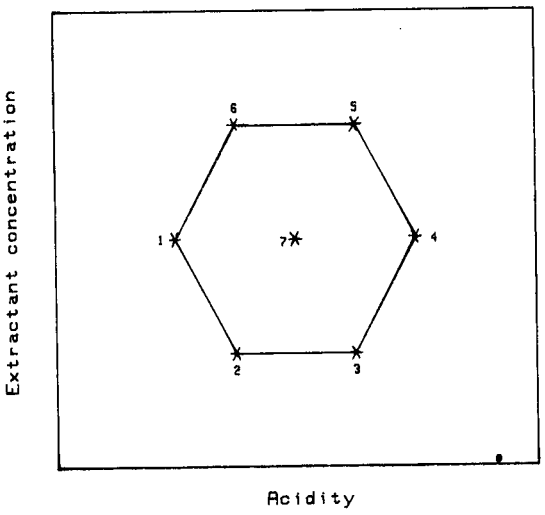

Fig. 1. Hexagon design for two-factor effects.

$$R_F = b_0 + b_1X_1 + b_2X_2 + b_{11}X_1^2 + b_{22}X_2^2 + b_{12}X_1X_2 \quad (1)$$

where X_1 and X_2 are the two factors of unrelated variables and b_0, b_1, b_2, b_{11}, b_{22} and b_{12} are constants characteristic of a given compound. According to eqn. 1, the R_F values of the compounds can be predicted at all two-factor compositions within the rectangular region.

The difference between R_F values was used as the separation criterion for indication of chromatographic performance:

$$\Delta R_F = |R_{F(i)} - R_{F(j)}| \quad (2)$$

The method allows the determination of ΔR_F only for adjacent pairs of spots and not for all pairs. If n is the spot number, $n - 1$ spot pairs are calculated in each two-factor composition within the selected rectangle. The predicted R_F values of the solutes are arranged in order before calculating every ΔR_F in all two-factor compositions. The result is satisfactory even if not all the spots have the same relative order of R_F values in the experimental runs.

A ΔR_F contour map was constructed to calculate all adjacent pair ΔR_F values and to select the minimum ΔR_F in every two-factor composition. A maximum ΔR_F was then selected in all two-factor compositions. The maximum ΔR_F was selected for the worst separated spot pair as the separation criterion. All other spot pairs have larger ΔR_F values.

The computer program DOS-T (di-factor optimization system for TLC) was used for the optimization of the separation of a mixture of ten rare earths. Good results were obtained between the predicted data and experimental results.

EXPERIMENTAL

Materials

All chemicals were of analytical-reagent grade. Test solutions of rare earths were prepared by dissolving appropriate amount of the oxides (>99.9%) in 7.2 *M* nitric acid and evaporating to dryness, followed by dissolution in 0.1 *M* nitric acid to give a 5 mg/ml metal solution. Commercially available precoated HPTLC silica plates from Merck (Darmstadt, Germany) were used. All plates were preliminarily developed with the 2.5 *M* ammonium nitrate solution as the mobile phase, then heated at *ca.* 70°C for 1 h before use.

The mobile phase components were mixed in different ratios as given in Table I. The four constituents were (A) 4-methyl-2-pentanone, (B) tetrahydrofuran (THF), (C) nitric acid and (D) the mono-2-ethylhexyl ester of 2-ethylhexylphosphonic acid (P507, No. 1 Chemical Reagent Factory, Tianjin, China).

Apparatus

A CAMAG (Muttenz, Switzerland) Nanomat sampler, linear developing chamber and TLC plate heater II were used.

All computer studies were carried out on a Model HP-220 microcomputer (Hewlett-Packard, Palo Alto, CA, USA) with an HP-9133A disk drive and HP-7470A graphics plotter. The DOS-T program was written in HP BASIC 4.

Chromatography

Volumes of 200 nl of aqueous solutions were spotted by means a Pt–Ir pointed glass capillary. Separation was carried out using linear development with the mobile phases given in Table I. A typical development required the solvent front to move 50 mm from the origin. After development, the HPTLC plate was dried thoroughly by blowing warm air and the positions of the rare earths were revealed by

TABLE I

R_F VALUES OF TEN RARE EARTHS MEASURED BY HPTLC USING DIFFERENT MOBILE PHASE COMPOSITIONS

Mobile phase composition (ml)[a]				R_F[b]									
A	B	C	D	La	Ce	Pr	Nd	Sm	Eu	Gd	Tb	Ho	Er
3.00	1.50	0.40	0.42	0.05	0.11	0.15	0.21	0.42	0.49	0.54	0.62	0.69	0.78
3.00	1.50	0.58	0.14	0.02	0.04	0.05	0.07	0.13	0.15	0.15	0.20	0.34	0.39
3.00	1.50	0.94	0.14	0.01	0.01	0.02	0.03	0.06	0.07	0.08	0.11	0.16	0.22
3.00	1.50	1.12	0.42	0.01	0.03	0.04	0.06	0.11	0.14	0.17	0.26	0.35	0.43
3.00	1.50	0.94	0.70	0.02	0.06	0.08	0.09	0.23	0.29	0.31	0.45	0.64	0.73
3.00	1.50	0.58	0.70	0.06	0.14	0.21	0.27	0.54	0.63	0.69	1.0	1.0	1.0
3.00	1.50	0.76	0.42	0.02	0.04	0.07	0.08	0.18	0.20	0.25	0.35	0.44	0.46

[a] For designation of A, B, C and D, see the text.
[b] R_F values are the mean of four measurements; the relative standard deviation is less than 6% on different plates.

spraying with saturated alizarin–ethanol solution and then treatment with ammonia vapour, followed by gentle heating. The rare earths were all detected as violet spots on a pale yellow background.

RESULTS AND DISCUSSION

A series of ten rare earths were applied for two-factor (volume of HNO_3 and P507) optimization. The measured R_F values used in the optimization are listed in Table I and the coefficients b in Table II.

In Table I the R_F values of the rare earths increase with increasing concentration of P507 and decrease with increasing concentration of HNO_3. The effects of P507 and HNO_3 on R_F are complicated, so the selction of the optimum composition of P507 and HNO_3 is difficult. DOS-T can be selct the composition of P507 and HNO_3 with only seven preliminary experiments.

Figs. 2 and 3 show the DOS-T ΔR_F contour maps (stereo and planar). Note that in Fig. 3 the white region is designated as the optimum two-factor composition, where the value of ΔR_F between all possible spot pairs is equal to or better than the desired value ($\Delta R_F = 0.04$). The point of the maximum ΔR_F value (0.05) is marked by with a cross; here the optimum condition of the two-factor composition is 0.46 ml each of HNO_3 and P507. In practice the composition 4-methyl-2-pentanone–

TABLE II

VALUES OF COEFFICIENTS $b_0, b_1, b_2, b_{11}, b_{22}$ AND b_{12} FOR TEN RARE EARTHS AND CORRELATION COEFFICIENT (r), F-TEST (F) AND STANDARD DEVIATION (s)

Rare earth	b_0	b_1	b_2	b_{11}	b_{22}	b_{12}	r	F	s
La	0.0553	−0.1150	0.1042	0.0772	0.0638	−0.1488	0.9964	83.727	0.0024
Ce	0.1670	−0.3727	0.1617	0.2315	0.1913	−0.2480	0.9943	51.741	0.0071
Pr	0.1052	−0.2608	0.4261	0.1929	0.1754	−0.4960	0.9924	38.980	0.0118
Nd	0.2367	−0.5941	0.5322	0.4244	0.2710	−0.6944	0.9913	34.057	0.0165
Sm	0.4004	−0.9599	1.0074	0.6559	0.4943	−1.1905	0.9978	137.147	0.0165
Eu	0.5590	−1.3256	1.0025	0.8873	0.7175	−1.2897	0.9984	185.783	0.0165
Gd	0.4274	−1.1366	1.5213	0.8102	0.3986	−1.5377	0.9982	167.554	0.0188
Tb	0.2257	−0.7269	2.0288	0.6944	0.8610	−2.2818	0.9881	24.744	0.0660
Ho	0.6820	−1.1281	0.8928	0.6173	0.9566	−0.8929	0.9929	41.785	0.0471
Er	1.1287	−2.0201	0.4261	1.1188	1.1320	−0.4960	0.9985	195.464	0.0212

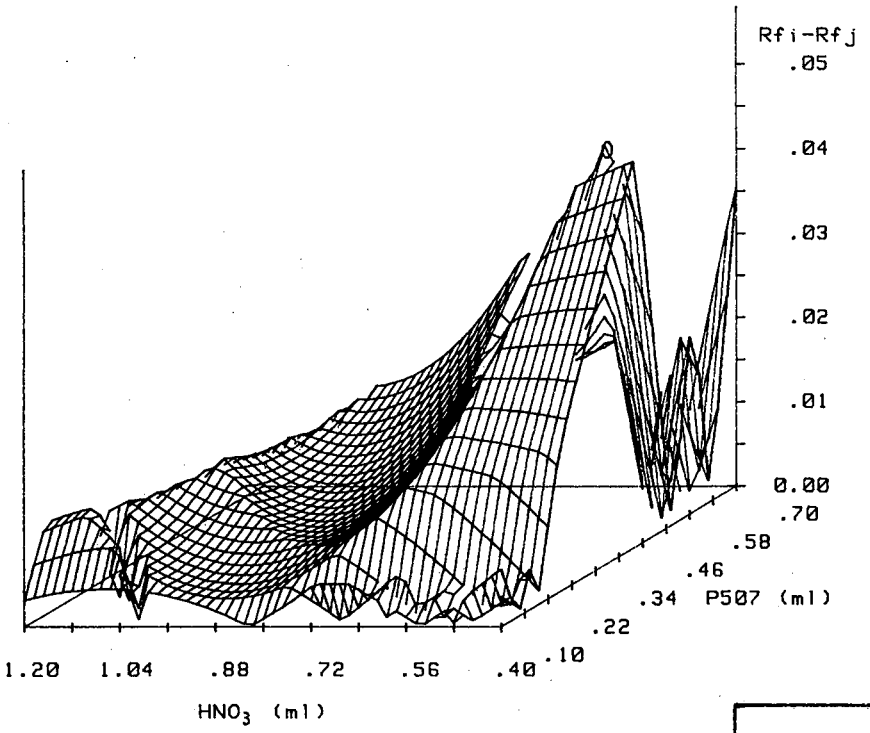

Fig. 2. ΔR_F stereo resolution map for ten rare earths in HPTLC.

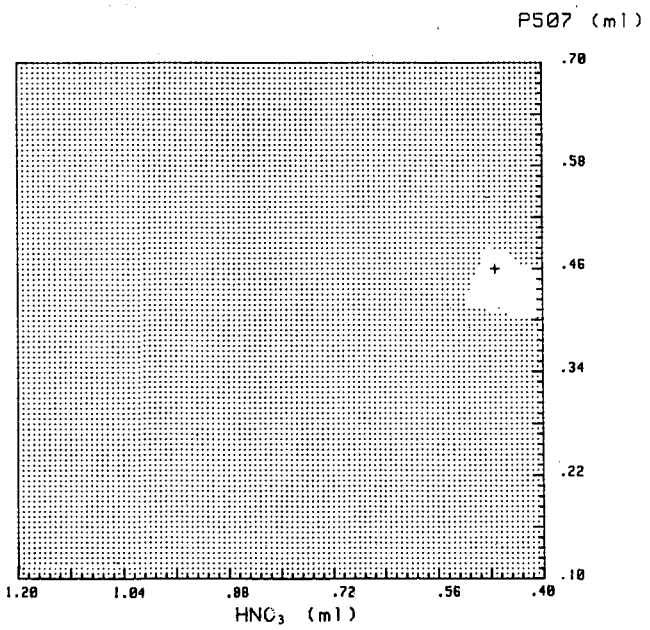

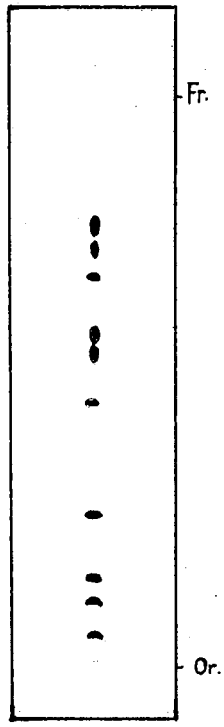

Fig. 3. ΔR_F planar map for ten rare earths in HPTLC.

Fig. 4. Chromatogram of the ten rare earths using the optimum mobile phase composition: 4-methyl-2-pentanone–THF–HNO_3–P507 (3.00:1.50:0.46:0.46).

TABLE III

COMPARISON OF PREDICTED AND OBSERVED R_F VALUES FOR TEN RARE EARTHS UNDER OPTIMUM CONDITIONS

R_F	La	Ce	Pr	Nd	Sm	Eu	Gd	Tb	Ho	Er
Predicted	0.05	0.11	0.15	0.21	0.41	0.48	0.54	0.67	0.72	0.77
Observed[a]	0.06	0.12	0.16	0.27	0.47	0.55	0.59	0.69	0.74	0.78

[a] R_F values are the means of four measurements, the relative standard deviation is less than 5% on different plates.

THF–HNO_3–P507 = 3.00:1.50:0.46:0.46 (v/v/) was used for separation and the results are shown in Fig. 4. Table III gives the experimental and predicted results using this optimum condition composition; they are in good agreement.

ACKNOWLEDGEMENT

This work was support by the National Natural Science Foundation of China.

REFERENCES

1 H. Specher and A. Hufnagel, *Fresenius' Z. Anal. Chem.*, 318 (1984) 198.
2 H. Specher and C. Pomp, *Fresenius' Z. Anal. Chem.*, 322 (1985) 292.
3 W. Y. Ding, B. Y. Qian and G. L. Yang, *J. Chin. Rare Earth Soc.*, 3 (1985) 79.
4 K. Ishida, S. Ninomiya, Y. Takeda and K. Watanabe, *J. Chromatogr.*, 351 (1986) 489.
5 K. Ishida, S. Ninomiya and N. Osawa, *Fresenius' Z. Anal. Chem.*, 328 (1987) 228.
6 Z. F. Hsu, X. P. Jia and C. S. Hu, *Talanta*, 33 (1986) 455.
7 J. Wang and Z. S. Hu, *Chin. J. Chromatogr.*, 6 (1988) 105.
8 R. Bhushan, S. P. Srivastava and R. S. Chauhan, *Ann. Lett.*, 18 (1985) 1549.
9 L. G. Sabate and X. Tomas, *J. High Resolut. Chromatogr. Chromatogr. Commun.*, 7 (1984) 104.
10 C. K. Baune and C. Y. Ma, *J. Liq. Chromatogr.*, 10 (1987) 3529.
11 Q. S. Wang, R. Y. Gao and H. Y. Wang, *Chromatographia*, 28 (1989) 285.
12 Q. S. Wang and H. Y. Wang, *J. Planar Chromatogr.*, 3 (1990) 15.
13 R. E. Tecklenburg, Jr., G. H. Fricke and D. Nurok, *J. Chromatogr.*, 290 (1984) 75.
14 C. K. Bayne and C. Y. Ma, *J. Liq. Chromatogr.*, 12 (1989) 235.
15 Q. S. Wang and B. W. Yan, *Chromatographia*, 28 (1989) 473.
16 Q. S. Wang and W. Q. Xie, *J. Planar Chromatogr.*, 3 (1990) 153.
17 D. H. Dochlert, *Appl. Stat.*, 19 (1970) 231.

Journal of Chromatography, 587 (1991) 364–367
Elsevier Science Publishers B.V., Amsterdam

CHROM. 23 695

Short Communication

Capillary tube isotachophoretic separation of catecholamines using cyclodextrin in the leading electrolyte

Shunitz Tanaka, Takashi Kaneta, Mitsuhiko Taga* and Hitoshi Yoshida

Department of Chemistry, Faculty of Science, Hokkaido University, Sapporo 060 (Japan)

Hirokazu Ohtaka

Department of Polymer Science, Faculty of Science, Hokkaido University, Sapporo 060 (Japan)

(First received May 14th, 1991; revised manuscript received August 14th, 1991)

ABSTRACT

The isotachophoretic separation of catecholamines based on inclusion complex formation with β-cyclodextrin (β-CD) was investigated. Separability was improved with increasing concentration of β-CD in the leading electrolyte. It was found that a neutral surfactant, added to suppress the electroosmotic flow and to form sharp zone boundaries, affects the resolution. Six catecholamines were separated by using complex formation with β-CD.

INTRODUCTION

Capillary isotachophoresis (CITP) is widely applied in separations of many ionic species. It is important to maximize the differences in the effective mobilities of the sample ions because the separation mechanism is based on the differential mobilities between analytes [1]. The use of complex-forming equilibria can be used to control the effective mobilities of analyte ions in CITP, and the optimum migration system can easily be established so that this technique has broad utility. Typically, a charged ligand or a metal ion is added to the leading electrolyte as a complexing counter ion in this method [2,3]. In recent years, methods utilizing the interaction between sample ions and a neutral ligand in the leading electrolyte have been developed. Especially utilizing cyclodextrin (CD) as the neutral ligand, optical isomers and structural isomers can be separated [4–7]. This technique will be able to improve the separation of many species in CITP.

The separation of catecholamines has been investigated by many techniques, such as high-performance liquid chromatography [8,9], capillary electrophoresis [10–13] and micellar electrokinetic capillary chromatography [14,15]. Although CITP is also an excellent separation technique, the separation of catecholamines by CITP is difficult because of the similarity of their structures and characteristics. We therefore attempted the separation of catecholamines by CITP using β-CD in the leading electrolyte.

0021-9673/91/$03.50

EXPERIMENTAL

Apparatus

A Model IP-3A capillary tube isotachophoretic analyser (Shimadzu, Kyoto, Japan), equipped with a potential gradient detector and a column system (Shimadzu) consisting of a PTFE preseparation capillary (80 × 0.7 mm I.D.) and a fused-silica analytical capillary column (170 × 0.2 mm I.D.), was used. The current was kept constant at 10 μA after migration at 360 μA for 4 min. The capillary tube was filled with the leading and terminating electrolytes using a peristaltic pump.

The R_E value, which is the ratio of the potential gradient of the sample zone to that of the leading zone, is used as an index of effective mobility.

Reagents

Potassium acetate, acetic acid, β-alanine, hydrochloric acid, Triton *X*-100 and poly(vinyl alcohol) (PVA) were of analytical-reagent grade from Wako (Osaka, Japan) and used without further purification, and α-β-cyclodextrins were purchased from Tokyo Kasei Kogyo (Tokyo, Japan).

Stock solutions of catecholamines were prepared by dissolving dopamine hydrochloride, *dl*-normetanephrine hydrochloride, *dl*-metanephrine hydrochloride (Nacalai, Tesque, Kyoto, Japan), 3,4-dihydroxybenzylamine, (+)-norepinephrine (Aldrich, Milwaukee, WI, USA), *dl*-epinephrine and *dl*-isoproterenol hydrochloride (Wako) in water.

Electrolytes

The operating systems used are given in Table I. The leading electrolyte was prepared by diluting a stock solution of 1 *M* potassium acetate and 5% PVA or 10% Triton X-100 and adjusting the pH to 5.0 by adding acetic acid. The terminating electrolyte was prepared by dissolving β-alanine and adjusting the pH to 1.7 by adding hydrochloric acid.

TABLE I

OPERATING SYSTEMS

Parameter	Leading electolyte	Terminating electrolyte
Cation	K^+	β-Alanine
Counter ion	CH_3COO^-	Cl^-
Concentration of cation	5 m*M*	10 m*M*
Additive	β-CD	None
Surfactant	0.05% PVA or 0.10% Triton X-100	None
pH	5.0	1.7

RESULTS AND DISCUSSION

The interaction between CD and catecholamines is a host–guest interaction, the intensity of which depends on the sizes of the CD cavity and of a guest molecule. First, we investigated the effect of adding α-CD. When α-CD was added to the leading electrolyte, no change in the separability of catecholamines was found. The cavity of α-CD accommodates molecules the size of benzene, but the catecholamines investigated here have two hydroxyl groups or one hydroxyl and one methoxy group, and are larger than benzene. We therefore studied the effect of β-CD.

Effect of β-CD on effective mobilities of catecholamines

The effective mobilities of catecholamines were dramatically changed on adding β-CD to the leading electrolyte. Fig. 1 shows the relationship be-

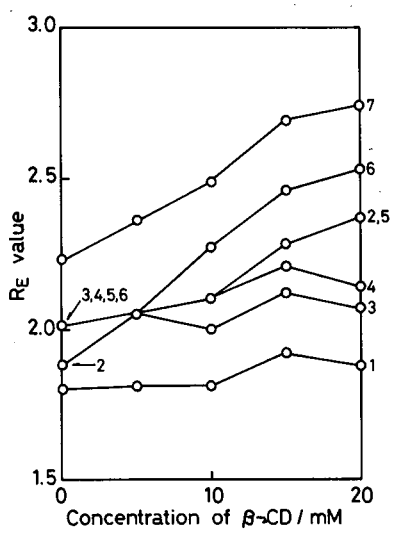

Fig. 1. Effect of β-CD concentration on R_E values of catecholamines. 1 = 3,4-Dihydroxybenzylamine; 2 = dopamine; 3 = normetanephrine; 4 = metanephrine; 5 = norepinephrine; 6 = epinephrine; 7 = isoproterenol.

tween the concentration of β-CD in a leading electrolyte containing 0.05% PVA and the R_E values of catecholamines. The R_E values increase and the effective mobilities decrease with increase in the β-CD concentration. This decrease in the effective mobilities is due to the increase in the size of the migrating species. As catecholamines complexed with β-CD are larger than the free catecholamines, the effective mobilities will decrease. The intensities of interaction of metanephrine and normetanephrine are smaller than those of the others because the decreases in their effective mobilities are very small.

In Fig. 1, the order of the decrease in the effective mobilities of catecholamines (*i.e.*, the order of the association constants of catecholamines with β-CD) is epinephrine > norepinephrine > metanephrine > normetanephrine, which indicates that the cavity of β-CD fits epinephrine and norepinephrine better than metanephrine and normetanephrine. Epinephrine and norepinephrine have two hydroxyl groups, whereas metanephrine and normetanephrine have one hydroxyl and one methoxy group. The structures of the aminoalkyl groups in metanephrine and normetanephrine are the same as those in epinephrine and norepinephrine, respectively. The methoxy group is larger than the hydroxyl group so that metanephrine and normetanephrine will not be able to interact with the β-CD cavity, and also the side of the catecholamines molecule bearing hydroxyl groups interacts with the cavity of β-CD.

Effect of surfactant

In CITP, an electrically neutral surfactant is usually added to the leading electrolyte in order to form a sharp zone boundary. We investigated two surfactants, PVA and Triton X-100. Table II gives the R_E values of catecholamines obtained utilizing two leading electrolytes containing PVA and Triton X-100. Metanephrine and norepinephrine can be separated in PVA solution, whereas they form a mixed zone in Triton X-100 slution. This may be due to phenyl groups existing in Triton X-100. As β-CD interacts with the phenyl groups of Triton X-100, the concentration of the free form CD in the leading electrolyte, that is, the concentration of β-CD interacting with catecholamines, decreases:

$$CD + Triton \rightleftharpoons CD(Triton)$$

TABLE II

EFFECT OF SURFACTANTS ON R_E VALUES OF CATECHOLAMINES

β-CD concentration is 20 m*M*.

Sample	R_E	
	0.05% PVA	0.10% Triton X-100
3,4-Dihydroxybenzylamine	1.88	1.93
Dopamine	2.37	2.30
Normetanephrine	2.07	2.17
Metanephrine	2.14	2.30
Norepinephrine	2.37	2.30
Epinephrine	2.53	2.48
Isoproterenol	2.74	2.72

Further, in the presence of Triton X-100, ligand-exchange equilibria may be achieved as follows:

$$CD(Triton) + CA \rightleftharpoons CD(CA) + Triton$$

where CA is catecholamine. In these instances, because the interaction between β-CD and catecholamines becomes weak, the differences in the effective mobilities of the catecholamines are also small. On the other hand, PVA will hardly interact with β-CD because of its linear structure and catecholamines can be sufficiently complexed with β-CD. As shown in Table II, PVA is preferred to Triton X-100 from the point of view of the separability.

An isotachopherogram of catecholamines using 0.05% PVA as a surfactant in the leading electrolyte is shown in Fig. 2. The concentration of β-CD

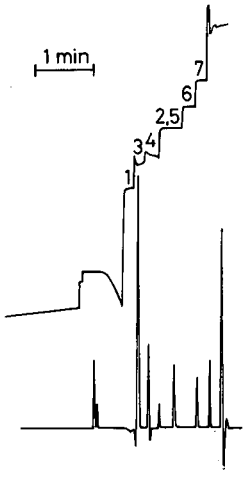

Fig. 2. Isotachopherogram of catecholamines. The β-CD concentration is 20 m*M*. Symbols as in Fig. 1.

is 20 m*M*. Six catecholamines were separated, the order of migration being 3,4-dihydroxybenzylamine > normetanephrine > metanephrine > dopamine = norepinephrine > epinephrine > isoproterenol.

REFERENCES

1 F. M. Everaerts, J. L. Beckers and Th. P. E. M. Verheggen, *Isotachophoresis*, Elsevier, Amsterdam, Oxford, New York, 1976.
2 P. Boček, I. Miedziak, M. Delm and J. Janák, *J. Chromatogr.*, 137 (1977) 83.
3 I. Nukatsuka, M. Taga and H. Yoshida, *J. Chromatogr.*, 205 (1981) 95.
4 J. Snopek, I. Jelínek and E. Smolková-Keulemansová, *J. Chromatogr.*, 411 (1987) 153.
5 J. Snopek, I. Jelínek and E. Smolková-Keulemansová, *J. Chromatogr.*, 438 (1988) 211.
6 S. Fanali and M. Sinibaldi, *J. Chromatogr.*, 442 (1988) 371.
7 I. Jelínek, J. Dohnal, J. Snopek and E. Smolková-Keulemansová, *J. Chromatogr.*, 464 (1989) 139.
8 R. M. Riggin and P. T. Kissinger, *Anal. Chem.*, 49 (1977) 2109.
9 G. C. Davis, P. T. Kissinger and R. E. Shoup, *Anal. Chem.*, 53 (1981) 156.
10 R. A. Wallingford and A. G. Ewing, *Anal. Chem.*, 59 (1987) 1762.
11 S. Fanali, *J. Chromatogr.*, 474 (1989) 441.
12 S. Tanaka, T. Kaneta and H. Yoshida, *Anal. Sci.*, 6 (1990) 467.
13 T. Kaneta, S. Tanaka and H. Yoshida, *J. Chromatogr.*, 538 (1991) 385.
14 R. A. Wallingford and A. G. Ewing, *Anal. Chem.*, 60 (1988) 258.
15 R. A. Wallingford and A. E. Ewing, *J. Chromatogr.*, 441 (1988) 299.

Journal of Chromatography, 587 (1991) 368
Elsevier Science Publishers B.V., Amsterdam

CHROM. 23 704

Book Review

Quantitative chemical analysis, by D. C. Harris, 1991, W. H. Freeman & Co., San Francisco, CA, 3rd ed., 758 pp., price £ 21.95 (paperback) £ 42.95 (hardcover), ISBN 0-7167 - 2171-6 (paperback), 0-7167 - 2170-8 (hardcover).

The course book *Quantitative chemical analysis* contains 25 chapters, covering general aspects, *e.g.*, units, tools such as the balance and glassware, errors and statistics, chemical equilibrium, "wet-chemical" methods, *e.g.*, gravimetry and precipitation, acid–base, EDTA and redox titrations, electrochemistry, spectrophotometry and atomic spectrometry and analytical separations and chromatography. A separate chapter on sample preparation and a chapter with illustrative experiments are also provided. The usefulness of the latter can be questioned: the number of experiments is too small to provide sufficient training in manual analytical practice, and a chemical textbook is far from ideal to be used at the bench in the laboratory.

The book is primarily an introductory course in analytical chemistry. One of the difficulties one faces in writing such an introductory course is that the text should simultaneously provide a sound physical understanding of the principles of analytical chemistry and also present the various topics in a way that is interesting for students for whom analytical chemistry is not their subject of prime interest. The reviewer considers that the author has succeeded in solving the problems associated with this challenge. The text is written in an open and understandable way, providing both the necessary in-depth physico-chemical knowledge and topics of more general interest, and also demonstrating the perspective and applicability of that knowledge. Various means are used to strengthen this. Each chapter contains, in addition to the main text, some illustrative examples, a short summary, a list of terms to understand, exercises and problems. Detailed solutions to the exercises are provided, and brief numerical answers to the problems are given; detailed solutions to the problems appear in a separate booklet (*Solutions manual to accompany quantitative chemical analysis*). Short notes on important points in the text are given in the text margin, which aids in clarification. Unfortunately, some of the figures and most of the figure captions and boxed challenging questions are also given in this text margin, obscuring the text clarifications. Further, topics of special interest, *e.g.*, piezoelectric crystal detectors, standard reference materials, oxygen sensors and chelation therapy, are discussed in grey boxes, providing a broader perspective. A set of colour plates in the middle of the book nicely illustrate some of the colourful aspects of analytical chemistry. The book ends with an extensive glossary of terms, a set of appendices and an elaborate index.

One of the features of the text is that SI units are used. Although SI units are officially accepted by scientists, many still use other, older units. However, especially in teaching, one should try to provide the correct units, hoping that some day a new generation will work in the officially accepted units.

In conclusion, this book is a worthwhile textbook for an introductory course in analytical chemistry. It provides the main topics of analytical chemistry in a sound but readable format, and also provides discussion on more advanced topics. It compares well with other introductory books on analytical chemistry.

Leiden (Netherlands) W. M. A. Niessen

Journal of Chromatography, 587 (1991) 369–370
Elsevier Science Publishers B.V., Amsterdam

CHROM. 23 705

Book Review

Non-chromatographic continuous separation techniques, by M. Valcárcel and M. D. Luque de Castro, Royal Society of Chemistry, Cambridge, 1991, XII + 290 pp., price £ 42.50, ISBN 0-85186-986-6.

In spite of its title, this book is of considerable interest for the chromatographer as it contains thorough reviews of various extraction and enrichment techniques, which are not usually treated together and which could become (and in some instances already are) useful for sample pre-processing before chromatographic separations. The meaning of the word "continuous" is that the techniques considered are performed in flow systems.

After a first introductory chapter, with a mainly philosophical and sometimes obvious content, the main body of the book is divided into three large chapters: Gas–liquid, liquid–liquid and liquid–solid systems.

The most significant (for the chromatographer) part of the chapter on gas–liquid systems treats the technique of gas diffusion through membranes. With this techniques volatile analytes can be efficiently separated from mainly aqueous matrices. In some instances, considerable enrichment is also possible. Its use in flow-injection analysis (FIA) is described in some detail, but there is no reference to direct combination with chromatography. The chapter also treats topics such as hydride and mercury vapour generation for atomic spectroscopy and micro-distillation. There is also a short description of continuous evaporation techniques.

The chapter on liquid–liquid systems first deals with dialysis. The theory of this technique should preferably be studied in alternative publications, but there are detailed descriptions of equipment and applications, both in FIA and in liquid chromatography. Also, the important application of in-line microdialysis is covered, *i.e.*, direct sampling and analysis of body fluids in living animals. The technique of aqueous–aqueous extraction with a liquid membrane is also mentioned. This technique can be seen as an extension to dialysis, additionally permitting selectivity and enrichment for certain sample classes.

Liquid–liquid extraction in flow systems is thoroughly covered with regard to the principles, equipment and applications of this important technique. Of special interest may be the section dealing with on-line coupling to gas and liquid chromatographic instrumentation. In the case of liquid chromatography both pre- and post-column arrangements are presented.

Most of the chapter on liquid-solid systems is not of immediate interest in combination with chromatography, except for a section which in a general way covers various uses for precolumns in liquid chromatography. Other techniques treated in the chapter include the use of ion-exchange columns in the atomic spectroscopy of metals and electrochemical stripping techniques.

The chapter also discusses methods for continuous precipitation, filtration, dissolution and leaching, none of which seem to have been used for chromatographic purposes, but which should not be excluded from potential future application in some instances.

The last chapter provides summarizing comments and comparisons regarding the techniques described earlier in the book. It also contains short descriptions of two additional techniques, which, admittedly, formally fall into the category defined by the title of the book, but add nothing to the general scope. The techniques of field-flow fractionation and isotachophoresis (the latter seemingly slightly mixed up with capillary electrophoresis) are better summarized in other publications, and their inclusion is probably a result of the authors' sometimes exaggerated urge to classify and systematize.

Also frustrating is the fact that the authors in most instances start by describing in detail material and apparatus before any general information is given about the general scope of use of a certain method.

The book contains very little useful theory, but a large number of instructive illustrations, mainly flow diagrams and details of equipment. There are also over 600 references, which further increase the value of this book as an important source of practical information about this timely topic.

Lund (Sweden) Jan Åke Jönsson

Author Index

PUBLICATION SCHEDULE FOR 1992

Journal of Chromatography and *Journal of Chromatography, Biomedical Applications*

MONTH	O 1991	N 1991	D 1991	
Journal of Chromatography	585/1	585/2 586/1 586/2 587/1	587/2 588/1 + 2	The publication schedule for further issues will be published later
Cumulative Indexes, Vols. 551–600				
Bibliography Section				
Biomedical Applications				

INFORMATION FOR AUTHORS

(Detailed *Instructions to Authors* were published in Vol. 558, pp. 469–472. A free reprint can be obtained by application to the publisher, Elsevier Science Publishers B.V., P.O. Box 330, 1000 AH Amsterdam, The Netherlands.)

Types of Contributions. The following types of papers are published in the *Journal of Chromatography* and the section on *Biomedical Applications:* Regular research papers (Full-length papers), Review articles and Short Communications. Short Communications are usually descriptions of short investigations, or they can report minor technical improvements of previously published procedures; they reflect the same quality of research as Full-length papers, but should preferably not exceed five printed pages. For Review articles, see inside front cover under Submission of Papers.

Submission. Every paper must be accompanied by a letter from the senior author, stating that he/she is submitting the paper for publication in the *Journal of Chromatography*.

Manuscripts. Manuscripts should be typed in double spacing on consecutively numbered pages of uniform size. The manuscript should be preceded by a sheet of manuscript paper carrying the title of the paper and the name and full postal address of the person to whom the proofs are to be sent. As a rule, papers should be divided into sections, headed by a caption (*e.g.*, Abstract, Introduction, Experimental, Results, Discussion, etc.). All illustrations, photographs, tables, etc., should be on separate sheets.

Introduction. Every paper must have a concise introduction mentioning what has been done before on the topic described, and stating clearly what is new in the paper now submitted.

Abstract. All articles should have an abstract of 50–100 words which clearly and briefly indicates what is new, different and significant.

Illustrations. The figures should be submitted in a form suitable for reproduction, drawn in Indian ink on drawing or tracing paper. Each illustration should have a legend, all the *legends* being typed (with double spacing) together on a *separate sheet.* If structures are given in the text, the original drawings should be supplied. Coloured illustrations are reproduced at the author's expense, the cost being determined by the number of pages and by the number of colours needed. The written permission of the author and publisher must be obtained for the use of any figure already published. Its source must be indicated in the legend.

References. References should be numbered in the order in which they are cited in the text, and listed in numerical sequence on a separate sheet at the end of the article. Please check a recent issue for the layout of the reference list. Abbreviations for the titles of journals should follow the system used by *Chemical Abstracts.* Articles not yet published should be given as "in press" (journal should be specified), "submitted for publication" (journal should be specified), "in preparation" or "personal communication".

Dispatch. Before sending the manuscript to the Editor please check that the envelope contains four copies of the paper complete with references, legends and figures. One of the sets of figures must be the originals suitable for direct reproduction. Please also ensure that permission to publish has been obtained from your institute.

Proofs. One set of proofs will be sent to the author to be carefully checked for printer's errors. Corrections must be restricted to instances in which the proof is at variance with the manuscript. "Extra corrections" will be inserted at the author's expense.

Reprints. Fifty reprints of Full-length papers and Short Communications will be supplied free of charge. Additional reprints can be ordered by the authors. An order form containing price quotations will be sent to the authors together with the proofs of their article.

For Superior Chiral Separation From Analytical To Preparative.

The finest from DAICEL·····

Why look beyond DAICEL? We have developed the finest CHIRALCEL, CHIRALPAK and CROWNPAK with up to 17 types of HPLC columns, all providing superior resolution of racemic compounds.

NEW CHIRALPAK AS

● CHIRALPAK AS

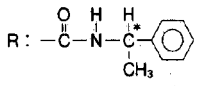

for β-Lactam antibiotics

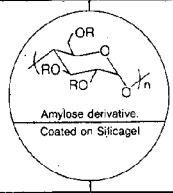

NEW CHIRALPAK AD

● CHIRALPAK AD

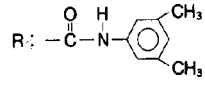

1-Acetoxy-2-azetidine

Eluant : Hexane/Ethanol = 8/2
Flow rate : 1.0ml/min
Temperature: r.t.
Detection : UV254nm

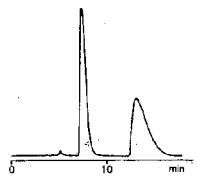

Oxyphencyclimine

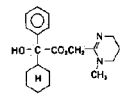

Eluant : Hexane/2-Propagol = 9/1
Flow rate : 1.0ml/min
Temperature: r.t.
Detection : UV254nm

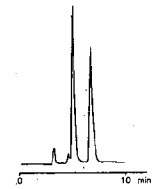

Ofloxacine methyl ester

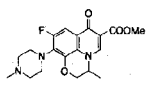

Eluant : Hexane/EtOH=8/2
Flow rate : 1.2ml/min
Temperature: 40°C
Detection : UV254nm

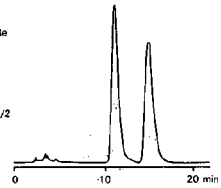

Verapamil

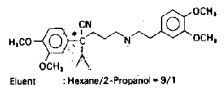

Eluant : Hexane/2-Propanol = 9/1
Flow rate : 1.0ml/min
Temperature: r.t.
Detection : UV254nm

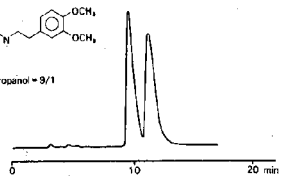

Analytical column 0.46cm×25cm(10μm)

CHIRALCEL OA
OB
OC
OD
OJ
OF
OG
OK

CHIRALPAK AS
AD

Normal Phase

Semi-preparative column 2cm×25cm(10μm)

You can have Pure enantiomer quickly!!

■Separation Service

- A pure enantiomer separation in the amount of 100g~10kg is now available.
- Please contact us for additional information regarding the manner of use and application of our chiral columns and how to procure our separation service.

DAICEL CHEMICAL INDUSTRIES, LTD.

chiral chemicals division.
8-1, Kasumigaseki 3-chome, Chiyoda-ku, Tokyo 100 Japan Phone: 03 (507) 3151 FAX: 03 (507) 3193

DAICEL(U.S.A.), INC.
Fort Lee Executive Park
Two Executive Drive, Fort Lee,
New Jersey 07024
Phone: (201) 461-4466
FAX: (201) 461-2776

DAICEL(U.S.A.), INC.
23456 Hawthorne Blvd
Bldg. 5, Suit 130
Torrance, CA 90505
Phone: (213) 791-2030
FAX: (213) 791-2031

DAICEL(EUROPA)GmbH
Oststr. 22
4000 Düsseldorf 1, F.R. Germany
Phone: (211) 369848
Telex: (41) 8588042 DCEL D
FAX: (211) 364429

DAICEL CHEMICAL(ASIA)PTE. LTD.
65 Chulia Street #40-07
OCBC Centre, Singapore 0104
Phone: 5332511
FAX: 5326454